

See discussions, stats, and author profiles for this publication at: <https://www.researchgate.net/publication/24381098>

# An improved model of the Earth's gravitational field: GEM-T1

Article · August 1987

Source: NTRS

---

CITATIONS

50

READS

342

10 authors, including:



Braulio V. Sanchez

Retired

49 PUBLICATIONS 877 CITATIONS

[SEE PROFILE](#)



David Edmund Smith

MIT

445 PUBLICATIONS 10,167 CITATIONS

[SEE PROFILE](#)



Erricos C. Pavlis

University of Maryland, Baltimore County

239 PUBLICATIONS 5,255 CITATIONS

[SEE PROFILE](#)

Some of the authors of this publication are also working on these related projects:



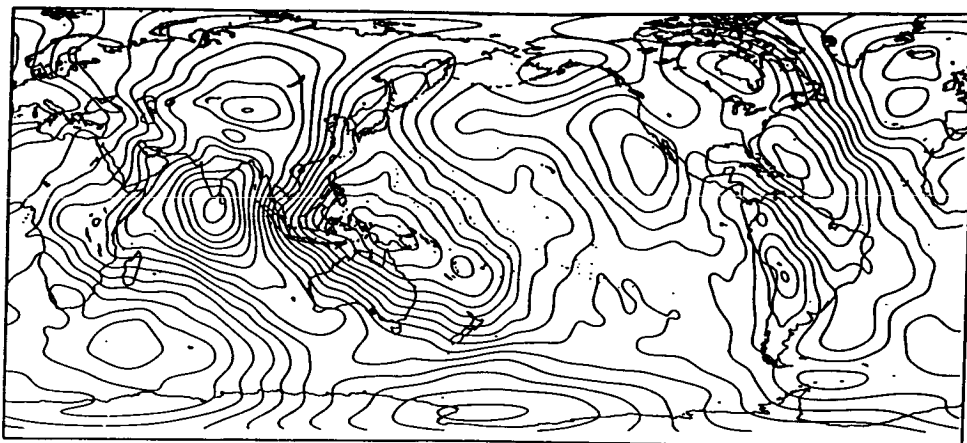
Project Spacetime Metrology and Relativistic Geodesy [View project](#)



Project Satellite Laser Ranging [View project](#)

# NASA Technical Memorandum 4019

## An Improved Model of the Earth's Gravitational Field: \*GEM-T1\*



J. G. Marsh, F. J. Lerch, B. H. Putney,  
D. C. Christodoulidis, T. L. Felsentreger,  
B. V. Sanchez, D. E. Smith, S. M. Klosko,  
T. V. Martin, E. C. Pavlis, J. W. Robbins,  
R. G. Williamson, O. L. Colombo,  
N. L. Chandler, K. E. Rachlin, G. B. Patel,  
S. Bhati, and D. S. Chinn

(NASA-TM-4019) AN IMPROVED MODEL OF THE  
EARTH'S GRAVITATIONAL FIELD: GEM-T1 (NASA)  
351 p Avail: NTIS HC A16/MF A01 CSCL 08G

N87-29967

H1/46 Unclassified  
0099843

JULY 1987



# NASA Technical Memorandum 4019

## An Improved Model of the Earth's Gravitational Field: \*GEM-T1\*

J. G. Marsh, F. J. Lerch, B. H. Putney,  
D. C. Christodoulidis, T. L. Felsentreger,  
B. V. Sanchez, and D. E. Smith  
*Geodynamics Branch*

S. M. Klosko, T. V. Martin, E. C. Pavlis,  
J. W. Robbins, R. G. Williamson,  
O. L. Colombo, N. L. Chandler, and  
K. E. Rachlin

*EG&G Washington Analytical Services  
Center, Inc.*

G. B. Patel, S. Bhati, and D. S. Chinn  
*Science Applications and Research  
Corporation*

JULY 1987



National Aeronautics and  
Space Administration

Goddard Space Flight Center

1987

## TABLE OF CONTENTS

|         |   |    |
|---------|---|----|
| 1.0     | INTRODUCTION . . . . .  | 1  |
| 2.0     | THE GEODYN AND SOLVE SYSTEMS . . . . .  | 9  |
| 2.1     | SOFTWARE DESCRIPTION . . . . .  | 9  |
| 2.1.1   | Vectorization of SOLVE . . . . .  | 11 |
| 2.1.2   | Evolution of GEODYN . . . . .   | 12 |
| 2.1.2.1 | GEODYN II Design Philosophy . . .   | 13 |
| 2.1.2.2 | GEODYN II Benefits . . . . .  | 20 |
| 2.1.3   | GEODYN II, SOLVE and the TOPEX Gravity Models . . . . .                           | 21 |
| 2.2     | OPERATIONS . . . . .  | 25 |
| 3.0     | REFERENCE FRAME . . . . .   | 29 |
| 3.1     | INTRODUCTION . . . . .  | 29 |
| 3.2     | DESCRIPTION OF THE CONTRIBUTING DATA . . . . .                                    | 29 |
| 3.3     | DISCREPANCIES BETWEEN DATA SETS . . . . .   | 30 |
| 3.4     | MATHEMATICAL FORMULATION . . . . .  | 33 |
| 3.5     | DYNAMIC POLAR MOTION . . . . .  | 38 |
| 3.6     | SUMMARY . . . . .   | 41 |
| 4.0     | A PRIORI CONSTANTS ADOPTED IN THE GENERATION OF THE TOPEX GRAVITY MODEL . . . . . | 43 |
| 4.1     | COMMON PARAMETERS . . . . .   | 43 |
| 4.1.1   | Earth Tides . . . . .   | 43 |
| 4.1.2   | Ocean Tides . . . . .   | 43 |
| 4.1.3   | Tidal Deformations . . . . .  | 44 |
| 4.1.4   | Earth Parameters . . . . .  | 44 |
| 4.1.5   | Polar Motion and A1-UT1 . . . . .   | 44 |
| 4.1.6   | Station Coordinates . . . . .   | 45 |
| 4.1.7   | Third Body Effects . . . . .  | 45 |
| 4.1.8   | Z-Axis Definition . . . . .   | 45 |
| 4.1.9   | Coordinate System . . . . .   | 45 |
| 4.1.10  | Relativity . . . . .  | 46 |
| 4.1.11  | A Priori Gravity Modeling . . . . .   | 46 |

*PRECEDING PAGE BLANK NOT FILMED*

*PREVIOUS PAGE BLANK NOT FILMED*

TABLE OF CONTENTS (cont.)

|          |   |     |
|----------|---|-----|
| 4.1.11.1 | Selection of an A Priori Gravity Model: General Vs. Several Tailored Fields . . . . .         | 47  |
| 4.1.11.2 | Simulations for Geopotential Solution Using Tailor-Made Vs. General A Priori Models . . . . . | 49  |
| 5.0      | TRACKING DATA . . . . .   | 59  |
| 5.1      | DATA SELECTION . . . . .  | 60  |
| 5.2      | INDIVIDUAL SATELLITE ANALYSES . . . . .   | 68  |
| 5.2.1    | Analysis of SEASAT Doppler and Laser Data . . . . .   | 68  |
| 5.2.2    | Analysis of OSCAR Doppler Data . . . . .  | 69  |
| 5.2.3    | Analysis of GEOS-1 Laser Ranging Data . . . . .   | 78  |
| 5.2.4    | GEOS-3 Analysis of Laser Ranging Data . . . . .   | 84  |
| 5.2.5    | Analysis of STARLETTE Laser Ranging Data . . . . .  | 89  |
| 5.2.6    | Analysis of LAGEOS Laser Ranging Data . . . . .   | 98  |
| 5.2.7    | Analysis of GEOS-2 Laser Ranging Data . . . . .   | 107 |
| 5.2.8    | Analysis of Optical and Low Inclination Satellite Observations . . . . .                      | 108 |
| 5.2.9    | Analysis of BE-C Laser Ranging Data . . . . .   | 128 |
| 6.0      | DEFINITION OF A PRIORI GEOCENTRIC TRACKING STATION COORDINATES . . . . .                      | 133 |
| 6.1      | COORDINATE SYSTEM DEFINITION . . . . .  | 133 |
| 6.2      | INITIAL STATUS OF STATION COORDINATES . . . . .   | 134 |
| 6.3      | THE TRANSFORMATION MODELS . . . . .   | 134 |
| 6.3.1    | Seven Parameter Transformation . . . . .  | 136 |
| 6.3.2    | The Linear Translation . . . . .  | 137 |
| 6.4      | NUMERICAL RESULTS . . . . .   | 137 |
| 6.4.1    | NAD 27 to SL-6 Transformation . . . . .   | 139 |
| 6.4.2    | GEM-9 to SL-6 Transformation . . . . .  | 139 |
| 6.4.3    | GSFC-73 to GEM-9 Transformation . . . . .   | 139 |
| 6.4.4    | Other Transformations . . . . .   | 140 |
| 6.5      | DISCUSSION . . . . .  | 140 |
| 6.5.1    | Transformation Parameters and Accuracies . . . . .  | 140 |
| 6.5.2    | Precision of the Transformations . . . . .  | 142 |
| 6.5.3    | Error Sources . . . . .   | 144 |
| 6.5.4    | Distortion in the NAD 27 Datum . . . . .  | 145 |
| 6.6      | SUMMARY OF STATION DEFINITION . . . . .   | 147 |

TABLE OF CONTENTS (cont.)

|         |   |     |
|---------|---|-----|
| 7.0     | FORCE MODELING . . . . .  | 149 |
| 7.1     | POTENTIAL EFFECTS . . . . .   | 149 |
| 7.1.1   | Mathematical Formulation of the Potentials .  | 149 |
| 7.1.2   | The A Priori Static Geopotential Models . .   | 152 |
| 7.1.3   | The A Priori Body Tide Model . . . . .  | 154 |
| 7.1.4   | A Priori Ocean Tides Models . . . . .   | 154 |
| 7.2     | ATMOSPHERIC DRAG AND SOLAR RADIATION PRESSURE . . . .                                   | 170 |
| 7.2.1   | Mathematical Formulation of the Models . . . .  | 170 |
| 7.2.2   | Atmospheric Drag Model Testing . . . . .  | 171 |
| 7.2.2.1 | Orbit Comparison Results . . . . .  | 173 |
| 7.2.2.2 | Evaluation of Apparent Timing . . . .   | 177 |
| 7.2.2.3 | Errors . . . . .  | 177 |
| 7.2.2.3 | Conclusions . . . . .   | 179 |
| 8.0     | SOLUTION DESIGN . . . . .   | 183 |
| 8.1     | COLLOCATION . . . . .   | 183 |
| 8.2     | STRATEGY FOR DATA WEIGHTING AND FIELD CALIBRATION . .                                   | 187 |
| 8.3     | PROBLEMS AND ASSOCIATED BENEFITS WITH A "SATELLITE-ONLY"<br>36 x 36 SOLUTIONS . . . . . | 198 |
| 9.0     | THE GEM-T1 SOLUTION RESULTS . . . . .   | 209 |
| 9.1     | THE GRAVITY MODEL . . . . .   | 209 |
| 9.2     | OCEAN TIDE SOLUTION . . . . .   | 209 |
| 9.3     | STATION COORDINATE SOLUTIONS AND COMPARISONS . . . . .                                  | 229 |
| 9.3.1   | Introduction . . . . .  | 229 |
| 9.3.2   | GEM-T1 Stations . . . . .   | 229 |
| 9.3.3   | Laser Station Solutions . . . . .   | 230 |
| 9.3.4   | Doppler Station Solutions . . . . .   | 232 |
| 9.3.5   | Summary . . . . .   | 235 |
| 9.4     | EVALUATION OF THE SOLVED POLAR MOTION . . . . .   | 235 |
| 9.4.1   | Introduction . . . . .  | 235 |
| 9.4.2   | The 1980-84 Solution . . . . .  | 236 |
| 9.4.3   | The Annual and Chandler Cycles . . . . .  | 240 |
| 9.4.4   | Summary . . . . .   | 248 |

TABLE OF CONTENTS (cont.)

|               |  |     |
|---------------|--|-----|
| 10.0          | A CALIBRATION OF GEM-T1 MODEL ACCURACY . . . . .   | 249 |
| 10.1          | THE GEM-T1 CALIBRATION OF A SATELLITE MODEL'S ERRORS<br>USING GRAVITY ANOMALY DATA . . . . . | 254 |
| 10.2          | CALIBRATION BASED UPON FIELD SUBSET SOLUTION TESTING .                                       | 263 |
| 10.3          | COMPARISONS BETWEEN GEM-T1 AND GEM-L2 . . . . .  | 277 |
| 10.4          | THE NEED FOR LOW INCLINATION DATA--REVISITED . . . .   | 280 |
| 10.5          | SUMMARY . . . . .  | 287 |
| 11.0          | GRAVITY FIELD TESTING ON GEM-T1 . . . . .  | 289 |
| 11.1          | ORBIT TESTING . . . . .  | 289 |
| 11.1.1        | Orbital Tests on Laser Satellites . . . . .  | 290 |
| 11.1.2        | Orbit Tests On Doppler Satellites . . . . .  | 302 |
| 11.1.3        | Tests Using Low Inclination Data . . . . .   | 304 |
| 11.1.4        | Radial Accuracy on SEASAT . . . . .  | 307 |
| 11.1.5        | Tests Using the Longitudinal Acceleration<br>on Ten 24 Hour Satellites . . . . .             | 310 |
| 11.2          | GEOID MODELING . . . . .   | 312 |
| 11.3          | ESTIMATED TOPEX/POSEIDON ORBITAL ACCURACY . . . .  | 313 |
| 11.4          | ORTHOMETRIC HEIGHTS COMPARISONS . . . . .  | 318 |
| 12.0          | SUMMARY . . . . .  | 325 |
|               | ACKNOWLEDGEMENTS . . . . .   | 327 |
|               | REFERENCES . . . . .   | 329 |
| APPENDIX I:   | TOPEX GEODETIC FILE: TRANET DOPPLER, LASER, S-BAND<br>TRACKING SITES . . . . .               | 337 |
| APPENDIX II:  | TOPEX GEODETIC FILE: OPTICAL AND EARLY DOPPLER TRACKING<br>SITES . . . . .                   | 343 |
| APPENDIX III: | <u>A PRIORI</u> OCEAN TIDAL MODEL . . . . .  | 347 |

## SECTION 1.0

### INTRODUCTION

Ground-based tracking of artificial satellites has provided an observational data set which has been used to develop spherical harmonic models of the global long wavelength gravity field of the earth. Analyses of these data by the authors and many others have provided a major advance in the field of Geodesy. Since the creation of the National Geodetic Satellite Program in the middle 1960's, a continuous effort has been underway at NASA/Goddard Space Flight Center (GSFC) and other research centers (notably the Smithsonian Astrophysical Observatory, the U.S. Department of Defense, and a cooperative effort between Germany's Deutsches Geodaetisches Forschungsinstitut and France's Groupe de Recherches de Geodesie Spatiale -- to name a few) to use satellite observations to improve our understanding of the gravity field and enhance our capabilities for modeling near-earth satellite orbital motion. Better knowledge of the geopotential has created dramatic advances in point positioning, in the study of the earth's kinematics and tectonics, in understanding the earth's rheology and interior, and in the study of global oceanic processes with spaceborne instrumentation.

The geopotential models developed by GSFC are known by their acronym, GEM, standing for Goddard Earth Models. The GEM have generally kept pace with the rapid advances made in the precision by which near-earth satellites are tracked and the orbital accuracy requirements of the missions themselves. However, new NASA missions foreseen for the 1990's require further gravity model improvement to achieve their mission objectives. Of most immediate concern is geodetic support (e.g., for orbit computations and the marine geoid) for the TOPEX oceanographic satellite which is under development for launch in 1991. The 10 to 15 cm radial orbit accuracy requirement of TOPEX, driven by the radar altimeter system, is at least a factor of three beyond the

capability of gravity models existing in 1985. There is an additional need for an Interim model which enhances our present knowledge of the earth's gravity field at intermediate and short wavelengths to the accuracy needed to support a low orbiting Geopotential Research Mission which is under consideration as a new flight project by NASA. Both of these objectives can be satisfied with a substantial improvement in global gravity modeling and the development of an Interim Model.

The recovery of a gravity model from satellite observations is both costly and time consuming. It requires the arduous analysis of large numbers of observations spanning diverse data types and the building of large numerical systems of equations permitting a simultaneous solution of several thousand unknowns. Consequently, the preparation of an improved model requires extensive pre-launch research.

To achieve the accuracy required for TOPEX, an experimental plan has been devised which builds towards a final geopotential solution in stages with harmonics extending to higher degree as the earth's gravity field is more completely sampled. Therein, each type of data is to be carefully scrutinized and separately evaluated to extract optimal subset gravity solutions. The final model, and one that will satisfy the TOPEX criterion, will be obtained from the combination of all of these validated data. This model will utilize a large amount of available laser, altimeter, satellite-to-satellite tracking and surface gravimetric observations.

This report describes the first of these preliminary gravity models, GEM-T1, which is exclusively based upon direct satellite tracking observations. This spherical harmonic model, complete to degree and order 36 is a direct result of the gravity field improvement effort which has been undertaken by GSFC and the University of Texas' Center for Space Research to produce an Interim Model. This "satellite-only" model was developed by GSFC and is reported herein. In regard to data selection, GEM-T1 although more complete in spherical harmonics, is

like earlier GSFC models, for example, GEM-9 (Lerch et al., 1979) and GEM-L2 (Lerch et al., 1982) which also exclusively used satellite tracking observations. Models which will include satellite-to-satellite tracking, spaceborne radar altimeter observations and surface gravity measurements are in the planning stages. These later fields will all be built upon the long wavelength information contained within GEM-T1.

The demands of future orbital missions made the recovery of a more accurate gravity model necessary and required their extension to higher degree. The availability of the CYBER 205 "super-computer" at GSFC played a major role in making this task both feasible within the time constraints imposed upon us and practical from a resource assessment. Adapting our orbit determination GEODYN Program and the SOLVE least squares solution system to the Cyber vector processor was a major step in laying the foundation for a complete and total re-iteration of our previous gravity modeling activities. The last recalculation of all least-squares normal matrices occurred more than ten years ago in preparation for GEM-7 (Wagner, et al., 1977).

In the computation of the GEM-T1 model a total re-iteration of the data analysis and matrix generation activities was performed. This permitted a consistency lacking in the earlier GEM models in terms of adopted constants, data treatment, non-conservative force modeling and in the definition of a reference frame. In particular, the aliasing error has been reduced by consistently evaluating all orbital data in the normal equations for a spherical harmonic representation to degree and order 36. For many data sets, terms extending to degree 50 are available although they have not been used to solve GEM-T1. In the past, as the state of the science evolved, only the most recent data sets benefitted from improved modeling. The inconsistencies associated with an evolving science and the lag-time required for their implementation in our data analysis have been avoided by design in the creation of GEM-T1. A model with improved parentage has now been produced which is based largely upon the standard set of constants

adopted for the MERIT Campaign (Melbourne, et al 1983) with some significant improvements. Additionally, other NASA Geodynamics research activities like the Crustal Dynamics Program, have provided improved a priori tracking station coordinates and earth rotation series which have been used in the development of GEM-T1. These models, values and treatments are described in detail within this report. In subsequent models planned for the next few years, a simultaneous solution including tracking station adjustments with the gravity field will also be explored.

Although the title of this report might indicate otherwise, there is more than one gravitational model discussed within its pages. We deliberately sacrificed brevity for the sake of completeness to permit a more thorough discussion of the approach we have pursued to design, compute, calibrate, and test the GEM-T1 solution. In so doing, we have presented material pertaining to many additional fields which were in some cases developed specifically for test purposes. Generally, these models were used to illustrate specific points and show the response of the model to new weights and/or new data contributions. As an aide in keeping track of them all and to assist in an easy understanding of their differences, these models are summarized in Table 1. Therein we present a brief description of these fields, and a cross reference which highlights specific tables, figures and sections where they are used.

**TABLE 1. KEY TO GSFC GRAVITATIONAL FIELDS:  
DESCRIPTIVE SUMMARY AND  
CROSS REFERENCE**

| <u>FIELD NAME</u> | <u>DESCRIPTION</u>   |
|-------------------|--|
| <b>GEM-T1</b>     | is a "satellite-only" gravitational field model developed from tracking data acquired on 17 unique satellite orbits (Table 5.4). A summary of the observations utilized is presented on Table 5.3 and the weighting used is shown in Figure 8.4. The spherical harmonic coefficients for GEM-T1 are found in Table 9.1 and their uncertainties are shown in Figure 10.1. This model is the focus of this manuscript. GEM-T1 had an internal GSFC field number of PGS 3113. Note also, certain data sets were corrected to improve the overall model. |
| <b>PGS-T2</b>     | is an earlier model presented at the American Geophysical Union Meeting in the spring of 1986. It did not contain data from 6 low inclination satellite (Section 5.2.8 and 10.4) and contained a serious GEOS-2 matrix back-substitution problem (Figure 8.3).   |

|                  |   |
|------------------|---|
| <b>PGS-T2'</b>   | is the PGS-T2 field (above) with the GEOS-2 problem corrected.  |
| <b>GEM-9</b>     | is a pre-Lageos "satellite-only" model (Lerch et al, 1977).   |
| <b>GEM-L2'</b>   | is the GEM-L2 model (Lerch et al, 1982) solved with the C,S (2,1) coefficients constrained to equal zero. This was GSFC's general recommended "satellite only" model prior to the completion of GEM-T1. |
| <b>PGS-1331'</b> | is the PGS-1331 model (Marsh et al, 1985), like Gem-L2, solved with C,S(2,1) constrained to equal zero. PGS-1331 was a model "tailored" for the Starlette satellite orbital computations.               |
| <b>PGS-S4'</b>   | is the PGS-S4 model (Lerch et al, 1982b ) solved with the C,S (2,1) coefficients constrained to equal zero. PGS-S4 was a model "tailored" for SEASAT orbital computations.                              |
| <b>GEM-10B'</b>  | is the GEM-10B model ( Lerch et al, 1981) solved with the C,S (2,1) coefficients constrained to equal zero. GEM-10B is a comprehensive model which contained altimetry and surface gravimetry.          |

**PGS-3013**

is the PGS-T2 model where the data weight was increased by a factor of 5 with respect to the collocation matrix (Table 8.2) and was used to give an example of the adequacy of the calibration method in Figure 10.12.

**PGS-3167**

was made from the GEM-T1 normal equations but solved to be of a smaller size--being complete to degree and order 20 (like GEM-L2) and not 36, which was the truncation limit of GEM-T1 (Figure 8.7).

**PGS-3163**

was a combination solution combining GEM-T1 with SEASAT altimeter matrices. The altimetry in this field was given a weak weight of 0.1 (Figure 8.5, Figure 10.3.1, and Figure 10.10).

**PGS-3164**

was the PGS-3163 field, solved giving greater weight of 0.5 to the altimetry (Figure 10.11).

SECTION 2.0  
THE GEODYN AND SOLVE SYSTEMS

The Cyber 205 computing system was obtained by Goddard Space Flight Center in 1982. An effort was immediately undertaken (and continues today) to improve our principal analysis tools, GEODYN and SOLVE, to efficiently use the Cyber's vector processing capabilities. This section describes the design decisions, status, and most importantly, the enormous benefits which accrued as a result of these software development activities.

#### 2.1 SOFTWARE DESCRIPTION

The primary software tools utilized by the GSFC TOPEX gravity modeling team were the SOLVE program and the GEODYN system of programs.

GEODYN provides state-of-the-art orbit determination and geodetic parameter estimation capabilities [Putney, 1977; Martin et al., 1980, Martin et al., 1987]. Using a fixed-integration-step, high-order Cowell integrator, GEODYN numerically integrates the spacecraft Cartesian state and the force model partial derivatives. The forcing function includes a spherical harmonic representation for Earth gravitation as well as models for point mass lunar, solar and planetary gravitation, solar radiation pressure, Earth atmospheric drag, and dynamical Earth and ocean tides. Observation modeling includes Earth precession and nutation, polar motion and Earth rotation, and tracking stations displacements due to solid tides and ocean loading. Tracking measurement corrections are provided for tropospheric and parallactic refraction, annual and diurnal aberration, antenna axis displacement and spacecraft center of gravity offset. Dynamic data editing is performed as the Bayesian least squares estimator is iterated to solution convergence. Estimable parameters include measurement and timing biases, and tracking

station coordinates, as well as the orbit state and force model parameters in all of the above mentioned models. The normal equations formed within GEODYN may be output to a file for inclusion in large parameter estimations and error analyses.

The SOLVE computer program selectively combines and edits the least squares normal equations formed by the GEODYN Program to form solutions for the gravity field, tracking station coordinates, polar motion, earth rotation, ocean tides and other geodetic parameters. The SOLVE Program provides a highly flexible tool for the computation of the solutions.

This software has evolved over the last 20 years to include the processing of many satellite tracking data types using sophisticated geophysical models. In the past, the research has been heavily constrained by the capabilities of the available computers. Typically, computer runs to create and solve large normal matrices for the solution of geodetic parameters required several CPU hours. As additional geophysical models were added, the increase in the number of estimable parameters was clearly limited by computer resources.

In 1982, the Cyber 205 vector computer was installed at GSFC. For more than a year before the installation, both GEODYN I and SOLVE were upgraded for the Cyber 205. The GEODYN program required some basic redesign to optimally use the vector hardware. This entailed a complete rewrite of the original scalar version of GEODYN, creating the GEODYN II Program. The SOLVE program, which intrinsically dealt with large arrays, was modified in sections to take advantage of the vector architecture.

From the beginning of this activity, considerable effort has been devoted to improve computational efficiencies on the Cyber. For GEODYN II, completely rewriting the software has taken several years. For SOLVE, I/O redesign has become necessary, since in a typical run, I/O time is now twice that of CPU time.

### 2.1.1 Vectorization of SOLVE

The SOLVE [Estes and Major, 1986] program has been vectorized for the Cyber 205. The solution section of the code is now fully vectorized and optimally partitioned for CPU and I/O performance. The CPU usage is so small that the algorithm is now clearly I/O bound. Minimizing the I/O time has led to the utilization of special I/O packages. Large quantities of data are moved simultaneously from different disk packs residing on separate I/O channels when possible.

Typically, many hundreds of matrices, each representing a single orbital arc, are required for a solution. Techniques are employed to limit the amount of data processed by SOLVE at any one time; these include combining several matrices into a single "combined" matrix or C-Matrix. SOLVE is capable of performing this function with the option of eliminating satellite arc dependent parameters through back substitution at the same time. There are two types of parameters that are solved for. Some are satellite specific (e.g., the satellite's initial state vector at some epoch time). These so-called "arc" parameters are seldom the ones of major interest. The "common" parameters include those of geodetic interest that are global in nature. They can be gravity coefficients, earth orientation parameters, tidal terms, etc., and it is the set of values of these parameters alone which normally constitute a solution. The process of combining matrices may be done when summing the normals of individual data sets to form C-matrices or at a later stage, when combining C-Matrices to form a second level of C-Matrices. This affords tremendous data compression and creates a final matrix with the smallest possible number of parameters through the back-substitution of all arc-parameters. When this matrix is inverted by SOLVE, corrections to the total set of common parameters are produced without the added expense of carrying along unnecessary arc parameters.

The SOLVE program has the capability to perform a linear shift on the right-hand side of the normal equations. This may be done during the combining stage so that all parameters converged using different values of the global parameters may be transformed to a common reference. The solution also may be referenced to any set of starting values. Other SOLVE capabilities include dynamical suppression of parameters based on numerical stability, application of weights to individual matrices or C-Matrices when combining, and carrying out a partitioned Cholesky decomposition to optionally compute (a) the parameter solution, (b) the parameter solution plus standard deviations or (c) the parameter solution plus a full variance/covariance matrix, as the user requires.

An example of the reduction in computing time which has been achieved is provided for the full inversion of a 1921 x 1921 matrix. On the IBM 3081 this process took 116 minutes of CPU time and 31 minutes of I/O time. On the Cyber 205 (with four million words of computer memory) the process required only 90 seconds of CPU time and 142 seconds of I/O time. This is a factor of 77 improvement in CPU and a factor of 13 improvement in I/O!

#### 2.1.2 Evolution of GEODYN

The original GEODYN system (GEODYN I) was designed for IBM mainframe computers. In this form, GEODYN I was optimized to take full advantage of its environment. When NASA began the procurement process for a vector computer, it became immediately apparent that a redesign of the GEODYN system was necessary to make a cost-effective utilization of the vector computing environment. Also of great importance was the vastly increased speed achievable for large parameter solutions if this approach was undertaken. Additionally the GEODYN I software contained a number of outdated approximations which needed to be eliminated in the system redesign.

With these concepts in mind, a two-pronged approach was taken which led to a new and highly efficient GEODYN operating within the vector processing environment.

Because GEODYN's historical computing environment - the IBM 360/95, was to be replaced, a scalar version of GEODYN I for the Cyber 205 computer was created directly from the IBM version. This program has been commonly referred to as Cyber GEODYN I.

In a parallel effort, a totally new GEODYN program was designed to take full advantage of the vector-processing environment. This new program is called GEODYN II and has been developed in such a fashion that those functions which are I/O intensive are performed on the "front-end" to the vector computer and the CPU intensive functions are performed either on the vector computer or on the "front-end" computer at the specification of the user.

These two efforts have permitted a smooth transition of operations from the IBM 360/95 to the Vector Processing Facility at GSFC. Because the GEODYN II system required a development period of about 5 years, the Cyber GEODYN I was used in the interim. A more thorough discussion of the GEODYN II design philosophy and its impact on the TOPEX gravity model effort are presented below.

#### 2.1.2.1 GEODYN II Design Philosophy

There were a number of key considerations that went into the design of the GEODYN II system. They are briefly presented below and individually discussed in the following paragraphs.

- o All data formats were made a uniform 64-bit floating point.

- o I/O intensive operations were off-loaded from the vector computer.
- o Observation processing was adapted to vectorization.
- o Interpolation and partial derivative chaining were fully vectorized.
- o Force model evaluations and partial derivatives were vectorized where appropriate.
- o Numerical integration of the orbit was vectorized where possible.
- o Numerical integration of force model partial derivatives was fully vectorized.
- o Formulation of normal equations was fully vectorized.
- o Large parameter solutions exhibit different vectorization problems than routine orbit determination solutions. Therefore capabilities were provided to allow optimization of vectorization based upon the type of problem to be solved.

Figure 2-1 presents the data flow structure of the GEODYN II system. It also indicates the operating environment of the various programs in the system. No explicit references to this figure are made in the following paragraphs, but an awareness of its contents may be useful to the reader.

Transmissions of data between the Cyber 205 vector computer and its "front-end", the Amdahl V7 computer, require data conversions if the data are to be used by both computer systems. These data conversions are

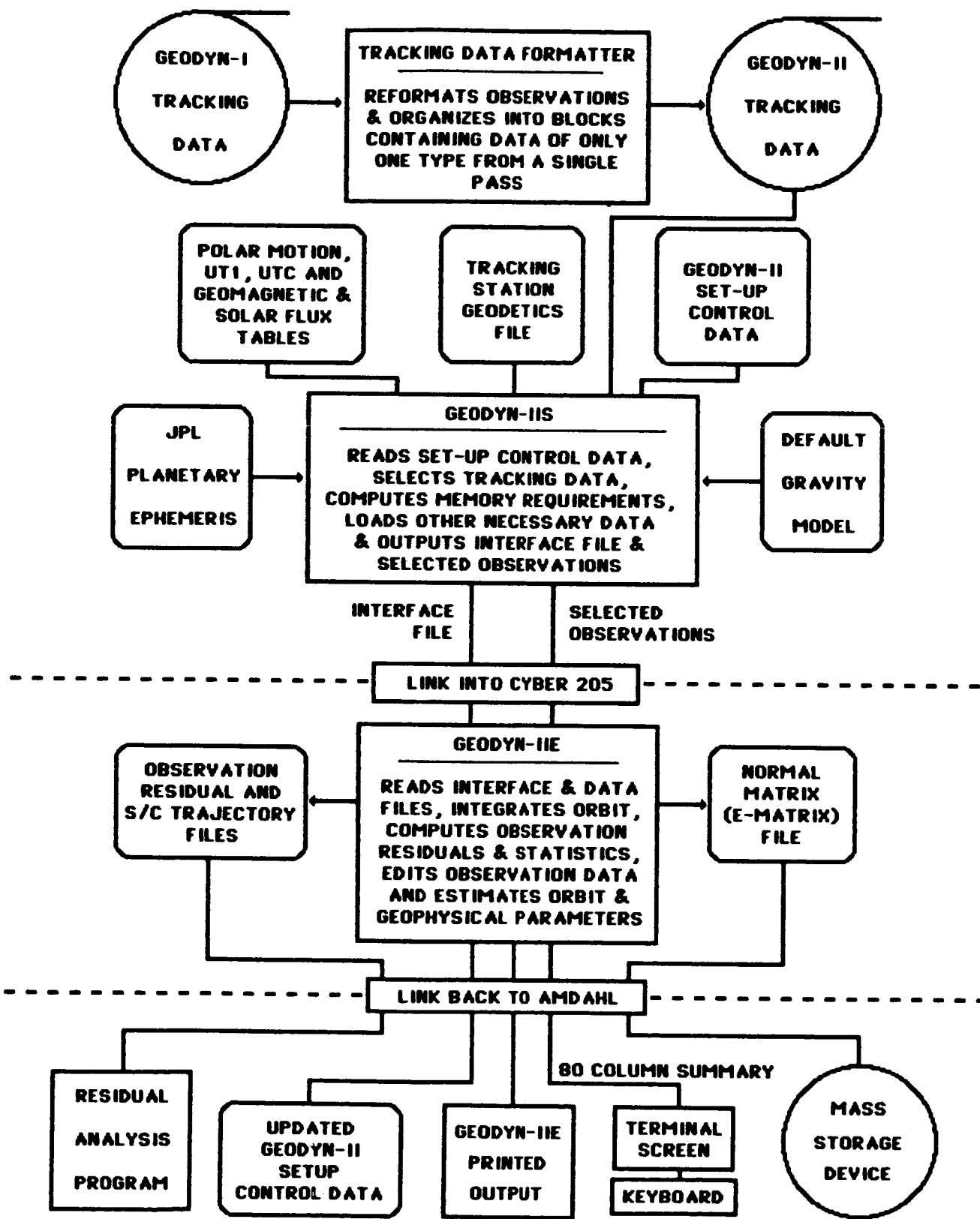


Figure 2.1 GEODYN-II Flow Diagram.

greatly facilitated and performed at a higher speed if the data are all of one FORTRAN variable type. For these reasons, all observation data and all output files from the Cyber 205 exclusively use 64-bit floating point words. The Tracking Data Formatter (TDF) program has been designed as the part of the GEODYN II system that converts all observation data into a common 64-bit floating point format.

The Cyber 205 is well-suited to the performance of operations that take advantage of vector pipeline commands. For this reason the basic input data processing, which is fundamentally serial, is performed on the Amdahl V7 computer by the GEODYN II-S program. This involves reading the various input files and selecting those subsets of data required to perform the numerical computations. The GEODYN II-S program also performs the bookkeeping functions of the system and transmits this information along with the data subsets to the computationally intensive component of the GEODYN II system.

The GEODYN II-E program is the computing engine of the GEODYN II system. This program has been designed in such a fashion that it may be used on both the "IBM type" computer or on the Cyber 205 vector processor. It is in this segment of the system where the CPU intensive operations are performed. GEODYN II-E has been optimized for the vector processing environment, and as a consequence, is most efficient when utilizing the Cyber 205 computer.

Observation processing has been vectorized within the GEODYN II system. This has been made possible by carrying this theme throughout all of the above programs:

Beginning with the TDF, the observations are organized by measurement type and tracking station into data blocks. Each data block contains observations of only one data type from a single tracking pass. The observations within each block are chronologically

ordered and the blocks themselves are chronologically ordered with respect to block start times.

The GEODYN II-S program retains an observation block structure in the data that it selects and passes on to GEODYN II-E. However, at this stage the data blocks may be subdivided to facilitate later processing.

GEODYN II-E processes data blocks by treating each observation identically within the same block. This allows the application of vector operations to the data processing algorithms. It further permits the vector interpolation of orbit and force model dynamical partial derivatives obtained from the numerical integration of the variational equations and the vector chaining of partial derivatives.

The primary time consuming algorithms in the numerical integration of satellite orbits and force model parameters are associated with 1) spherical harmonic evaluation of the Earth's gravitation field, 2) evaluation of variational derivatives, 3) numerical integration of the equations of motion, 4) evaluation of force model partial derivatives, 5) numerical integration of force model variational equations, and 6) the evaluation of other force model perturbations. The relative importance of each of these items depends on the specific circumstances pertaining to each problem. In the typical orbit determination problem items 1-3 will be expected to dominate computation times. When a tide model including 300 pairs of coefficients is evaluated, item 6 will become a very significant factor. Or, if a full gravity field normal matrix is to be calculated, items 4-5 will have substantial impact.

Because all of the above factors enter into the numerical integration problem, a very high level of vectorization is required in these areas. To deal in an efficient manner with these various problems GEODYN II-E has been vectorized in the following fashion:

- 1) Spherical harmonic evaluation has been fully vectorized including the Legendre polynomial recursions.
- 2) Spherical harmonic variational derivatives have been fully vectorized.
- 3) Numerical integration of the equations of motion is fundamentally sequential in nature, however some vectorization has been performed in this area.
- 4) Force model partial derivatives for terrestrial gravity and Earth and ocean tides have been fully vectorized.
- 5) Numerical integration of force model partial derivatives has been fully vectorized.
- 6) Evaluation of Earth and ocean tidal perturbations has been fully vectorized.

For large problems, the greatest speed improvements may be achieved through vectorization of the formation of the normal equations. Computations in this area are linearly proportional to the number of observations and proportional to the square of the number of adjusted parameters. This segment of the code has been fully vectorized in GEODYN II-E.

Problem-oriented intelligent optimization has also been performed within GEODYN II.

For simple orbit determination problems, the number of force model parameters is generally substantially smaller than the number of observations within each data block. Under these circumstances the matrix of partial derivatives is dimensioned such that partial derivative interpolation, chaining and normal summation will be vectorized based on the number of observations in the block.

For solutions with a large number of adjusted parameters, the problem is sufficiently complex that the normal equations for each data arc must be put in a file for later combination with the normal equations of other data arcs. In this situation the matrix of partial derivatives is dimensioned such that the partial derivative interpolation, chaining and normal summation will be vectorized based upon the number of adjusted parameters. Improvements achieved in this area result primarily from linearization of the relationship between computation time and the number of adjusted parameters.

Another problem addressed by GEODYN II occurs when the normal equations become sufficiently large that the program and its arrays no longer fit into computer memory. If left to its own devices the computer's virtual memory paging system will interminably thrash about consuming exorbitant amounts of computer time. For this reason the GEODYN II system has been optimized to partition the matrix summation problem. GEODYN II-E temporarily stores the measurement partial derivatives on disk and forms the normal matrix in the minimum number of segments necessary to allow summation without paging.

### 2.1.2.2 GEODYN II Benefits

The benefits of this extensive effort to reconstruct GEODYN for the vector processing environment are several:

- o The switch to the normalized Legendre recursion formulation in GEODYN II permits the numerically stable computation of gravitational coefficient accelerations and partial derivatives to degrees in excess of 360.
- o The computation of the Right Ascension of Greenwich is performed more precisely, eliminating annual discontinuities on the order of 100 microns.
- o Precession and nutation are included in the integration of the adjusted force model parameters resulting in more accurate force model partial derivatives.
- o Two-way range is strictly modeled as such, removing errors on the order of one micron for satellites at altitudes of one Earth radius. Errors of much greater magnitude are eliminated for more distant satellites.
- o The JPL DE-200 ephemeris using the Wahr nutations and the year 2000 precession model has been implemented.
- o Spherical harmonic contributions to the variational equations are fully computed automatically whenever normal matrices are output.
- o Time dependent non-conservative forces are now modeled.

and last, but not least,

- o Typical orbit determination runs are 6.5 times faster on the Cyber using GEODYN II than on the IBM 3081 using the original GEODYN I.
- o Gravity model normal matrix generations are at least 90 times faster using GEODYN II on the Cyber than original GEODYN I on the IBM 360/95. This factor of 90 is based upon duplication within GEODYN II, of the original GEODYN I processing of non-altimeter, satellite only, dynamical normals for inclusion in the GEM-10B gravity model.

#### 2.1.3 GEODYN II, SOLVE and the TOPEX Gravity Models

The TOPEX gravity modeling effort presented the first large scale problem to be solved using the GEODYN II system and the Cyber optimized SOLVE.

From the viewpoint of GEODYN II operations, three classes of satellite data arcs were used in the TOPEX gravity modeling effort. These classes were: optical data arcs, laser data arcs, and Doppler data arcs. The primary computational performance difference between the optical and laser data arcs derives from the number of estimated parameters included in the normal matrices generated. The Doppler data arcs not only include the greatest number of parameters but also include nearly an order of magnitude greater number of observations.

Figure 2-2 graphically illustrates the relationship between GEODYN II running time on the Cyber, the number of adjusted parameters and the number of observations in a data arc. The numbers shown are typical for the analysis of both optical and laser data. Similar

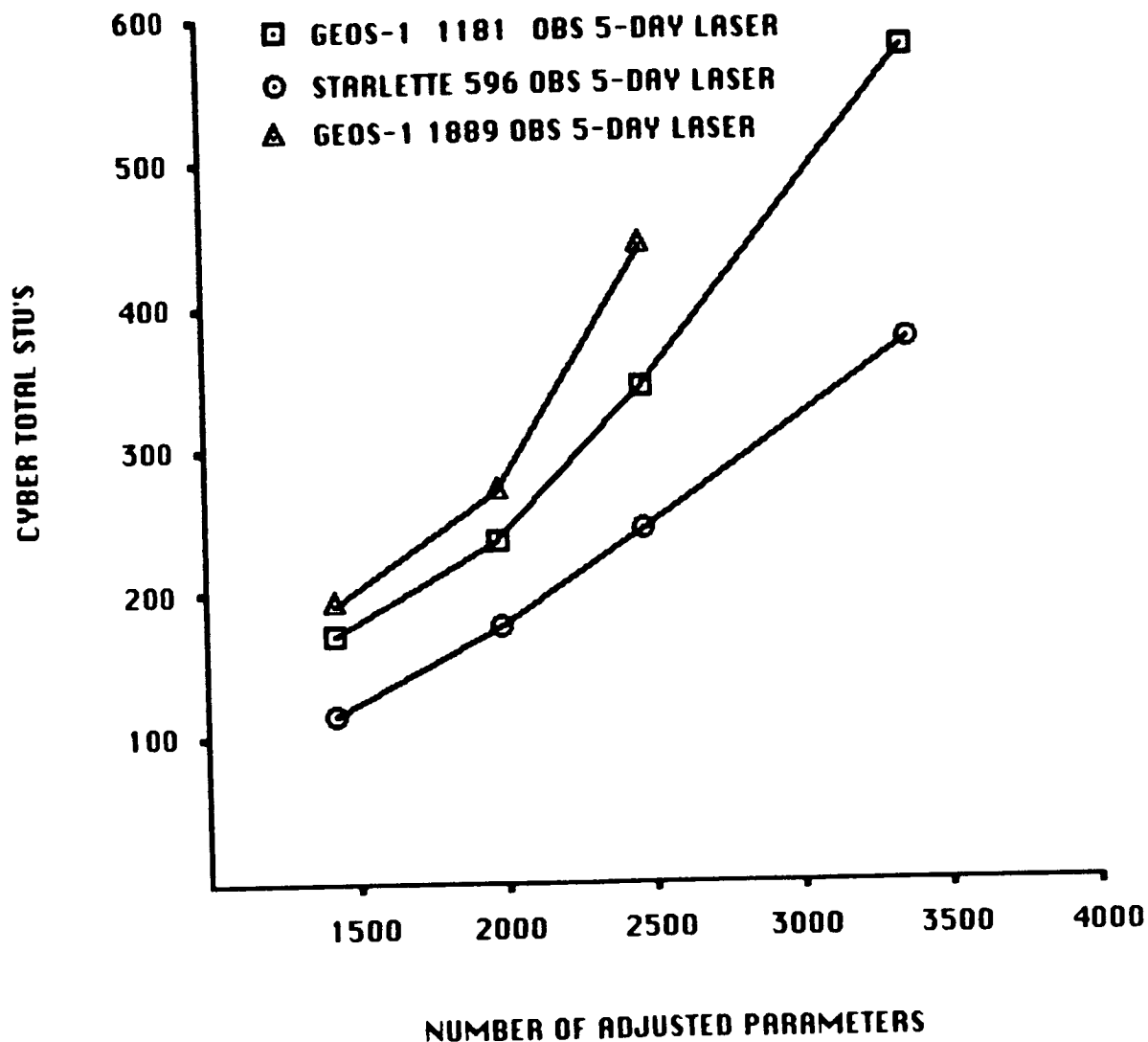


Figure 2.2 Computer Time Required for Generation of Normal Equations by GEODYN-II.

relationships exist for Doppler processing, with an approximately ten-fold increase in running time associated with the ten-fold increase in weighted observations.

Of particular note in Figure 2-2 is the strong linearity of all profiles as the number of adjusted parameters is increased. This should be compared with the quadratic increase in running time associated with the generation of normal matrices on scalar computers such as the IBM 360/95 and the IBM 3081.

Using a conservative speed-increase factor of 90 for GEODYN II on the Cyber versus the original GEODYN I on the IBM 360/95 (which is comparable in speed to the IBM 3081), the following estimates merit consideration.

- o Cyber 205 computer time required to generate 580 normal matrices of 2000 parameters and 1380 observations should be 44 hours.
- o IBM 360/95 computer time required to generate 580 normal matrices of 2000 parameters and 1380 observations should be 3,960 hours.

Using a factor of 6.5 speed increase for GEODYN II on the Cyber versus the original GEODYN I on the IBM 3081, estimates of the resources to converge each of the data arcs used in the gravity model determination are as follows:

- o Cyber 205 computer time required to converge 580 satellite data arcs, using 12 iterations each, should be 178 hours.
- o IBM 3081 computer time required to converge 580 satellite data arcs, using 12 iterations each, should be 1156 hours.

Using that same factor of 6.5, the following are estimates of the resources required to converge 720 data arcs used to evaluate the test gravity model solutions.

- o Cyber 205 computer time required to converge 720 satellite data arcs, using 6 iterations each should be 110 hours.
- o IBM 3081 computer time required to converge 720 satellite data arcs, using 6 iterations each should be 718 hours.

Translated into other terms, the projected resource requirements for the convergence and formation of 580 normal matrices and the testing of gravity model solutions would require the exclusive utilization of an IBM 3081 computer by the project for the period of nine full months.

This same computational burden, when placed on the Cyber 205 computer using the GEODYN II system, constitutes less than five percent of the annual resource allocation of the computer.

In fact the total computer resource budget for this TOPEX gravity model effort was only 500 hours of Cyber 205 time spent over a period of approximately one year. This figure also includes the computer resources used by SOLVE to combine the 580 normal matrices, remove all arc parameters through back-substitution, and produce some 120 test gravity fields. Such a concentrated effort to produce these TOPEX gravity models would not have been logically possible using the original GEODYN I and SOLVE even with a dedicated IBM 3081 computer.

## 2.2 OPERATIONS

With thousands of arcs to be processed by a dozen individuals at GSFC, the operation of the gravity field modelling effort was standardized as much as possible.

This was achieved in several ways. Each satellite was given a two character abbreviation and a three digit number so that required data sets and matrix numbers could be related to the satellite automatically. Generic setups were created to provide common control language and common model constants for ease of operation and quality control of input data streams. Naming conventions were defined for satellite observation data sets. The summary page output of the GEODYN program was modified to include more summary information. The normal equations were numbered to provide satellite and arc information as well as version number (see Figure 2-3). An on-line file was created to provide a reservoir of information for sharing and documenting the status of arcs completed and for combining arcs in the solution.

The actual task of arc processing and matrix generation was divided into subtasks by satellite and data type. After the processing for an arc had been completed, matrix numbers and mass storage cartridge and backup tape location was stored in an on-line data file.

The job submission was done on the Amdahl V-7, which is the front-end for the Cyber 205. It has an MVS operating system with the TSO interactive capability. TSO command files, or CLISTS, were created for the job submittal. Typically, the submittal of any of the job steps in the GEODYN or SOLVE program required the typing of only one line of controlling input containing the epoch date of the data arc, the satellite identifier, and the type of processing to be performed. The CLISTS, given this information, filled in the required data sets and

|  |   |                                   |
|--|---|-----------------------------------|
| <b>E MATRIX</b>  | <b>USSSTDDDDDER</b>                                     | <b>13 DIGITS<br/>(USUALLY 12)</b> |
|  | <b>EXAMPLE: 460176022701</b>                            |                                   |
|  | <b>VERSION 1 GEOS-3<br/>LASER DATE 760227</b>           |                                   |
| <b>LEVEL 1<br/>C MATRIX<br/>(CONTAINS ARC<br/>PARAMETER)</b> | <b>SSSTUARCCC</b>                                       | <b>10 DIGITS</b>                  |
|  | <b>EXAMPLE: 2403110205</b>                              |                                   |
|  | <b>BE-B OPTICAL VERSION 1<br/>10 ARCS CARTRIDGE 205</b> |                                   |
| <b>LEVEL 2<br/>C MATRIX</b>                                  | <b>TTSSSRAUU - ONE SATELLITE</b>                        | <b>9 DIGITS</b>                   |
|  | <b>EXAMPLE: 112601201</b>                               |                                   |
|  | <b>LASER BE-C 12 ARCS VERSION 1</b>                     |                                   |
| <b>(NO ARC PARAMETERS)</b>                                   | <b>TTBBAARRU - MULTIPLE SATELLITES</b>                  | <b>9 DIGITS</b>                   |
|  | <b>EXAMPLE: 110412001</b>                               |                                   |
|  | <b>LASER 4 SATELLITES 120 ARCS<br/>VERSION 1</b>        |                                   |

**WHERE:**

**AA OR AAA = NO. OF ARCS**

**SSS = SATELLITE NUMBER**

**BB = NO. OF SATELLITES**

**TT = DATA TYPE ENTERED TWICE**

**CCC = CARTRIDGE NUMBER**

**VER OR UU OR U = VERSION NUMBER**

**DDDDDD = DATE**

Figure 2.3 Matrix Numbering Scheme.

submitted the runs. In addition, various types of output were collected for further processing, documentation or continuation of the arc processing. This process automation has proven invaluable throughout the TOPEX gravity modeling project.

Data management for the normal equations was a nontrivial problem. A 2400 parameter matrix requires 2.9 million 8-byte words. Consequently, only 6 matrices fit onto a 6250-bits-per-inch magnetic tape. The storage of 1000 matrices requires 166 tapes. Consequently 332 tapes were required to maintain the minimal two copies that prudence demanded. The matrices to be used were stored on the mass storage device attached to the Amdahl V-7 computer. Cartridges were used to store the individual normal equations, and the combined normal equations. Typically, six normal equations were output from the GEODYN program onto a mass storage cartridge. These six were combined to form a Level 1 C-Matrix. This combined matrix was stored on the mass storage device as well. The arc parameters (state, drag, solar radiation, biases etc.) were maintained through the Level 1 C-Matrix. When 6 C-Matrices were completed they were combined into a Level 2 C-Matrix. At this point the arc parameters were eliminated from the matrix. The aim was to produce a single matrix from each satellite with a single data type. This would allow weighting of matrices in the solutions by satellite and data type. Some satellite data sets could also be combined, since they would be handled alike. This was true of the optical and some of the laser satellites. The record keeping and numbering/naming conventions are vital in such a large data management problem. It was important that the matrix number indicate the satellite or number of satellites, combined matrix level, version number, and the number of arcs or date of arc. Figure 2-3 shows how the different levels of combined matrices were numbered to maintain control of the data problem. In addition, combining matrices requires a fair amount of computer time. Therefore, it was necessary that a normal matrix compression occur at each successive level so that a sufficiently small

number of matrices would be created to permit a good turnaround of experimental solutions.

These operational concepts have paid off in providing a high degree of quality control, offering flexibility to the analyst in preparing arcs for inclusion in the gravity computation, and allowing control of the overall model and in the use of constants. The GSFC TOPEX gravity modeling project has benefitted immensely from this effort.

## SECTION 3.0

### REFERENCE FRAME

#### 3.1 INTRODUCTION

A uniform series for connecting the Conventional Inertial Reference System (CIRS) realized by the orbital dynamics, with the Conventional Terrestrial System (CTRS) realized by the global network of tracking stations was a requirement for our new gravity solution. This was one of the preliminary activities undertaken for the development of the TOPEX field. A desirable technical constraint on the origin of these series requires that it be as close as possible to the average pole of the mid-70's to mid-80's interval. This required a redefinition of the origin to coincide with the LAGEOS estimated 1979-84 six-year average pole. The major characteristics of the new series are its uniformity, its new origin, and its consistency with other conventional models used in the transformation CIRS <=> CTRS, namely the nutation model (Wahr's) and the precession model (Lieske's).

#### 3.2 DESCRIPTION OF THE CONTRIBUTING DATA

The polar motion and UT1-UTC data available to us were as follows:

- (1) the somewhat poorly documented but well maintained file of polar motion values contained in GEODYN I,
- (2) two series based on BIH data (Feissel, private communication),
- (3) the series resulting from the LAGEOS SL6 solution.

The source(s) for the first data set is not clear, especially for the earliest years. The BIH series were obtained from the BIH Circular D data set with additional corrections to reference them to the IAU 1980 nutation theory (Wahr, 1979) and contained some weak Vondrak smoothing to remove periodicities shorter than 35 days. The third and last set of data, that obtained by GSFC from LAGEOS, was used as the basis for unifying the series. This set was adopted for it is more consistent with the rest of the mathematical model than any other. Details about the periods covered by each data set are given in Table 3.1. The BIH series are shown in Figure 3.1.

### 3.3 DISCREPANCIES BETWEEN DATA SETS

The discrepancies reconciled here were different for each of the data sets, even though for the most part, they all amount to a different origin of the local frame in which the pole coordinates are reported. As a first step we compared each of the above with the SL6 series. The origin of the BIH 1967-85 series could be easily and rigorously related to that of SL6 since the two series overlapped for a considerable time interval. The six year period (1979-84) was selected as the most appropriate for determining the transformation parameters between the two series for several reasons. First, this period is where the LAGEOS-determined polar motion is the strongest due to the robustness of the tracking data set. Second it covers most of the period over which very accurate tracking data are available for analysis under this project. A six year period was selected to properly average both the annual as well as the Chandlerian cycles of the polar motion.

Table 3.1

**POLAR MOTION  
AND EARTH ROTATION SERIES**

• SELECTED DATA FOR POLAR MOTION

| <i>SOURCE</i>                 | <i>PERIOD</i>       |
|-------------------------------|---------------------|
| - OLD GEODYN FILE             | 58 09 18 - 61 12 31 |
| - BIH CIRCULAR D (OLD SYSTEM) | 62 01 05 - 66 12 30 |
| - BIH CIRCULAR D (NEW SYSTEM) | 67 01 04 - 78 12 27 |
| - LAGEOS SOLUTION SL-6        | 79 01 01 - 84 12 30 |

• EARTH ROTATION SERIES

|                   |                     |
|-------------------|---------------------|
| - OLD GEODYN FILE | 58 09 18 - 61 12 31 |
| - BIH CIRCULAR D  | 62 01 05 - 84 12 30 |

• MAJOR DISCREPANCY

THE REFERENCE FRAME DIFFERENCE BETWEEN THE  
BIH CIRCULAR D SERIES AND THE LAGEOS SL-6 SERIES.

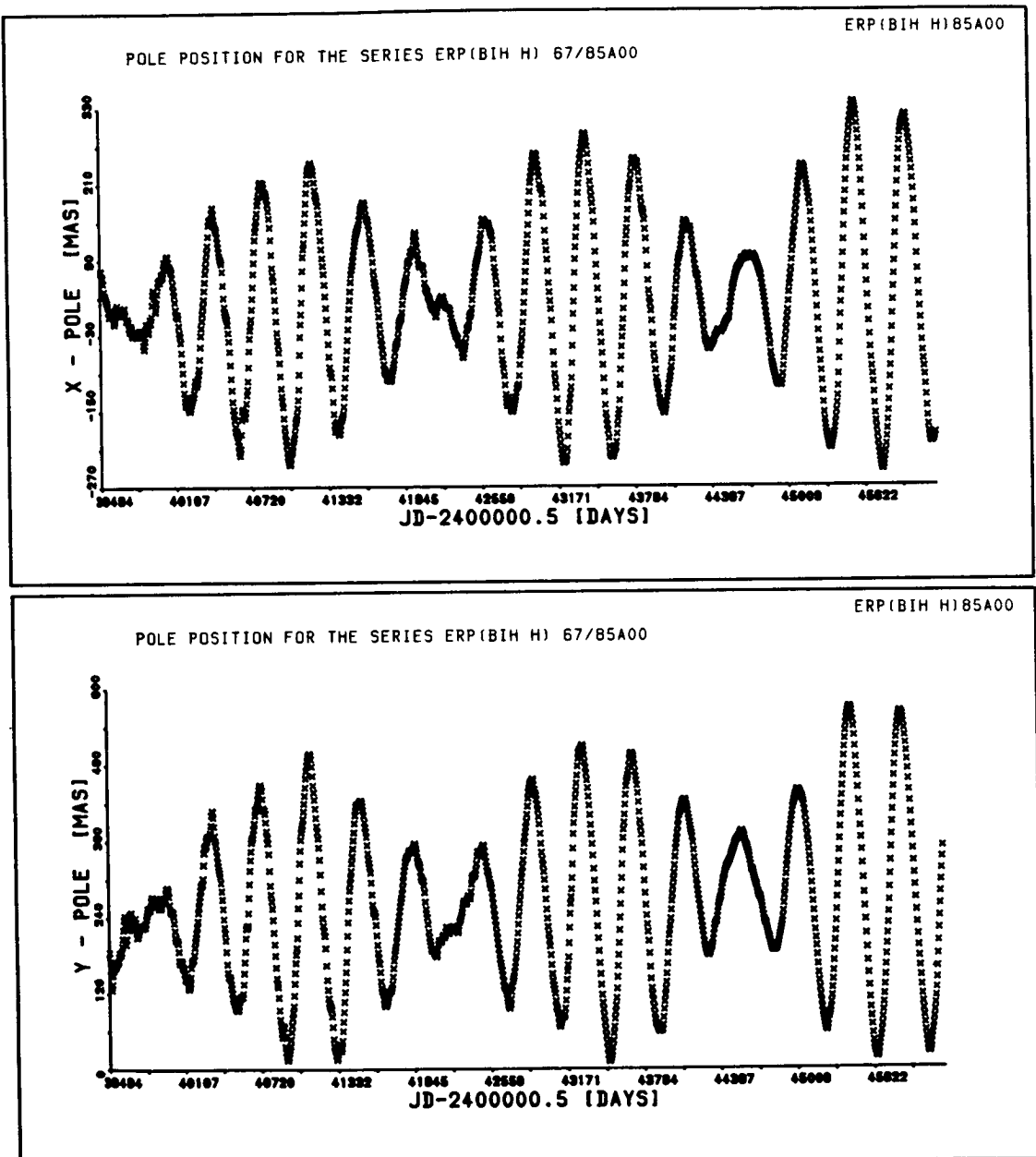


Figure 3.1 BIH Polar Motion.

### 3.4 MATHEMATICAL FORMULATION

The general theory on which we based our reference frame transformations is detailed in the recommendations report made by COTES (IAG/IAU Joint Working Group on the Establishment and Maintenance of a Conventional Terrestrial Reference System) to the MERIT Steering Committee (CSTG Bulletin, June 9, 1982). Since the LAGEOS-derived Earth Rotation variations (UT1-UTC) do not provide a continuous uniform series we limited our analysis to that of the polar motion series. We thereby adopted the BIH-provided UT1-UTC series with no changes whatsoever. A general picture of the geometry and notation utilized in this analysis is shown in Figure 3.2. With the third rotation eliminated by virtue of the fact that the two Earth Rotation series are identical, the mathematical model relating the  $x_p$ ,  $y_p$  discrepancies to the systematic transformation parameters is as follows:

#### THE MERIT/COTES WORKING GROUP MODEL

$$\Delta y = \alpha_1 \cos \theta + \alpha_2 \sin \theta - \beta_1 \quad (3.1)$$

$$\Delta x = -\alpha_1 \sin \theta + \alpha_2 \cos \theta - \beta_2$$

where:

$\alpha_1$ ,  $\alpha_2$ : implied inertial frame misalignment

$\beta_1$ ,  $\beta_2$ : implied terrestrial frame misalignment

$\theta$  : Greenwich Mean Sidereal Angle

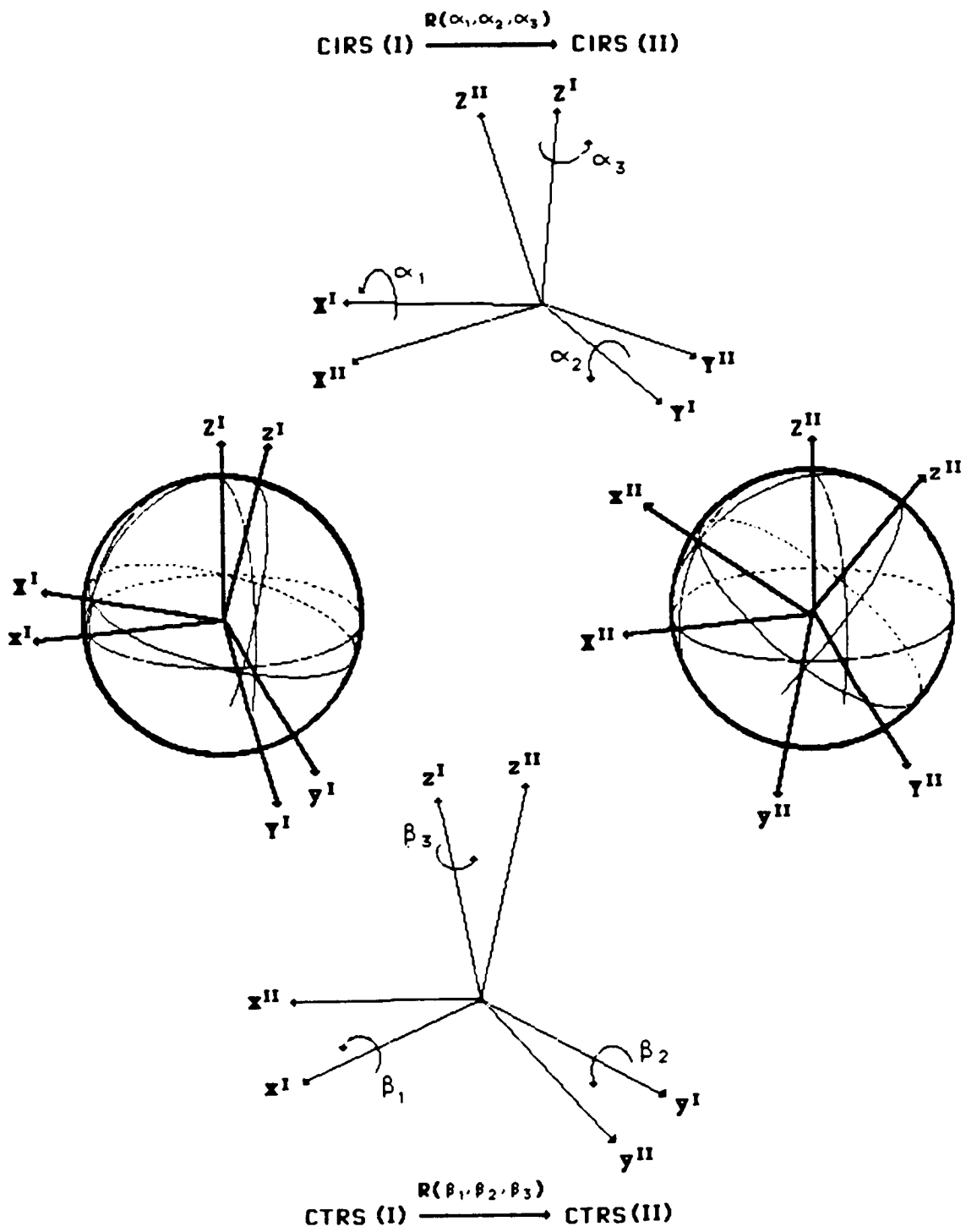


Figure 3.2 Geometry for Coordinate Transformations.

Application of this model to the selected 6-year BIH-SL6 polar motion discrepancies resulted in the determination of the misalignment angles listed in Table 3.2. These parameters were used to transform all of the BIH polar motion series from 1962 to the end of 1978 into the SL6 reference frame. The average values of the  $x_p, y_p$  listed in this table were used to define the new origin of the local plane coordinate system to which the coordinates of the pole refer. The reason for this is apparent after a discussion of the dynamic polar motion. Since this origin coincides with the Z-axis of our terrestrial system of reference, we have, in effect, redefined that axis as well. To be consistent therefore we must apply the appropriate rotations to the station coordinates to make them compatible with this new Z-axis. The geometry and the relationship of these coordinate systems at the pole are shown in Figure 3.3. The redefinition of this origin was realized for this new polar motion series through a simple subtraction of the above average values. In the case of the station coordinates we must apply these two rotations about the X-axis ( $y_p$ ) and Y-axis ( $x_p$ ). Since the angles are small, the cosines are basically equal to one and the sines can be approximated by the angles in radians. The transformation equations then are:

$$\begin{aligned} x_T &= x_S - \bar{x}_p z_S \\ y_T &= y_S + \bar{y}_p z_S \\ z_T &= z_S + \bar{x}_p x_S - \bar{y}_p y_S \end{aligned} \tag{3.2}$$

where the subscript S stands for the SL6 coordinates and the T for the new frame for TOPEX.

TABLE 32

BIH (1979-84) TO LAGEOS (SL-6)  
POLAR MOTION SERIES  
TRANSFORMATION PARAMETERS

$\beta_1 = 1.46 \pm 0.3$  mas

$\beta_2 = -3.80 \pm 0.3$  mas

$\alpha_1 = -0.22 \pm 0.3$  mas

$\alpha_2 = 0.62 \pm 0.3$  mas

RMS ( $\Delta x$ ) : 6.5 mas

RMS ( $\Delta y$ ) : 6.2 mas

SIX YEAR AVERAGE

$x = 38.2 \pm 0.9$

$y = 280.3 \pm 2.2$

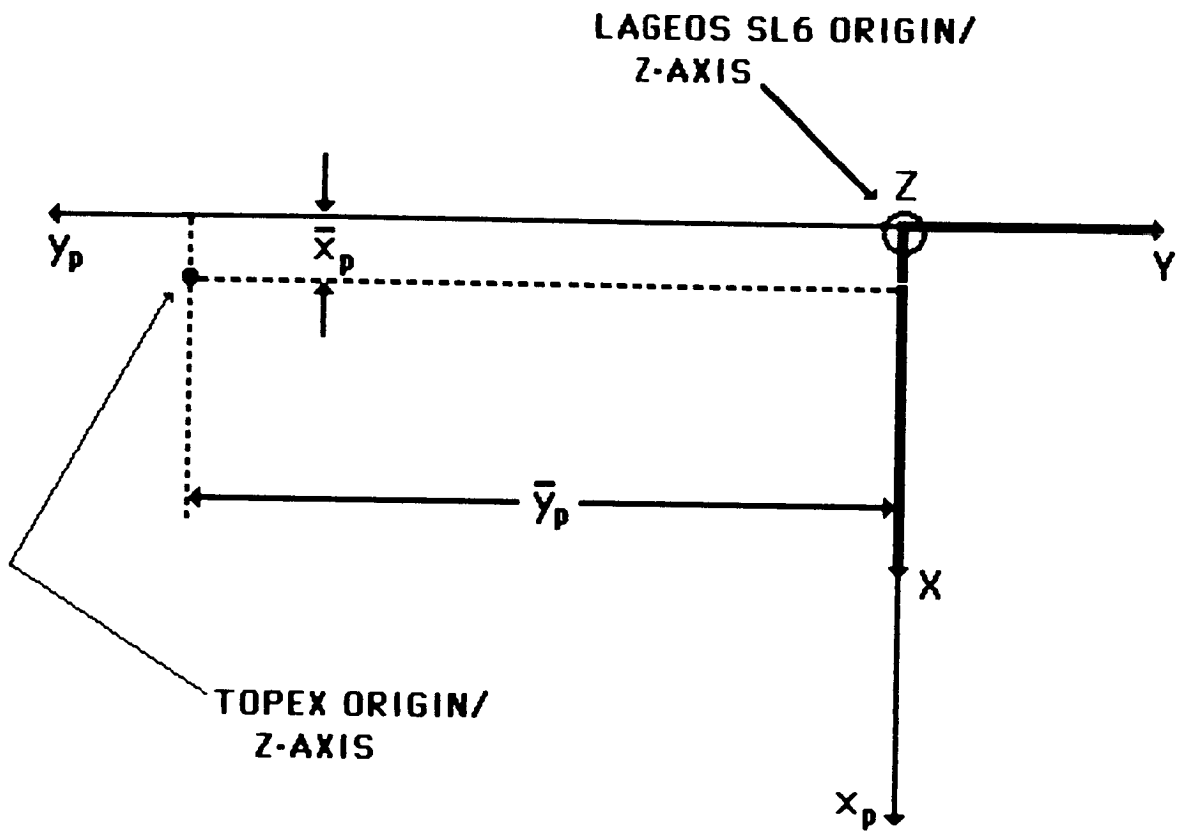


Figure 3.3 Relationship of Coordinate System Origins.

### 3.5 DYNAMIC POLAR MOTION

The non-rigidity of our planet is clearly manifested in the temporal variability of the Earth's moments of inertia in response to both rotational and tidal deformations. The Earth's axis of figure, which is the principal axis of angular momentum, exhibits two periodic motions. There is daily motion with an amplitude that can reach 60 meters due to the Earth's response to the tidal deformation. The tides are modeled elsewhere and therefore this motion is accounted for. The much smaller motion, with a period similar to that of the Chandlerian wobble, is the Earth's response to the rotational deformation. The geometry of the motions involved is depicted in Figure 3.4.

Most of the theories developed so far [Gaposchkin, 1972], [Lambeck, 1971 and 1972], [McClure, 1973] concluded that this motion is proportional to the main wobble. The proportionality factor when the geopotential is referenced on the CTRS is about 1/3 and depends on the Earth's elastic properties. Because our capability to determine  $C(2,1)$  and  $S(2,1)$  is of higher accuracy than our knowledge of the Earth's elasticity parameters, it is only prudent to parameterize this factor. It is well known [Heiskanen and Moritz, 1967] that the orientation of the axis of figure with respect to some arbitrary frame of reference is reflected in the values of the second degree, order one, harmonics of the spherical harmonic expansion of the gravitational field of the body ( $C, S(2,1)$ ). Based on the equations given in [ibid.] relating the moments of inertia to the  $C(2,1)$  and  $S(2,1)$  harmonics (through  $C(2,0)$ ), we can derive a general formulation which accounts for the temporal variations of the figure axis through the application of proportional variations of the  $C, S(2,1)$  harmonics. Denoting this proportionality factor by  $k$  (to be determined), the resulting model is:

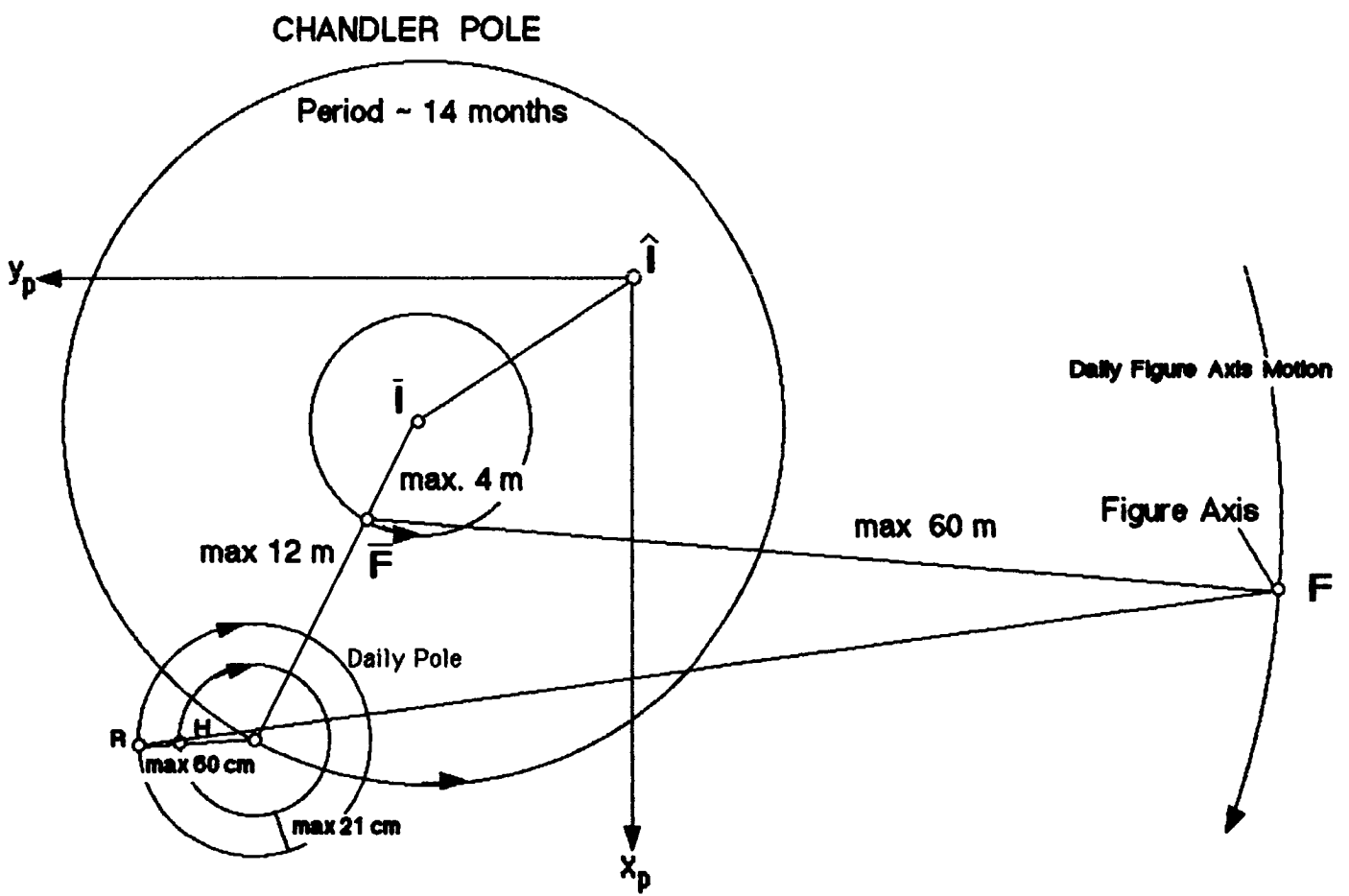


Figure 3.4 Dynamic Polar Motion Model.

$$c_{2,1}(t) = \hat{c}_{2,1}(t_0) + \dot{c}_{2,1}(t-t_0) + kx_p(t) \hat{c}_{2,0} \quad (3.3)$$

$$s_{2,1}(t) = \hat{s}_{2,1}(t_0) + \dot{s}_{2,1}(t-t_0) - ky_p(t) \hat{c}_{2,0}$$

where the harmonics with the carets refer to the value of these harmonics relative to the CTRS at the initial epoch,  $t_0$ . It should be clear that the periodic part, which is represented by the last term, will average out in each Chandler cycle; any mean offsets in the polar motion series cause there to be a need for nonzero first terms. The center of the polar motion migrates slowly, and after some time, accumulates as an offset. To the extent that this offset becomes much larger than that of the periodic part, the second term is included to compensate for this future secular motion. If we were to reference our gravitational expansion to a CTRS whose third axis coincides with the average wobble center at  $t_0$ , then the first terms are identically equal to zero. Over a short period of time (several years) the second term is negligible; and as argued above, the third term will average out if we analyze data over full Chandler cycles.

Our current software does not completely model this effect. Plans to implement it have been developed. Therefore with the current SL6 coordinate system very close to that of BIH, the average pole for the recent years (which contain the most accurate and more important tracking data) would be about 10 meters off at an azimuth of about 270 degrees. The first term in the above model therefore would be nonzero and very significant. By redefining the origin and the Z-axis of our CTRS we have avoided these implications and at the same time, we can still use the available software. Additionally, when the full model is implemented we lose nothing since we can always apply it with the initial harmonics at  $t_0$  equal to zero.

### 3.6 SUMMARY

The methodology used for creating a uniform series for the coordinates of the pole over the period Sep. 18, 1958 through Dec. 30, 1984 based on series provided primarily by the BIH and the LAGEOS SL6 system has been presented. The resulting series realizes a modified SL6 CTRS, modified in the sense that its Z-axis and thus the origin of the local plane system to which the pole coordinates  $x_p, y_p$  refer, coincide with the axis through the center of the 1979-84 six-year wobble. This deviation from the SL6 CTRS makes it possible to set  $C(2,1)$  and  $S(2,1)$  identically equal to zero with no further modeling for the dynamic polar motion and still claim a model accuracy which is only slightly inferior to the ideal model described herein.

SECTION 4.0  
A PRIORI CONSTANTS ADOPTED IN THE GENERATION  
OF THE TOPEX GRAVITY MODEL

The constants that were adopted and used in the development of the a priori TOPEX gravity model delineate the physical parameters within which the solution exists. These constants were chosen after considerable thought and debate. This brief chapter describes the adopted parameters and updates a similar monograph found in Marsh and Tapley (1985). The constants and procedures are listed by parameter type in the following section on common parameters. By common parameters it is meant parameters which are not satellite dependent (e.g. parameters regarding the Earth).

#### 4.1 COMMON PARAMETERS

##### 4.1.1 Earth Tides

A total of eight tidal harmonics were used from Wahr's frequency dependent model (Wahr, 1979), providing the a priori standard. All other solid earth tides were modeled through a closed formula for their combined 2nd degree tidal potential using  $k_2=0.30$  and a zero phase lag. Partials were included for each of the specific frequency-dependent solid earth tidal terms, as well  $k_2$ ,  $\epsilon_2$  and  $k_3$ , to add some flexibility in our tidal analysis (see Section 7.1 for a complete description of the earth tide modeling).

##### 4.1.2 Ocean Tides

The a priori ocean tide model was developed by Christodoulidis, et al. (1986b) in which 600 individual terms representing 32 major and

PRECEDING PAGE BLANK NOT FILMED

minor tides were calculated from point admittances. For diurnal and semi-diurnal constituents, the tidal expansion was carried out in spherical harmonics to degree 6 for both the prograde and retrograde parts of that expansion. For long period tides only prograde terms were used. The a priori terms were predicted from admittances over each band using the values and errors found in the Schwiderski (NSWC) oceanographic models. Details on the algorithm can be found elsewhere (Section 7.1) in this document. Partials were computed for the 6 prograde terms giving long period orbital perturbations for each of 12 tidal frequencies.

#### 4.1.3 Tidal Deformations

The Love and Shida numbers  $h_2$  and  $l_2$  had, as a priori values, the values adopted for the MERIT Campaign standards, (Melbourne et al., 1983);  $h_2 = .609$ ,  $l_2 = .0852$ . Partials were included for  $h_2$  and  $l_2$ .

#### 4.1.4 Earth Parameters

The a priori value adopted for the product of the gravitational constant and the Earth's mass, GM, was  $398600.436 \text{ km}^3/\text{s}^2$ . The speed of light adopted was set at  $299792.458 \text{ km/s}$ . The semi-major axis of the Earth was set at  $6378137\text{m}$ . The Earth's flattening chosen as  $1/298.257$ . These values are consistent with the adopted laser tracking station coordinates used as a priori values for the orbital recoveries.

#### 4.1.5 Polar Motion and A1-UT1

In conjunction with a more consistent definition of the geometric and gravimetric reference frames, a zero-mean set of polar motions has been adopted. Partials have been calculated for average five-day polar

motion and earth rotation values. Details regarding the a priori values used for this zero-mean set of polar coordinates can be found elsewhere in this document.

#### 4.1.6 Station Coordinates

A priori station coordinate files were constructed based upon the global laser station coordinate solution SL-6. The MERIT adopted reference longitude for the laser station at McDonald, TX, was implemented and the coordinates were rotated to comply with the zero mean pole definition mentioned before. Station parameter partials were computed for further analysis and quality checks. Further details on this subject are presented in Section 6.

#### 4.1.7 Third Body Effects

Gravitational potential perturbations have been modeled for all of the planets except Pluto.

#### 4.1.8 Z-Axis Definition

The Z-reference for the gravity field is provided by the instantaneous spin axis of the Wahr model.

#### 4.1.9 Coordinate System

The J2000 reference epoch and associated precession constants as adopted by the IAU have been utilized throughout. The nutation model used is that of Wahr.

#### 4.1.10 Relativity

Relativistic effects were not applied.

#### 4.1.11 A Priori Gravity Modeling

An a priori gravity model is necessary in order to converge the orbits and to construct the matrices required for a linear differential correction to form a new gravity solution. Four gravity models were used in this regard. The LAGEOS data were prepared by using the GEM-L2' model of Lerch et al (1982). The prime denotes that the model (in spherical harmonic form) was obtained through a new solution which contained all of the original GEM-L2 data but now constrained the C(2,1) and S(2,1) coefficients to zero. Justification for this constraint is discussed in detail in Section 3. The STARLETTE data were prepared by using the PGS-1331' model; a model that has been tailored for STARLETTE analysis (Marsh et al, 1985). The SEASAT data were prepared by using the PGS-S4' model; a model that has also been tailored for SEASAT analysis (Lerch et al, 1982). All other satellites contributing in the solution were prepared by using the GEM-10B' model (Lerch et al, 1981) which is GSFC's preferred general gravity model. Note that all the models mentioned here have been resolved constraining the C(2,1) and S(2,1) coefficients to have zero values (as denoted by the primes). The adoption of several gravity models means that differing a priori parameters were used with different data sets. This approach was adopted after conducting the following study.

#### 4.1.11.1 Selection of an A Priori Gravity Model: General Vs. Several Tailored Fields

The question of which gravitational field should be chosen as the a priori model was investigated. The central concern was whether adopting one model or several specialized models, or even some new "ad hoc" ones, would be better for the linearization of the observation equations. This question was of concern because of the known properties of general and "tailored" fields. Tailored models fit the data from one specific satellite orbit very well. However, the individual coefficients in these models can be at times, geophysically unrealistic. The general models, on the other hand, have the best set of coefficients overall, but they may poorly model a specific "lumped harmonic" on an important satellite. The result is larger data residuals and a less accurate orbit.

One approach implies the linearization of all equations with one single set of starting values prior to a series of iterative linear adjustments, which is correct for the Gauss-Newton method implemented in our orbit and field estimation programs. However, a modification of this approach could provide quicker convergence in the particular problem at hand. This second approach was to use "tailor-made" fields, adjusted to each of the main data sets (of which fields several are already available from previous projects) in order to ensure that the computed orbits, along which the linearized equations and residuals are calculated, are as close to the true orbits as possible. This latter approach seeks to minimize the non-linearities associated with mis-modeling the orbit's evolution. This implies using different fields as a priori. All of these various "starting points" are made approximately compatible with the single field chosen for actual improvement, by way of linear transformations (or "shifts") in the right-hand sides of the normal equations. A question which required answering was whether non-linear aspects of the problem could adversely affect these transformations. Nevertheless, it is important to note that in preparation for the normal

equation generation, the use of "tailored fields" improved upon our ability to eliminate spurious data due to tighter editing than is possible when using a single, more general model.

The main purpose here was to select a procedure that was likely to converge to the correct solution (within the accuracy allowed by the data). In order to clarify which of the two methods, the "unique starting field" or the "multiple, tailored fields," was likely to satisfy our needs best, a number of small-scale simulations of the problem were carried out. The idea was to reproduce the main characteristics of the adjustment for either approach in a reasonably inexpensive way. A more complete description of the results of the simulations is given in the next section. These simulations had the respective properties of tailored and global models. In the a priori tailored fields, some potential coefficients adjusted to provide accurate orbits were clearly geophysically unrealistic. On the other hand, the general a priori model did not fit the simulated data for a particular arc nearly as well as the corresponding tailored model.

If the problem was sufficiently close to being perfectly linear, either method should give virtually the same results, in which case the choice becomes trivial from a theoretical point of view. (There are practical operational differences even in this case.) This would happen if the non-linear problem had such a well-behaved geometry in a neighborhood of the actual solution, that in it, the hypersurface defined by each normal equation could be regarded as flat in this neighborhood, and all the different "starting fields" fell within this region. As shown in the following section, this seems to have been the situation in the cases simulated.

#### 4.1.11.2 Simulations for Geopotential Solution Using Tailor-Made vs General A Priori Models

##### A. Simulations Design

A set of 21 spherical harmonic coefficients were recovered using simulated laser data on 3 satellites with 13th order resonance. Data from a simulated global set of laser stations were employed for the normal equations using one 9-day arc on each satellite. The geopotential model used to simulate the observations consisted of the 21 coefficients to be recovered plus a base model complete through degree and order 4 with values obtained from GEM-9. The general a priori model contained 21 perturbed GEM-9 coefficients. When it was used in the orbital recovery, only the state parameters were solved for on each arc. The tailor-made model had the same perturbed coefficients but each arc permitted certain geopotential coefficients to adjust (i.e., tailor the field) for each satellite individually. These coefficients were then "shifted" to the common values of the general a priori model before solving the normals. The state parameters consisted of six orbital elements plus two drag parameters ( $C_D$ ,  $\dot{C}_D$ ) for each of the three satellite arcs. Two cases involving different data quality were considered. One case had 5 cm Gaussian random noise applied to the range observations and the other case had perfect data, that is, with no noise applied.

##### B. Coefficient Terms Recovered

The 21 coefficient terms of the spherical harmonics that were recovered in the solution consisted of:

| <u>Zonals</u> | <u>Tesseral</u> s | <u>Resonant Tesseral</u> s |
|---------------|-------------------|----------------------------|
| $C(3,0)$      | $CS(2,2)$         | $CS(15,13)$                |
| $C(4,0)$      | $CS(10,4)$        | $CS(17,13)$                |
| $C(7,0)$      | $CS(19,17)$       | $CS(19,13)$                |
| $C(16,0)$     | $CS(25,23)$       | $CS(27,13)$                |
| $C(17,0)$     |                   |                            |

### Lumped Coefficients Solved by Satellite for Tailored Model

To "tailor" each individual satellite's model, lumped coefficient terms were solved for on individual arcs. These were:

$$C(16,0), C(17,0), CS(27,13)$$

### Starting Values of Coefficients (A Priori)

Except for the base  $4 \times 4$  terms, the a priori model (starting values) was GEM-9  $\pm 3\sigma$  where the  $\sigma$  values represent the published errors in the GEM-9 field. Since  $C, S(25,23)$  was not recovered in GEM-9 the  $\sigma$  value was computed from Kaula's rule ( $10^{-5}/l^2$  for  $l=25$ ). The coefficients  $C(16,0)$ ,  $C(17,0)$ , and  $CS(27,13)$  were solved for on the individual satellite arcs to obtain a priori values for the tailored models, and the true values of these terms from GEM-9 were used as the a priori for the general model. Notice, for example, in Table D the very large adjustment made on  $C(23,13)$  to tailor a local gravity model to fit the data on 5BN-2. The same is true for the  $C, S(23,13)$  adjustments for ANNA. But note that, although these coefficient adjustments were large when "tailoring" the satellite-specific fields, these tailored models fit the simulated data many times better than the constant a priori field. In the constant a priori field, no coefficient errors were greater than  $3\sigma$ . The "tailored" model for 5BN.2 had a coefficient error for  $C(23,13)$  of nearly 50 $\sigma$ . (See Section D for comparisons.)

### C. Satellite Orbital Characteristics

| <u>Satellite</u> | <u>a</u> | <u>e</u> | <u>I</u> | <u>Mean Motion</u><br>(rev/day) | <u>Primary Resonant Period</u><br>(days) | <u>Drag</u><br>( $C_D=2$ )<br><u>m/day<sup>2</sup></u> |
|------------------|----------|----------|----------|---------------------------------|--|--|
| DI-D             | 7622 km  | .0848    | 39.5°    | 13.05                           | 8.4                                      | 70   |
| ANNA             | 7501     | .0082    | 50.1°    | 13.37                           | 4.8                                      | 4  |
| 5BN-2            | 7462     | .0058    | 89.9°    | 13.46                           | 2.4                                      | 10   |

D. A Priori Satellite Arc Residuals and Lumped Coefficients

| <u>Satellite</u> | No. of<br>Observations<br>( $\pm 5$ cm noise) | <u>A Priori Residuals</u> |                      |
|------------------|---|---------------------------|----------------------|
|                  |   | Tailor Model<br>rms       | General Model<br>rms |
| DI-D             | 6937  | 110 cm                    | 383 cm               |
| ANNA             | 6124  | 133                       | 730                  |
| 5BN-2            | 3637  | 192                       | 725                  |

| Adjusted<br>Tailored Model<br>Lumped<br>Coefficients | Coefficient Units $10^{-9}$ |             |               | Correct<br>Answer:<br><u>GEM-9</u> |
|--|-----------------------------|-------------|---------------|------------------------------------|
|  | <u>DI-D</u>                 | <u>ANNA</u> | <u>5BN-2</u>  |                                    |
| C(16,0)  | - 5.4                       | - 7.8       | - 18.5        | - 8.5                              |
| C(17,0)  | 19.2                        | 14.5        | - 7.8         | 16.2                               |
| C(23,13)   | -12.8                       | <u>28.7</u> | <u>-202.2</u> | - 7.7                              |
| S(23,13)   | -18.9                       | <u>75.9</u> | - 78.4        | -10.7                              |

E. Recovery of Geopotential

The normal equations were solved using both the tailor-made a priori model and the general a priori model. Errors in the solutions of the 21 geopotential coefficients were plotted for comparison of the two methods. An ideal TOPEX accuracy goal of 1/4 the errors in the GEM-9 model (i.e., 25% of GEM-9's uncertainties) was also plotted to show the significance of the differences between the solutions of each method. Both cases of simulation, with noise on the data (Figure 4.2) and without noise (Figure 4.3) were plotted. The following additional information has been plotted in Figure 4.1: (a) the general a priori starting values ( $\text{GEM-9} \pm 3\sigma$ ), (b) the standard deviations (error estimate) of the recovered coefficients for the case where noise was applied to the data, and (c) the Topex accuracy goal of 1/4 GEM-9 error  $\sigma$ 's for comparison. A log scale was used since over 6 orders of magnitude are seen in the plots.

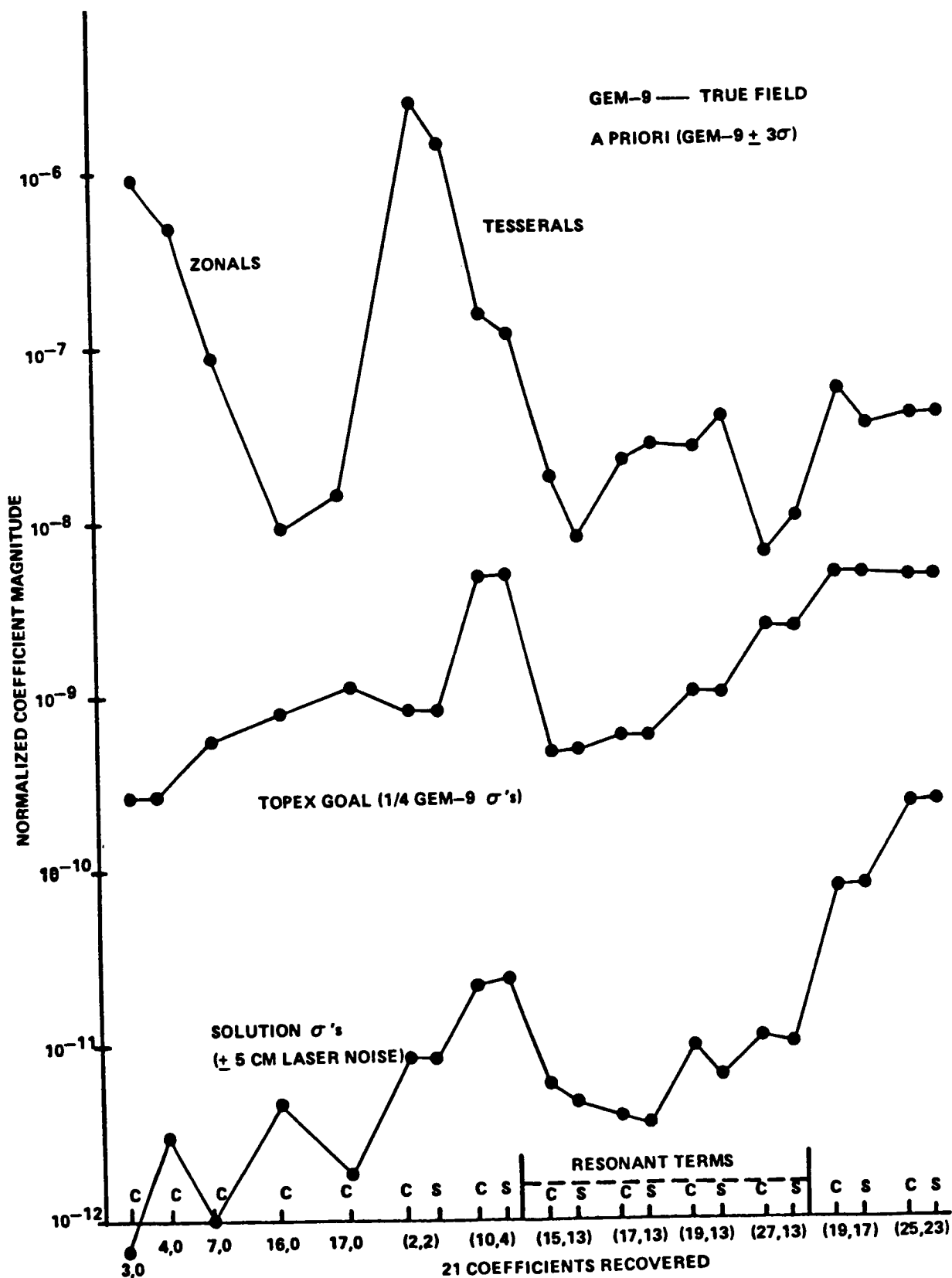


Figure 4.1 Geopotential Simulation Information.

F. Summary and Conclusions

In Figure 4.2 (with noise applied to the data) the errors are approximately the same for the two methods except for the C(7,0) value. Moreover, these differences are small and based upon the TOPEX goal, there is not a significant difference between the two methods. The main feature of these errors (Figure 4.3) is that the general model (with smaller errors for most of the zonal terms but with larger errors for most of the other terms) has a larger spread in the errors than the tailored model which gives a much more consistent error. These errors are much less significant when compared to the TOPEX goal than the previous set of errors of Figure 4.2 where noise was applied to the data.

The solutions were compared through post-solution fits to the simulated range observations on DI-D using the "true" data (no noise). The rms of the residuals gave the following results:

| <u>Model</u> | <u>RMS</u> |
|--------------|------------|
| General      | .116 cm    |
| "Tailored"   | .025 cm    |

The conclusion of this simulation is that the tailored model gives slightly better results (especially in the perfect data case) but the improvement seen is sufficiently small that, considering the goals of TOPEX, or the present state-of-the-art, either method may be used.

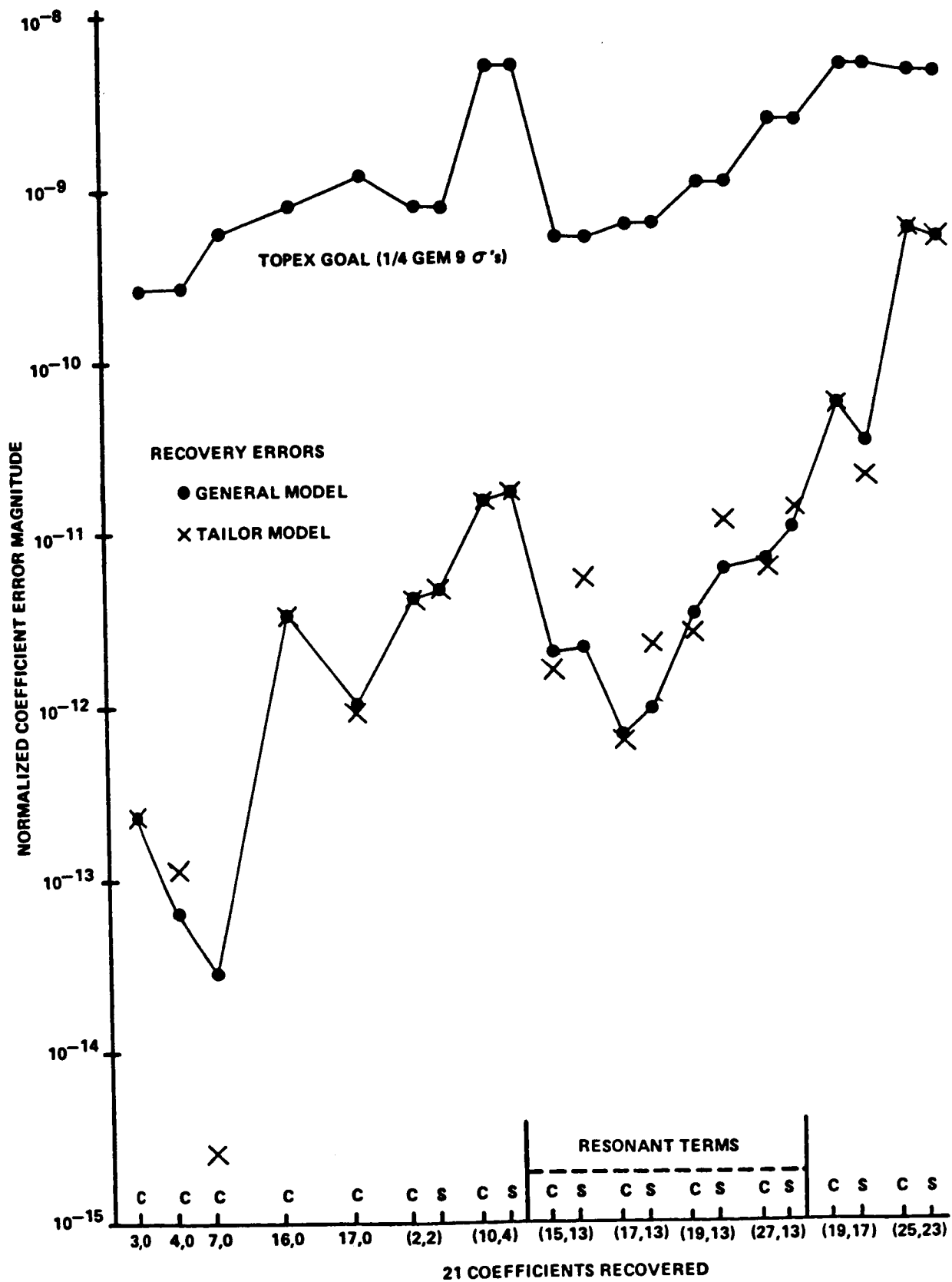


Figure 4.2 Gravity Recovery from Noise.

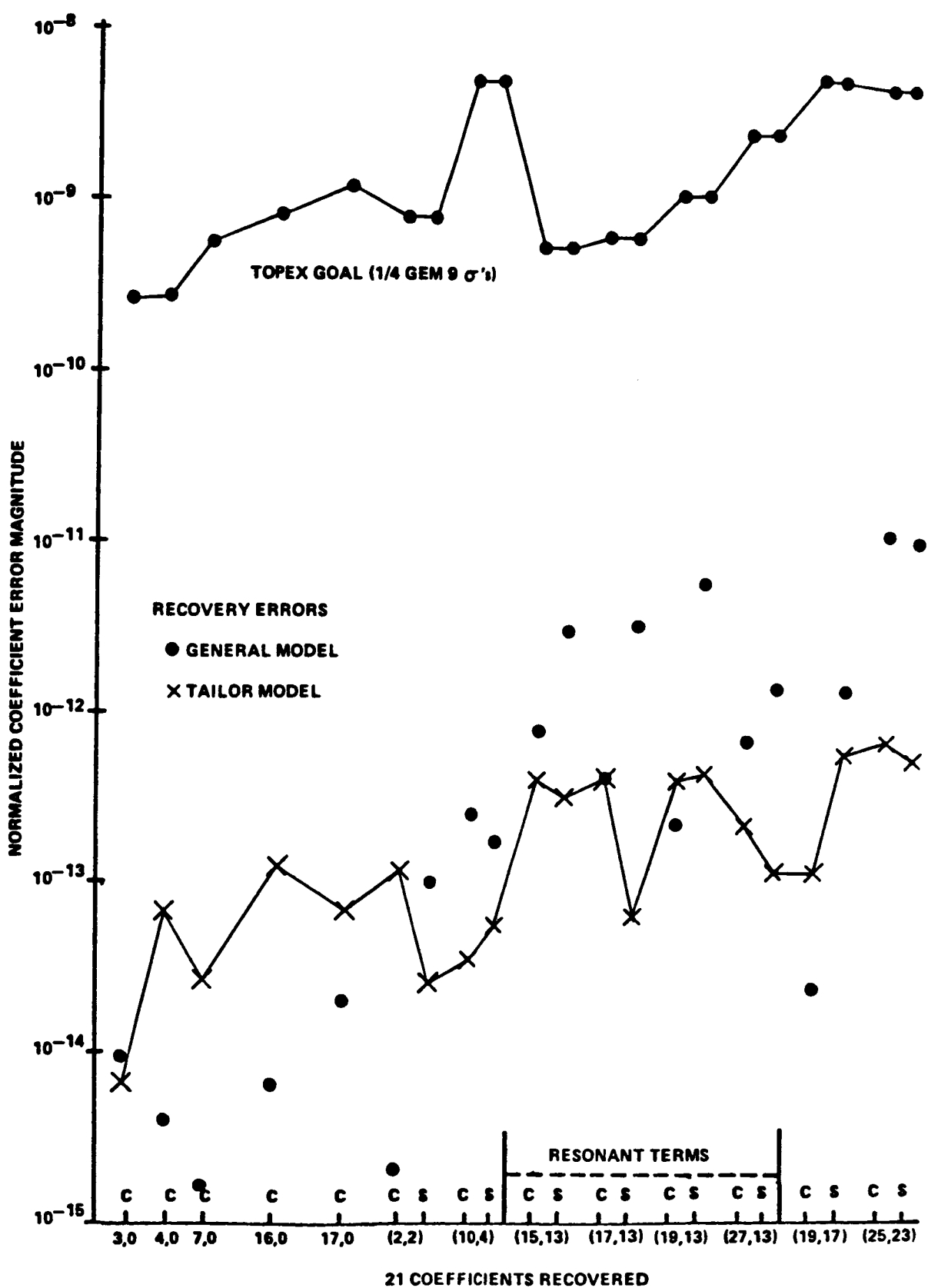


Figure 4.3 Gravity Recovery without Noise.

#### G. Interpretation of Results and Future Investigation

Even though the simulation shows that the difference in the results between the two approaches is not clearly significant, it is interesting to interpret the difference. First, it is clear that non-linear effects in the system cause the different geopotential results. An explanation for the improved results of the tailored approach is that some non-linear effects in the residuals are removed with the lumped (tailored) coefficients in the iteration used to converge the orbit. These effects remain filtered-out when a linear shift is made to adjust the tailored coefficients to the common values of the general model.

The approach using the general model as well as that using the tailored model may both benefit from the adjustment of additional orbit parameters. This is evident in the present results, where the drag parameters apparently are removing non-linear effects from the residuals in the process of converging the orbits. Both cases, tailored vs. general a priori models, have obtained better geopotential results with the application of drag parameters as compared to results where drag was not applied.

The present simulation is quite simplified since most of the gravity field was considered perfectly known in the recovery of the 21 coefficients and of those adjusting, 40% were 13th order resonant terms. Yet, this work is important since in practice both methods have been employed in the recovery of past geopotential models. We however felt safe in concluding that there were no inherent ill-effects in using "tailored" models to reduce the data and shift the resulting normals to a common base in the final solution. Since this approach had the benefit of improving our data editing and orbit convergence activities, it was adopted in the development of GEM-T1.

On the other hand, it was not necessary to compute tailored models for each satellite. We were able to adopt an approach of using available tailored fields for certain satellite analyses, and a general model elsewhere.

One should exercise caution before accepting our conclusions as completely general. We have not attempted to assess the impact of using a truly poor model as a priori. Furthermore, the effects of non-linearity becomes more severe in the solution as the matrix conditioning degrades. Hence this simulation would have been more conclusive if a more complete set of coefficients were employed in the solution instead of the simplified subset actually used. However, the present results provided a basis for additional insight into the choice of an a priori model, and revealed little significant problem with the approach we ultimately adopted.

SECTION 5.0  
TRACKING DATA

The earliest satellite tracking systems were quite crude by today's standards. Camera images and Minitrack interferometric tracking yield satellite single-point positioning of from 10 to 100 meters. Although the observations themselves were somewhat imprecise, a large group of satellites having diverse orbital characteristics were tracked by these systems. Therefore, these observations (especially those obtained on twenty or so different orbits by a globally deployed network of Baker-Nunn and MOTS cameras) have formed the basis for earlier gravity modeling activities at GSFC and elsewhere.

In the early and mid-1970's electronic tracking of considerably higher precision than that obtained by cameras became the routine method for locating operational satellites. The main operational tracking network for NASA became the Unified S-Band Electronic Network. These electronic tracking systems acquired data in all weather conditions but provided data of significantly lesser precision than that produced by the early laser technologies of this era.

Laser systems are currently the most accurate and advanced means of precision satellite tracking. These ranging systems have substantially evolved and have undergone nearly a ten-fold improvement in system precision every three years of the last decade. The evolution of laser systems typify the progress which has been made in monitoring the motion of near-earth satellites and has resulted in much more stringent demands for geopotential models capable of utilizing data which now are accurate to a few centimeters. The only limitation found with the lasers is their dependence on weather and the somewhat restricted number of satellites which carried corner cubes enabling them to be tracked by ground laser systems. Historically, there are ten satellites which have been tracked by NASA's laser systems.

PRECEDING PAGE BLANK NOT FILMED

The parallel capability of S-Band and laser tracking provided flexibility within NASA's operational environment. The laser network provided NASA with the means of obtaining high quality data on geodetic missions which required precision rather than mere operational orbital accuracies. Satellite missions with less stringent orbit determination requirements were supported by the S-Band Network.

The routine tracking obtained by the S-Band Network has been utilized in past GSFC gravity solutions. The S-band stations operationally tracked using a single frequency. Ionospheric refraction effects are significant in S-band average range-rate observations. These data have not been used within GEM-T1 pending the implementation of either a reliable general ionospheric refraction model or some method for deleting data significantly corrupted by this effect.

#### 5.1 DATA SELECTION

There are perhaps sixty satellites which received sufficient tracking to warrant their consideration for inclusion in the GSFC gravity modeling activities. The TOPEX orbit determination requirements are such that a four-fold improvement over existing field accuracies is necessary. Such an improvement can only be accomplished with greatly improved data handling and data validation directed at existing data sets, particularly the older ones. Therefore some manageable framework for selecting, qualifying and processing those data which were deemed most important was developed as a preliminary step in the creation of GEM-T1.

One of the first tasks was a selection of the most important data sets upon which a "satellite-only" field could be computed. The sixty objects which had geodetic quality data sets and orbits which were reasonably free of large perturbations due to air drag were evaluated

according to certain criteria: (a) the quality, quantity and global distribution of their tracking data sets, (b) the uniqueness of orbital perturbations on the satellite (d) the similarity of the orbit to that anticipated for TOPEX (e) the distribution of the data set over the satellite's apsidal period and (f) the sensitivity of the satellite's orbit to present weaknesses in existing gravity models.

The satellites which were considered are described in Table 5.1 which also shows their orbital characteristics. The satellite physical dimensions, shape and weight are also given in Table 5.1. Based upon an evaluation scheme detailed in (Marsh and Born, 1985) the ranking of the satellite data sets can be found in Table 5.2. GEM-T1 has been computed from seventeen of the top thirty ranked data sets. Almost all objects rated in the top ten have been utilized. To achieve a better sampling of inclinations, six satellites of low inclination were selected (see Section 5.2.8). Future models containing additional orbits, altimetry, surface gravity and satellite-tracking-satellite data are being planned.

In all, 17 satellites were included in the GEM-T1 solution. A data summary for the GEM-T1 solution is presented in Table 5.3. Table 5.4 describes the orbital characteristics of the satellites used in the formation of GEM-T1. The distribution of the selected satellite's orbital characteristics are shown in Figure 5.1.a. The temporal distribution of the data used is summarized in Figure 5.1.b. As is obvious from the summaries in Table 5.3, precise laser tracking played a dominant role in defining the GEM-T1 gravity and tidal models. The LAGEOS and STARLETTE laser satellites especially, played a central role in both the tidal and gravity field recoveries. These satellites are completely passive orbiting objects whose sole functions are to serve as space-based laser targets. Both satellites are extremely dense spheres (area to mass ratios of .00069 and .00096  $\text{m}^2 \text{ kg}^{-1}$  respectively) covered by laser corner cubes and are in orbits designed to minimize non-conservative forcing effects. LAGEOS orbits at nearly an earth radius

TABLE 5.1

## SATELLITE CHARACTERISTICS FOR GEOPOTENTIAL IMPROVEMENT

| NAME         | DATE   | AREA   | MASS    | SHAPE        | $\dot{\omega}$ | PR HI   | AP HI    | ECC    | INCL   |
|--------------|--------|--------|---------|--------------|----------------|---------|----------|--------|--------|
| TELSTAR      | 621115 | 0.581  | 77.0    | sphere       | 1.986          | 955.89  | 5649.96  | 0.2426 | 44.80  |
| GEOS-1       | 651116 | 1.23   | 172.5   | oct. Sphere  | 0.659          | 1107.54 | 2276.53  | 0.0725 | 59.37  |
| TIROS-9      | 660115 | 0.6    | 138.0   | cylinder     | - 2.165        | 706.10  | 2572.67  | 0.1166 | 96.40  |
| SECOR-5      | 651201 | 0.288  | 18.0    | sphere       | - 0.792        | 1140.15 | 2446.97  | 0.0801 | 69.23  |
| OVI-2        | 661028 | 0.697  | 22.7    | cyl.hemis.   | 4.839          | 414.80  | 3467.11  | 0.1835 | 144.27 |
| ECHO-1RB     | 600920 | 0.23   | 23.0    | cylinder     | 2.976          | 1505.89 | 1702.09  | 0.0123 | 47.23  |
| BE-C         | 660405 | 1.139  | 52.6    | octagon      | 5.158          | 945.07  | 1321.12  | 0.0250 | 41.19  |
| DI-D         | 670219 | 0.697  | 22.7    | cylinder     | 5.372          | 595.89  | 1888.31  | 0.0848 | 39.46  |
| DI-C         | 670224 | 0.697  | 22.7    | cylinder     | 5.913          | 586.62  | 1359.39  | 0.0526 | 40.00  |
| ANNA-1B      | 640229 | 0.657  | 158.8   | spheroid     | 2.970          | 1076.81 | 1181.81  | 0.0070 | 50.13  |
| GEOS-2       | 680310 | 1.23   | 211.8   | oct.pyramid  | - 1.621        | 1092.09 | 1600.23  | 0.0330 | 105.79 |
| OSCAR-7      | 660422 | 1.25   | 50.0    | cylinder     | - 2.934        | 876.40  | 1222.86  | 0.0233 | 89.70  |
| 5B-1-2       | 650426 | 1.139  | 61.0    | octagon      | - 2.862        | 1096.16 | 1133.10  | 0.0025 | 89.95  |
| COURIER-1B   | 670127 | 1.327  | 230.0   | sphere       | 8.230          | 963.38  | 1225.28  | 0.0175 | 28.33  |
| GRS          | 650623 | 0.889  | 99.3    | cylinder     | 3.501          | 415.54  | 1309.79  | 0.0618 | 49.76  |
| TRANSIT-4A   | 610902 | 0.897  | 79.0    | cylinder     | - 0.694        | 902.89  | 1015.66  | 0.0077 | 66.83  |
| BE-B         | 670316 | 1.139  | 52.6    | octagon      | - 2.543        | 889.08  | 1087.64  | 0.0135 | 79.69  |
| OGO-2        | 660521 | 4.645  | 486.9   | box          | - 3.050        | 428.22  | 1512.96  | 0.0739 | 87.37  |
| INJUN-1      | 610916 | 0.19   | 22.0    | sphere cyl.  | - 0.6927       | 888.40  | 1007.86  | 0.0082 | 66.80  |
| AGENA-RB     | 640615 | 28.0   | 1000.0  | cylinder     | - 1.276        | 929.08  | 934.80   | 0.0004 | 69.90  |
| MIDAS-4      | 641110 | 84.5   | 1600.0  | cylinder     | - 0.980        | 3490.52 | 3752.47  | 0.0131 | 95.83  |
| VANGUARD-2RB | 660128 | 1.275  | 68.0    | cylinder     | 5.273          | 572.15  | 3285.55  | 0.1634 | 32.89  |
| VANGUARD-2   | 600505 | 1.275  | 23.0    | sphere       | 5.256          | 573.94  | 3302.49  | 0.1641 | 32.90  |
| VANGUARD-3   | 600115 | 3.0    | 68.0    | roc.-sph.rod | 4.859          | 513.84  | 3754.57  | 0.1904 | 33.35  |
| ALOU-2       | 690721 | 1.0    | 145.0   | oblate sph.  | - 1.906        | 507.65  | 2946.21  | 0.1505 | 79.82  |
| LANSAT-1     | 720801 | 7.030  | 816.0   | conc         | - 2.728        | 924.20  | 938.78   | 0.0010 | 99.12  |
| PEOLE        | 710202 | 1.539  | 70.0    | sphere       | 13.121         | 520.93  | 745.25   | 0.0160 | 15.00  |
| SAS          | 710103 | 2.041  | 143.0   | cylinder     | 14.914         | 522.09  | 563.62   | 0.0030 | 3.04   |
| VANGUARD-1   | 581204 | 0.080  | 1.47    | sphere       | 4.421          | 652.11  | 3947.09  | 0.1900 | 34.25  |
| EXPLORER-7   | 671205 | 1.014  | 41.5    | double cone  | 3.417          | 562.75  | 1080.22  | 0.0360 | 50.31  |
| TIROS-1RB    | 671106 | 2.168  | 24.0    | cylinder     | 4.143          | 691.50  | 734.04   | 0.0030 | 48.39  |
| A04          | 661107 | 2.168  | 24.0    | cylinder     | - 3.012        | 614.92  | 856.79   | 0.0170 | 98.69  |
| RELAY-1      | 630101 | 1.883  | 78.0    | oct.prism    | 1.213          | 1325.31 | 7436.43  | 0.2840 | 47.49  |
| TELSTAR-2    | 630602 | 2.54   | 79.4    | spheroid     | 1.217          | 969.98  | 10808.11 | 0.4010 | 42.73  |
| MIDAS-7      | 630803 | 42.412 | 2000.0  | cylinder     | - 1.001        | 3670.26 | 3730.72  | 0.0030 | 88.41  |
| SECOR-1      | 640204 | 0.496  | 18.0    | rect.box     | - 1.271        | 922.92  | 952.11   | 0.0020 | 69.89  |
| LCS-1        | 650605 | 7.1    | 34.0    | sphere       | 3.623          | 2710.42 | 2875.39  | 0.0090 | 32.11  |
| NIMBUS-2     | 660606 | 7.03   | 414.0   | cone         | - 2.348        | 1105.93 | 1181.12  | 0.0050 | 100.35 |
| EXPLORER-39  | 770407 | 42.084 | 9.3     | sphere       | - 2.170        | 687.19  | 2170.52  | 0.0950 | 80.66  |
| LANDSAT-2    | 750202 | 7.03   | 953.0   | cone         | - 2.729        | 926.32  | 940.90   | 0.0010 | 99.09  |
| LANDSAT-3    | 780403 | 7.03   | 960.0   | cone         | - 2.730        | 914.89  | 929.46   | 0.0010 | 99.14  |
| LANDSAT-4    | 810915 | 13.935 | 1496.86 | cone         | - 3.099        | 705.29  | 705.43   | 0.0001 | 98.20  |
| NIMBUS-6     | 750705 | 7.03   | 827.0   | cone         | - 2.429        | 1098.47 | 1108.94  | 0.0007 | 99.96  |
| NIMBUS-7     | 781106 | 9.935  | 832.0   | cone         | - 2.666        | 959.37  | 969.63   | 0.0007 | 99.29  |
| HEAO-1       | 770901 | 43.731 | 2720.0  | cylinder     | 12.835         | 433.68  | 447.31   | 0.0010 | 22.76  |
| HEAO-3       | 791002 | 43.731 | 2720.0  | cylinder     | 6.222          | 494.37  | 508.11   | 0.0010 | 43.61  |
| SMM          | 800303 | 28.903 | 2315.0  | cylinder     | 10.570         | 568.83  | 571.61   | 0.0020 | 28.51  |
| SME          | 810701 | 19.97  | 437.0   | cylinder     | - 3.435        | 531.27  | 535.41   | 0.0003 | 97.55  |
| STARLETTE    | 750527 | 0.045  | 47.25   | sphere       | 3.296          | 812.19  | 1114.80  | 0.0206 | 49.83  |
| LAGEOS       | 790812 | 0.2827 | 411.0   | sphere       | - 0.214        | 5834.25 | 5944.82  | 0.0045 | 109.84 |
| GEOS-3       | 750531 | 1.4365 | 345.909 | oct.pyramid  | - 0.349        | 841.10  | 857.55   | 0.0011 | 114.98 |
| SEASAT       | 780921 | 25.31  | 2213.6  | cylinder     | - 1.722        | 812.00  | 818.59   | 0.0005 | 108.01 |
| EXPLORER-38  | 680801 | 4.58   | 190.0   | tub.cross    | 0.152          | 5855.43 | 5865.21  | 0.0004 | 120.64 |

**Table 5.2**  
**FINAL SATELLITE SELECTION RANKING**

| NAME  | INCL. | ACU | GLB | PAS | TOTAL DATA | UNI. | ACL. | TOP SIMILY | GRY SENS | APSD COVR | TOTAL SCORE | ACCURACY OF DATA |     |     | GLOBAL DISTRIBUTION OF DATA |      |            | QUANTITY OF DATA |           |             | TOTAL FOR DATA: |  |  |
|-------|-------|-----|-----|-----|------------|------|------|------------|----------|-----------|-------------|------------------|-----|-----|-----------------------------|------|------------|------------------|-----------|-------------|-----------------|--|--|
|       |       |     |     |     |            |      |      |            |          |           |             | ACU              | GLB | PAS | UNI.                        | ACL. | TOP SIMILY | GRY SENS         | APSD COVR | TOTAL SCORE |                 |  |  |
| SME   | 97.6  | 8.  | 4.  | 3.  | 9.         | 7.   | 3.   | 4.         | 3.       | 7.        | -4.         |                  |     |     |                             |      |            |                  |           |             |                 |  |  |
| EXP39 | 80.7  | 7.  | 4.  | 4.  | 8.         | 7.   | 2.   | 4.         | 4.       | 2.        | -2.         |                  |     |     |                             |      |            |                  |           |             |                 |  |  |
| 0V12  | 144.3 | 7.  | 2.  | 1.  | 13.        | 2.   | 15.  | 2.         | 2.       | 2.        | 0.          |                  |     |     |                             |      |            |                  |           |             |                 |  |  |
| SAS   | 3.0   | 2.  | 3.  | 2.  | 2.         | 6.   | 5.   | 12.        | 2.       | 2.        | 4.          |                  |     |     |                             |      |            |                  |           |             |                 |  |  |
| ADR   | 98.7  | 7.  | 3.  | 2.  | 6.         | 5.   | 12.  | 13.        | 1.       | 1.        | 10.         |                  |     |     |                             |      |            |                  |           |             |                 |  |  |
| VANI  | 34.3  | 7.  | 4.  | 2.  | 6.         | 5.   | 12.  | 13.        | 1.       | 1.        | 14.         |                  |     |     |                             |      |            |                  |           |             |                 |  |  |
| HEAD1 | 22.8  | 8.  | 4.  | 6.  | 12.        | 13.  | 12.  | 13.        | 1.       | 1.        | 10.         |                  |     |     |                             |      |            |                  |           |             |                 |  |  |
| VAN2  | 32.9  | 7.  | 6.  | 3.  | 9.         | 5.   | 10.  | 12.        | 2.       | 2.        | 17.         |                  |     |     |                             |      |            |                  |           |             |                 |  |  |
| TMR   | 48.4  | 7.  | 4.  | 2.  | 6.         | 6.   | 12.  | 12.        | 2.       | 2.        | 17.         |                  |     |     |                             |      |            |                  |           |             |                 |  |  |
| VAN3  | 33.4  | 7.  | 6.  | 4.  | 4.         | 2.   | 5.   | 10.        | 2.       | 2.        | 17.         |                  |     |     |                             |      |            |                  |           |             |                 |  |  |
| SEC1  | 69.9  | 7.  | 3.  | 3.  | 6.         | 5.   | 3.   | 5.         | 2.       | 2.        | 19.         |                  |     |     |                             |      |            |                  |           |             |                 |  |  |
| EXPL7 | 50.3  | 7.  | 3.  | 3.  | 6.         | 5.   | 7.   | 5.         | 3.       | 3.        | 19.         |                  |     |     |                             |      |            |                  |           |             |                 |  |  |
| TEL2  | 42.7  | 7.  | 5.  | 4.  | 4.         | 4.   | 8.   | 4.         | 2.       | 2.        | 19.         |                  |     |     |                             |      |            |                  |           |             |                 |  |  |
| EXP38 | 120.6 | 7.  | 3.  | 3.  | 3.         | 6.   | 7.   | 1.         | 0.       | 0.        | 20.         |                  |     |     |                             |      |            |                  |           |             |                 |  |  |
| HEAO3 | 43.6  | 8.  | 4.  | 4.  | 4.         | 4.   | 12.  | 15.        | 2.       | 2.        | 19.         |                  |     |     |                             |      |            |                  |           |             |                 |  |  |
| DSR7  | 89.7  | 7.  | 5.  | 5.  | 5.         | 5.   | 9.   | 5.         | 2.       | 2.        | 19.         |                  |     |     |                             |      |            |                  |           |             |                 |  |  |
| LAND4 | 98.2  | 8.  | 10. | 3.  | 5.         | 5.   | 10.  | 15.        | 1.       | 2.        | 21.         |                  |     |     |                             |      |            |                  |           |             |                 |  |  |
| PEOPE | 15.0  | 10. | 10. | 5.  | 5.         | 5.   | 10.  | 11.        | 7.       | 2.        | 21.         |                  |     |     |                             |      |            |                  |           |             |                 |  |  |
| LAND3 | 99.1  | 8.  | 8.  | 5.  | 5.         | 5.   | 11.  | 11.        | 3.       | 2.        | 22.         |                  |     |     |                             |      |            |                  |           |             |                 |  |  |
| MJMI  | 66.8  | 7.  | 5.  | 5.  | 5.         | 5.   | 12.  | 12.        | 2.       | 2.        | 22.         |                  |     |     |                             |      |            |                  |           |             |                 |  |  |
| GRS   | 49.8  | 7.  | 5.  | 5.  | 5.         | 5.   | 12.  | 12.        | 2.       | 2.        | 22.         |                  |     |     |                             |      |            |                  |           |             |                 |  |  |
| LAND1 | 99.1  | 8.  | 5.  | 5.  | 5.         | 5.   | 12.  | 12.        | 2.       | 2.        | 22.         |                  |     |     |                             |      |            |                  |           |             |                 |  |  |
| SECS5 | 69.2  | 7.  | 3.  | 3.  | 2.         | 3.   | 11.  | 11.        | 3.       | 2.        | 22.         |                  |     |     |                             |      |            |                  |           |             |                 |  |  |
| VM2R  | 32.9  | 7.  | 6.  | 5.  | 5.         | 5.   | 11.  | 11.        | 3.       | 2.        | 22.         |                  |     |     |                             |      |            |                  |           |             |                 |  |  |
| LAND2 | 99.1  | 8.  | 7.  | 6.  | 5.         | 5.   | 11.  | 11.        | 3.       | 2.        | 22.         |                  |     |     |                             |      |            |                  |           |             |                 |  |  |
| 0602  | 87.4  | 7.  | 7.  | 7.  | 7.         | 7.   | 12.  | 12.        | 2.       | 2.        | 22.         |                  |     |     |                             |      |            |                  |           |             |                 |  |  |
| TMR9  | 96.4  | 2.  | 2.  | 2.  | 2.         | 2.   | 12.  | 12.        | 1.       | 1.        | 23.         |                  |     |     |                             |      |            |                  |           |             |                 |  |  |
| SBH2  | 90.0  | 7.  | 7.  | 7.  | 7.         | 7.   | 12.  | 12.        | 2.       | 2.        | 23.         |                  |     |     |                             |      |            |                  |           |             |                 |  |  |
| NHNB2 | 100.4 | 8.  | 10. | 5.  | 5.         | 5.   | 11.  | 11.        | 3.       | 2.        | 23.         |                  |     |     |                             |      |            |                  |           |             |                 |  |  |
| NHNB7 | 99.3  | 8.  | 8.  | 5.  | 5.         | 5.   | 11.  | 11.        | 3.       | 2.        | 23.         |                  |     |     |                             |      |            |                  |           |             |                 |  |  |
| TRRAA | 66.3  | 7.  | 7.  | 7.  | 7.         | 7.   | 11.  | 11.        | 3.       | 2.        | 23.         |                  |     |     |                             |      |            |                  |           |             |                 |  |  |
| AGENR | 69.9  | 7.  | 4.  | 4.  | 4.         | 4.   | 12.  | 12.        | 4.       | 2.        | 23.         |                  |     |     |                             |      |            |                  |           |             |                 |  |  |
| DIC   | 40.0  | 10. | 10. | 5.  | 5.         | 5.   | 11.  | 11.        | 3.       | 2.        | 23.         |                  |     |     |                             |      |            |                  |           |             |                 |  |  |
| LCS1  | 32.1  | 7.  | 5.  | 5.  | 5.         | 5.   | 11.  | 11.        | 3.       | 2.        | 23.         |                  |     |     |                             |      |            |                  |           |             |                 |  |  |
| MID7  | 88.4  | 7.  | 7.  | 7.  | 7.         | 7.   | 11.  | 11.        | 3.       | 2.        | 23.         |                  |     |     |                             |      |            |                  |           |             |                 |  |  |
| NHNB6 | 100.0 | 8.  | 5.  | 5.  | 5.         | 5.   | 11.  | 11.        | 3.       | 0.        | 24.         |                  |     |     |                             |      |            |                  |           |             |                 |  |  |
| DID   | 89.5  | 10. | 4.  | 4.  | 4.         | 4.   | 11.  | 11.        | 2.       | 2.        | 24.         |                  |     |     |                             |      |            |                  |           |             |                 |  |  |
| RELY1 | 47.5  | 7.  | 2.  | 2.  | 2.         | 2.   | 12.  | 12.        | 3.       | 2.        | 24.         |                  |     |     |                             |      |            |                  |           |             |                 |  |  |
| SEAST | 108.0 | 12. | 4.  | 4.  | 4.         | 4.   | 12.  | 12.        | 3.       | 2.        | 24.         |                  |     |     |                             |      |            |                  |           |             |                 |  |  |
| MID4  | 95.8  | 7.  | 7.  | 6.  | 6.         | 6.   | 12.  | 12.        | 3.       | 2.        | 24.         |                  |     |     |                             |      |            |                  |           |             |                 |  |  |
| ALOU2 | 79.8  | 2.  | 5.  | 5.  | 5.         | 5.   | 12.  | 12.        | 4.       | 4.        | 24.         |                  |     |     |                             |      |            |                  |           |             |                 |  |  |
| COUR1 | 28.3  | 7.  | 7.  | 7.  | 7.         | 7.   | 12.  | 12.        | 4.       | 4.        | 24.         |                  |     |     |                             |      |            |                  |           |             |                 |  |  |
| GBB   | 79.7  | 10. | 5.  | 5.  | 5.         | 5.   | 12.  | 12.        | 4.       | 4.        | 24.         |                  |     |     |                             |      |            |                  |           |             |                 |  |  |
| TEL1  | 44.8  | 7.  | 7.  | 7.  | 7.         | 7.   | 12.  | 12.        | 5.       | 2.        | 24.         |                  |     |     |                             |      |            |                  |           |             |                 |  |  |
| SMM   | 28.5  | 8.  | 8.  | 8.  | 8.         | 8.   | 12.  | 12.        | 5.       | 2.        | 24.         |                  |     |     |                             |      |            |                  |           |             |                 |  |  |
| ECH14 | 47.2  | 7.  | 7.  | 7.  | 7.         | 7.   | 12.  | 12.        | 4.       | 4.        | 24.         |                  |     |     |                             |      |            |                  |           |             |                 |  |  |
| BEC   | 41.2  | 12. | 4.  | 4.  | 4.         | 4.   | 12.  | 12.        | 4.       | 4.        | 24.         |                  |     |     |                             |      |            |                  |           |             |                 |  |  |
| ANNA1 | 50.1  | 7.  | 5.  | 5.  | 5.         | 5.   | 12.  | 12.        | 4.       | 4.        | 24.         |                  |     |     |                             |      |            |                  |           |             |                 |  |  |
| GEOS1 | 59.4  | 13. | 5.  | 5.  | 5.         | 5.   | 12.  | 12.        | 5.       | 2.        | 24.         |                  |     |     |                             |      |            |                  |           |             |                 |  |  |
| STRLT | 49.8  | 14. | 5.  | 5.  | 5.         | 5.   | 12.  | 12.        | 5.       | 2.        | 24.         |                  |     |     |                             |      |            |                  |           |             |                 |  |  |
| GEOS2 | 105.8 | 12. | 4.  | 4.  | 4.         | 4.   | 12.  | 12.        | 5.       | 2.        | 24.         |                  |     |     |                             |      |            |                  |           |             |                 |  |  |
| GEOS3 | 115.0 | 15. | 5.  | 5.  | 5.         | 5.   | 12.  | 12.        | 5.       | 2.        | 24.         |                  |     |     |                             |      |            |                  |           |             |                 |  |  |
| LAD05 | 109.8 | 15. | 5.  | 5.  | 5.         | 5.   | 12.  | 12.        | 5.       | 2.        | 24.         |                  |     |     |                             |      |            |                  |           |             |                 |  |  |

**Table 5.3**  
**DATA UTILIZED IN PRELIMINARY**  
**TOPEX GRAVITY MODEL: 1986**

| <u>SATELLITE</u>    | <u>DATA TYPE</u> | <u>NUMBER OF<br/>NORMAL MATRICES</u> | <u>NUMBER OF<br/>OBSERVATIONS</u> |
|---------------------|------------------|--------------------------------------|-----------------------------------|
| LAGEOS              | LASER            | 58                                   | 144527                            |
| STARLETTE           |                  | 46                                   | 57356                             |
| GEOS-1              |                  | 48                                   | 71287                             |
| GEOS-2              |                  | 28                                   | 26613                             |
| GEOS-3              |                  | 36                                   | 42407                             |
| BE-C                |                  | 39                                   | 64240                             |
| SEASAT              |                  | 14                                   | 14923                             |
| D1-C                |                  | 4                                    | 7455                              |
| D1-D                |                  | 6                                    | 11487                             |
| PEOLE               |                  | 6                                    | 4113                              |
| SUB-TOTAL - LASER   |                  | 285                                  | 444,408                           |
| SEASAT              | DOPPLER          | 15                                   | 138042                            |
| OSCAR-14            |                  | 13                                   | 63098                             |
| SUB-TOTAL - DOPPLER |                  | 28                                   | 201,140                           |
| GEOS-1              | CAMERA           | 43                                   | 60750                             |
| GEOS-2              |                  | 46                                   | 61403                             |
| ANNA                |                  | 30                                   | 4463                              |
| TELSTAR             |                  | 30                                   | 3962                              |
| BE-C                |                  | 50                                   | 7501                              |
| BE-B                |                  | 20                                   | 1739                              |
| COURIER 1B          |                  | 10                                   | 2476                              |
| VANGUARD-2RB        |                  | 10                                   | 686                               |
| VANGUARD-2          |                  | 10                                   | 1299                              |
| D1-C                |                  | 10                                   | 2712                              |
| D1-D                |                  | 9                                    | 6111                              |
| PEOLE               |                  | 6                                    | 38                                |
| SUB-TOTAL - CAMERA  |                  | 273                                  | 153,140                           |
| TOTAL               |                  | 580*                                 | 798,688                           |

\*PEOLE arcs contained both optical and laser data.

**TABLE 5.4**  
**SATELLITE ORBITAL CHARACTERISTICS**

| SATELLITE<br>NAME | SATELLITE<br>ID NO. | SEMI-MAJOR<br>AXIS | ECC   | INCL.<br>(DEG.) | DATA*<br>TYPE |
|-------------------|---------------------|--------------------|-------|-----------------|---------------|
| ANNA-1B           | 620601              | 7501.              | .0082 | 50.12           | O             |
| BE-B              | 640841              | 7354.              | .0135 | 79.69           | O             |
| BE-C              | 650321              | 7507.              | .0257 | 41.19           | L,O           |
| COURIER-1B        | 600131              | 7469.              | .0161 | 28.31           | O             |
| D1-C              | 670111              | 7341.              | .0532 | 39.97           | L,O           |
| D1-D              | 670141              | 7622.              | .0848 | 39.46           | L,O           |
| GEOS-1            | 650891              | 8075.              | .0719 | 59.39           | L,O           |
| GEOS-2            | 680021              | 7711.              | .0330 | 105.79          | L,O           |
| GEOS-3            | 750271              | 7226.              | .0008 | 114.98          | L             |
| LAGEOS            | 760391              | 12273.             | .0038 | 109.85          | L             |
| OSCAR             | 670921              | 7440.              | .0029 | 89.27           | D             |
| PEOLE             | 701091              | 7006.              | .0164 | 15.01           | L,O           |
| SEASAT            | 780641              | 7170.              | .0021 | 108.02          | D,L           |
| STARLETTE         | 750101              | 7331.              | .0204 | 49.80           | L             |
| TELESTAR-1        | 620291              | 9669.              | .2429 | 44.79           | O             |
| VANGUARD-2RB      | 590012              | 8496.              | .1832 | 32.92           | O             |
| VANGUARD-2        | 590011              | 8298.              | .1641 | 32.89           | O             |

\* D = Doppler  
 L = Laser  
 O = Optical

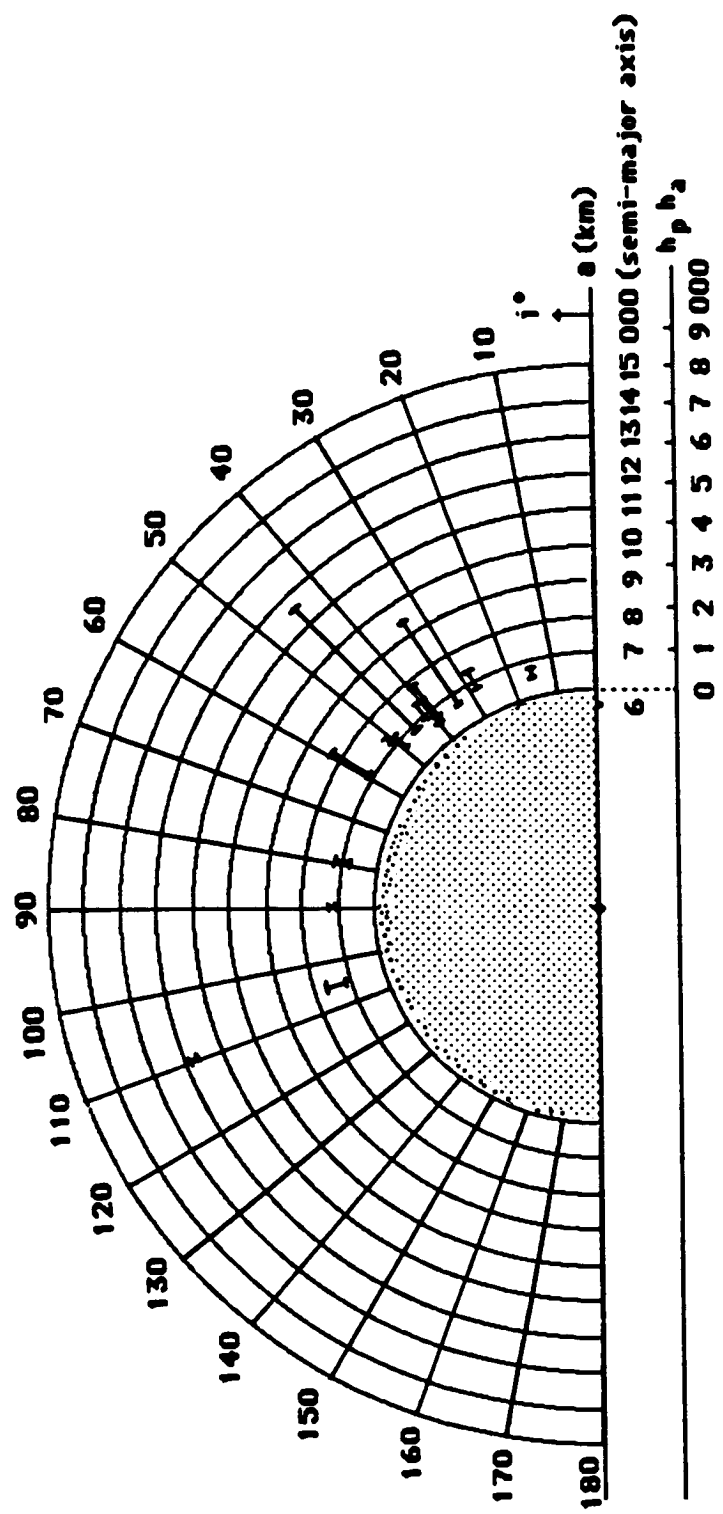


Figure 5.1a. Orbital Characteristics of the GEM-T1 Satellites.

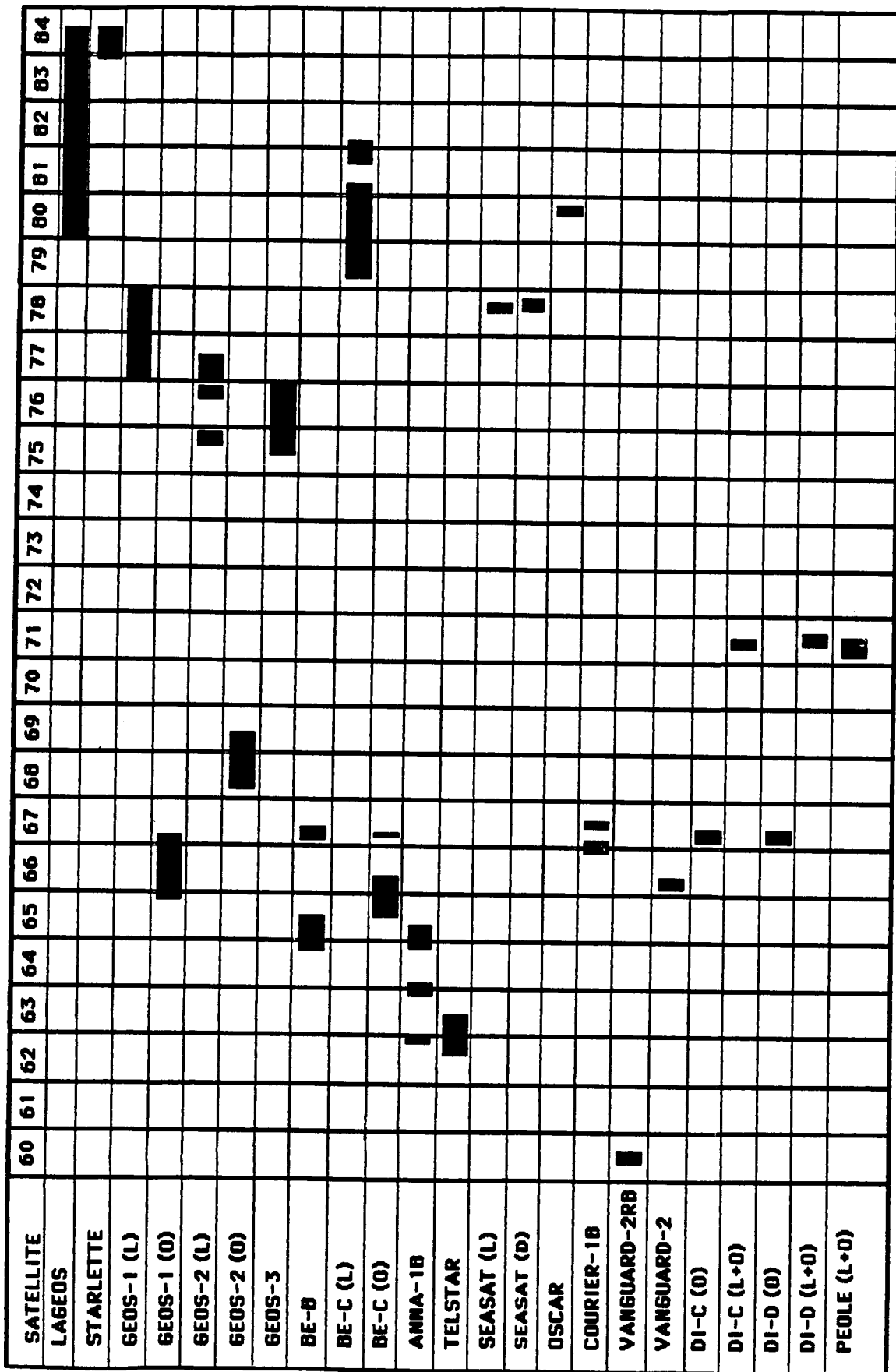


Figure 5.1b. Time Line of Satellite Tracking.

above the earth, and senses only the longest wavelength gravity and tidal effects. STARLETTE, orbiting at a much lower altitude of about 1000 km, experiences a rich spectrum of tidal and gravity perturbations and is highly complementary to LAGEOS for the separation of long and short wavelength gravity and tidal terms. Both of these satellites are tracked on a high priority basis by a global network of laser tracking stations and have extensive observation sets which have been supported by NASA's Crustal Dynamics Project activities, Project MERIT, and the WEGENER Campaign.

The following sub-sections as reported by the individual analysis managers, describe the data analysis activities which were undertaken for the high-priority satellites utilized in forming GEM-T1.

#### 5.2.1 Analysis of SEASAT Doppler and Laser Data

SEASAT was launched on June 28, 1978. The SEASAT satellite is of major significance because it has four distinct data types; S-Band, laser, Doppler and altimetry.

The nominal orbit parameters used in processing the SEASAT Doppler and laser arcs are listed in Table 5.2.1a.

Orbit computations using the PGS-S4' gravity model in the GSFC GEODYN-2 computer program have been performed on 14 arcs of both Doppler and laser data covering the span from July 27, 1978 to October 11, 1978. These arcs were of 6-day duration with the exception of those arcs between August 8 and September 17, which were shortened or lengthened due to maneuvers during this period (Table 5.2.1b). In the computation of the orbital solution for each Doppler arc, the six orbital elements, daily atmospheric drag coefficients ( $C_D$ ), and a single solar radiation pressure coefficient ( $C_R$ ) were determined. Pass-by-pass measurement biases were also determined for each station in the solution.

The Doppler data in the SEASAT orbital solutions were pre-edited by passing the residuals from the initial orbits through a residual edit analysis program. This program produced delete cards for passes of data that exceeded the maximum RMS value of 1.5 cm/sec, fell below an elevation cutoff of 5° and/or has a maximum timing bias of 5 ms. Passes with less than 5 data points were also edited. The program also produced the initial measurement bias values for input into GEODYN-2.

The laser orbits were computed by constraining the converged Doppler orbits and passing them through the laser data. Solar radiation pressure and the daily atmospheric drag parameters were also constrained at their Doppler determined values. This was done to permit proper combination of laser and Doppler orbital arcs with flexibility remaining for defining the relative weight of Doppler vs. laser observations. The nominal weighting sigma used on the Doppler data was 1 cm/sec for all stations. A sigma of 1 meter was used for all of the laser stations except 7833 (KOOTWIJK), which had a sigma of 2 meters applied. For the laser orbits, Kootwijk was sampled at every 2nd observation and the GSFC lasers were sampled at every 3rd observation. Stations 7804 (SAFLAS), 7842 (GRASSE) and 7834 (WETTZEL) were deleted from the solutions.

An estimate of the "true" noise was 0.6 cm/sec for the Doppler data and 10 cm for the laser data. The overall RMS of fit obtained for the Doppler orbits was about 0.75 cm/sec and 1.23 meters for the laser orbits (Table 5.2.1c and 5.2.1d) based on the a priori PGS-S4 gravity model.

### 5.2.2 Analysis of OSCAR Doppler Data

The OSCAR-14 satellite, launched in 1967, is one of the U.S. Navy navigation satellites. Data for this satellite were obtained as part of the MEDOC Campaign, an international Doppler data program. The data is

**Table 5.2.1a**

**NOMINAL ORBIT PARAMETERS FOR SEASAT**

|                        |                            |
|------------------------|----------------------------|
| <b>AREA:</b>           | <b>25.31 m<sup>2</sup></b> |
| <b>MASS:</b>           | <b>2213.6 kg</b>           |
| <b>ECCENTRICITY:</b>   | <b>0.001</b>               |
| <b>INCLINATION:</b>    | <b>108°</b>                |
| <b>PERIGEE HEIGHT:</b> | <b>7171 km</b>             |
| <b>APOGEE HEIGHT:</b>  | <b>7183 km</b>             |
| <b>PERIOD:</b>         | <b>100 minutes</b>         |

Table 5.2.1b

SEASAT PRECISION ORBITS

| <u>ARC NO.</u> | <u>START<br/>YYMMDD HHMM</u> | <u>STOP<br/>YYMMDD HHMM</u> |
|----------------|------------------------------|-----------------------------|
| 1              | 780727 0000                  | 780802 0000                 |
| 2              | 780802 0000                  | 780808 0000                 |
| 3              | 780808 0000                  | 780815 0730                 |
| 4              | 780815 0743                  | 780818 0748                 |
| 5              | 780818 0749                  | 780823 0921                 |
| 6              | 780823 0922                  | 780826 0927                 |
| 7              | 780826 0928                  | 780901 0000                 |
| 8              | 780901 0000                  | 780905 0000                 |
| 9              | 780905 0000                  | 780910 0105                 |
| 10             | 780910 0123                  | 780917 0000                 |
| 11             | 780917 0000                  | 780923 0000                 |
| 12             | 780923 0000                  | 780929 0000                 |
| 13             | 780929 0000                  | 781005 0000                 |
| 14             | 781005 0000                  | 781011 0000                 |

LAUNCHED: JUNE 28, 1978

FAILED: OCTOBER 10, 1978

HEIGHT: 800 km ALTITUDE

INCLINATION: 108<sup>0</sup>

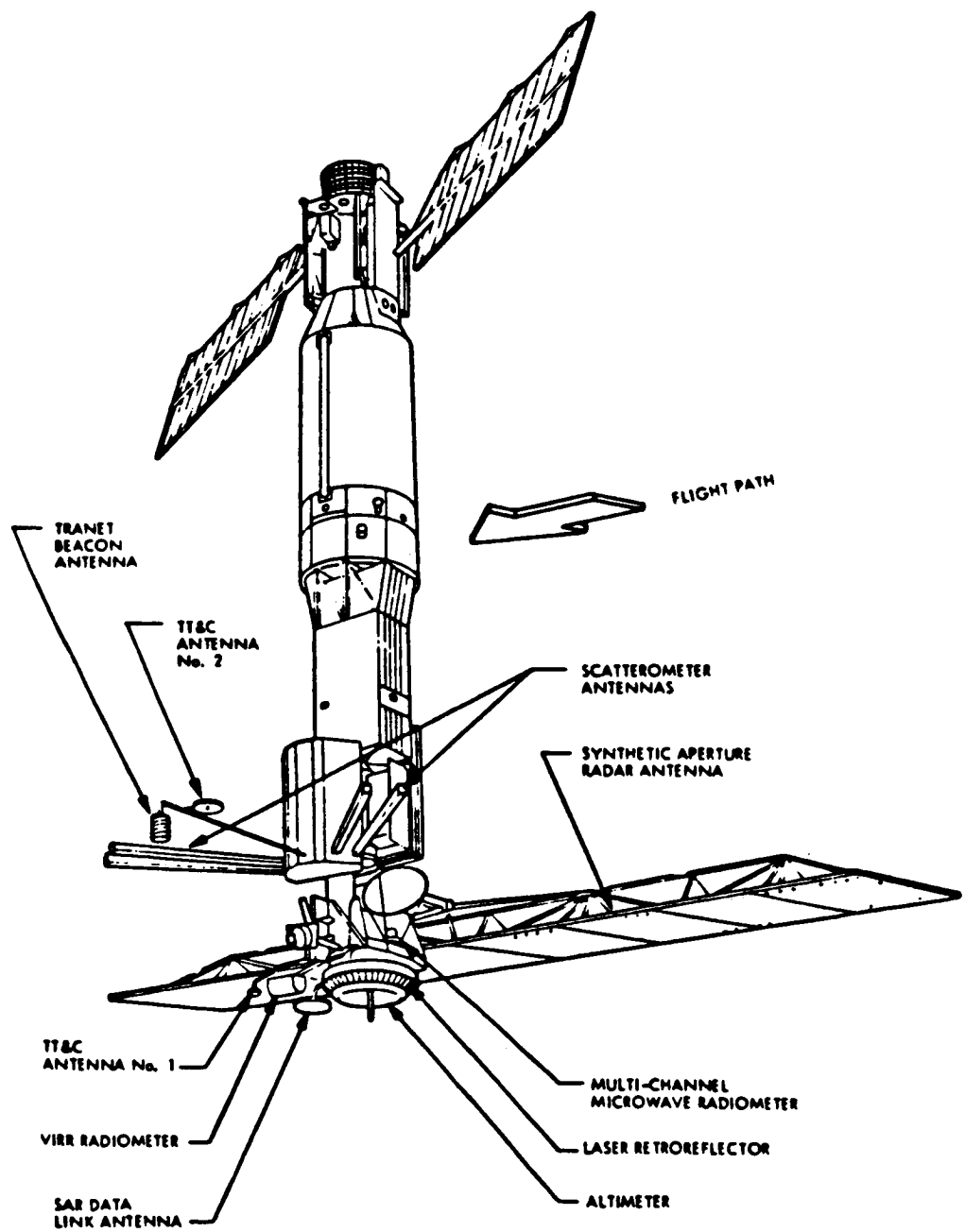


Figure 5.2.1. SEASAT

Table 5.2.1c

**EMAT SUMMARY FOR SEASAT DOPPLER**

| <u>EPOCH</u> | <u>NUMBER OF<br/>OBSERVATIONS</u> | <u>WEIGHTED<br/>RMS (cm/sec)</u> | <u>NUMBER OF<br/>STATIONS</u> | <u>ARGUMENT<br/>OF PERIGEE<br/>(AT EPOCH)</u> |
|--------------|-----------------------------------|----------------------------------|-------------------------------|---|
| 780721       | 7100                              | 1.7822                           | 35                            | 180.573                                       |
| 780727       | 14860                             | .7318                            | 35                            | 193.017                                       |
| 780802       | 13511                             | .7135                            | 35                            | 153.474                                       |
| 780808       | 15203                             | .7662                            | 34                            | 116.081                                       |
| 780815       | 6041                              | .6708                            | 34                            | 146.012                                       |
| 780818       | 6723                              | .7109                            | 34                            | 141.374                                       |
| 780823       | 5369                              | .6704                            | 33                            | 124.192                                       |
| 780826       | 10808                             | .7030                            | 33                            | 51.376  |
| 780901       | 7369                              | .7058                            | 34                            | 99.272  |
| 780905       | 8453                              | .8914                            | 34                            | 292.590                                       |
| 780910       | 10404                             | .7498                            | 34                            | 115.672                                       |
| 780917       | 9592                              | .7399                            | 33                            | 93.448  |
| 780923       | 8934                              | .7483                            | 33                            | 122.805                                       |
| 781005       | 6982                              | .7656                            | 32                            | 56.247  |

Table 5.2.1d

**EMAT SUMMARY FOR SEASAT LASER**

| <u>EPOCH</u> | <u>NUMBER OF<br/>OBSERVATIONS</u> | <u>WEIGHTED<br/>RMS (m)</u> | <u>NUMBER OF<br/>STATIONS</u> | <u>ARGUMENT<br/>OF PERIGEE<br/>(AT EPOCH)</u> |
|--------------|-----------------------------------|-----------------------------|-------------------------------|---|
| 780727       | 676                               | 1.4265                      | 8                             | 193.018                                       |
| 780802       | 986                               | 1.3541                      | 8                             | 153.474                                       |
| 780808       | 1522                              | 1.1539                      | 8                             | 116.082                                       |
| 780815       | 424                               | 1.3371                      | 4                             | 146.013                                       |
| 780818       | 483                               | .9859                       | 3                             | 141.375                                       |
| 780823       | 355                               | .6760                       | 4                             | 124.193                                       |
| 780826       | 1129                              | .8644                       | 5                             | 51.377  |
| 780901       | 627                               | 1.0067                      | 4                             | 99.273  |
| 780905       | 664                               | 2.0218                      | 9                             | 292.591                                       |
| 780910       | 1289                              | 1.7256                      | 10                            | 115.672                                       |
| 780917       | 1725                              | 1.2234                      | 10                            | 93.449  |
| 780923       | 1785                              | 1.3231                      | 9                             | 122.806                                       |
| 780929       | 1915                              | 1.7240                      | 9                             | 281.185                                       |
| 781005       | 1343                              | 1.8012                      | 9                             | 56.248  |

of particular importance because the satellite is in a polar orbit giving complete global sampling of the gravity field. This is the first time a strong polar orbit has been incorporated into the determination of GSFC gravity fields.

The nominal orbit parameters used in processing OSCAR-14 data were as follows:

|                 |                   |
|-----------------|-------------------|
| Area:           | 25 m <sup>2</sup> |
| Mass:           | 1000 kg           |
| Eccentricity:   | .004              |
| Inclination:    | 89°               |
| Perigee Height: | 1040 km           |
| Apogee Height:  | 1085 km           |
| Period:         | 106 minutes       |

Orbit computations for OSCAR-14 utilized the GEM-10B' gravity model. Thirteen 7-day arcs were analyzed using the GSFC GEODYN-2 computer program. The data coverage was from August 1, 1980 through October 24, 1980 (Table 5.2.2a). Computation of orbital solutions for these arcs included the adjustment of the six orbital elements, daily atmospheric drag parameters ( $C_D$ ), a single solar radiation pressure coefficient ( $C_R$ ), and observation biases for each pass. Timing biases were computed for SHANGHAI (743) and PURPLE MT. (7185). Data from GRAZ (425) were deleted from the solution. The sigma on all the data was nominally 1 cm/sec.

An estimate of the "true" noise for the Doppler data was ~1.2 cm/sec, largely due to the large variety of receivers which tracked. The overall RMS obtained for the OSCAR-14 orbits was about 1.59 cm/sec (Table 5.2.2b).

Table 5.2.2a

OSCAR-14 PRECISION ORBITS

| <u>ARC NO.</u> | <u>START<br/>YYMMDD</u> | <u>STOP<br/>YYMMDD</u> |
|----------------|-------------------------|------------------------|
| 1              | 800801                  | 800808                 |
| 2              | 800808                  | 800815                 |
| 3              | 800815                  | 800822                 |
| 4              | 800822                  | 800829                 |
| 5              | 800829                  | 800905                 |
| 6              | 800905                  | 800912                 |
| 7              | 800912                  | 800919                 |
| 8              | 800919                  | 800926                 |
| 9              | 800926                  | 801003                 |
| 10             | 801003                  | 801010                 |
| 11             | 801010                  | 801017                 |
| 12             | 801017                  | 801024                 |
| 13             | 801024                  | 801031                 |

Table 5.2.2b

**EMAT SUMMARY FOR OSCAR 14**

| <u>EPOCH</u> | <u>NUMBER OF<br/>OBSERVATIONS</u> | <u>WEIGHTED<br/>RMS (m)</u> | <u>NUMBER OF<br/>STATIONS</u> | <u>ARGUMENT<br/>OF PERIGEE<br/>(AT EPOCH)</u> |
|--------------|-----------------------------------|-----------------------------|-------------------------------|---|
| 800801       | 5867                              | 1.4677                      | 16                            | 357.420                                       |
| 800808       | 5559                              | 1.3992                      | 16                            | 337.814                                       |
| 800815       | 6227                              | 1.4702                      | 17                            | 336.019                                       |
| 800822       | 5635                              | 1.5358                      | 17                            | 277.827                                       |
| 800829       | 5812                              | 1.5332                      | 18                            | 273.059                                       |
| 800905       | 5944                              | 1.5991                      | 17                            | 240.671                                       |
| 800912       | 5993                              | 1.6518                      | 17                            | 209.115                                       |
| 800919       | 6015                              | 1.6174                      | 16                            | 187.183                                       |
| 800926       | 4519                              | 1.5773                      | 18                            | 187.551                                       |
| 801003       | 5500                              | 1.5881                      | 17                            | 136.816                                       |
| 801010       | 2251                              | 1.8217                      | 13                            | 140.581                                       |
| 801017       | 1881                              | 1.6457                      | 10                            | 119.267                                       |
| 801024       | 1895                              | 1.7754                      | 9                             | 97.921  |

### 5.2.3 Analysis of GEOS-1 Laser Ranging Data

GEOS-1 laser data from the period January 20, 1977 to December 14, 1978 have been chosen for analysis. This period spans more than one cycle of the argument of perigee, thus providing good temporal coverage. The data involves both SAO and NASA stations.

The first step in the procedure was to catalog the data and divide it into 5-day arcs, eliminating those time periods with little or no coverage. Attention was given to the number of passes and the number of stations involved in any 5-day period. A total of 104 arcs survived this scrutiny. Tables 5.2.3a and 5.2.3b provide summaries of the satellite's orbit and the tracking data.

The NASA data was provided at a frequency of one measurement/sec, with one measurement/7.5 sec for the SAO data. It was decided to select every third NASA observation and every SAO observation to get a more even balance in the data weighting. Using estimates of the position and velocity vectors of the satellite, nominal values for air drag, solar radiation pressure and solid earth tidal parameters, an ocean tide model, and the GEM-10B' gravity field, the arcs were converged. In the convergence process, the position and velocity vectors, air drag and solar radiation pressure parameters were adjusted for each arc. The purpose of the convergence is twofold: (1) to obtain more accurate position and velocity vectors preparatory to the creation of the matrix of normal equations ("E"-matrix) to be used in the gravity field solution, and (2) to identify and delete nonreliable measurements and/or passes. One air drag coefficient ( $C_D$ ) for each day of a 5-day arc and one solar radiation pressure ( $C_R$ ) coefficient for the whole arc were solved for. A total of 101 arcs survived this procedure.

**Table 5.2.3a**  
**ORBITAL DATA FOR GEOS-1**

|                                   |                           |
|-----------------------------------|---------------------------|
| <b>Semi-major axis:</b>           | <b>8080 km</b>            |
| <b>Eccentricity:</b>              | <b>.07</b>                |
| <b>Inclination:</b>               | <b>59°4'</b>              |
| <b>Perigee Height:</b>            | <b>1135 km</b>            |
| <b>Apogee Height:</b>             | <b>2270 km</b>            |
| <b>Year of Launch:</b>            | <b>1965</b>               |
| <b>Area:</b>                      | <b>1.23 m<sup>2</sup></b> |
| <b>Mass:</b>                      | <b>172.5 kg</b>           |
| <b>Period:</b>                    | <b>120 minutes</b>        |
| <b>Period of Arg. of Perigee:</b> | <b>540 days</b>           |

**Table 5.2.3b**

**TRACKING DATA SUMMARY**

|                          |                    |
|--------------------------|--------------------|
| ● SATELLITE:             | GEOS-1             |
| ● TIME PERIOD:           | 1/20/77 - 12/14/78 |
| ● DATA:                  | SAO + NASA LASER   |
| ● ARC LENGTH:            | 5 DAYS             |
| ● NO. ARCS (INCL. NASA): | 101 (58)           |
| ● NO. OBSERVATIONS:      | 129,371            |

**Table 5.2.3c**  
**SUMMARY OF GEOS-1 ORBITS**

| ARC EPOCH<br>YYMMDD | NO. OBS. | RMS (m) |
|---------------------|----------|---------|
| 770120              | 838      | 0.886   |
| 126                 | 904      | 0.721   |
| 207                 | 724      | 0.821   |
| 213                 | 752      | 0.848   |
| 311                 | 616      | 0.850   |
| 321                 | 1169     | 0.744   |
| 329                 | 978      | 0.463   |
| 403                 | 1303     | 0.816   |
| 408                 | 1359     | 0.658   |
| 413                 | 1589     | 1.088   |
| 418                 | 1061     | 0.890   |
| 423                 | 1649     | 0.794   |
| *                   | 428      | 2084    |
| *                   | 503      | 1778    |
| *                   | 508      | 1525    |
| *                   | 524      | 1085    |
| *                   | 603      | 1520    |
| *                   | 608      | 1830    |
| *                   | 613      | 1331    |
| *                   | 618      | 1245    |
| *                   | 623      | 1637    |
| *                   | 628      | 1240    |
| *                   | 703      | 1235    |
| *                   | 708      | 1255    |
| *                   | 713      | 1238    |
| *                   | 718      | 1095    |
| *                   | 723      | 704     |
| *                   | 729      | 1512    |
| *                   | 803      | 1728    |
| *                   | 808      | 1513    |
| *                   | 818      | 1151    |
| *                   | 825      | 1614    |
| *                   | 830      | 1364    |
| *                   | 904      | 1739    |
| *                   | 916      | 1661    |
| *                   | 921      | 2343    |
| *                   | 928      | 1804    |
| *                   | 1003     | 908     |
| *                   | 1008     | 1207    |
| *                   | 1013     | 1647    |
| *                   | 1024     | 1706    |
| *                   | 1029     | 1598    |

\*Includes NASA data

Table 5.2.3c *cont.*

| ARC EPOCH<br>YYMMDD | NO. OBS. | RMS (m) |
|---------------------|----------|---------|
| 771103              | 1195     | 1.815   |
| * 1110              | 1295     | 0.742   |
| * 1116              | 1359     | 1.137   |
| 1126                | 961      | 0.859   |
| 1201                | 1089     | 0.649   |
| 1211                | 1114     | 0.915   |
| 1216                | 801      | 0.876   |
| 780123              | 1196     | 0.804   |
| 201                 | 1075     | 0.880   |
| * 209               | 1039     | 0.798   |
| * 217               | 1280     | 0.868   |
| * 222               | 1644     | 0.783   |
| * 308               | 864      | 0.806   |
| * 314               | 985      | 0.754   |
| * 322               | 827      | 0.767   |
| * 330               | 885      | 0.821   |
| * 404               | 942      | 0.804   |
| 413                 | 894      | 0.761   |
| 419                 | 940      | 0.681   |
| 424                 | 1465     | 0.937   |
| 429                 | 960      | 1.010   |
| 504                 | 1313     | 0.815   |
| 509                 | 1810     | 0.932   |
| * 514               | 1049     | 0.838   |
| * 520               | 1065     | 0.789   |
| 528                 | 1092     | 0.871   |
| 602                 | 1443     | 0.860   |
| 607                 | 1700     | 0.982   |
| * 613               | 1533     | 0.841   |
| * 625               | 1478     | 0.949   |
| * 630               | 1329     | 0.805   |
| * 705               | 1670     | 1.199   |
| * 710               | 1440     | 0.928   |
| * 715               | 1212     | 0.697   |
| * 720               | 938      | 0.997   |
| * 725               | 632      | 0.773   |
| 730                 | 1329     | 0.925   |
| 804                 | 1318     | 1.112   |
| * 809               | 742      | 0.933   |
| * 820               | 683      | 0.852   |
| * 825               | 771      | 0.793   |
| * 830               | 961      | 0.488   |
| * 906               | 789      | 0.529   |
| * 919               | 1770     | 0.718   |

\*Includes NASA data

**Table 5.2.3c cont.**

| ARC EPOCH<br>YYMMDD | NO. OBS. | RMS (m) |
|---------------------|----------|---------|
| * 780924            | 1315     | 0.793   |
| * 929               | 1468     | 0.908   |
| * 1004              | 1620     | 1.044   |
| * 1009              | 1975     | 0.579   |
| * 1014              | 1890     | 0.969   |
| * 1019              | 1189     | 0.807   |
| * 1024              | 2034     | 0.701   |
| * 1029              | 1278     | 0.826   |
| * 1105              | 1169     | 0.967   |
| * 1110              | 1227     | 0.709   |
| * 1115              | 1380     | 0.753   |
| * 1120              | 1571     | 0.973   |
| * 1125              | 865      | 0.658   |
| * 1204              | 1362     | 1.019   |
| * 1209              | 912      | 0.843   |

Average rms = 0.912 m

\*Includes NASA data

Finally, one E-matrix (matrix of normal equations) was prepared for each arc. RMS of fit values for the arcs provide an indication of the overall fit to the data. They are presented in Table 5.2.3c

The RMS values ranged from 0.4 m to 1.8 m, with an average of 0.91 m. This is quite good, considering the vintage of the data. The GEOS-1 laser data provided an important contribution to the determination of the Earth's gravity field.

#### 5.2.4 GEOS-3 Analysis of Laser Ranging Data

The Geodynamics Earth and Ocean Satellite, GEOS-3, was launched on April 9, 1975. The satellite characteristics and the nominal orbital parameters are the following:

|                             |                       |
|-----------------------------|-----------------------|
| Area:                       | 1.4365 m <sup>2</sup> |
| Mass:                       | 345.909 kg            |
| Eccentricity:               | 0.00114               |
| Inclination:                | 115°                  |
| Perigee Height:             | 840 km                |
| Apogee Height:              | 860 km                |
| Orbital Period:             | 102 minutes           |
| Argument of Perigee Period: | 1039 days             |

The available data were obtained by both NASA and SAO laser tracking stations during the years 1975 and 1976. It is distributed as follows:

|        |                         |
|--------|-------------------------|
| 1975:  | 196916 meas.            |
| 1976:  | 193405 meas.            |
| Total: | 389421 meas. (SAO: 18%) |

Past experience at GSFC indicates that a 5 to 7 day arc length is optimum for the analysis of data acquired on geodetic satellites at 800 to 1000 km orbit heights. This time span provides strong gravitational information without excessive contamination from nonconservative force effects such as atmospheric drag and solar radiation pressure. A 5-day arc for GEOS-3 covers approximately the period of the effect produced by the resonant 14th order coefficients of the Earth's gravitational field. This effect can reach magnitudes of 150 meters in the along-track component. The gravitational field used in the computations was the GEM-10B' model complete to degree and order 36, derived from satellite tracking data, surface gravity and altimetry. The atmospheric density was that of the Jacchia 1971 model.

Forty-eight arcs covering the time period from May, 1975 to December, 1976, have been analyzed using the GEODYN Program. The editing applied to the data consisted of several stages. There was a preliminary selection based on existing knowledge concerning the quality of the data obtained by different stations at different times. The internal consistency of the data was checked on a pass by pass basis. Finally, the dynamic editing inherent in GEODYN was applied also.

The atmospheric drag model formulation allowed the estimation of a daily drag coefficient ( $C_D$ ), and the force model for the solar radiation pressure incorporated a single coefficient  $C_R$  for every 5-day arc. The solid earth tidal effects were modeled after Wahr's formulation, the ocean tides force model used a spherical harmonics approach due to D. Christodoulidis, et al. (1986b): the long wavelength components of approximately 600 constituents were used in the calculations and the coefficients of about 60 are actually estimated when computing a solution.

The trajectory generated using these estimated parameters was used to compute an RMS value for each 5-day arc, which provided an

**Table 5.2.4a**  
**GEO-S-3 ORBIT DETERMINATION RESULTS**

| <u>ARC EPOCH</u> | <u>NO. OF MEAS.</u> | <u>RMS (METERS)</u> |
|------------------|---------------------|---------------------|
| 750519           | 356                 | 0.510               |
| 750524           | 435                 | 0.273               |
| 750614           | 910                 | 0.559               |
| 750619           | 662                 | 0.679               |
| 750629           | 926                 | 0.633               |
| 750709           | 1120                | 0.757               |
| 750724           | 796                 | 0.469               |
| 750729           | 876                 | 0.363               |
| 750828           | 1705                | 0.596               |
| 750902           | 1240                | 0.459               |
| 750907           | 1501                | 0.527               |
| 750929           | 336                 | 0.571               |
| 751118           | 537                 | 0.613               |
| 751123           | 488                 | 0.593               |
| 751216           | 1333                | 0.485               |
| 760108           | 903                 | 1.542               |
| 760113           | 1533                | 1.454               |
| 760205           | 1219                | 1.202               |
| 760210           | 2078                | 1.237               |
| 760217           | 1450                | 0.809               |
| 760222           | 1184                | 0.869               |
| 760227           | 1801                | 1.300               |
| 760404           | 1009                | 1.487               |
| 760409           | 1217                | 1.282               |
| 760417           | 1178                | 1.186               |
| 760422           | 1112                | 1.380               |
| 760427           | 2307                | 1.443               |
| 760502           | 1866                | 1.391               |
| 760507           | 1193                | 1.079               |
| 760523           | 1010                | 1.218               |
| 760601           | 1003                | 1.231               |
| 760606           | 974                 | 1.374               |
| 760614           | 900                 | 1.465               |
| 760621           | 804                 | 1.319               |
| 760913           | 848                 | 1.480               |
| 761004           | 1641                | 1.309               |
| 761009           | 1085                | 1.432               |
| 761018           | 878                 | 0.904               |
| 761023           | 1031                | 1.145               |
| 761028           | 1072                | 1.641               |
| 761102           | 810                 | 1.547               |
| 761107           | 1634                | 1.126               |
| 761112           | 984                 | 0.965               |
| 761117           | 1394                | 1.369               |
| 761122           | 1527                | 1.386               |
| 761127           | 955                 | 1.294               |
| 761202           | 610                 | 1.383               |
| 761207           | 839                 | 1.306               |

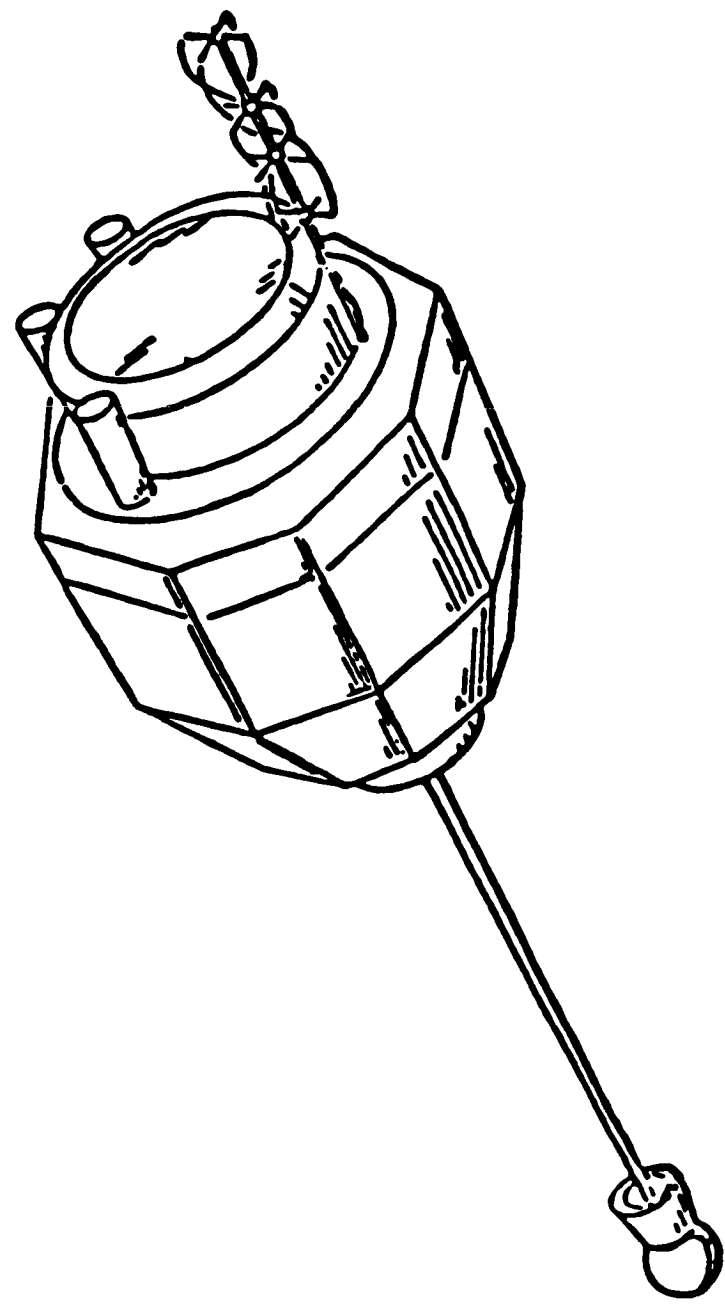


Figure 5.2.4a. GEOS-3 Spacecraft.

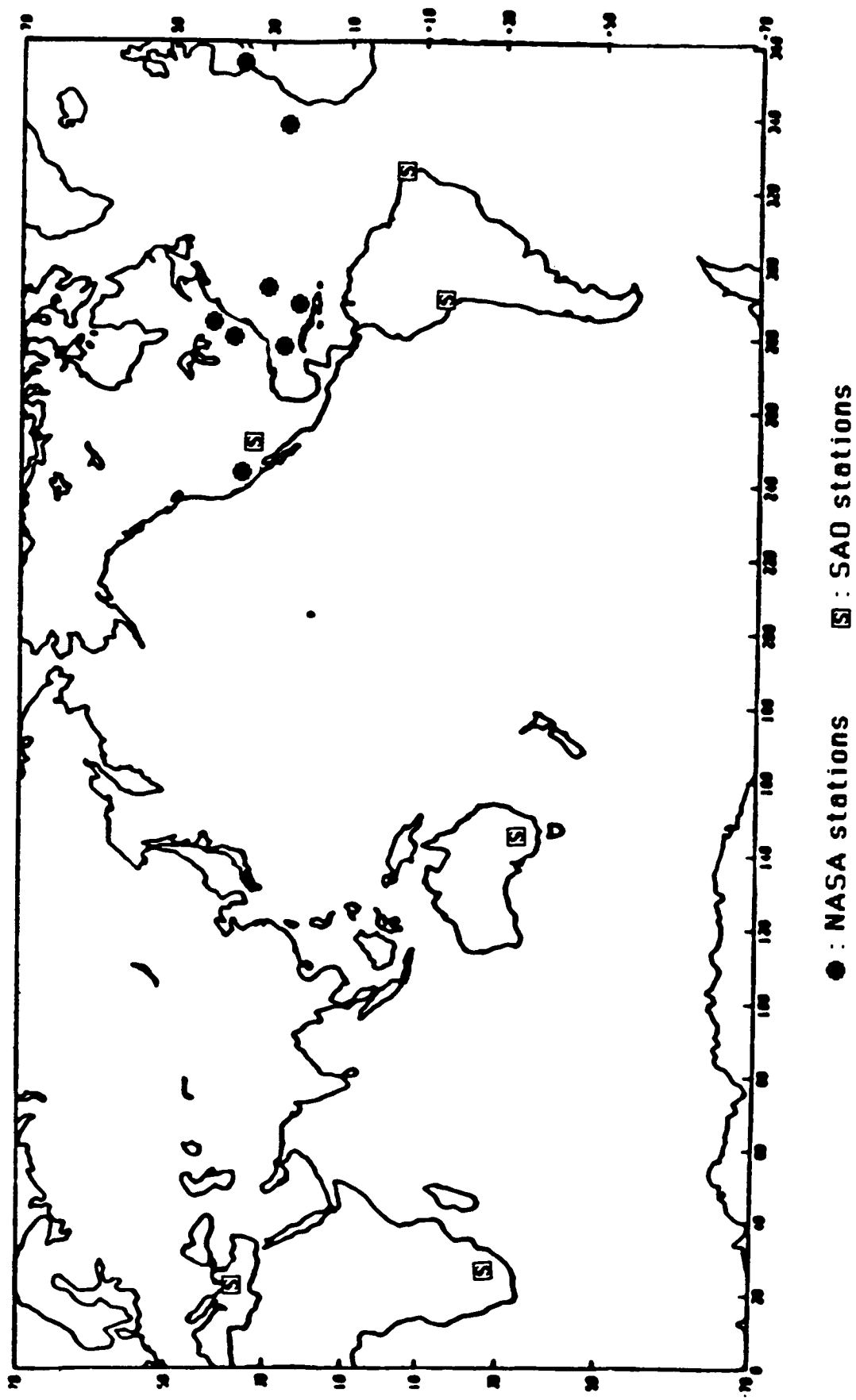


Figure 5.2.4b. Position of Stations Used in Tracking GEOS-1 and GEOS-3.

indication of the overall fit to the data for each arc. The results are given in Table 5.2.4a below. The converged arcs were used to compute the normal equations.

The higher RMS values in the 1976 arcs are due to the presence of data from the SAO stations, which are less accurate than the NASA stations. The SAO stations provide a global coverage which would be lacking with the use of NASA data alone.

#### 5.2.5 Analysis of STARLETTE Laser Ranging Data

This section documents the various stages of the data reduction effort in connection with the STARLETTE laser ranging data set. The data which fulfilled the editing criteria were subsequently used to form the normal equations contributing to the estimation of the TOPEX model parameters.

STARLETTE is a geodetic satellite launched by the French Space Agency in 1975. Information on its size, shape, mass and orbital characteristics is given in Table 5.2.5a. The STARLETTE data used in this effort consist of a set of raw ranges sampled in such a way that each station has about one range per six seconds (whenever available). Based on previous experience we decided that this procedure produced results similar to those obtained using normal points. The laborious process of forming normal points was thus avoided. We have only completed the analysis of the data covering the first eight months of 1984, with much more data being available.

These data that have been selected for analysis cover the January 1984 through August 1984 period. Table 5.2.5b shows the amount of tracking available for analysis from each station. The breakdown in terms of passes and individual ranges per station gives a rough

Table 5.2.5a

**ORBITAL AND PHYSICAL CHARACTERISTICS  
OF STARLETTE (7501001)**

---

|                          |                        |
|--------------------------|------------------------|
| APOGEE HEIGHT            | 1105 km                |
| PERIGEE HEIGHT           | 610 km                 |
| ECCENTRICITY             | 0.02                   |
| INCLINATION              | 49°.8                  |
| PERIOD                   | 104 min.               |
| ASCENDING NODE RATE      | -3.94 °/day            |
| ARGUMENT OF PERIGEE RATE | 3.30 °/day             |
| AREA                     | 0.04524 m <sup>2</sup> |
| MASS                     | 47.250 kg              |
| SHAPE                    | SPHERE                 |
| RADIUS                   | 12 cm                  |
| ONBOARD INSTRUMENTATION  | RETROREFLECTORS        |

indication of the varying repetition rates in this network. Based on prior experience with STARLETTE and considering the quality of our a priori models, a 5-day nominal arc length was chosen. The data were edited using the GEODYN-II software package appended with editing programs to perform post-fit residual analysis on station-by-station and pass-by-pass basis. Table 5.2.5c gives a summary of the constants and models used in the dynamical orbit determination process. The residual analysis package was invaluable in locating data problems and eliminating outliers. The philosophy here was to edit data points that looked suspect where documentation was lacking for curable station problems. Given the abundance of data, this process was beneficial in creating a stable and bias-free set of tracking data. Figure 5.2.5a shows a residual plot where one can clearly see an edited outlier and a number of residuals of questionable quality. The latter had to be edited manually and the whole process repeated until it converged. To give an insight into what was achieved through this process, we have included Tables 5.2.5d and 5.2.5e which show the apriori model fits and those based on our first generation TOPEX model, the PGS-T2. The improvement is highly significant. Table 5.2.5f gives a summary of the statistics by station based again on the same set of data and the same models as the previous two tables. We have analyzed forty-six 5-day arcs covering a period from January 1984 through August 1984. These arcs sample 2.2 periods of the argument of perigee and 2.6 periods of the ascending node. We chose to start the editing process with the more recent data since this period is characterized by intense tracking due to the ongoing (at the time) MERIT campaign. The large amount of data and the participation of new tracking stations for which we had no prior performance records on any satellite made the editing effort more complicated and tedious, but at the same time more important.

Starting with the "raw" data fits at the 1-2 meters level the editing process resulted in a very significant reduction to about 60 cm which was the typical RMS fit at the "normal-equation-forming" stage. A

Table 5.2.5b

**STARLETTE DATA CATALOG**  
**JANUARY 1983 - AUGUST 1984**

**SUMMARY BY STATIONS**

| LOCATION          | NAME   | NUMBER | PASSES | POINTS |
|-------------------|--------|--------|--------|--------|
| POTSDAM, DDR      | POTSDM | 1181   | 59     | 1271   |
| SAN DIEGO, CA.    | ML0306 | 7062   | 3      | 30     |
| AUSTRALIA         | ML0502 | 7090   | 64     | 3649   |
| GREENBELT, MD.    | ML0501 | 7102   | 1      | 5      |
| GREENBELT, MD.    | ML0702 | 7105   | 105    | 5499   |
| QUINCY, CA.       | ML0802 | 7109   | 288    | 18247  |
| MONUMENT PEAK, CA | ML0402 | 7110   | 270    | 12059  |
| PLATTEVILLE, CO.  | ML0201 | 7112   | 208    | 8589   |
| HUAHINE, FR.POL.  | ML0101 | 7121   | 41     | 1033   |
| MAZATLN, MEXICO   | ML0601 | 7122   | 54     | 2733   |
| MAUII, HAWAII     | HOLLAS | 7210   | 37     | 1441   |
| METSÄHOVI, FINN.  | FINLAS | 7805   | 12     | 209    |
| HELWAN, EGYPT     | HELWAN | 7831   | 12     | 376    |
| KOOTWIJK, HOLLAND | KOOLAS | 7833   | 32     | 419    |
| WEITZELL, FRG     | WETZEL | 7834   | 50     | 1602   |
| GRASSE, FRANCE    | GRASSE | 7835   | 7      | 111    |
| SIMOSATO, JAPAN   | SHOLAS | 7838   | 124    | 4690   |
| GRAZ, AUSTRIA     | GRAZ   | 7839   | 106    | 3665   |
| HERSTMONCEUX, UK  | RGO    | 7840   | 56     | 1609   |
| AREQUIPA, PERU    | ARELAS | 7907   | 939    | 44344  |
| MATERA, ITALY     | MATERA | 7939   | 289    | 15089  |
| DIONYSOS, GREECE  | DIOLAS | 7940   | 6      | 81     |
| ZIMMERWALD, SWIZ  |        | 7810   | 29     | 691    |

TOTAL NO. OF PASSES = 2792  
TOTAL NO. OF OBSERVATIONS = 127442

Table 5.2.5c

**DATA REDUCTION MODEL  
FOR  
STARLETTE DATA EDITING**

---

**GENERAL PARAMETERS**

|                           |  |
|---------------------------|--|
| GM                        | $3.98600436 \times 10^{14} \text{ m}^3/\text{s}^2$ |
| SPEED OF LIGHT            | 299792458.0 m/s                                    |
| $a_e$                     | 6378137.0 m  |
| $1/f$                     | 298.257  |
| JPL EPHEMERIDES           | DE-200/LE-200                                      |
| ATMOSPHERIC DENSITY MODEL | JACCHIA 1971                                       |

**GLOBAL PARAMETERS**

|                               |                      |
|-------------------------------|----------------------|
| GEOPOTENTIAL                  | PGS1331' (36 x 36)   |
| TIDES                         | APRIORI TOPEX MODEL  |
| POLAR MOTION & EARTH ROTATION | APRIORI TOPEX SERIES |
| STATION POSITIONS             | LAGEOS SL6 SOLUTION  |

**ARC PARAMETERS**

|                             |      |
|-----------------------------|------|
| STATE VECTOR                | 6    |
| DRAG COEFFICIENT            | 1    |
| SOLAR RADIATION COEFFICIENT | 1    |
| MEASUREMENT BIASES          | NONE |

**ORIGINAL DATA IS  
OF POOR QUALITY**

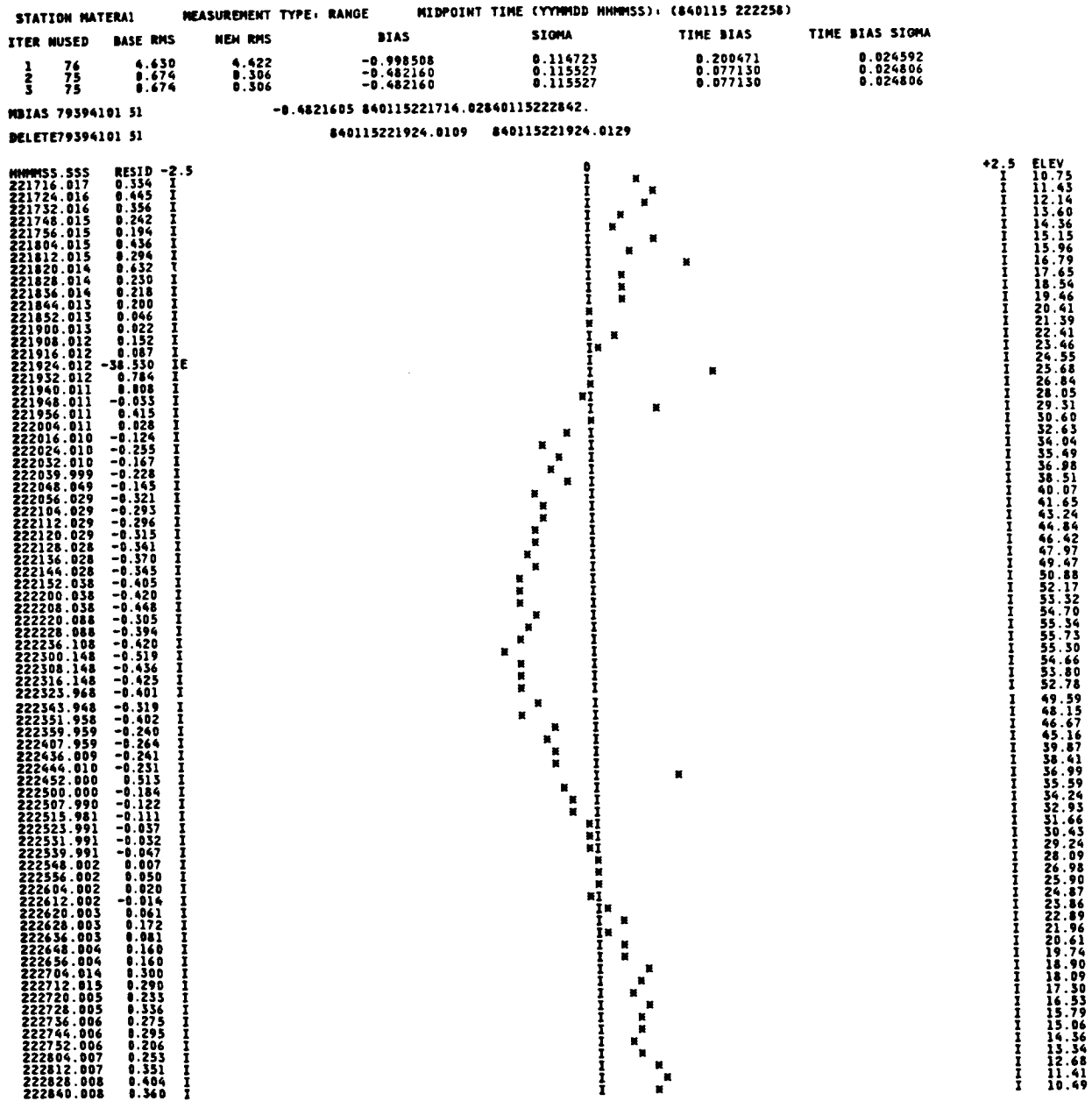


Figure 5.2.5a. Example of Residual Analysis Package Diagnostic Plot from Starlette: Matera Residuals Plotted Versus Time.

Table 5.2.5d. Example of Residual Analysis for Starlette Laser Passes During Period of January 3 to 7, 1984: Statistics Based on Apriori Model (Pgs 1331')

| STANAM                      | ISTA     | MTYPE | YYMMDD | HHMMSS | NPTS | ITER | USED | BIAS   | SIGMA | T. BIAS | SIGMA | FIT RMS | BASE RMS | MAXEL |
|-----------------------------|----------|-------|--------|--------|------|------|------|--------|-------|---------|-------|---------|----------|-------|
| GRAZ1                       | 78393401 | RANGE | 840103 | 12643  | 55   | 5    | 55   | -2.661 | 0.178 | 0.539   | 0.080 | 0.157   | 2.211    | 42.6  |
| GRAZ1                       | 78393401 | RANGE | 840105 | 20521  | 46   | 5    | 46   | -0.529 | 0.148 | 0.263   | 0.043 | 0.088   | 0.885    | 80.8  |
| GRAZ1                       | 78393401 | RANGE | 840105 | 35558  | 10   | 5    | 10   | 0.131  | 0.965 | 0.367   | 0.385 | 0.046   | 0.417    | 67.6  |
| GRAZ1                       | 78393401 | RANGE | 840106 | 5400   | 59   | 5    | 59   | 0.597  | 0.161 | 0.147   | 0.065 | 0.044   | 0.582    | 45.3  |
| GRAZ1                       | 78393401 | RANGE | 840106 | 22454  | 56   | 5    | 56   | 0.590  | 0.134 | -0.083  | 0.040 | 0.071   | 0.486    | 81.8  |
| GRAZ1                       | 78393401 | RANGE | 840106 | 41468  | 25   | 5    | 25   | 0.039  | 0.206 | -0.273  | 0.065 | 0.045   | 0.925    | 71.6  |
| GRAZ1                       | 78393401 | RANGE | 840107 | 5416   | 9    | 5    | 9    | -0.048 | 0.821 | 0.357   | 0.388 | 0.049   | 0.661    | 64.0  |
| TOTAL POINTS THIS STATION:  |          | 218   |        |        |      |      |      |        |       |         |       |         |          |       |
| RMS OF UNADJUSTED DATA:     |          | 1.048 |        |        |      |      |      |        |       |         |       |         |          |       |
| RMS OF ADJUSTED DATA:       |          | 0.089 |        |        |      |      |      |        |       |         |       |         |          |       |
| STANAM                      | ISTA     | MTYPE | YYMMDD | HHMMSS | NPTS | ITER | USED | BIAS   | SIGMA | T. BIAS | SIGMA | FIT RMS | BASE RMS | MAXEL |
| LAQU1102                    | 71100402 | RANGE | 840107 | 74460  | 16   | 3    | 16   | -1.157 | 0.324 | 0.178   | 0.078 | 0.276   | 0.993    | 50.6  |
| LAQU1102                    | 71100402 | RANGE | 840107 | 93513  | 34   | 3    | 34   | -1.209 | 0.341 | 0.309   | 0.106 | 0.043   | 0.630    | 36.2  |
| TOTAL POINTS THIS STATION:  |          | 50    |        |        |      |      |      |        |       |         |       |         |          |       |
| RMS OF UNADJUSTED DATA:     |          | 0.743 |        |        |      |      |      |        |       |         |       |         |          |       |
| RMS OF ADJUSTED DATA:       |          | 0.153 |        |        |      |      |      |        |       |         |       |         |          |       |
| STANAM                      | ISTA     | MTYPE | YYMMDD | HHMMSS | NPTS | ITER | USED | BIAS   | SIGMA | T. BIAS | SIGMA | FIT RMS | BASE RMS | MAXEL |
| MATERA1                     | 79394101 | RANGE | 840103 | 50554  | 81   | 6    | 77   | 0.153  | 0.114 | -0.920  | 0.030 | 0.097   | 0.199    | 39.6  |
| MATERA1                     | 79394101 | RANGE | 840104 | 33518  | 64   | 5    | 61   | 0.585  | 0.129 | 0.887   | 0.033 | 0.219   | 0.684    | 39.2  |
| TOTAL POINTS THIS STATION:  |          | 138   |        |        |      |      |      |        |       |         |       |         |          |       |
| RMS OF UNADJUSTED DATA:     |          | 0.474 |        |        |      |      |      |        |       |         |       |         |          |       |
| RMS OF ADJUSTED DATA:       |          | 0.161 |        |        |      |      |      |        |       |         |       |         |          |       |
| STANAM                      | ISTA     | MTYPE | YYMMDD | HHMMSS | NPTS | ITER | USED | BIAS   | SIGMA | T. BIAS | SIGMA | FIT RMS | BASE RMS | MAXEL |
| PLATVL1                     | 71120201 | RANGE | 840105 | 104850 | 40   | 4    | 38   | -1.100 | 0.208 | -0.002  | 0.059 | 0.118   | 1.140    | 41.0  |
| TOTAL POINTS THIS STATION:  |          | 38    |        |        |      |      |      |        |       |         |       |         |          |       |
| RMS OF UNADJUSTED DATA:     |          | 1.140 |        |        |      |      |      |        |       |         |       |         |          |       |
| RMS OF ADJUSTED DATA:       |          | 0.118 |        |        |      |      |      |        |       |         |       |         |          |       |
| STANAM                      | ISTA     | MTYPE | YYMMDD | HHMMSS | NPTS | ITER | USED | BIAS   | SIGMA | T. BIAS | SIGMA | FIT RMS | BASE RMS | MAXEL |
| QUIN1092                    | 71090802 | RANGE | 840105 | 85703  | 31   | 3    | 31   | 0.259  | 0.439 | -0.062  | 0.125 | 0.026   | 0.214    | 38.8  |
| QUIN1092                    | 71090802 | RANGE | 840106 | 91659  | 39   | 3    | 39   | 1.688  | 0.649 | -0.369  | 0.147 | 0.065   | 0.444    | 60.5  |
| TOTAL POINTS THIS STATION:  |          | 70    |        |        |      |      |      |        |       |         |       |         |          |       |
| RMS OF UNADJUSTED DATA:     |          | 0.356 |        |        |      |      |      |        |       |         |       |         |          |       |
| RMS OF ADJUSTED DATA:       |          | 0.051 |        |        |      |      |      |        |       |         |       |         |          |       |
| STANAM                      | ISTA     | MTYPE | YYMMDD | HHMMSS | NPTS | ITER | USED | BIAS   | SIGMA | T. BIAS | SIGMA | FIT RMS | BASE RMS | MAXEL |
| SIMOSATA                    | 78383601 | RANGE | 840105 | 231608 | 9    | 3    | 9    | 0.649  | 3.752 | 0.673   | 0.795 | 0.120   | 4.333    | 46.3  |
| TOTAL POINTS THIS STATION:  |          | 9     |        |        |      |      |      |        |       |         |       |         |          |       |
| RMS OF UNADJUSTED DATA:     |          | 4.333 |        |        |      |      |      |        |       |         |       |         |          |       |
| RMS OF ADJUSTED DATA:       |          | 0.120 |        |        |      |      |      |        |       |         |       |         |          |       |
| STANAM                      | ISTA     | MTYPE | YYMMDD | HHMMSS | NPTS | ITER | USED | BIAS   | SIGMA | T. BIAS | SIGMA | FIT RMS | BASE RMS | MAXEL |
| YARAG1                      | 78900501 | RANGE | 840105 | 134412 | 72   | 3    | 72   | -0.178 | 0.118 | -0.057  | 0.026 | 0.063   | 0.317    | 65.0  |
| YARAG1                      | 78900501 | RANGE | 840106 | 121434 | 54   | 7    | 49   | -0.097 | 0.144 | 0.095   | 0.039 | 0.020   | 0.380    | 40.4  |
| TOTAL POINTS THIS STATION:  |          | 121   |        |        |      |      |      |        |       |         |       |         |          |       |
| RMS OF UNADJUSTED DATA:     |          | 0.341 |        |        |      |      |      |        |       |         |       |         |          |       |
| RMS OF ADJUSTED DATA:       |          | 0.050 |        |        |      |      |      |        |       |         |       |         |          |       |
| TOTAL POINTS INPUT=         |          | 658   |        |        |      |      |      |        |       |         |       |         |          |       |
| TOTAL USED=                 |          | 644   |        |        |      |      |      |        |       |         |       |         |          |       |
| TOTAL EL CUT=               |          | 0     |        |        |      |      |      |        |       |         |       |         |          |       |
| TOTAL OTHER EDITS=          |          | 14    |        |        |      |      |      |        |       |         |       |         |          |       |
| NUMBER OF PASSES PROCESSED= |          | 17    |        |        |      |      |      |        |       |         |       |         |          |       |
| NUMBER DELETED ENTIRELY=    |          | 0     |        |        |      |      |      |        |       |         |       |         |          |       |
| RMS OF UNADJUSTED DATA:     |          | 0.077 |        |        |      |      |      |        |       |         |       |         |          |       |
| RMS OF ADJUSTED DATA:       |          | 0.108 |        |        |      |      |      |        |       |         |       |         |          |       |

C - 3

Table 5.2.5e. Post Fit Residual Analysis for Starlette Laser Passes During Period of January 3 to 7, 1984: Statistics Based on Pgs-T2.

| STANAM                      | ISTA     | MTYPE | YYMMDD | HHMMSS | NPTS | ITER | USED | BIAS   | SIGMA | T. BIAS | SIGMA | FIT RMS | BASE RMS | MAXEL |
|-----------------------------|----------|-------|--------|--------|------|------|------|--------|-------|---------|-------|---------|----------|-------|
| GRAZI                       | 78393401 | RANGE | 840103 | 12643  | 33   | 2    | 33   | -0.087 | 0.178 | 0.104   | 0.080 | 0.049   | 0.242    | 42.6  |
| GRAZI                       | 78393401 | RANGE | 840105 | 20521  | 46   | 2    | 46   | -0.397 | 0.148 | -0.041  | 0.043 | 0.080   | 0.428    | 80.8  |
| GRAZI                       | 78393401 | RANGE | 840105 | 35558  | 10   | 2    | 10   | 0.115  | 0.960 | -0.038  | 0.381 | 0.046   | 0.064    | 67.6  |
| GRAZI                       | 78393401 | RANGE | 840106 | 3600   | 39   | 2    | 39   | 0.024  | 0.161 | -0.122  | 0.063 | 0.028   | 0.320    | 45.3  |
| GRAZI                       | 78393401 | RANGE | 840106 | 22454  | 56   | 2    | 56   | -0.092 | 0.134 | -0.019  | 0.040 | 0.047   | 0.126    | 81.8  |
| GRAZI                       | 78393401 | RANGE | 840106 | 41448  | 25   | 2    | 25   | -0.199 | 0.206 | -0.103  | 0.063 | 0.069   | 0.454    | 71.6  |
| GRAZI                       | 78393401 | RANGE | 840107 | 5416   | 9    | 2    | 9    | -0.303 | 0.818 | -0.056  | 0.386 | 0.049   | 0.233    | 64.0  |
| TOTAL POINTS THIS STATION:  |          |       | 218    |        |      |      |      |        |       |         |       |         |          |       |
| RMS OF UNADJUSTED DATA:     |          |       | 0.302  |        |      |      |      |        |       |         |       |         |          |       |
| RMS OF ADJUSTED DATA:       |          |       | 0.055  |        |      |      |      |        |       |         |       |         |          |       |
| <br>                        |          |       |        |        |      |      |      |        |       |         |       |         |          |       |
| STANAM                      | ISTA     | MTYPE | YYMMDD | HHMMSS | NPTS | ITER | USED | BIAS   | SIGMA | T. BIAS | SIGMA | FIT RMS | BASE RMS | MAXEL |
| LAGU1102                    | 71100402 | RANGE | 840107 | 74440  | 16   | 2    | 16   | -0.231 | 0.324 | -0.001  | 0.078 | 0.094   | 0.262    | 50.6  |
| LAGU1102                    | 71100402 | RANGE | 840107 | 95313  | 34   | 2    | 34   | -0.042 | 0.341 | -0.026  | 0.106 | 0.036   | 0.130    | 36.2  |
| TOTAL POINTS THIS STATION:  |          |       | 50     |        |      |      |      |        |       |         |       |         |          |       |
| RMS OF UNADJUSTED DATA:     |          |       | 0.177  |        |      |      |      |        |       |         |       |         |          |       |
| RMS OF ADJUSTED DATA:       |          |       | 0.059  |        |      |      |      |        |       |         |       |         |          |       |
| <br>                        |          |       |        |        |      |      |      |        |       |         |       |         |          |       |
| STANAM                      | ISTA     | MTYPE | YYMMDD | HHMMSS | NPTS | ITER | USED | BIAS   | SIGMA | T. BIAS | SIGMA | FIT RMS | BASE RMS | MAXEL |
| MATERAI                     | 79394101 | RANGE | 840103 | 30540  | 76   | 2    | 76   | 0.158  | 0.115 | -0.018  | 0.050 | 0.095   | 0.201    | 39.6  |
| MATERAI                     | 79394101 | RANGE | 840104 | 33518  | 61   | 3    | 60   | 0.156  | 0.130 | -0.023  | 0.033 | 0.118   | 0.196    | 39.2  |
| TOTAL POINTS THIS STATION:  |          |       | 136    |        |      |      |      |        |       |         |       |         |          |       |
| RMS OF UNADJUSTED DATA:     |          |       | 0.198  |        |      |      |      |        |       |         |       |         |          |       |
| RMS OF ADJUSTED DATA:       |          |       | 0.105  |        |      |      |      |        |       |         |       |         |          |       |
| <br>                        |          |       |        |        |      |      |      |        |       |         |       |         |          |       |
| STANAM                      | ISTA     | MTYPE | YYMMDD | HHMMSS | NPTS | ITER | USED | BIAS   | SIGMA | T. BIAS | SIGMA | FIT RMS | BASE RMS | MAXEL |
| PLATVLL1                    | 71120201 | RANGE | 840105 | 104855 | 38   | 2    | 38   | -0.237 | 0.208 | 0.084   | 0.059 | 0.073   | 0.254    | 41.0  |
| TOTAL POINTS THIS STATION:  |          |       | 38     |        |      |      |      |        |       |         |       |         |          |       |
| RMS OF UNADJUSTED DATA:     |          |       | 0.254  |        |      |      |      |        |       |         |       |         |          |       |
| RMS OF ADJUSTED DATA:       |          |       | 0.073  |        |      |      |      |        |       |         |       |         |          |       |
| <br>                        |          |       |        |        |      |      |      |        |       |         |       |         |          |       |
| STANAM                      | ISTA     | MTYPE | YYMMDD | HHMMSS | NPTS | ITER | USED | BIAS   | SIGMA | T. BIAS | SIGMA | FIT RMS | BASE RMS | MAXEL |
| QUIN1092                    | 71090802 | RANGE | 840105 | 85703  | 31   | 2    | 31   | 0.193  | 0.438 | 0.058   | 0.125 | 0.026   | 0.512    | 38.8  |
| QUIN1092                    | 71090802 | RANGE | 840106 | 91659  | 39   | 2    | 39   | 0.270  | 0.648 | -0.035  | 0.147 | 0.032   | 0.135    | 60.5  |
| TOTAL POINTS THIS STATION:  |          |       | 70     |        |      |      |      |        |       |         |       |         |          |       |
| RMS OF UNADJUSTED DATA:     |          |       | 0.227  |        |      |      |      |        |       |         |       |         |          |       |
| RMS OF ADJUSTED DATA:       |          |       | 0.029  |        |      |      |      |        |       |         |       |         |          |       |
| <br>                        |          |       |        |        |      |      |      |        |       |         |       |         |          |       |
| STANAM                      | ISTA     | MTYPE | YYMMDD | HHMMSS | NPTS | ITER | USED | BIAS   | SIGMA | T. BIAS | SIGMA | FIT RMS | BASE RMS | MAXEL |
| SIMOSATA                    | 78383601 | RANGE | 840105 | 231608 | 9    | 2    | 9    | -0.656 | 3.503 | -0.364  | 0.743 | 0.117   | 2.691    | 46.3  |
| TOTAL POINTS THIS STATION:  |          |       | 9      |        |      |      |      |        |       |         |       |         |          |       |
| RMS OF UNADJUSTED DATA:     |          |       | 2.691  |        |      |      |      |        |       |         |       |         |          |       |
| RMS OF ADJUSTED DATA:       |          |       | 0.117  |        |      |      |      |        |       |         |       |         |          |       |
| <br>                        |          |       |        |        |      |      |      |        |       |         |       |         |          |       |
| STANAM                      | ISTA     | MTYPE | YYMMDD | HHMMSS | NPTS | ITER | USED | BIAS   | SIGMA | T. BIAS | SIGMA | FIT RMS | BASE RMS | MAXEL |
| YARAGI                      | 70900501 | RANGE | 840105 | 134412 | 72   | 2    | 72   | -0.031 | 0.118 | -0.015  | 0.026 | 0.040   | 0.088    | 65.0  |
| YARAGI                      | 70900501 | RANGE | 840106 | 121436 | 53   | 2    | 53   | -0.158 | 0.158 | 0.046   | 0.038 | 0.047   | 0.252    | 40.4  |
| TOTAL POINTS THIS STATION:  |          |       | 125    |        |      |      |      |        |       |         |       |         |          |       |
| RMS OF UNADJUSTED DATA:     |          |       | 0.175  |        |      |      |      |        |       |         |       |         |          |       |
| RMS OF ADJUSTED DATA:       |          |       | 0.043  |        |      |      |      |        |       |         |       |         |          |       |
| <br>                        |          |       |        |        |      |      |      |        |       |         |       |         |          |       |
| TOTAL POINTS INPUT=         | 647      |       |        |        |      |      |      |        |       |         |       |         |          |       |
| TOTAL USED=                 | 646      |       |        |        |      |      |      |        |       |         |       |         |          |       |
| TOTAL EL CUT=               | 0        |       |        |        |      |      |      |        |       |         |       |         |          |       |
| TOTAL OTHER EDITS=          | 1        |       |        |        |      |      |      |        |       |         |       |         |          |       |
| NUMBER OF PASSES PROCESSED= | 17       |       |        |        |      |      |      |        |       |         |       |         |          |       |
| NUMBER DELETED ENTIRELY=    | 0        |       |        |        |      |      |      |        |       |         |       |         |          |       |
| RMS OF UNADJUSTED DATA:     | 8.367    |       |        |        |      |      |      |        |       |         |       |         |          |       |
| RMS OF ADJUSTED DATA:       | 0.067    |       |        |        |      |      |      |        |       |         |       |         |          |       |

Circles indicate points  
of poor quality

**Table 5.2.5f**

**STARLETTE RESIDUAL  
STATISTICS SUMMARY**

**APRIORI MODEL (PGS 1331')**

| STANAM   | ISTA     | MTYPE | YYMMDD | HHMMSS | NPTS | ITER | USED | BIAS   | SIGMA | T. BIAS | SIGMA | FIT RMS | BASE RMS | MAXEL |
|----------|----------|-------|--------|--------|------|------|------|--------|-------|---------|-------|---------|----------|-------|
| GRAZ1    | 78393401 | RANGE | 840103 | 12643  | 33   | 5    | 33   | -2.041 | 0.178 | 0.539   | 0.080 | 0.157   | 2.211    | 42.6  |
| GRAZ1    | 78393401 | RANGE | 840105 | 20521  | 46   | 5    | 46   | -0.329 | 0.148 | 0.223   | 0.043 | 0.088   | 0.883    | 80.8  |
| GRAZ1    | 78393401 | RANGE | 840105 | 35558  | 10   | 5    | 10   | 0.131  | 0.965 | 0.097   | 0.383 | 0.046   | 0.617    | 67.6  |
| GRAZ1    | 78393401 | RANGE | 840106 | 3600   | 39   | 5    | 39   | 0.397  | 0.161 | 0.147   | 0.063 | 0.044   | 0.582    | 45.3  |
| GRAZ1    | 78393401 | RANGE | 840106 | 22654  | 56   | 5    | 56   | 0.390  | 0.134 | -0.083  | 0.040 | 0.091   | 0.486    | 81.8  |
| GRAZ1    | 78393401 | RANGE | 840106 | 41648  | 25   | 5    | 25   | 0.039  | 0.206 | -0.273  | 0.063 | 0.045   | 0.923    | 71.6  |
| GRAZ1    | 78393401 | RANGE | 840107 | 5616   | 9    | 5    | 9    | -0.048 | 0.021 | 0.337   | 0.388 | 0.049   | 0.861    | 64.0  |
| LAGU1102 | 71100402 | RANGE | 840107 | 74460  | 16   | 5    | 16   | 1.157  | 0.324 | 0.178   | 0.078 | 0.276   | 0.993    | 50.6  |
| LAGU1102 | 71100402 | RANGE | 840107 | 93513  | 34   | 5    | 34   | -1.209 | 0.341 | 0.309   | 0.106 | 0.043   | 0.630    | 36.2  |
| MATERA1  | 79394101 | RANGE | 840103 | 50554  | 81   | 6    | 77   | 0.153  | 0.114 | -0.020  | 0.030 | 0.097   | 0.199    | 39.4  |
| MATERA1  | 79394101 | RANGE | 840104 | 33518  | 64   | 5    | 61   | 0.585  | 0.129 | 0.087   | 0.033 | 0.219   | 0.684    | 39.2  |
| PLATV11  | 71120201 | RANGE | 840105 | 104850 | 40   | 4    | 38   | -1.100 | 0.208 | -0.002  | 0.059 | 0.118   | 1.140    | 61.0  |
| QUIN1092 | 71090802 | RANGE | 840105 | 85703  | 31   | 3    | 31   | 0.259  | 0.639 | -0.062  | 0.125 | 0.026   | 0.114    | 38.8  |
| QUIN1092 | 71090802 | RANGE | 840106 | 91659  | 39   | 3    | 39   | 1.688  | 0.649 | -0.349  | 0.147 | 0.065   | 0.644    | 60.5  |
| SIMOSATA | 78383601 | RANGE | 840105 | 231608 | 9    | 5    | 9    | 0.649  | 3.752 | 0.673   | 0.795 | 0.120   | 4.333    | 46.3  |
| YARAG1   | 70900501 | RANGE | 840105 | 134612 | 72   | 5    | 72   | 0.178  | 0.118 | -0.057  | 0.026 | 0.063   | 0.317    | 65.0  |
| YARAG1   | 70900501 | RANGE | 840106 | 121436 | 54   | 7    | 49   | -0.097 | 0.144 | 0.095   | 0.039 | 0.020   | 0.380    | 40.4  |

**TOPEX MODEL PGS - T2**

| STANAM   | ISTA     | MTYPE | YYMMDD | HHMMSS | NPTS | ITER | USED | BIAS   | SIGMA | T. BIAS | SIGMA | FIT RMS | BASE RMS | MAXEL |
|----------|----------|-------|--------|--------|------|------|------|--------|-------|---------|-------|---------|----------|-------|
| GRAZ1    | 78393401 | RANGE | 840103 | 12643  | 33   | 2    | 33   | -0.007 | 0.178 | 0.104   | 0.080 | 0.049   | 0.242    | 42.6  |
| GRAZ1    | 78393401 | RANGE | 840105 | 20521  | 46   | 2    | 46   | -0.397 | 0.148 | -0.041  | 0.043 | 0.080   | 0.428    | 80.8  |
| GRAZ1    | 78393401 | RANGE | 840105 | 35558  | 10   | 2    | 10   | 0.115  | 0.960 | -0.038  | 0.381 | 0.046   | 0.064    | 67.6  |
| GRAZ1    | 78393401 | RANGE | 840106 | 3600   | 39   | 2    | 39   | 0.024  | 0.161 | -0.122  | 0.063 | 0.028   | 0.520    | 45.3  |
| GRAZ1    | 78393401 | RANGE | 840106 | 22654  | 56   | 2    | 56   | -0.092 | 0.134 | -0.019  | 0.040 | 0.047   | 0.126    | 81.8  |
| GRAZ1    | 78393401 | RANGE | 840106 | 41648  | 25   | 2    | 25   | -0.199 | 0.206 | -0.103  | 0.063 | 0.069   | 0.354    | 71.6  |
| GRAZ1    | 78393401 | RANGE | 840107 | 5616   | 9    | 2    | 9    | -0.303 | 0.018 | -0.056  | 0.386 | 0.049   | 0.233    | 64.0  |
| LAGU1102 | 71100402 | RANGE | 840107 | 74460  | 16   | 2    | 16   | -0.231 | 0.324 | -0.001  | 0.078 | 0.094   | 0.262    | 50.6  |
| LAGU1102 | 71100402 | RANGE | 840107 | 93513  | 34   | 2    | 34   | -0.042 | 0.341 | -0.026  | 0.106 | 0.036   | 0.130    | 36.2  |
| MATERA1  | 79394101 | RANGE | 840103 | 50550  | 76   | 2    | 76   | 0.158  | 0.115 | -0.018  | 0.030 | 0.095   | 0.201    | 39.4  |
| MATERA1  | 79394101 | RANGE | 840104 | 33518  | 61   | 3    | 60   | 0.150  | 0.130 | 0.023   | 0.033 | 0.118   | 0.196    | 39.2  |
| PLATV11  | 71120201 | RANGE | 840105 | 104855 | 38   | 2    | 38   | -0.237 | 0.208 | 0.084   | 0.059 | 0.073   | 0.254    | 41.0  |
| QUIN1092 | 71090802 | RANGE | 840105 | 85703  | 31   | 2    | 31   | 0.103  | 0.638 | 0.058   | 0.125 | 0.026   | 0.312    | 38.8  |
| QUIN1092 | 71090802 | RANGE | 840106 | 91659  | 39   | 2    | 39   | 0.270  | 0.648 | -0.035  | 0.167 | 0.032   | 0.155    | 60.5  |
| SIMOSATA | 78383601 | RANGE | 840105 | 231608 | 9    | 2    | 9    | -0.656 | 3.503 | -0.366  | 0.743 | 0.117   | 2.691    | 46.3  |
| YARAG1   | 70900501 | RANGE | 840105 | 134612 | 72   | 2    | 72   | -0.031 | 0.118 | -0.015  | 0.026 | 0.040   | 0.088    | 65.0  |
| YARAG1   | 70900501 | RANGE | 840106 | 121436 | 53   | 2    | 53   | -0.138 | 0.138 | 0.046   | 0.038 | 0.047   | 0.252    | 40.4  |

detailed picture of the individual 5-day arc normal equations is shown in Table 5.2.5g. The STARLETTE normal equations allowed for the adjustment of geopotential harmonics, the selected subset of tidal coefficients, the Earth orientation parameters, the station positions, and the orbital arc parameters. The 46 matrices were subsequently combined (after the elimination of the arc parameters) into a single matrix, the STARLETTE C-mat. This allowed for an easier combination and weighting of the data. The RMS of fit values from Table 5.2.5g are shown pictorially in Figure 5.2.5b.

Forty six five-day arcs of recent (1984) STARLETTE laser ranging data have been analyzed. The resulting normal equations have contributed in the determination of the latest interim TOPEX model, GEM-T1. Extensive data editing and a general overhauling of the physical and mathematical models used in this analysis resulted in a remarkably improved performance of these data. This is very encouraging in light of the fact that the altitude of STARLETTE is relatively low and its orbit is strongly influenced by gravity and tidal perturbations. Its sensitivity to these forces however, coupled with the robustness of the edited data set and STARLETTE's orbital similarities with TOPEX make its contribution to the solution a very important one.

#### 5.2.6 Analysis of LAGEOS Laser Ranging Observations

The utilization of Satellite Laser Ranging for monitoring the earth's motions (both tectonic and rotational) has been greatly enhanced by the May, 1976 launch of the LAGEOS satellite. LAGEOS stands for the LAser GEodynamics Satellite and is the first NASA satellite to be launched exclusively to serve as a space-based laser target. The nominal orbital characteristics for LAGEOS are described in Table 5.2.6a. The high altitude of the LAGEOS orbit reduces errors arising from short-wavelength gravity, tidal and drag effects, leaving a strong

Table 5.2.5g

**EMAT SUMMARY FOR STARLETTE**

| <u>EPOCH</u> | <u>NUMBER OF<br/>OBSERVATIONS</u> | <u>WEIGHTED<br/>RMS (m)</u> | <u>NUMBER OF<br/>STATIONS</u> | <u>ARGUMENT<br/>OF PERIGEE<br/>(AT EPOCH)</u> |
|--------------|-----------------------------------|-----------------------------|-------------------------------|---|
| 840102       | 633                               | .5736                       | 7                             | 328.219                                       |
| 840107       | 682                               | .5172                       | 9                             | 343.032                                       |
| 840112       | 1043                              | .6436                       | 10                            | 1.779   |
| 840117       | 1012                              | .7107                       | 10                            | 17.217  |
| 840122       | 2270                              | .4651                       | 9                             | 32.676  |
| 840127       | 958                               | .4331                       | 10                            | 50.280  |
| 840201       | 847                               | .3903                       | 7                             | 64.865  |
| 840206       | 1499                              | .5625                       | 8                             | 83.486  |
| 840211       | 398                               | .6710                       | 6                             | 97.697  |
| 840216       | 338                               | .4215                       | 5                             | 113.218                                       |
| 840221       | 502                               | .8665                       | 8                             | 129.760                                       |
| 840226       | 841                               | .7439                       | 7                             | 144.077                                       |
| 840302       | 451                               | .8990                       | 5                             | 162.843                                       |
| 840312       | 716                               | .6586                       | 5                             | 194.533                                       |
| 840317       | 741                               | .4125                       | 6                             | 212.022                                       |
| 840322       | 1289                              | .6363                       | 9                             | 227.683                                       |
| 840327       | 1971                              | .5744                       | 8                             | 247.627                                       |
| 840401       | 2069                              | .5924                       | 7                             | 262.668                                       |
| 840406       | 2212                              | .5219                       | 6                             | 279.917                                       |
| 840411       | 3084                              | .5851                       | 8                             | 297.023                                       |
| 840416       | 827                               | .6289                       | 8                             | 312.347                                       |
| 840421       | 1437                              | .6480                       | 7                             | 332.052                                       |
| 840426       | 893                               | .8068                       | 9                             | 347.073                                       |
| 840501       | 619                               | .5879                       | 5                             | 4.323   |
| 840506       | 874                               | .8000                       | 4                             | 20.754  |
| 840511       | 905                               | .7750                       | 4                             | 36.110  |
| 840516       | 574                               | .6051                       | 8                             | 54.741  |
| 840521       | 2250                              | .7150                       | 8                             | 68.645  |
| 840526       | 1437                              | .7178                       | 8                             | 85.147  |
| 840531       | 2012                              | .6031                       | 8                             | 100.373                                       |
| 840605       | 1279                              | .5656                       | 11                            | 115.013                                       |
| 840610       | 2160                              | .7684                       | 10                            | 133.685                                       |
| 840615       | 2323                              | .5638                       | 12                            | 148.093                                       |
| 840620       | 1480                              | .5611                       | 9                             | 165.902                                       |
| 840625       | 3451                              | .6866                       | 10                            | 181.369                                       |
| 840630       | 1429                              | .4409                       | 8                             | 197.607                                       |
| 840705       | 1197                              | .6200                       | 7                             | 216.576                                       |
| 840710       | 550                               | .4866                       | 5                             | 231.370                                       |
| 840715       | 486                               | .5503                       | 5                             | 249.614                                       |
| 840720       | 824                               | .7427                       | 4                             | 265.374                                       |
| 840725       | 350                               | .4617                       | 3                             | 281.668                                       |
| 840730       | 754                               | .4867                       | 5                             | 301.339                                       |
| 840804       | 749                               | .6397                       | 6                             | 316.584                                       |
| 840809       | 921                               | .5161                       | 7                             | 335.486                                       |
| 840814       | 1170                              | .5073                       | 8                             | 350.581                                       |
| 840819       | 2849                              | .4891                       | 8                             | 7.096   |
| 46 EMATS     | 57356                             | .6120                       |                               |   |

**STARLETTE E-MAT SUMMARY**  
**WEIGHTED RMS**  
**(APRIORI)**

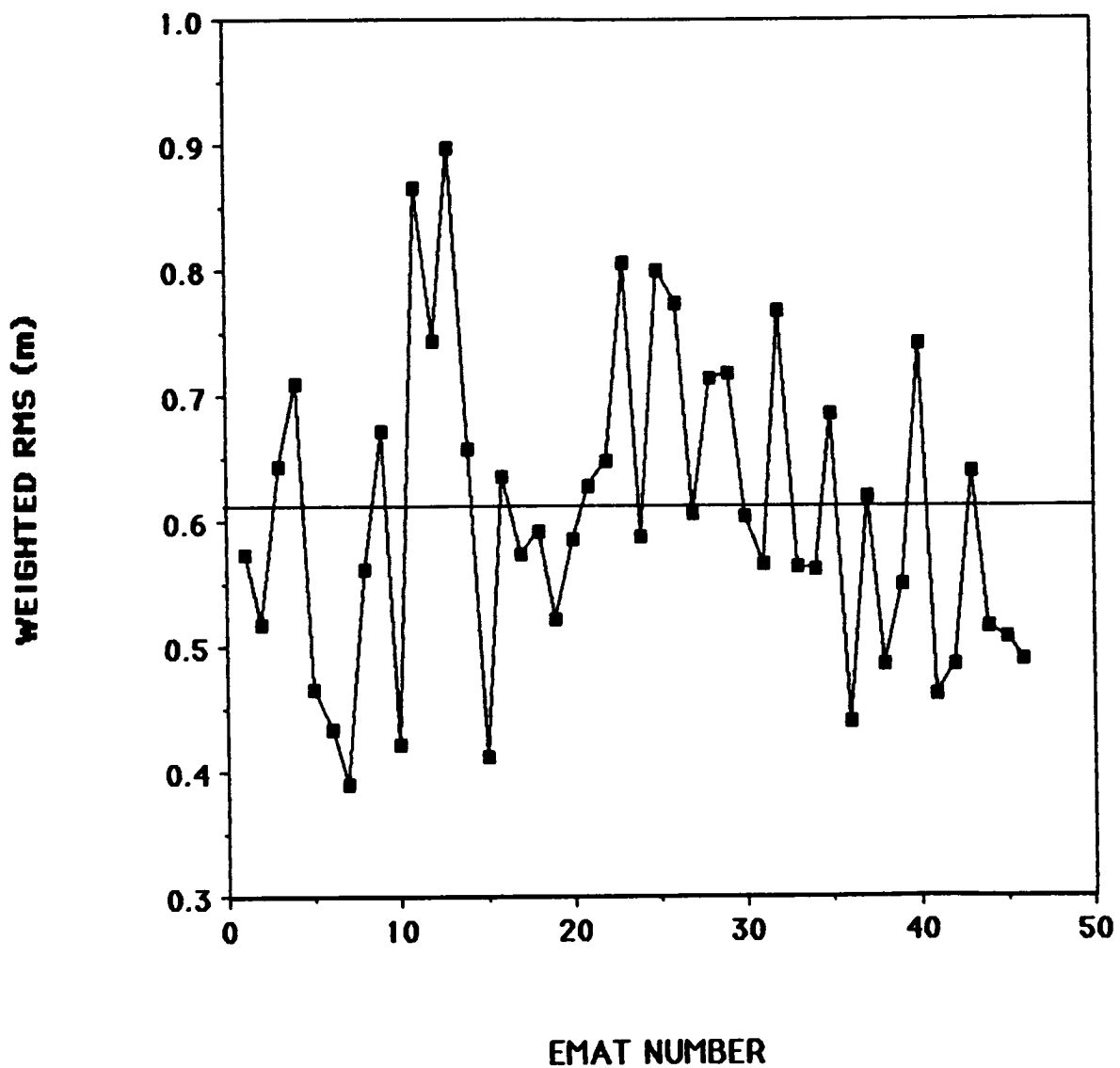


Figure 5.2.5b. STARLETTE E-MAT Summary.

signal for the longest wavelength portion of the gravitational field. Furthermore, by being extremely dense and having a perfectly spherical shape (see figure 5.2.6a), LAGEOS also minimizes errors arising from non-conservative forces like solar radiation pressure and albedo re-radiation. Therefore, LAGEOS is an ideal satellite for improving the determination of the long wavelength gravity field. A significant distinction of LAGEOS over previous laser satellite missions is the extensive international cooperation which has occurred to enhance global laser coverage. There is now a worldwide network of third generation laser stations which is tracking LAGEOS as their highest priority target. These constitute the largest and best distributed set of laser observations which have ever been collected. In our present analysis, 5 years of laser data acquired on LAGEOS have been used in the GEM-T1 solution. These ranges have been condensed into laser "normal-points" at two minute intervals. The time span selected contains the most outstanding set of these data encompassing the years 1980 through to the end of 1984. The NASA mobile laser systems were first deployed in late 1979 so early data sets are somewhat unsatisfactory. The additional data from 1985, which is now available, will be added to the solution over the next year. It is desirable to have at least six years of these observations in our gravity solutions. Six years of tracking is somewhat important because it corresponds to the beat period of the two dominant polar motion terms, that of the annual and Chandler periods. And LAGEOS data make a strong contribution to the definition of the pole obtained within our solution. The LAGEOS data were reduced in monthly arc lengths with a solar radiation pressure and along track acceleration parameter allowed to adjust along with the epoch state elements. These observations were carefully edited, and post-processing analysis of these data indicate RMS of fits for monthly arcs of between 4.5 to 10 cm. A summary of the LAGEOS arcs used to generate the normal equations is presented in Table 5.2.6b.

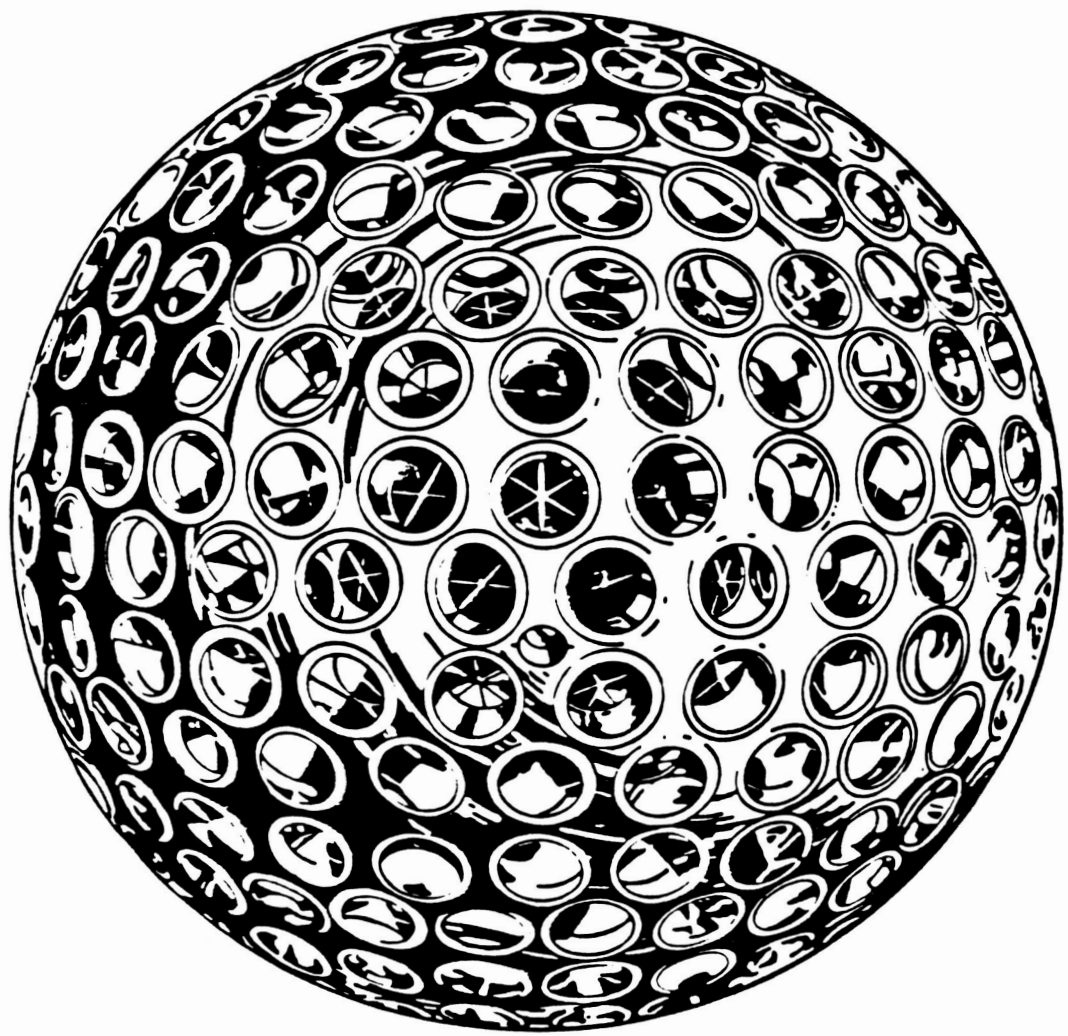


Figure 5.2.6. LAGEOS Satellite.

**Table 5.2.6a**  
**LAGEOS**  
**(LASER GEODYNAMICS SATELLITE)**

**Launch:** May 4, 1976

**Spacecraft:** Spherical, 60 cm diameter  
406.965 kg  
426 laser retro-reflectors, 3.8 cm diameter

|               |                             |                |
|---------------|-----------------------------|----------------|
| <b>Orbit:</b> | <b>Semi-major axis</b>      | 12265 km       |
|               | <b>Inclination</b>          | 109.8 degrees  |
|               | <b>Eccentricity</b>         | 0.004          |
|               | <b>Perigee height</b>       | 5858 km        |
|               | <b>Apogee height</b>        | 5958 km        |
|               | <b>Node rate</b>            | +0.343 deg/day |
|               | <b>Perigee rate</b>         | -0.214 deg/day |
|               | <b>Semi-major axis rate</b> | -1.1 mm/day    |

Table 5.2.6b

**EMAT SUMMARY FOR LAGEOS**

| <u>EPOCH</u> | <u>NUMBER OF<br/>OBSERVATIONS</u> | <u>WEIGHTED<br/>RMS (m)</u> | <u>NUMBER OF<br/>STATIONS</u> | <u>ARGUMENT<br/>OF PERIGEE<br/>(AT EPOCH)</u> |
|--------------|-----------------------------------|-----------------------------|-------------------------------|---|
| 791230       | 1455                              | .2065                       | 13                            | 345.174                                       |
| 800129       | 2319                              | .2210                       | 14                            | 338.042                                       |
| 800228       | 2639                              | .2475                       | 14                            | 330.814                                       |
| 800329       | 2231                              | .2228                       | 14                            | 321.579                                       |
| 800428       | 1543                              | .2396                       | 10                            | 311.512                                       |
| 800528       | 1926                              | .2336                       | 9                             | 313.865                                       |
| 800702       | 1801                              | .2241                       | 13                            | 297.302                                       |
| 800801       | 3187                              | .2237                       | 13                            | 290.785                                       |
| 800831       | 3496                              | .1934                       | 16                            | 287.046                                       |
| 800930       | 3336                              | .2088                       | 18                            | 281.014                                       |
| 801030       | 2751                              | .2191                       | 14                            | 271.071                                       |
| 801129       | 1413                              | .2022                       | 11                            | 260.453                                       |
| 801229       | 794                               | .1736                       | 8                             | 255.325                                       |
| 810128       | 1287                              | .1784                       | 9                             | 253.457                                       |
| 810227       | 2739                              | .1787                       | 13                            | 240.940                                       |
| 810329       | 1943                              | .1913                       | 11                            | 232.084                                       |
| 810428       | 1884                              | .2057                       | 9                             | 226.531                                       |
| 810528       | 1944                              | .2512                       | 11                            | 221.412                                       |
| 810627       | 2187                              | .2555                       | 12                            | 217.269                                       |
| 810727       | 2168                              | .1948                       | 13                            | 201.207                                       |
| 810826       | 2821                              | .2065                       | 14                            | 199.978                                       |
| 810925       | 3143                              | .2308                       | 16                            | 194.745                                       |
| 811025       | 1972                              | .2095                       | 12                            | 188.166                                       |
| 811124       | 1573                              | .2126                       | 12                            | 181.017                                       |
| 811224       | 1314                              | .3018                       | 12                            | 168.490                                       |
| 820123       | 1878                              | .2427                       | 12                            | 172.349                                       |
| 820222       | 1883                              | .2125                       | 15                            | 162.371                                       |
| 820329       | 1926                              | .2007                       | 12                            | 153.177                                       |
| 820428       | 3084                              | .2055                       | 12                            | 148.207                                       |
| 820602       | 2488                              | .1811                       | 11                            | 142.263                                       |
| 820702       | 2980                              | .2022                       | 11                            | 134.020                                       |
| 820801       | 2027                              | .2197                       | 13                            | 126.356                                       |
| 820831       | 2720                              | .2154                       | 14                            | 127.720                                       |
| 820930       | 3596                              | .1788                       | 15                            | 118.145                                       |
| 821030       | 1938                              | .1604                       | 12                            | 110.051                                       |
| 821129       | 2041                              | .1788                       | 11                            | 104.642                                       |
| 821229       | 1699                              | .1990                       | 11                            | 101.347                                       |

**LAGEOS** *CONTD...*

| <u>EPOCH</u> | <u>NUMBER OF<br/>OBSERVATIONS</u> | <u>WEIGHTED<br/>RMS (m)</u> | <u>NUMBER OF<br/>STATIONS</u> | <u>ARGUMENT<br/>OF PERIGEE<br/>(AT EPOCH)</u> |
|--------------|-----------------------------------|-----------------------------|-------------------------------|---|
| 830128       | 1494                              | .2204                       | 12                            | 97.008  |
| 830227       | 2010                              | .2378                       | 14                            | 87.259  |
| 830329       | 2187                              | .2079                       | 14                            | 79.935  |
| 830428       | 2405                              | .2180                       | 13                            | 79.208  |
| 830627       | 1920                              | .1511                       | 8                             | 64.706  |
| 830727       | 2751                              | .1796                       | 8                             | 57.853  |
| 830831       | 2520                              | .1425                       | 11                            | 54.654  |
| 830930       | 3761                              | .1760                       | 17                            | 48.845  |
| 831030       | 31??                              | .2306                       | 17                            | 36.054  |
| 831229       | 2729                              | .2583                       | 17                            | 30.879  |
| 840128       | 2425                              | .2172                       | 16                            | 23.527  |
| 840227       | 2437                              | .2519                       | 22                            | 16.220  |
| 840329       | 3817                              | .2267                       | 20                            | 9.126   |
| 840428       | 4129                              | .2554                       | 22                            | 1.119   |
| 840528       | 4541                              | .2468                       | 20                            | 3.869   |
| 840627       | 4372                              | .2724                       | 19                            | 349.233                                       |
| 840801       | 4857                              | .2617                       | 22                            | 344.696                                       |
| 840831       | 4611                              | .2408                       | 21                            | 338.433                                       |

LAGEOS E-MAT SUMMARY  
WEIGHTED RMS  
(APRIORI)

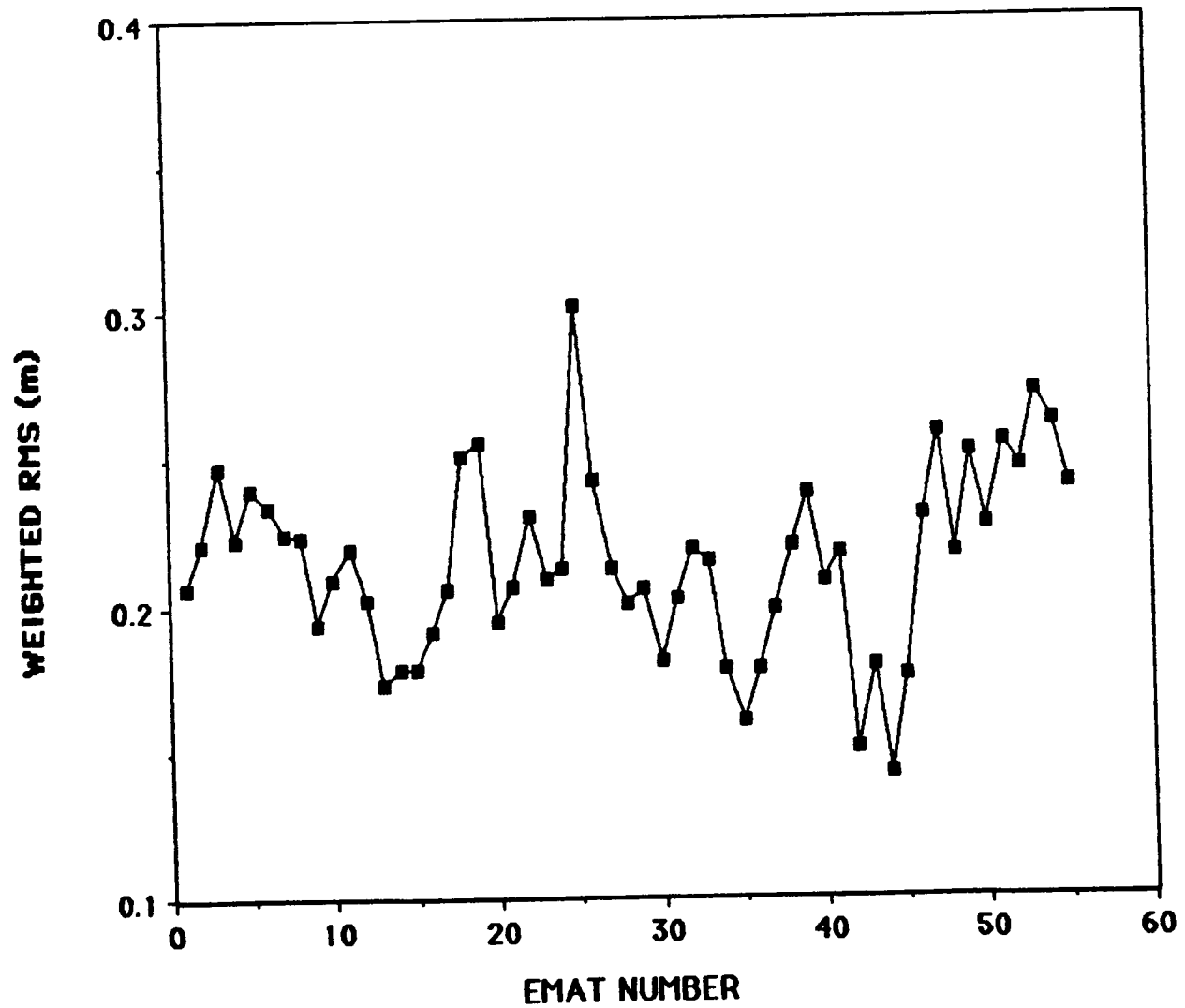


Figure 5.2.6b. LAGEOS E-MAT Summary.

### 5.2.7 Analysis of GEOS-2 Laser Tracking Data

The GEOS-2 satellite was launched on April 28, 1968. This satellite was one of the earliest geodetic missions initiated by NASA and served several purposes. First and foremost, GEOS-2 carried flashing lamps which allowed it to be photographed (as was GEOS-1) by a globally distributed network of optical observatories. The National Geodetic Satellite Program had an objective to unify the world's tracking datums to the 5 to 10 m level of uncertainty with respect to the geocenter. This was to be accomplished through an accurate reduction of these satellite photographic positions for use in solutions (both geometric and dynamic) of camera locations within a global reference system. It was an analysis of these early observations (NASA, 1977; Marsh et al, 1973) which satisfied the NGSP objectives. Of secondary interest was the calibration of NASA's Minitrack Network. Cameras were located at all of the worldwide Minitrack installations and the direction cosines obtained by these electronic fences were calibrated against those simultaneous right ascension and declination measurements acquired photographically. Fortunately, GEOS-2 also carried corner cubes and served as a target of opportunity for early laser ranging experiments.

The characteristics of the GEOS-2 orbit are given in Table 5.2.7a. GEOS-2 was intermittently tracked on a low priority basis by the lasers for much of the 1970's. Tracking apparently ceased in the middle of 1977. We thereby had a sparse data set to utilize for gravity modeling investigations from third generation laser systems which started to appear in the 1975 timeframe. Consequently, after an evaluation of data catalogues, we found only a limited number of possible arcs for GEOS-2. To have a reasonably large sample, we were forced to use the 1975 SAO data although these systems were not upgraded until late 1975 to early 1976. Some of the earlier 1975 SAO data was found to have range biases which were seen to be a function of range. The SAO

data taken during 1975 were heavily edited, but a subset of them were found to be satisfactory for inclusion in our GEM-T1 solution.

Five day arc lengths were used in the GEOS-2 data reduction and normal equation solutions. In these arcs, a drag parameter per day, a solar radiation coefficient per arc and the orbital state were all permitted to adjust. The normal equations for 28 of these arcs were generated and are summarized in Table 5.2.7b. Note that even when including SAO lasers in many of the 1975 arcs, only 3 or 4 stations were tracking over this time period.

Table 5.2.7a  
Orbital Characteristics of GEOS-2

|                    |               |
|--------------------|---------------|
| Apogee Height      | 1569 km       |
| Perigee Height     | 1077 km       |
| Eccentricity       | 0.03          |
| Inclination        | 105.8 degrees |
| Anomalistic Period | 112.1 minutes |

#### 5.2.8 Analysis of Optical and Low Inclination Satellite Observations

The optical observations acquired by a global network of predominantly SAO Baker Nunn observatories were the state-of-the-art in satellite tracking throughout the 1960's. A reasonable data set was acquired for over 60 satellites, rocket bodies, fragments, and space-borne balloons of this era. These observations provided the data base for the first comprehensive satellite-based gravity solution, that of the Smithsonian Astrophysical Observatory in 1966. Surprisingly, these observations are still making important contributions to the gravity solution even though they have an observational noise which is four orders of magnitude greater than that which is obtained by the best laser tracking of the 1980's.

Table 5.2.7b

**EMAT SUMMARY FOR GEOS-2**

| <u>EPOCH</u> | <u>NUMBER OF OBSERVATIONS</u> | <u>WEIGHTED RMS (m)</u> | <u>NUMBER OF STATIONS</u> | <u>ARGUMENT OF PERIGEE (AT EPOCH)</u> |
|--------------|-------------------------------|-------------------------|---------------------------|---------------------------------------|
| 750708       | 595                           | 1.3994                  | 4                         | 55.162                                |
| 750803       | 638                           | 1.6999                  | 3                         | 14.673                                |
| 750815       | 472                           | 1.0250                  | 3                         | 354.021                               |
| 750825       | 732                           | .8124                   | 5                         | 337.992                               |
| 750901       | 416                           | 1.0606                  | 4                         | 327.452                               |
| 750906       | 573                           | .6148                   | 5                         | 319.665                               |
| 750915       | 357                           | 1.5540                  | 5                         | 301.713                               |
| 750923       | 785                           | 1.8013                  | 5                         | 289.163                               |
| 751006       | 475                           | 1.4644                  | 4                         | 268.194                               |
| 751021       | 923                           | 1.1042                  | 4                         | 244.037                               |
| 751027       | 1351                          | 2.1442                  | 6                         | 233.716                               |
| 751102       | 1204                          | 2.0522                  | 6                         | 223.079                               |
| 760829       | 544                           | 1.4113                  | 5                         | 95.276                                |
| 760927       | 894                           | 2.0713                  | 5                         | 49.825                                |
| 761009       | 1435                          | 1.6547                  | 4                         | 33.373                                |
| 761019       | 1184                          | 1.7588                  | 7                         | 17.469                                |
| 761025       | 1389                          | 1.9487                  | 7                         | 7.638                                 |
| 761103       | 1418                          | 1.9838                  | 6                         | 349.358                               |
| 761108       | 1364                          | 1.0963                  | 7                         | 341.704                               |
| 761115       | 1475                          | 1.2160                  | 7                         | 331.432                               |
| 770120       | 701                           | 1.5675                  | 5                         | 222.343                               |
| 770320       | 784                           | 1.4755                  | 6                         | 125.612                               |
| 770403       | 1412                          | 1.2887                  | 6                         | 103.939                               |
| 770409       | 1277                          | 1.5900                  | 5                         | 95.076                                |
| 770425       | 1040                          | 1.4304                  | 3                         | 70.440                                |
| 770430       | 881                           | 1.1608                  | 3                         | 59.898                                |
| 770607       | 1196                          | 1.2060                  | 6                         | 1.945                                 |
| 770613       | 1098                          | 1.6737                  | 4                         | 351.478                               |

The reason for this importance is found in the diversity of objects which have been optically tracked. Any given satellite orbit samples the earth's gravity field in a way which causes it to sense certain perturbative frequencies. Each of these perturbations may be mathematically described as some linear combination of the spherical harmonics used to represent the gravity field. These sums (or "lumped-harmonics") can be very accurately determined although they are satellite specific. Past experience has shown that data analyzed on many orbits over a wide range of inclinations and mean motions yield a sufficiently large set of "lumped harmonics" to permit an accurate deconvolution of this signal into well determined individual spherical harmonic coefficients comprising a global gravity model. The optical satellites continue to play an important role in filling in the inclination gaps found within the data sets available from other tracking systems. In point of fact, the optical satellites are one of the best sources of gravity information for low inclination objects. Results will be discussed later showing the very important role these observations have in resolving accurate values for the zonal harmonic terms ( $m=0$  coefficients). Initially, six optically tracked satellites, only one of which was exclusively camera tracked, were selected for inclusion in the gravity solution. These satellites were : ANNA-1B, TELESTAR-1, BE-B, BE-C, GEOS-1 and GEOS-2. TELESTAR-1 is solely an optical satellite. While tracking data for them exists from other systems, only optical data for ANNA-1B and BE-B have been used at present to obtain GEM-T1. ANNA-1B's Doppler tracking and the very limited laser data taken on BE-B are yet to be used. Both of the GEOS satellites flew flashing lamps which permitted unlimited nighttime visibility for observing instruments. The flashing lamp data sets from the two GEOS were much more robust than those from the other four satellites. These other satellites were passively observed, requiring solar illumination of the objects against a dark sky. Therefore, data collection was restricted to the dusk period or before dawn.

A summary of the data, RMS of fit, perigee coverage and number of stations found in each of the optical arcs are shown in tables 5.2.8a through 5.2.8f. These data comprised the total optical data set found in the PGS-T2 field (Marsh et al, 1986) which is a precursor of GEM-T1.

The optical data have a precision of approximately two seconds of arc. The weighted observation residuals (whose RMS values are given in Tables 5.2.8a to 5.2.8f) were calculated as:

$$\text{declination: } \Delta\delta_w = \frac{\Delta\delta}{2}$$

$$\text{right ascension: } \Delta\alpha_w = \left[ \frac{\Delta\alpha}{2} \right] \cos\delta$$

where

$\Delta\delta$ ,  $\Delta\alpha$  are the observation residuals in declination and right ascension from the orbital fit, and

$\Delta\delta_w$ ,  $\Delta\alpha_w$  are their corresponding weighted residuals.

Figure 5.2.8a presents the uncertainties for the PGS-T2 field obtained from a scaled covariance of the solution. These values can be compared to figure 5.2.8b which is a similiar result from the GEM-L2 field. What is strikingly different between the two sets of uncertainties is the degradation of the accuracy for the zonal harmonics within PGS-T2. This degradation is confirmed when the values for the zonals are compared to those found in GEM-L2. The (PGS-T2) minus (GEM-L2) zonal harmonic differences are many times greater than the uncertainty in the GEM-L2 determination of these terms (see Figure 5.2.8c). Therefore, we concluded that an inadequate coverage of orbital inclinations was used in obtaining PGS-T2 with significant information being absent from low inclination objects.

ERRORS X 10<sup>9</sup>

| RMS | DEGREE | ORDER  |
|-----|--------|--|
| 1   | 1      | 10   |
| 1   | 2      | 10   |
| 1   | 3      | 10   |
| 1   | 4      | 10   |
| 1   | 5      | 10   |
| 1   | 6      | 10   |
| 1   | 7      | 10   |
| 1   | 8      | 10   |
| 1   | 9      | 10   |
| 1   | 10     | 10   |
| 1   | 11     | 10   |
| 1   | 12     | 10   |
| 1   | 13     | 10   |
| 1   | 14     | 10   |
| 1   | 15     | 10   |
| 1   | 16     | 10   |
| 1   | 17     | 10   |
| 1   | 18     | 10   |
| 1   | 19     | 10   |
| 1   | 20     | 10   |
| 1   | 21     | 10   |
| 1   | 22     | 10   |
| 1   | 23     | 10   |
| 1   | 24     | 10   |
| 1   | 25     | 10   |
| 1   | 26     | 10   |
| 1   | 27     | 10   |
| 1   | 28     | 10   |
| 1   | 29     | 10   |
| 1   | 30     | 10   |
| 1   | 31     | 10   |
| 1   | 32     | 10   |
| 1   | 33     | 10   |
| 1   | 34     | 10   |
| 1   | 35     | 10   |
| 1   | 36     | 10   |
| RMS |        | 10 10 11 11 10 9 9 8 8 7 6 5 4 4 5 6 6 7 7 7 7 7 6 6 5 4 4 5 5 6 6 6 6 6 6 5 |

Figure 5.2.8a. Estimated Errors for PGS-T2 Coefficients.

ERRORS X  $10^9$

| RMS | DEGREE | ORDER |    |    |    |    |    |    |    |    |    |    |    |    |    |    |    |    |    |    |    |    |    |    |    |    |    |    |    |    |  |
|-----|--------|-------|----|----|----|----|----|----|----|----|----|----|----|----|----|----|----|----|----|----|----|----|----|----|----|----|----|----|----|----|--|
|     |        | 0     | 1  | 2  | 3  | 4  | 5  | 6  | 7  | 8  | 9  | 10 | 11 | 12 | 13 | 14 | 15 | 16 | 17 | 18 | 19 | 20 | 21 | 22 | 23 | 24 | 25 | 26 | 27 | 28 |  |
| 1.3 | 3      | 4.5   | 6  | 7  | 6  | 5  | 2  |    |    |    |    |    |    |    |    |    |    |    |    |    |    |    |    |    |    |    |    |    |    |    |  |
| 1.3 | 4      | 6     | 7  | 6  | 5  | 3  | 2  |    |    |    |    |    |    |    |    |    |    |    |    |    |    |    |    |    |    |    |    |    |    |    |  |
| 1.3 | 5      | 7     | 8  | 9  | 8  | 9  | 10 | 9  | 11 | 6  | 9  | 10 | 15 |    |    |    |    |    |    |    |    |    |    |    |    |    |    |    |    |    |  |
| 1.3 | 6      | 8     | 9  | 10 | 11 | 12 | 13 | 14 | 15 | 16 | 17 | 18 | 19 | 17 | 14 | 10 | 10 | 11 | 16 | 5  | 3  | 2  | 2  |    |    |    |    |    |    |    |  |
| 1.3 | 7      | 9     | 10 | 11 | 12 | 13 | 14 | 15 | 16 | 17 | 18 | 19 | 19 | 19 | 18 | 14 | 15 | 11 | 15 | 14 | 11 | 6  | 3  | 2  | 1  | 5  | 12 | 21 |    |    |  |
| 1.3 | 8      | 10    | 11 | 12 | 13 | 14 | 15 | 16 | 17 | 18 | 19 | 19 | 19 | 19 | 18 | 18 | 15 | 14 | 11 | 15 | 14 | 11 | 6  | 3  | 2  | 1  | 5  | 12 | 17 |    |  |
| 1.3 | 9      | 11    | 12 | 13 | 14 | 15 | 16 | 17 | 18 | 19 | 19 | 19 | 19 | 19 | 18 | 18 | 15 | 14 | 11 | 15 | 14 | 11 | 6  | 3  | 2  | 1  | 5  | 12 | 17 |    |  |
| 1.3 | 10     | 12    | 13 | 14 | 15 | 16 | 17 | 18 | 19 | 17 | 19 | 19 | 19 | 19 | 18 | 18 | 15 | 14 | 11 | 15 | 14 | 11 | 6  | 3  | 2  | 1  | 5  | 12 | 17 |    |  |
| 1.3 | 11     | 13    | 14 | 15 | 16 | 17 | 18 | 19 | 17 | 19 | 17 | 19 | 19 | 19 | 19 | 18 | 18 | 15 | 14 | 11 | 15 | 14 | 11 | 6  | 3  | 2  | 1  | 5  | 12 | 17 |  |
| 1.3 | 12     | 14    | 15 | 16 | 17 | 18 | 19 | 17 | 19 | 17 | 19 | 19 | 19 | 19 | 18 | 18 | 15 | 14 | 11 | 15 | 14 | 11 | 6  | 3  | 2  | 1  | 5  | 12 | 17 |    |  |
| 1.3 | 13     | 15    | 16 | 17 | 18 | 19 | 17 | 19 | 17 | 19 | 19 | 19 | 19 | 19 | 18 | 18 | 15 | 14 | 11 | 15 | 14 | 11 | 6  | 3  | 2  | 1  | 5  | 12 | 17 |    |  |
| 1.3 | 14     | 16    | 17 | 18 | 19 | 17 | 19 | 17 | 19 | 19 | 19 | 19 | 19 | 19 | 18 | 18 | 15 | 14 | 11 | 15 | 14 | 11 | 6  | 3  | 2  | 1  | 5  | 12 | 17 |    |  |
| 1.3 | 15     | 17    | 18 | 19 | 17 | 19 | 17 | 19 | 19 | 19 | 19 | 19 | 19 | 19 | 18 | 18 | 15 | 14 | 11 | 15 | 14 | 11 | 6  | 3  | 2  | 1  | 5  | 12 | 17 |    |  |
| 1.3 | 16     | 18    | 19 | 17 | 19 | 17 | 19 | 19 | 19 | 19 | 19 | 19 | 19 | 19 | 18 | 18 | 15 | 14 | 11 | 15 | 14 | 11 | 6  | 3  | 2  | 1  | 5  | 12 | 17 |    |  |
| 1.3 | 17     | 19    | 18 | 19 | 17 | 19 | 17 | 19 | 19 | 19 | 19 | 19 | 19 | 19 | 18 | 18 | 15 | 14 | 11 | 15 | 14 | 11 | 6  | 3  | 2  | 1  | 5  | 12 | 17 |    |  |
| 1.3 | 18     | 19    | 19 | 17 | 19 | 17 | 19 | 19 | 19 | 19 | 19 | 19 | 19 | 19 | 18 | 18 | 15 | 14 | 11 | 15 | 14 | 11 | 6  | 3  | 2  | 1  | 5  | 12 | 17 |    |  |
| 1.3 | 19     | 19    | 19 | 19 | 17 | 19 | 17 | 19 | 19 | 19 | 19 | 19 | 19 | 19 | 18 | 18 | 15 | 14 | 11 | 15 | 14 | 11 | 6  | 3  | 2  | 1  | 5  | 12 | 17 |    |  |
| 1.3 | 20     | 21    | 22 | 23 | 24 | 25 | 26 | 27 | 28 | 29 | 29 | 29 | 29 | 29 | 29 | 29 | 29 | 29 | 29 | 29 | 29 | 29 | 29 | 29 | 29 | 29 | 29 | 29 | 29 | 29 |  |
| 1.3 | 21     | 22    | 23 | 24 | 25 | 26 | 27 | 28 | 29 | 29 | 29 | 29 | 29 | 29 | 29 | 29 | 29 | 29 | 29 | 29 | 29 | 29 | 29 | 29 | 29 | 29 | 29 | 29 | 29 | 29 |  |
| 1.3 | 22     | 23    | 24 | 25 | 26 | 27 | 28 | 29 | 29 | 29 | 29 | 29 | 29 | 29 | 29 | 29 | 29 | 29 | 29 | 29 | 29 | 29 | 29 | 29 | 29 | 29 | 29 | 29 | 29 | 29 |  |
| 1.3 | 23     | 24    | 25 | 26 | 27 | 28 | 29 | 29 | 29 | 29 | 29 | 29 | 29 | 29 | 29 | 29 | 29 | 29 | 29 | 29 | 29 | 29 | 29 | 29 | 29 | 29 | 29 | 29 | 29 | 29 |  |
| 1.3 | 24     | 25    | 26 | 27 | 28 | 29 | 29 | 29 | 29 | 29 | 29 | 29 | 29 | 29 | 29 | 29 | 29 | 29 | 29 | 29 | 29 | 29 | 29 | 29 | 29 | 29 | 29 | 29 | 29 | 29 |  |
| 1.3 | 25     | 26    | 27 | 28 | 29 | 29 | 29 | 29 | 29 | 29 | 29 | 29 | 29 | 29 | 29 | 29 | 29 | 29 | 29 | 29 | 29 | 29 | 29 | 29 | 29 | 29 | 29 | 29 | 29 | 29 |  |
| 1.3 | 26     | 27    | 28 | 29 | 29 | 29 | 29 | 29 | 29 | 29 | 29 | 29 | 29 | 29 | 29 | 29 | 29 | 29 | 29 | 29 | 29 | 29 | 29 | 29 | 29 | 29 | 29 | 29 | 29 | 29 |  |
| 1.3 | 27     | 28    | 29 | 29 | 29 | 29 | 29 | 29 | 29 | 29 | 29 | 29 | 29 | 29 | 29 | 29 | 29 | 29 | 29 | 29 | 29 | 29 | 29 | 29 | 29 | 29 | 29 | 29 | 29 | 29 |  |
| 1.3 | 28     | 29    | 29 | 29 | 29 | 29 | 29 | 29 | 29 | 29 | 29 | 29 | 29 | 29 | 29 | 29 | 29 | 29 | 29 | 29 | 29 | 29 | 29 | 29 | 29 | 29 | 29 | 29 | 29 | 29 |  |
| 1.3 | 29     | 29    | 29 | 29 | 29 | 29 | 29 | 29 | 29 | 29 | 29 | 29 | 29 | 29 | 29 | 29 | 29 | 29 | 29 | 29 | 29 | 29 | 29 | 29 | 29 | 29 | 29 | 29 | 29 | 29 |  |
| 1.3 | 30     | 29    | 29 | 29 | 29 | 29 | 29 | 29 | 29 | 29 | 29 | 29 | 29 | 29 | 29 | 29 | 29 | 29 | 29 | 29 | 29 | 29 | 29 | 29 | 29 | 29 | 29 | 29 | 29 | 29 |  |

Figure 5.2.8b. Estimated Errors for GEM-L2 Coefficients.

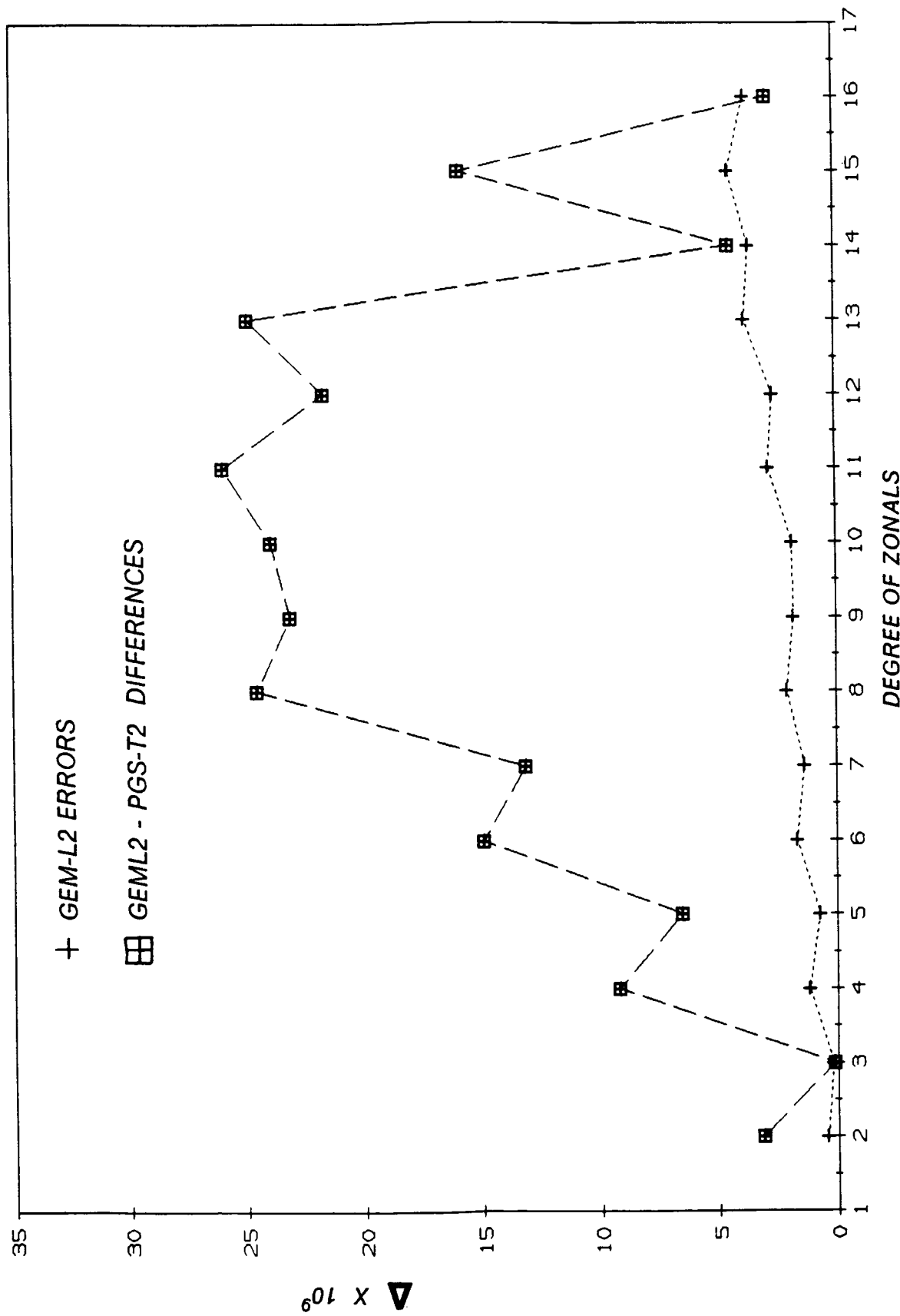


Figure 5.2.8c. Zonal Coefficients.

*Table 5.2.8a*  
**ANNA-1B OPTICAL 7-DAYS ARCS**

| NO.            | EPOCH  | NO. OF OBS. | WEIGHTED RMS ARCSEC/2 | NO. OF STATIONS | ARGUMENT OF PERIGEE (AT EPOCH) |
|----------------|--------|-------------|-----------------------|-----------------|--------------------------------|
| 1              | 621101 | 157         | 1.294                 | 9               | 207.7                          |
| 2              | 621115 | 126         | 1.413                 | 10              | 248.1                          |
| 3              | 621122 | 154         | 1.212                 | 6               | 274.3                          |
| 4              | 621129 | 158         | 1.221                 | 9               | 294.2                          |
| 5              | 621213 | 258         | 1.201                 | 10              | 343.6                          |
| 6              | 621220 | 262         | 1.155                 | 11              | 358.1                          |
| 7              | 631107 | 64          | 1.149                 | 4               | 228.4                          |
| 8              | 631114 | 98          | 1.109                 | 10              | 245.9                          |
| 9              | 631121 | 78          | 1.479                 | 9               | 269.3                          |
| 10             | 631128 | 36          | 1.028                 | 6               | 295.7                          |
| 11             | 631205 | 118         | 1.293                 | 7               | 316.6                          |
| 12             | 631212 | 183         | 1.360                 | 8               | 336.0                          |
| 13             | 631219 | 232         | 1.577                 | 7               | 3.2                            |
| 14             | 631226 | 56          | 1.173                 | 6               | 17.5                           |
| 15             | 640102 | 36          | 0.940                 | 4               | 39.8                           |
| 16             | 640110 | 56          | 0.875                 | 9               | 65.9                           |
| 17             | 640117 | 82          | 1.226                 | 8               | 75.2                           |
| 18             | 651128 | 162         | 1.017                 | 11              | 294.9                          |
| 19             | 660116 | 130         | 0.905                 | 6               | 85.4                           |
| 20             | 660123 | 102         | 1.076                 | 6               | 101.1                          |
| 21             | 660130 | 120         | 1.122                 | 7               | 119.9                          |
| 22             | 660215 | 184         | 0.994                 | 7               | 163.3                          |
| 23             | 660222 | 250         | 1.063                 | 6               | 188.8                          |
| 24             | 660301 | 96          | 1.169                 | 4               | 206.9                          |
| 25             | 660308 | 147         | 0.899                 | 6               | 227.9                          |
| 26             | 660315 | 318         | 1.132                 | 6               | 255.4                          |
| 27             | 660329 | 132         | 1.311                 | 7               | 297.7                          |
| 28             | 660410 | 264         | 1.079                 | 7               | 325.4                          |
| <b>AVERAGE</b> |        | <b>148</b>  | <b>1.160</b>          | <b>7</b>        |                                |
| <b>TOTAL</b>   |        | <b>4151</b> |                       |                 |                                |

Table 5.2.8b

## BE-B 7-DAYS ARCS

| NO.     | EPOCH  | NO. OF OBS. | WEIGHTED RMS ARCSEC/2 | NO. OF STATIONS | ARGUMENT OF PERIGEE (AT EPOCH) |
|---------|--------|-------------|-----------------------|-----------------|--------------------------------|
| 1       | 641026 | 38          | 1.427                 | 8               | 104.7                          |
| 2       | 641102 | 60          | 1.309                 | 11              | 85.3                           |
| 3       | 641109 | 38          | 1.021                 | 3               | 74.8                           |
| 4       | 650112 | 52          | 1.173                 | 6               | 266.7                          |
| 5       | 650203 | 32          | 1.139                 | 4               | 213.1                          |
| 6       | 650323 | 54          | 1.005                 | 9               | 92.0                           |
| 7       | 650406 | 30          | 1.329                 | 6               | 59.4                           |
| 8       | 650415 | 46          | 1.555                 | 8               | 41.2                           |
| 9       | 650424 | 30          | 1.300                 | 6               | 14.7                           |
| 10      | 650613 | 50          | 1.357                 | 5               | 242.7                          |
| 11      | 650627 | 40          | 1.166                 | 8               | 196.1                          |
| 12      | 650716 | 30          | 1.451                 | 8               | 149.2                          |
| 13      | 670226 | 211         | 1.181                 | 9               | 100.2                          |
| 14      | 670305 | 56          | 1.258                 | 4               | 88.8                           |
| 15      | 670312 | 128         | 0.909                 | 6               | 65.7                           |
| 16      | 670319 | 228         | 1.109                 | 6               | 52.6                           |
| 17      | 670507 | 60          | 1.148                 | 4               | 284.8                          |
| 18      | 670514 | 154         | 1.461                 | 5               | 269.2                          |
| 19      | 670521 | 232         | 1.064                 | 12              | 245.7                          |
| 20      | 670528 | 170         | 0.983                 | 8               | 233.4                          |
| AVERAGE |        | 87          | 1.217                 | 7               |                                |
| TOTAL   |        | 1739        |                       |                 |                                |

Table 5.2.8c

## BE-C OPTICAL 7-DAYS ARCS

| NO.     | EPOCH  | NO. OF OBS. | WEIGHTED RMS ARCSEC/2 | NO. OF STATIONS | ARGUMENT OF PERIGEE (AT EPOCH) |
|---------|--------|-------------|-----------------------|-----------------|--------------------------------|
| 1       | 650619 | 64          | 1.381                 | 4               | 327.6                          |
| 2       | 650626 | 56          | 0.998                 | 6               | 1.5                            |
| 3       | 650703 | 52          | 1.326                 | 7               | 38.7                           |
| 4       | 650710 | 56          | 1.113                 | 8               | 73.9                           |
| 5       | 650717 | 94          | 1.104                 | 9               | 109.0                          |
| 6       | 650724 | 155         | 1.225                 | 9               | 145.3                          |
| 7       | 650731 | 80          | 1.080                 | 11              | 180.3                          |
| 8       | 650807 | 48          | 1.079                 | 10              | 217.7                          |
| 9       | 650814 | 62          | 0.871                 | 8               | 253.7                          |
| 10      | 650821 | 74          | 0.983                 | 9               | 135.8                          |
| 11      | 650828 | 50          | 1.190                 | 5               | 237.9                          |
| 12      | 650904 | 38          | 1.124                 | 7               | 4.8                            |
| 13      | 650911 | 66          | 1.002                 | 9               | 38.9                           |
| 14      | 650918 | 64          | 0.848                 | 8               | 77.4                           |
| 15      | 650925 | 58          | 1.084                 | 11              | 109.2                          |
| 16      | 651002 | 38          | 1.188                 | 5               | 147.5                          |
| 17      | 651009 | 42          | 1.220                 | 9               | 182.1                          |
| 18      | 651016 | 66          | 1.164                 | 9               | 218.9                          |
| 19      | 651023 | 54          | 1.200                 | 9               | 255.7                          |
| 20      | 651030 | 56          | 0.965                 | 8               | 293.3                          |
| 21      | 651106 | 68          | 1.346                 | 4               | 329.0                          |
| 22      | 651113 | 58          | 0.940                 | 8               | 6.0                            |
| 23      | 651120 | 38          | 1.155                 | 6               | 41.4                           |
| 24      | 651127 | 34          | 1.060                 | 9               | 77.5                           |
| 25      | 651210 | 48          | 1.114                 | 7               | 142.5                          |
| 26      | 651217 | 32          | 0.865                 | 8               | 179.8                          |
| 27      | 651225 | 54          | 1.337                 | 9               | 219.2                          |
| 28      | 660101 | 73          | 1.079                 | 9               | 258.7                          |
| 29      | 660108 | 92          | 0.970                 | 7               | 293.7                          |
| 30      | 660115 | 67          | 0.983                 | 6               | 331.4                          |
| 31      | 660301 | 216         | 1.107                 | 9               | 201.5                          |
| 32      | 660308 | 301         | 0.985                 | 10              | 238.2                          |
| 33      | 660315 | 374         | 0.957                 | 9               | 275.6                          |
| 34      | 660322 | 544         | 0.897                 | 6               | 311.4                          |
| 35      | 660329 | 269         | 1.096                 | 7               | 349.5                          |
| 36      | 660405 | 235         | 0.992                 | 7               | 24.2                           |
| 37      | 660412 | 274         | 0.854                 | 9               | 60.7                           |
| 38      | 660419 | 299         | 0.994                 | 8               | 95.7                           |
| 39      | 660426 | 346         | 1.051                 | 8               | 130.9                          |
| 40      | 660503 | 210         | 1.145                 | 9               | 167.8                          |
| 41      | 660510 | 270         | 0.986                 | 9               | 201.9                          |
| 42      | 660517 | 257         | 0.858                 | 9               | 241.4                          |
| 43      | 660524 | 189         | 0.886                 | 7               | 275.9                          |
| 44      | 670312 | 185         | 1.089                 | 9               | 346.0                          |
| 45      | 670319 | 327         | 1.090                 | 9               | 23.5                           |
| 46      | 670326 | 207         | 1.062                 | 7               | 57.8                           |
| 47      | 670402 | 472         | 1.116                 | 8               | 94.0                           |
| 48      | 670410 | 235         | 1.173                 | 10              | 135.7                          |
| 49      | 670417 | 250         | 1.187                 | 10              | 169.4                          |
| 50      | 670424 | 204         | 1.074                 | 8               | 206.4                          |
| AVERAGE |        | 150         | 1.071                 | 8               |                                |
| TOTAL   |        | 7501        |                       |                 |                                |

Table 5.2.8d

## GEOS-1 OPTICAL 7-DAYS ARCS

| NO.     | EPOCH  | NO. OF OBS. | WEIGHTED RMS ARCSEC/2 | NO. OF STATIONS | ARGUMENT OF PERIGEE (AT EPOCH) |
|---------|--------|-------------|-----------------------|-----------------|--------------------------------|
| 1       | 651108 | 244         | 0.920                 | 9               | 150.5                          |
| 2       | 651115 | 331         | 1.051                 | 10              | 154.7                          |
| 3       | 651122 | 1692        | 0.727                 | 17              | 159.9                          |
| 4       | 651129 | 883         | 0.785                 | 22              | 164.4                          |
| 5       | 651213 | 1177        | 0.829                 | 22              | 173.5                          |
| 6       | 651220 | 1426        | 1.001                 | 25              | 177.3                          |
| 7       | 651227 | 1291        | 1.126                 | 30              | 182.2                          |
| 8       | 660103 | 769         | 1.231                 | 24              | 187.5                          |
| 9       | 660110 | 1524        | 1.036                 | 29              | 191.4                          |
| 10      | 660117 | 1722        | 0.980                 | 26              | 196.0                          |
| 11      | 660124 | 1296        | 0.862                 | 27              | 200.9                          |
| 12      | 660131 | 838         | 0.961                 | 22              | 205.2                          |
| 13      | 660207 | 364         | 0.901                 | 18              | 209.4                          |
| 14      | 660214 | 773         | 0.954                 | 21              | 214.8                          |
| 15      | 660221 | 1249        | 0.836                 | 25              | 218.6                          |
| 16      | 660228 | 967         | 0.889                 | 26              | 223.7                          |
| 17      | 660307 | 1506        | 1.038                 | 36              | 228.8                          |
| 18      | 660314 | 2673        | 0.823                 | 30              | 232.9                          |
| 19      | 660404 | 1781        | 0.865                 | 30              | 246.6                          |
| 20      | 660411 | 1879        | 0.805                 | 30              | 250.8                          |
| 21      | 660425 | 2034        | 0.778                 | 31              | 260.6                          |
| 22      | 660502 | 2079        | 0.771                 | 28              | 265.0                          |
| 23      | 660509 | 1471        | 0.770                 | 24              | 270.3                          |
| 24      | 660516 | 743         | 0.724                 | 17              | 274.7                          |
| 25      | 660523 | 263         | 0.649                 | 11              | 280.0                          |
| 26      | 660709 | 3485        | 0.780                 | 31              | 310.5                          |
| 27      | 660716 | 3780        | 0.857                 | 30              | 315.6                          |
| 28      | 660723 | 3433        | 0.781                 | 28              | 319.9                          |
| 29      | 660730 | 3039        | 0.792                 | 25              | 324.5                          |
| 30      | 660806 | 1791        | 0.688                 | 28              | 329.7                          |
| 31      | 660813 | 1506        | 0.667                 | 20              | 333.9                          |
| 32      | 660820 | 1091        | 0.704                 | 16              | 338.2                          |
| 33      | 660827 | 594         | 0.585                 | 11              | 343.5                          |
| 34      | 660903 | 702         | 0.615                 | 15              | 348.0                          |
| 35      | 660922 | 2218        | 0.919                 | 9               | 359.7                          |
| 36      | 661006 | 2378        | 0.892                 | 22              | 9.8                            |
| 37      | 661013 | 1721        | 0.803                 | 24              | 13.7                           |
| 38      | 661020 | 1446        | 0.809                 | 24              | 18.6                           |
| 39      | 661115 | 1141        | 0.707                 | 14              | 35.1                           |
| 40      | 670226 | 214         | 0.987                 | 10              | 101.9                          |
| 41      | 670305 | 575         | 0.931                 | 8               | 106.2                          |
| 42      | 670312 | 375         | 0.928                 | 11              | 110.1                          |
| 43      | 670319 | 286         | 0.971                 | 7               | 115.1                          |
| AVERAGE |        | 1413        | 0.854                 | 22              |                                |
| TOTAL   |        | 60750       |                       |                 |                                |

Table 5.2.8e

## GEOS-2 OPTICAL 7-DAYS ARCS

| NO.     | EPOCH  | NO. OF OBS. | WEIGHTED RMS ARCSEC/2 | NO. OF STATIONS | ARGUMENT OF PERIGEE (AT EPOCH) |
|---------|--------|-------------|-----------------------|-----------------|--------------------------------|
| 1       | 680315 | 1378        | 0.857                 | 26              | 67.1                           |
| 2       | 680322 | 1938        | 0.865                 | 27              | 53.5                           |
| 3       | 680329 | 1664        | 0.803                 | 32              | 44.6                           |
| 4       | 680405 | 1613        | 0.753                 | 33              | 34.6                           |
| 5       | 680412 | 1607        | 0.986                 | 32              | 21.7                           |
| 6       | 680419 | 2132        | 1.040                 | 36              | 11.0                           |
| 7       | 680426 | 1772        | 0.737                 | 35              | 357.4                          |
| 8       | 680503 | 1696        | 0.826                 | 30              | 347.7                          |
| 9       | 680510 | 1427        | 0.798                 | 27              | 338.7                          |
| 10      | 680517 | 1619        | 0.720                 | 24              | 324.3                          |
| 11      | 680524 | 1390        | 0.724                 | 26              | 313.2                          |
| 12      | 680531 | 1196        | 0.702                 | 18              | 301.3                          |
| 13      | 680607 | 2098        | 0.754                 | 30              | 289.1                          |
| 14      | 680614 | 2775        | 0.723                 | 31              | 279.8                          |
| 15      | 680621 | 2978        | 0.709                 | 34              | 266.6                          |
| 16      | 680628 | 417         | 0.702                 | 17              | 255.0                          |
| 17      | 680719 | 1712        | 0.727                 | 30              | 220.0                          |
| 18      | 680814 | 1172        | 0.668                 | 15              | 177.2                          |
| 19      | 680828 | 1220        | 0.922                 | 30              | 154.9                          |
| 20      | 680904 | 1793        | 0.920                 | 29              | 143.3                          |
| 21      | 680911 | 1242        | 0.808                 | 29              | 134.2                          |
| 22      | 680918 | 2863        | 0.766                 | 35              | 121.8                          |
| 23      | 680925 | 1650        | 0.829                 | 28              | 109.5                          |
| 24      | 681002 | 2007        | 0.932                 | 29              | 100.2                          |
| 25      | 681009 | 1954        | 0.851                 | 30              | 87.4                           |
| 26      | 681016 | 1254        | 0.850                 | 29              | 77.4                           |
| 27      | 681023 | 1616        | 0.852                 | 29              | 67.6                           |
| 28      | 681116 | 869         | 0.832                 | 14              | 28.5                           |
| 29      | 681217 | 463         | 0.970                 | 13              | 336.4                          |
| 30      | 690128 | 729         | 1.030                 | 9               | 269.1                          |
| 31      | 690204 | 908         | 1.099                 | 13              | 256.0                          |
| 32      | 690211 | 912         | 0.995                 | 12              | 244.6                          |
| 33      | 690218 | 579         | 1.085                 | 9               | 235.3                          |
| 34      | 690225 | 429         | 0.969                 | 11              | 221.3                          |
| 35      | 690304 | 760         | 0.931                 | 13              | 210.1                          |
| 36      | 690311 | 908         | 0.927                 | 13              | 198.3                          |
| 37      | 690318 | 847         | 0.851                 | 12              | 186.9                          |
| 38      | 690325 | 675         | 0.874                 | 12              | 178.2                          |
| 39      | 690331 | 861         | 0.770                 | 19              | 167.9                          |
| 40      | 690407 | 1068        | 0.758                 | 22              | 155.4                          |
| 41      | 690414 | 839         | 0.762                 | 11              | 143.3                          |
| 42      | 690421 | 1259        | 0.816                 | 23              | 133.5                          |
| 43      | 690428 | 778         | 0.774                 | 18              | 121.7                          |
| 44      | 690505 | 1160        | 0.761                 | 20              | 110.7                          |
| 45      | 690512 | 491         | 0.669                 | 9               | 100.5                          |
| 46      | 690519 | 685         | 0.778                 | 9               | 87.4                           |
| AVERAGE |        | 1335        | 0.846                 | 22              |                                |
| TOTAL   |        | 61403       |                       |                 |                                |

Table 5.2.8f

## TELSTAR-1 OPTICAL 7-DAYS ARCS

| NO.     | EPOCH  | NO. OF OBS. | WEIGHTED RMS ARCSEC/2 | NO. OF STATIONS | ARGUMENT OF PERIGEE (AT EPOCH) |
|---------|--------|-------------|-----------------------|-----------------|--------------------------------|
| 1       | 620713 | 39          | 1.096                 | 5               | 170.1                          |
| 2       | 620725 | 80          | 1.211                 | 10              | 193.9                          |
| 3       | 620801 | 74          | 1.112                 | 7               | 207.8                          |
| 4       | 620808 | 128         | 0.989                 | 9               | 221.8                          |
| 5       | 620816 | 138         | 1.482                 | 7               | 237.7                          |
| 6       | 620823 | 106         | 1.113                 | 7               | 251.7                          |
| 7       | 620830 | 116         | 0.936                 | 5               | 265.5                          |
| 8       | 620913 | 153         | 1.127                 | 6               | 293.2                          |
| 9       | 620920 | 105         | 1.102                 | 7               | 307.2                          |
| 10      | 620927 | 166         | 1.043                 | 10              | 321.2                          |
| 11      | 621004 | 209         | 1.122                 | 9               | 335.2                          |
| 12      | 621018 | 154         | 1.225                 | 11              | 3.0                            |
| 13      | 621025 | 210         | 1.171                 | 11              | 16.9                           |
| 14      | 621101 | 124         | 1.037                 | 10              | 30.8                           |
| 15      | 621108 | 94          | 1.256                 | 7               | 44.5                           |
| 16      | 621115 | 138         | 1.187                 | 9               | 58.5                           |
| 17      | 621122 | 114         | 1.004                 | 7               | 72.4                           |
| 18      | 621206 | 68          | 1.405                 | 9               | 100.2                          |
| 19      | 621213 | 58          | 0.898                 | 7               | 114.1                          |
| 20      | 630207 | 64          | 1.047                 | 6               | 225.3                          |
| 21      | 630214 | 147         | 0.840                 | 10              | 239.3                          |
| 22      | 630221 | 139         | 0.965                 | 10              | 253.2                          |
| 23      | 630228 | 122         | 0.853                 | 11              | 267.0                          |
| 24      | 630307 | 129         | 0.806                 | 7               | 280.9                          |
| 25      | 630314 | 193         | 0.783                 | 8               | 294.7                          |
| 26      | 630328 | 144         | 1.095                 | 8               | 322.7                          |
| 27      | 630414 | 118         | 1.033                 | 10              | 356.5                          |
| 28      | 630421 | 110         | 0.767                 | 10              | 11.0                           |
| 29      | 630526 | 180         | 0.884                 | 5               | 79.9                           |
| 30      | 630616 | 342         | 0.764                 | 12              | 121.0                          |
| AVERAGE |        | 132         | 1.045                 | 8               |                                |
| TOTAL   |        | 3962        |                       |                 |                                |

Table 5.2.09

LOW INCLINATION ( $1 < 40^\circ$ ) SATELLITE DATA

FOR GEM-T1

| <u>SATELLITE</u> | <u># OF OBS</u> | <u>CAMERA DATA</u> | <u>LASER DATA</u> | <u># OF ARCS</u> | <u>PERIGEE HEIGHT (KM)</u> | <u>E</u> | <u>I (DEG)</u> |
|------------------|-----------------|--------------------|-------------------|------------------|----------------------------|----------|----------------|
| COURIER-1B       | 2476            | ----               | ----              | 10               | 989                        | .0161    | 28.3           |
| VANGUARD-2RB     | 686             | ----               | ----              | 10               | 562                        | .1832    | 32.9           |
| VANGUARD-2       | 1299            | ----               | ----              | 10               | 562                        | .1641    | 32.9           |
| DI-C             | 2712            | ----               | ----              | 10               | 587                        | .0532    | 39.9           |
| DI-C             | 159             | 7455               | 4                 | ----             |                            |          |                |
| DI-D             | 6111            | ----               | ----              | 9                | 589                        | .0848    | 39.5           |
| DI-D             | 146             | 11487              | 6                 | ----             |                            |          |                |
| PEOLE            | 38              | 4113               | 6                 | 515              | .0164                      | 15.0     |                |

*Table 5.2.8h*

**PEOLE LASER+OPTICAL 7-DAYS ARCS**

| NO.     | EPOCH  | NO. OF OBS. | WEIGHTED RMS ARCSEC/2 | NO. OF STATIONS | ARGUMENT OF PERIGEE (AT EPOCH) |
|---------|--------|-------------|-----------------------|-----------------|--------------------------------|
| 1       | 710225 | 736         | 2.840                 | 4               | 104.7                          |
| 2       | 710304 | 663         | 1.730                 | 4               | 191.6                          |
| 3       | 710507 | 815         | 1.400                 | 5               | 324.3                          |
| 4       | 710527 | 1594        | 2.810                 | 4               | 220.4                          |
| 5       | 710610 | 104         | 4.270                 | 1               | 55.5                           |
| 6       | 710623 | 239         | 0.680                 | 2               | 222.3                          |
| AVERAGE |        | 692         | 2.29                  | 3               |                                |
| TOTAL   |        | 4151        |                       |                 |                                |

Table 5.2.8*i*

## DI-D OPTICAL 7-DAYS ARCS

| NO.     | EPOCH  | NO. OF OBS. | WEIGHTED RMS ARCSEC/2 | NO. OF STATIONS | ARGUMENT OF PERIGEE (AT EPOCH) |
|---------|--------|-------------|-----------------------|-----------------|--------------------------------|
| 1       | 670219 | 164         | 1.138                 | 7               | 156.2                          |
| 2       | 670226 | 250         | 1.113                 | 10              | 194.5                          |
| 3       | 670305 | 432         | 1.066                 | 7               | 232.1                          |
| 4       | 670312 | 275         | 0.957                 | 8               | 270.1                          |
| 5       | 670319 | 174         | 1.030                 | 7               | 308.1                          |
| 6       | 670430 | 1003        | 0.967                 | 11              | 173.7                          |
| 7       | 670507 | 1367        | 1.020                 | 11              | 211.4                          |
| 8       | 670514 | 1592        | 0.934                 | 12              | 249.5                          |
| 9       | 670521 | 854         | 1.360                 | 14              | 287.1                          |
| AVERAGE |        | 679         | 1.065                 | 10              |                                |
| TOTAL   |        | 6111        |                       |                 |                                |

## DI-D LASER + OPTICAL 7-DAYS ARCS

| NO.     | EPOCH  | NO. OF OBS. | WEIGHTED RMS ARCSEC/2 | NO. OF STATIONS | ARGUMENT OF PERIGEE (AT EPOCH) |
|---------|--------|-------------|-----------------------|-----------------|--------------------------------|
| 1       | 710423 | 3463        | 1.040                 | 6               | 108.1                          |
| 2       | 710507 | 1824        | 1.930                 | 9               | 183.4                          |
| 3       | 710514 | 2027        | 0.950                 | 10              | 221.5                          |
| 4       | 710703 | 1604        | 1.480                 | 2               | 132.5                          |
| 5       | 710710 | 2368        | 1.870                 | 2               | 169.7                          |
| 6       | 710719 | 347         | 1.890                 | 4               | 218.7                          |
| AVERAGE |        | 1939        | 1.530                 | 5               |                                |
| TOTAL   |        | 11633       |                       |                 |                                |

*Table 5.2.8j*

VANGUARD-2 7-DAYS ARCS

| NO.     | EPOCH  | NO. OF OBS. | WEIGHTED RMS ARCSEC/2 | NO. OF STATIONS | ARGUMENT OF PERIGEE (AT EPOCH) |
|---------|--------|-------------|-----------------------|-----------------|--------------------------------|
| 1       | 660202 | 42          | 1.121                 | 6               | 252.4                          |
| 2       | 660209 | 70          | 0.868                 | 6               | 290.0                          |
| 3       | 660216 | 136         | 1.192                 | 8               | 326.9                          |
| 4       | 660223 | 170         | 1.039                 | 8               | 3.8                            |
| 5       | 660302 | 136         | 1.243                 | 9               | 41.3                           |
| 6       | 660309 | 163         | 1.003                 | 9               | 77.9                           |
| 7       | 660316 | 249         | 0.885                 | 6               | 114.9                          |
| 8       | 660323 | 231         | 1.221                 | 8               | 152.0                          |
| 9       | 660330 | 64          | 1.194                 | 8               | 188.8                          |
| 10      | 660407 | 38          | 1.165                 | 8               | 231.3                          |
| AVERAGE |        | 130         | 1.093                 | 8               |                                |
| TOTAL   |        | 1299        |                       |                 |                                |

*Table 5.2.8k*

VANGUARD-2RB 7-DAYS ARCS

| NO.     | EPOCH  | NO. OF OBS. | WEIGHTED RMS ARCSEC/2 | NO. OF STATIONS | ARGUMENT OF PERIGEE (AT EPOCH) |
|---------|--------|-------------|-----------------------|-----------------|--------------------------------|
| 1       | 600402 | 42          | 1.273                 | 4               | 357.5                          |
| 2       | 600409 | 30          | 0.846                 | 2               | 31.7                           |
| 3       | 600417 | 40          | 1.643                 | 5               | 71.3                           |
| 4       | 600427 | 30          | 1.007                 | 7               | 120.7                          |
| 5       | 600505 | 74          | 1.298                 | 5               | 160.3                          |
| 6       | 600512 | 92          | 1.427                 | 6               | 194.6                          |
| 7       | 600519 | 124         | 1.020                 | 7               | 229.4                          |
| 8       | 600526 | 94          | 1.173                 | 8               | 226.3                          |
| 9       | 600608 | 55          | 0.920                 | 6               | 328.6                          |
| 10      | 600717 | 105         | 1.259                 | 8               | 0.0                            |
| AVERAGE |        | 69          | 1.187                 | 6               |                                |
| TOTAL   |        | 686         |                       |                 |                                |

*Table 5.2.81*  
**DI-C OPTICAL 7-DAYS ARCS**

| NO.     | EPOCH  | NO. OF OBS. | WEIGHTED RMS ARCSEC/2 | NO. OF STATIONS | ARGUMENT OF PERIGEE (AT EPOCH) |
|---------|--------|-------------|-----------------------|-----------------|--------------------------------|
| 1       | 670220 | 164         | 1.061                 | 4               | 217.9                          |
| 2       | 670227 | 158         | 1.195                 | 7               | 259.0                          |
| 3       | 670306 | 300         | 1.071                 | 10              | 301.5                          |
| 4       | 670313 | 201         | 1.049                 | 7               | 343.6                          |
| 5       | 670320 | 127         | 0.949                 | 4               | 24.8                           |
| 6       | 670416 | 244         | 0.921                 | 8               | 183.6                          |
| 7       | 670423 | 400         | 1.055                 | 8               | 226.7                          |
| 8       | 670430 | 720         | 1.001                 | 9               | 267.8                          |
| 9       | 670507 | 196         | 0.902                 | 9               | 308.8                          |
| 10      | 670514 | 202         | 1.003                 | 10              | 351.9                          |
| AVERAGE |        | 271         | 1.021                 | 8               |                                |
| TOTAL   |        | 2712        |                       |                 |                                |

**DI-C LASER + OPTICAL 7-DAYS ARCS**

| NO.     | EPOCH  | NO. OF OBS. | WEIGHTED RMS ARCSEC/2 | NO. OF STATIONS | ARGUMENT OF PERIGEE (AT EPOCH) |
|---------|--------|-------------|-----------------------|-----------------|--------------------------------|
| 1       | 710401 | 751         | 0.780                 | 4               | 165.6                          |
| 2       | 710608 | 698         | 1.320                 | 10              | 213.0                          |
| 3       | 710615 | 3783        | 2.580                 | 8               | 255.9                          |
| 4       | 710622 | 2382        | 2.230                 | 8               | 297.8                          |
| AVERAGE |        | 1903        | 1.720                 | 7               |                                |
| TOTAL   |        | 7614        |                       |                 |                                |

*Table 5.2.8m*  
**COURIER-1B 7-DAYS ARCS**

| NO.     | EPOCH  | NO. OF OBS. | WEIGHTED RMS ARCSEC/2 | NO. OF STATIONS | ARGUMENT OF PERIGEE (AT EPOCH) |
|---------|--------|-------------|-----------------------|-----------------|--------------------------------|
| 1       | 661224 | 334         | 1.130                 | 9               | 95.5                           |
| 2       | 670107 | 307         | 1.183                 | 8               | 211.8                          |
| 3       | 670114 | 368         | 1.072                 | 8               | 273.6                          |
| 4       | 670121 | 301         | 1.087                 | 10              | 332.1                          |
| 5       | 670128 | 237         | 1.059                 | 9               | 27.8                           |
| 6       | 670602 | 97          | 0.971                 | 5               | 343.6                          |
| 7       | 670609 | 97          | 1.150                 | 5               | 40.5                           |
| 8       | 670616 | 151         | 1.074                 | 7               | 94.1                           |
| 9       | 670623 | 258         | 1.010                 | 7               | 150.2                          |
| 10      | 670708 | 326         | 1.244                 | 7               | 276.6                          |
| AVERAGE |        | 248         | 1.098                 | 8               |                                |
| TOTAL   |        | 2476        |                       |                 |                                |

To remedy this situation, data sets of six additional satellites were selected for inclusion in the model. These satellites were COURIER-1B, VANGUARD 2 rocket body, VANGUARD 2, DI-C, DI-D, and PEOLE. The later three of these satellites were tracked by the first generation laser systems in the early 1970's. Tables 5.2.8g through 5.2.9m summarize the data contribution of these low inclination satellites. As it will be discussed later, the inclusion of these data had a dramatic positive impact on the resulting GEM-T1 gravity solution.

#### 5.2.9 Analysis of BE-C Laser Observations

Beacon Explorer-C was launched from Wallops Flight Facility, Wallops Island, Virginia in 1965. The satellite was magnetically stabilized, had reasonably large solar panels and fortunately also carried a ring of laser retro-reflectors. Because of its low inclination, BE-C became a favorite target for early North American crustal motion studies. BE-C at times, was visible to laser sites located in the United States on three to four successive revolutions. Therefore, a large BE-C data set could be acquired in a short time interval enabling short arcs to be utilized in station position determination solutions. To support these studies, the global laser network tracked BE-C often, yielding a reasonably robust data set. However, given this satellite's magnetic stabilization and the location of its corner cubes at its lowest end, BE-C unfortunately was not visible to lasers located beyond the equatorial region of the Southern Hemisphere.

The orbital characteristics for BE-C are presented in Table 5.2.9a. This satellite was studied using 5 day arcs. A drag parameter per day, a solar radiation pressure coefficient and the orbital state vector were adjusted within each arc. In general, the laser data taken on BE-C were quite good, being data from third generation systems which were globally deployed to support the LAGEOS mission. Since this object

was and remains a satellite of interest, data from 1979 onwards were sufficient to have this satellite well represented in our gravity modeling solutions. The normal equations generated from BE-C tracking data are shown in Table 5.2.9b. In all, 39 arcs of BE-C laser data were used in the GEM-T1 solution with other additional arcs being available for field testing.

Extensive tests of the drag parameterization on BE-C were performed and are found summarized in Section 7.2.2.

Table 5.2.9a. Orbital Characteristics of BE-C

|                 |                       |
|-----------------|-----------------------|
| Semi-Major Axis | 7507 km               |
| Apogee Height   | 1320 km               |
| Perigee Height  | 940 km                |
| Eccentricity    | 0.0257                |
| Inclination     | 41.19 degrees         |
| Mean Motion     | 13.35 revolutions/day |
| Beat Period     | 5.5 days              |

Table 5.2.9b

**EMAT SUMMARY FOR BEC**

| <u>EPOCH</u> | <u>NUMBER OF OBSERVATIONS</u> | <u>WEIGHTED RMS (m)</u> | <u>NUMBER OF STATIONS</u> | <u>ARGUMENT OF PERIGEE (AT EPOCH)</u> |
|--------------|-------------------------------|-------------------------|---------------------------|---------------------------------------|
| 790320       | 1153                          | 1.2126                  | 8                         | 18.204                                |
| 790402       | 1535                          | 1.7486                  | 8                         | 81.950                                |
| 790411       | 2472                          | 1.4003                  | 8                         | 128.830                               |
| 790417       | 3596                          | 1.2484                  | 9                         | 161.207                               |
| 790426       | 3265                          | 1.1535                  | 8                         | 207.915                               |
| 790501       | 1904                          | 1.3096                  | 6                         | 232.713                               |
| 790512       | 3136                          | 1.2258                  | 6                         | 291.352                               |
| 790523       | 1173                          | 1.4735                  | 4                         | 349.258                               |
| 790813       | 614                           | 1.3281                  | 5                         | 51.989                                |
| 791022       | 1254                          | 1.1893                  | 8                         | 54.306                                |
| 791112       | 1765                          | 1.1033                  | 7                         | 161.403                               |
| 791202       | 986                           | 1.4961                  | 9                         | 265.595                               |
| 791217       | 1002                          | 1.3430                  | 7                         | 344.681                               |
| 800115       | 973                           | .6662                   | 7                         | 133.182                               |
| 800122       | 1022                          | .7459                   | 10                        | 168.528                               |
| 800129       | 2202                          | 1.1481                  | 7                         | 206.047                               |
| 800205       | 1710                          | .9070                   | 7                         | 239.858                               |
| 800408       | 1460                          | 1.2113                  | 8                         | 206.400                               |
| 800505       | 1551                          | 1.1468                  | 8                         | 349.147                               |
| 800528       | 644                           | 2.1713                  | 4                         | 106.631                               |
| 800602       | 1197                          | 1.2983                  | 6                         | 131.798                               |
| 800728       | 1215                          | 1.5013                  | 8                         | 62.832                                |
| 800802       | 1175                          | 2.0744                  | 10                        | 89.221                                |
| 800915       | 1683                          | 1.4970                  | 7                         | 99.180                                |
| 800923       | 1564                          | 1.5275                  | 10                        | 359.756                               |
| 801006       | 1412                          | 1.6996                  | 10                        | 63.421                                |
| 801013       | 1419                          | 1.7794                  | 9                         | 101.679                               |
| 801124       | 632                           | 1.0837                  | 5                         | 319.695                               |
| 801201       | 1010                          | 1.4706                  | 6                         | 355.343                               |
| 801215       | 1076                          | 1.2099                  | 7                         | 67.447                                |
| 810303       | 1911                          | 1.5659                  | 9                         | 111.785                               |
| 810317       | 1760                          | 1.1450                  | 7                         | 181.514                               |
| 810728       | 1357                          | 1.3487                  | 7                         | 149.842                               |
| 810817       | 1266                          | 1.3525                  | 5                         | 254.153                               |
| 810924       | 2039                          | 1.4846                  | 7                         | 92.630                                |
| 811006       | 3997                          | 1.4363                  | 8                         | 150.636                               |
| 811012       | 2717                          | 1.7980                  | 8                         | 182.613                               |
| 811019       | 2258                          | 1.0116                  | 7                         | 221.105                               |
| 820201       | 1135                          | 1.2684                  | 6                         | 46.323                                |

SECTION 6.0  
DEFINITION OF A PRIORI GEOCENTRIC  
TRACKING STATION COORDINATES

In order to compute an improved preliminary gravity field model for the TOPEX mission, the coordinates of all contributing tracking stations must be referred to one unified coordinate system. The reference frame for this work will be briefly described in the course of this section as well as the procedures and transformations required to bring existing station coordinates into a unique system. The existing station coordinates are in a variety of coordinate systems from various solutions made in past years. The coordinate system chosen for the TOPEX work is closely related to GSFC's laser coordinate system, SL-6.

#### 6.1 COORDINATE SYSTEM DEFINITION

The unified coordinate system developed for the a priori station positions needed for the TOPEX gravity model project is based upon the laser coordinate system developed by GSFC from LAGEOS tracking, known as the SL-6 system [for a description of a typical laser coordinate solution, see Smith et al. (1985)]. The longitude definition was adopted from that used in the MERIT campaign [Melbourne, et al. (1983)]. Thus all of the station coordinates that were transformed into the SL-6 system were ultimately rotated by +0.144525 arcsec in longitude to accommodate the McDonald Observatory reference meridian definition. A zero mean pole position was adopted to better model the mean figure and rotation axes, and all station coordinates were rotated further to this zero mean pole origin. This issue is considered in more detail elsewhere in this document. The resulting coordinate frame will be referred to as the TOPEX Coordinate System (TCS). The station coordinates are put in Cartesian form for use in the data-reduction and

PRECEDING PAGE BLANK NOT PLEATED

the E-matrix generation runs, but, for the purpose of cataloging, the coordinates have also been transformed to geodetic form. The geodetic coordinates refer to an ellipsoid with a semi-major axis of 6378137 m and a flattening of 1/298.257.

## 6.2 INITIAL STATUS OF STATION COORDINATES

The station positions to be transformed into the TCS exist in a variety of coordinate systems. These include local datum coordinates and dynamically derived coordinates from solutions such as GEM-9 [Lerch et al. (1979)], and GSFC-73 [Marsh et al. (1973)]. The means for determining the transformations is provided by a set of laser sites for which both the SL-6 coordinates and the datum or dynamically determined coordinates are known. Table 6.1 lists the laser sites and their unmodified SL-6 coordinates that were used in this work. The approximate epoch for these stations is 1982.

## 6.3 THE TRANSFORMATION MODELS

Two transformation models were used to complete this task. The first model utilizes the coordinates for widely distributed laser stations known in both coordinate systems, the SL-6 system and the other coordinate system of interest (e.g., local datum or dynamically determined system) for which we wish to establish a rigorous transformation. The second model employs a simple linear transformation for stations which are in close proximity to one of the laser stations listed in Table 1. By "close proximity", we mean that station separations do not exceed 100 km. Beyond this distance, the errors committed by ignoring scale and rotation parameters can grow rapidly to a size of a few meters. This aspect will be described shortly.

Table 6.1 Laser sites known from the SL6 dynamic solution

| Station |      | latitude |    |         | longitude |    |         | ellipsoidal height |
|---------|------|----------|----|---------|-----------|----|---------|--------------------|
| NAME    | no.  | d        | m  | s       | d         | m  | s       |                    |
| QUINY   | 7051 | 39       | 58 | 24.5710 | 239       | 3  | 37.5530 | 1052.8800          |
| EASTER  | 7061 | -27      | 8  | 52.1650 | 250       | 36 | 58.9940 | 110.5550           |
| SANDIE  | 7062 | 32       | 36 | 2.6580  | 243       | 9  | 32.7810 | 981.4700           |
| STALAS  | 7063 | 39       | 1  | 13.3620 | 283       | 10 | 19.7950 | 12.1670            |
| GSFCLS  | 7064 | 39       | 1  | 15.1040 | 283       | 10 | 18.6050 | 10.1530            |
| BDILAS  | 7067 | 32       | 21 | 13.7620 | 295       | 20 | 37.927  | -30.1170           |
| GRKLAS  | 7068 | 21       | 27 | 37.7710 | 288       | 52 | 5.0330  | -25.7760           |
| RAMLAS  | 7069 | 28       | 13 | 40.6520 | 279       | 23 | 39.2980 | -30.6690           |
| BEARLK  | 7082 | 41       | 56 | 0.8960  | 248       | 34 | 45.5370 | 1955.9060          |
| OVRLAS  | 7084 | 37       | 13 | 55.6560 | 241       | 42 | 15.1130 | 1171.0190          |
| GOLDLS  | 7085 | 35       | 25 | 27.9630 | 243       | 6  | 48.9170 | 958.3230           |
| FTDAVS  | 7086 | 30       | 40 | 37.3040 | 255       | 59 | 2.4810  | 1954.3160          |
| YARLAS  | 7090 | -29      | 02 | 47.4100 | 115       | 20 | 48.1070 | 234.2260           |
| HAYLAS  | 7091 | 42       | 37 | 21.6890 | 288       | 30 | 44.3390 | 84.9250            |
| KWJLAS  | 7092 | 9        | 23 | 37.6890 | 167       | 28 | 32.4860 | 25.7920            |
| SAMLAS  | 7096 | -14      | 20 | 7.5170  | 189       | 16 | 30.3570 | 41.8820            |
| GSF100  | 7100 | 39       | 1  | 15.4510 | 283       | 10 | 47.6350 | 3.1100             |
| GSF101  | 7101 | 39       | 1  | 16.2050 | 283       | 10 | 42.8350 | 1.3140             |
| GSF102  | 7102 | 39       | 1  | 14.3800 | 283       | 10 | 18.7920 | 10.8910            |
| GSF103  | 7103 | 39       | 1  | 14.6070 | 283       | 10 | 18.7950 | 10.8330            |
| GSF104  | 7104 | 39       | 1  | 17.0820 | 283       | 10 | 36.8380 | 2.8980             |
| GSF105  | 7105 | 39       | 1  | 14.1640 | 283       | 10 | 20.1580 | 12.0840            |
| QUILAS  | 7109 | 39       | 58 | 30.0020 | 239       | 03 | 18.9490 | 1099.2260          |
| MONLAS  | 7110 | 32       | 53 | 30.0020 | 243       | 34 | 38.2580 | 1831.8602          |
| PLALAS  | 7112 | 40       | 10 | 58.0010 | 255       | 16 | 26.3360 | 1494.4826          |
| OVRLAS  | 7114 | 37       | 13 | 57.2120 | 241       | 42 | 22.2150 | 1170.9230          |
| GOLLAS  | 7115 | 35       | 14 | 53.9000 | 243       | 12 | 28.9490 | 1031.5171          |
| MUILAS  | 7120 | 20       | 42 | 27.3920 | 203       | 44 | 38.1020 | 3060.6295          |
| HUANIL  | 7121 | -16      | 44 | 0.6830  | 208       | 57 | 31.7780 | 40.1250            |
| MAULAS  | 7210 | 20       | 42 | 25.9960 | 203       | 44 | 38.6000 | 3061.2004          |
| FINLAS  | 7805 | 60       | 13 | 2.2880  | 24        | 23 | 40.2110 | 71.2110            |
| KOOLAS  | 7833 | 52       | 10 | 42.2450 | 5         | 48 | 35.1190 | 86.4620            |
| WETLAS  | 7834 | 49       | 08 | 41.7770 | 12        | 52 | 40.9670 | 654.0907           |
| GRALAS  | 7835 | 43       | 45 | 16.8840 | 6         | 55 | 15.8640 | 1315.9275          |
| SHOLAS  | 7838 | 33       | 34 | 39.7210 | 135       | 56 | 13.1890 | 94.3156            |
| RGOLAS  | 7840 | 50       | 52 | 2.5610  | 0         | 20 | 9.8620  | 68.2651            |
| FORLAS  | 7885 | 30       | 40 | 37.3060 | 255       | 59 | 2.4780  | 1954.2694          |
| QUILAS  | 7886 | 39       | 58 | 30.0180 | 239       | 3  | 18.0180 | 1102.4716          |
| VANLAS  | 7887 | 34       | 33 | 58.3570 | 239       | 29 | 57.9780 | 597.2122           |
| HOPLAS  | 7888 | 31       | 41 | 6.3150  | 249       | 7  | 18.5000 | 2327.6088          |
| YUMLAS  | 7894 | 32       | 56 | 20.9340 | 245       | 47 | 48.6070 | 234.6146           |
| ARELAS  | 7907 | -16      | 27 | 56.7010 | 288       | 30 | 24.6030 | 2485.1860          |
| HOPLAS  | 7921 | 31       | 41 | 3.2220  | 249       | 7  | 18.8370 | 2345.8548          |
| NATLAS  | 7929 | -5       | 55 | 40.1350 | 324       | 50 | 7.2190  | 32.4910            |
| MATLAS  | 7939 | 40       | 38 | 55.7930 | 16        | 42 | 16.6860 | 528.8756           |
| ORRLAS  | 7943 | -35      | 37 | 29.7560 | 148       | 57 | 17.1240 | 941.8380           |
| ARESAO  | 9907 | -16      | 27 | 56.7010 | 288       | 30 | 24.6030 | 2485.1860          |
| HOPSAO  | 9921 | 31       | 41 | 3.2220  | 249       | 7  | 18.8370 | 2345.8548          |
| NATSAO  | 9929 | -5       | 55 | 40.1350 | 324       | 50 | 7.2190  | 32.4910            |

$$a_e = 6378144.11, f = 1/298.255$$

### 6.3.1 Seven Parameter Transformation

The seven parameter transformation, also sometimes known as the Bursa/Wolf transformation [Leick & van Gelder (1975)], is a rigorous transformation relating two geodetic coordinate systems when only small rotations are involved. The transformation has the form

$$\begin{bmatrix} \text{---} \\ X \\ Y \\ Z \\ \text{---} \end{bmatrix}_i^{\text{SL6}} = \begin{bmatrix} \text{---} \\ \Delta X \\ \Delta Y \\ \Delta Z \\ \text{---} \end{bmatrix} + (1 + \Delta L) \begin{bmatrix} 1 & \omega & -\psi \\ -\omega & 1 & \epsilon \\ \psi & -\epsilon & 1 \end{bmatrix} \begin{bmatrix} \text{---} \\ X \\ Y \\ Z \\ \text{---} \end{bmatrix}_i^{\text{dat}} \quad (6.1)$$

where

$\begin{bmatrix} \text{---} \\ X \\ Y \\ Z \\ \text{---} \end{bmatrix}_i^{\text{dat}}$  is the  $i^{\text{th}}$  station's Cartesian coordinates referred to the local datum (or other coordinate systems, depending on the case),

$\omega$ ,  $\psi$ , and  $\epsilon$  are small Euler rotations about the  $Z, Y, X$  axes respectively,

$\Delta L$  is a scale factor, and

$\Delta X, \Delta Y, \Delta Z$  are translations between the local datum (or other coordinate systems) and the SL-6 system.

The seven parameters are determined in a least squares solution by comparing the laser station coordinates in both systems for which the transformation is desired. Further details and a derivation are found in Rapp (1983).

### 6.3.2 The Linear Translation

The approximate linear translation of the  $i^{\text{th}}$  station into the SL-6 system is found from

$$\begin{aligned}\phi_i^{\text{SL6}} &= \phi_i^{\text{dat}} + (\phi_j^{\text{SL6}} - \phi_j^{\text{dat}}) \\ \lambda_i^{\text{SL6}} &= \lambda_i^{\text{dat}} + (\lambda_j^{\text{SL6}} - \lambda_j^{\text{dat}}) \\ H_i^{\text{SL6}} &= H_i^{\text{dat}} + (H_j^{\text{SL6}} - H_j^{\text{dat}})\end{aligned}\quad (6.2)$$

where  $j$  denotes the near-by  $j^{\text{th}}$  laser station having its coordinates known in both coordinate systems (e.g., in SL6 and in the local datum (dat)). Some errors can be expected to arise in this model primarily due to neglecting scale and rotation parameters. This is especially true when stations  $i$  and  $j$  are relatively far apart. A computation was made to ascertain the size of these errors as a function of distance using the NAD to SL-6 transformation. It was found that errors in longitude grow most rapidly and the magnitude of the error can be as large as 3 meters at a distance of 100 km. The linear method was primarily used to determine older optical and doppler sites in our new system when they were situated near laser tracking stations.

## 6.4 NUMERICAL RESULTS

This section will highlight the numerical aspects of the transformations used to establish the table of TOPEX a priori station positions. Table 6.2 lists the stations used to determine the transformation parameters relating: NAD 27 to SL-6; GEM-9 to SL-6; and GSFC-73 to GEM-9. The TOPEX a priori station coordinates given here are currently regarded as being the best, but they may be changed when better information becomes available.

**Table 6.2. Stations used in least-squares determination  
of the seven parameter transformations.  
(i.e. solutions from program STC)**

**NAD 27 → SL-6**

|               |               |
|---------------|---------------|
| 7062 : SANDIE | 7109 : QUILAS |
| 7069 : RAMLAS | 7110 : MONLAS |
| 7082 : BEARLK | 7112 : PLALAS |
| 7086 : FTDAVS | 7114 : OVRLAS |
| 7091 : HAYLAS | 7115 : GOLLAS |
| 7105 : GSF105 | 7921 : HOPLAS |

**GEM 9 → SL-6**

|                |               |
|----------------|---------------|
| 1038 : 10RORL  | 7907 : ARELAS |
| 7063 : STALAS  | 7921 : HOPLAS |
| 7067 : BDILAI1 | 7929 : NATLAS |
| 7068 : GRKLAS  | 9012 : 1MAUI0 |

**GSFC-73 → SL-6**

|                |               |
|----------------|---------------|
| 9001 : 1ORGAN  | 9007 : 1QUIPA |
| 9002 : 1OLFAN  | 9009 : 1CURAC |
| 9004 : 1SPRAIN | 9011 : 1VILDO |
| 9005 : 1TOKYO  | 9012 : 1MAUI0 |
| 9006 : 1NATAL  | 9021 : HOPKIN |

#### 6.4.1 NAD 27 to SL-6 Transformation

The NAD 27 to SL-6 transformation parameters were determined from 12 stations distributed over the United States as shown in Figure 6.1. These parameters were then used to transform NAD 27 optical and Doppler tracking station coordinates into SL-6. The NAD 27 coordinates were used since the terrestrial coordinates are considered more accurate than coordinates determined from camera and Doppler solutions made in previous years. Small rotations for longitude definition and zero mean pole definition were applied to these stations to complete the transformation into TCS.

#### 6.4.2 GEM-9 to SL-6 Transformation

The GEM-9 to SL-6 transformation parameters were determined from 8 stations distributed around the globe. These parameters were then used to transform tracking stations located around the globe with the exception of stations in Europe. The European stations are discussed in the next paragraph. The GEM-9 to SL-6 transformation was used since the local datum coordinates for most of these stations are not very well known or are of dubious origin. Again, the small rotations for zero mean pole and longitude definition were applied to bring these coordinates into the TCS.

#### 6.4.3 GSFC-73 to GEM-9 Transformation

The GSFC-73 solution was used because a European Datum to SL-6 transformation could not be determined due to insufficiencies in the terrestrial data and because the European GSFC-73 dynamically derived positions are considered more reliable than the GEM-9 dynamically derived positions. It may appear rather odd that the transformation relates GSFC-73 to GEM-9 rather than to SL-6. This was done since a direct GSFC-73 to SL-6 transformation could not be established due to

insufficient data. To get around this problem, a two-step procedure was used. The transformation parameters relating GSFC-73 to GEM-9 were determined from 10 stations distributed globally. The European stations were then transformed into GEM-9 via these parameters, followed by the GEM-9 to SL-6 transformation mentioned in the previous paragraph. Small rotations again were applied, accounting for the zero mean pole and our new longitude definition, to bring these stations into the TCS.

#### 6.4.4 Other Transformations

After some analysis, it became apparent that a few of the stations positions were causing larger than anticipated residuals. The network of S-band tracking stations was one such case. The S-band tracking stations (used to track SEASAT) were transformed into SL-6 by determining the GEM-9 to SL-6 parameters found exclusively from S-band position data known in both systems. Six S-band stations were used to determine these parameters. Thirteen other S-band stations were then transformed via these parameters into the SL-6 system. Likewise, similar rotations as mentioned above were employed to these sites to bring them into the TCS.

### 6.5 DISCUSSION

#### 6.5.1 Transformation Parameters and Accuracies

The determination of the seven parameters in the transformations were performed in a least-squares based program known as STC (STation Comparison). The transformation parameters relating the coordinate systems described in the previous sections as computed by STC are given in Table 6.3.

**Table 6.3. Transformation Parameters**

| parameter      | NAD → SL-6 | GEM9 → SL-6 | GSFC73 → GEM9 |
|----------------|------------|-------------|---------------|
| $\Delta X$ (m) | -31.4805   | -0.9451     | 2.5460        |
| $\Delta Y$ (m) | 172.5176   | -1.7602     | 2.6820        |
| $\Delta Z$ (m) | 182.7296   | 0.8776      | -0.2535       |
| $\Delta L$     | 1.6015E-6  | -3.5305E-7  | 9.0237E-8     |
| $\omega$ (")   | -0.77841   | 0.32384     | -0.00924      |
| $\psi$ (")     | -0.01160   | -0.08520    | -0.02139      |
| $\epsilon$ (") | -0.31494   | 0.04528     | -0.04434      |

**Table 6.4. Quality of the transformations  
(RMS about the mean, see text)**

| parameter     | NAD → SL-6 | GEM9 → SL-6 | GSFC73 → GEM9 |
|---------------|------------|-------------|---------------|
| X (m)         | 3.158      | 1.404       | 4.663         |
| Y (m)         | 2.422      | 1.133       | 3.014         |
| Z (m)         | 2.826      | 0.469       | 3.128         |
| $\phi$ (")    | 0.1161     | 0.0464      | 0.1615        |
| $\lambda$ (") | 0.1166     | 0.0233      | 0.1080        |
| H (m)         | 1.784      | 1.537       | 3.158         |

The translation parameters in the NAD 27 to SL-6 transformation are large (i.e., tens and hundreds of meters) since NAD 27 is not a center of mass system. The magnitude of the translations is consistent with other investigations reported in Bomford (1980), p. 635 with the exception of the  $\Delta Y$  translation component. The value we determined for  $\Delta Y$  is 15 meters larger than that found by other investigators. The seven parameter determination by STC is highly dependent upon the distribution of stations. As can be noted in Figure 6.1, our determination will be stronger in the western United States. This is the case since the LAGEOS tracking network is concentrated in the more tectonically active west coast. Although the distribution is far from optimal, the resulting transformation has suited our needs and is of adequate precision (to be discussed below).

The other two transformations, GEM-9 to SL-6 and GSFC-73 to GEM-9, have smaller parameters since all three coordinate systems are supposedly center of mass systems. However, significant differences are present which are most likely due in part to differences in the longitude origin of the systems. The  $\Delta Z$  translational component is at least an order of magnitude smaller than the equatorial plane components,  $\Delta X$  and  $\Delta Y$ . In the equatorial plane, the SL-6 center of mass falls nearly half-way between the center of mass of the GEM-9 and GSFC-73 coordinate systems.

#### 6.5.2 Precision of the Transformations

The precision of the transformations can be gauged from the RMS scatter of the residuals after the transformation has been made. The RMS scatter is given by

$$\bar{\chi}_\sigma = \left[ \sum_i (\bar{\chi}_{if} - T(\Delta X, \Delta Y, \Delta Z, \omega, \psi, \epsilon, \Delta L) \bar{\chi}_{ia})^2 \right]^{1/2} \quad (6.3)$$

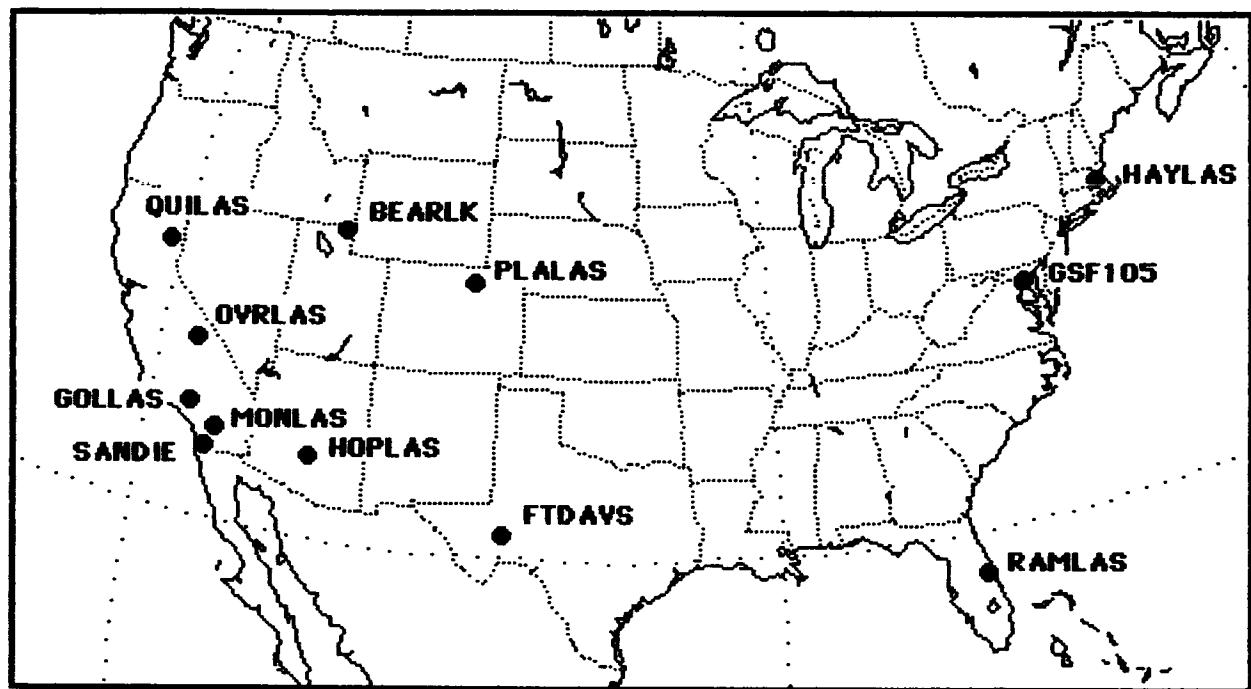


Figure 6.1. Laser Tracking Station Locations used in Determining the Seven Parameter Transformation between NAD 27 and SL-6.

where

$\bar{x}_{if}$  are the known coordinates for tracking station i in the unified coordinate system (e.g., SL-6),

$\bar{x}_{ia}$  are the known coordinates in the a priori coordinate system (e.g., NAD 27, GEM-9, etc.), and

T denotes the seven parameter transformation.

This actually provides a measure of how well the stations that were used to determine the parameters of T agree when T is applied to their a priori coordinates. The RMS quantities for the three transformations described here are given in Table 6.4. It can be seen in Table 6.4 that the GEM-9 to SL-6 transformation is the strongest of the three with residuals averaging in the 1 to 1.5 meter range. The NAD 27 to SL-6 transformation is weaker with residuals in the 2.5 to 3 meter range. Finally, the GSFC-73 to GEM-9 transformation is the weakest with 3.5 to 4 meter residuals. This latter result is not too surprising since the GSFC-73 coordinates are based upon early camera and laser data with a solution accuracy goal of 5 meters. As mentioned earlier, though the uncertainties of the GSFC-73 coordinates may seem large by today's standards, in some cases (especially the European and other remote or abandoned sites), the GSFC-73 coordinates are the best available. GEM-9 used much of the same data, and therefore must share in the resulting station uncertainties.

### 6.5.3 Error Sources

Errors in the coordinates of the stations in the TCS can be as large as a few meters. This is especially true for stations having their a priori coordinates determined from an early dynamic solution.

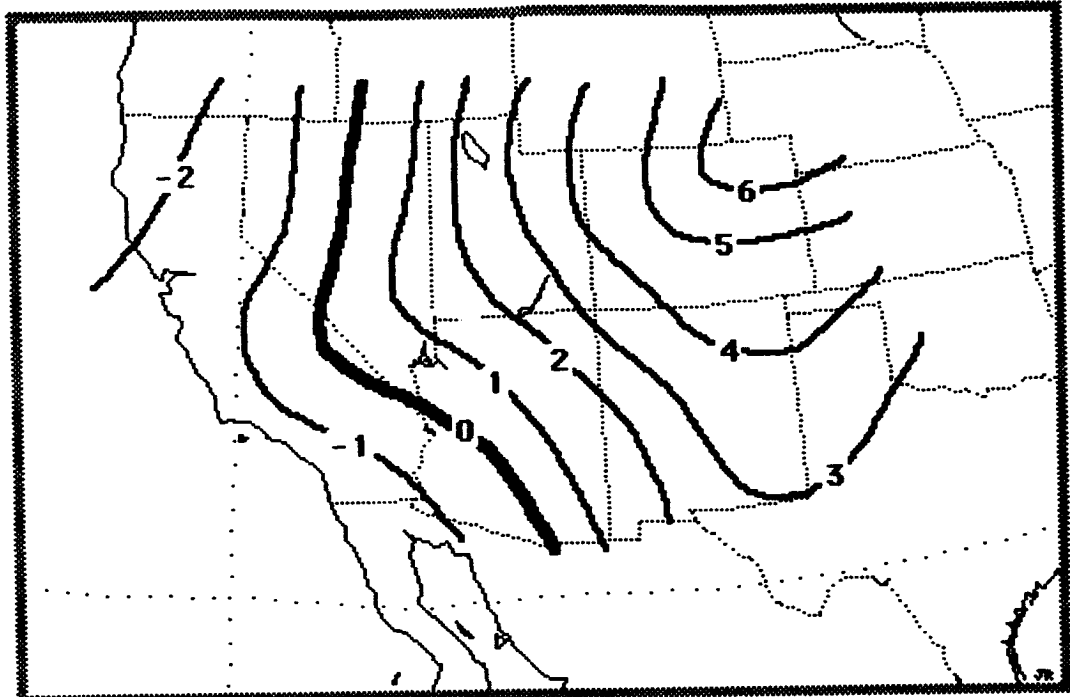
Stations in this category very likely have limited tracking histories and will never be positioned accurately from available early tracking observations. On the other hand, most of the laser stations coming directly from the SL-6 solution will have their coordinates determined to an accuracy in the sub-decimeter range: This is especially true for stations with robust tracking histories. Stations that have come from the GEM-9 solution have their coordinates known to an accuracy of 1 to 2 meters; again, those stations with strong tracking histories will be better determined.

The seven parameters of the transformations are thus susceptible to errors in the coordinates of the stations in both the a priori and the SL-6 coordinate systems. These coordinate errors will be mapped into the seven parameters directly. In running the STC Program, stations were selected such that 1) good geographical distribution was maintained, and 2) all coordinates (a priori and SL-6) were well determined. The STC Program unfortunately, uses equal weights for the stations when estimating the transformation parameters. For the remaining stations to be transformed, in addition to the transformation parameter uncertainties, the errors of the a priori coordinates map directly into the resulting unified coordinates.

The linear translations suffer from the fact that rotation and scale are not considered. These errors can grow as large as three meters when the stations involved are separated by 100 km. However, only a small number of optical and doppler stations were transformed in this way; all of them had station separations of less than 3 km.

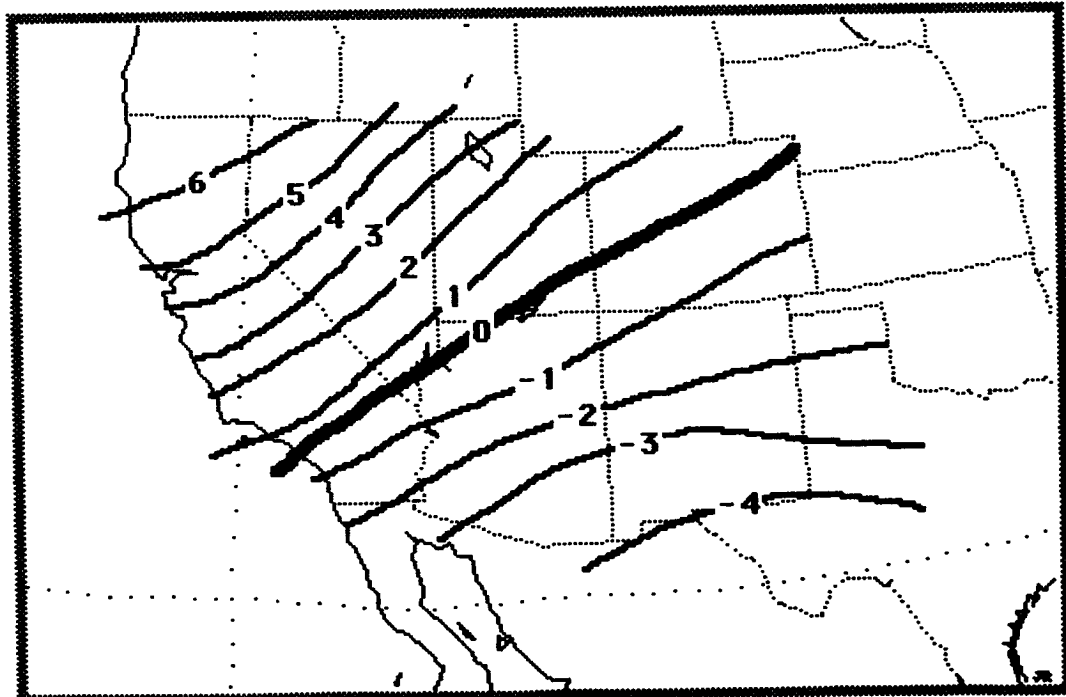
#### 6.5.4 Distortion in the NAD 27 Datum

The STC program provides the residuals for each station's coordinates after the transformation is applied. These residuals, when viewed geographically, can illustrate the relative distortion between two



**CONTOUR INTERVAL: 1 meter**

Figure 6.2. Longitude Distortion Based Upon SL-6 vs. NAD.



**CONTOUR INTERVAL: 1 meter**

Figure 6.3. Latitude Distortion Based Upon SL-6 vs. NAD.

datums. The NAD 27 is a terrestrially determined network established by classical geodetic surveying techniques and adjusted by Gaussian least squares. The distortions of the NAD 27 with respect to SL-6 can be determined by utilizing the more densely distributed stations in the western United States (Figure 6.1). The distortions in longitude and latitude are shown as contour maps in Figures 6.2 and 6.3. Regions of negative distortion indicate areas where NAD 27's longitude or latitude is larger than SL-6's. Leick & Van Gelder (1975) published similar maps comparing NAD 27 to the NWL9D Doppler satellite center of mass system. Their results agree quite well with those of the present analysis.

## 6.6 SUMMARY OF STATION DEFINITION

Station positions from a variety of sources have been transformed into a unified geocentric coordinate system (the TCS) to aid in the creation of a preliminary gravity field model to support the TOPEX mission. Complete lists of the stations in the TCS system are found in Appendices 1 and 2. Appendix 1 has the currently maintained TOPEX geodetic file which consists primarily of active laser and Doppler sites. Appendix 2 consists of older optical sites, many of which are no longer active. The transformations used are anticipated to yield station coordinates with an accuracy of 2 to 5 meters in all coordinates for the NAD 27 transformed stations, and 3 to 7 meters for the dynamically determined coordinates transformed into the modified SL-6 system. The stations which appeared in Table 1 are assessed to have coordinate uncertainties in the range of a few centimeters since they have been determined in recent laser/dynamic solutions. Error sources have been identified and attempts have been made to eliminate, as best as possible, their effects on the resulting transformed coordinates. NAD 27 distortions have been estimated in a limited region and are in good agreement with previous studies. Maintenance of the station coordinates as a geodetic file is an ongoing project. As new solutions and data become available, this file will be updated. Since the station

coordinates come from a variety of sources, an associated epoch cannot be assigned generally. It is planned that as the TCS geodetic file improves, epoch dates can either be assigned to individual stations or the stations will be rotated to a particular epoch using a set of plate motion parameters. The effects of plate motion will continue to grow as tracking histories lengthen in time.

## SECTION 7.0

### FORCE MODELING

The force model used for the GEM-T1 development consists of the conservative geopotential forces and the non-conservative solar radiation pressure and drag forces. This section describes the specific application of the models and provides the general basis for the details of the modeling.

#### 7.1 POTENTIAL EFFECTS

The geopotential consists of both a static part, which is defined by the unperturbed mass distribution of the Earth, and a dynamic part, commonly known as the tidal potential, which is due to the mass deformation of the Earth caused by the gravitational forces of the Sun and Moon. The force is computed as the gradient of the potential.

##### 7.1.1 Mathematical Formulation of the Potentials

The standard form of the geopotential is given by:

$$U^S = \frac{\mu}{r} \left[ 1 + \sum_{n=2}^{n_{\max}} \sum_{m=0}^n \left[ \frac{a_e}{r} \right]^n \bar{P}_{nm}(\sin \phi) \left[ \bar{C}_{nm} \cos m\lambda + \bar{S}_{nm} \sin m\lambda \right] \right] \quad (7.1)$$

where  $\mu$  is the gravitational constant of the Earth (elsewhere referred to as GM),  $r$  is the geocentric satellite distance,  $\phi$  is the satellite geocentric latitude,  $\lambda$  is the satellite east longitude,  $\bar{P}_{nm}(\sin \phi)$  are the associated Legendre functions of the first kind, and  $\bar{C}_{nm}$  and  $\bar{S}_{nm}$  are the geopotential coefficients. The use of the normalized harmonics is

indicated by the overbar. The relationship between the normalized and unnormalized functions is

$$\overline{P}_{nm} = \left[ \frac{(n-m)! (2\ell+1) (2-\delta_{om})}{(n+m)!} \right]^{1/2} P_{nm} \quad (7.2)$$

where  $\delta_{om}$  is the Kronecker delta, which equals 1 when  $m$  is 0 and otherwise equals 0.

The tidal potential adopted consists of the body tide potential and the ocean tide potential. The body tide potential is modeled based on the frequency dependent elastic response of the Wahr Earth model. The ocean tide model is based upon the spherical harmonic expansion of a simple surface density layer model. Both of these potentials may be expressed in the standard form given above, where the coefficients vary with time. However, tidal potentials are more conventionally expressed in terms of amplitude and phase, where the amplitudes are related to either  $c_m$  of tide height or to the contribution to the elasticity parameter  $k_2$ .

The body tide potential is given by

$$U^B = \sum_f A_f k_{2,f} \left[ \frac{a_e}{r} \right]^3 P_{2m}(\sin \phi) \cos (\sigma_f^B + \delta_{2,f}) \quad (7.3)$$

and the ocean tide potential is similarly expressed as

$$U^O = \sum_f \sum_{\ell,q,\pm} K_\ell C_{\ell q}^\pm \left[ \frac{a_e}{r} \right]^{\ell+1} P_{\ell q}(\sin \phi) \cos (\sigma_{\ell q,f}^\pm + \epsilon_{\ell q,f}^\pm) \quad (7.4)$$

where

$\sum_f$  indicates summation over all tidal constituents f.

$\Lambda_f$  is a body tide constant associated with constituent f.

$\sigma_f^B$  is the angular argument associated with constituent f of the body tide.

$k_{2,f}, \delta_{2,f}$  are the Love number amplitude and phase respectively which describe the body response of the Earth.

m is the order associated with f and is 0 for the long period tides, 1 for the diurnal tides, and 2 for the semi-diurnal tides.

$K_\lambda$  is an ocean tide constant associated with degree  $\lambda$ .

$\sigma_{\lambda q, f}^\pm$  is the angular argument associated with the  $(\lambda, q, \pm)$  subharmonic of the ocean tide generated by constituent f.

$C_{\lambda q}^\pm, \epsilon_{\lambda q, f}^\pm$  are the amplitude and phase of the  $(\lambda, q, \pm)$  subharmonic of the ocean tide generated by constituent f.

Each constituent f is associated with an unique frequency. It should be noted that if

$$k_{2,f} = k_2$$

$$\delta_{2,f} = \delta_2 \quad (7.5)$$

for all f, then the total body tide potential may be simply computed in the time domain using the potential

$$U^B = \sum_d \frac{k_2}{2} \frac{\mu_d a_e^2}{r_d^3} \left[ \frac{a_e}{r} \right]^3 \left[ 3 \left[ \frac{\frac{r_d}{r} \cdot \frac{r}{r_d}}{r_d r} \right]^2 - 1 \right] \quad (7.6)$$

where  $\bar{r}_d$  is the geocentric vector to the Sun or Moon and  $\mu_d$  is the gravitational constant of the Sun or Moon. For a frequency dependent model for the Love numbers, most of the variations are concentrated in a single band (the diurnal). It is computationally efficient to use a simple background model and correct terms for which the Love numbers differ significantly from the background reference values. This procedure was adopted.

The tidal constituent  $f$  is uniquely identified by the Doodson argument number. Table 7.1 identifies the principal tidal frequencies and gives the (approximate) matching Darwinian symbol for each corresponding Doodson number. The frequencies are based upon the ecliptic element rates. Note that these same frequencies are also present in the ocean tide effects.

#### 7.1.2 The a priori Static Geopotential Models

The a priori models adopted for the GEM-T1 development are:

|           |                          |
|-----------|--------------------------|
| GEM-L2'   | for LAGEOS               |
| PGS-1331' | for Starlette            |
| PGS-S4'   | for SEASAT               |
| GEM-10B'  | for all other satellites |

These gravity models were analytically corrected to zero mean pole, modern ellipsoid parameters ( $a_e=6378137\text{m}$ ,  $f^{-1}=298.257$ ), and the adopted definition of the new speed of light ( $c=2.99792458 \times 10^8 \text{m/sec}$ ).

TABLE 7.1

| Darwinian<br>Symbol | Doodson's<br>Argument<br>Number | Period<br>(hr) | Description                          |
|---------------------|---------------------------------|----------------|--------------------------------------|
| $M_2$               | 255.555                         | 12.42          | Principal lunar semidiurnal          |
| $S_2$               | 273.555                         | 12.00          | Principal solar semidurnal           |
| $N_2$               | 245.655                         | 12.66          | Larger lunar elliptic<br>semidiurnal |
| $K_2$               | 275.555                         | 11.97          | Lunar/Solar semidiurnal              |
| $L_2$               | 265.455                         | 12.19          | Smaller lunar elliptic               |
| $K_1$               | 165.555                         | 23.93          | Lunar/Solar diurnal                  |
| $O_1$               | 145.555                         | 25.82          | Principal lunar diurnal              |
| $P_1$               | 163.555                         | 24.07          | Principal solar diurnal              |
| $M_f$               | 075.555                         | 13.66d         | Lunar fortnightly                    |
| $M_m$               | 065.455                         | 27.55d         | Lunar monthly                        |
| $S_{sa}$            | 057.555                         | 188.62d        | Solar semi-annual                    |

### 7.1.3 The a priori Body Tide Model

Table 7.2 gives the Love numbers computed by Wahr (1979), based upon the Earth Model 1066A of Gilbert & Dziewonski (1975). Note that  $\delta_{2,f}$  is zero for this elastic model, i.e., the model is free of dissipation. These Love numbers fully characterize the response of the 1066A Earth to the non-loading tide generating potential.

### 7.1.4 A priori Ocean Tides Models

The response of the oceans to the tide generating potential is a set of constituent tide heights

$$\xi_f(P) = A_f(P) \cos(\omega_f - \psi_f(P)) \quad (7.7)$$

where  $\omega_f$  is the angular argument associated with constituent  $f$  and  $A_f(P)$  and  $\psi_f(P)$  are the tidal amplitude and phase respectively at point  $P$ . The amplitudes and phases are computed from numerical solutions of the Laplace Tide Equations. Such solutions involve a high computational burden and presently such models are available for only a limited number of tidal constituents.

The tidal heights are expanded into spherical harmonics by:

$$\xi_f(P) = \sum_{l,q,\pm} C_{lq,f}^{\pm} P_{lq}(\sin \phi) \cos(\sigma_{lq,f}^{\pm} \epsilon_{lq,f}^{\pm}) \quad (7.8)$$

Given the global tidal heights, the coefficients  $C_{lq,f}^{\pm}$  and phases  $\epsilon_{lq,f}^{\pm}$  necessary for the evaluation of the potential can be computed.

TABLE 7.2  
WAHR LOVE NUMBERS FOR 1077A

| <u>Band</u>  | <u>Tidal Line</u> | <u><math>k_{2,f}</math></u> |
|--------------|-------------------|-----------------------------|
| Long Period  | All               | .299                        |
| Diurnal      | 145555 (O1)       | .298                        |
|              | 163555 (P1)       | .287                        |
|              | 165545            | .259                        |
|              | 165555 (K1)       | .256                        |
|              | 165565            | .253                        |
|              | 166554 (PSI)      | .466                        |
| Semi-Diurnal | All               | .302                        |

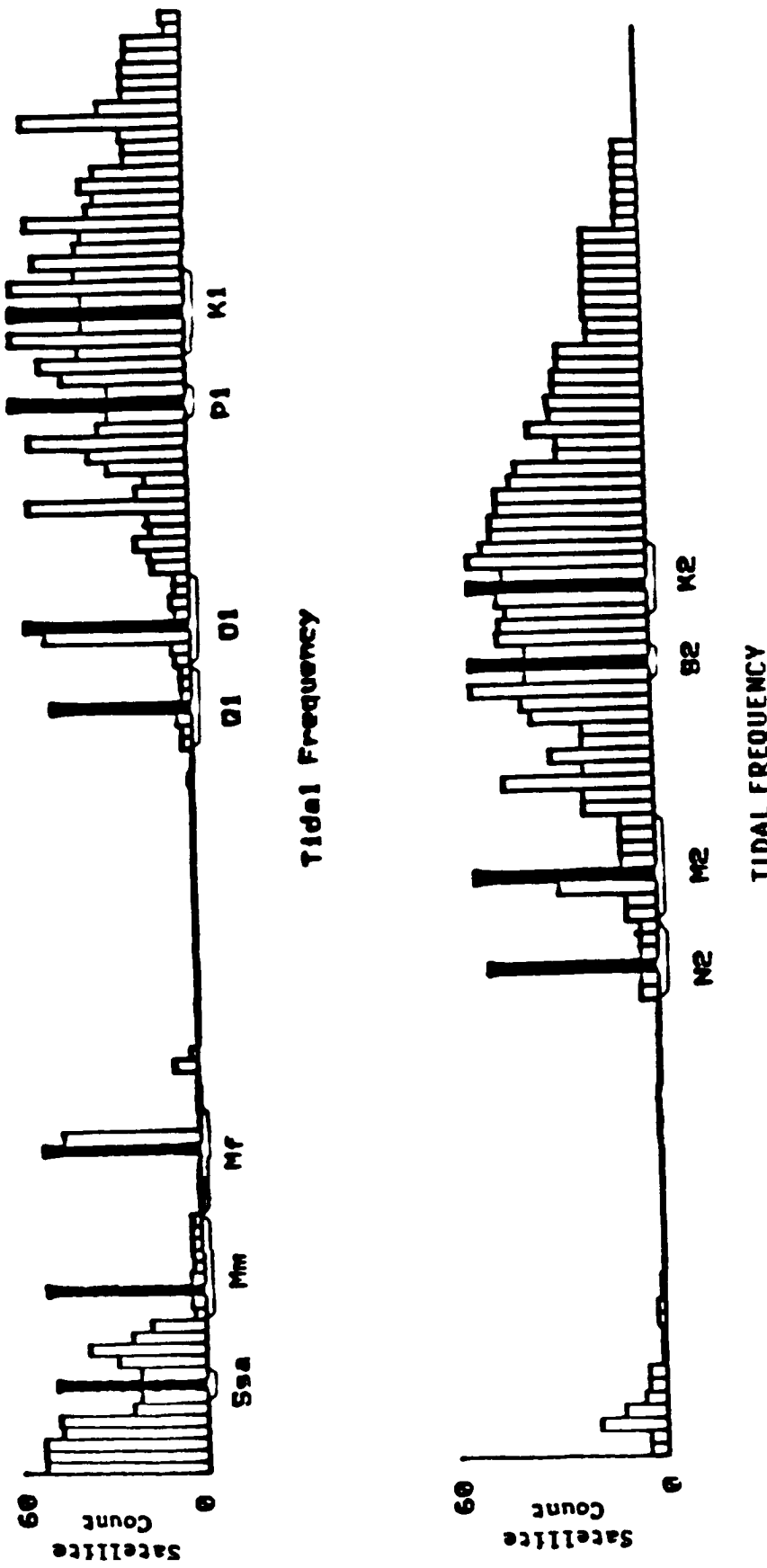
Observed tide models for 11 major tide constituents in the semidiurnal, diurnal, and long period bands have been computed on a  $1^{\circ} \times 1^{\circ}$  global grid by E.W. Schwiderski using an integration scheme which incorporates the available deep sea tide gauge data. These tidal constituents should account for over 90% of the total ocean tide amplitude at any point. However, no models are available for the minor tide constituents, which although small in amplitude, can have significant perturbing effects on a satellite's orbit.

Table 7.3 shows the estimated radial perturbation amplitude due to the major ocean tide constituents on the proposed TOPEX orbit and on the GEOS-3 orbit. This analysis was based upon a Kaula-type first order linear orbit perturbation theory. More than half of the constituents have effects which exceed 1 decimeter radially. These terms must be modeled. It is probable that the associated minor tides for some of these also must be modeled if the minor tide response is proportional to the tide raising potential of the major tide.

Figure 7.1 presents a qualitative analysis of 53 satellites, whose tracking data might contribute to an improved geopotential model. A crude estimate of the ocean tide effect is about 10% of the body tide. The 53 satellite orbits were evaluated for their nominal ocean tide perturbations at 230 tidal frequencies. These 53 orbits represent a variety of orbital inclinations and altitudes, and all have reasonable tracking data histories. Figure 7.1 shows the number of satellites having effects over .001 arcsec in the inclination as a function of tidal frequency. Satellites were also included if the principal third degree terms from an ocean tide decomposition produced a perturbation in the orbit eccentricity greater than 1 ppm. In this analysis, the amplitude of the ocean tide coefficients was assumed to be 1 cm. Note that the criterion of 1 ppm perturbation in the eccentricity is equivalent to the criterion of a .001 arcsec perturbation in the inclination.

TABLE 7.3 OCEAN TIDE RADIAL PERTURBATION AMPLITUDES ON SATELLITE ORBITS

| <u>Schwiderski Tide Model</u> | <u>Tide Frequency (cycles/Day)</u> | <u>GEOSS-3 Amplitude (cm)</u> | <u>TOPEX Amplitude (cm)</u> |
|-------------------------------|------------------------------------|-------------------------------|-----------------------------|
| $S_{sa}$                      | 0.005                              | 10                            | 6                           |
| $M_m$                         | 0.036                              | 1                             | 1                           |
| $M_f$                         | 0.073                              | 1                             | 1                           |
| $Q_1$                         | 0.083                              | 2                             | 2                           |
| $O_1$                         | 0.930                              | 13                            | -                           |
| $P_1$                         | 0.997                              | 24                            | 24                          |
| $K_1$                         | 1.003                              | 125                           | 116                         |
| $N_2$                         | 1.896                              | 3                             | 2                           |
| $M_2$                         | 1.932                              | 3                             | 1.3                         |
| $S_2$                         | 2.000                              | 29                            | 70                          |
| $K_2$                         | 2.005                              | 13                            | 13                          |
| SEMI-DIURNAL                  |                                    |                               |                             |



Histogram of the number of satellites with strong sensitivity to various tidal frequencies. The tidal frequency axis is not linear. The 11 major constituent tidal families are marked by brackets. Numerical tide models exist only for the principal tidal frequency of each family shown by the black bars.

Figure 7.1 Histogram of the Number of Satellites with Strong Sensitivity to Various Tidal Frequencies.

This analysis revealed more than 150 possibly significant tidal constituents. A substantial number of these are associated, not with the main tidal frequencies, but with the nearby sideband frequencies. The periodicities of the satellite orbital motion are convolved with those of the tides as seen on the Earth to produce the frequencies seen at the satellite. Some of the sideband terms are closer to exciting orbital resonance than the dominant tidal terms due to their commensurability with orbital frequencies. However, only the low degree and order terms in the spherical harmonic expansion of the tides can have significant potential effects on the satellites because of the attenuation with distance of these effects on orbiting objects. Our fundamental concern is thus with the long wavelength character of the tides.

The most complete set of a priori ocean tides available represents only the main tidal frequencies. A procedure was developed in order to provide estimates and their errors for the sideband terms from existing oceanographic models in order to both perform a quantitative error analysis and to better assess the recoverability of the low degree and order spherical harmonic tidal terms in a true simultaneous solution with the terms of the geopotential. The complete ocean tidal model which was used as a priori is given in Appendix 3.

The procedure is based upon the concept of admittance, as detailed below. Models were derived for some 36 minor tides, which are on a one degree global grid matching that of Schwiderski. These models have also been converted to spherical harmonics for the subsequent satellite studies. The use of the admittance was motivated by the study of Munk and Cartwright (1977).

The tide raising potential at time  $t$  and at latitude  $\phi$  and longitude  $\lambda$  is given by

$$\Gamma(\phi, \lambda, t) = \sum_{\beta} \Gamma_{\beta}(\phi, \lambda, t) = \sum_{\beta} g \eta_{\beta} P_{2m}(\sin \phi) \cos[\sigma_{\beta} t + \chi_{\beta} + m\lambda] \quad (7.9)$$

where  $\beta$  designates the particular constituent of frequency  $\sigma_\beta$  and equilibrium tide amplitude  $n_\beta$ .  $x_\beta$  is the phase constant associated with the ephemerides of the Sun or Moon for the epoch of January 0, 1900. The gravitational acceleration at the Earth's surface is represented by  $g$ .  $P_{2m}$  is the associated Legendre function of degree 2 and order  $m$ . The terms for degree greater than 2 are of negligible effect (e.g. Munk and Cartwright, 1977). Note that in specifying  $\beta$ ,  $m$  is also specified.

The response to this perturbing potential is the set of constituent tide heights

$$\xi_\beta(\phi, \lambda, t) = A_\beta(\phi, \lambda) \cos[\sigma_\beta t + x_\beta - \psi_\beta(\phi, \lambda)] \quad (7.10)$$

where  $A_\beta(\phi, \lambda)$  and  $\psi_\beta(\phi, \lambda)$  are the amplitude and phase respectively. The admittance function relating the complex exponential signal  $\Gamma'_\beta$  corresponding to the input signal  $\Gamma_\beta$  with the complex output signal  $\xi'_\beta$  for the constituent  $\beta$  is given by

$$Z_\beta(\phi, \lambda) = \frac{A_\beta}{g n_\beta P_{2m}} e^{-j(\psi_\beta + m\lambda)} \quad (7.11)$$

These admittances are readily computed from the known tides. If, on the other hand, the admittance is known for constituent  $\beta$ , then one may compute

$$\xi_\beta = R_e[\xi'_\beta] = R_e[Z_\beta \Gamma'_\beta] \quad (7.12)$$

Thus, if reasonable admittance function descriptions could be obtained from the known tides, the unknown tides could be estimated.

The major tide constituent data, the Schwiderski models (1980a, 1980b), were obtained in the form of a standard NSWC GOTD-1981 tape, i.e. tide values for  $A_\beta$  and  $\psi_\beta$  on a one degree global grid. The rms values of these constituents, computed from their spherical harmonic representation, are tabulated in Table 7.4. Also shown are NSWC's estimated errors for the semidiurnal and diurnal tides and each constituent's equilibrium tide amplitude,  $\eta_\beta$ . NSWC did not provide us with estimated errors for the long period tides. Nominal errors for the long period band were estimated as being proportionately as well determined relative to the equilibrium tide as  $M_2$ , i.e., 12.8%. The model errors are available only in an overall rms sense - the geographic distribution of the estimated errors is not available. Note that there are only four semidiurnal, four diurnal, and three long period tides available.

From the outset, we chose to do separate analyses for the semidiurnal, diurnal, and long period bands so that the range of frequency being represented was more limited. The procedure assumes that the tidal admittance is locally a linear function of frequency, i.e. within each band at each particular  $\phi, \lambda$  point on the Earth's surface. This linearity assumption was adopted because global nonlinearities are anticipated to be small, and also, for the practical reason that there are only at best four points to interpolate over (or extrapolate from) in each band. The procedure is illustrated in Figure 7.2. Proportionally, there is a much greater span of frequency variation in the long period band than in the diurnal or semidiurnal band. However, only three long period tides are available, so this frequency band cannot be further segmented to reduce the range of interpolation. Also, the NSWC  $M_m$  and  $M_f$  tides are smaller by a factor of 3 or 4 compared to their equilibrium values. This suggests a conflict with the assumption of linearity of the admittances across the long period tidal band.

TABLE 7.4  
NSWC TIDE MODELS

Cumulative RMS Tide Values Summed to Degree 30 and their RMS Errors

| Tide Constituent | Equilibrium Tide Amplitude $n_B$ (cm) | NSWC RMS (cm) | NSWC Model Errors (cm & deg)* |       |
|------------------|---------------------------------------|---------------|-------------------------------|-------|
|                  |                                       |               | Amplitude                     | Phase |
| M <sub>2</sub>   | 24.2                                  | 30.0          | 3.11                          | 3.72  |
| S <sub>2</sub>   | 11.3                                  | 12.2          | 1.28                          | 4.24  |
| M <sub>2</sub>   | 4.6                                   | 6.5           | 0.51                          | 4.12  |
| K <sub>2</sub>   | 3.1                                   | 3.4           | 0.23                          | 3.13  |
| K <sub>1</sub>   | 14.1                                  | 10.9          | 0.94                          | 9.95  |
| O <sub>1</sub>   | 10.1                                  | 7.9           | 0.57                          | 3.42  |
| P <sub>1</sub>   | 4.7                                   | 3.5           | 0.20                          | 4.14  |
| Q <sub>1</sub>   | 1.9                                   | 1.7           | 0.08                          | 2.41  |
| M <sub>f</sub>   | 4.2                                   | 1.0           | --                            | --    |
| M <sub>m</sub>   | 2.2                                   | 0.8           | --                            | --    |
| S <sub>sa</sub>  | 1.9                                   | 1.6           | --                            | --    |

\*From Table of Comparison of Empirical and Modeled Ocean Tides at 195 Island and Deep-Sea Stations (used and not used), E.W. Schwiderski, private communications.

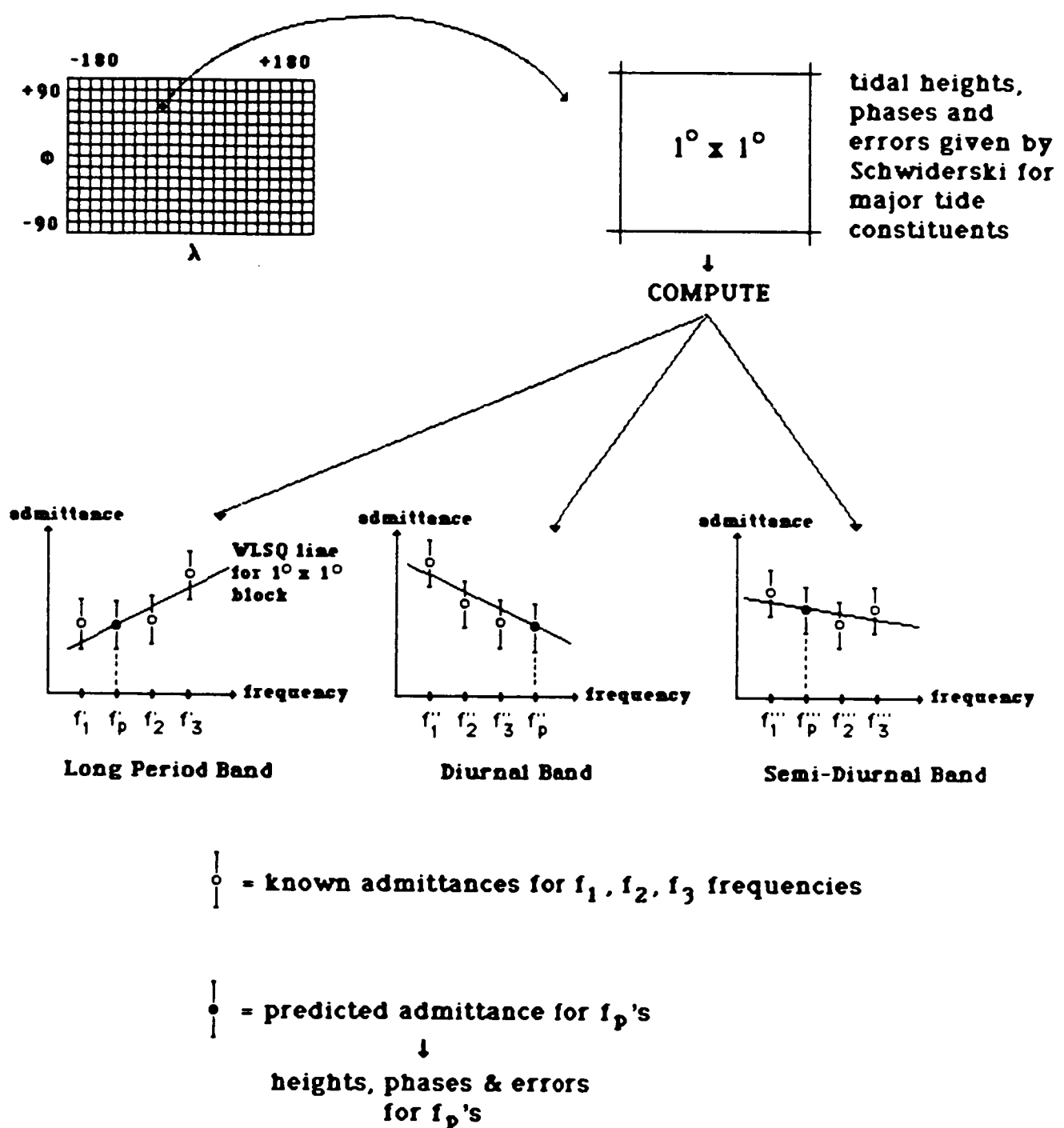


Figure 7.2. Background Tides Model Development.

The residuals from the fitting process reflect the disagreement of the NSWC tides with this hypothesis. The fitting process is a least squares linear regression weighting each  $A_\beta \cos \psi_\beta$  or  $A_\beta \sin \psi_\beta$  according to the specified NSWC estimated errors:

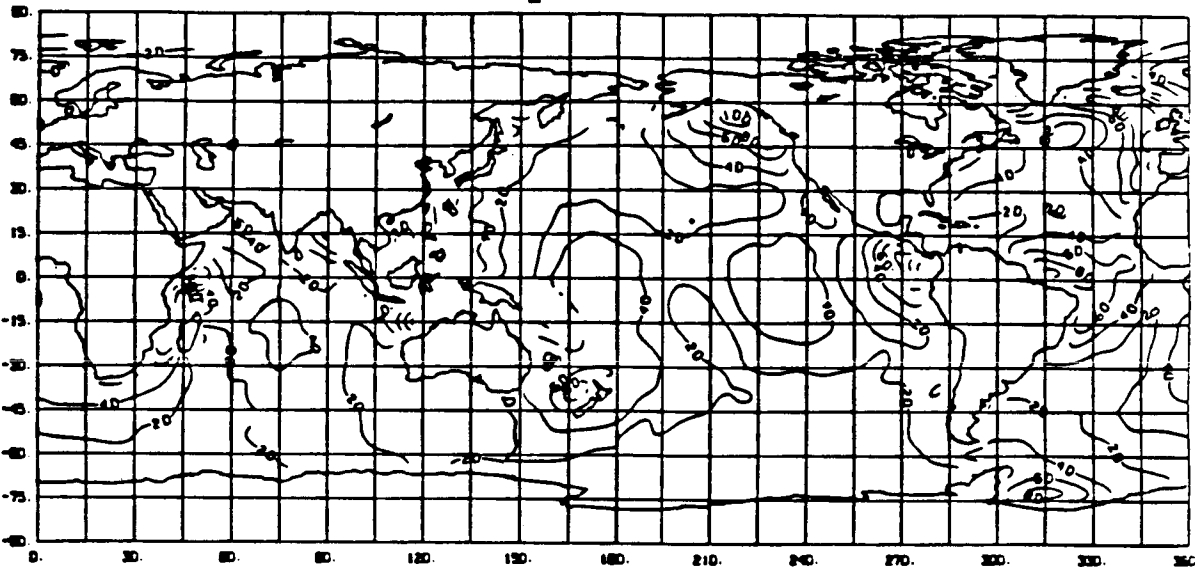
$$\text{weight} = (\delta a^2 + A_\beta^2 \delta \psi^2)^{-1} \quad (7.13)$$

where  $\delta a$  represents the error in  $A_\beta(\phi, \lambda)$  and  $\delta \psi$  represents the error in  $\psi_\beta(\phi, \lambda)$ . For the long period tides, we estimated that the error was proportionally the same as for  $M_2$ , which is 12.8% of the equilibrium tide amplitude. Because we are dealing with tide models as data, our residuals should be dominated by local nonlinearities in areas such as the Patagonian Shelf and the more global nonlinearities due to the Earth's diurnal resonance. The differential response to solar radiation will be present. These residuals will also reflect nonlinearities in the physical modeling of Schwiderski (1980a, 1980b) and any systematic data errors specific to a particular tide. Clearly, if a nonlinear hypothesis were to be adopted to replace the linear arc based on the admittance concept, a physically justifiable nonlinear model would be essential.

The global amplitudes and phases for the  $M_2$  tide as computed by Schwiderski and our numerical model are compared in Figures 7.3 and 7.4. The models are qualitatively the same, which indicates that, in a global sense, we have not seriously mismodeled this important tide. This is true for all of the semidiurnal and diurnal tides. The upper part of Figure 7.5 shows the global amplitude of the residuals in  $M_2$  (vector magnitude). As expected, local areas such as the Patagonian Shelf dominate the residuals. There are also significant differences in the general area of the Marquesas Islands and the western Atlantic. The lower part of Figure 7.5 shows the percentage relative error, indicating that the error is typically less than 20%. The regions of high relative error, greater than 20%, generally correspond to amphidrome locations

CHART NO. 13  
OF POOR QUALITY

Schwiderski  $M_2$  Tide – Amplitude in Cm



Interpolated  $M_2$  Tide – Amplitude in Cm.

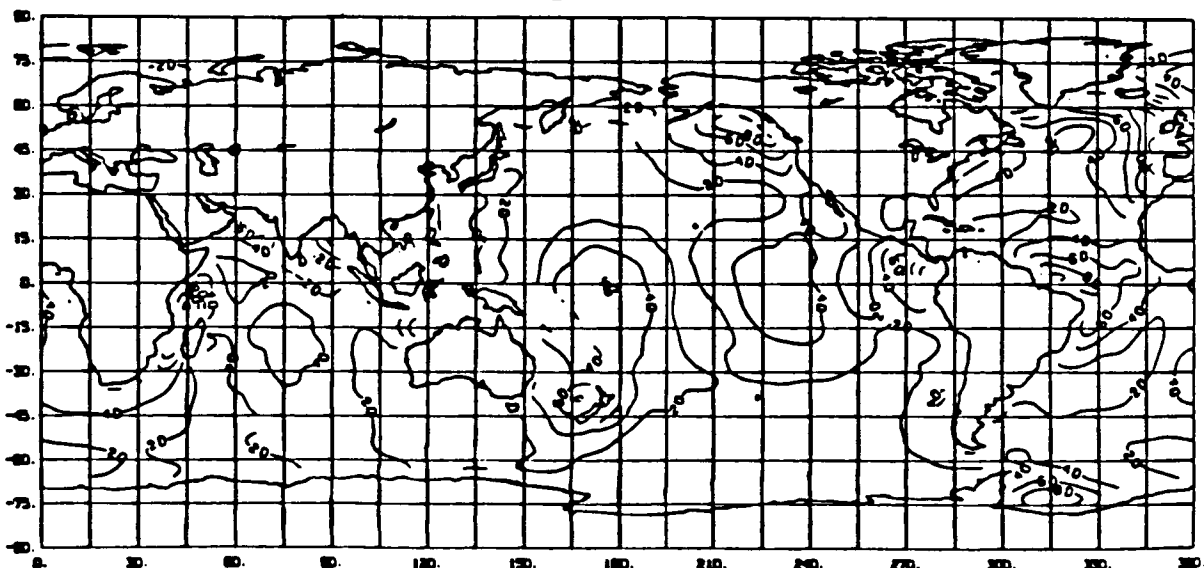
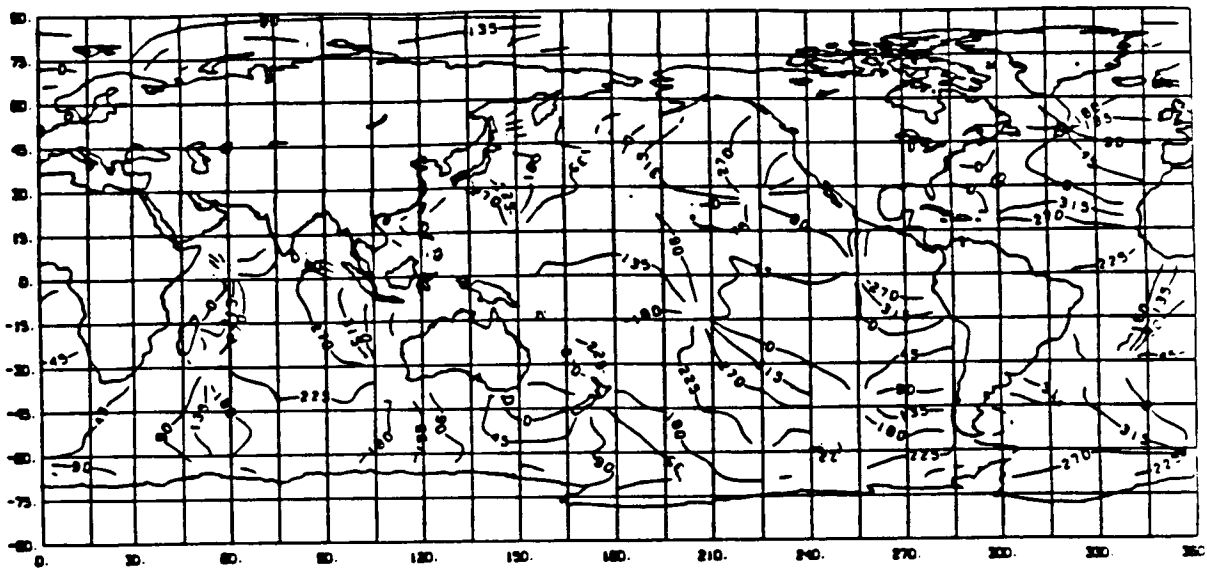


Figure 7.3. Comparison of  $M_2$  Tide Amplitudes.

Schwiderski  $M_2$  Tide – Phases in Deg.



Interpolated  $M_2$  Tide – Phases in Deg.

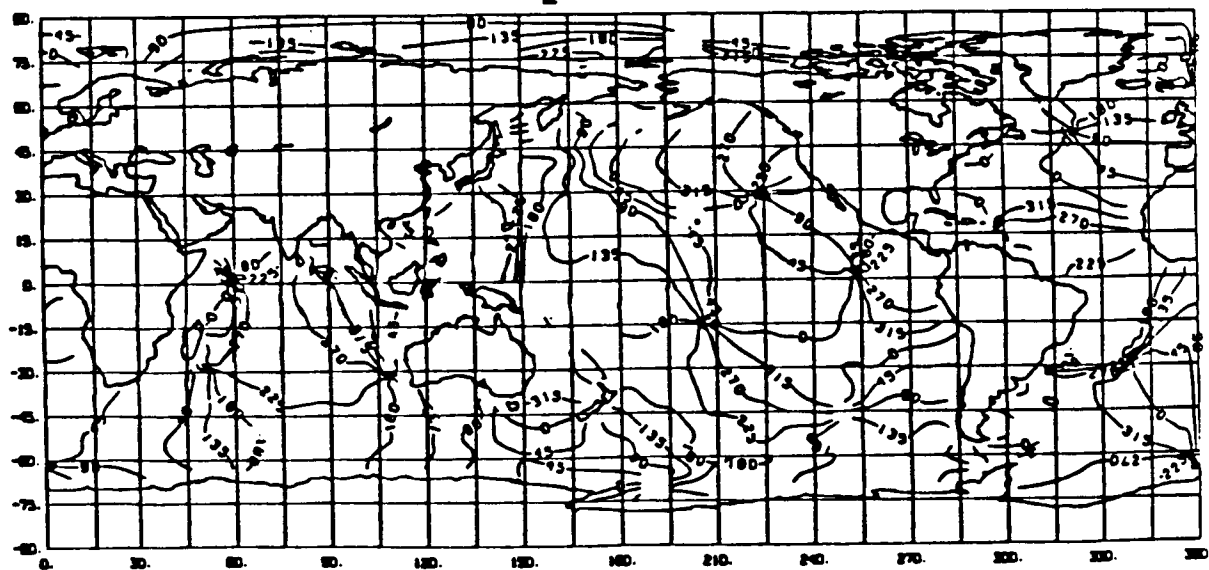
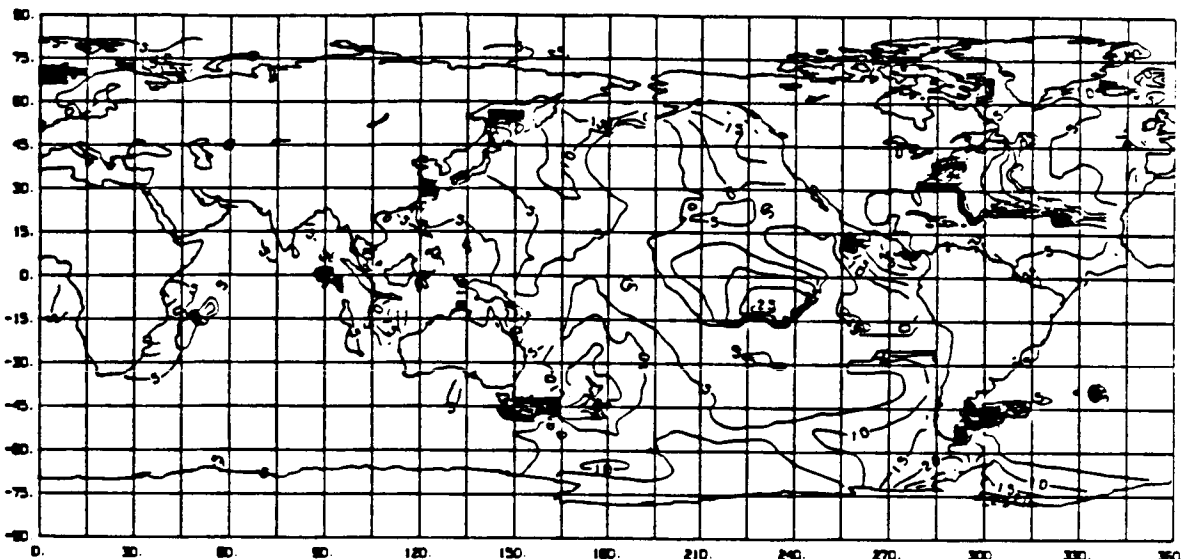


Figure 7.4. Comparison of  $M_2$  Tide Phases.

ORIGINAL DATA IS  
OF POOR QUALITY

Amplitude of Error in Cm



Relative Error in Percent



Figure 7.5. Error in Interpolated  $M_2$  Tide.

where the amplitude variability is small. This example is typical of the results we obtained for all of the tides in the diurnal and semidiurnal bands.

Similar comparisons for the long period tides show large regions of high relative error, over 100%, which indicates that our approach has difficulties with the long period tidal band. These difficulties were not unexpected given the substantial frequency range within this band. However, as there are only three major tides available in this band, there is no practical alternative.

Table 7.5 presents the global statistical summary for each of the NSWC tides. The rms of fit in cm shown was computed from the rms admittance. With the exception of  $O_1$  and  $M_2$ , the rms global fit in each of the semidiurnal and diurnal bands shows that the linear model disagrees with the NSWC input by approximately the estimated error in NSWC.  $O_1$  and  $M_2$  disagree by a factor of two in this quantity.  $M_2$ , the worst case, has a weighted rms disagreement of 7 cm out of a total 30 cm, yet still has an error in power of less than 5%. The fits in the long period band confirm the conclusion that these tides are not adequately modeled with this procedure, in that the weighted rms residual amplitude is on the order of the entire NSWC rms tide amplitude. However, the weighted rms residual amplitude is only twice our 12.8% of the equilibrium tide amplitude. As can be seen in Table 7.4, the NSWC  $M_m$  and  $M_f$  tide amplitudes are quite different from the equilibrium tide amplitudes.

The standard deviations of unit weight given in Table 7.5 provide the factors by which the NSWC rms amplitude errors need to be adjusted in order to map the weighted residuals into the unit normal distribution. The semidiurnal and diurnal bands are near unity, but the long period band is off by a factor of 2.5. Thus the linear model is not inconsistent with the semidiurnal and diurnal data, but it is

TABLE 7.5 SUMMARY OF AMPLITUDES AND ERRORS

| Band | Tide     | Equilibrium Tide<br>Amplitude $K_\beta$ (cm) | NSWC RMS<br>Ampl. (cm)  | RMS<br>Ampl. Err. (cm) | NSWC RMS<br>Mod. Admittance | RMS Residual<br>Amplitude (cm) | Stand. Dev.<br>of Unit Wt.                   | Estimated RMS<br>Ampl. Error (cm) |
|------|----------|--|-------------------------|------------------------|-----------------------------|--------------------------------|--|-----------------------------------|
| i    | j        | $\bar{a}_{ij}$                               | $\bar{\sigma}_{a_{ij}}$ | $\delta \bar{M}_{ij}$  | $\hat{\delta} \bar{a}_{ij}$ | $\hat{\sigma}_{o_1}$           | $\hat{\sigma}_{o_1} * \bar{\sigma}_{a_{ij}}$ |                                   |
| 0    | $S_{sa}$ | 1.9  | 1.6                     | 0.2*                   | 0.27                        | 0.5                            | 2.5  | 0.5                               |
|      | $M_m$    | 2.2  | 0.8                     | 0.3*                   | 0.37                        | 0.8                            |  | 0.8                               |
|      | $M_f$    | 4.2  | 1.0                     | 0.5*                   | 0.16                        | 0.7                            |  | 1.3                               |
| 1    | $Q_1$    | 1.9  | 1.7                     | 0.1                    | 0.05                        | 0.1                            | 1.1  | 0.1                               |
|      | $O_1$    | 10.1   | 7.9                     | 0.6                    | 0.12                        | 1.2                            |  | 0.7                               |
|      | $P_1$    | 4.7  | 3.5                     | 0.2                    | 0.03                        | 0.2                            |  | 0.2                               |
|      | $K_1$    | 14.1   | 10.9                    | 0.9                    | 0.06                        | 0.9                            |  | 1.0                               |
| 2    | $N_2$    | 4.6  | 6.5                     | 0.5                    | 0.18                        | 0.8                            | 1.3  | 0.7                               |
|      | $M_2$    | 24.2   | 30.0                    | 3.1                    | 0.29                        | 7.0                            |  | 4.0                               |
|      | $S_2$    | 11.3   | 12.2                    | 1.3                    | 0.13                        | 1.5                            |  | 1.7                               |
|      | $K_2$    | 3.1  | 3.4                     | 0.2                    | 0.07                        | 0.2                            |  | 0.3                               |

\*Estimated

inconsistent for the long period tides assuming the projected error estimates for these tides are correct. However, rms fits are still less than 40% of the equilibrium amplitude for these long period tides, and are only about twice the estimated nominal error in these tides.

In addition to computing the unknown tides, we have also computed the associated errors of these tides based on errors which have been corrected to attain unit variance. The error at a point is simply obtained by propagating the covariance matrix associated with each point to the desired frequency.

## 7.2 ATMOSPHERIC DRAG AND SOLAR RADIATION PRESSURE

The non-conservative forces which are of concern in modeling the evolution of the spacecraft orbit are the forces of atmospheric drag and solar radiation pressure.

### 7.2.1 Mathematical Formulation of the Models

In GEODYN, the acceleration due to atmospheric drag is

$$\bar{A}_D = -\frac{1}{2} C_D \left[ \frac{A}{M} \right] \rho_D v_r \bar{v}_r \quad (7.14)$$

where  $C_D$  is the satellite drag coefficient,  $A$  is the cross-sectional area of the satellite,  $M$  is the mass of the satellite,  $\rho_D$  is the density of the atmosphere,  $\bar{v}_r$  is the velocity vector of the satellite relative to the atmosphere and  $v_r$  is its modulus. The atmosphere model is the 1971 Jacchia; the atmosphere is presumed to rotate with the Earth.

The acceleration due to solar radiation pressure is given by

$$\bar{A}_R = -v C_R \left| \frac{A}{M} \right| P_s \frac{r_s^P}{r_s^2} \hat{r}_s \quad (7.15)$$

where  $v$  is the eclipse factor accounting for shadowing of the satellite by the body of the Earth,  $C_R$  is the satellite radiation pressure coefficient,  $A$  and  $M$  are as before,  $P_s$  is the solar radiation pressure in the vicinity of the Earth,  $r_s$  is the distance from the satellite to the sun in AU, and  $\hat{r}_s$  is the geocentric unit vector pointing toward the Sun.

Both of these models assume the satellite is a sphere. However, the adjustment of the drag and/or radiation pressure coefficient accommodates much of the model error associated with the spacecraft shape. Errors in the density model are similarly accommodated, but, because the atmosphere varies with time, multiple drag coefficients are often required to accommodate the observed drag variations. GEODYN has the capability to model either the drag or solar pressure effects using piecewise discontinuous coefficients over specified time intervals, and, within each time interval, the coefficient can vary according to

$$C = C_0 + \dot{C} (t-t_0) \quad (7.16)$$

For the present efforts, we are only using this capability with the drag modeling.

### 7.2.2 Atmospheric Drag Model Testing

Almost all of the satellites used in our analyses are significantly perturbed by drag. Given that there are model errors in both the shape of the spacecraft and in the atmospheric density model, the major

question to be answered was how best to parameterize the drag so as to minimize the atmospheric drag error within the orbital solutions. The parameterization options investigated were:

- (a) a constant scale parameter,  $C_D$ , adjusted once in the arc
- (b) a  $C_D$  and  $\dot{C}_D$  adjusted over the length of the arc, or
- (c) solution for several  $C_D$  values over specified time intervals,  
(i.e. once per day) over the arc length.

This investigation was most conveniently performed using the GEODYN I software, as it has variable area modeling capabilities and a selection of atmospheric density models -- specifically both the 65 and 71 Jacchia models (Jacchia, 1965, 1971). The BE-C satellite was used as the basis for this investigation.

The BE-C orbit has received a good deal of attention from its contributions to the San Andreas Fault Experiment and the analysis of laser ranging to determine intersite station distances within California (see for example Smith et al., 1977). Of the set of laser satellites which were used in the creation of GEM-T1, BE-C presented one of the most difficult atmospheric drag modeling problems. It was magnetically stabilized, which caused its in-plane cross-sectional area to vary significantly over each orbital revolution. BE-C also has a somewhat eccentric orbit ( $e=0.0257$ ) with a perigee height of 940km. A variable cross-section surface area model for BE-C was developed by Safran, 1975. Given that BE-C also has a reasonably strong set of laser ranging data, tests of drag modeling error could be designed using orbit intercomparisons and analysis of along track errors sensed at the observing sites using the real tracking data and resulting orbits directly.

Several five-day arcs were selected. These arcs were chosen so as to represent the full spectrum of tracking available on BE-C. For example, a well tracked arc (epoch of 790417) having a total of 78 passes was used. On the other hand a somewhat weaker arc having only 30 passes (epoch of 800201) was also selected. Table 7.6 shows the geographic distribution of the data found in each of these arcs.

#### 7.2.2.1 Orbit Comparison Results

The representation and solution of drag parameters was tested preliminarily through a series of trajectory comparisons. Each of the approaches ((a) through (c) outlined above where (c) was tried two ways-with a coefficient adjusted every 12hrs. and once per day) was utilized to converge each of the five day arcs. Both the Jacchia 1965 and 1971 models were employed. All of these resulting trajectories were intercompared every minute over their respective 5 day intervals as shown in Table 7.6.

Table 7.6 summarizes the RMS along track trajectory component differences for each of these comparisons as shown in Figure 7.7. In all cases, drag predominantly perturbed the along track component of the orbit, with radial and cross track RMS differences always being less than 0.6m. The data sets and non-drag force models were the same in all orbits with the same epoch. The differences in the trajectories are due to drag modeling differences which can be construed as an estimate of drag model error. The effects of this drag error are to be minimized through the solution of drag scaling parameters. Therefore, where different density models show the greatest agreement, this minimization has been effective. There is also some concern that over-parameterization of the drag effects could result in an aliasing of drag and long period gravity signals. Therefore, it was desirable that the number of degrees of freedom devoted to drag scale parameters be held to a minimum unless strong evidence was present indicating a need for

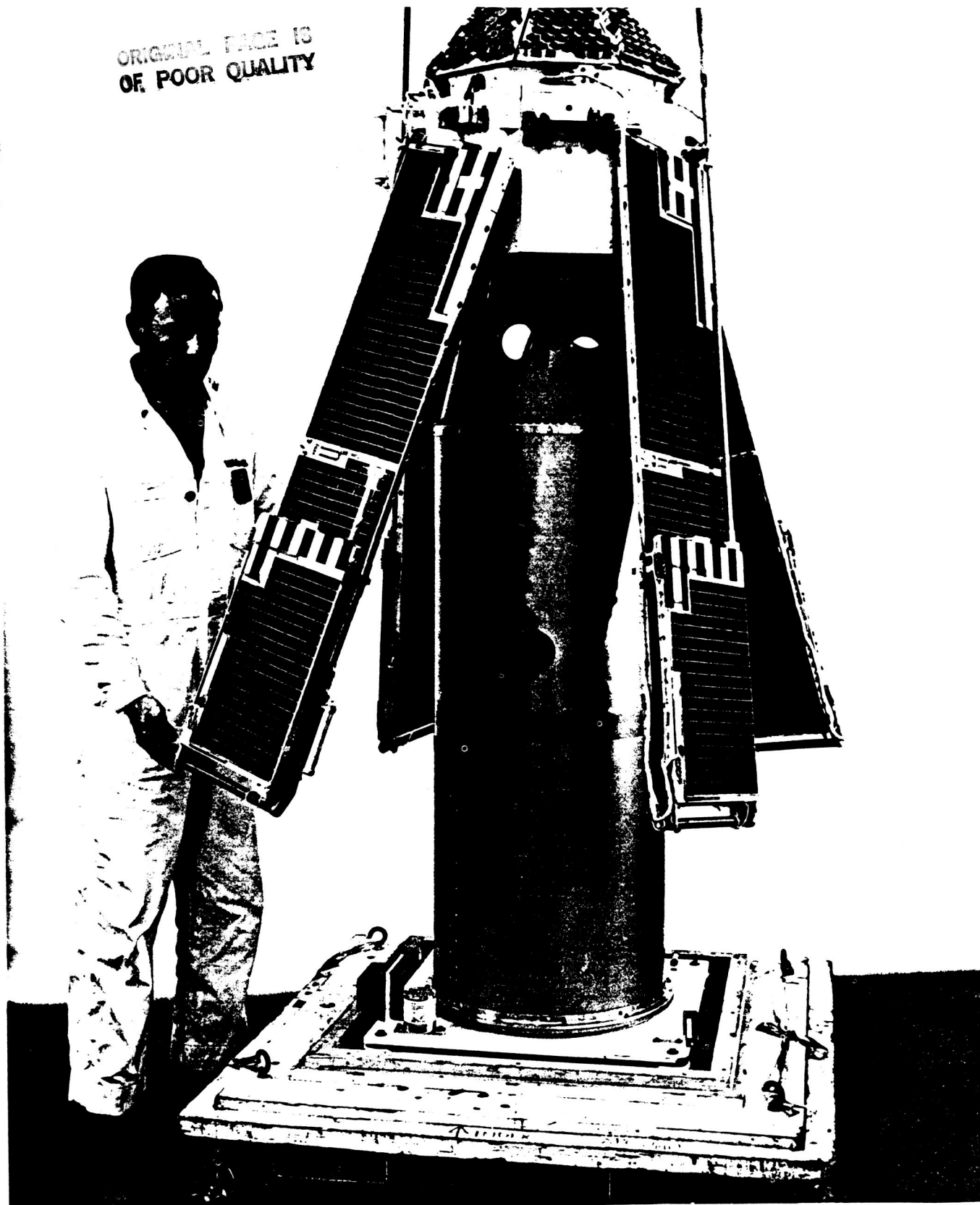


Figure 7.6. BE-C.

**Table 7 6**

**BE-C DRAG MODELING ORBITAL COMPARISONS**

**TEST ARCS: 5 DAY ARC LENGTHS**

790417                  800201

**No. of passes:**

|        |    |    |
|--------|----|----|
| W. USA | 51 | 24 |
| E. USA | 24 | 1  |
| S. Am. | 3  | 0  |
| Hawaii | 0  | 5  |
| TOTAL  | 78 | 30 |

**790417: ORBIT COMPARISONS: RMS ALONG TRACK DIFFERENCES (m)**

| J71 CD+CDOT |     |            | J65 CD+CDOT |            |     |
|-------------|-----|------------|-------------|------------|-----|
| J71 CD/DAY  |     | J71 CD/12H |             | J65 CD/DAY |     |
| J71 CD/DAY  | 3.0 | 3.4        | 0.8         | 1.6        | 4.3 |
| J71 CD/12H  |     |            |             | 4.7        |     |
| J65 CD+CDOT | 1.6 |            |             |            |     |
| J65 CD/DAY  | 3.0 | 1.2        | 1.2         | 4.1        |     |
| J65 CD/12H  | 3.6 | 1.9        | 1.4         | 4.6        | 1.1 |

**800201: ORBIT COMPARISONS: RMS ALONG TRACK DIFFERENCES (m)**

| J71 CD+CDOT |      |            | J65 CD+CDOT |            |      |
|-------------|------|------------|-------------|------------|------|
| J71 CD/DAY  |      | J71 CD/12H |             | J65 CD/DAY |      |
| J71 CD/DAY  | 9.3  | 9.2        | 1.5         | 8.5        |      |
| J71 CD/12H  |      |            |             |            |      |
| J65 CD+CDOT | 1.4  | 8.7        | 2.7         | 2.9        | 10.7 |
| J65 CD/DAY  | 11.5 |            |             |            |      |
| J65 CD/12H  | 11.2 | 3.1        |             | 2.5        | 10.4 |
|             |      |            |             |            | 1.5  |

**RMS Cross Track and Radial Differences are all less than 0.6 m**

**J65 CD/DAY VS. J71 CD/DAY**

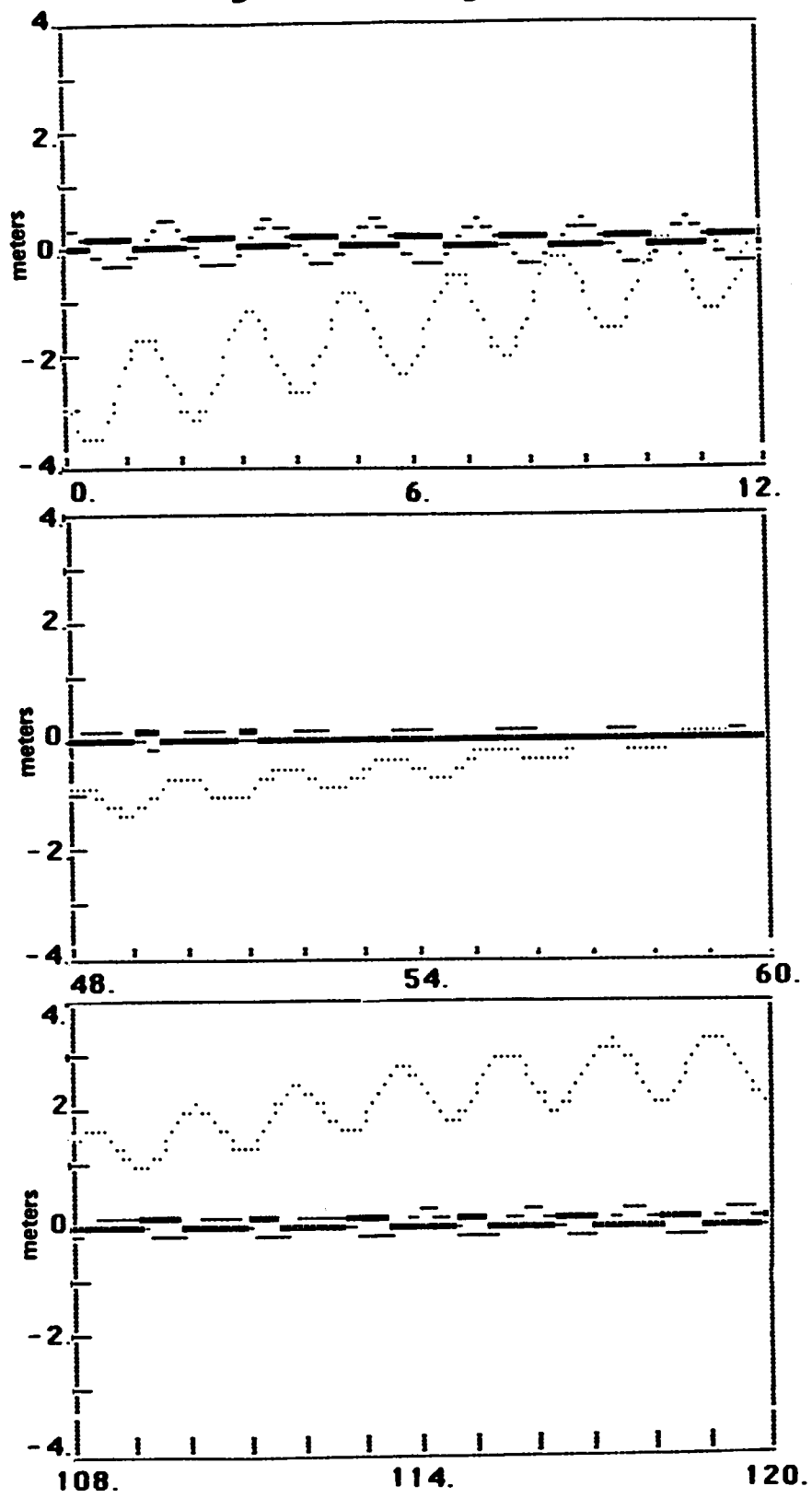


Figure 7.7. Trajectory Differences: BE-C 5 Day Arcs.

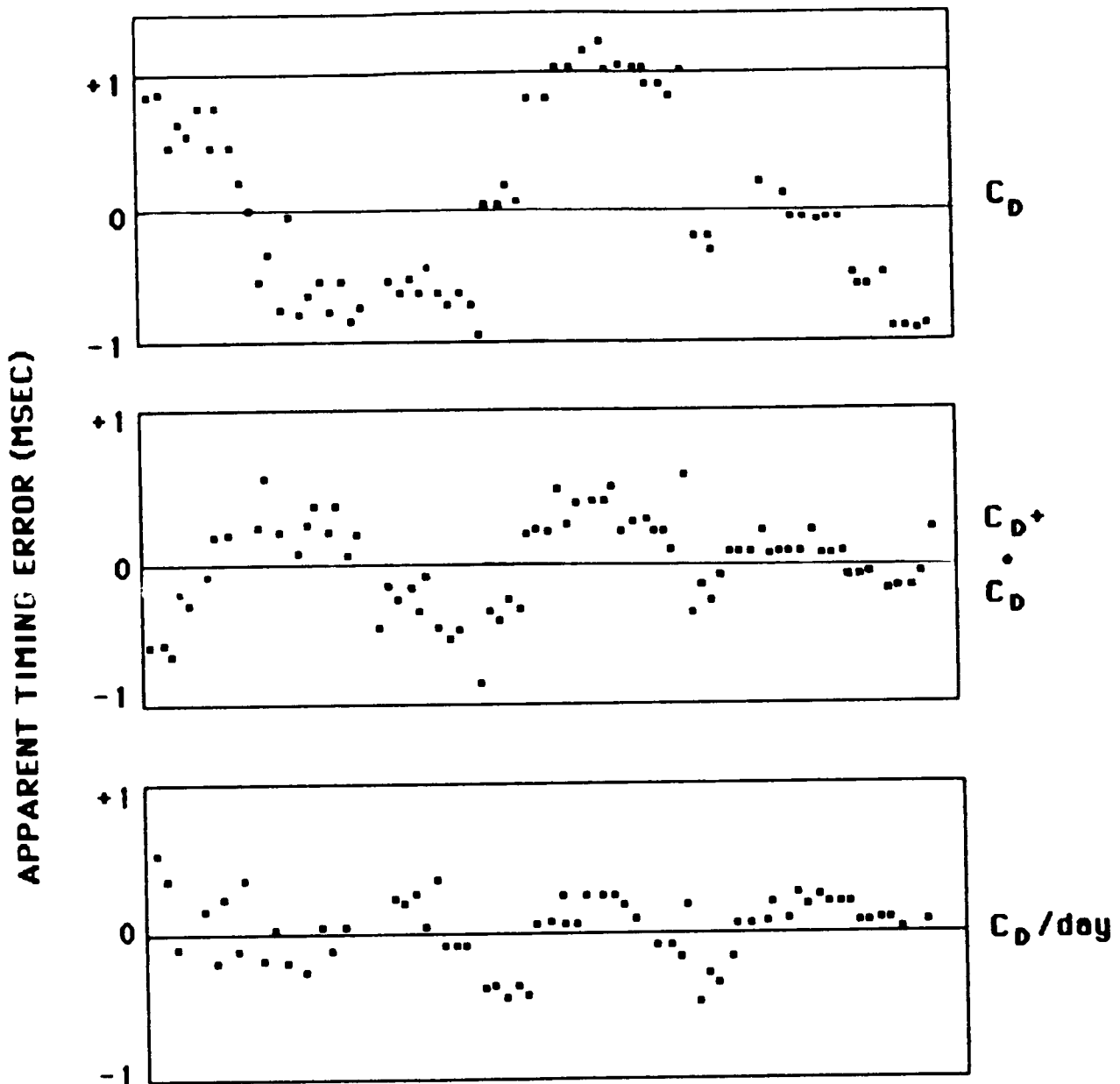
additional drag parameters. The drag/day and drag/12hr representations clearly had the best overall performance for reducing drag error and producing the most similar orbits. This representation yielded results which on the arcs with the strongest tracking showed agreement of better than 2m RMS along track between trajectories calculated using different density models. Even for the weaker second arc, results no worse than 3.1 m RMS were obtained. Since there was no clear improvement to be seen in the  $C_D/12hr$  drag parameterization, the  $C_D/day$  approach was adopted as the most desirable on the basis of these tests.

These orbits were tested invoking the variable cross-sectional area model and compared with trajectories calculated modeling a constant satellite surface area. No significant improvement was found when the variable area model was utilized. As the variable area modeling was not available in GEODYN II, the data analysis proceeded using constant satellite cross-sectional area values.

#### 7.2.2.2 Evaluation of Apparent Timing Errors

This second approach is based upon analysis of the apparent timing errors seen in each pass of tracking data. As most of the satellite's motion is in its orbital plane, an error in the calculated orbit causes the acquisition time at a station to appear either early or late with respect to the actual observations--these are the so-called apparent "timing errors" which are analyzed. Figure 7.8 presents the apparent timing errors seen in a 5 day arc (epoch 811012) when different parameterizations are employed for the minimization of drag errors.

The intercomparison of the spectra of the timing errors associated with the various types of drag parameterization provided the basis for the evaluation. It is assumed that, if one could completely eliminate drag model errors through some parameterization, then the



**PASSES TAKEN CHRONOLOGICALLY  
OVER 5<sup>D</sup> ARC (EPOCH 790417)**

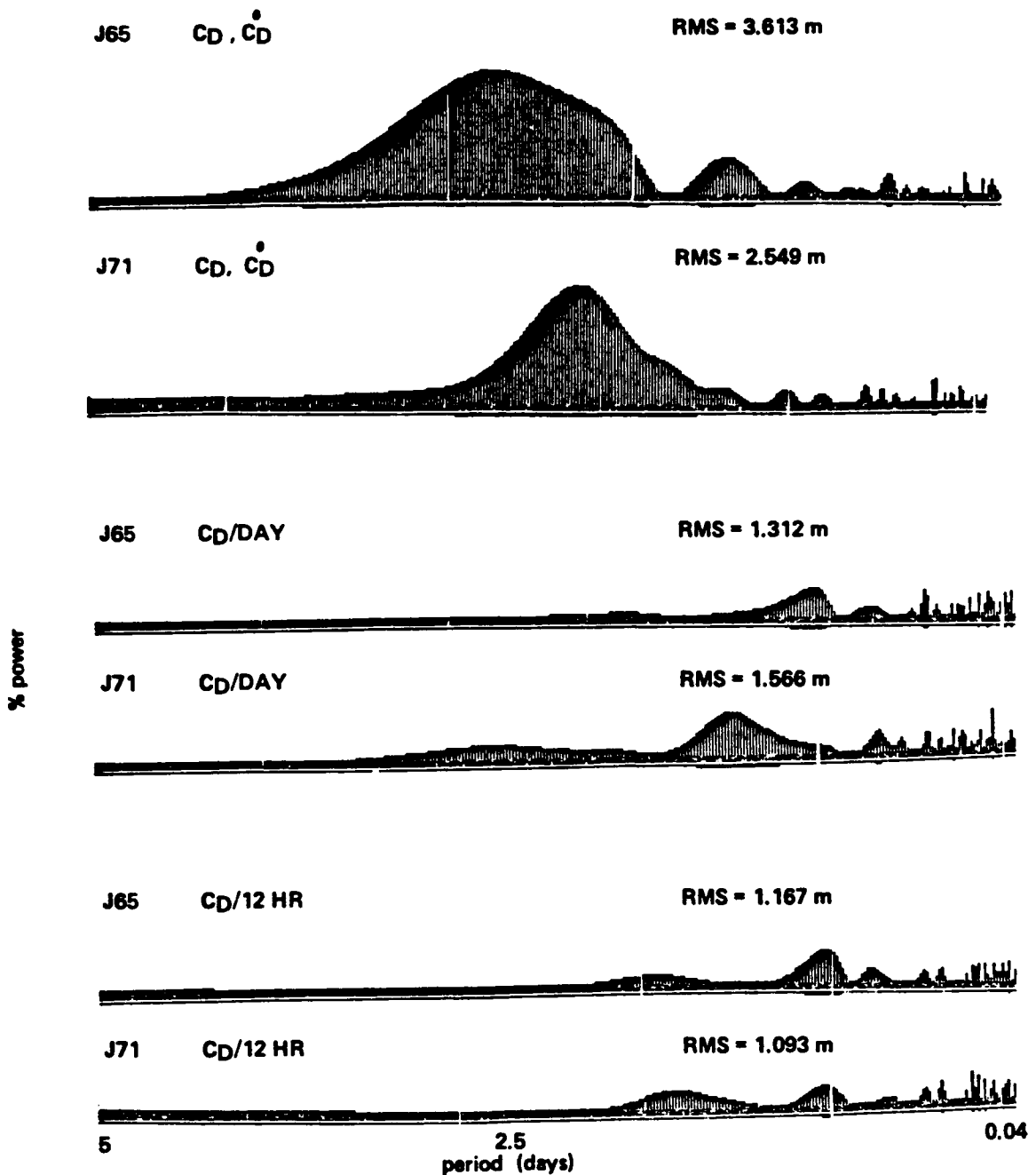
Figure 7.8. Apparent Timing Errors in Laser Passes within a Five Day Arc of BE-C Using Different Representations of Drag Parameterization.

resulting spectra would be unaffected by the density model used. Conversely, if the same representation of drag yielded very different timing error spectra when different density models were used, then it is expected that there would be a strong residual drag related aliasing signal corrupting the computed orbit. Figure 7.9 compares the timing error spectra using different density models for each of the drag parameterizations described above. The difference in the spectra when drag is represented by a  $C_D$  and a  $\dot{C}_D$  strongly indicates that there is considerable residual drag error left within each of the calculated trajectories. This large error is greatly reduced when a  $C_D/\text{day}$  or  $C_D/12\text{hr}$  modeling is used. Other arcs were tested and gave the same strong evidence that a  $C_D/\text{day}$  coefficient recovery was the most desirable representation requiring a limited set of solution parameters.

#### 7.2.2.3 Conclusions

The BE-C atmospheric drag investigation led to the adoption of the  $C_D/\text{day}$  parameterization for the orbital data reductions and normal equation generations for the GEM-T1 solution. This representation was used on all near-Earth laser, flashing lamp optical and Doppler satellites. It was not possible to use this approach for the passive optical satellites whose data were too sparse to support daily drag parameter recoveries. LAGEOS and STARLETTE, given their extremely high density and insensitivity to atmospheric drag, required a solution of a single drag parameter for each orbital arc. Table 7.7 summarizes the treatment of the orbital specific parameters by satellite in the analysis and normal equation generation phases of the GEM-T1 investigation.

Further investigations of this nature are planned for future iterations of the gravitational field models. Tests involving the atmospheric model of Barlier (1978) are to be included.



**SPECTRUM OF APPARENT STATION TIMING ERRORS FOR A BE-C  
FIVE DAY ARC WITH GOOD GLOBAL DATA DISTRIBUTION:**

**NO. of PASSES:**

|        |    |
|--------|----|
| S. Am. | 16 |
| W. USA | 21 |
| E. USA | 18 |
| Haw    | 12 |

**811012 EPOCH :**

Figure 7.9. Atmospheric Drag Parameterization Test.

Table 7.7

**SATELLITE ARC  
DEPENDENT PARAMETERS USED IN  
THE DATA ANALYSIS & NORMAL  
EQUATION GENERATION**

| <u>SATELLITE</u> | <u>ARC LENGTH</u> | <u>DRAG</u>      | <u>SOL. RAD.</u> | <u>ACCEL.</u> |
|------------------|-------------------|------------------|------------------|---------------|
| LAGEOS           | 30°               | -                | $C_r, \dot{C}_r$ | $a, \dot{a}$  |
| STARLETTE        | 5°                | $C_D$            | $C_r$            | —             |
| OTHER LASER      | 5°                | $C_D / DAY$      | $C_r, \dot{C}_r$ | —             |
| DOPPLER          | 6°, 7°            | $C_D / DAY$      | $C_r, \dot{C}_r$ | —             |
| FLASHING LAMP    | 7°                | $C_D / DAY$      | $C_r, \dot{C}_r$ | —             |
| PASSIVE OPTICAL  | 7°                | $C_D, \dot{C}_D$ | $C_r, \dot{C}_r$ | —             |

\*We have written partial derivatives permitting solution for  $\dot{C}_r$  and  $\ddot{a}$ . These parameters have not yet been allowed to adjust from their a priori value of zero.

## SECTION 8.0

### SOLUTION DESIGN

The design of a comprehensive gravity field solution is complicated by imperfections and incomplete knowledge in the mathematical models used to describe the tracking observations. Therefore, a certain degree of experimentation and testing of preliminary models is necessary. This section describes the method of solution adopted for GEM-T1, and relates how difficult decisions concerning data weighting were made.

#### 8.1 LEAST SQUARES COLLOCATION

The use of a modified least squares method was implemented in recent GEM models (Lerch et al., 1977) to permit a meaningful, stable solution of the satellite field to high degree and order. With the exception of GEM-10B and 10C, all of the post-GEM-7 solutions used this modified form of least squares, which includes a priori information on the power of the field. A general mathematical description of this method follows, with specific details relating to the development of GEM-T1 shown in the next subsection 8.2.

Conventional least squares simply minimizes the observation residuals (noise). However, high correlation between certain high degree and order coefficients in gravity solutions is a persistent problem when large fields are estimated. If uncontrolled, this results in excessively large values for the adjusted coefficients in the conventional least squares solution. By applying constraints in the form of a priori weights for the unknowns we essentially minimize both the signal (e.g., the size of the harmonic coefficients) and the noise (observation residuals) within the solution, thereby preventing an unreasonably powerful gravity solution.

The principle of least squares collocation is to minimize (see Moritz, 1980, Eq. 21.38):

$$Q = s^T K^{-1} s + n^T D^{-1} n \quad (8.1)$$

with respect to the unknowns  $y$ , where

$y$  - complete set of solution parameters for the geopotential, stations, earth orientation, tides and the orbit

$n$  - adjusted satellite observation residuals

$D$  - diagonal matrix for satellite observation residuals whose diagonal elements are the variances of the observations

$s$  - signal, which in our application consists of the harmonic (potential) coefficients representing a subset of  $y$ , with an expected value of zero

$K$  - diagonal matrix, where the diagonal elements are the degree variances per coefficient (see Moritz (*ibid*) Eqs. 21.23 and 21.52) of the potential.

In principle, there are infinitely many harmonics in the spectrum of the gravitational field, so  $K$  would be an infinite matrix. However, at satellite altitude, only a finite number of (lower degree) harmonics perturb orbits to the extent that these perturbations can be observed and separated from the measurement noise. Therefore, for space applications, it is reasonable to make the approximation of assuming that the expansion of the field is finite. This leads to a finite matrix  $K$ , which, as is shown, can readily be incorporated into the

adjustment. This is accomplished by adding  $K^{-1}$  to the usual normal matrix of Bayesian least squares created by GEODYN, which gives the desired normal matrix for minimizing (8.1). Further consideration on the wisdom of using this type of approximation can be found in Schwarz (1976, 1978) and Moritz (ibid) Chapter 21.

Let  $s$  represent the subset of  $y$  corresponding to the potential coefficients and  $x$  the subset of the other parameters. The  $y$  can be partitioned as:

$$y = \begin{bmatrix} x \\ s \end{bmatrix}. \quad (8.2)$$

Using the linear terms in the Taylor's series expansion of the measured variable (data)  $d$  and calling,

$$\lambda = d \text{ (observed)} - d \text{ (computed)},$$

one gets

$$\begin{aligned} \lambda &= Ax + Bs + n && \text{(where } A \text{ and } B \text{ are matrices of} \\ &&& \text{partial derivatives; this is} \\ &&& \text{Eq. (16.1) in Moritz (ibid))}. \end{aligned} \quad (8.3)$$

then minimizing  $Q$  in (8.1) above gives the normal equations

$$\begin{bmatrix} A^T D^{-1} A & A^T D^{-1} B \\ B^T D^{-1} A & B^T D^{-1} B + K^{-1} \end{bmatrix} \begin{bmatrix} x \\ s \end{bmatrix} = \begin{bmatrix} A^T D^{-1} \lambda \\ B^T D^{-1} \lambda \end{bmatrix} \quad (8.4)$$

which are the equations formed and solved with GEODYN and SOLVE, when the elements of  $K^{-1}$  are added to the main diagonals of the submatrix  $B^T D^{-1} B$  and the a priori values of  $s$  are chosen as zero. Moritz (ibid) employs a different formulation of the normal equations to arrive at the expressions needed for specific applications of least squares

collocation. We wish to show that equations (8.4) above are equivalent to those special cases of Moritz's equations that he and others have derived for satellite applications. For this purpose we may write the second matrix row equation of (8.4) as follows:

$$s = (B^T D^{-1} B + K^{-1})^{-1} (B^T D^{-1} \ell - B^T D^{-1} Ax) \quad (8.5)$$

and by substituting into this equation the matrix identity

$$(B^T D^{-1} B + K^{-1})^{-1} B^T D^{-1} = K B^T (BKB^T + D)^{-1} \quad (8.6)$$

it follows that

$$s = KB^T (BKB^T + D)^{-1} (\ell - Ax) \quad (8.7)$$

with

$$x = [A^T (BKB^T + D)^{-1} A] A^T (BKB^T + D)^{-1} \ell.$$

In Moritz ((ibid), Chapter 16), starting from (Eq. 16.1), which is the equivalent of (Eq. 8.3) above, he derives (Eq. 16.37):

$$s = C_{st} \bar{C}^{-1} (\ell - Ax) \quad \text{where, in Moritz's notation,}$$

$$C_{st} = KB^T, \quad \bar{C}^{-1} = (BKB^T + D)^{-1}.$$

Hence, in equation (8.7),  $(BK B^T + D)$  represents Moritz's autocovariance matrix  $\bar{C}$ , and  $KB^T$  is the cross-covariance matrix  $C_{st}$ , for a field with a "finite" harmonic expansion.

## 8.2 STRATEGY FOR DATA WEIGHTING AND FIELD CALIBRATION

As described in the previous section, the solution for high degree gravity coefficients is made reliable through the introduction of least squares collocation. For simplicity, and to permit a more thorough discussion of data weighting, let (8.1) be rewritten (see also Moritz (ibid), Chapter 28) as:

$$Q = \bar{f} \sum_{l,m} \frac{\bar{C}_{l,m}^2 + \bar{S}_{l,m}^2}{\sigma_l^2} + f \sum_{t \text{ obs}} \sum \frac{r_{it}^2}{\sigma_t^2} \quad (8.8)$$

where the calibration factors  $\bar{f}$  and  $f$  compensate for errors in the nominal  $\sigma_l^2$  and  $\sigma_t^2$ , as explained in what follows:

The values of the degree variances per coefficient  $\sigma_l^2$  are based on previous studies (Kaula, 1966), which show that they follow the general approximate rule:

$$\sigma_l = 10^{-5}/l^2 \quad (8.9)$$

(This means the power spectrum for the signal is referenced here to the ellipsoid instead of a more advanced geoidal model such as that found in contemporary gravity models. The signal matrix  $K^{-1}$  corresponds to the full power of the gravity field and not some correction to an existent model. In this way, our solution is independent of the coefficient values from earlier gravity models.)

Expression (8.9) has been obtained from the analysis of early sets of surface gravimetry and is known as "Kaula's rule" (1966). In (8.8),  $r_i$  is the  $i^{\text{th}}$  observation tracking residual from the  $t^{\text{th}}$  homogeneous data subset (e.g. laser ranging on LAGEOS). The weight  $\sigma_t^2$  given to these observations, is constant for all data in the  $t^{\text{th}}$  subset\* and largely reflects the accuracy of such data as reflected by the residuals seen in the solution.

Two factors,  $\bar{f}$  and  $f$  are introduced to scale the two terms in (8.1) relative to each other. The  $\bar{f}$  parameter, however, is not a free scaling parameter, for if

$$\bar{f} = 2 \quad (8.10)$$

is chosen, it improves Kaula's rule (8.9) so that the signal matrix better reflects the observed power found in contemporary gravity modeling studies (Wagner and Colombo, 1979; Lerch et al., 1979). The  $f$  parameter plays an equally important role. The use of data noise alone as a weighting factor in the solution causes the formal estimate of error to be optimistic due to the neglect of unmodeled effects other than noise as solution contaminants. Therefore,  $f$  is introduced to scale the least squares normal equations so that the resulting solution has more realistic error estimates, as shown by calibrations using independent data sources (see Section 10). The accuracy of the solution represented by (8.4) is also improved which is most important. In 8.4  $D^{-1}$  is scaled by  $f$  and  $K^{-1}$  by  $\bar{f}$ . Iteration on the solution weighting factors  $f$  and  $\bar{f}$  is generally required to converge on a near optimal answer.

---

\* with an occasional variation for a certain station as described in Section 5.

The GEM-9 and GEM-L2 solutions were based upon the size of the coefficients and the scaling of the standard errors in GEM-7. We used  $\bar{f} = 2$  and  $f = 1/10$  in GEM-9 and GEM-L2. Therefore, the noise only formal errors were scaled by  $\sqrt{10}$  to yield more realistic error estimates. The accuracy assessments for both GEM-9 and GEM-L2 were re-evaluated in Lerch et al (1985) and proved to be realistic, although for most terms the resulting uncertainties seemed pessimistic by about 30%.

Returning to expression (8.8), both the observation residuals,  $r_i$ , and the overall size of the gravity coefficients,  $\bar{C}_{l,m}$ ,  $\bar{S}_{l,m}$  are to be simultaneously minimized. The relationship between the scale factors,  $f$  and  $\bar{f}$ , needs to be chosen prior to the solution, and the weighting for specific data sets,  $\sigma_t^2$ , needs to be established and tested. A natural starting point for scaling the solution is to choose values for  $f$  and  $\bar{f}$  which were found to be optimal in earlier GEM solutions and then experimentally adjust these parameters. Each  $\sigma_t^2$  is nominally adopted and improved upon based on experience with the data. The final determination of  $\sigma_t^2$  must also take into account systematic errors enlarging a specific satellite's residuals due to errors in the modeling of non-conservative forces. Objects experiencing large drag perturbations, for example, are more likely to have larger drag modeling errors. These data sets must be downweighted to some (to be determined) level. The determination of all of these scaling parameters is described below.

If:

$N_t$  is the satellite normal matrix for a given observation type on a specific satellite with a priori weight  $w_{ot} = 1/\sigma_{ot}^2$  and scaled weight

$$w_t = \sigma_t^{-2} = w_t w_{ot}$$

where  $w_t$  is an additional weighting factor for  $N_t$ .

$K^{-1}$  is the scaled ( $f=2$ ) normal signal matrix for the potential coefficients (diagonal elements only) and is based on the observed power seen in the previous GEM-10B satellite gravity model as shown in (8.10):

$$K_{\ell,m}^{-1} = 1/\sigma_\ell^2 = 2\ell^4 \times 10^{10} \quad (8.11)$$

Then the combined reduced normal matrix for the gravity solution is given by:

$$C = K^{-1} + f \sum_t W_t M_t \quad (8.12)$$

(Ordinarily, to reduce the size of the combined normal matrix,  $M_t$  is used, and not  $N_t$ , where  $M_t$  is the reduced satellite normal matrix after back-substitution for the satellite specific orbital parameters.)

Ideally,  $W_t$  represents the formal accuracy of the data. In practice, this weight is adjusted to account for the general problem of incomplete information, where there are unmodeled and correlated errors in the observation residuals.  $W_t$  therefore is also used to balance the solution, ensuring that satellite residuals with large (systematic) unmodeled errors do not overwhelm it.

The  $K^{-1}$  matrix has certain important properties. First, it is unbiased in the sense that it does not favor any single gravity model, as the total field (above some degree and order), and not its adjustment, is minimized. To take an example, suppose a given coefficient does not contribute to the satellite signal. In the final solution, the determined value for this coefficient will be zero with the resulting uncertainty being 100% of its expected power. Although biased towards zero power, this is the best collocation estimate for any coefficient if no satellite information is present for its solution.  $K^{-1}$  is applied to terms above a certain degree cutoff. In GEM-T1, this cutoff was degree

5;  $K^{-1}$  has not directly been applied to the lowest degree and order terms (i.e., the corresponding diagonal terms in  $K^{-1}$  are set equal to zero).

The scaled error covariance for the coefficients is obtained as:

$$[\sigma_{\ell m}] = C^{-1} = [K^{-1} + f \sum W_t M_t]^{-1} \quad (8.13)$$

where choosing the overall scale factor of  $f=1$  produces errors from the diagonal elements of  $C^{-1}$  which are overly optimistic. Therefore,  $f$  is adjusted to produce realistic error estimates for the optimally weighted solution.

Table 8.1 presents a list of the independent data tests used to evaluate the scaling and data weights of the solution. Many of these test results are described more fully in the accuracy and calibration sections of this report. An example of the tests spanning different solutions are shown in Table 8.2. Herein, the factor,  $f$ , and certain data weights were varied. Differing results were obtained since  $\bar{f}$ , as expected, was held constant. Therefore, the relative balance of the  $K^{-1}$  and the rest of the normal matrix has been altered. The models which were obtained were tested here using:

- An estimate of gravity model error for the field truncated respectively at degrees 10, 20 and 36 obtained from intercomparisons with global surface gravimetry (described fully in Section 10);
- An estimate of complete gravity model error at degree 36 obtained from comparisons with  $5 \times 5$  degree gravity anomaly blocks determined from SEASAT altimetry; and
- The weighted residual obtained from the models when they are used to predict the longitude acceleration of 10 independently studied 24-hour satellites.

Table 8.2 presents results for a small subset of the testing that the fields undergo, and it shows clearly that experimentally varying the data weights can significantly alter the tested performance of the gravity model solutions. In particular, notice the degradation in field performance which results when  $f$  is increased from .02 to .1 as was done in the computation of PGS 3013. This is especially apparent in the test against independent surface gravity data. (PGS 3013 is discussed further in Section 10.2).

The values employed for  $W_t$  in (8.13) are also critically evaluated. As shown in Table 8.3, the post-solution RMS of fit of the data using an improved geopotential model can give preliminary values for these parameters.

In an ideal case, the potential coefficient diagonal elements of each satellite's combined normal matrix would reflect the total sensitivity this orbit had to a given gravity harmonic. This ideal case requires complete global coverage and complete orbital information at every point along the orbit (not the incomplete information that a typical tracking observation, for example, a range to the satellite, contains). The sizes of the actual diagonal elements are important when balancing a multi-satellite solution, but the off-diagonal information must also be considered. This is certainly the case when dealing with real (limited) observation histories.

Information obtained through a study of the diagonal elements on the contributions  $M_t$  of the individual satellites normal matrices are useful in determining  $W_t$ . Figure 8.1 shows the RMS contribution (percentage by degree) for each of the satellite-specific normals to the diagonal elements of the combined normal matrix when the data are weighted using the  $W_t$  values finally adopted for GEM-T1. (The four laser data sets from BE-C, GEOS-1, GEOS-2 and GEOS-3 are combined into

TABLE 8.1

DATA AND CRITERIA EMPLOYED  
FOR EVALUATING AND ADJUSTING  
WEIGHTS IN SOLUTIONS

- SATELLITE TRACKING DATA ON SELECTED ORBITAL ARCS
- $5^\circ \times 5^\circ$  SET OF SEASAT ALTIMETER DERIVED ANOMALIES
- KAULA ERROR ESTIMATE OF GRAVITY ANOMALY FOR SATELLITE DERIVED MODEL BASED UPON A  $5^\circ \times 5^\circ$  SET OF GLOBAL TERRESTRIAL GRAVITY ANOMALY DATA
- SATELLITE ACCELERATIONS IN LONGITUDE FOR 24 HR. ORBITS DERIVED BY WAGNER (private communication) FOR TEN SATELLITES TO TEST LOW DEGREE ( $\ell \leq 6$ ) TERMS
- SEASAT ALTIMETER CROSSOVERS
- DIAGONAL TERMS OF WEIGHTED NORMAL EQUATIONS OF EACH SATELLITE OBS. DATA TYPE FOR RELATIVE SENSITIVITY ANALYSIS
- PERCENT REDUCTION OF ERROR VARIANCES OF GRAVITY COEFFICIENTS DUE TO EACH SATELLITE DATA TYPE IN SOLUTION
- CONDITION NUMBERS OF SOLUTION PARAMETERS
- EFFECT ON SOLUTION TESTS BY REMOVAL OF SATELLITE DATA TYPES FROM SOLUTION

Table 8.2  
TEST RESULTS FOR  
EVALUATING AND ADJUSTING  
WEIGHTS

| MODEL    | DESCRIPTION                     | KAULA       |   |                 | 24 HR.                 |                           |
|----------|---------------------------------|-------------|---|-----------------|------------------------|---------------------------|
|          |                                 | DATA WEIGHT | GRAV. ANOM.<br>ERROR (MGAL <sup>2</sup> ) | DEG. TRUNCATION | SEASAT ANOM.<br>RESID. | SAT. ACCEL.<br>(WEIGHTED) |
|          |                                 | 1           | 10  | 20              | 36                     | MGAL <sup>2</sup>         |
| PGS-T2   | TOPEX AGU SOL.                  | .02         | 2.3                                       | 5               | 8                      | 35                        |
| PGS-3013 | 5 X DATA WT.<br>OF T2           | .10         | 3.0                                       | 13              | 31                     | 48                        |
| PGS-3016 | GEOSS-2 DOWN-<br>WEIGHTED IN T2 | .02         | 2.2                                       | 4               | 6                      | 33                        |
| PGS-T3   | T2 DATA WITH<br>3 LOW-INC SATS  | .02         | 1.1                                       | 3               | 5                      | 31                        |
| PGS-3026 | 2 X DATA WT.<br>OF T3           | .04         | 1.2                                       | 4               | 10                     | 32                        |
| GEM-T1   | NEW TOPEX FIELD                 | .02         | 1.1                                       | 3               | 5                      | 29                        |

Table 8.3

## RELATIVE WEIGHT ESTIMATES TEST CASE

RMS OF SATELLITE OBSERVATION RESIDUALS  
FROM TEST FIELD (PGS-T2 TYPE)

$$w_t^* = \sigma_{ot}^2 / RMS_t^2$$

| <u>TYPE j</u><br><u>(LASER DATA)</u> | <u>APRIORI</u><br><u><math>\sigma_{obj}</math></u> | <u>RMS<sub>t</sub></u> | <u>w<sub>t</sub>**</u> |
|--------------------------------------|--|------------------------|------------------------|
| LAGEOS                               | 1 m  | .1 m                   | 100                    |
| STARLETTE                            | 1  | .2                     | 25                     |
| BE-C                                 | 1  | .5                     | 4                      |
| GEOS-1                               | 1  | .7                     | 2                      |
| GEOS-2                               | 1  | .8                     | 1.6                    |
| GEOS-3                               | 1  | .7                     | 2                      |
| <hr/>                                |  |                        |                        |
| <u>DOPPLER</u>                       |  |                        |                        |
| OSCAR                                | 1 cm/sec   | 1.2                    | 0.7                    |
| SEASAT                               | 1  | .6                     | 2.8                    |

\*  $w_t = w_t^* / \sigma_{ot}^2 = 1 / RMS_t^2$  where  $\sigma_{ot}^2$  is the a priori value in the normal equations  $N_t$ .

\*\* Because of the relative amounts of data quantity and other factors, further adjustment is considered for relative weighting.

one matrix labeled "4-LASER-SATS" in Figure 8.1). The diagonal elements per se tell an incomplete story. STARLETTE seems to contribute a disproportionately large amount of information to the solution based on Figure 8.1. However, when the individual satellites are evaluated in terms of their specific contribution to the reduction of the error degree-variances within the combined solution (looking at the aposteriori variance-covariance matrix), one sees (Figure 8.2) that the 4-LASER and LAGEOS data now control the solution for low degree terms through degree 13, and STARLETTE is no longer dominant. The impact of optical observations on the solution is nearly completely lost in Figure 8.1, showing an insignificant contribution to the solution's diagonal elements. However, as shown in Figure 8.2, the optical data makes significant contributions to the solution (which must be through off-diagonal conditioning) for the resonance ( $m=11$  through 15) and zonal ( $m=0$ ) orders. Generally, it is desirable to obtain a solution which has significant contributions from many satellite data sets (as is evidenced in Figure 8.2), for this tends to average-out satellite-specific error sources. Summing up: the data weights used in GEM-T1 (Figure 8.2) have been selected in an attempt to assure a balanced multi-satellite solution.

The diagonal elements can also be used diagnostically. A study of the diagonal elements of the four-laser satellites (which were combined to form a single matrix), revealed an anomaly for GEOS-2. This is shown in Figure 8.3. The diagonal elements for this satellite's contribution were originally too large. A physical explanation for this effect was not found through a study of the magnitude of first-order gravity perturbation estimates for this satellite. Therefore an error in our processing of the normal equations from this satellite was investigated. A software problem in the back-substitution of the orbital parameters, when a priori weights were introduced on the drag parameters, was uncovered and corrected in GEM-T1. The PGS-T2 model contained this erroneous treatment of the GEOS-2 matrices and was also

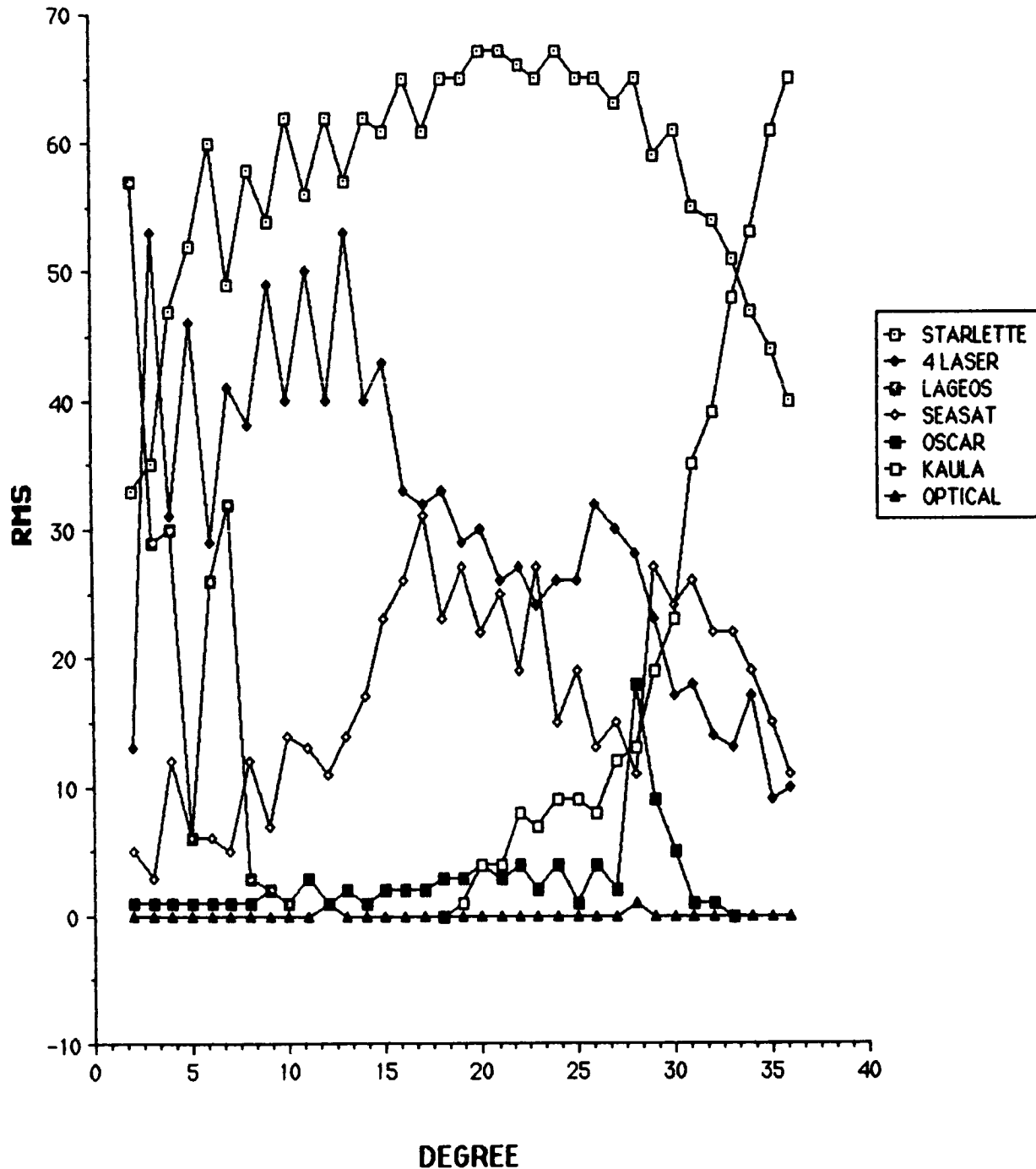


Figure 8.1. RMS of Percentages of Ratios of Diagonals Per Degree  
Comparing Major Data Types in PGS-T2.

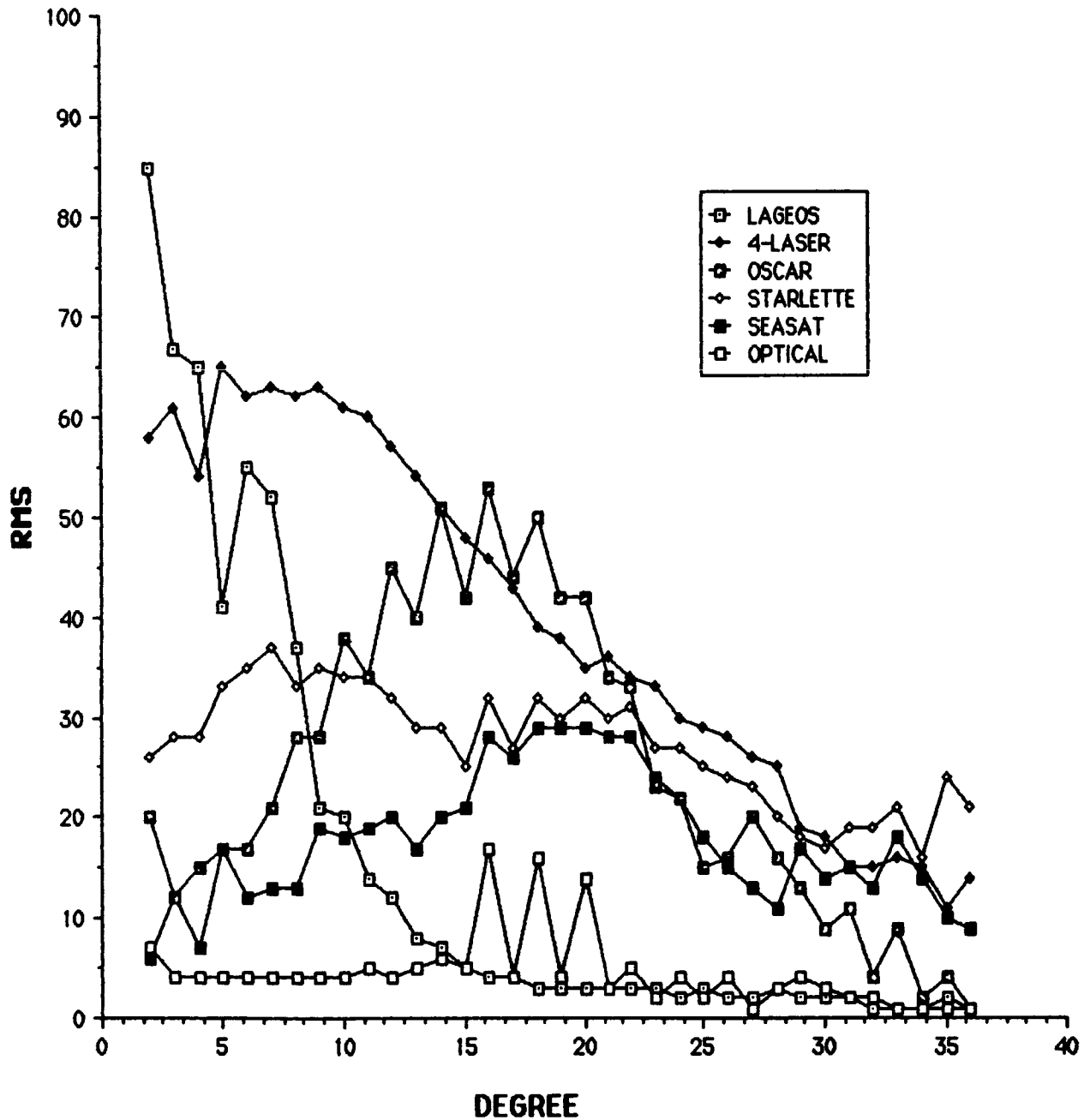


Figure 8.2. Percent Reduction of Error Variances Due to Major Data Types in Solution.

### OF 4-LAS DATA IN COMPARISON WITH PGS-T2

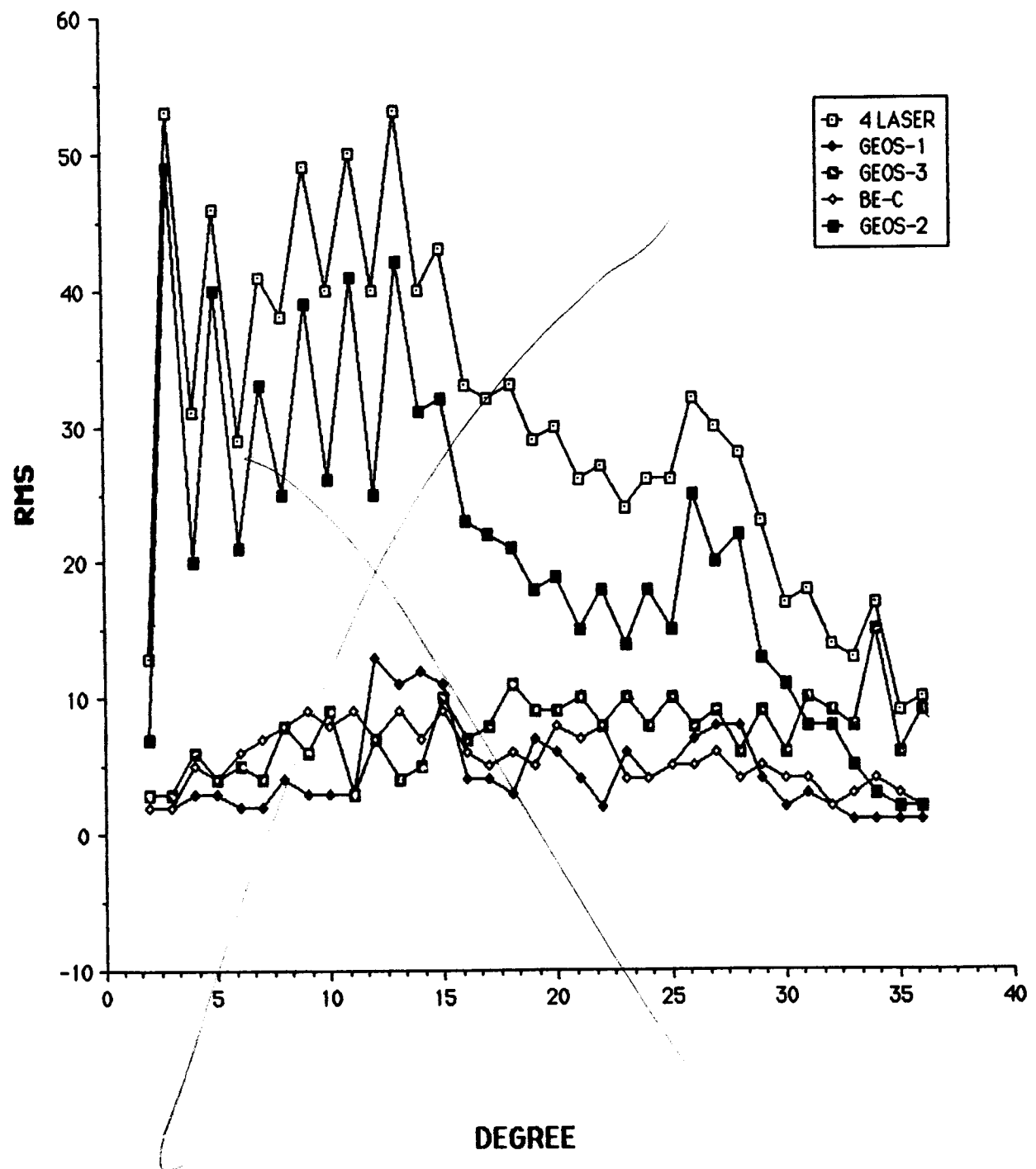


Figure 8.3. RMS of Percentages of Ratios of Diagonals Per Degree.

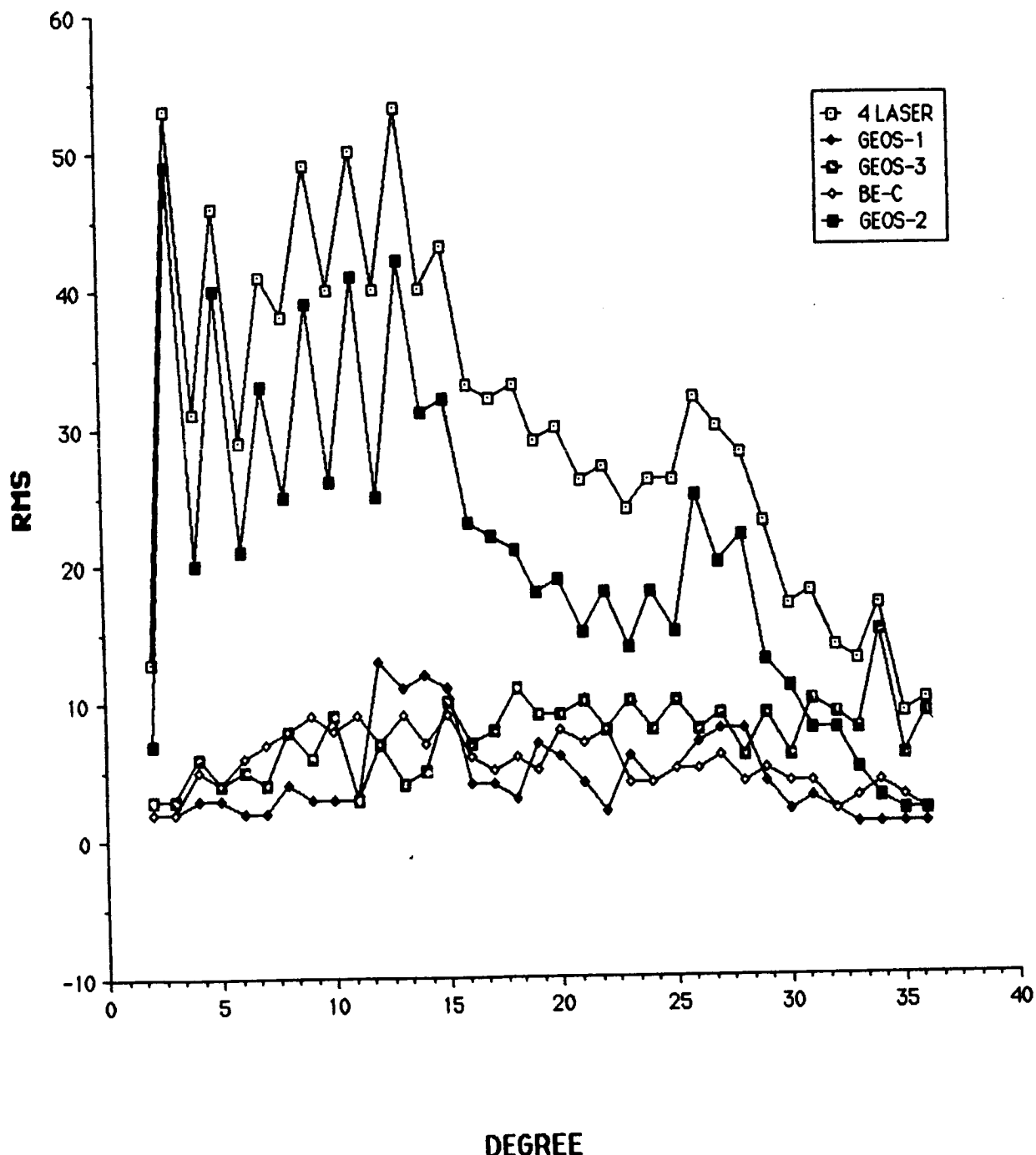


Figure 8.3. RMS of Percentages of Ratios of Diagonals Per Degree Comparing the 4 Laser Satellite Contributions Within PGS-T2.

| <u>TOTAL DATA</u>   |             |            | <u>GEM-T1 RELATIVE WEIGHTS (<math>w_t</math>)</u> |               |
|---|-------------|------------|---|---------------|
| <u>SAT</u>  | <u>ARCS</u> | <u>OBS</u> | <u>PGS-T2</u>                                     | <u>GEM-T1</u> |
| LAGEOS  | 58          | 144529     | 40  | 40            |
| STARLETTE   | 46          | 57356      | 10  | 10            |
| 4-LAS*  | 151         | 204547     | 1   | 1*            |
| SEASAT LASER  | 14          | 14923      | 1   | 1             |
| SEASAT DOPPLER  | 14          | 129604     | 1   | 1             |
| OSCAR DOPPLER   | 13          | 63098      | 1   | 0.75          |
| 6-OPT*  | 219         | 139818     | 5   | 5*            |
| LOW INC (OPT)*  | 49          | 4461       | --  | 5*            |
| LOW INC (LAS)*  | 16          | 23055      | --  | 1*            |
| <b>WEIGHT MULTIPLYING FACTOR (<math>f</math>) . . . . .</b> |             |            | <b>.02</b>  | <b>.02</b>    |
| <b>KAULA WT. (<math>10^{-5}/\theta^2</math>) . . . . .</b>  |             |            | <b>2</b>  | <b>2</b>      |

\*GEM-T1 ADDITIONAL SCALE FACTOR ( $w_t$ )

| <u>4-LAS</u> | <u>ARCS</u> | <u>OBS</u> | <u><math>w_t</math></u> | <u>LOW INCLIN</u>  | <u>ARCS</u> | <u>OBS</u> | <u><math>w_t</math></u> |
|--------------|-------------|------------|-------------------------|--------------------|-------------|------------|-------------------------|
| GEOS-1       | 48          | 71287      | 1.13                    | COURIER-1B (OPT)   | 10          | 2476       | 2.00                    |
| GEOS-2       | 28          | 26613      | .75                     | VANGUARD-2RB (OPT) | 10          | 686        | 2.00                    |
| GEOS-3       | 36          | 42407      | .75                     | VANGUARD-2 (OPT)   | 10          | 1299       | 2.00                    |
| BE-C         | 39          | 64240      | 1.50                    | DI-C (OPT)         | 10          | 2712       | .75                     |
|              |             |            |                         | DI-C (LAS/<br>OPT) | 4           | 7455       | .75                     |
| <u>6-OPT</u> |             |            |                         |                    |             | 159        |                         |
| BE-B         | 20          | 1739       | 2.0                     |                    |             |            |                         |
| BE-C         | 50          | 7501       | 1.3                     | DI-D (OPT)         | 9           | 6111       | .50                     |
| GEOS-1       | 43          | 60750      | .5                      | DI-D (LAS/<br>OPT) | 6           | 11487      | .75                     |
| GEOS-2       | 46          | 61403      | .5                      |                    |             | 146        |                         |
| ANNA-1B      | 30          | 4463       | 2.0                     | PEOLE (LAS)        | 6           | 4113       | .75                     |
| TELSTAR      | 30          | 3962       | 2.0                     |                    |             |            |                         |
| <b>ALTIM</b> |             |            |                         |                    |             |            |                         |
| SEASAT       | 8           | 14093      |                         |                    |             |            |                         |

| DATA ERRORS ( $\sigma$ ) FOR WEIGHT = 1 |                                       |
|---|---------------------------------------|
| <u>DATA</u>                             | <u><math>\sigma</math> (A PRIORI)</u> |
| LASER                                   | 1 m                                   |
| DOPPLER                                 | 1 cm/sec                              |
| OPTICAL                                 | 2 arc seconds                         |
| ALTIM                                   | 1 m                                   |

Figure 8.4. GEM-T1 TOPEX Data and Weighting.

sensitivity to resolve every coefficient to this degree. Therefore, an external estimate of the size of the coefficients was used as a constraint to stabilize the solution. There is an important benefit in solving for a complete 36 X 36 field. We have found that aliasing in the middle degrees of the model has been avoided through this relatively high degree and order solution. And the destabilizing lack of sensitivity to a subset of the coefficients is compensated through the application of least squares collocation, which keeps coefficient errors within less than 100% of the size of the coefficients predicted from independent gravimetry. However, there are certain problems in carrying out such a large solution that need to be discussed.

Firstly, the application of Kaula's rule as a constraint is equivalent to introducing a set of additional observations of the coefficients where their expected values are all zero, with a scaled version of Kaula's power estimate used as a variance on these "observations". This rule represents a mild use of a priori information on the determination of low degree terms, constraining the coefficient only to the approximate power spectrum of gravimetry. However, because some sensitivity is lacking for high degree terms, this collocation constraint has caused the coefficients in GEM-T1 above degree 25 to have less power than the "true" gravity field. And at degree 36, GEM-T1 power is about 1/3 to 1/2 of that seen in fields which used altimetry and surface gravity. While this is troublesome, it should be noted that if no adjustment is made of these high degree terms (i.e., the harmonic model is truncated at a lower degree cutoff) then these terms would be absolutely constrained to zero (as are all terms above the field limits). Hence, with least squares collocation there is a gradual decay in the power spectrum instead of a sharp drop to zero at the point of truncation within the field. In this sense, collocation can be viewed as permitting more power in the solved for short wavelength gravity field, for the model, although constrained, can be extended to much higher degree through the use of this technique.

Altimetry and surface gravimetry provide strong sensitivity to harmonics up to degree 360 and higher in the gravity model. Eventual use of this data in future solutions will overcome the shortcomings of GEM-T1, where a total reliance on satellite data, due to attenuation, causes incomplete resolution of all higher degree gravity terms. Figure 8.5 presents a comparison of the degree variances found in GEM-T1 with those in GEM-10B. GEM-10B is a comprehensive model which used GEOS-3 altimetry and surface gravity data and therefore did not require any form of constraint on the size of the coefficients. The lack of high-degree power for the GEM-T1 model is evident. Interestingly, when preliminary altimetry data sets are even weakly introduced into GEM-T1, (forming PGS3163), the power is much closer to the level seen in GEM-10B (see Figure 8.5). PGS3163 is discussed further in the Calibration Section (Section 10) of this report.

We also believe that the use of Kaula's rule as a constraint may have altered the high-degree terms' covariances, indicating less cross-correlation among these coefficients than is truly found in the overall orbital signal sampled by our selection of satellites. Therefore, calibrations using objects passing through deep resonance may be biased if the full covariance of GEM-T1 is utilized.

However, tests against independent altimeter data show there is valuable information in GEM-T1 above degree 25 and although the coefficients are small, they do improve the orbital fits obtained by this field. Therefore, this 36 degree level of truncation was adopted for GEM-T1. Plans for future efforts are to merge the GEM-T1 database with other observations obtained by altimetric, satellite-to-satellite tracking, and surface gravity data sources. These more comprehensive solutions will be free of the constraint imposed on the GEM-T1 "satellite-only" model. In spite of some limitations, the GEM-T1 solution is a very accurate model at long and intermediate wavelengths, as shown in the next paragraph.

**DEGREE VARIANCES OF  
GEM-T1, GEM 10B AND  
PGS-3163 (GEM T1 + ALTIMETRY)**

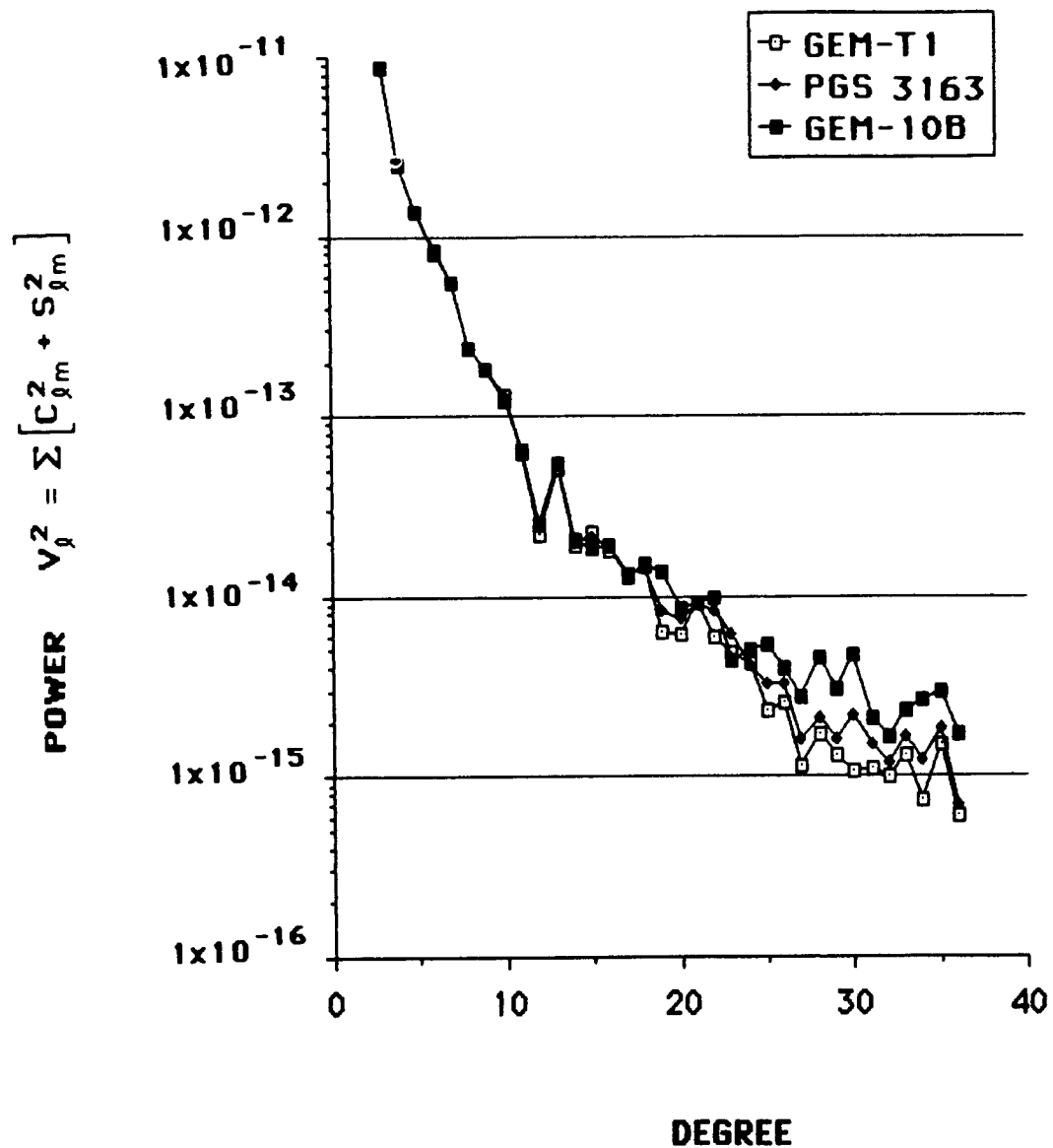


Figure 8.5. Degree Variance Comparison for Recent Models.

An experiment was conducted showing the effect on the GEM-T1 solution of removing the collocation term  $\bar{f}K^{-1}$ . This was accomplished by setting  $\bar{f}=0$ . Figure 8.6 compares this test model and GEM-T1 with independent  $5^\circ \times 5^\circ$  gravity anomalies derived from SEASAT altimetry (Rapp, 1983a) at different levels of field truncation. In the case of the test field, the ordinary least squares method (with  $\bar{f}=0$ ) could not be successfully solved beyond degree 25. The comparison in Figure 8.6 shows that a gravity solution which lacks collocation rapidly becomes unreliable above degree 18, with an excessively large power spectrum found for terms beyond this point.

Although GEM-T1 has a weak power spectrum for its terms beyond degree 25, there are strong benefits achieved in solving for a complete  $36 \times 36$  model and using a least squares collocation approach. This is demonstrated in Figure 8.7 where GEM-T1 has been solved only complete to degree  $20 \times 20$  (yielding PGS-3167) which is the same size as the earlier GSFC GEM-L2 (Lerch et al., 1983) solution. The same gravity anomaly comparison as described in the previous paragraph shows little improvement of PGS-3167 over that of GEM-L2, and clearly inferior field performance compared to what has been achieved in GEM-T1.

The addition of the Cyber 205 computer allowed evaluation and solution of larger gravity models with a consistent reduction and formation of normal matrices for all data sets which was not possible during earlier times. This factor greatly contributed to the development of a complete  $36 \times 36$  model. GEM-T1 was the result. Previously, this  $36 \times 36$  option could not be explored due to the enormous computer resources which would have been required.

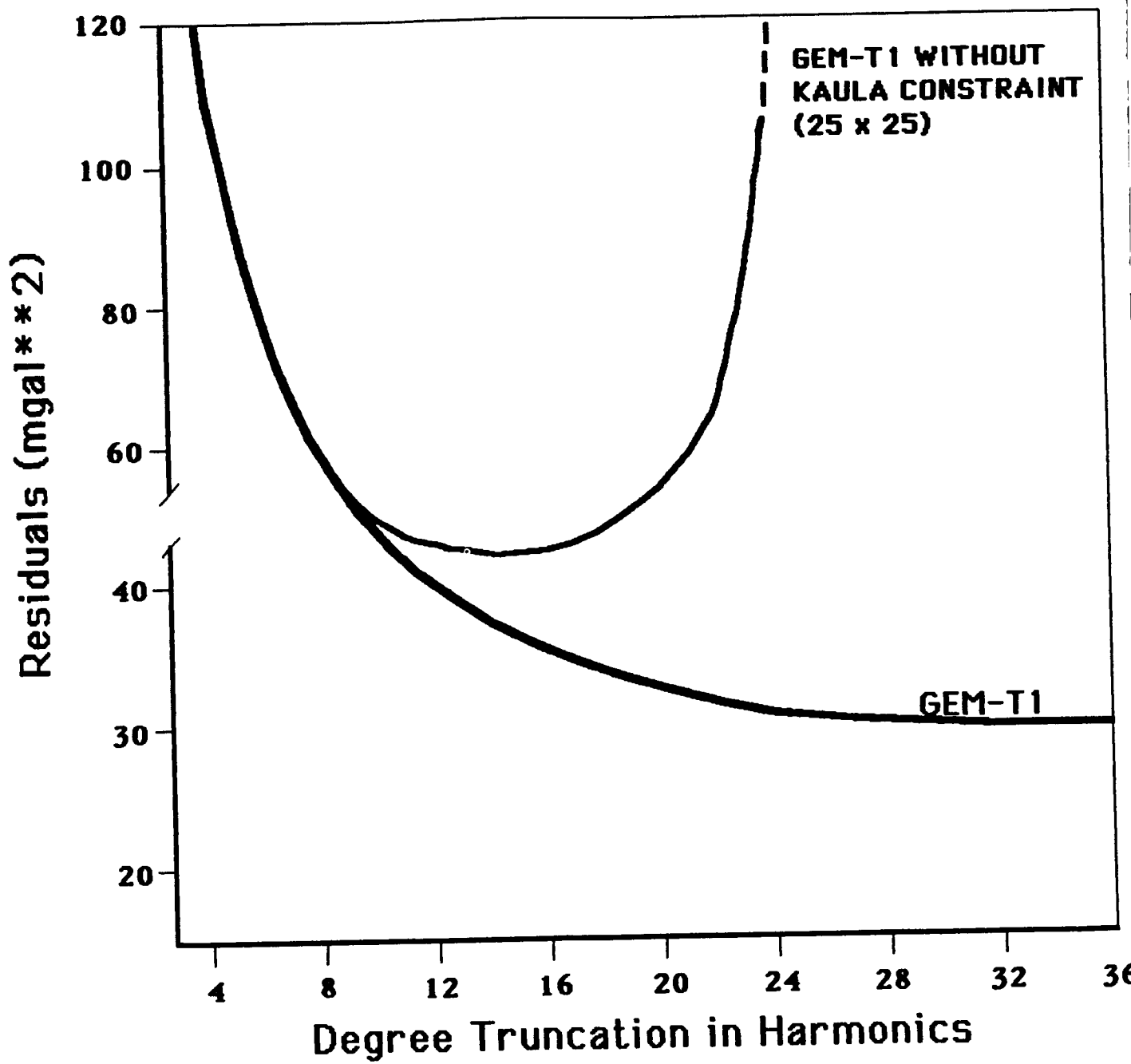


Figure 8.6. Gravity Model Comparison with 1114  $5^\circ \times 5^\circ$  SEASAT Gravity Anomalies: GEM-T1 With and Without Collocation.

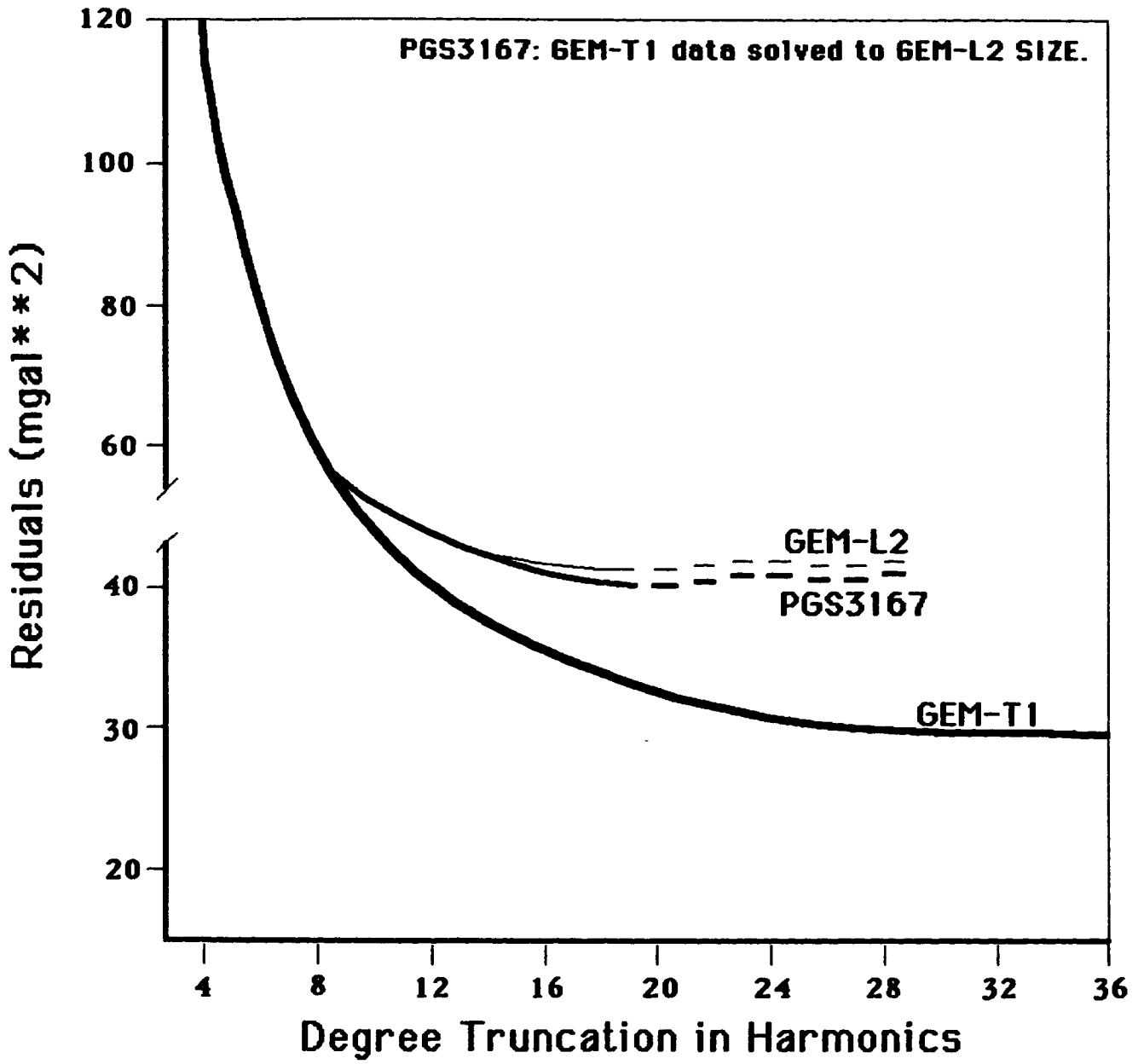


Figure 8.7. Gravity Model Comparison With 1114  $5^\circ \times 5^\circ$  SEASAT Gravity Anomalies: GEM-T1 Solved to  $20 \times 20$ .

SECTION 9.0  
THE GEM-T1 SOLUTION RESULTS

9.1 THE GRAVITY MODEL

Table 9-1 presents the coefficient values which were obtained for the GEM-T1 gravity model. The model is complete to degree and order 36, and has been obtained from a data set consisting exclusively of ground based satellite tracking. To stabilize the coefficient adjustment (see Section 8), a mild constraint on the size of the coefficients was used to eliminate unstable adjustment of correlated high degree terms. This model is more complete than previous GSFC "satellite-only" models, which in the past were only solved completely to degree 20, with isolated higher degree resonant and zonal terms (GEM-9:Lerch et al, 1979; GEM-L2: Lerch et al, 1982). The remainder of this document discusses the GEM-T1 parameters and their calibrated accuracies in detail. An extensive error analysis to establish field uncertainty is described in Sections 10 and 11. A contour map of the GEM-T1 geoid is presented in Figure 9.0. The geoid was computed using the potential coefficients of Table 9.1 in Brun's formula (Heiskanen and Moritz, 1967, p. 85).

9.2 OCEAN TIDE SOLUTION

With the advent of centimeter level satellite geodesy and geodynamics, it has become necessary to accurately model the deformation of the earth and its oceans due to tides, i.e., the temporal variations of the geopotential, in order to obtain accurate estimates of the static geopotential coefficients. This is in part because the data distribution in time and space cannot be selected so that the effects of these temporal variations average out.

PRECEDING PAGE BLANK AND FOLDED

Table 9.1  
GEM-T1 NORMALIZED COEFFICIENTS  
UNITS OF  $10^{-6}$

| ZONALS                   |       |              |            |       |            |            |            |            |       |            |            |
|--------------------------|-------|--------------|------------|-------|------------|------------|------------|------------|-------|------------|------------|
| INDEX                    | VALUE | INDEX        | VALUE      | INDEX | VALUE      | INDEX      | VALUE      | INDEX      | VALUE | INDEX      | VALUE      |
| N                        | N     | N            | N          | N     | N          | N          | N          | N          | N     | N          | N          |
| 2                        | 0     | -484.1649906 | 3          | 0     | 0.9572375  | 4          | 0          | 0.5387322  | 5     | 0          | 0.0687802  |
| 7                        | 0     | 0.0905337    | 8          | 0     | 0.0459023  | 9          | 0          | 0.0283764  | 10    | 0          | 0.0572211  |
| 12                       | 0     | 0.0320806    | 13         | 0     | 0.0422319  | 14         | 0          | -0.0197327 | 15    | 0          | 0.0018731  |
| 17                       | 0     | 0.0203968    | 18         | 0     | 0.0112912  | 19         | 0          | -0.0046084 | 20    | 0          | 0.0153150  |
| 22                       | 0     | -0.0048440   | 23         | 0     | -0.0241260 | 24         | 0          | -0.0009556 | 25    | 0          | 0.0068867  |
| 27                       | 0     | 0.0041234    | 28         | 0     | -0.0058541 | 29         | 0          | -0.0039091 | 30    | 0          | -0.0002749 |
| 32                       | 0     | 0.0000819    | 33         | 0     | 0.0022286  | 34         | 0          | -0.0024803 | 35    | 0          | 0.0012731  |
| SECTORIALS AND TESSERALS |       |              |            |       |            |            |            |            |       |            |            |
| INDEX                    | C     | VALUE        | S          | INDEX | C          | VALUE      | S          | INDEX      | C     | VALUE      | S          |
| N                        | M     |              |            | N     | M          | C          |            | N          | M     | C          |            |
| 2                        | 2     | 2.4389280    | -1.3998397 |       |            |            |            |            |       |            |            |
| 3                        | 1     | 2.0297737    | 0.2495946  | 3     | 2          | 0.9035491  | -0.6204198 | 3          | 3     | 0.7209866  | 1.4131694  |
| 4                        | 1     | -0.5334272   | -0.4751189 | 4     | 2          | 0.3470021  | 0.6640304  | 4          | 3     | 0.9909779  | -0.2006215 |
| 4                        | 4     | -0.1900348   | 0.3084595  |       |            |            |            |            |       |            |            |
| 5                        | 1     | -0.0589503   | -0.0955435 | 5     | 2          | 0.6557902  | -0.3234056 | 5          | 3     | -0.4482036 | -0.2151363 |
| 5                        | 4     | -0.2948236   | 0.0524087  | 5     | 5          | 0.1777563  | -0.6660281 |            |       |            |            |
| 6                        | 1     | -0.0813751   | 0.0238900  | 6     | 2          | 0.0516096  | -0.3749956 | 6          | 3     | 0.0619709  | 0.0464430  |
| 6                        | 4     | -0.0927975   | -0.4733069 | 6     | 5          | -0.2657650 | -0.5377472 | 6          | 6     | 0.0090593  | -0.2363344 |
| 7                        | 1     | 0.2770971    | 0.9978177  | 7     | 2          | 0.3177108  | 0.0916083  | 7          | 3     | 0.2507429  | -0.2091639 |
| 7                        | 4     | -0.2737404   | -0.1220207 | 7     | 5          | 0.0034750  | 0.0196519  | 7          | 6     | -0.3578527 | 0.1509175  |
| 7                        | 7     | 0.0015976    | 0.0220013  |       |            |            |            |            |       |            |            |
| 8                        | 1     | 0.0288561    | 0.0547223  | 8     | 2          | 0.0703801  | 0.0684494  | 8          | 3     | -0.019664  | -0.0869367 |
| 8                        | 4     | -0.2460639   | 0.0677453  | 8     | 5          | -0.0249335 | 0.0853003  | 8          | 6     | -0.0664178 | 0.3128323  |
| 8                        | 7     | 0.0704248    | 0.0748626  | 8     | 8          | -0.1188827 | 0.1223320  |            |       |            |            |

*Table 9.1*  
**GEM-T1 NORMALIZED COEFFICIENTS (continued)**  
 UNITS OF  $10^{-6}$

SECTORIALS AND TESSERALS

| INDEX |    |            | INDEX      |    |    | INDEX      |            |    | INDEX |            |            |
|-------|----|------------|------------|----|----|------------|------------|----|-------|------------|------------|
| N     | M  | C          | N          | M  | S  | N          | M          | C  | N     | M          | S          |
| 9     | 1  | 0.1480447  | 0.0245251  | 9  | 2  | 0.0311365  | -0.0323882 | 9  | 3     | -0.1553742 | -0.0840158 |
| 9     | 4  | -0.0128303 | 0.0232637  | 9  | 5  | -0.0141122 | -0.0600627 | 9  | 6     | 0.0705263  | 0.2166285  |
| 9     | 7  | -0.1186233 | -0.1005510 | 9  | 8  | 0.1844954  | -0.0018494 | 9  | 9     | -0.0555457 | 0.0975889  |
| 10    | 1  | 0.0769655  | -0.1381110 | 10 | 2  | -0.0805212 | -0.0513356 | 10 | 3     | 0.0013119  | -0.1614824 |
| 10    | 4  | -0.0973123 | -0.0693825 | 10 | 5  | -0.0504401 | -0.0438269 | 10 | 6     | -0.0347366 | -0.0777189 |
| 10    | 7  | 0.0097468  | -0.0042901 | 10 | 8  | 0.0437468  | -0.0924808 | 10 | 9     | 0.1281797  | -0.0481860 |
| 10    | 10 | 0.0945596  | -0.0201041 |    |    |            |            |    |       |            |            |
| 11    | 1  | 0.0095019  | -0.0278111 | 11 | 2  | 0.0090541  | -0.092414  | 11 | 3     | -0.0288895 | -0.1324693 |
| 11    | 4  | -0.0332108 | -0.0700036 | 11 | 5  | 0.0459086  | 0.0552848  | 11 | 6     | 0.0084723  | 0.0242910  |
| 11    | 7  | 0.0096093  | -0.0918891 | 11 | 8  | -0.0063530 | 0.0225827  | 11 | 9     | -0.0387774 | 0.0402849  |
| 11    | 10 | -0.0520582 | -0.0176126 | 11 | 11 | 0.0543322  | -0.0547288 |    |       |            |            |
| 12    | 1  | -0.0492610 | -0.0496520 | 12 | 2  | 0.076400   | 0.0349183  | 12 | 3     | 0.0324198  | 0.0179438  |
| 12    | 4  | -0.0653020 | -0.0030125 | 12 | 5  | 0.0306040  | -0.0014745 | 12 | 6     | 0.0013881  | 0.0458328  |
| 12    | 7  | -0.0126975 | 0.0348291  | 12 | 8  | -0.0212177 | 0.0169046  | 12 | 9     | 0.0469380  | 0.0132223  |
| 12    | 10 | -0.0091273 | 0.0316782  | 12 | 11 | 0.0054143  | -0.0095228 | 12 | 12    | -0.0035280 | -0.0117964 |
| 13    | 1  | -0.0540617 | 0.0434555  | 13 | 2  | 0.0534361  | -0.0575844 | 13 | 3     | -0.0140259 | 0.0836615  |
| 13    | 4  | -0.0881882 | -0.0003732 | 13 | 5  | 0.0596176  | 0.0574460  | 13 | 6     | -0.0223869 | -0.0118360 |
| 13    | 7  | 0.0035736  | -0.0061717 | 13 | 8  | -0.0122964 | -0.0110925 | 13 | 9     | 0.0203827  | 0.0457820  |
| 13    | 10 | 0.0433028  | -0.0380383 | 13 | 11 | -0.0401906 | 0.0055015  | 13 | 12    | -0.0280059 | 0.0864102  |
| 13    | 13 | -0.0615483 | 0.0682661  |    |    |            |            |    |       |            |            |
| 14    | 1  | -0.0187462 | 0.0232244  | 14 | 2  | -0.0348122 | -0.0060681 | 14 | 3     | 0.0369311  | 0.0224222  |
| 14    | 4  | -0.088329  | 0.0018783  | 14 | 5  | 0.0227952  | -0.016078  | 14 | 6     | -0.0031868 | 0.0065119  |
| 14    | 7  | 0.0374843  | -0.0033588 | 14 | 8  | -0.0329416 | -0.0131814 | 14 | 9     | 0.0371609  | 0.0179332  |
| 14    | 10 | 0.0369953  | -0.0027966 | 14 | 11 | 0.0080835  | -0.0413614 | 14 | 12    | 0.0089681  | -0.0320668 |
| 14    | 13 | 0.0315333  | 0.0446234  | 14 | 14 | -0.0505657 | -0.0063741 |    |       |            |            |
| 15    | 1  | 0.0082868  | 0.0142124  | 15 | 2  | -0.0216258 | -0.0364425 | 15 | 3     | 0.0446271  | 0.0265447  |
| 15    | 4  | -0.0443760 | 0.0126416  | 15 | 5  | 0.0160742  | 0.0108864  | 15 | 6     | 0.0272318  | -0.0517077 |
| 15    | 7  | 0.0667130  | 0.014545   | 15 | 8  | -0.0406660 | -0.0247325 | 15 | 9     | 0.0134441  | 0.0410187  |
| 15    | 10 | 0.0095928  | 0.0160812  | 15 | 11 | 0.0017171  | 0.0289322  | 15 | 12    | -0.0283317 | 0.0124872  |
| 15    | 13 | -0.0281051 | -0.0049829 | 15 | 14 | 0.0061707  | -0.0256132 | 15 | 15    | -0.0180968 | -0.0080854 |

*Table 9.1*  
**GEM-T1 NORMALIZED COEFFICIENTS (continued)**  
 UNITS OF  $10^{-6}$

SECTORIALS AND TESSERALS

| INDEX<br>N<br>M | C<br>VALUE | S          | INDEX<br>N<br>M | C<br>VALUE | S          | INDEX<br>N<br>M | C<br>VALUE | S           |
|-----------------|------------|------------|-----------------|------------|------------|-----------------|------------|-------------|
| 16 1            | 0.0317099  | 0.0173493  | 16 2            | -0.0156437 | 0.0245431  | 16 3            | -0.0320841 | -0.0450272  |
| 16 4            | 0.0365123  | 0.0438559  | 16 5            | -0.0077242 | -0.0016773 | 16 6            | 0.0179449  | -0.0267835  |
| 16 7            | 0.0030511  | -0.0090737 | 16 8            | -0.0134376 | 0.0022804  | 16 9            | -0.0165750 | -0.0509825  |
| 16 10           | -0.0104171 | 0.0066056  | 16 11           | 0.0160156  | -0.0064368 | 16 12           | 0.0208803  | 0.0057370   |
| 16 13           | 0.0130754  | 0.006134   | 16 14           | -0.0191226 | -0.0382895 | 16 15           | -0.0125321 | -0.0322958  |
| 16 16           | -0.0324114 | -0.0043686 |                 |            |            |                 |            |             |
| 17 1            | -0.0309381 | -0.0268459 | 17 2            | -0.0057800 | 0.0171247  | 17 3            | 0.0101214  | 0.0098939   |
| 17 4            | 0.0125878  | 0.0312242  | 17 5            | -0.0111472 | -0.0056031 | 17 6            | 0.0002920  | -0.0304166  |
| 17 7            | 0.0229520  | -0.019809  | 17 8            | 0.0311564  | 0.087750   | 17 9            | -0.0032015 | -0.0343246  |
| 17 10           | 0.0021050  | 0.0201193  | 17 11           | -0.0171108 | 0.0175019  | 17 12           | 0.0342734  | 0.0172570   |
| 17 13           | 0.0169075  | 0.0201122  | 17 14           | -0.0133370 | 0.017613   | 17 15           | 0.0049435  | 0.0057493   |
| 17 16           | -0.0290683 | 0.0018848  | 17 17           | -0.0383106 | -0.0206234 |                 |            |             |
| 18 1            | -0.0002253 | -0.0456055 | 18 2            | 0.0084083  | 0.0168428  | 18 3            | -0.0010020 | -0.0070483  |
| 18 4            | 0.0634167  | 0.0060924  | 18 5            | 0.0017426  | 0.0211276  | 18 6            | 0.0311991  | -0.0855669  |
| 18 7            | -0.0007957 | 0.0067159  | 18 8            | 0.0457191  | 0.0004305  | 18 9            | -0.0135216 | 0.0192446   |
| 18 10           | 0.0090063  | -0.0108619 | 18 11           | -0.0127989 | -0.0005971 | 18 12           | -0.0261819 | -0.0165262  |
| 18 13           | -0.0065815 | -0.0351551 | 18 14           | -0.0092828 | -0.0109400 | 18 15           | -0.0377619 | -0.0198247  |
| 18 16           | 0.0097880  | 0.0050024  | 18 17           | 0.0061142  | 0.0087663  | 18 18           | -0.0044692 | -0.0050647  |
| 19 1            | -0.0115942 | 0.0053764  | 19 2            | 0.0084369  | -0.0104744 | 19 3            | 0.0014391  | 0.0141955   |
| 19 4            | 0.0025699  | 0.0076747  | 19 5            | -0.0024457 | 0.0173789  | 19 6            | -0.0062545 | 0.0039169   |
| 19 7            | 0.0051463  | -0.0016620 | 19 8            | 0.0148626  | -0.0113273 | 19 9            | 0.0017566  | 0.0086593   |
| 19 10           | -0.0353538 | -0.0026556 | 19 11           | 0.0164804  | 0.0134748  | 19 12           | 0.0032037  | 0.0043292   |
| 19 13           | -0.0060894 | -0.0291709 | 19 14           | -0.0051227 | -0.0126448 | 19 15           | -0.0183164 | -0.0127675  |
| 19 16           | -0.0199047 | -0.0119326 | 19 17           | 0.0279459  | -0.0108837 | 19 18           | -0.0216467 | -0.0031131  |
| 19 19           | 0.0064638  | 0.0104244  |                 |            |            |                 |            |             |
| 20 1            | 0.0145119  | -0.0212711 | 20 2            | 0.0198772  | 0.0032259  | 20 3            | 0.0082691  | 0.0137151   |
| 20 4            | -0.0017951 | 0.008281   | 20 5            | -0.0104182 | 0.0003034  | 20 6            | 0.0127607  | 0.0096662   |
| 20 7            | -0.0077913 | 0.0489558  | 20 8            | -0.0020109 | -0.0012912 | 20 9            | 0.0228121  | 0.0072350   |
| 20 10           | -0.0224201 | -0.0080926 | 20 11           | 0.013787   | -0.0239305 | 20 12           | -0.0040581 | 0.0172980   |
| 20 13           | 0.0266491  | 0.048913   | 20 14           | 0.0103228  | -0.0117620 | 20 15           | -0.0227306 | -0.00294135 |
| 20 16           | -0.0106685 | 0.016919   | 20 17           | 0.0042934  | -0.0089776 | 20 18           | -0.0105771 | -0.0013024  |
| 20 19           | -0.0070980 | 0.0084586  | 20 20           | 0.0017085  | -0.0135051 |                 |            |             |

*Table 9.1*  
**GEM-T1 NORMALIZED COEFFICIENTS (continued)**  
 UNITS OF  $10^{-6}$

SECTORIALS AND TESSERALS

| INDEX<br>N<br>M | C<br>VALUE | S<br>INDEX<br>N<br>M | C<br>VALUE | S<br>INDEX<br>N<br>M | C<br>VALUE | S<br>INDEX<br>N<br>M |            |
|-----------------|------------|----------------------|------------|----------------------|------------|----------------------|------------|
| 21 1            | -0.0153942 | 0.0417459            | 21 2       | 0.0009874            | -0.0026067 | 21 3                 | 0.0019941  |
| 21 4            | -0.0002550 | 0.0069894            | 21 5       | 0.0177593            | -0.0158911 | 21 6                 | 0.0042146  |
| 21 7            | -0.0122279 | -0.0014058           | 21 8       | -0.0181008           | 0.0025208  | 21 9                 | 0.0173205  |
| 21 10           | 0.0036543  | 0.0018356            | 21 11      | 0.0092806            | -0.0367834 | 21 12                | 0.0028236  |
| 21 13           | -0.0181694 | 0.0115969            | 21 14      | 0.0187760            | 0.0086994  | 21 15                | 0.0166205  |
| 21 16           | -0.0087331 | -0.0051553           | 21 17      | -0.0067459           | 0.0008396  | 21 18                | 0.0168304  |
| 21 19           | -0.0209515 | 0.0158790            | 21 20      | -0.0190411           | 0.0185361  | 21 21                | 0.0024775  |
| 22 1            | 0.0083946  | -0.0167250           | 22 2       | -0.0162925           | 0.0020958  | 22 3                 | 0.0067253  |
| 22 4            | -0.0094462 | 0.0167100            | 22 5       | -0.0046335           | -0.0001257 | 22 6                 | 0.0146261  |
| 22 7            | 0.0127538  | 0.0013042            | 22 8       | -0.0098173           | -0.068267  | 22 9                 | 0.0125106  |
| 22 10           | 0.0050062  | 0.0203830            | 22 11      | -0.0093740           | -0.0183775 | 22 12                | 0.0074377  |
| 22 13           | -0.0169455 | -0.0178453           | 22 14      | 0.0087280            | 0.0102407  | 22 15                | 0.0279373  |
| 22 16           | 0.00892    | -0.009265            | 22 17      | 0.0138079            | -0.011258  | 22 18                | 0.0070311  |
| 22 19           | 0.0066210  | -0.0046952           | 22 20      | -0.0133152           | 0.0147789  | 22 21                | -0.0132244 |
| 22 22           | -0.0014623 | 0.0047182            |            |                      |            |                      | 0.0075983  |
| 23 1            | 0.0008657  | 0.0145970            | 23 2       | -0.0005313           | -0.0017780 | 23 3                 | -0.0045642 |
| 23 4            | -0.0100336 | -0.0016696           | 23 5       | 0.0019941            | -0.0079407 | 23 6                 | 0.009988   |
| 23 7            | -0.0023282 | 0.0026452            | 23 8       | 0.0042209            | -0.0067954 | 23 9                 | -0.0040274 |
| 23 10           | 0.0199758  | -0.0037585           | 23 11      | 0.0038490            | 0.0136794  | 23 12                | -0.0215777 |
| 23 13           | -0.0104578 | -0.0075112           | 23 14      | 0.0046108            | -0.0032727 | 23 15                | -0.0166812 |
| 23 16           | 0.0049029  | 0.0117671            | 23 17      | -0.0072125           | -0.0066031 | 23 18                | -0.0177318 |
| 23 19           | -0.0086827 | 0.0074916            | 23 20      | 0.0172248            | -0.0090475 | 23 21                | -0.0019656 |
| 23 22           | -0.0009034 | -0.0021445           | 23 23      | 0.0008446            | 0.0002030  |                      | 0.0108195  |
| 24 1            | 0.0081178  | -0.0291987           | 24 2       | -0.0058515           | 0.0052022  | 24 3                 | 0.0069148  |
| 24 4            | 0.0060580  | 0.0181145            | 24 5       | -0.0140838           | -0.0079805 | 24 6                 | -0.0003055 |
| 24 7            | -0.0025113 | 0.0050662            | 24 8       | -0.0024330           | 0.0075574  | 24 9                 | -0.0038940 |
| 24 10           | 0.0173535  | 0.0092954            | 24 11      | 0.0127396            | 0.0121180  | 24 12                | -0.0123406 |
| 24 13           | -0.0036235 | -0.0003824           | 24 14      | -0.0186436           | 0.0014570  | 24 15                | 0.0098097  |
| 24 16           | -0.0004908 | 0.0062766            | 24 17      | -0.0084625           | 0.0018817  | 24 18                | 0.0043072  |
| 24 19           | 0.0005274  | -0.0150179           | 24 20      | -0.0060619           | -0.0003298 | 24 21                | 0.0105744  |
| 24 22           | -0.0017322 | -0.0013033           | 24 23      | -0.0021435           | -0.0090055 | 24 24                | -0.0023438 |

*Table 9.1*  
**GEM-T1 NORMALIZED COEFFICIENTS (continued)**  
 UNITS OF  $10^{-6}$

SECTORIALS AND TESSERALS

| INDEX<br>N M |    | C          | VALUE      | S  | INDEX<br>N M | C          | VALUE      | S  | INDEX<br>N M | C          | VALUE      | S |
|--------------|----|------------|------------|----|--------------|------------|------------|----|--------------|------------|------------|---|
| 25           | 1  | 0.0037145  | 0.0043498  | 25 | 2            | 0.0037220  | 0.0052068  | 25 | 3            | -0.0032642 | -0.0031087 |   |
| 25           | 4  | 0.0063503  | -0.0015335 | 25 | 5            | -0.0024585 | -0.0023514 | 25 | 6            | 0.0059358  | -0.0067430 |   |
| 25           | 7  | 0.002632   | 0.0034596  | 25 | 8            | 0.0014256  | -0.0041241 | 25 | 9            | -0.0060297 | 0.0094442  |   |
| 25           | 10 | 0.0056907  | -0.0044669 | 25 | 11           | 0.0055793  | -0.0012766 | 25 | 12           | -0.0055425 | 0.0110100  |   |
| 25           | 13 | 0.0073795  | -0.0151883 | 25 | 14           | -0.0219418 | 0.0132058  | 25 | 15           | -0.0019899 | -0.0022710 |   |
| 25           | 16 | 0.0030419  | -0.0127972 | 25 | 17           | -0.0083083 | 0.0005500  | 25 | 18           | -0.0013004 | -0.016697  |   |
| 25           | 19 | 0.0091802  | 0.0021317  | 25 | 20           | -0.0037315 | -0.0066217 | 25 | 21           | 0.0053968  | 0.0031404  |   |
| 25           | 22 | -0.0018741 | -0.0017578 | 25 | 23           | 0.0045743  | -0.0024633 | 25 | 24           | 0.0036065  | -0.0038584 |   |
| 25           | 25 | 0.0049455  | 0.0040141  |    |              |            |            |    |              |            |            |   |
| 26           | 1  | 0.0049741  | -0.0172518 | 26 | 2            | -0.0052887 | 0.0002522  | 26 | 3            | -0.0002621 | -0.0037215 |   |
| 26           | 4  | 0.0053222  | 0.0048968  | 26 | 5            | 0.0043007  | 0.0106472  | 26 | 6            | 0.0085388  | 0.0031968  |   |
| 26           | 7  | 0.0054524  | 0.0025831  | 26 | 8            | 0.0030889  | -0.0021407 | 26 | 9            | 0.0025191  | -0.006592  |   |
| 26           | 10 | -0.0048370 | 0.0016645  | 26 | 11           | 0.0032045  | -0.0050467 | 26 | 12           | -0.0196457 | 0.0054338  |   |
| 26           | 13 | 0.0027230  | 0.0014151  | 26 | 14           | 0.0039290  | 0.0056350  | 26 | 15           | -0.013797  | 0.0047010  |   |
| 26           | 16 | 0.0058241  | -0.0041510 | 26 | 17           | -0.0048890 | 0.0082820  | 26 | 18           | -0.0090168 | 0.0075516  |   |
| 26           | 19 | 0.0016260  | -0.007199  | 26 | 20           | 0.0094830  | -0.0109488 | 26 | 21           | -0.0003907 | -0.0024147 |   |
| 26           | 22 | 0.0109119  | 0.0091610  | 26 | 23           | 0.0023537  | 0.0089516  | 26 | 24           | -0.0013736 | 0.0121837  |   |
| 26           | 25 | -0.0039876 | 0.0082488  | 26 | 26           | 0.0034281  | -0.0042690 |    |              |            |            |   |
| 27           | 1  | 0.0005230  | 0.0066113  | 27 | 2            | 0.0102174  | -0.0028223 | 27 | 3            | -0.0051035 | -0.0018585 |   |
| 27           | 4  | 0.0029164  | -0.0006401 | 27 | 5            | -0.0015884 | 0.0037103  | 27 | 6            | 0.001746   | -0.0021342 |   |
| 27           | 7  | 0.0069279  | -0.0028217 | 27 | 8            | -0.0041794 | -0.0044059 | 27 | 9            | 0.0003990  | 0.0021553  |   |
| 27           | 10 | -0.0083100 | 0.0060112  | 27 | 11           | -0.0011883 | -0.0030951 | 27 | 12           | -0.0004228 | -0.0017182 |   |
| 27           | 13 | -0.0059813 | 0.0061287  | 27 | 14           | 0.0119702  | 0.0066379  | 27 | 15           | -0.0043373 | 0.0001002  |   |
| 27           | 16 | 0.0065849  | -0.0041072 | 27 | 17           | 0.0055505  | 0.0015914  | 27 | 18           | -0.0051898 | 0.0059394  |   |
| 27           | 19 | 0.0009254  | -0.0062305 | 27 | 20           | 0.0029525  | 0.0030106  | 27 | 21           | -0.0020712 | -0.0045432 |   |
| 27           | 22 | -0.0001430 | 0.0029341  | 27 | 23           | -0.003881  | -0.0027372 | 27 | 24           | -0.0019361 | -0.0026238 |   |
| 27           | 25 | 0.0118014  | 0.0031453  | 27 | 26           | -0.0050080 | 0.0040035  | 27 | 27           | 0.0068945  | 0.0034538  |   |

*Table 9.1*  
**GEM-T1 NORMALIZED COEFFICIENTS (continued)**  
 UNITS OF  $10^{-6}$

SECTORIALS AND TESSERALS

| INDEX |    |            | INDEX      |    |    | INDEX      |            |    | INDEX |            |            |
|-------|----|------------|------------|----|----|------------|------------|----|-------|------------|------------|
| N     | M  | C          | N          | M  | S  | N          | M          | C  | N     | M          | S          |
| 28    | 1  | 0.0065294  | -0.0100251 | 28 | 2  | -0.0084276 | -0.0115524 | 28 | 3     | -0.0002646 | 0.0011662  |
| 28    | 4  | 0.0028786  | -0.0024855 | 28 | 5  | -0.009222  | -0.002361  | 28 | 6     | -0.0083296 | 0.0020029  |
| 28    | 7  | -0.0046459 | -0.0015444 | 28 | 8  | -0.005655  | -0.0031778 | 28 | 9     | 0.0029414  | -0.0030550 |
| 28    | 10 | -0.0072826 | -0.0012046 | 28 | 11 | -0.006214  | -0.008290  | 28 | 12    | -0.0004024 | 0.0024269  |
| 28    | 13 | 0.0000983  | 0.0035308  | 28 | 14 | -0.0021064 | -0.0065025 | 28 | 15    | -0.0082106 | 0.0053751  |
| 28    | 16 | -0.0083073 | -0.0076860 | 28 | 17 | 0.0045201  | -0.0042606 | 28 | 18    | 0.0003645  | -0.0008295 |
| 28    | 19 | 0.0044182  | 0.0138003  | 28 | 20 | -0.0009805 | -0.0011271 | 28 | 21    | 0.0024900  | 0.0002697  |
| 28    | 22 | -0.0048465 | 0.0005118  | 28 | 23 | -0.0026403 | 0.0063891  | 28 | 24    | 0.0068762  | -0.0150341 |
| 28    | 25 | 0.0011295  | -0.0048096 | 28 | 26 | 0.0034421  | 0.0016811  | 28 | 27    | -0.0099247 | 0.0013336  |
| 28    | 28 | 0.0067689  | 0.0019493  |    |    |            |            |    |       |            |            |
| 29    | 1  | 0.0034699  | 0.0024176  | 29 | 2  | 0.0094632  | -0.0043311 | 29 | 3     | -0.0043864 | -0.0017609 |
| 29    | 4  | -0.0063641 | 0.0007289  | 29 | 5  | 0.0034464  | 0.0035422  | 29 | 6     | -0.0002960 | -0.0024663 |
| 29    | 7  | 0.0011830  | -0.0072940 | 29 | 8  | -0.0064245 | 0.0025406  | 29 | 9     | -0.0016394 | 0.0024790  |
| 29    | 10 | 0.0000602  | 0.0060144  | 29 | 11 | -0.0093226 | 0.0004548  | 29 | 12    | -0.0008339 | -0.0049254 |
| 29    | 13 | -0.0011458 | -0.0019753 | 29 | 14 | -0.0051525 | 0.0019409  | 29 | 15    | -0.0012718 | -0.0024918 |
| 29    | 16 | -0.0021980 | -0.0055327 | 29 | 17 | -0.0045708 | -0.0027849 | 29 | 18    | -0.0002095 | -0.0001378 |
| 29    | 19 | -0.0021920 | 0.0015059  | 29 | 20 | -0.0047996 | 0.0031625  | 29 | 21    | -0.0003986 | -0.0059494 |
| 29    | 22 | 0.0096562  | 0.0044395  | 29 | 23 | -0.0050118 | -0.0000780 | 29 | 24    | -0.0025342 | -0.0037024 |
| 29    | 25 | 0.0083057  | 0.0036286  | 29 | 26 | 0.0062584  | -0.0036878 | 29 | 27    | -0.0074725 | -0.0021507 |
| 29    | 28 | 0.0103226  | -0.0019625 | 29 | 29 | 0.0086366  | 0.0031601  |    |       |            |            |
| 30    | 1  | -0.0016171 | -0.0090886 | 30 | 2  | -0.0040515 | -0.0053645 | 30 | 3     | -0.0016075 | 0.0014770  |
| 30    | 4  | -0.0021102 | -0.0039250 | 30 | 5  | 0.0033916  | 0.0006983  | 30 | 6     | -0.0032177 | 0.0041679  |
| 30    | 7  | -0.0001720 | -0.0001291 | 30 | 8  | 0.0029536  | 0.0005720  | 30 | 9     | -0.0001665 | -0.0039351 |
| 30    | 10 | 0.0012265  | -0.0010402 | 30 | 11 | -0.0016207 | 0.00050752 | 30 | 12    | 0.0037915  | -0.0034240 |
| 30    | 13 | 0.0146742  | -0.0000192 | 30 | 14 | -0.0000327 | -0.0025522 | 30 | 15    | 0.002816   | -0.0092780 |
| 30    | 16 | 0.0006189  | 0.0056597  | 30 | 17 | 0.0010057  | -0.0015438 | 30 | 18    | 0.0003035  | 0.0008530  |
| 30    | 19 | -0.0056266 | -0.0026384 | 30 | 20 | -0.0000276 | 0.0035666  | 30 | 21    | -0.0074518 | -0.0030982 |
| 30    | 22 | 0.0032458  | -0.0055410 | 30 | 23 | -0.0015833 | -0.0053377 | 30 | 24    | -0.0025120 | -0.0000377 |
| 30    | 25 | 0.0088475  | -0.0056062 | 30 | 26 | -0.0032087 | 0.0081399  | 30 | 27    | -0.0019206 | 0.0078152  |
| 30    | 28 | -0.0089658 | -0.0051589 | 30 | 29 | 0.0048227  | 0.0001240  | 30 | 30    | -0.0015075 | -0.0004221 |

*Table 9.1*  
**GEM-T1 NORMALIZED COEFFICIENTS (continued)**  
 UNITS OF  $10^{-6}$

SECTORIALS AND TESSERALS

| INDEX |    | C          | VALUE      | S  | INDEX | C           | VALUE      | S  | INDEX | C          | VALUE      | S |
|-------|----|------------|------------|----|-------|-------------|------------|----|-------|------------|------------|---|
| N     | M  |            |            |    | N     | M           |            |    | N     | M          |            |   |
| 31    | 1  | 0.0051782  | 0.0023829  | 31 | 2     | 0.0066008   | 0.0008362  | 31 | 3     | -0.0018668 | -0.0040769 |   |
| 31    | 4  | -0.0049509 | -0.0016392 | 31 | 5     | 0.0009096   | 0.0014649  | 31 | 6     | -0.0005622 | 0.0007667  |   |
| 31    | 7  | 0.0014817  | -0.0017479 | 31 | 8     | 0.000872    | -0.0011845 | 31 | 9     | -0.0038941 | -0.0017016 |   |
| 31    | 10 | 0.0025178  | -0.0037447 | 31 | 11    | -0.0016631  | 0.0058521  | 31 | 12    | 0.0001491  | 0.0046159  |   |
| 31    | 13 | 0.0056871  | 0.0013250  | 31 | 14    | -0.0072828  | 0.0012481  | 31 | 15    | 0.0004541  | -0.0043732 |   |
| 31    | 16 | -0.0045141 | 0.0048013  | 31 | 17    | -0.0059335  | 0.0025686  | 31 | 18    | 0.0025645  | 0.0038491  |   |
| 31    | 19 | 0.0020172  | 0.0028162  | 31 | 20    | 0.0018947   | 0.0005595  | 31 | 21    | 0.0023358  | 0.0035767  |   |
| 31    | 22 | -0.0062664 | -0.0057325 | 31 | 23    | 0.0095047   | 0.0056544  | 31 | 24    | -0.0038298 | -0.0019101 |   |
| 31    | 25 | -0.0077449 | -0.002757  | 31 | 26    | -0.0046923  | 0.003639   | 31 | 27    | 0.0069960  | 0.012525   |   |
| 31    | 28 | 0.0003428  | 0.0017261  | 31 | 29    | -0.0054215  | -0.0059502 | 31 | 30    | -0.0024527 | 0.0084230  |   |
| 31    | 31 | -0.0002319 | -0.000737  |    |       |             |            |    |       |            |            |   |
| 32    | 1  | -0.0091529 | -0.0092451 | 32 | 2     | 0.0018649   | 0.0043749  | 32 | 3     | -0.0006663 | 0.0029992  |   |
| 32    | 4  | 0.0020179  | -0.0033825 | 32 | 5     | -0.0000480  | -0.0027949 | 32 | 6     | -0.0038310 | 0.0002190  |   |
| 32    | 7  | -0.0030832 | 0.0018611  | 32 | 8     | 0.0008818   | -0.0033226 | 32 | 9     | 0.0019461  | 0.0007681  |   |
| 32    | 10 | 0.0072556  | -0.0019507 | 32 | 11    | -0.0024010  | -0.0006463 | 32 | 12    | -0.0017118 | 0.0041940  |   |
| 32    | 13 | 0.0029187  | 0.0022229  | 32 | 14    | 0.0046569   | -0.0069216 | 32 | 15    | 0.0039107  | -0.0049375 |   |
| 32    | 16 | 0.0030881  | 0.0041010  | 32 | 17    | -0.0036602  | 0.0018909  | 32 | 18    | 0.0022105  | -0.0014795 |   |
| 32    | 19 | 0.0046595  | 0.007455   | 32 | 20    | -0.0015881  | 0.0014199  | 32 | 21    | 0.0011690  | 0.0058848  |   |
| 32    | 22 | -0.0131730 | 0.0077043  | 32 | 23    | 0.0038573   | 0.0015337  | 32 | 24    | -0.0065905 | 0.0053251  |   |
| 32    | 25 | 0.0015717  | 0.0023530  | 32 | 26    | -0.0010511  | -0.0033428 | 32 | 27    | -0.0030949 | -0.0030221 |   |
| 32    | 28 | -0.0007616 | -0.0027125 | 32 | 29    | 0.0007277   | 0.0005068  | 32 | 30    | 0.0082893  | 0.0016713  |   |
| 32    | 31 |            |            |    |       |             |            |    |       |            |            |   |
| 33    | 1  | 0.0012672  | 0.0021258  | 33 | 2     | -0.0010231  | 0.0009548  | 33 | 3     | -0.0017027 | -0.0028776 |   |
| 33    | 4  | -0.0002362 | 0.0003938  | 33 | 5     | -0.0005132  | 0.0032353  | 33 | 6     | 0.0013824  | -0.0012542 |   |
| 33    | 7  | -0.000405  | 0.0017756  | 33 | 8     | -0.0000823  | 0.0015750  | 33 | 9     | -0.0002939 | 0.0018691  |   |
| 33    | 10 | 0.0002341  | -0.0009449 | 33 | 11    | 0.0055568   | -0.0004803 | 33 | 12    | 0.005208   | 0.0041268  |   |
| 33    | 13 | 0.0036684  | -0.0067767 | 33 | 14    | 0.0092319   | -0.0025099 | 33 | 15    | -0.0030055 | 0.0021726  |   |
| 33    | 16 | -0.0003879 | 0.0019724  | 33 | 17    | -0.0021426  | 0.0030432  | 33 | 18    | 0.0008702  | -0.0012393 |   |
| 33    | 19 | 0.0016796  | 0.0002369  | 33 | 20    | -0.0020822  | -0.0007525 | 33 | 21    | 0.0007319  | -0.0008394 |   |
| 33    | 22 | -0.0040992 | 0.0010974  | 33 | 23    | -0.0006277  | -0.0043975 | 33 | 24    | 0.003903   | -0.0004821 |   |
| 33    | 25 | -0.0012628 | -0.0048224 | 33 | 26    | 0.00081343  | 0.0055386  | 33 | 27    | -0.0103323 | -0.0021297 |   |
| 33    | 28 | -0.0108851 | 0.0018952  | 33 | 29    | -0.0213209  | 0.0001932  | 33 | 30    | 0.0025217  | -0.0134935 |   |
| 33    | 31 | 0.0001745  | 0.0011566  |    |       | -0.00024100 | -0.0000219 | 33 | 32    | -0.0003603 | -0.0002676 |   |

*Table 9.1*  
**GEM-T1 NORMALIZED COEFFICIENTS (continued)**  
 UNITS OF  $10^{-6}$

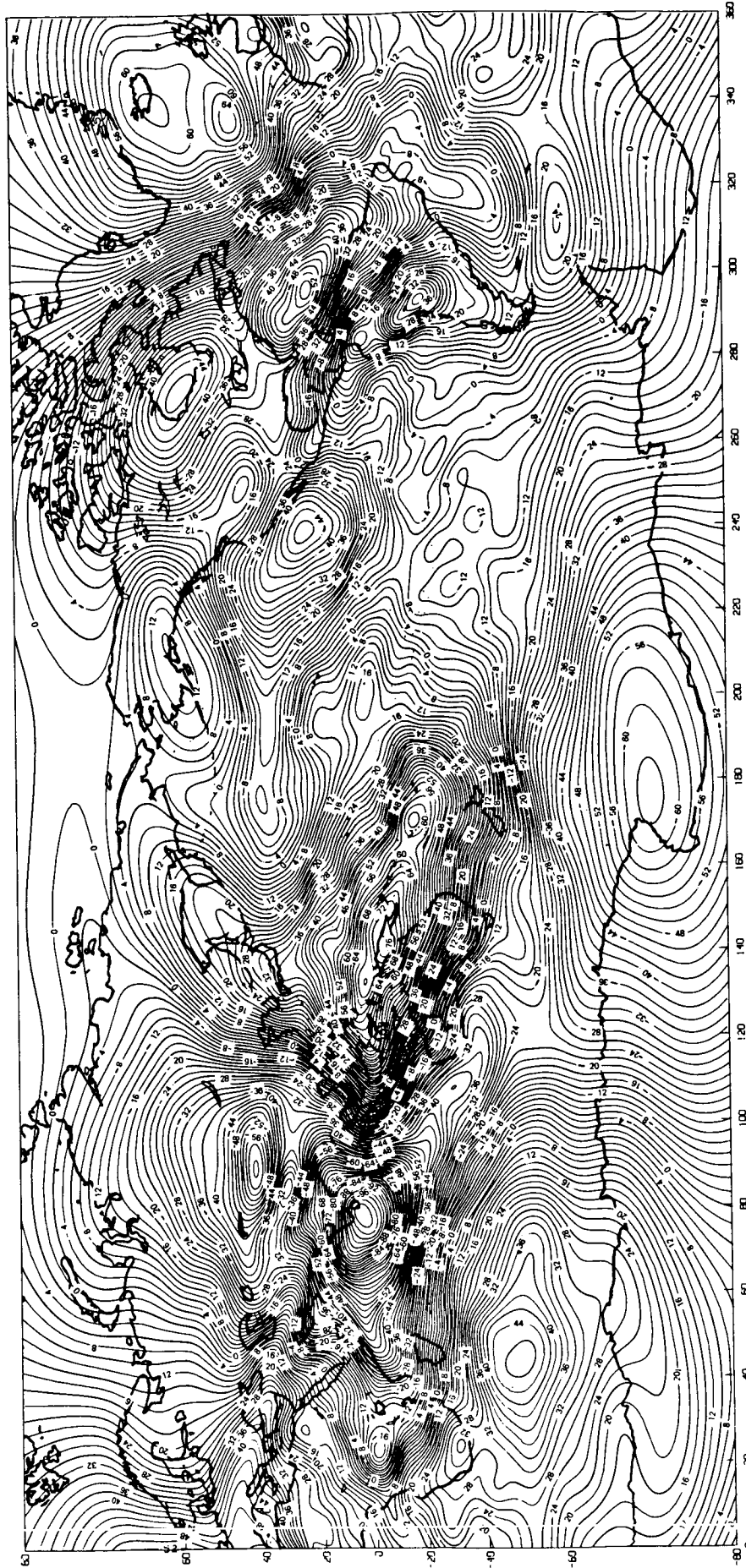
**SECTORIALS AND TESSERALS**

| INDEX<br>N | INDEX<br>M | C          | VALUE       | S  | INDEX<br>N | INDEX<br>M | C          | VALUE | S  | INDEX<br>N | INDEX<br>M | C | VALUE | S |
|------------|------------|------------|-------------|----|------------|------------|------------|-------|----|------------|------------|---|-------|---|
| 34         | 1          | -0.0015608 | -0.0091011  | 34 | 2          | 0.0035817  | 0.0051783  | 34    | 3  | -0.0005145 | 0.0022065  |   |       |   |
| 34         | 4          | 0.0028502  | -0.0018773  | 34 | 5          | -0.0012952 | 0.000401   | 34    | 6  | 0.0005808  | -0.0003220 |   |       |   |
| 34         | 7          | 0.0023148  | 0.0001028   | 34 | 8          | 0.0007083  | -0.0007860 | 34    | 9  | 0.0012660  | 0.0015093  |   |       |   |
| 34         | 10         | -0.0014879 | -0.0000093  | 34 | 11         | 0.00012406 | -0.0038325 | 34    | 12 | 0.0004550  | 0.0024876  |   |       |   |
| 34         | 13         | -0.0080803 | 0.0012768   | 34 | 14         | -0.0010431 | -0.0002878 | 34    | 15 | 0.0007643  | 0.003005   |   |       |   |
| 34         | 16         | 0.0011337  | -0.0026578  | 34 | 17         | 0.0003626  | 0.0025764  | 34    | 18 | -0.0027232 | -0.0000869 |   |       |   |
| 34         | 19         | 0.0005953  | -0.0010032  | 34 | 20         | 0.0008917  | -0.0003975 | 34    | 21 | 0.0013743  | -0.0006590 |   |       |   |
| 34         | 22         | 0.0008294  | 0.0004221   | 34 | 23         | -0.0009300 | -0.0021403 | 34    | 24 | 0.0067267  | 0.0008511  |   |       |   |
| 34         | 25         | 0.0062516  | 0.0082080   | 34 | 26         | 0.0010816  | -0.009061  | 34    | 27 | 0.0068974  | -0.0005442 |   |       |   |
| 34         | 28         | 0.0045502  | -0.0081979  | 34 | 29         | -0.0038113 | 0.0044842  | 34    | 30 | -0.0061161 | 0.0000268  |   |       |   |
| 34         | 31         | 0.0023534  | 0.0022983   | 34 | 32         | -0.0008166 | -0.0011610 | 34    | 33 | -0.0010234 | 0.0013813  |   |       |   |
| 34         | 34         | -0.0002093 | -0.0006039  |    |            |            |            |       |    |            |            |   |       |   |
| 35         | 1          | -0.0019069 | 0.0020110   | 35 | 2          | -0.0025529 | 0.0010277  | 35    | 3  | 0.0006733  | 0.0006861  |   |       |   |
| 35         | 4          | 0.0027442  | 0.00014864  | 35 | 5          | -0.0002351 | -0.0007374 | 35    | 6  | 0.0008304  | -0.0014752 |   |       |   |
| 35         | 7          | 0.0007448  | -0.0014313  | 35 | 8          | 0.0002679  | -0.001772  | 35    | 9  | 0.0010826  | -0.0020731 |   |       |   |
| 35         | 10         | -0.0014313 | -0.0008354  | 35 | 11         | 0.0006785  | -0.0036583 | 35    | 12 | 0.0014841  | -0.0020619 |   |       |   |
| 35         | 13         | -0.001849  | 0.0044812   | 35 | 14         | -0.0004836 | -0.0001238 | 35    | 15 | 0.0002609  | 0.0028304  |   |       |   |
| 35         | 16         | 0.0001314  | -0.0013369  | 35 | 17         | 0.0033863  | -0.0024391 | 35    | 18 | 0.0015093  | -0.0005937 |   |       |   |
| 35         | 19         | -0.0029031 | 0.0005932   | 35 | 20         | -0.0007745 | -0.0008763 | 35    | 21 | 0.0013843  | 0.0027357  |   |       |   |
| 35         | 22         | 0.0000159  | -0.0033003  | 35 | 23         | -0.0023783 | -0.0015551 | 35    | 24 | 0.0025277  | 0.0021953  |   |       |   |
| 35         | 25         | -0.0038892 | 0.0015231   | 35 | 26         | -0.0143438 | -0.0001412 | 35    | 27 | 0.0027787  | -0.0191290 |   |       |   |
| 35         | 28         | -0.0108936 | -0.0233542  | 35 | 29         | 0.0081878  | -0.0031532 | 35    | 30 | 0.0037128  | -0.0028852 |   |       |   |
| 35         | 31         | 0.0013305  | 0.0010339   | 35 | 32         | -0.0039791 | 0.005664   | 35    | 33 | -0.0002881 | 0.0016655  |   |       |   |
| 35         | 34         | -0.0005168 | 0.0001237   | 35 | 35         | 0.0000938  | -0.0001450 |       |    |            |            |   |       |   |
| 36         | 1          | 0.0028774  | -0.0058408  | 36 | 2          | 0.0001790  | 0.0012922  | 36    | 3  | -0.0008129 | -0.0013852 |   |       |   |
| 36         | 4          | 0.0013157  | -0.00001181 | 36 | 5          | -0.0011798 | 0.0003403  | 36    | 6  | -0.0005757 | -0.0008988 |   |       |   |
| 36         | 7          | -0.0001662 | -0.0004199  | 36 | 8          | -0.0010487 | -0.0005378 | 36    | 9  | -0.0003170 | 0.0005484  |   |       |   |
| 36         | 10         | -0.0003570 | 0.0004671   | 36 | 11         | -0.0005880 | -0.0007308 | 36    | 12 | -0.0002182 | -0.0016668 |   |       |   |
| 36         | 13         | 0.0007685  | 0.0037948   | 36 | 14         | -0.0048384 | -0.0040665 | 36    | 15 | 0.0018223  | 0.0018634  |   |       |   |
| 36         | 16         | 0.0013405  | -0.0020055  | 36 | 17         | 0.0021679  | -0.0008490 | 36    | 18 | 0.000693   | 0.0005306  |   |       |   |
| 36         | 19         | -0.0002562 | -0.0000695  | 36 | 20         | -0.0009128 | -0.0008661 | 36    | 21 | 0.0007411  | -0.0021175 |   |       |   |
| 36         | 22         | 0.0005732  | 0.0006864   | 36 | 23         | -0.0012168 | -0.0005518 | 36    | 24 | 0.0006589  | -0.0014201 |   |       |   |
| 36         | 25         | 0.0000270  | 0.0086477   | 36 | 26         | 0.0084469  | 0.0110849  | 36    | 27 | -0.0101912 | 0.0042305  |   |       |   |
| 36         | 28         | 0.0069480  | 0.0056619   | 36 | 29         | -0.0013415 | -0.0024474 | 36    | 30 | -0.0015551 | -0.0020261 |   |       |   |
| 36         | 31         | -0.0035516 | 0.0013604   | 36 | 32         | -0.0008804 | -0.0003000 | 36    | 33 | -0.0023972 | -0.0026170 |   |       |   |
| 36         | 34         | 0.0008324  | 0.00017560  | 36 | 35         | -0.0002152 | -0.0007347 | 36    | 36 | 0.0001484  | 0.0004197  |   |       |   |

# GEOID HEIGHTS

REFERRED TO GRS-80 ELLIPSOID  
 $a_e = 6378137 \text{ m}$   $1/f = 298.257$

Figure 9.0. The GEM-T1 Geoid.



The artificial satellites suitable for geopotential recovery are sensitive to the low degree and order harmonics in the global spherical harmonic expansions of the tides. In fact, these satellites form a sensitive measurement system for monitoring these effects. (Table 9.2 shows the periods of the principal long period tidal perturbations on the orbits for the major satellites used in GEM-T1. The diurnal and semidiurnal bands are particularly variable in frequency relative to the corresponding periodicities of the tides on the Earth's surface since the satellite's nodal precession and not the earth's rotation makes the largest contribution to these periodicities.)

The approach we have used in the development of GEM-T1 is to recover the relevant tidal parameters directly in the simultaneous least squares data reduction process along with the other geodetic and geodynamic parameters. The rationale for this approach is dictated largely by the present uncertainty of these tidal coefficients which are known only to about 10% of their values. This approach was demonstrated with great success in single satellite analyses using STARLETTE (Williamson and Marsh, 1985; Marsh et al., 1985) and LAGEOS (Christodoulidis et al., 1986a).

The a priori values for the ocean tides were derived as detailed in Section 7.1.4. The body tides were held fixed according to the Wahr values as given in Section 7.1.3 and the adopted precession and nutation are the IAU 1980 models. Because the body tides are not separable from the ocean tides, only the ocean tides were adjusted. The ocean tides recovered actually represent a determination of the total temporal variations of the geopotential exterior to the Earth's atmosphere in the presence of a fixed solid earth tidal model.

Table 9.3 summarizes the ocean tidal terms which were modeled or adjusted in the GEM-T1 solution. Due to the altitudes of the satellites, the background model is only required to degree 6. Coefficients associated with the primary tidal terms were adjusted. This restriction of

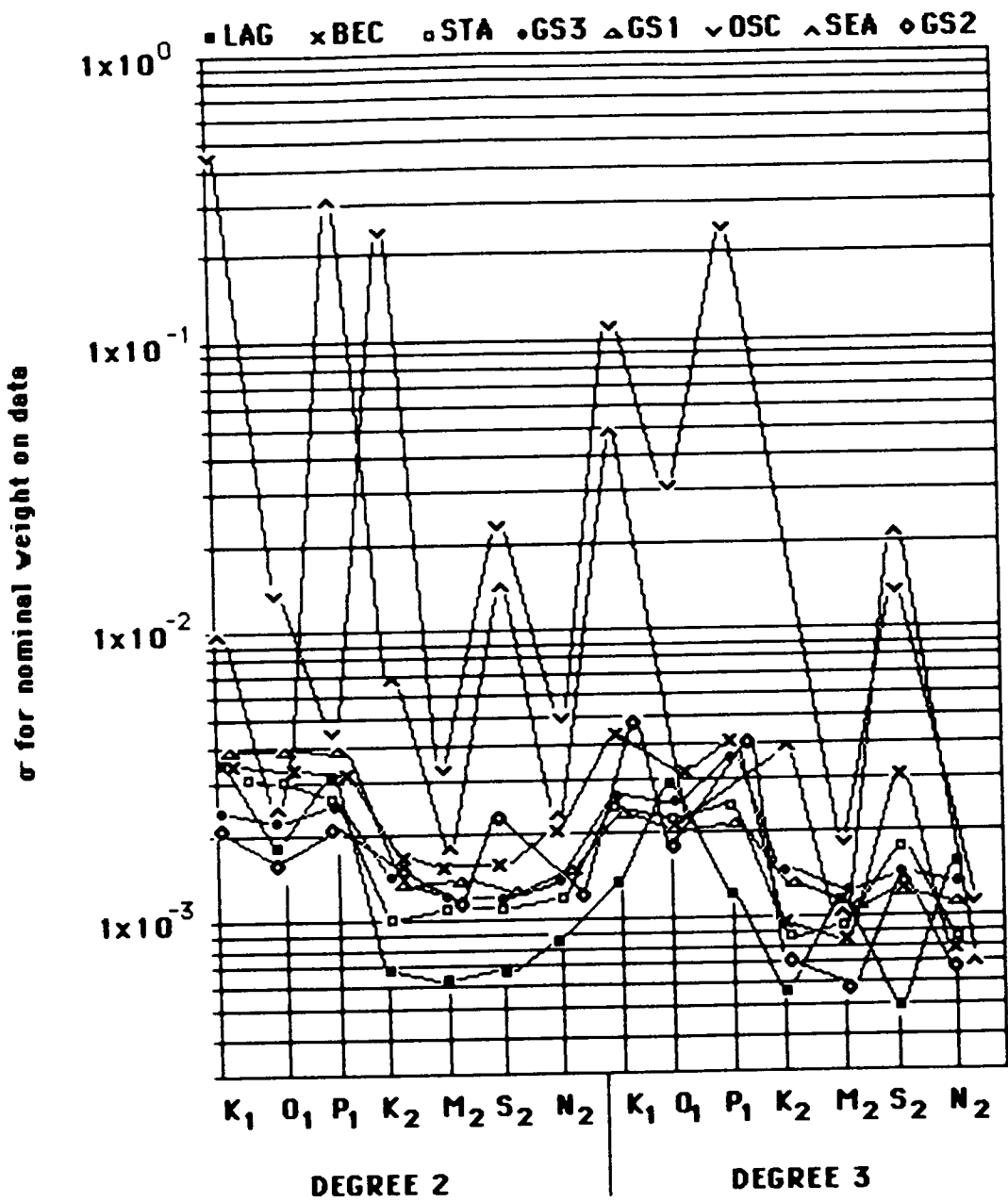


Figure 9.1. Satellite Tidal Sensitivities from Single Satellite Solutions for  $5 \times 5$  Gravity Coefficients and 2nd and 3rd Degree Tidal Terms.

Table 9.2

**PERIODS (DAYS) OF PRINCIPAL LONG PERIOD  
SATELLITE PERTURBATIONS  
DUE TO SOLID EARTH AND OCEAN TIDES  
FOR 12 MAJOR TIDE CONSTITUENTS**

|                  | <b>056.5545</b>      | <b>057.5555</b>       | <b>065.4555</b>      | <b>075.5555</b>      | <b>145.5555</b>      | <b>163.5555</b>      | <b>165.5555</b>      | <b>245.6555</b>      | <b>255.5555</b>      | <b>272.5565</b>      | <b>273.5555</b>      | <b>275.5555</b>      |
|------------------|----------------------|-----------------------|----------------------|----------------------|----------------------|----------------------|----------------------|----------------------|----------------------|----------------------|----------------------|----------------------|
| <b>SATELLITE</b> | <b>S<sub>a</sub></b> | <b>S<sub>aa</sub></b> | <b>M<sub>m</sub></b> | <b>M<sub>f</sub></b> | <b>O<sub>1</sub></b> | <b>P<sub>1</sub></b> | <b>K<sub>1</sub></b> | <b>N<sub>2</sub></b> | <b>M<sub>2</sub></b> | <b>T<sub>2</sub></b> | <b>S<sub>2</sub></b> | <b>K<sub>2</sub></b> |
| LAGEOS           | <b>365</b>           | <b>183</b>            | <b>27.6</b>          | <b>13.7</b>          | <b>13.8</b>          | <b>221</b>           | <b>1050</b>          | <b>9.20</b>          | <b>14.0</b>          | <b>159</b>           | <b>280</b>           | <b>524</b>           |
| STARLETTE        | <b>365</b>           | <b>183</b>            | <b>27.6</b>          | <b>13.7</b>          | <b>11.9</b>          | <b>60.8</b>          | <b>91.0</b>          | <b>7.61</b>          | <b>10.5</b>          | <b>33.1</b>          | <b>36.4</b>          | <b>45.5</b>          |
| GEOS-1           | <b>365</b>           | <b>183</b>            | <b>27.6</b>          | <b>13.7</b>          | <b>12.6</b>          | <b>85.4</b>          | <b>160</b>           | <b>8.20</b>          | <b>11.7</b>          | <b>48.3</b>          | <b>55.7</b>          | <b>80.2</b>          |
| GEOS-2           | <b>365</b>           | <b>183</b>            | <b>27.6</b>          | <b>13.7</b>          | <b>14.4</b>          | <b>629</b>           | <b>257</b>           | <b>9.83</b>          | <b>15.3</b>          | <b>2250</b>          | <b>436</b>           | <b>129</b>           |
| GEOS-3           | <b>365</b>           | <b>183</b>            | <b>27.6</b>          | <b>13.7</b>          | <b>15.2</b>          | <b>482</b>           | <b>132</b>           | <b>10.6</b>          | <b>17.2</b>          | <b>145</b>           | <b>104</b>           | <b>66.2</b>          |
| BE-B             | <b>365</b>           | <b>183</b>            | <b>27.6</b>          | <b>13.7</b>          | <b>13.1</b>          | <b>118</b>           | <b>332</b>           | <b>8.66</b>          | <b>12.6</b>          | <b>70.2</b>          | <b>87.0</b>          | <b>166</b>           |
| BE-C             | <b>365</b>           | <b>183</b>            | <b>27.6</b>          | <b>13.7</b>          | <b>11.8</b>          | <b>57.9</b>          | <b>84.8</b>          | <b>7.51</b>          | <b>10.3</b>          | <b>31.5</b>          | <b>34.4</b>          | <b>42.4</b>          |
| SEASAT           | <b>365</b>           | <b>183</b>            | <b>27.6</b>          | <b>13.7</b>          | <b>14.8</b>          | <b>7130</b>          | <b>178</b>           | <b>10.2</b>          | <b>16.1</b>          | <b>331</b>           | <b>174</b>           | <b>89.0</b>          |
| TELSTAR-1        | <b>365</b>           | <b>183</b>            | <b>27.6</b>          | <b>13.7</b>          | <b>12.8</b>          | <b>93.9</b>          | <b>193</b>           | <b>8.34</b>          | <b>12.0</b>          | <b>53.9</b>          | <b>63.2</b>          | <b>96.7</b>          |
| ANNA             | <b>365</b>           | <b>183</b>            | <b>27.6</b>          | <b>13.7</b>          | <b>12.0</b>          | <b>64.4</b>          | <b>99.4</b>          | <b>7.71</b>          | <b>10.7</b>          | <b>35.3</b>          | <b>39.1</b>          | <b>49.7</b>          |
| OSCAR            | <b>365</b>           | <b>183</b>            | <b>27.6</b>          | <b>13.7</b>          | <b>13.6</b>          | <b>180</b>           | <b>11700</b>         | <b>9.12</b>          | <b>13.6</b>          | <b>119</b>           | <b>177</b>           | <b>5830</b>          |

**Table 9.3**  
**OCEAN TIDE MODELING**  
**FOR**  
**GRAVITY RECOVERY**

• LONG PERIOD TIDES •

| <u>Doodson<br/>No.</u> | <u>Darwin<br/>Name</u> | <u>Modeled</u>   | <u>Adjusted</u> |
|------------------------|------------------------|------------------|-----------------|
| 056.554                | S <sub>a</sub>         | deg. 2→6         | deg. 2          |
| 057.555                | S <sub>sa</sub>        | prograde<br>only | deg. 2          |
| 058.554                |                        |                  | none            |
| 065.455                | M <sub>m</sub>         |                  | deg. 2          |
| 075.555                | M <sub>f</sub>         |                  | deg. 2          |
| 075.565                |                        |                  | none            |

• DIURNAL •

|         |                 |                   |              |
|---------|-----------------|-------------------|--------------|
| 135.655 | Q <sub>1</sub>  | deg. 2→6          | none         |
| 145.545 |                 | prograde          | none         |
| 145.555 | O <sub>1</sub>  | and<br>retrograde | deg. 2, 3, 4 |
| 155.455 |                 |                   | none         |
| 155.655 | M <sub>1</sub>  |                   | none         |
| 162.556 | P <sub>1</sub>  |                   | none         |
| 163.555 | P <sub>1</sub>  |                   | deg. 2, 3, 4 |
| 164.556 | S <sub>1</sub>  |                   | none         |
| 165.545 |                 |                   | none         |
| 165.555 | K <sub>1</sub>  |                   | deg. 2, 3, 4 |
| 165.565 |                 |                   | none         |
| 166.554 |                 |                   | none         |
| 167.555 |                 |                   | none         |
| 175.455 | S <sub>1</sub>  |                   | none         |
| 185.555 | OO <sub>1</sub> |                   | none         |

• SEMI-DIURNAL •

| <u>Doodson<br/>No.</u> | <u>Darwin<br/>Name</u> | <u>Modeled</u> | <u>Adjusted</u> |
|------------------------|------------------------|----------------|-----------------|
| 245.655                | N <sub>2</sub>         | deg. 2→6       | deg. 2, 3, 4, 5 |
| 255.545                |                        | prograde       | none            |
| 255.555                | M <sub>2</sub>         | and            | deg. 2, 3, 4, 5 |
| 265.455                | L <sub>2</sub>         | retrograde     | none            |
| 271.557                |                        |                | none            |
| 272.556                | T <sub>2</sub>         |                | deg. 2, 3, 4, 5 |
| 273.555                | S <sub>2</sub>         |                | deg. 2, 3, 4, 5 |
| 274.554                | R <sub>2</sub>         |                | none            |
| 275.555                | K <sub>2</sub>         |                | deg. 2, 3, 4, 5 |
| 285.455                |                        |                | none            |
| 295.555                |                        |                | none            |



adjusting the coefficients of the primary terms was adopted because of computer limitations. The background tidal terms are less significant in their orbital perturbations than those from the primary terms, and errors in these terms are not expected to be of consequence now that they are somewhat reliably modeled (we estimate 10 to 20% uncertainty).

Tables 9.4 through 9.7 present the recovered ocean tidal coefficients by degree. The values shown for the coefficient and phase uncertainties were obtained from the covariance analysis which produced the properly calibrated gravity coefficients as described in Section 10. These uncertainties are believed to give realistic estimates for the error in the total exterior tidal potential. Tables 9.4 to 9.7 also compare our GEM-T1 ocean tide coefficients with those obtained from the Schwiderski and Parke models, which were conventionally obtained by solution of the Laplace Tidal Equations using deep ocean tide guage data. The variation seen between the two oceanographic tidal solutions is often larger than the uncertainty in our recovered solution. Generally the satellite results are in reasonable agreement with the Schwiderski and Parke models. A more complete discussion of the GEM-T1 tidal solution is found in Christodoulidis et al., 1987.

A limited test was performed to assess the relative contribution of each of the major satellites in the solution to the tide coefficient recovery. Figure 9.1 shows the relative standard deviations of the second and third degree diurnal and semidiurnal tides from solutions based on individual satellites. Each test solution included the adjustment of a (5x5) gravity model simultaneously with the second and third degree tidal terms. The weights in these solutions were 1 meter on range and 1 cm/sec on range-rate. LAGEOS dominates the second degree semidiurnal recovery, and the polar OSCAR Doppler satellite is not strongly contributing to the solution. Otherwise, the individual satellites contribute nearly equally to within a factor of two or three.

Table 9.4

**VALUES FOR DYNAMICALLY ESTIMATED  
2ND DEGREE TIDES  
COMPARED TO OCEANOGRAPHIC DETERMINATIONS**

| TIDE (r)             | AMPLITUDE (cm) |             |               | PHASE (deg)    |             |               |
|----------------------|----------------|-------------|---------------|----------------|-------------|---------------|
|                      | OBSERVED       |             | OCEANOGRAPHIC | OBSERVED       |             | OCEANOGRAPHIC |
|                      | SATELLITE      | SCHWIDERSKI | PARKE         | SATELLITE      | SCHWIDERSKI | PARKE         |
| LONG PERIOD (m = 0)  |                |             |               |                |             |               |
| H <sub>in</sub>      | .36 ± .50      | 1.06        | ---           | 274.10 ± 76.60 | 258.9       | ---           |
| S <sub>a</sub>       | 2.44 ± .77     | ---         | ---           | 31.03 ± 18.75  | ---         | ---           |
| H <sub>r</sub>       | 1.80 ± .41     | 1.70        | ---           | 245.35 ± 13.08 | 252.0       | ---           |
| S <sub>sa</sub>      | 1.68 ± .72     | 1.24        | ---           | 223.12 ± 26.44 | 221.6       | ---           |
| DIURNAL (m = 1)      |                |             |               |                |             |               |
| K <sub>1</sub>       | 2.61 ± .23     | 2.82        | 2.46          | 328.50 ± 5.02  | 315.1       | 312.0         |
| O <sub>1</sub>       | 2.69 ± .17     | 2.42        | 1.88          | 318.53 ± 3.63  | 313.7       | 309.0         |
| P <sub>1</sub>       | 0.81 ± .23     | 0.90        | 0.76          | 296.83 ± 16.07 | 313.9       | 311.7         |
| SEMI-DIURNAL (m = 2) |                |             |               |                |             |               |
| K <sub>2</sub>       | 0.31 ± .05     | 0.26        | ---           | 302.14 ± 9.79  | 315.11      | ---           |
| H <sub>2</sub>       | 3.26 ± .05     | 2.96        | 3.38          | 320.93 ± 0.92  | 310.6       | 313.1         |
| S <sub>2</sub>       | 0.80 ± .05*    | 0.93        | 0.88          | 301.93 ± 3.73* | 314.0       | 300.8         |
| N <sub>2</sub>       | 0.70 ± .07     | 0.65        | 0.58          | 334.01 ± 5.52  | 321.8       | 324.5         |
| T <sub>2</sub>       | 0.09 ± .05     | ---         | ---           | 19.76 ± 34.80  | ---         | ---           |

\*combined ocean/atmospheric effect

Table 9.5

**VALUES FOR DYNAMICALLY ESTIMATED  
3RD DEGREE TIDES  
COMPARED TO OCEANOGRAPHIC DETERMINATIONS**

| TIDE (t)             | AMPLITUDE (cm)               |                                     |                                | PHASE (deg)                  |                                     |                                |
|----------------------|------------------------------|-------------------------------------|--------------------------------|------------------------------|-------------------------------------|--------------------------------|
|                      | OBSERVED<br><u>SATELLITE</u> | OCEANOGRAPHIC<br><u>SCHWIDERSKI</u> | OCEANOGRAPHIC<br><u>PARKER</u> | OBSERVED<br><u>SATELLITE</u> | OCEANOGRAPHIC<br><u>SCHWIDERSKI</u> | OCEANOGRAPHIC<br><u>PARKER</u> |
| K <sub>1</sub>       | 0.57 ± .10                   | 0.89                                | 1.04                           | 50.96 ± 10.38                | 33.7                                | 16.2                           |
| M <sub>1</sub>       | 1.73 ± .21                   | 1.31                                | 1.54                           | 77.59 ± 6.85                 | 83.6                                | 74.9                           |
| O <sub>1</sub>       | 0.33 ± .10                   | 0.29                                | 0.36                           | 2.09 ± 10.14                 | 39.9                                | 33.8                           |
| P <sub>1</sub>       |                              |                                     |                                |                              |                                     |                                |
| DIURNAL (m = 1)      |                              |                                     |                                |                              |                                     |                                |
| K <sub>2</sub>       | 0.51 ± .04                   | 0.09                                | ---                            | 206.35 ± 4.88                | 195.0                               | ---                            |
| M <sub>2</sub>       | 0.20 ± .08                   | 0.36                                | 0.39                           | 152.39 ± 22.28               | 168.6                               | 219.7                          |
| S <sub>2</sub>       | 0.38 ± .04                   | 0.26                                | 0.48                           | 237.37 ± 6.14                | 201.9                               | 222.5                          |
| N <sub>2</sub>       | 0.10 ± .09                   | 0.11                                | 0.12                           | 84.93 ± 51.64                | 171.9                               | 174.5                          |
| T <sub>2</sub>       | 0.15 ± .04                   | ---                                 | ---                            | 214.52 ± 16.02               | ---                                 | ---                            |
| SEMI-DIURNAL (m = 2) |                              |                                     |                                |                              |                                     |                                |
| K <sub>2</sub>       | 0.51 ± .04                   | 0.09                                | ---                            | 206.35 ± 4.88                | 195.0                               | ---                            |
| M <sub>2</sub>       | 0.20 ± .08                   | 0.36                                | 0.39                           | 152.39 ± 22.28               | 168.6                               | 219.7                          |
| S <sub>2</sub>       | 0.38 ± .04                   | 0.26                                | 0.48                           | 237.37 ± 6.14                | 201.9                               | 222.5                          |
| N <sub>2</sub>       | 0.10 ± .09                   | 0.11                                | 0.12                           | 84.93 ± 51.64                | 171.9                               | 174.5                          |
| T <sub>2</sub>       | 0.15 ± .04                   | ---                                 | ---                            | 214.52 ± 16.02               | ---                                 | ---                            |

Table 9.6

**VALUES FOR DYNAMICALLY ESTIMATED  
4TH DEGREE TIDES  
COMPARED TO OCEANOGRAPHIC DETERMINATIONS**

| TIDE ( <i>t</i> )           | AMPLITUDE (cm)               |                                     |                         | PHASE (deg)                  |                                     |                         |
|-----------------------------|------------------------------|-------------------------------------|-------------------------|------------------------------|-------------------------------------|-------------------------|
|                             | OBSERVED<br><u>SATELLITE</u> | OCEANOGRAPHIC<br><u>SCHWIDERSKI</u> | PARKER<br><u>PARKER</u> | OBSERVED<br><u>SATELLITE</u> | OCEANOGRAPHIC<br><u>SCHWIDERSKI</u> | PARKER<br><u>PARKER</u> |
| K <sub>1</sub>              | 2.62 ± .34                   | 1.91                                | 1.72                    | 254.42 ± 9.24                | 254.2                               | 241.2                   |
| O <sub>1</sub>              | 1.83 ± .32                   | 1.43                                | 1.46                    | 203.30 ± 9.57                | 276.3                               | 267.2                   |
| P <sub>1</sub>              | 0.35 ± .32                   | 0.63                                | 0.57                    | 234.91 ± 52.62               | 258.3                               | 253.6                   |
| <u>DIURNAL (m = 1)</u>      |                              |                                     |                         |                              |                                     |                         |
| K <sub>2</sub>              | 0.19 ± .07                   | 0.11                                | ---                     | 75.96 ± 21.23                | 103.5                               | ---                     |
| H <sub>2</sub>              | 0.93 ± .07                   | 1.01                                | 1.29                    | 127.41 ± 4.61                | 124.7                               | 120.3                   |
| S <sub>2</sub>              | 0.41 ± .07                   | 0.21                                | 0.19                    | 86.53 ± 11.18                | 141.8                               | 125.4                   |
| N <sub>2</sub>              | 0.17 ± .08                   | 0.37                                | 0.39                    | 137.28 ± 25.62               | 103.0                               | 84.8                    |
| T <sub>2</sub>              | 0.07 ± .08                   | ---                                 | ---                     | 46.02 ± 65.50                | ---                                 | ---                     |
| <u>SEMI-DIURNAL (m = 2)</u> |                              |                                     |                         |                              |                                     |                         |

Table 9.7

**VALUES FOR DYNAMICALLY ESTIMATED  
5TH DEGREE TIDES  
COMPARED TO OCEANOGRAPHIC DETERMINATIONS**

| TIDE (t)       | SEMI-DIURNAL (m = 2)         |                                     |                                | C <sup>+</sup><br>C <sub>5m,f</sub> | AMPLITUDE (cm) | OBSERVED<br><u>SATELLITE</u> | OCEANOGRAPHIC<br><u>SCHWIDERSKI</u> | OCEANOGRAPHIC<br><u>PARKER</u> | PHASE (deg)<br>E <sup>+</sup><br>E <sub>5m,f</sub> |
|----------------|------------------------------|-------------------------------------|--------------------------------|-------------------------------------|----------------|------------------------------|-------------------------------------|--------------------------------|--|
|                | OBSERVED<br><u>SATELLITE</u> | OCEANOGRAPHIC<br><u>SCHWIDERSKI</u> | OCEANOGRAPHIC<br><u>PARKER</u> |                                     |                |                              |                                     |                                |  |
| K <sub>2</sub> | 0.10 ± .05                   | 0.04                                | ---                            |                                     | 56.10 ± 31.38  | 0.41                         |                                     |                                | ---  |
| M <sub>2</sub> | 0.28 ± .06                   | 0.28                                | 0.25                           |                                     | 17.62 ± 12.02  | 356.60                       | 15.9                                |                                |  |
| S <sub>2</sub> | 0.21 ± .06                   | 0.14                                | 0.12                           |                                     | 34.42 ± 17.97  | 3.77                         | 30.1                                |                                |  |
| N <sub>2</sub> | 0.11 ± .06                   | 0.08                                | 0.05                           |                                     | 3.56 ± 31.76   | 5.03                         | 352.3                               |                                |  |
| T <sub>2</sub> | 0.14 ± .06                   | ---                                 | ---                            |                                     | 39.03 ± 23.96  | ---                          |                                     |                                |  |

## 9.3 STATION COORDINATE SOLUTIONS AND COMPARISONS

### 9.3.1 Introduction

As has been discussed for some time, geopotential modeling has been the dominant source of error in previous station coordinate solutions (Smith et al, 1979). More recently, these uncertainties have been diminishing with the collection of more tracking data and the recovery of refined gravity models. In Smith et al (1985), the uncertainties in the geopotential model (GEM-L2) were estimated to have a degrading effect of less than 5 cm in the coordinate solutions. The development of the improved TOPEX gravity model offers an opportunity to compute new coordinate solutions whereby many of the uncertainties associated with the geopotential model have been further minimized. As part of these efforts, better models for describing tides, polar motion, and non-conservative forces have been developed thereby minimizing uncertainties arising from these parameters. This section restricts itself to preliminary solutions for station coordinates and an assessment of the quality of station positioning which has been achieved.

### 9.3.2 GEM-T1 STATIONS

The GEM-T1 solution was made holding the station coordinates fixed in the TCS system at the values described in Section 6. However, with the arrival of GEM-T1 force modeling, two solutions have been performed and tested against the a priori values. These solutions included:

- \* Doppler station coordinates from a combination of SEASAT and OSCAR data and
- \* A laser solution from 5 years of LAGEOS observations.

The laser solution used the GEM-T1 gravity and tide models. The Doppler solution used an earlier GEM-T1 model which contained GEM T1's entire doppler data set but was otherwise incomplete.

### 9.3.3 Laser Station Solutions

We will concern ourselves, for the moment, with the laser network. A solution for coordinates for stations tracking LAGEOS has been computed utilizing the SOLVE software package. This solution incorporates five years of LAGEOS tracking data and also solves for polar motion, A1-UT1, GM, and the Love numbers  $h_2$ ,  $k_2$ . The GEM-T1 gravity model was used in this solution. This coordinate solution is equivalent to a first iteration using a new gravity model and is not equivalent to making a simultaneous solution for station positions and gravity field. This means that part of the a priori coordinate uncertainties may possibly have been absorbed in the adjustment for the gravity field (i.e. the computation for GEM-T1) since the gravity field and the station positions may be, in some way, correlated.

To test for the internal consistency of the solution, the solved for coordinates were compared to the a priori set of coordinates in the TOPEX geodetic file. This comparison (as well as those that follow) was performed using software which determines the seven parameter transformation between the two sets of coordinates in a least squares algorithm. This is the same software used in creating the geodetic file (see Section 6 on Station Coordinates).

Within the transformation parameters, the translational components provide an internal check of the stability of the origin of the coordinate system. For the LAGEOS solution, these parameters reveal an encouraging picture. The results discussed here are summarized in

TABLE 9.8  
SEVEN PARAMETER COMPARISONS BETWEEN STATION COORDINATE SOLUTIONS

| PARAMETER  | LASER: NEW vs. A PRIORI | DOPPLER: NEW vs. A PRIORI | DOPPLER : NEW vs. PTGF-2 |
|------------|-------------------------|---------------------------|--------------------------|
| $\Delta X$ | 0.26 cm                 | 11.64 cm                  | -24 cm                   |
| $\Delta Y$ | 1.46 cm                 | 4.16 cm                   | -5 cm                    |
| $\Delta Z$ | -2.54 cm                | -93.89 cm                 | -4 cm                    |
| scale      | 0.005 ppm               | 0.011 ppm                 |                          |
| omega      | 0.23 mas                | 30.7 mas                  |                          |
| psi        | -1.48 mas               | -10.5 mas                 |                          |
| epsilon    | -1.11 mas               | 1.86 mas                  |                          |
| RMS X      | 5.42 cm                 | 55.58 cm                  | 131 cm                   |
| RMS Y      | 4.40 cm                 | 63.30 cm                  | 114 cm                   |
| RMS Z      | 4.23 cm                 | 54.66 cm                  | 59 cm                    |
| stations   | 43                      | 35                        | 28                       |

Table 9.8 along with results from the Doppler solutions. The 2.5 cm value (and less) for the origin translation implies that the coordinate system and reference frame were properly maintained in the development of the TOPEX gravity model effort. The rotational elements of the transformation provide information regarding mismodeling of the axes definition. The values for these rotations are at the milli-arc second level.

Differences in cartesian and geodetic coordinates can be analyzed after the transformation has been made. With these differences, aberrant stations can be isolated easily and the RMS value of all of the differences allows an assessment of the consistency between the two sets of coordinates. Upon removing a small set of weakly determined stations, a 43 station comparison was made. The RMS value of the differences for these 43 stations is 5 cm or less for each Cartesian coordinate. Thus one can conclude that the a priori positions (the SL-6 values) for the LAGEOS tracking stations were well determined and that, in general, these positions are known relatively to better than 5 cm in any direction.

#### 9.3.4 Doppler Station Solutions

The Doppler results are not as encouraging as the laser results. The GSFC group has computed a set of solutions for Doppler station coordinates based on the complete SEASAT and OSCAR tracking data. The station coordinates from this solution are thought to be among the best available and are given in Table 9.9. The University of Texas Center for Space Research has also made a similar solution based on one of their preliminary TOPEX gravity models.

First, we will discuss the comparison results for the GSFC SEASAT/OSCAR solution with the a priori station coordinates in the TOPEX geodetic file. Referring again to Table 9.8, it can be noted that the

Table 9.9 Doppler Station coordinates based upon PGS-T2' gravity field.

| name    | num.  | X  | Y       | Z          | dd mm ss.ssss | dd mm ss.ssss | longitude | latitude | height |
|---------|---|--|---------|------------|---------------|---------------|-----------|----------|--------|
| SJEDOP  | 8   | 4083913.573800-4209803.360600-2499113.610600 | -23 12  | 2.9371     | 314           | 7 49.3604     | 612.9718  |          |        |
| MCMDDOP | 19-1310714.327500                                 | 310460.178800-6213366.135200                 | -77     | 50 51.7210 | 166 40        | 27.5393       | -13.3333  |          |        |
| MAHDOP  | 20 3602881.466600                                 | 5238221.052500-515942.091700                 | -4      | 40 14.4561 | 55 28         | 46.4214       | 554.4624  |          |        |
| UCLDOP  | 21 4027833.675100                                 | 307023.119300 4919537.009200                 | 50 47   | 54.9566    | 4 21          | 32.2662       | 158.6962  |          |        |
| SMGDDOP | 22-3088047.766000                                 | 5333058.457000 1638810.773500                | 14 59   | 16.0794    | 120 4         | 21.0223       | 56.5049   |          |        |
| GWMDDOP | 23-5059776.901400                                 | 3591211.911800 1472781.612500                | 13 26   | 22.8662    | 144 38        | 4.2254        | 95.4591   |          |        |
| TAFDOP  | 24-6100051.346100                                 | -997193.869001-1568316.457900                | -14 19  | 45.3816    | 189 17        | 3.0985        | 45.7365   |          |        |
| MSADOP  | 27-3857199.252000                                 | 3108663.581400 4004043.602400                | 39 8    | 6.5598     | 141 8         | 0.0168        | 122.0553  |          |        |
| PRTDOP  | 105 5051979.361600                                | 2725636.047000-2774471.714200                | -25 56  | 48.6545    | 28 20         | 51.6482       | 1607.9857 |          |        |
| VIRDOP  | 107 1090139.925300                                | -4842520.544000 3991980.602100               | 38 59   | 43.7271    | 282 41        | 12.6026       | 85.1699   |          |        |
| STFDOP  | 112-3942239.972800                                | 3468854.894100-3608206.038100                | -34 40  | 26.4843    | 138 39        | 17.3286       | 36.9684   |          |        |
| NMXDOP  | 113-1556216.300000                                | -5169444.400000 3387248.800000               | 32 16   | 43.9534    | 253 14        | 45.7268       | 1183.4922 |          |        |
| ANCDOP  | 114-2656164.814100-1544366.619100                 | 5570654.124900                               | 61 17   | 0.4266     | 210 10        | 29.5907       | 76.3954   |          |        |
| BSEDOP  | 116 4004965.181300                                | -96560.012500 4946540.225700                 | 51 11   | 4.5330     | 358 37        | 7.9032        | 125.3628  |          |        |
| TULDOP  | 118 539846.322900-1                               | 388555.012600 6180979.992300                 | 76 32   | 9.0740     | 291 14        | 42.8136       | 68.8087   |          |        |
| ALTDOP  | 127-3850349.491000                                | 397642.607500 5052347.981900                 | 52 43   | 41.8761    | 174 6         | 13.3734       | 73.0156   |          |        |
| OTTDOP  | 128 1091450.648500-4351284.681200                 | 4518703.573000                               | 45 23   | 59.8860    | 284 4         | 52.3730       | 47.3492   |          |        |
| TEXDOP  | 192 -740293.468700-5457073.249600                 | 3207243.561400                               | 30 23   | 1.1022     | 262 16        | 28.3874       | 218.3548  |          |        |
| FLODOP  | 641 4522403.122800                                | 898011.711900 4392485.926100                 | 43 48   | 13.6560    | 11 13         | 51.9826       | 147.7314  |          |        |
| ACSDOP  | 68 6119385.149700-1571426.518600                  | -871690.023200                               | -7 54   | 28.1648    | 345 35        | 52.5543       | 46.1535   |          |        |
| KWJDOP  | 214-6160998.307900                                | 1339621.205200 960416.180000                 | 8 43    | 6.9609     | 167 43        | 58.0634       | 36.7855   |          |        |
| QUIDOP  | 121 1280855.854900-6250961.221400                 | -10806.752400                                | 0 5     | 51.6884    | 281 34        | 47.7330       | 2711.3358 |          |        |
| SHIDOP  | 123 6104424.398300                                | -611087.365300-1740830.800000                | -15 56  | 34.8304    | 354 17        | 0.2890        | 604.1717  |          |        |
| HONDOP  | 188-5511608.514600-2226970.831300                 | 2303885.073100                               | 21 18   | 52.5097    | 202 0         | 4.3898        | 19.9707   |          |        |
| STODOP  | 280 1743940.076400-5022701.153800-3512034.477600  | -33 37                                       | 26.0465 | 289 8      | 51 51.3386    | 449.1890      |           |          |        |
| CALDOP  | 414-1659604.047400-3676718.989500                 | 4925497.766500                               | 50 52   | 17.0968    | 245 42        | 23.2188       | 1247.6164 |          |        |
| NAPDOP  | 448-4923683.766500                                | 270897.300000-4031783.343900                 | -39 27  | 31.6075    | 176 51        | 2.8991        | 19.1794   |          |        |
| EASDOP  | 730-1888663.201600-53355677.966300-2893871.401500 | -27 9  | 30.1475 | 250 34     | 29.8560       | 49.7576       |           |          |        |
| TIEDOP  | 793-5037686.183500                                | 3301866.756900-2090791.616000                | -19 15  | 43.8999    | 146 45        | 28.2094       | 66.2392   |          |        |
| BGKDOP  | 800-1139090.620500                                | 6089775.302400 1510692.144300                | 13 47   | 32.9671    | 100 35        | 41.0243       | -13.2719  |          |        |
| DGCDOP  | 939 1915631.941000                                | 6030276.444000-801057.498700                 | -7 15   | 49.0991    | 72 22         | 35.6174       | -57.5421  |          |        |
| LADOP   | 966 4432069.311200-2268085.806300                 | 3973469.226100                               | 38 46   | 51.2986    | 332 53        | 56.9995       | 131.8420  |          |        |
| BRADOP  | 967 22933703.881200-1883222.108500                | 3390597.138100                               | 32 19   | 16.9383    | 295 9         | 35.8834       | -5.3777   |          |        |
| PERDOP  | 968-2353565.897200                                | 4877202.957400-3358334.837400                | -31 58  | 39.4718    | 115 45        | 37.1351       | 13.5722   |          |        |
| CNIDOP  | 970 5384988.497500-1576475.750800                 | 3023842.298400                               | 28 54   | 47.18      | 343 40        | 56.6697       | 625.9310  |          |        |
| UKIDOP  | 1960-2713391.978100-4144609.641000                | 4004304.375500                               | 39 8    | 16.1970    | 236 47        | 16.9567       | 169.9827  |          |        |

Semi-major axis: 6378137.00

Flattening: 1/298.257

center of mass offset between the two sets of coordinates is quite small in the equatorial plane but the magnitude of the axial displacement in the Z direction is nearly -1 meter. This result is similar to that observed in earlier, and unfortunately unreported, GSFC studies dealing with laser tracking sites determined in similar coordinate systems. In the earlier work, a pair of solutions for laser coordinates was made, one based on the SL-6 system and the other based on a coordinate system associated with the PGS-S4 gravity model. The earlier station comparison between these two sets of coordinates showed, as does our station comparison, this -1m Z coordinate offset. Since our a priori stations are based on the SL-6 system, it seems that in the adjustment for the Doppler stations, the stations are adjusting towards those computed in the PGS-S4 based solution. The scale parameter is at the 11 parts per billion level, this slight scale change is most likely attributable to the adjustment of GM. The RMS of the differences between the transformed coordinates is at the 60 cm level (an order of magnitude worse than the lasers). A portion of the RMS disagreement is attributable to errors in the Doppler tracking systems and in part due to the larger SEASAT orbit errors.

A comparison of the GSFC SEASAT/OSCAR solution has been made with a similar solution by University of Texas utilizing their PTGF-2 gravity model (the comparison was provided courtesy of C.K. Shum). This comparison is also summarized in Table 9.8. The translational components of the seven parameter transformation are of the same magnitude as those seen in the previous discussion except that the  $\Delta Z$  shift is now quite small. Thus, the adjusted Doppler station coordinates in both the GSFC and UT solutions appear to agree well with regard to the coordinate system origin. By the same token, the RMS differences of the positions after transformation are on the 0.5 to 1.5 m level. This leads one to conclude that the station positions are still not resolvable to a level below 50 cm with Doppler data.

The causes for the poor resolution at the Doppler sites are still being studied at this time. The RMS differences after transformation are consistent with the formal uncertainties of 20 to 50 cm observed in the Doppler solution. Modeling the Doppler data as one way average range-rate with pass by pass measurement bias adjustments is the major reason that the solution is formally weak. Additional areas of investigation to improve the determination of the Doppler sites include a re-assessment of editing procedures and re-evaluation of deficiencies in the measurement model, among others. If ten centimeter positioning is expected from TOPEX Doppler tracking, these issues must be resolved.

#### 9.3.5 Summary

The preliminary station solutions basically demonstrate two general conclusions. First, the laser sites in general are very well determined in the a priori geodetic file. Second, the Doppler station coordinates have an uncertainty of 50cm to 1m at some sites. The laser station result comes as no surprise since the a priori laser site positions were determined in a dynamic solution (SL-6) made at GSFC which is very similar in character to the TOPEX laser solution. We note, in conclusion, that we are currently capable of obtaining with the LAGEOS laser data more than an order of magnitude better station location accuracy than with Doppler data.

### 9.4 EVALUATION OF THE ADJUSTED EARTH ORIENTATION PARAMETERS

#### 9.4.1 Introduction

Accurate determination of the coordinates of the pole requires a robust, accurate and uniformly distributed set of tracking data. Satellites with minimal short periodic perturbations due to the Earth's gravity field are always preferred in this task (e.g. LAGEOS).

Considering the data on which our gravity solution is based and taking into account the above, we decided at present to adjust the pole positions during the 1980-84 period. During this period alone the a priori Earth Orientation Parameters (EOP) can be possibly improved in a combined solution.

#### 9.4.2 The 1980-84 Solution

The a priori polar motion series for the 1980-84 period are shown in Figure 9.2; the series that was simultaneously estimated with the GEM-T1 field is shown in Figure 9.3. Since we have kept the station positions fixed to their a priori values, we do not expect any large adjustments. This is clearly evident from the two figures. Within each 30-day arc of LAGEOS, a single value for A1-UT1 is held unadjusted to define the longitude of this satellite arc. This presents problems when the quality of the overall solution is to be assessed. The fact that our estimates of Earth rotation are recovered discontinuously from one 30-day interval to the next was overcome by the following procedure. The length of day variation series (LODR) were interpolated using cubic splines to determine the missing (constrained) values (i.e., those held fixed at the a priori values). Once this was done we formed a continuous A.1-UT1R series adopting only a starting value from BIH. Subsequently, the A.1-UT1R series were smoothed using a Vondrak filter with  $\epsilon=10^{-6}$ . This effectively suppresses periods below fifty to sixty days. The smoothed LODR series were obtained from the smoothed A.1-UT1R series by forward differencing. Both the a priori and estimated (smooth) series of Earth rotation (A.1-UT1R) and length of day variation (LODR) are shown in Figure 9.4. The next step was to remove the strong periodicities from the signals so that the underlying detailed structure could be revealed.

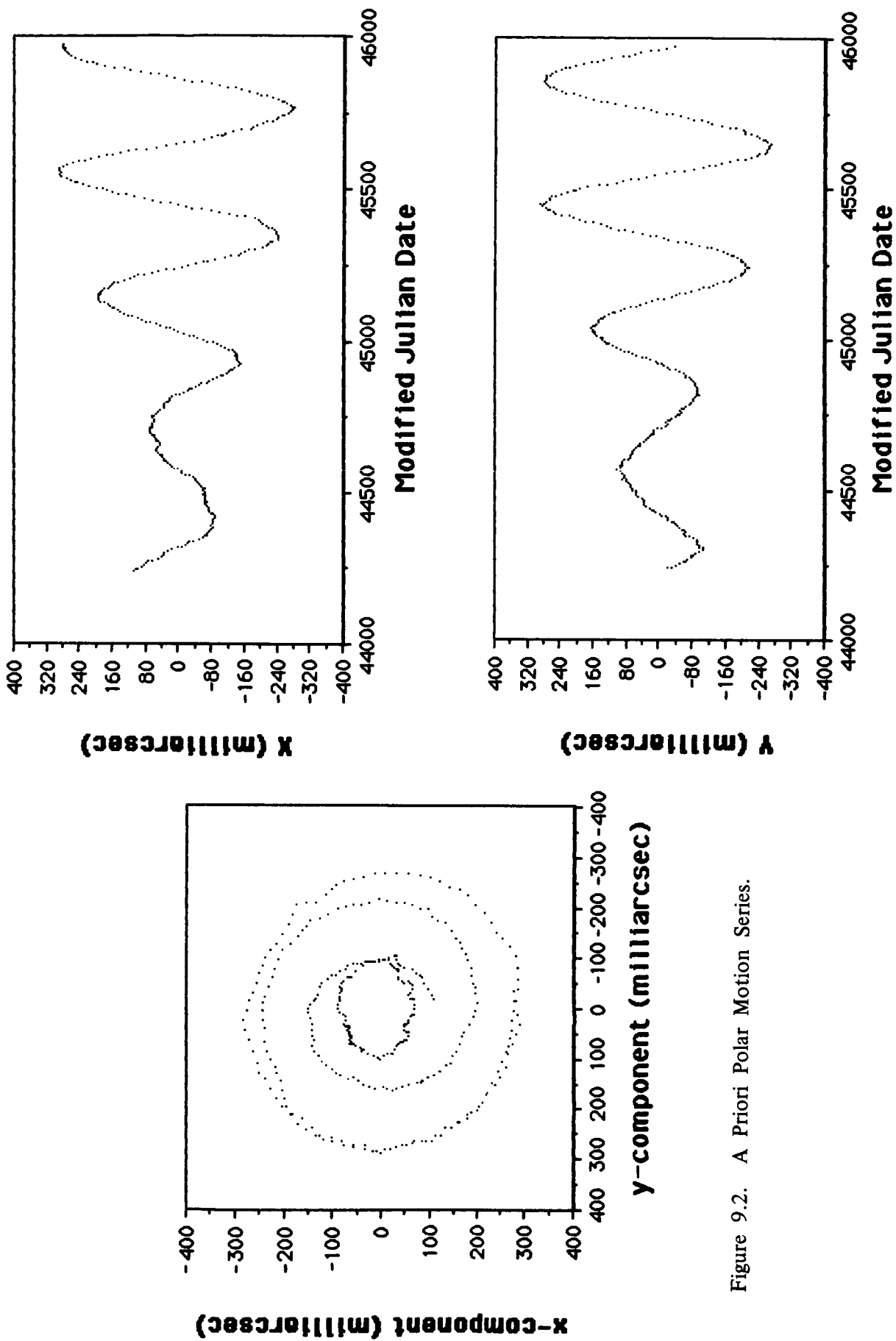


Figure 9.2. A Priori Polar Motion Series.

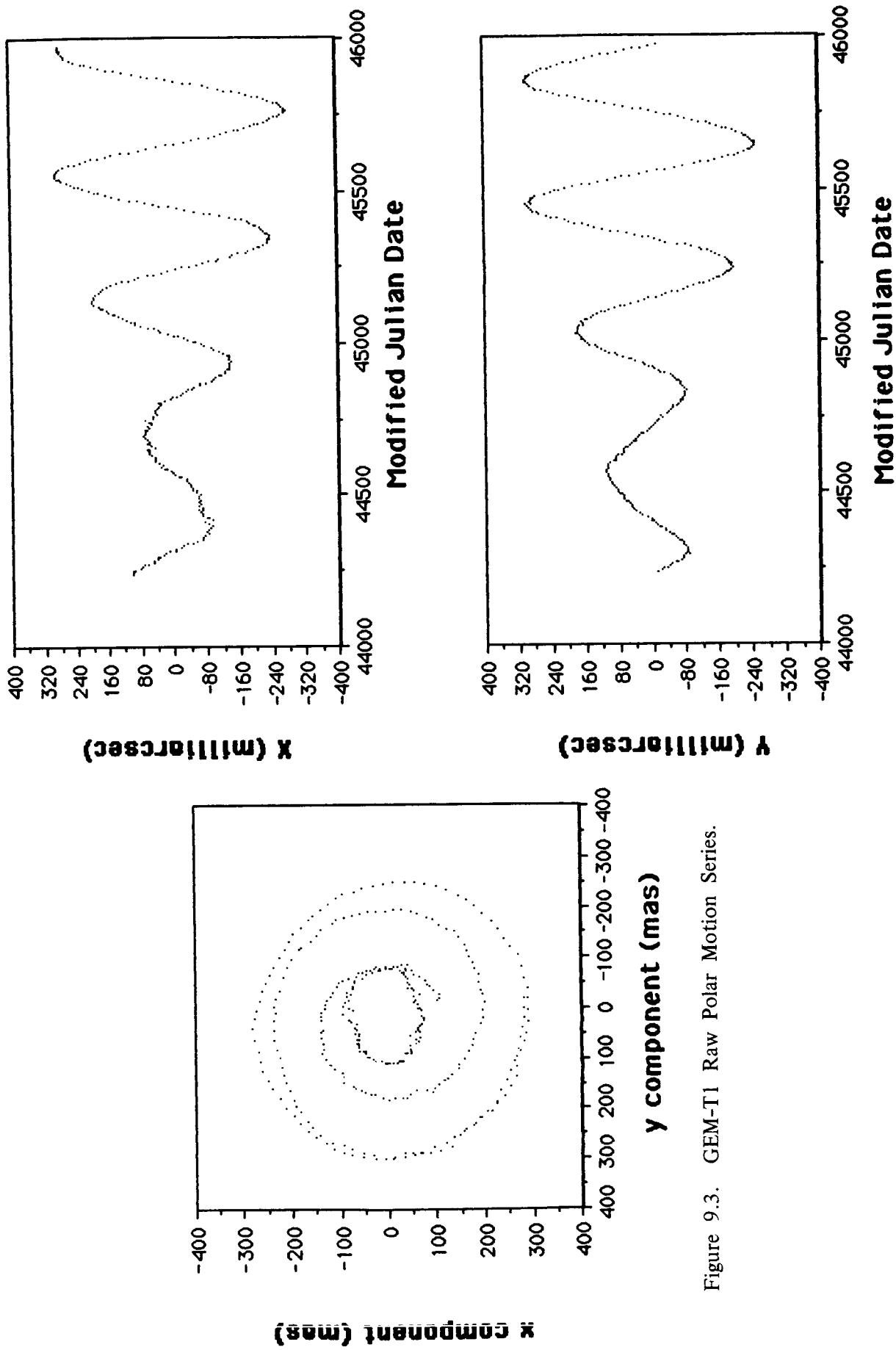


Figure 9.3. GEM-T1 Raw Polar Motion Series.

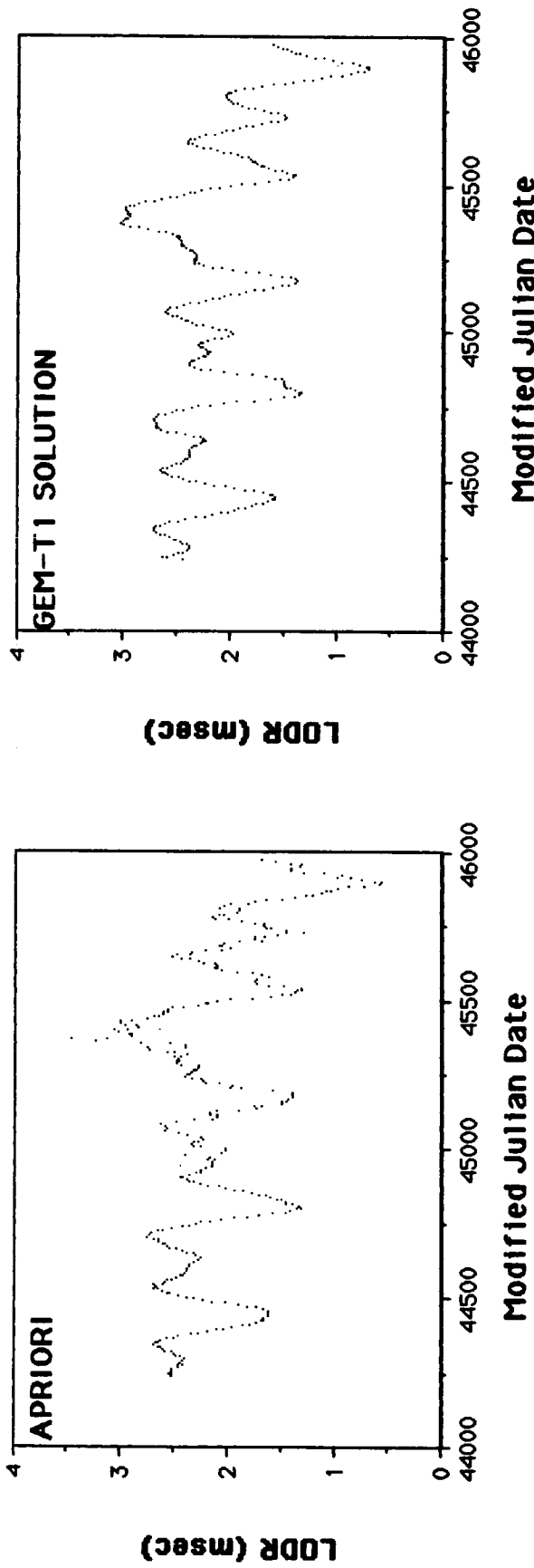
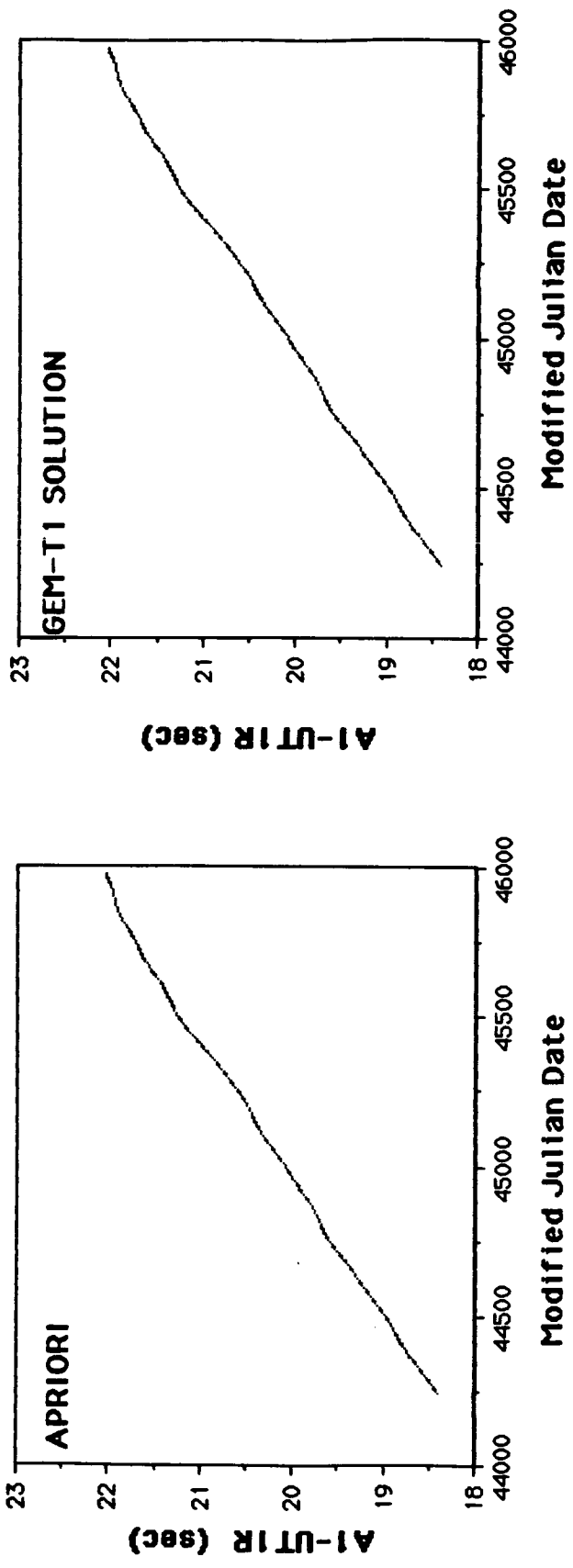


Figure 9.4. A Priori and GEM-T1 Vondrak Smoothed Earth Rotation Series.

#### 9.4.3 The Annual and Chandler Cycles

To remove the coordinate system dependence of this evaluation we first transformed the GEM-T1 solution to the a priori series frame of reference. This was accomplished by the same least squares process that was used to determine the transformation parameters between the LAGEOS SL6 series and the BIH series in the creation of the a priori series (see Section 3.0). The results of this transformation are given in Table 9.10. The raw differences due to our adjustment are shown in Figures 9.5 and 9.6 for the polar motion and Earth rotation series respectively. The large  $b_1$  rotation of 17.3 mas indicates a shift of the origin along the  $y_p$ -axis (that is in the negative Y-axis direction) as indicated in Figure 9.7. This has been resolved as an a priori bias of -18 mas along the Goddard meridian ( $\lambda \sim 283^\circ$ ) between the Z-axis of the a priori stations reference frame and the origin of the a priori polar motion. Since the station coordinates were held fixed during this solution, this rigid body rotation of the station network had to be accommodated by an opposite rotation of the estimated polar motion series.

An 18 mas rotation about an axis perpendicular to the Goddard meridian ( $\lambda \sim 283^\circ$ ) can be decomposed in two components along the  $x_p$  and  $y_p$  axes; the magnitudes of these turn out to be 4.0 mas and 17.5 mas respectively. It thus becomes apparent that there is no real change in the reference frame of the TOPEX solution for polar motion, and the Z-axis of the CTRS is retained.

An argument similar to the above explains the large systematic rotation  $\alpha_3 = 14.6$  mas about the Z-axis. This was derived on the assumption that  $\beta_3 = 0$ . This however turns out to be incorrect since the transformation between the a priori TOPEX stations and the stations compatible with the a priori Earth orientation series indicates a systematic longitudinal rotation of -6.9 mas. On top of that, the

Table 9.10

GEM-T1 TO APRIORI TOPEX  
EARTH ORIENTATION SERIES  
TRANSFORMATION PARAMETERS

REFERENCE FRAME ROTATIONS

$$\beta_1 = 17.3 \pm 0.2 \text{ mas}$$

$$\beta_2 = 2.3 \pm 0.2 \text{ mas}$$

$$\beta_3 \equiv 0.0 \text{ mas}$$

$$\alpha_1 = -0.13 \pm 0.2 \text{ mas}$$

$$\alpha_2 = -0.03 \pm 0.2 \text{ mas}$$

$$\alpha_3 = 14.1 \pm 0.2 \text{ mas}$$

EOP SERIES RAW DIFFERENCES

RMS ( $\Delta x$ ) : 4.0 mas

RMS ( $\Delta y$ ) : 3.5 mas

RMS ( $\Delta \text{UT}$ ) : 1.2 ms

RMS ( $\Delta \text{LOD}$ ) : 0.09 ms

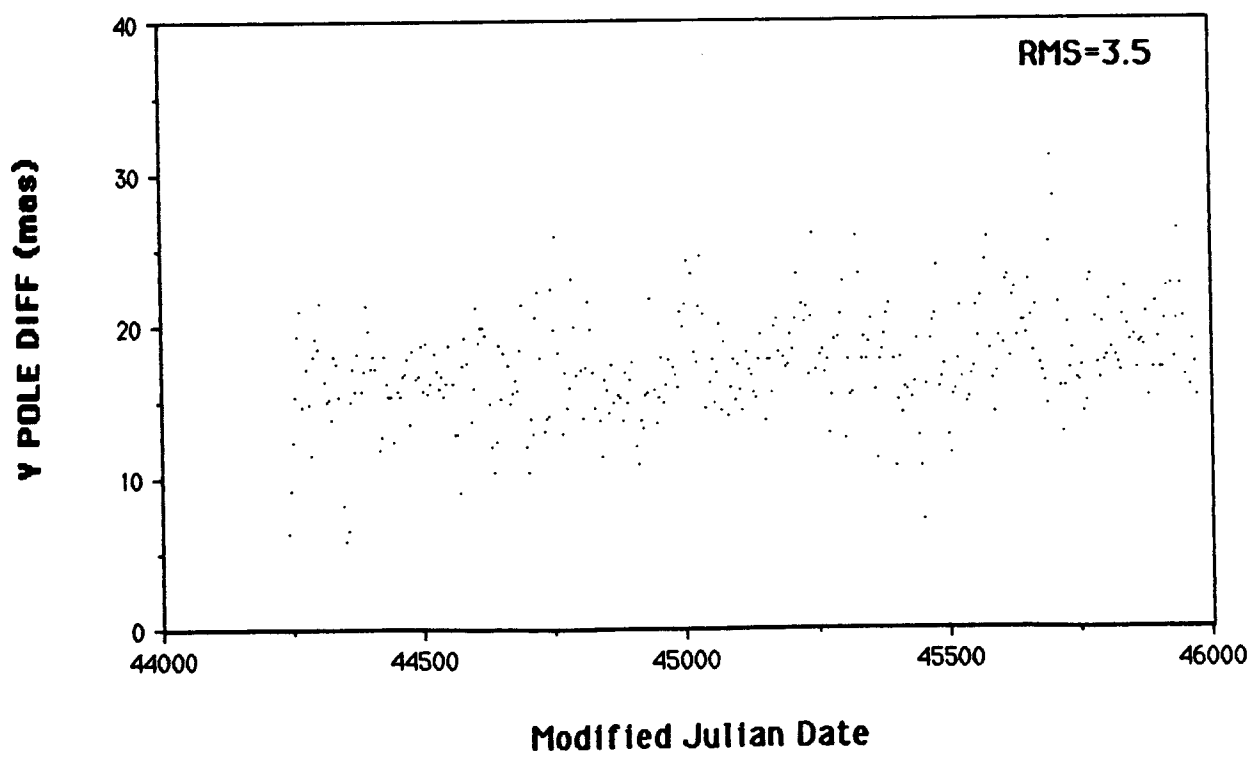
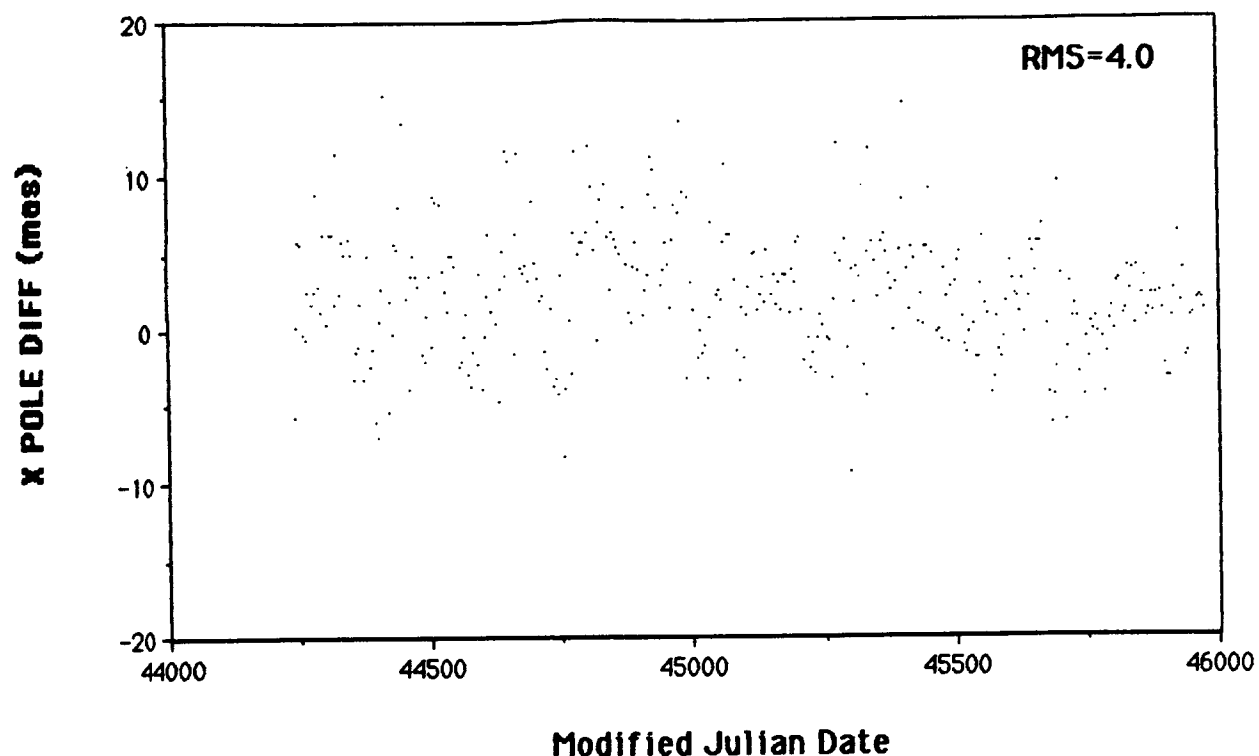


Figure 9.5. GEM-T1 Minus A Priori Polar Motion Series.

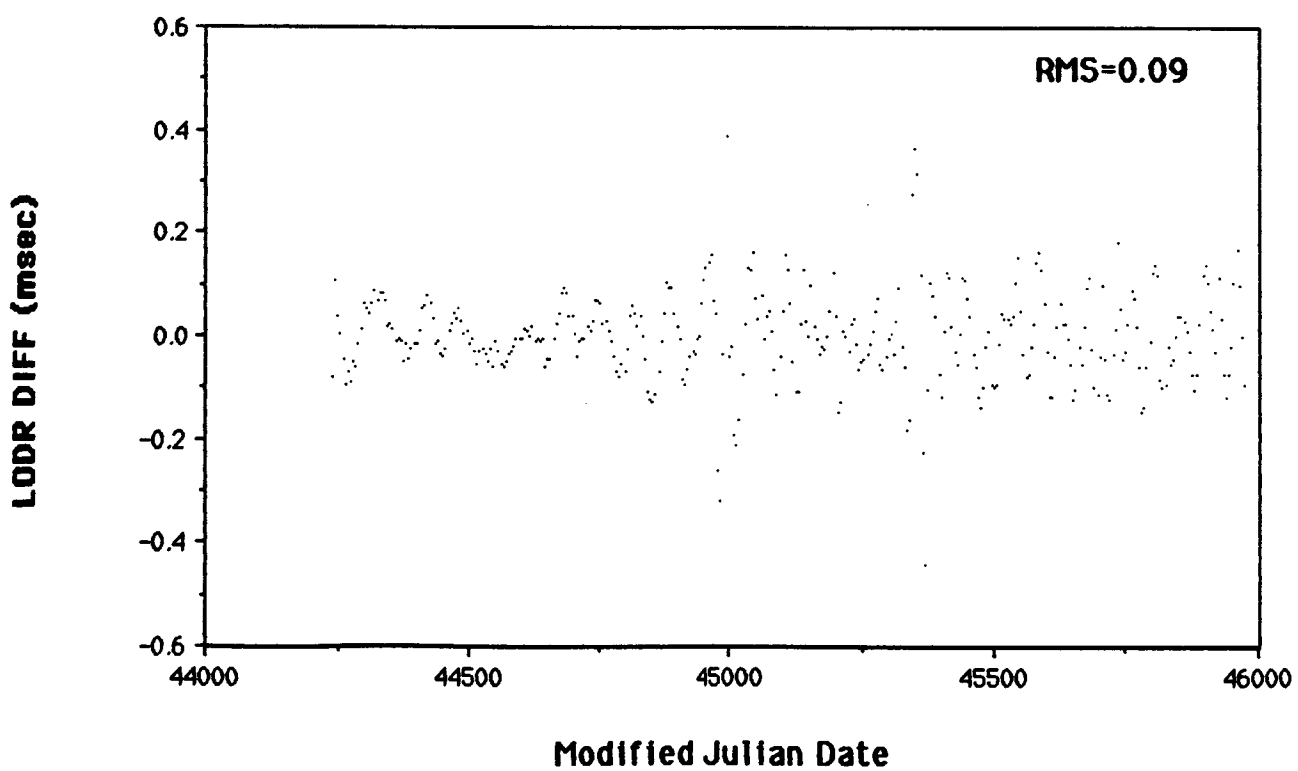
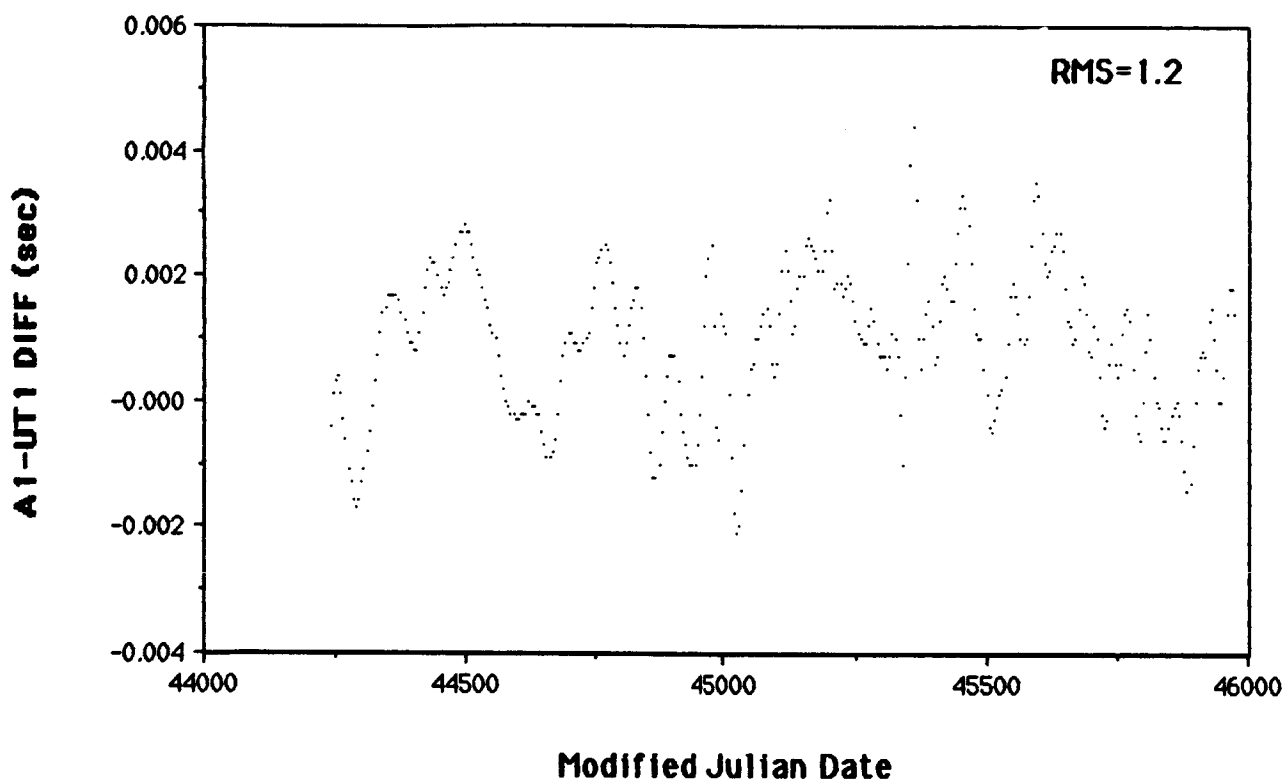


Figure 9.6. GEM-T1 (V-Smoothed) Minus A Priori Earth Rotation Series.

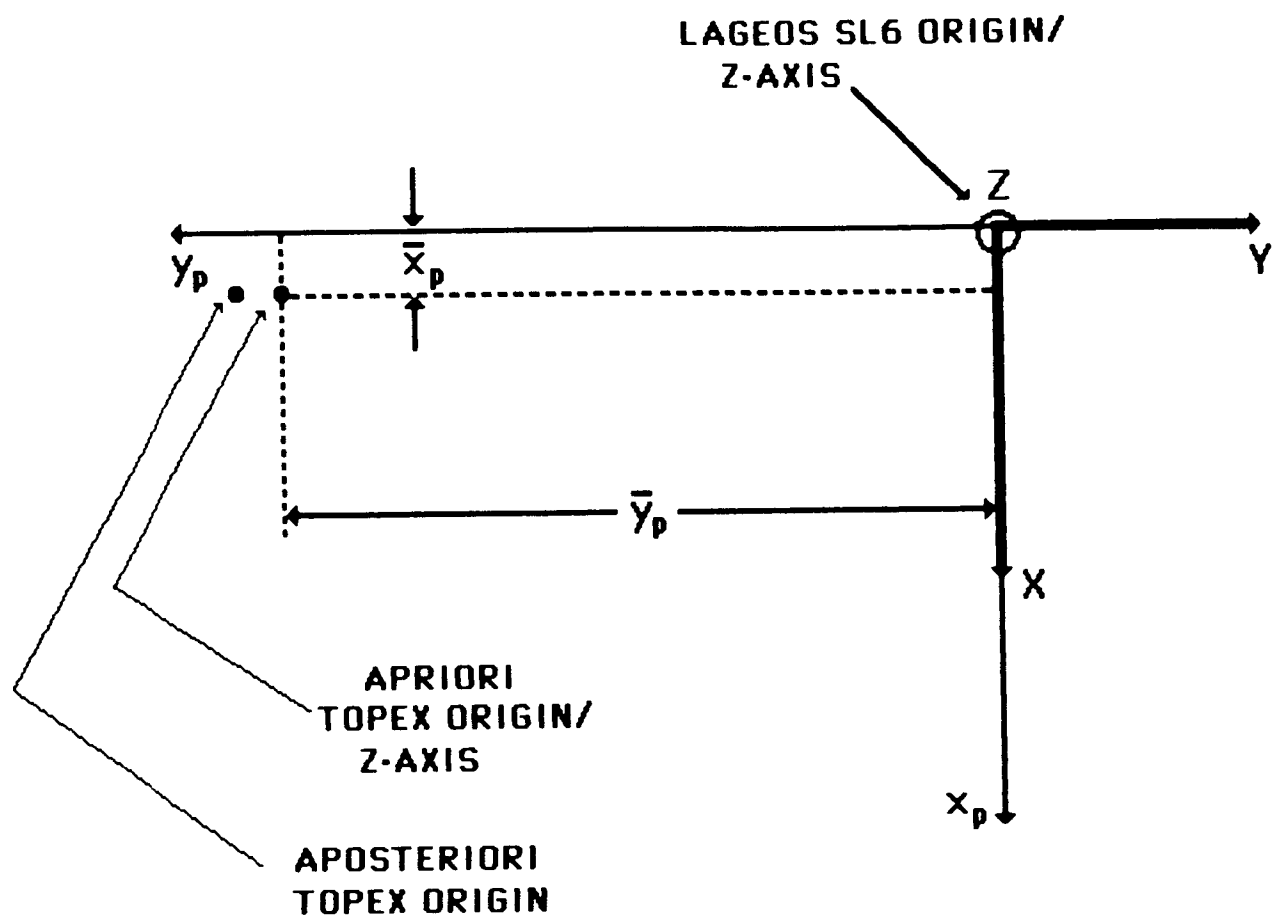


Figure 9.7. GEM-T1 Polar Motion Origin.

Starlette arcs that contributed to the GEM-T1 solution are based on a set of stations developed during MERIT that have an additional longitude offset of -8.8 mas with respect to the set of stations used for all other earlier satellite data sets. This discrepancy was largely accommodated by shifting the right-hand sides when combining normal matrices to produce a single matrix with a common station set. However, all stations are not common, and those which did not shift have to be accommodated somehow in the least squares process. Therefore we modify our original estimate of  $\beta_3 \approx 0$  mas to  $\beta_3 \approx -15.7$  mas and conclude that  $\alpha_3 \approx -1.2$  mas which is an acceptable change considering the fact that this solution is based on the simultaneous adjustment of several arcs from various satellites through an intricate weighted least squares process. The a priori Earth rotation series is based largely on astrometry (75%) and only in the very recent years on the preliminary VLBI results (25%). The results of fitting the EOP series with the two frequency models are presented in Tables 9.11 and 9.12. Since aliasing is possible due to the incomplete coverage of the beat period (short by 1.25 years), the estimates listed here are only meant for relative comparisons. They should not be used to compare with those resulting from the analysis of series covering other time periods. It is rather clear that the GEM-T1 solution agrees to a great extent with the a priori series. This is what we expected and hoped for since the two series share the strongest data set over the intercomparison period, namely, the LAGEOS SLR data. Comparing the rms of fit with the observed oscillations in the two components we conclude that the two frequency model explains satisfactorily more than 95% of the original signal. We have further analyzed the residuals to this model by creating their power spectra and subsequently the coherence spectra between the a priori and GEM-T1 series. There is a better than 80% agreement between all of the series at periods longer than sixty days.

Table 911

**COMPARISON OF  
POLAR MOTION SERIES PARAMETERS  
FOR THE  
TWO FREQUENCY MODEL**

$$\begin{matrix} x \\ y \end{matrix} = A + Bt + C_{\alpha} \cos \left( \frac{2\pi}{P_{\alpha}} t + \Phi_{\alpha} \right) + C_c \cos \left( \frac{2\pi}{P_c} t + \Phi_c \right)$$

| MODEL<br>PARAMETER    | SERIES    |           |           |           |
|-----------------------|-----------|-----------|-----------|-----------|
|                       | APRIORI   |           | GEM-T1    |           |
|                       | X         | Y         | X         | Y         |
| A (mas)               | -2.5±1.3  | 12.3±1.3  | -1.5±1.3  | 10.2±1.3  |
| B (mas/yr)            | 0.7±0.5   | -2.3±0.5  | 0.3±0.5   | -1.4±0.5  |
| C <sub>α</sub> (mas)  | 103.5±1.2 | 103.3±1.5 | 103.8±1.2 | 102.8±1.4 |
| P <sub>α</sub> (days) | 370.6±0.7 | 373.7±0.7 | 370.8±0.7 | 373.7±0.7 |
| Φ <sub>α</sub> (°)    | 138.1±1.7 | 237.4±1.8 | 138.1±1.7 | 237.5±1.7 |
| C <sub>c</sub> (mas)  | 180.1±1.2 | 179.0±1.5 | 180.1±1.2 | 178.4±1.5 |
| P <sub>c</sub> (days) | 432.7±0.5 | 433.1±0.7 | 432.5±0.5 | 433.1±0.6 |
| Φ <sub>c</sub> (°)    | 1.5±0.9   | 95.9±1.1  | 1.3±0.9   | 95.8±1.1  |
| RMS (mas)             | 11.9      | 11.8      | 12.0      | 11.2      |

t(days) = T - T<sub>0</sub>      T<sub>0</sub> = MJD 44239.0

Table 9.12

**COMPARISON OF  
EARTH ROTATION SERIES PARAMETERS  
FOR THE  
TWO FREQUENCY MODEL**

$$\left. \begin{array}{l} A1-UT1R \\ LODR \end{array} \right\} = A + Bt + C_{\alpha} \cos \left( \frac{2\pi}{P_{\alpha}} t + \phi_{\alpha} \right) + C_s \cos \left( \frac{2\pi}{P_s} t + \phi_s \right)$$

| MODEL<br>PARAMETER    | SERIES      |            |             |            |
|-----------------------|-------------|------------|-------------|------------|
|                       | APRIORI     |            | GEM-T1      |            |
|                       | A1-UT1      | LODR*      | A1-UT1      | LODR*      |
| A (ms)                | 18436.1±3.9 | 2.42±0.03  | 18436.8±3.9 | 2.42±0.03  |
| B (mas/yr)            | 791.9±1.5   | -0.13±0.01 | 792.0±1.5   | -0.13±0.01 |
| C <sub>α</sub> (ms)   | 24.9±2.8    | 0.40±0.02  | 25.0±2.7    | 0.40±0.02  |
| P <sub>α</sub> (days) | 340.8±4.3   | 365.0±2.3  | 338.7±4.2   | 363.6±2.2  |
| Φ <sub>α</sub> (°)    | 185.2±13.2  | 331.5±6.2  | 179.2±13.1  | 326.6±5.9  |
| C <sub>s</sub> (ms)   | 14.6±2.8    | 0.34±0.02  | 14.0±2.8    | 0.34±0.02  |
| P <sub>s</sub> (days) | 183.5±2.0   | 182.4±0.6  | 180.4±2.2   | 182.3±0.6  |
| Φ <sub>s</sub> (°)    | 71.3±21.5   | 136.9±6.9  | 52.9±23.4   | 137.5±6.6  |
| RMS (ms)              | 36.8        | 0.27       | 36.8        | 0.26       |

t(days) = T - T<sub>o</sub> ; T<sub>o</sub> = MJD 44239.0

\* NOTE: LODR values refer to 2.5 days prior to T.

#### 9.4.4 Summary

We have presented here an evaluation of the first Earth Orientation Parameters series obtained by the GEM-T1 solution. A continuous Earth rotation series was derived on the basis of the estimated Earth rotation variations (LODR). We have a viable technique to unify this inherently discontinuous series into a continuous one with satisfactory results and no apparent introduction of any distortions. The results indicate that all series agree very well with the a priori, a fact that was intuitively expected. A more comprehensive analysis of the EOPs will be possible (and more meaningful) when a complete solution (including station adjustments) becomes available.

SECTION 10.0  
A CALIBRATION OF GEM-T1 MODEL ACCURACY

One of the difficulties faced in a numerical solution for a large number of physical parameters is the determination of meaningful accuracy estimates for the result beyond what is learned from formal solution uncertainties. As is well known, the process of fitting a model to observations provides an internal measure of precision on the assumption that the model is exact, i.e., formal statistics. But the value of this estimate is generally optimistic with respect to the real accuracy attained since the observations are inevitably represented by an approximate (incomplete) mathematical model. Yet, in our case without a better estimate of the accuracy of the geopotential, the results may have limited value, especially in non-orbital investigations.

In recent GEM solutions, a considerable effort has gone into the calibration of the field errors. The accuracy assessments, for example those found in Lerch et al, (1985), have relied almost exclusively on tests using independent data. These calibrations have been strengthened by having "satellite-only" models which exclude altimetry and surface gravimetry. One of the best ways of obtaining realistic errors for the models comes from comparing satellite derived information to independent and globally well distributed gravity anomaly and altimetry observations. Although independent data are employed, the calibration needs to be well designed, for there is a wide range of wavelengths spanned within a geopotential solution. Although these tests are never complete for every harmonic term in fields containing 1000 or more coefficients, they need to be diverse enough so that the long, intermediate and short wavelength portions of the field are calibrated in an overall fashion.

In previous GEM models, the accuracies of the fields have been successfully calibrated through the application of a single scaling factor applied to the formal variances of the solution. This approach is again undertaken here. However, it should be noted that, while the method is generally satisfactory, the lowest degree and order portion of the field is somewhat optimistically evaluated with this approach (by approximately 30%). This problem was found in the calibration of GEM-L2 (Lerch et al, 1985) and seems to apply equally to the calibration performed here on our new GEM-T1. Apparently, although it is not too surprising, systematic errors arising from the orbit determination procedures seem to more adversely alias the long rather than short wavelength portion of the gravity model. Still, as percentages of the full coefficient values, the errors found in the long wavelength terms in the model are much smaller than those found elsewhere in the field. Therefore, we have continued to produce error estimates based on a single scaling factor because the complexity introduced by using multiple scaling factors is presently unjustified and the single coefficient approach (our experience has shown) produces a good overall calibration. To more fully understand this calibration, the method of solution for GEM-T1 found in Section 8 should be consulted.

Based upon the data weights and scaling factors described in Section 8.2, the uncertainty in the GEM-T1 gravity solution is shown in Figure 10.1. When compared pictorially to other GEM models, as is done in Figure 10.2, one sees clearly the major reduction in errors that has been achieved, with our new gravity field modeling capabilities, in the GEM-T1 solution. The adequacy of these estimates of error is the subject of the remainder of this section. (The calibrated uncertainties for GEM-L2 and PGS-T2 have been previously shown in Figures 5.2.8a and 5.2.8b and may be consulted for comparison purposes.)

An interesting manifestation of our use of least squares collocation can be seen upon examination of Figure 10.1. The

Figure 10.1. Estimated Errors for GEM-T1 Coefficients.

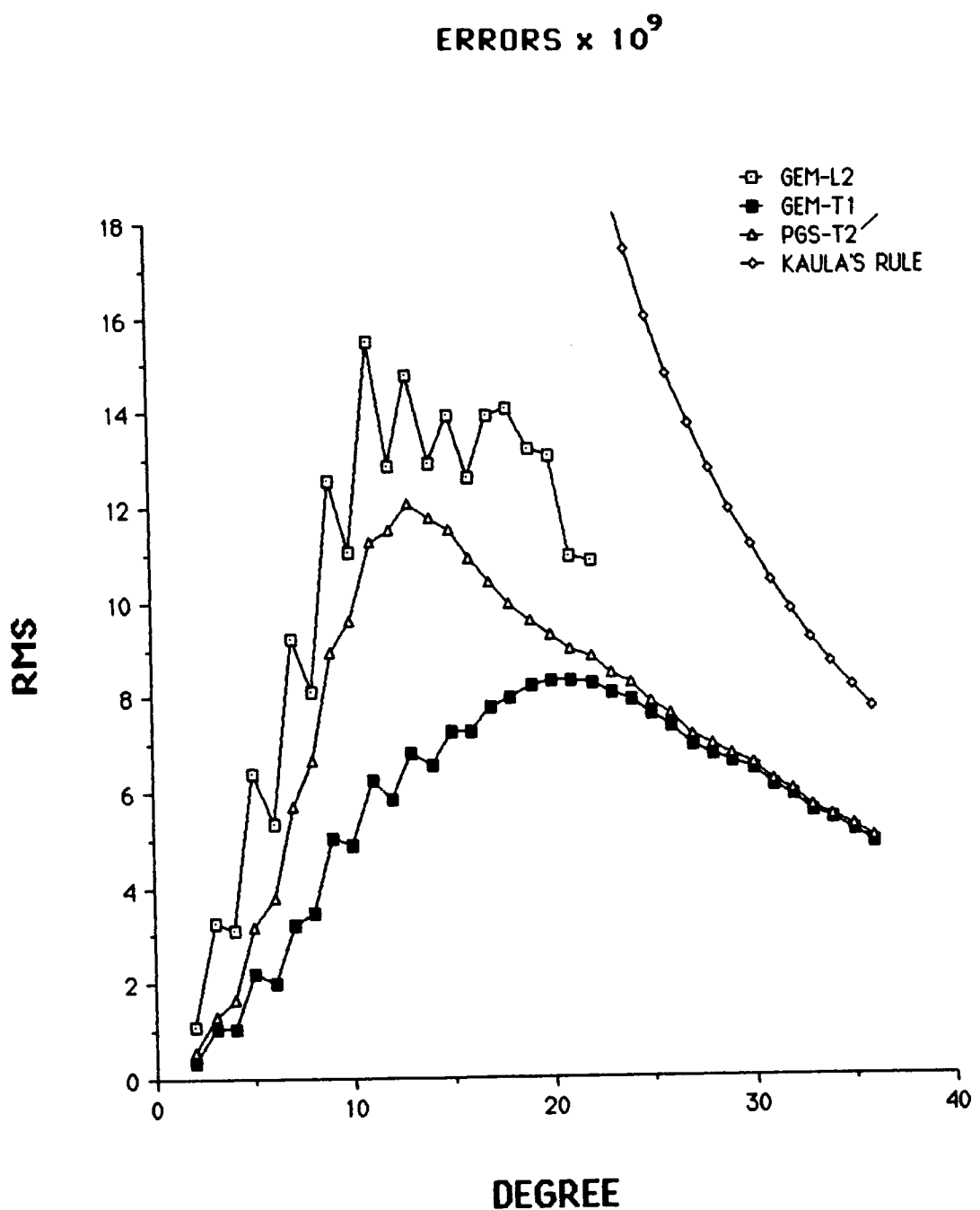


Figure 10.2. RMS of Coefficient Error Per Degree.

uncertainty for the highest degree terms in the model (except those of the zonal and resonant orders) are shown to be nearly 100% in error based upon their expected power. While collectively these terms contain valuable signal, individually, they are not well resolved. However, truncation of the field to a lower degree is unjustified, for as already shown in Figure 8.7, a significant amount of valuable information is lost by taking this approach. Nevertheless, based upon this preliminary scrutiny of the magnitude of the calibrated coefficient uncertainties, these high degree terms have been constrained to have no more than 100% of their expected power as their estimated error; and this is both a reasonable and desirable result for terms poorly resolved by dynamic orbital tracking data.

## 10.1 THE GEM-T1 CALIBRATION OF A SATELLITE MODEL'S ERRORS USING GRAVITY ANOMALY DATA

Mean free air gravity anomalies (on the geoid) can be calculated from the spherical harmonics of a gravity field as follows (Heiskanen and Moritz, 1967):

$$\Delta g_s = \sum_{\ell=2}^{\ell_{\max}} \sum_{m=0}^{\ell} \gamma(\ell-1) B_{\ell} \left( \frac{a_e}{r} \right)^{\ell} \bar{P}_{\ell m}(\sin\phi) [\bar{C}_{\ell m} \cos m\lambda + \bar{S}_{\ell m} \sin m\lambda] \quad (10.1)$$

where

$\gamma$  is the mean value of equatorial gravity.

$a_e$  is the earth's semi-major axis.

$r$  is the radius to the surface of the best fitting earth ellipsoid.

$\bar{P}_{\ell m}(\sin\phi)$  is the fully normalized associated Legendre function for geocentric latitude  $\phi$ .

$\lambda$  is the geographic longitude,

$B_{\ell}$  is Pellinen's smoothing factor (described in Katsambalos, 1979) corresponding to the block size over which  $\Delta g_s$  is averaged over. (Note:  $B_{\ell}=1$  for point anomaly values)

and

$\bar{C}_{\ell m}, \bar{S}_{\ell m}$  are the normalized spherical harmonics of the field with the reference ellipsoid zonal potential (even terms only) subtracted.

If

$\langle \rangle =$  global average value

$E =$  statistically expected value and

$\epsilon_s =$  Error in  $\Delta g_s$  from coefficient commission errors

then

$$E \langle \epsilon_s^2 \rangle = \sigma_{\text{Model}}^2(\Delta g_s) = \sum_{l=2}^{l_{\max}} \sum_{m=0}^l r^2(l-1)^2 \sigma^2(\bar{C}_{lm}, \bar{S}_{lm}) B_l^2 \quad (10.2)$$

where

$E \langle \epsilon_s^2 \rangle$  is the expected error in the gravity anomalies based upon the estimated errors in the satellite potential coefficients and  $\sigma^2(\bar{C}_{lm}, \bar{S}_{lm})$  is the variance of the pair of coefficients  $\bar{C}_{lm}, \bar{S}_{lm}$ .

Section 8.2 describes the data weights and scaling factors which have been determined to yield a well balanced solution for GEM-T1, and a solution which has realistic potential coefficient errors within its covariance. We wish to present the calibration this model has undergone based upon the best available and refined gravimetry and altimetry which we have employed as independent measures. Kaula (1966) showed how the errors (both of omission and commission) in a harmonic field can be estimated directly by comparison with independent global surface gravity data without forming harmonics for the surface information. The essential statistic is the difference between the global variance of the computed quantity and the covariance of computed and measured data. The expected value of this statistic is the expected global commission error of the model. If one also has reliable information on the errors in the surface data one can also estimate the omission (truncation) error in the harmonic field by computing the rms difference of the two data sets.

In terms of gravity anomalies as developed by Kaula (1966) the mean square commission errors are estimated for a given blocksize as:

$$E \langle \epsilon_s^2 \rangle = \langle \Delta g_s^2 \rangle - \langle \Delta g \Delta g_s \rangle \quad (10.3)$$

where the calculated value  $\Delta g_s$  is

$$\Delta g_s = \Delta g_{\text{true}} \text{ (for harmonics in the model)} + \epsilon_s \text{ averaged over a given blocksize}$$

and the measured  $\Delta g$  is

$$\Delta g = \Delta g_{\text{true}} + \Delta g_{\text{omission}} + \delta g_{\text{data}} \text{ averaged over the same block size; } \delta g \text{ is measurement noise in } \Delta g.$$

The omission errors are estimated as:

$$E \langle \Delta g_{\text{omission}}^2 \rangle = \langle (\Delta g - \Delta g_s)^2 \rangle - [\langle \Delta g_s^2 \rangle - \langle \Delta g \Delta g_s \rangle] - \langle \delta g_{\text{data}}^2 \rangle \quad (10.4)$$

To estimate a further scale factor in the coefficient uncertainties, we compare the estimated commission error from surface data, to model uncertainties and seek the scaling factor  $k$  in the equation:

$$\text{EST } \sigma_{\text{true}}(\Delta g_s) = E \langle \epsilon_s^2 \rangle = k \sigma_{\text{GEM-T1}} \quad (10.5)$$

where

$k$  is to be determined from this analysis.

Unfortunately, for gravity anomalies the omission error for low degree fields is large and this simple estimate for commission error (Eq. 10.3) is unreliable for these terms. But the technique appears to give reliable results for complete high degree models especially in comparisons with global anomalies including marine values derived from altimetry. This calibration is most sensitive to the high degree and order field. Table 10.1 presents results of this calibration for GEM-T1.

The data sets used to calibrate our satellite geopotential models were obtained from two sources. Terrestrial surface gravimetric anomalies were obtained from Rapp, (1981). They were in  $1^\circ \times 1^\circ$  observed (or geophysically predicted) areal means. Altimeter derived gravity anomalies from SEASAT were also used. These gravity anomalies were used in the form of  $5^\circ$  equal area mean anomalies computed from the original  $1^\circ$  values. The total estimated commission error for GEM-T1 based on the uncertainties in Figure 10.1 for  $5^\circ$  anomalies is given by:

$$\sigma_{\text{GEM T1}}(\Delta g_s) = \gamma \left[ \sum_{l=2}^{36} \sum_{m=0}^l B_l^2 (l-1)^2 \sigma_{lm}^2 (\bar{C}_{lm}, \bar{S}_{lm}) \right]^{1/2} = 4.5 \text{ mgals}$$

where:

$B_l$  is Pellinen's smoothing operator for  $5^\circ$  anomalies.

Table 10.1 presents the results of the calibrations in terms of the additional factor,  $k$ . This calibration, based on surface gravity alone, shows that our  $\sigma_{lm}$  have been estimated to within 4%. However, when altimetry is also utilized, it seems that we have been conservative in the estimation of our field model uncertainties by nearly a factor of 2. We have chosen the more conservative estimate of field uncertainty. This discrepancy was not found to this extent in the calibration of GEM-L2 (Lerch et al., 1985b) and it appears to occur in GEM-T1 due to

its solution for higher degree terms. These terms have relatively more constraint within the collocation solution and have lowered power which is known to be unrealistic. The error estimator used here (Kaula's) will give a biased answer which favors a field with lower power. This can be seen in Equation (10.3) where the errors in a field with lower power is seen to have underestimated errors.

Figure 10.3 shows the agreement of SEASAT altimetry with recent GEM gravity models more directly. Again we use Rapp's  $1^\circ \times 1^\circ$  estimates of oceanic gravity anomalies obtained from sea surface undulations. We have formed  $5^\circ \times 5^\circ$  blocks from these values. In Figure 10.3.1 we show the computed residual gravity anomaly for the GEM models at different degrees of truncation. Note the GEM-T1 "satellite-only" model agrees much better with the Seasat altimetric information than does the GEM-L2 model which is its predecessor. GEM-T1 performs nearly as well as GEM-10B which utilized altimeter data. PGS 3163, shown here for comparison purposes, is a version of GEM-T1 which contains SEASAT altimeter data, and as expected, performs best in this comparison. Note also, the improvement over PGS-T2' found with the GEM-T1 model.

Richard Rapp has recently made available to us a new set of altimetrically based ocean gravity anomalies and these have been compared to GEM-T1 as was done in Figure 10.3.1. A comparison of GEM-T1 with both the original (1981) and most recent (1985) SEASAT and GEOS-3 gravity anomalies underscores the point that while the altimetry is quite good and a source for independent testing of our fields, it too, is subject to improvement. It is encouraging to see that progress in both global gravity modeling and altimeter analyses are converging to an unique and absolute answer. We are making the necessary changes to incorporate this new altimetric gravity data set into future calibration activities.

As alluded to earlier, these gravity anomaly data sets are somewhat insensitive to the longer wavelength gravity field. Figure 10.4

TABLE 10.1 CALIBRATION OF GEM-T1 SATELLITE MODEL ERRORS  
 $\sigma_{\text{GEM T1}} (\Delta g_s) = 4.5 \text{ mgals}$  (using the preliminary estimate of commission  
 error out to degree 36 derived from the  $\sigma_{\text{km}}$  found  
 in Figure 10.1)

| Calibration Distribution | Data Test Cases ( $\Delta g^*$ )  | Satellite Model                           |                         |                  |
|--------------------------|---|---|-------------------------|------------------|
|                          |   | Gravity Anomaly EST $\sigma (\Delta g_s)$ | (from Kaula Statistics) | Errors Factor: k |
| Global                   | 5° equal area anomalies from surface gravimetry (Rapp, 1981 data set)                                       | 4.7 mgals                                 |                         | 1.04             |
| Global                   | 5° equal area anomalies from SEASAT altimetry over the oceans and surface gravimetry over land (Rapp, 1981) | 2.4                                       | .53                     |                  |

\*Data Sets Obtained From Rapp

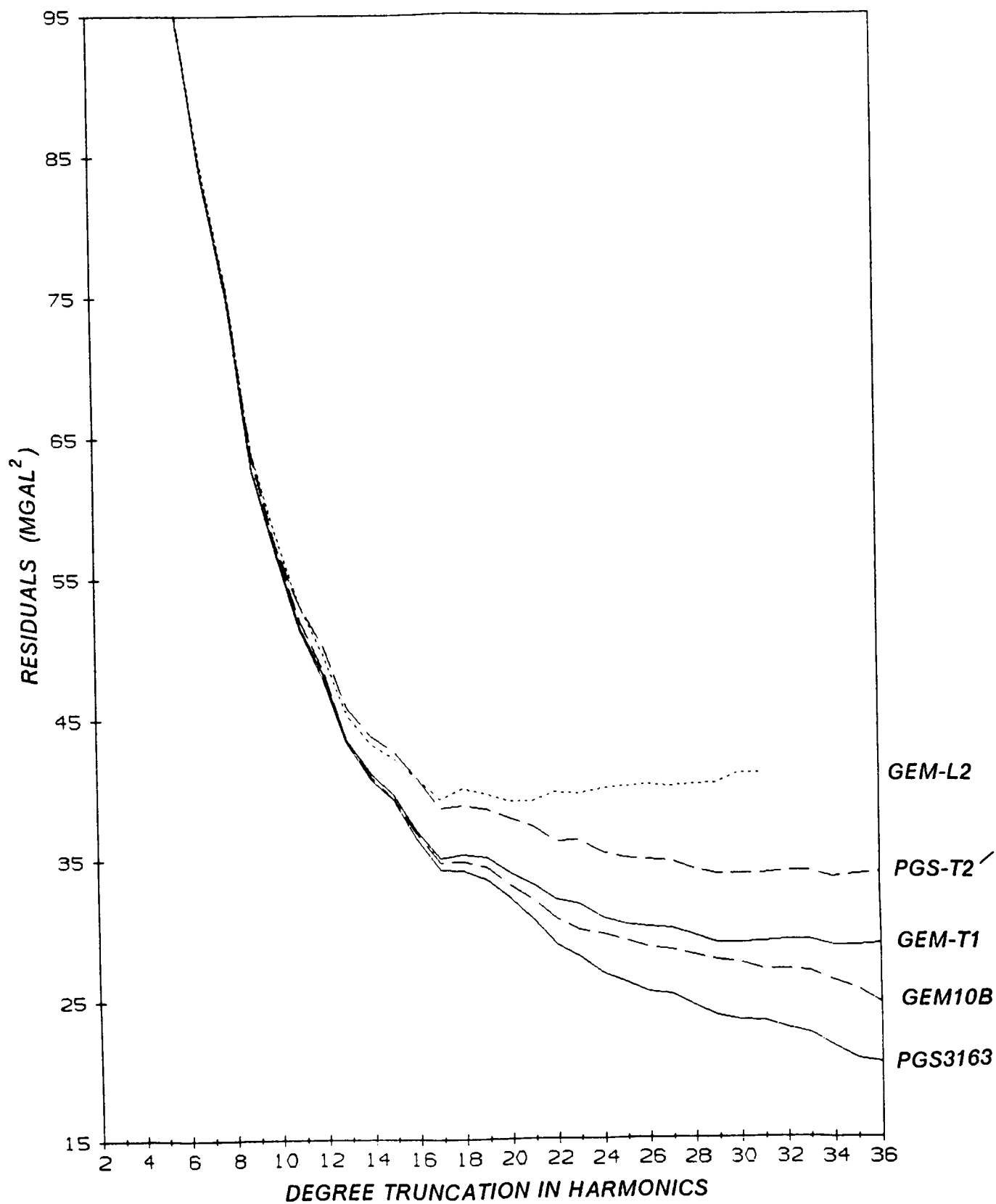


Figure 10.3.1. Gravity Model Comparison with 1114  $5^\circ \times 5^\circ$  SEASAT Gravity Anomalies.

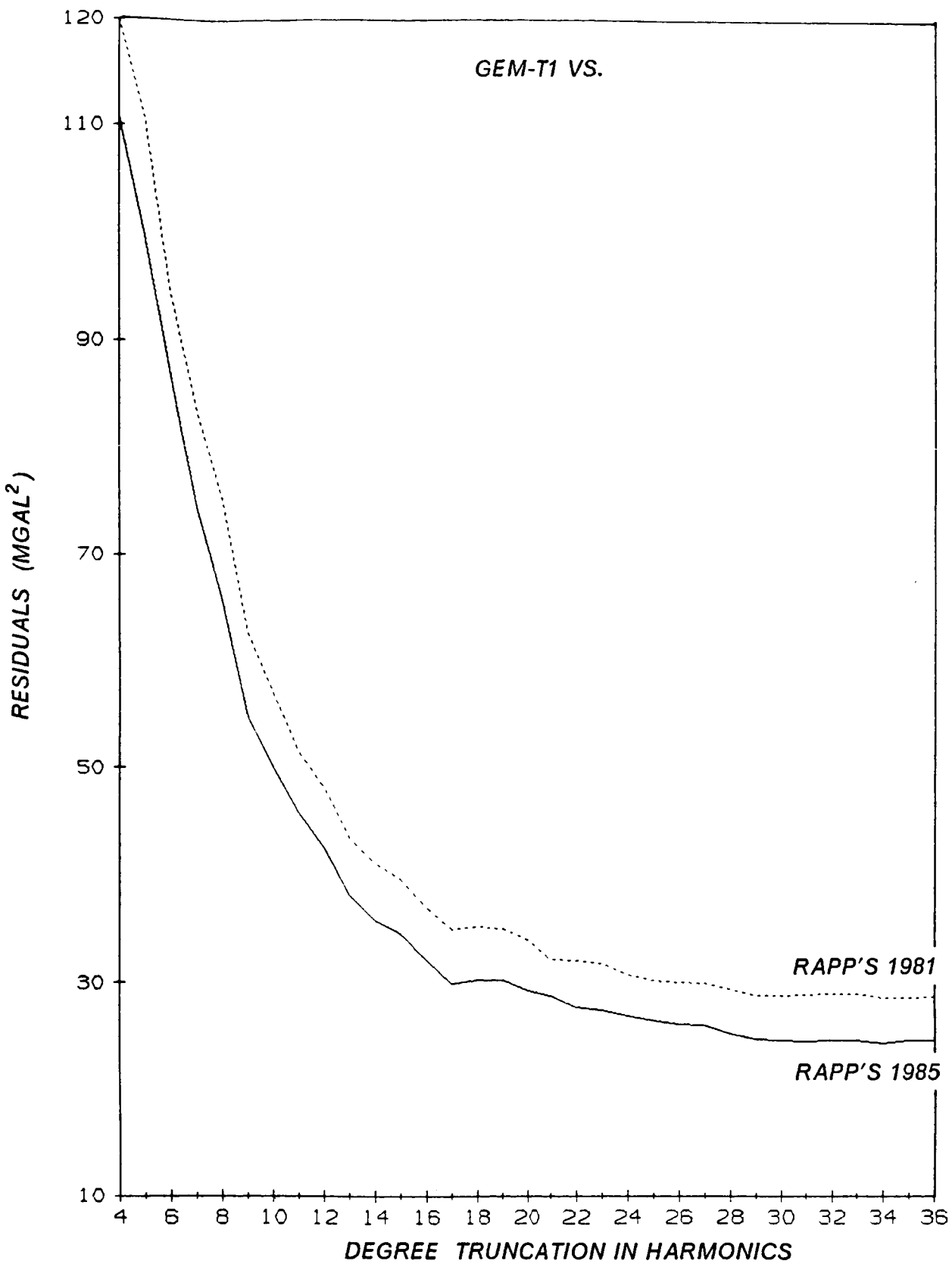


Figure 10.3.2. Gravity Model Comparison with  $5^\circ \times 5^\circ$  SEASAT Gravity Anomalies Using Two Recent Sets of Anomalies.

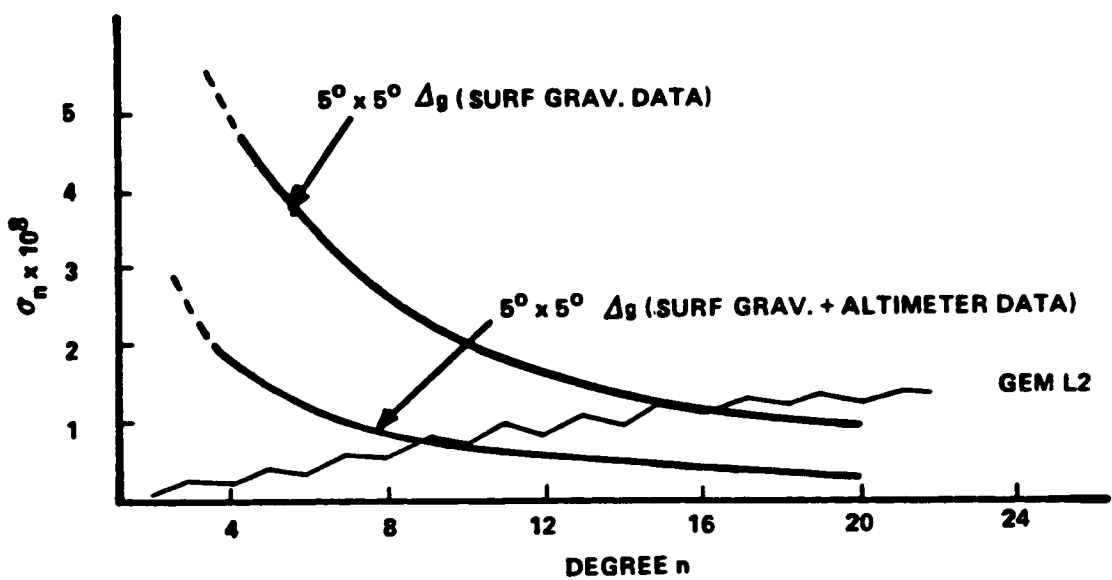


Figure 10.4. Coefficient Error Spectrum Per Degree  $n$ .

presents the error spectrum for GEM-L2 compared to that which is calculated from five-degree gravity anomalies. Based on Figure 10.4 the calibration described in Table 10.1 does not reliably test those terms below degree 8 in the GEM-T1 model. As indicated earlier the calibration for high degree terms may not be completely reliable because their low overall power in the GEM-T1 recovery may bias the Kaula error estimator. Hence we substantiate this calibration with additional tests as described throughout the remainder of this section.

## 10.2 CALIBRATION BASED UPON FIELD SUBSET SOLUTION TESTING

A new technique (Lerch, 1985a) has been developed for gravity model calibrations of errors and applied to GEM-T1. First the new method is reviewed along with test results which have verified the error estimates for GEM-L2. GEM-L2 has been previously calibrated by a number of different methods (Lerch et al., 1985b). If our new procedure yields comparable results to those found earlier for GEM-L2, then we have some verification of its performance.

A preliminary mathematical description of this new technique is given. We will define quantities used in the calibration of the geopotential coefficient errors between two fields,  $F$  and  $\bar{F}$  where:

$F : C_{\ell m}, S_{\ell m}, \sigma$ 's (coeff. standard deviations)

$\bar{F} : \bar{C}_{\ell m}, \bar{S}_{\ell m}, \bar{\sigma}$ 's (10.6)

$\Delta F : \Delta C_{\ell m} = (C_{\ell m} - \bar{C}_{\ell m}),$  likewise  $\Delta S_{\ell m}, \Delta \sigma$

(herein, the bar notation indicates the second model and is no longer used to denote field normalization.) The calibration quantities are further defined by

$$\text{RMS}_{\ell}(\Delta F) = \left[ \sum_{m=0}^{\ell} \frac{\Delta C_{\ell m}^2 + \Delta S_{\ell m}^2}{2\ell + 1} \right]^{1/2} \quad (\Delta: \text{difference operator})$$

$$\sigma_{\ell} = \left[ \sum_{m=0}^{\ell} \frac{\sigma_{(C_{\ell m})}^2 + \sigma_{(S_{\ell m})}^2}{2\ell + 1} \right]^{1/2} \quad (\text{similarly for } \bar{\sigma}_{\ell})$$

$$e_{\ell}^2 = E(\text{RMS}_{\ell})^2 \quad (10.7)$$

$$= \sigma_{\ell}^2 + \bar{\sigma}_{\ell}^2 \quad \text{when } F \text{ is independent of } \bar{F} \quad (10.7a)$$

$$= \sigma_{\ell}^2 - \bar{\sigma}_{\ell}^2 \quad \text{when data in } F \text{ are fully contained in } \bar{F}. \quad (10.7b)$$

Again, a calibration scale factor per degree,  $\ell$ , is denoted as  $k_{\ell}$  and is given by

$$k_{\ell} = \frac{\text{RMS}_{\ell}}{e_{\ell}}, \quad (10.8)$$

From equations (10.7) and (10.8) we have two methods for calibrating errors: the first when the fields  $F$  and  $\bar{F}$  are independent and contain no common data; the second when the data in  $F$  are wholly contained in  $\bar{F}$ . To satisfy the input criteria for this test the four models which were employed are described below:

- o GEM-9 is a satellite-only model which was published in Lerch et al, 1979. It is complete to degree and order 20. The gravity coefficients have no contributions from LAGEOS ranging, radar altimetry, or surface gravimetry. However, a limited amount of early STARLETTE laser data was utilized.
- o GEM-9A is a version of GEM-9 which was re-determined after removal of the STARLETTE data.
- o GEM-L2 is a satellite-only model which was published in Lerch et al., 1982. It was a solution which combined GEM-9 with LAGEOS laser ranging. Therefore, the data found within GEM-9 is entirely found within GEM-L2.
- o TEST FIELD was a special model developed from available sub-sets of normal equations. It contained recent LAGEOS and STARLETTE laser observations, surface gravimetry and SEASAT altimetry. It is therefore, by construction, a model whose data are completely independent of the data within GEM-9A described above.

Hence GEM-9A and TEST FIELD are evaluated with eq. (10.7a) for independent fields and GEM-9 and GEM-L2 are evaluated using eq. (10.7b) for dependent fields. Figure 10.5 presents the resulting calibration factors  $k_\ell$  determined from each of the methods. Also shown are the averages of the calibration factors for the two methods. Clearly, the two methods show a good agreement for field calibrations. More important, the values of the estimated calibration factors,  $k_\ell$ , are centered about  $k_\ell = 1$ , which indicates that the overall uncertainties estimated by these methods agree well with the extensive calibration results previously obtained for the GEM-9 and GEM-L2 models. It is interesting to note that, as explained in the introduction to this section, the lower degree terms in the models may be optimistically

calibrated through our use of a scaled covariance for field uncertainty estimation. As seen in Figure 10.5, the low degree terms have a calibration scaling factor which exceeds 1.0, but only at most by 30% at its largest offset from unity. Therefore the results of this method for gravity model calibration overall agree quite well with what had earlier been determined for GEM-L2 using different techniques.

The method selected for assessing the reliability of the estimated GEM-T1 uncertainties corresponds to using eq. (10.7b) in which two models are used, where the first is obtained from data totally contained within the more complete data set found in the second. These calibrations required making several experimental gravity models based on subsets of the data used to obtain GEM-T1.

For the tests on GEM-T1 we examine several additional statistics. We calculate:

$$\begin{aligned} \text{RMS}_{\ell m} &= (\Delta C_{\ell m}^2 + \Delta S_{\ell m}^2)^{1/2} \\ \epsilon_{\ell m} &= (\sigma_{\ell m}^2 - \bar{\sigma}_{\ell m}^2)^{1/2} \\ k_{\ell m} &= \text{RMS}_{\ell m} / \epsilon_{\ell m} \end{aligned} \quad (10.9)$$

Coefficient statistics both by degree and by order are also evaluated through

$$k_{\ell} = \left[ \sum_{m=0}^{\ell} k_{\ell m}^2 / (2\ell+1) \right]^{1/2} \quad (10.10)$$

$$k_m = \left[ \sum_{\ell=m}^{36} k_{\ell m}^2 / N_m \right]^{1/2}$$

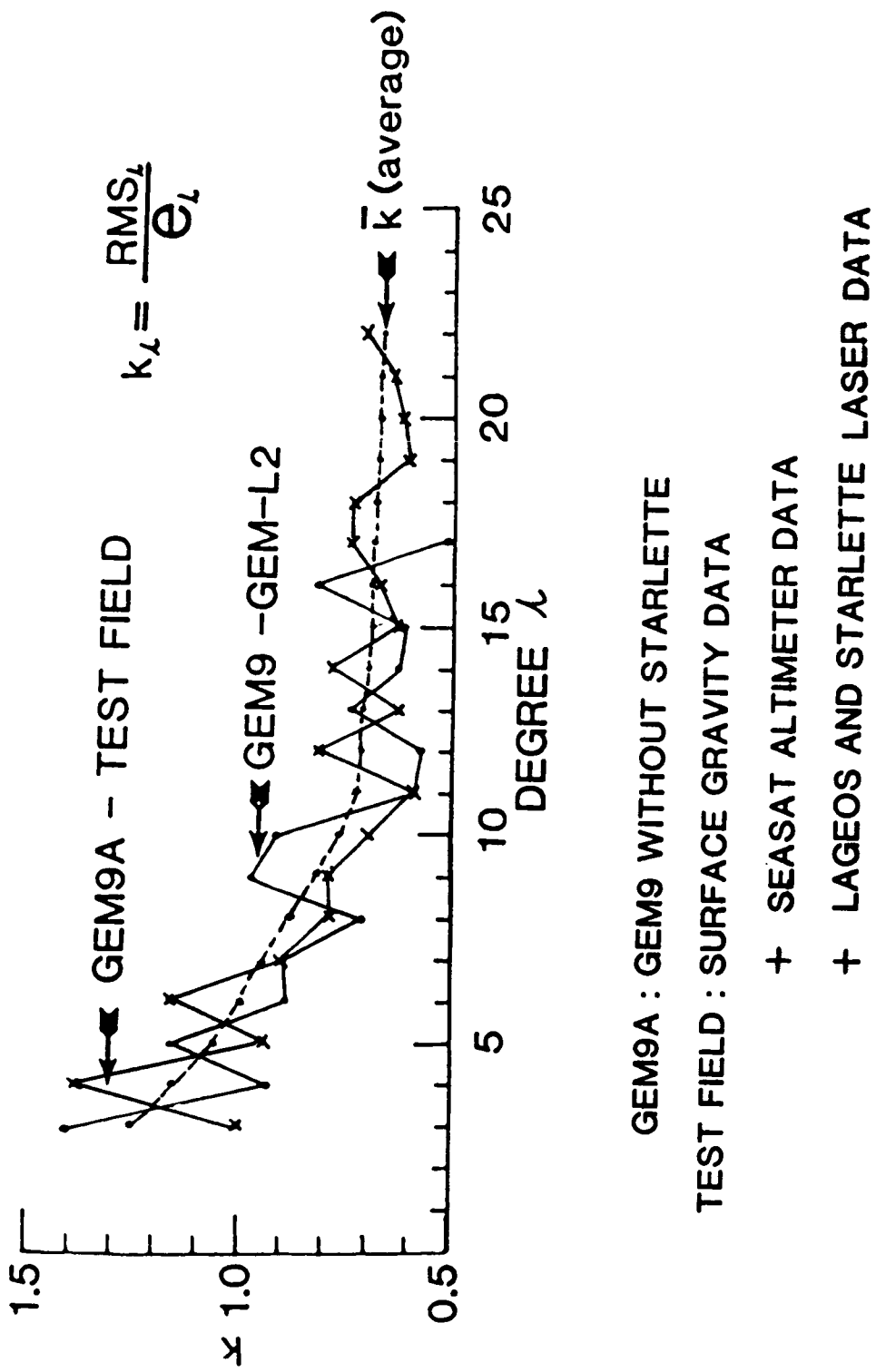


Figure 10.5. Scale Variability for Errors.

where  $N_m$  equals the number of terms of order  $m$  (i.e.,  $36-m+1$ ). As will be shown, similar results are obtained for either  $k_m$  or  $k_\ell$ .

The scale factors  $k_\ell$  are shown in Figure 10.6 for two cases:

- (1) GEM-T1 has been compared to an experimental version of GEM-T1 which lacked the STARLETTE data, and
- (2) GEM-T1 has been compared to a version of GEM-T1 which lacked the data from four laser satellites--BE-C, GEOS-1, GEOS-2 and GEOS-3.

The scale factors which were obtained by these calibrations (Figure 10.6) are close to unity for both cases with an overall average calibration factor of

$$\bar{k}_\ell = 1.1$$

(where the overbar indicates averaging)

The size of the subset of the potential coefficients used impacts the determination of these scaling parameters. For any individual coefficient, the factor would tend to be somewhat random. Therefore, the large subsets of coefficients (as indicated in (eq. 10.10)) provide a better determination of the overall calibration. Consequently, the slightly greater variability seen in Figure 10.6 for the low degree  $k_\ell$  possibly is explained by the limited number of coefficients which are sampled  $(2\ell + 1)$  at these lower degrees. Figure 10.7 shows the  $\sigma_\ell$ ,  $e_\ell$ , and  $RMS_\ell$  for the second case. Figure 10.8 presents results for the  $k_m$  scaling parameters determined from both of these cases, but now sampling the coefficient subsets by order. When examined by order, the average scale factor is found to be

## SCALE FACTOR PER DEGREE

$$k_l = \frac{RMS_l}{e_l}$$

### SUBSET SOLUTIONS:

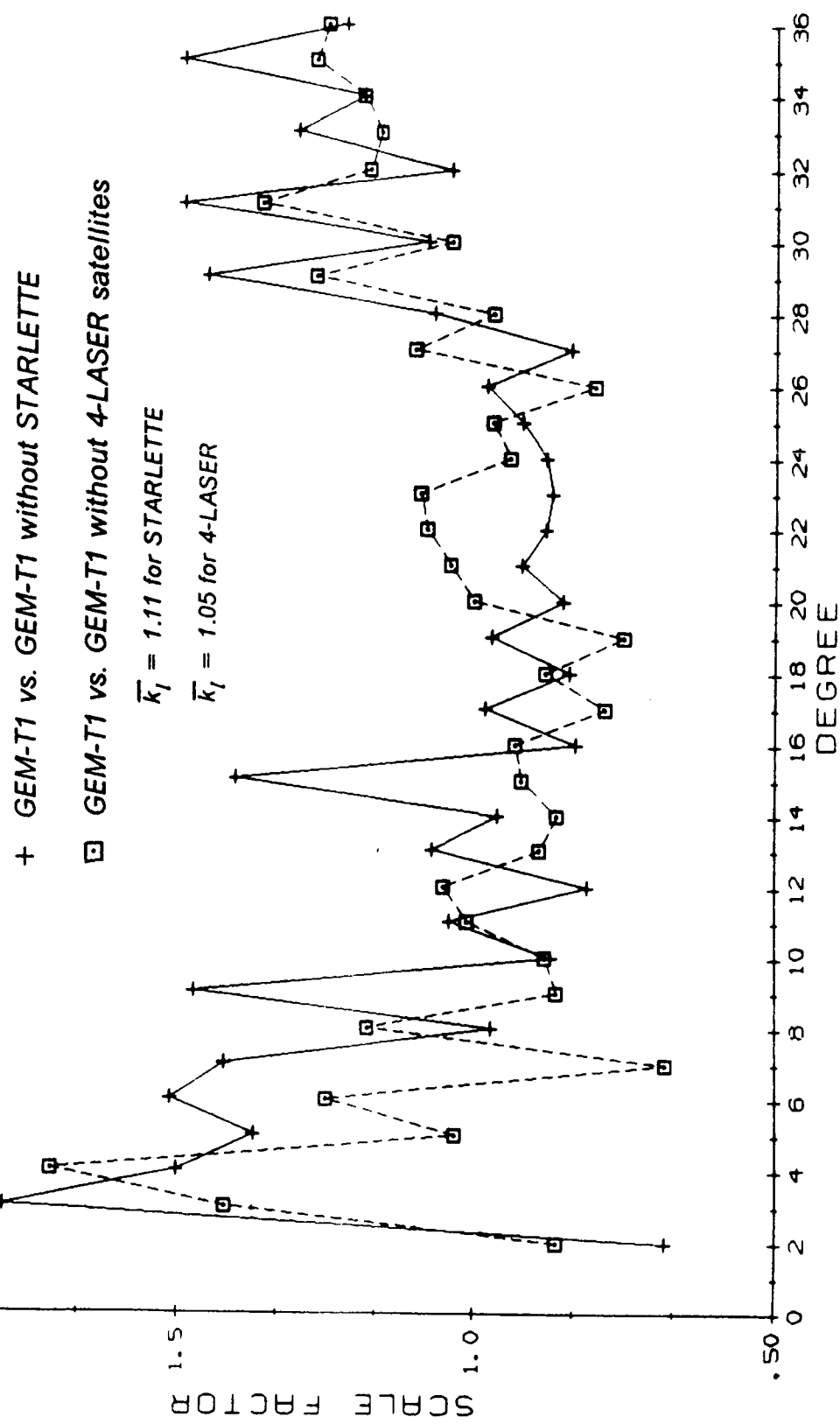


Figure 10.6. Calibration of Error Estimates Based Upon Subset Solutions.

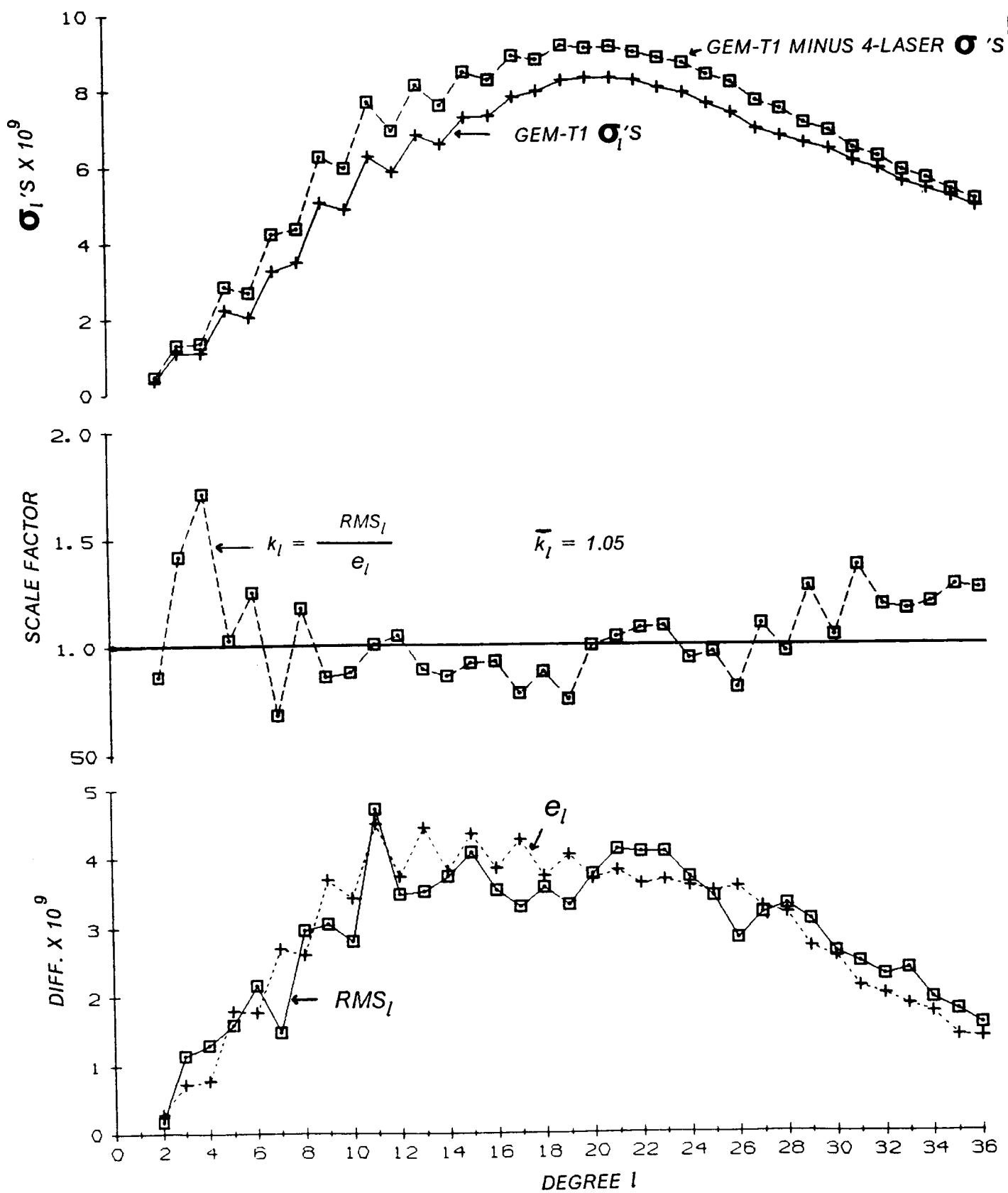


Figure 10.7. Calibration Statistics GEM-T1 vs. GEM-T1 Without 4-Laser Satellites.

## SCALE FACTOR PER ORDER

$$k_m = \frac{RMS_m}{e_m}$$

### SUBSET SOLUTIONS:

+ GEM-T1 vs. GEM-T1 without STARLETTE

□ GEM-T1 vs. GEM-T1 without 4-LASER satellites

$$\bar{k}_m = 1.16 \text{ for STARLETTE}$$

$$\bar{k}_m = 1.07 \text{ for 4-LASER}$$

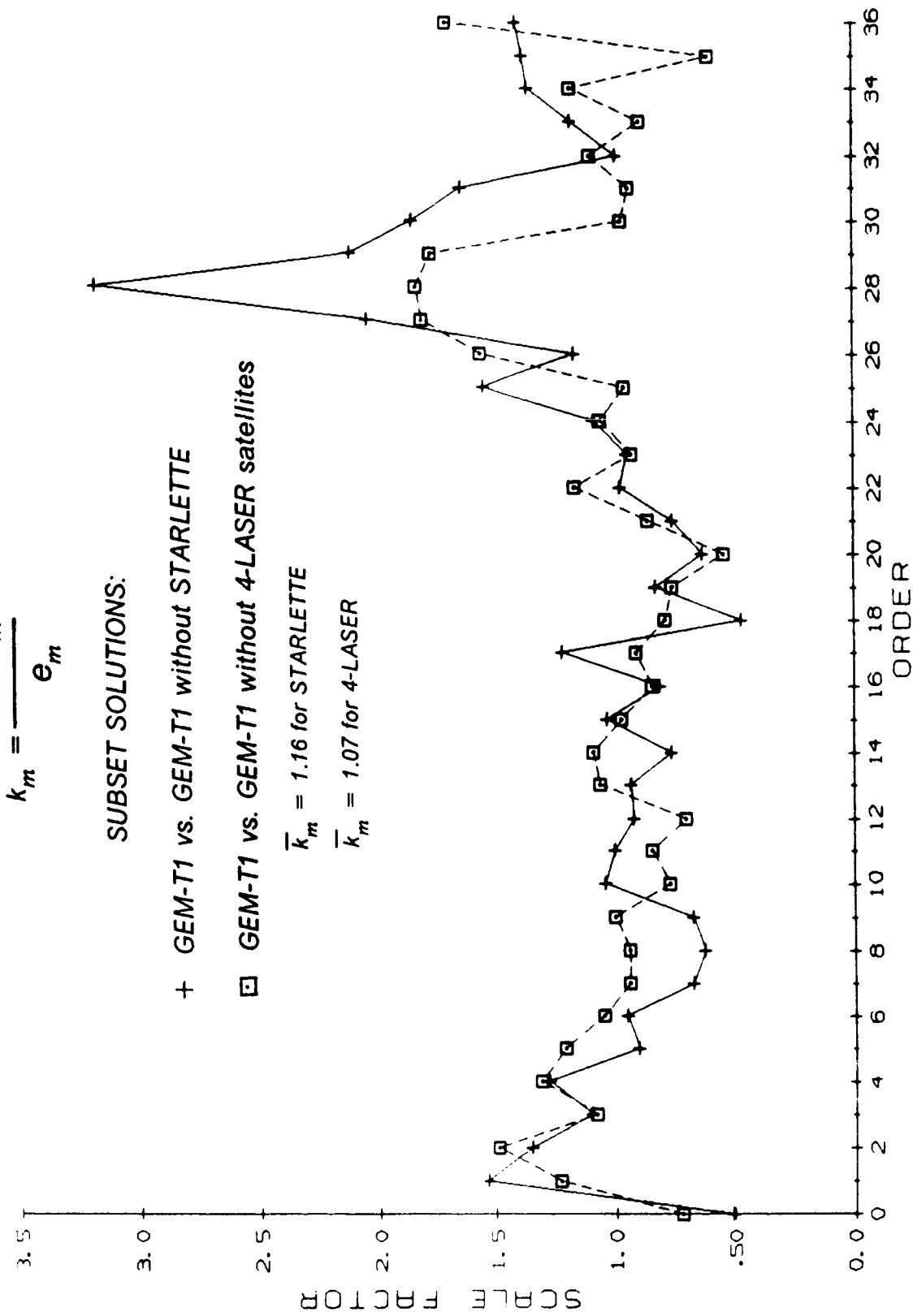


Figure 10.8. Calibration of Error Estimates Based Upon Subset Solutions.

$$\bar{k}_m = 0.99$$

Finally, the individual coefficient variability for these scaling parameters is shown in Figure 10.9. Overall, these fields seem to perform well when calibrated through these tests, and the overall scale factor obtained agrees well with that found using surface gravimetry and altimetry as described in Section 10.1.

Returning for a moment to Figure 10.8, one sees large scale factors for the orders where  $m=27$  through  $29$  when STARLETTE data is eliminated from the solution. These orders have a strong secondary resonance with the STARLETTE orbit, and STARLETTE senses resonant terms beyond the 36th degree of truncation used when solving GEM-T1. Therefore, unconsidered aliasing error (due to STARLETTE's unique sensitivity to these orders) is perturbing the determination of the scale parameters for these orders. We have calculated and stored satellite measurement partial derivatives for the gravity model (nearly) complete to degree 50. When altimetry and surface gravity are introduced into the solution, STARLETTE's resonance will contribute to the determination of these  $m=27$ ,  $28$ , and  $29$  terms to  $l=50$  and this source of aliasing will be eliminated.

Two additional calibration tests were made. The first was one in which the inclusion of a preliminary set of altimetry in the GEM-T1 solution was assessed (and calibrated). The second directly evaluated the effect of significantly changing the value of the scaling factor,  $f$ , given in (eq. 8.8).

When speculating about the effect of using altimeter data within the GEM-T1 solution, we are attempting to project into the future and assess the accuracy of some yet-to-be-determined solution. A great deal of work remains to be done on improving our treatment of the altimeter data to eliminate non-geoidal signal (and it is scheduled for late

AVERAGE PER DEGREE = 1.0    AVERAGE PER ORDER = 1.1

| RMS DEG |    | $\frac{RMS_{l,m}}{e_{l,m}}$ |
|---------|----|-----------------------------|
| 0.4     | 2  | 0.4                         |
| 1.1     | 5  | 1.5                         |
| 1.2     | 6  | 2.0                         |
| 1.3     | 7  | 2.5                         |
| 1.4     | 8  | 3.0                         |
| 1.5     | 9  | 3.5                         |
| 1.6     | 10 | 4.0                         |
| 1.7     | 11 | 4.5                         |
| 1.8     | 12 | 5.0                         |
| 1.9     | 13 | 5.5                         |
| 2.0     | 14 | 6.0                         |
| 2.1     | 15 | 6.5                         |
| 2.2     | 16 | 7.0                         |
| 2.3     | 17 | 7.5                         |
| 2.4     | 18 | 8.0                         |
| 2.5     | 19 | 8.5                         |
| 2.6     | 20 | 9.0                         |
| 2.7     | 21 | 9.5                         |
| 2.8     | 22 | 10.0                        |
| 2.9     | 23 | 10.5                        |
| 3.0     | 24 | 11.0                        |
| 3.1     | 25 | 11.5                        |
| 3.2     | 26 | 12.0                        |
| 3.3     | 27 | 12.5                        |
| 3.4     | 28 | 13.0                        |
| 3.5     | 29 | 13.5                        |
| 3.6     | 30 | 14.0                        |
| 3.7     | 31 | 14.5                        |
| 3.8     | 32 | 15.0                        |
| 3.9     | 33 | 15.5                        |
| 4.0     | 34 | 16.0                        |
| 4.1     | 35 | 16.5                        |
| 4.2     | 36 | 17.0                        |
| 4.3     | 0  | 1.0                         |
| 4.4     | 1  | 1.2                         |
| 4.5     | 2  | 1.4                         |
| 4.6     | 3  | 1.6                         |
| 4.7     | 4  | 1.8                         |
| 4.8     | 5  | 2.0                         |
| 4.9     | 6  | 2.2                         |
| 5.0     | 7  | 2.4                         |
| 5.1     | 8  | 2.6                         |
| 5.2     | 9  | 2.8                         |
| 5.3     | 10 | 3.0                         |
| 5.4     | 11 | 3.2                         |
| 5.5     | 12 | 3.4                         |
| 5.6     | 13 | 3.6                         |
| 5.7     | 14 | 3.8                         |
| 5.8     | 15 | 4.0                         |
| 5.9     | 16 | 4.2                         |
| 6.0     | 17 | 4.4                         |
| 6.1     | 18 | 4.6                         |
| 6.2     | 19 | 4.8                         |
| 6.3     | 20 | 5.0                         |
| 6.4     | 21 | 5.2                         |
| 6.5     | 22 | 5.4                         |
| 6.6     | 23 | 5.6                         |
| 6.7     | 24 | 5.8                         |
| 6.8     | 25 | 6.0                         |
| 6.9     | 26 | 6.2                         |
| 7.0     | 27 | 6.4                         |
| 7.1     | 28 | 6.6                         |
| 7.2     | 29 | 6.8                         |
| 7.3     | 30 | 7.0                         |
| 7.4     | 31 | 7.2                         |
| 7.5     | 32 | 7.4                         |
| 7.6     | 33 | 7.6                         |
| 7.7     | 34 | 7.8                         |
| 7.8     | 35 | 8.0                         |
| 7.9     | 36 | 8.2                         |

RMS      0.7 1.1 1.4 1.0 1.2 1.1 1.0 0.9 0.9 0.9 0.7 0.8 0.7 1.0 1.0 0.9 0.8 0.8 0.7 0.5 0.5 0.7 1.1 1.0 0.9 1.4 1.6 1.5 0.9 1.0 0.8 1.2 0.5 0.8

*4-LASER SATELLITES : BE-C , GEOS-1 , GEOS-2 , GEOS-3*

Figure 10.9. Calibration Ratio ( $k_{l,m}$ ) Based Upon GEM-T1 and GEM-T1 Without 4-Laser Satellites.

1987). However, the altimeter normal matrix we have obtained is similar to what will be available in the future, and for statistical purposes, it should be sufficient. Our first altimeter test model is PGS3163, whose gravity anomalies are compared to the SEASAT derived gravity anomalies in Figure 10.3. This model was computed giving very small weight to the altimeter data, since we did not wish to overwhelm the well calibrated GEM-T1 solution. However, for the present purposes, a second model was solved, called PGS3164, in which the altimetry was given five times the weight it had in PGS3163. The altimeter weight in PGS3164 more closely reflects the weight given to this data type in our previously published PGS-S4 solution. The calibration of this model is shown in Figure 10.10 where the overall scale factor of 1.02 which was obtained is in good agreement with those for either degree or order groupings of the coefficients. Shown in Figure 10.11 are the calibrated uncertainties for the PGS3164 model. The improvement over GEM-T1 is striking, and indicates that inclusion of the altimeter data in the future should have a substantial impact on further field improvements.

Finally, a calibration was performed on a field which was deliberately corrupted. In the discussion in Section 8.2, we show that a delicate balance of weights needs to be found to arrive at a good gravity model accompanied by realistic error covariances. We feel that this balance has been obtained in GEM-T1. However, looking at eq. (8.8) one can see that the value selected for  $f$  can alter both the overall scaling of the solution uncertainties and the balance between  $f$  and  $\bar{f}$ . A test solution, PGS3013, was made where  $f$  was multiplied upwards by a factor of 5 using a PGS-T2' base model (see Figure 8.4). The resulting standard deviations from this model, as expected, were about a factor of 2.5 better than those seen for GEM-T1. However, when this model was tested against surface gravity data, its performance was far worse (Table 8.2). PGS3013 was then calibrated using the same procedures which were utilized (as described in this section) for GEM-T1. For this model, the scaling parameter  $\bar{k}_f$  was found to be approximately 2.5. When

## GEM-T1 vs. GEM-T1 + SEASAT ALTIMETER

5 x ALTIMETER WEIGHT IN PGS3163

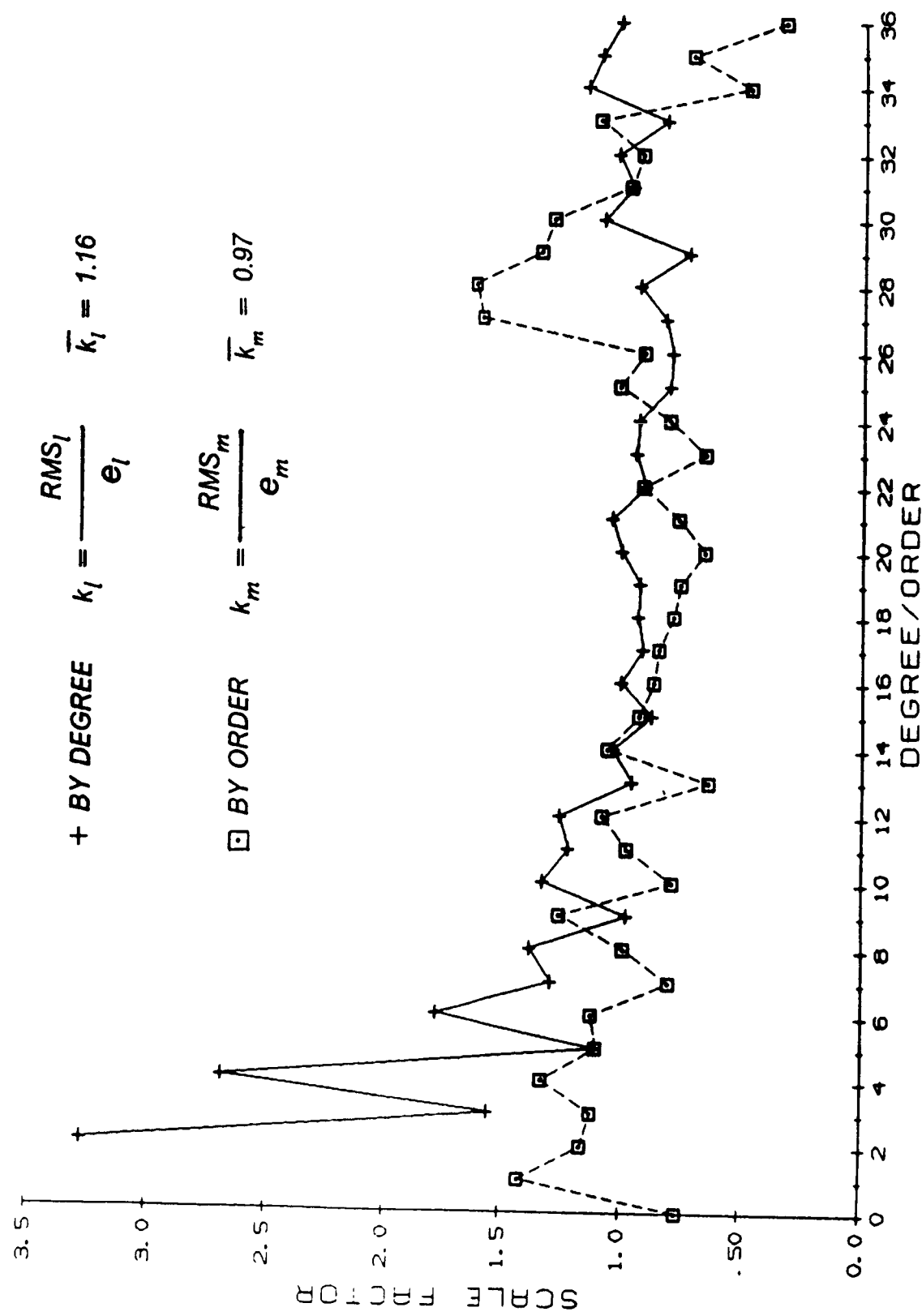


Figure 10.10. Calibration of Error Estimates Based Upon Subset Solutions.

| PGS3164 = GEM-T1 + SEASAT ALTIMETER |        | ORDER |
|-------------------------------------|--------|-------|
| RMS                                 | DEGREE |       |
| 0                                   | 0      | 36    |
| 0                                   | 1      | 35    |
| 0                                   | 2      | 35    |
| 0                                   | 3      | 35    |
| 0                                   | 4      | 35    |
| 0                                   | 5      | 35    |
| 0                                   | 6      | 35    |
| 0                                   | 7      | 35    |
| 0                                   | 8      | 35    |
| 0                                   | 9      | 35    |
| 0                                   | 10     | 35    |
| 0                                   | 11     | 35    |
| 0                                   | 12     | 35    |
| 0                                   | 13     | 35    |
| 0                                   | 14     | 35    |
| 0                                   | 15     | 35    |
| 0                                   | 16     | 35    |
| 0                                   | 17     | 35    |
| 0                                   | 18     | 35    |
| 0                                   | 19     | 35    |
| 0                                   | 20     | 35    |
| 0                                   | 21     | 35    |
| 0                                   | 22     | 35    |
| 0                                   | 23     | 35    |
| 0                                   | 24     | 35    |
| 0                                   | 25     | 35    |
| 0                                   | 26     | 35    |
| 0                                   | 27     | 35    |
| 0                                   | 28     | 35    |
| 0                                   | 29     | 35    |
| 0                                   | 30     | 35    |
| 0                                   | 31     | 35    |
| 0                                   | 32     | 35    |
| 0                                   | 33     | 35    |
| 0                                   | 34     | 35    |
| 0                                   | 35     | 35    |
| 0                                   | 36     | 35    |
| 1                                   | 1      | 35    |
| 1                                   | 2      | 35    |
| 1                                   | 3      | 35    |
| 1                                   | 4      | 35    |
| 1                                   | 5      | 35    |
| 1                                   | 6      | 35    |
| 1                                   | 7      | 35    |
| 1                                   | 8      | 35    |
| 1                                   | 9      | 35    |
| 1                                   | 10     | 35    |
| 1                                   | 11     | 35    |
| 1                                   | 12     | 35    |
| 1                                   | 13     | 35    |
| 1                                   | 14     | 35    |
| 1                                   | 15     | 35    |
| 1                                   | 16     | 35    |
| 1                                   | 17     | 35    |
| 1                                   | 18     | 35    |
| 1                                   | 19     | 35    |
| 1                                   | 20     | 35    |
| 1                                   | 21     | 35    |
| 1                                   | 22     | 35    |
| 1                                   | 23     | 35    |
| 1                                   | 24     | 35    |
| 1                                   | 25     | 35    |
| 1                                   | 26     | 35    |
| 1                                   | 27     | 35    |
| 1                                   | 28     | 35    |
| 1                                   | 29     | 35    |
| 1                                   | 30     | 35    |
| 1                                   | 31     | 35    |
| 1                                   | 32     | 35    |
| 1                                   | 33     | 35    |
| 1                                   | 34     | 35    |
| 1                                   | 35     | 35    |
| 1                                   | 36     | 35    |
| 2                                   | 1      | 35    |
| 2                                   | 2      | 35    |
| 2                                   | 3      | 35    |
| 2                                   | 4      | 35    |
| 2                                   | 5      | 35    |
| 2                                   | 6      | 35    |
| 2                                   | 7      | 35    |
| 2                                   | 8      | 35    |
| 2                                   | 9      | 35    |
| 2                                   | 10     | 35    |
| 2                                   | 11     | 35    |
| 2                                   | 12     | 35    |
| 2                                   | 13     | 35    |
| 2                                   | 14     | 35    |
| 2                                   | 15     | 35    |
| 2                                   | 16     | 35    |
| 2                                   | 17     | 35    |
| 2                                   | 18     | 35    |
| 2                                   | 19     | 35    |
| 2                                   | 20     | 35    |
| 2                                   | 21     | 35    |
| 2                                   | 22     | 35    |
| 2                                   | 23     | 35    |
| 2                                   | 24     | 35    |
| 2                                   | 25     | 35    |
| 2                                   | 26     | 35    |
| 2                                   | 27     | 35    |
| 2                                   | 28     | 35    |
| 2                                   | 29     | 35    |
| 2                                   | 30     | 35    |
| 2                                   | 31     | 35    |
| 2                                   | 32     | 35    |
| 2                                   | 33     | 35    |
| 2                                   | 34     | 35    |
| 2                                   | 35     | 35    |
| 2                                   | 36     | 35    |
| 3                                   | 1      | 35    |
| 3                                   | 2      | 35    |
| 3                                   | 3      | 35    |
| 3                                   | 4      | 35    |
| 3                                   | 5      | 35    |
| 3                                   | 6      | 35    |
| 3                                   | 7      | 35    |
| 3                                   | 8      | 35    |
| 3                                   | 9      | 35    |
| 3                                   | 10     | 35    |
| 3                                   | 11     | 35    |
| 3                                   | 12     | 35    |
| 3                                   | 13     | 35    |
| 3                                   | 14     | 35    |
| 3                                   | 15     | 35    |
| 3                                   | 16     | 35    |
| 3                                   | 17     | 35    |
| 3                                   | 18     | 35    |
| 3                                   | 19     | 35    |
| 3                                   | 20     | 35    |
| 3                                   | 21     | 35    |
| 3                                   | 22     | 35    |
| 3                                   | 23     | 35    |
| 3                                   | 24     | 35    |
| 3                                   | 25     | 35    |
| 3                                   | 26     | 35    |
| 3                                   | 27     | 35    |
| 3                                   | 28     | 35    |
| 3                                   | 29     | 35    |
| 3                                   | 30     | 35    |
| 3                                   | 31     | 35    |
| 3                                   | 32     | 35    |
| 3                                   | 33     | 35    |
| 3                                   | 34     | 35    |
| 3                                   | 35     | 35    |
| 3                                   | 36     | 35    |
| 4                                   | 1      | 35    |
| 4                                   | 2      | 35    |
| 4                                   | 3      | 35    |
| 4                                   | 4      | 35    |
| 4                                   | 5      | 35    |
| 4                                   | 6      | 35    |
| 4                                   | 7      | 35    |
| 4                                   | 8      | 35    |
| 4                                   | 9      | 35    |
| 4                                   | 10     | 35    |
| 4                                   | 11     | 35    |
| 4                                   | 12     | 35    |
| 4                                   | 13     | 35    |
| 4                                   | 14     | 35    |
| 4                                   | 15     | 35    |
| 4                                   | 16     | 35    |
| 4                                   | 17     | 35    |
| 4                                   | 18     | 35    |
| 4                                   | 19     | 35    |
| 4                                   | 20     | 35    |
| 4                                   | 21     | 35    |
| 4                                   | 22     | 35    |
| 4                                   | 23     | 35    |
| 4                                   | 24     | 35    |
| 4                                   | 25     | 35    |
| 4                                   | 26     | 35    |
| 4                                   | 27     | 35    |
| 4                                   | 28     | 35    |
| 4                                   | 29     | 35    |
| 4                                   | 30     | 35    |
| 4                                   | 31     | 35    |
| 4                                   | 32     | 35    |
| 4                                   | 33     | 35    |
| 4                                   | 34     | 35    |
| 4                                   | 35     | 35    |
| 4                                   | 36     | 35    |
| 5                                   | 1      | 35    |
| 5                                   | 2      | 35    |
| 5                                   | 3      | 35    |
| 5                                   | 4      | 35    |
| 5                                   | 5      | 35    |
| 5                                   | 6      | 35    |
| 5                                   | 7      | 35    |
| 5                                   | 8      | 35    |
| 5                                   | 9      | 35    |
| 5                                   | 10     | 35    |
| 5                                   | 11     | 35    |
| 5                                   | 12     | 35    |
| 5                                   | 13     | 35    |
| 5                                   | 14     | 35    |
| 5                                   | 15     | 35    |
| 5                                   | 16     | 35    |
| 5                                   | 17     | 35    |
| 5                                   | 18     | 35    |
| 5                                   | 19     | 35    |
| 5                                   | 20     | 35    |
| 5                                   | 21     | 35    |
| 5                                   | 22     | 35    |
| 5                                   | 23     | 35    |
| 5                                   | 24     | 35    |
| 5                                   | 25     | 35    |
| 5                                   | 26     | 35    |
| 5                                   | 27     | 35    |
| 5                                   | 28     | 35    |
| 5                                   | 29     | 35    |
| 5                                   | 30     | 35    |
| 5                                   | 31     | 35    |
| 5                                   | 32     | 35    |
| 5                                   | 33     | 35    |
| 5                                   | 34     | 35    |
| 5                                   | 35     | 35    |
| 5                                   | 36     | 35    |
| 6                                   | 1      | 35    |
| 6                                   | 2      | 35    |
| 6                                   | 3      | 35    |
| 6                                   | 4      | 35    |
| 6                                   | 5      | 35    |
| 6                                   | 6      | 35    |
| 6                                   | 7      | 35    |
| 6                                   | 8      | 35    |
| 6                                   | 9      | 35    |
| 6                                   | 10     | 35    |
| 6                                   | 11     | 35    |
| 6                                   | 12     | 35    |
| 6                                   | 13     | 35    |
| 6                                   | 14     | 35    |
| 6                                   | 15     | 35    |
| 6                                   | 16     | 35    |
| 6                                   | 17     | 35    |
| 6                                   | 18     | 35    |
| 6                                   | 19     | 35    |
| 6                                   | 20     | 35    |
| 6                                   | 21     | 35    |
| 6                                   | 22     | 35    |
| 6                                   | 23     | 35    |
| 6                                   | 24     | 35    |
| 6                                   | 25     | 35    |
| 6                                   | 26     | 35    |
| 6                                   | 27     | 35    |
| 6                                   | 28     | 35    |
| 6                                   | 29     | 35    |
| 6                                   | 30     | 35    |
| 6                                   | 31     | 35    |
| 6                                   | 32     | 35    |
| 6                                   | 33     | 35    |
| 6                                   | 34     | 35    |
| 6                                   | 35     | 35    |
| 6                                   | 36     | 35    |
| 7                                   | 1      | 35    |
| 7                                   | 2      | 35    |
| 7                                   | 3      | 35    |
| 7                                   | 4      | 35    |
| 7                                   | 5      | 35    |
| 7                                   | 6      | 35    |
| 7                                   | 7      | 35    |
| 7                                   | 8      | 35    |
| 7                                   | 9      | 35    |
| 7                                   | 10     | 35    |
| 7                                   | 11     | 35    |
| 7                                   | 12     | 35    |
| 7                                   | 13     | 35    |
| 7                                   | 14     | 35    |
| 7                                   | 15     | 35    |
| 7                                   | 16     | 35    |
| 7                                   | 17     | 35    |
| 7                                   | 18     | 35    |
| 7                                   | 19     | 35    |
| 7                                   | 20     | 35    |
| 7                                   | 21     | 35    |
| 7                                   | 22     | 35    |
| 7                                   | 23     | 35    |
| 7                                   | 24     | 35    |
| 7                                   | 25     | 35    |
| 7                                   | 26     | 35    |
| 7                                   | 27     | 35    |
| 7                                   | 28     | 35    |
| 7                                   | 29     | 35    |
| 7                                   | 30     | 35    |
| 7                                   | 31     | 35    |
| 7                                   | 32     | 35    |
| 7                                   | 33     | 35    |
| 7                                   | 34     | 35    |
| 7                                   | 35     | 35    |
| 7                                   | 36     | 35    |
| 8                                   | 1      | 35    |
| 8                                   | 2      | 35    |
| 8                                   | 3      | 35    |
| 8                                   | 4      | 35    |
| 8                                   | 5      | 35    |
| 8                                   | 6      | 35    |
| 8                                   | 7      | 35    |
| 8                                   | 8      | 35    |
| 8                                   | 9      | 35    |
| 8                                   | 10     | 35    |
| 8                                   | 11     | 35    |
| 8                                   | 12     | 35    |
| 8                                   | 13     | 35    |
| 8                                   | 14     | 35    |
| 8                                   | 15     | 35    |
| 8                                   | 16     | 35    |
| 8                                   | 17     | 35    |
| 8                                   | 18     | 35    |
| 8                                   | 19     | 35    |
| 8                                   | 20     | 35    |
| 8                                   | 21     | 35    |
| 8                                   | 22     | 35    |
| 8                                   | 23     | 35    |
| 8                                   | 24     | 35    |
| 8                                   | 25     | 35    |
| 8                                   | 26     | 35    |
| 8                                   | 27     | 35    |
| 8                                   | 28     | 35    |
| 8                                   | 29     | 35    |
| 8                                   | 30     | 35    |
| 8                                   | 31     | 35    |
| 8                                   | 32     | 35    |
| 8                                   | 33     | 35    |
| 8                                   | 34     | 35    |
| 8                                   | 35     | 35    |
| 8                                   | 36     | 35    |
| 9                                   | 1      | 35    |
| 9                                   | 2      | 35    |
| 9                                   | 3      | 35    |
| 9                                   | 4      | 35    |
| 9                                   | 5      | 35    |
| 9                                   | 6      | 35    |
| 9                                   | 7      | 35    |
| 9                                   | 8      | 35    |
| 9                                   | 9      | 35    |
| 9                                   | 10     | 35    |
| 9                                   | 11     | 35    |
| 9                                   | 12     | 35    |
| 9                                   | 13     | 35    |
| 9                                   | 14     | 35    |
| 9                                   | 15     | 35    |
| 9                                   | 16     | 35    |
| 9                                   | 17     | 35    |
| 9                                   | 18     | 35    |
| 9                                   | 19     | 35    |
| 9                                   | 20     | 35    |
| 9                                   | 21     | 35    |
| 9                                   | 22     | 35    |
| 9                                   | 23     | 35    |
| 9                                   | 24     | 35    |
| 9                                   | 25     | 35    |
| 9                                   | 26     | 35    |
| 9                                   | 27     | 35    |
| 9                                   | 28     | 35    |
| 9                                   | 29     | 35    |
| 9                                   | 30     | 35    |
| 9                                   | 31     | 35    |
| 9                                   | 32     | 35    |
| 9                                   | 33     | 35    |
| 9                                   | 34     | 35    |
| 9                                   | 35     | 35    |
| 9                                   | 36     | 35    |
| 10                                  | 1      | 35    |
| 10                                  | 2      | 35    |
| 10                                  | 3      | 35    |
| 10                                  | 4      | 35    |
| 10                                  | 5      | 35    |
| 10                                  | 6      | 35    |
| 10                                  | 7      | 35    |
| 10                                  | 8      | 35    |
| 10                                  | 9      | 35    |
| 10                                  | 10     | 35    |
| 10                                  | 11     | 35    |
| 10                                  | 12     | 35    |
| 10                                  | 13     | 35    |
| 10                                  | 14     | 35    |
| 10                                  | 15     | 35    |
| 10                                  | 16     | 35    |
| 10                                  | 17     | 35    |
| 10                                  | 18     | 35    |
| 10                                  | 19     | 35    |
| 10                                  | 20     | 35    |
| 10                                  | 21     | 35    |
| 10                                  | 22     | 35    |
| 10                                  | 23     | 35    |
| 10                                  | 24     | 35    |
| 10                                  | 25     | 35    |
| 10                                  | 26     | 35    |
| 10                                  | 27     | 35    |
| 10                                  | 28     | 35    |
| 10                                  | 29     | 35    |
| 10                                  | 30     | 35    |
| 10                                  | 31     | 35    |
| 10                                  | 32     | 35    |
| 10                                  | 33     | 35    |
| 10                                  | 34     | 35    |
| 10                                  | 35     | 35    |
| 10                                  | 36     | 35    |
| 11                                  | 1      | 35    |
| 11                                  | 2      | 35    |
| 11                                  | 3      | 35    |
| 11                                  | 4      | 35    |
| 11                                  | 5      | 35    |
| 11                                  | 6      | 35    |
| 11                                  | 7      | 35    |
| 11                                  | 8      | 35    |
| 11                                  | 9      | 35    |
| 11                                  | 10     | 35    |
| 11                                  | 11     | 35    |
| 11                                  | 12     | 35    |
| 11                                  | 13     | 35    |
| 11                                  | 14     | 35    |
| 11                                  | 15     | 35    |
| 11                                  | 16     | 35    |
| 11                                  | 17     | 35    |
| 11                                  | 18     | 35    |
| 11                                  | 19     | 35    |
| 11                                  | 20     | 35    |
| 11                                  | 21     | 35    |
| 11                                  | 22     | 35    |
| 11                                  | 23     | 35    |
| 11                                  | 24     | 35    |
| 11                                  | 25     | 35    |
| 11                                  | 26     | 35    |
| 11                                  | 27     | 35    |
| 11                                  | 28     | 35    |
| 11                                  | 29     | 35    |
| 11                                  | 30     | 35    |
| 11                                  | 31     | 35    |
| 11                                  | 32     | 35    |
| 11                                  | 33     | 35    |
| 11                                  | 34     | 35    |
| 11                                  | 35     | 35    |
| 11                                  | 36     | 35    |
| 12                                  | 1      | 35    |
| 12                                  | 2      | 35    |
| 12                                  | 3      | 35    |
| 12                                  | 4      | 35    |
| 12                                  | 5      | 35    |
| 12                                  | 6      | 35    |
| 12                                  | 7      | 35    |
| 12                                  | 8      | 35    |
| 12                                  | 9      | 35    |
| 12                                  | 10     | 35    |
| 12                                  | 11     | 35    |
| 12                                  | 12     | 35    |
| 12                                  | 13     | 35    |
| 12                                  | 14     | 35    |
| 12                                  | 15     | 35    |
| 12                                  | 16     | 35    |
| 12                                  | 17     | 35    |
| 12                                  | 18     | 35    |
| 12                                  | 19     | 35    |
| 12                                  | 20     | 35    |
| 12                                  | 21     | 35    |
| 12                                  | 22     | 35    |
| 12                                  | 23     | 35    |
| 12                                  | 24     | 35    |
| 12                                  | 25     | 35    |
| 12                                  | 26     | 35    |
| 12                                  | 27     | 35    |
| 12                                  | 28     | 35    |
| 12                                  | 29     | 35    |
| 12                                  | 30     | 35    |
| 12                                  | 31     | 35    |
| 12                                  | 32     | 35    |
| 12                                  | 33     | 35    |
| 12                                  | 34     | 35    |
| 12                                  | 35     | 35    |
| 12                                  | 36     | 35    |
| 13                                  | 1      | 35    |
| 13                                  | 2      | 35    |
| 13                                  | 3      | 35    |
| 13                                  | 4      | 35    |
| 13                                  | 5      | 35    |
| 13                                  | 6      | 35    |
| 13                                  | 7      | 35    |
| 13                                  | 8      | 35    |
| 13                                  | 9      | 35    |
| 13                                  | 10     | 35    |
| 13                                  | 11     | 35    |
| 13                                  | 12     | 35    |
| 13                                  | 13     | 35    |
| 13                                  | 14     | 35    |
| 13                                  | 15     | 35    |
| 13                                  | 16     | 35    |
| 13                                  | 17     | 35    |
| 13                                  | 18     | 35    |
| 13                                  | 19     | 35    |
| 13                                  | 20     | 35    |
| 13                                  | 21     | 35    |
| 13                                  | 22     | 35    |
| 13                                  | 23     | 35    |
| 13                                  | 24     | 35    |
| 13                                  | 25     | 35    |
| 13                                  | 26     | 35    |
| 13                                  | 27     | 35    |
| 13                                  | 28     | 35    |
| 13                                  | 29     | 35    |
| 13                                  | 30     | 35    |
| 13                                  | 31     | 35    |
| 13                                  |        |       |

Figure 10.11. Estimated Errors for PGS3164 Coefficients.

the PGS3013 errors are scaled by this factor one obtains the results shown in Figure 10.12 which reveals a significant degradation of the PGS-T2' field. It is encouraging to note that the scaled errors for PGS3013 are worse than even GEM-L2, as is its performance on all of our tests using independent surface gravimetry and altimeter data.

In summary, we believe that valid methods for gravity model calibration have been developed and tested. The results confirm those which were obtained from comparisons with surface gravity and altimetry and indicate that a dramatic improvement has been achieved over previous satellite-only, Goddard Earth Models like GEM-L2. As shown by these calibrations, the uncertainties given for the GEM-T1 models in Figures 10.1 and 10.2 are realistic and can be applied to TOPEX simulated orbit testing.

### 10.3 COMPARISONS BETWEEN GEM-T1 AND GEM-L2

One of the important gains achieved with the complete re-calculation of a satellite-only gravity model lies in the ability to replace older data sets with more precise data which previously were unavailable. When assessing GEM-T1 in this light, we find that all of the laser data from BE-C, GEOS-1, GEOS-2, SEASAT and STARLETTE were not utilized in GEM-L2. Nor were the Doppler data from OSCAR and SEASAT previously used. There is an overlap with regards to the LAGEOS ranging, for GEM-L2 employed 2.5 years of the full-rate observations spanning January 1979 through June 1981. In GEM-T1, five years of LAGEOS two-minute normal-points have now been analyzed covering the years 1980 through 1984. Therefore, there is a considerable independent wealth of GEM-T1 information (approximately 75%) which has not been previously used in earlier GEM solutions. It is principally the older optical/early laser data sets, especially those used having low inclination orbits, which are a source of commonality between recent GEM models and GEM-T1. But even in these

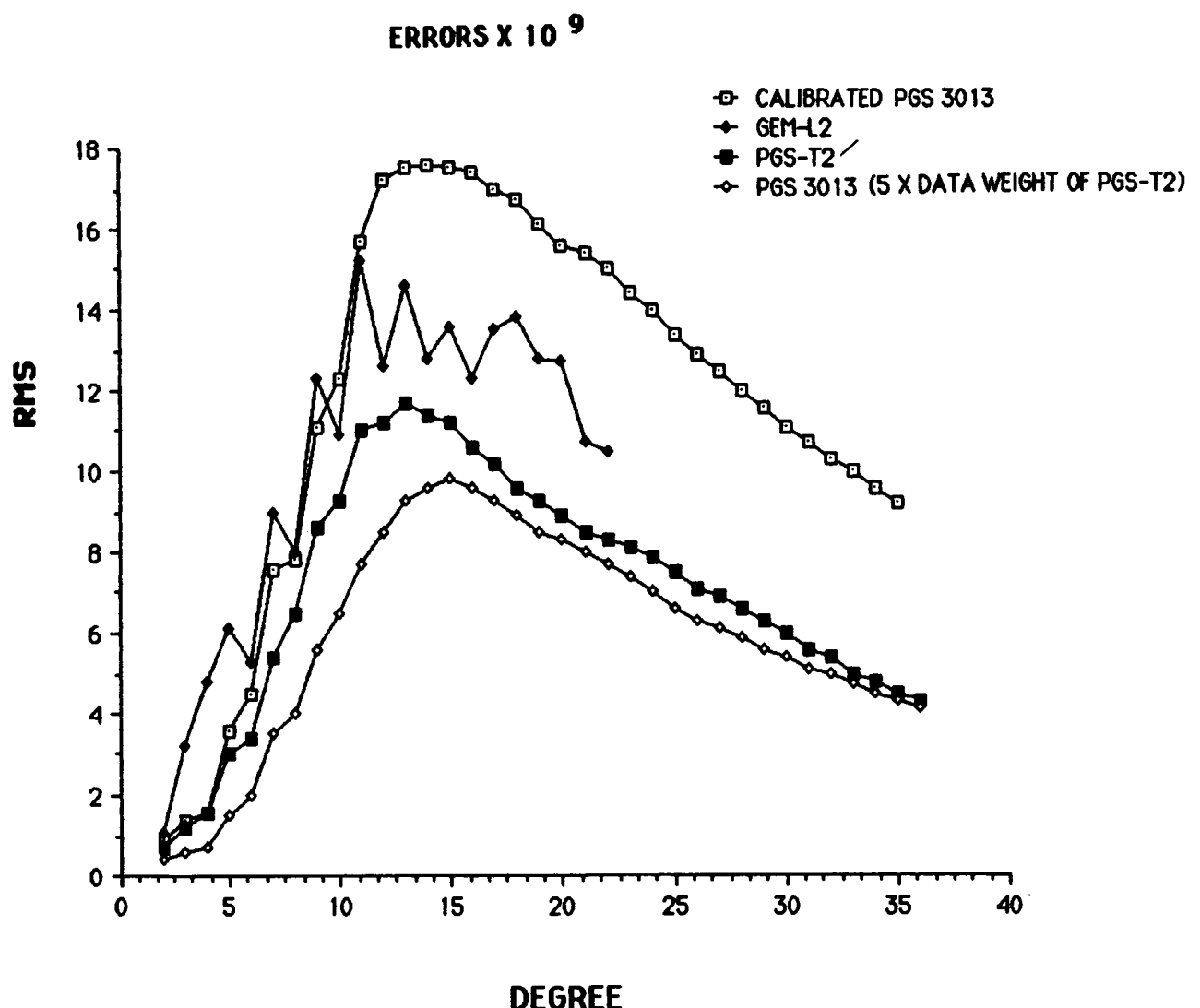


Figure 10.12. RMS of Coefficient Error Per Degree.

cases, changes of approximately 25% in data selection have been made overall. Also of note, GEM-L2 used an additional 14 satellites which have not yet been included in GEM-T1. Another significant departure from GEM-L2 is the extension of the "satellite-only" model from 20x20 to degree 36 as was done in GEM-T1.

In a paper by Lambeck and Coleman (1983) the uncertainties published for GEM-L2 were directly questioned. It is of interest to revisit this issue here, and go beyond our direct response to that paper found in Lerch et al, (1986). There is a high degree of independence between GEM-T1 and GEM-L2. The models have been developed (a) using different computer programs, (b) in the presence of different constants, (c) with completely different treatment of earth/ocean tides, (d) with a new set of station positions in a new earth-fixed reference frame, (e) using a new model for nutations and a new third-body ephemerides (J2000), (f) with nearly a completely different set of tracking observations and finally (g) with the extension of the field from degree 20 (in GEM-L2) to degree 36 (in GEM-T1) which more than doubles the size of the field. We feel that a direct comparison of these recent models can shed meaningful light on the adequacy of our previous calibration methods. Figure 10.13 presents a histogram of the percent change in the individual coefficients (between GEM-T1 and GEM-L2) as:

$$P_C = \frac{\Delta \bar{C}_{\ell,m}}{\sigma_{C_{\ell,m}}} \times 100 \quad (10.11)$$

$$P_S = \frac{\Delta \bar{S}_{\ell,m}}{\sigma_{S_{\ell,m}}} \times 100$$

where

$\Delta\bar{C}_{l,m}$  and  $\Delta\bar{S}_{l,m}$  are the normalized potential coefficient differences between the two models,

$\sigma_{C_{l,m}}$ ,  $\sigma_{S_{l,m}}$  are the published coefficient uncertainties found in Lerch et al, (1985) for the GEM-L2 model and

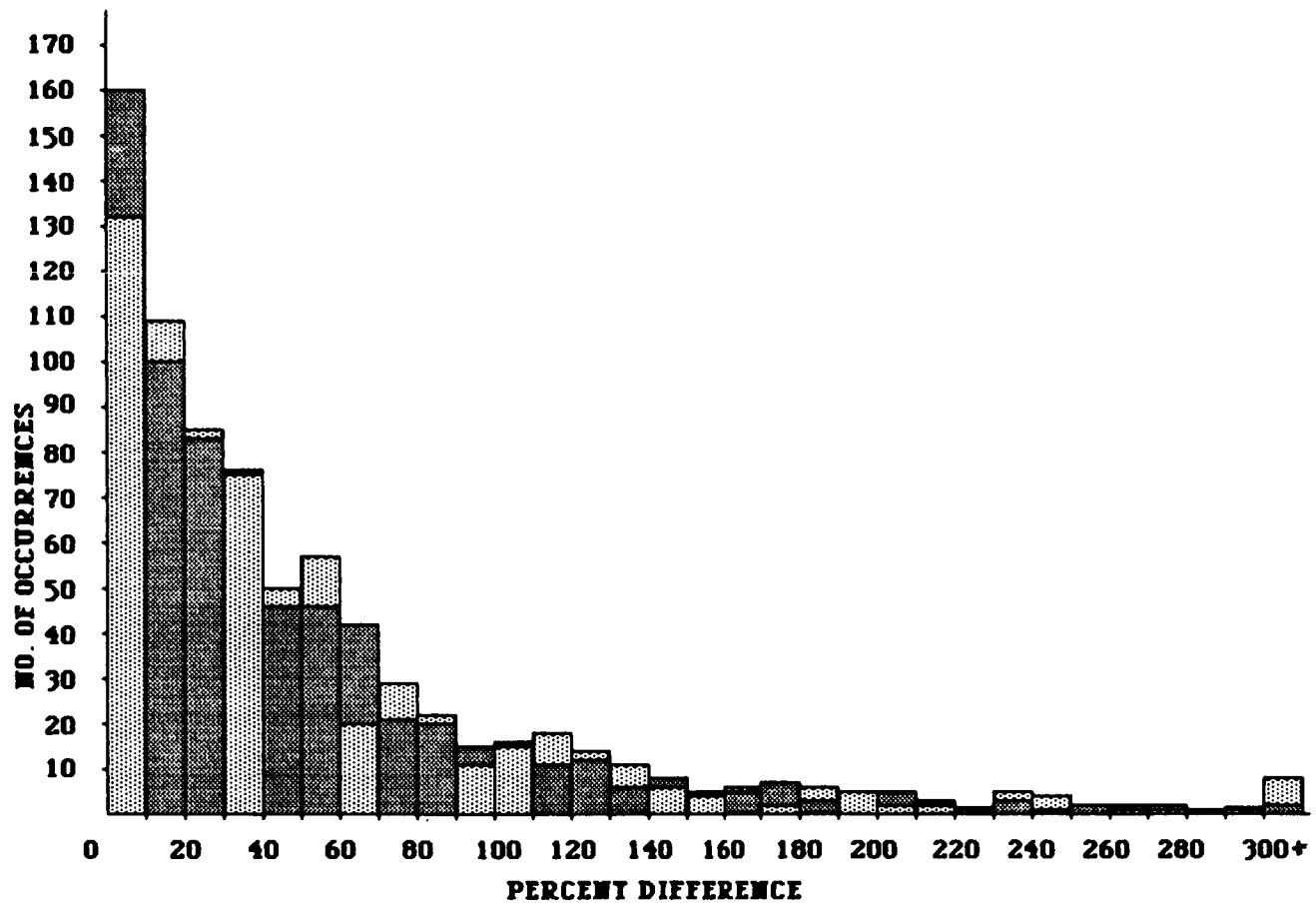
$P_C$ ,  $P_S$  are the percent changes in the coefficients.

It is clear from this figure, that nearly the entire GEM-T1 model is within one-sigma of GEM-L2.

Figure 10.14 shows the RMS coefficient differences by degree for both PGS-T2' and GEM-T1 with GEM-L2 again compared to the published estimate of GEM-L2's errors. (Again, PGS-T2' does not contain the low inclination satellite data.) Since the GEM-L2 errors are larger than those of GEM-T1 and PGS-T2', Figure 10.14 uses the GEM-L2 uncertainties as a basis for comparison. These last two figures show very good calibrated agreement between these nearly independent models and verify that our past calibration methods yielded reliable uncertainty estimates for GEM-L2.

#### 10.4 THE NEED FOR LOW INCLINATION DATA-- REVISITED

Section 5.2.8 described some of the analyses which led us to introduce six more satellite data sets into our earlier PGS-T2 model. As described therein, the zonal harmonic coefficients in PGS-T2 were unsatisfactory due to the lack of adequate orbital inclination sampling in the field. The PGS-T2' model which will be referred to in this section was a version of the original PGS-T2 corrected for the GEOS-2



█ = C

█ = S

$$\left[ \frac{\text{GEM-T1} - \text{GEM-L2}}{\sigma_{L2}} \right] \times 100 = z$$

Figure 10.13. Comparison of GEM-T1 and GEM-L2 with Calibrated GEM-L2 Uncertainties.

## *GEM-L2 vs. OTHER FIELDS*

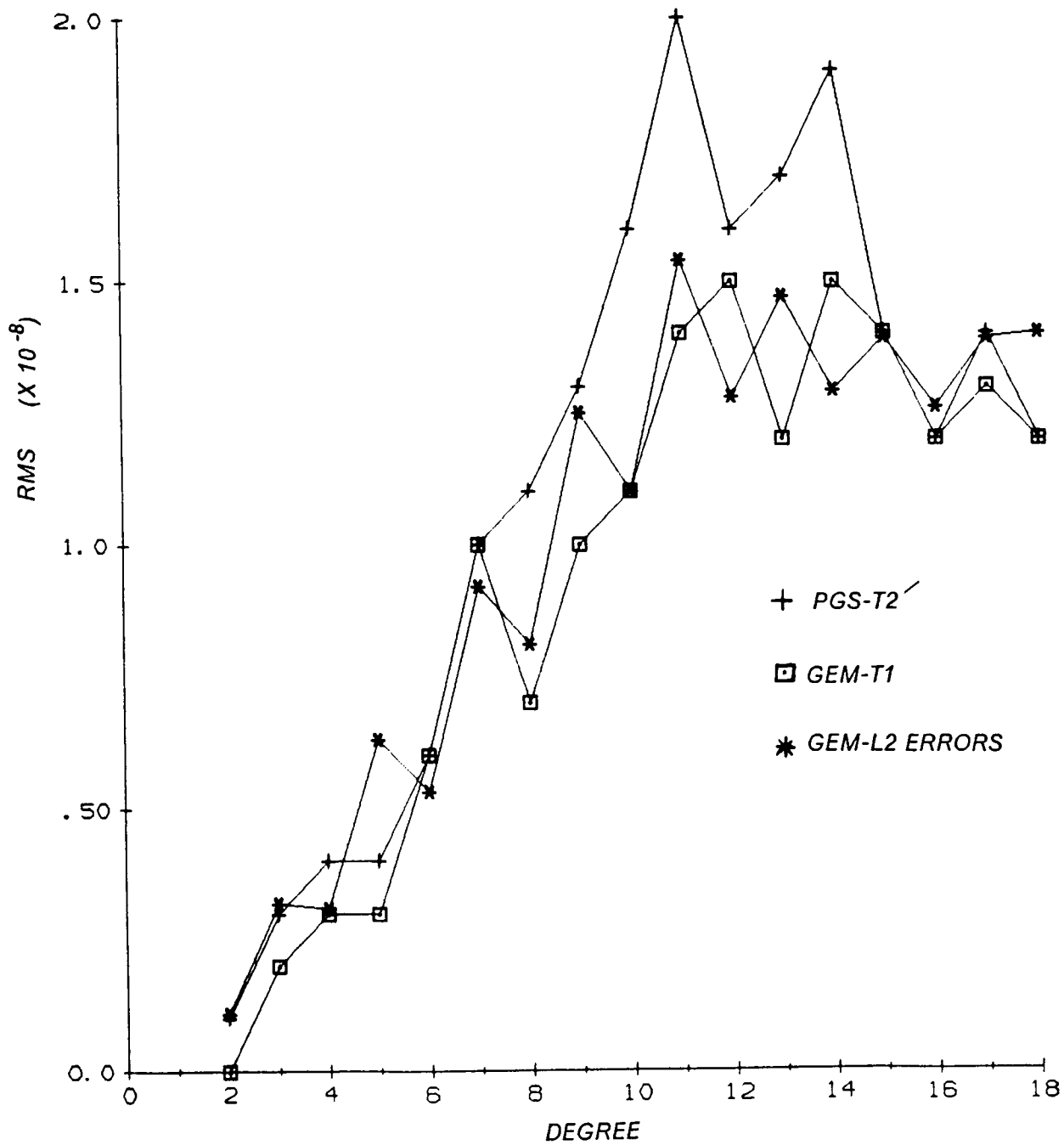


Figure 10.14. RMS Coefficient Difference by Degree.

problem described in Section 8.2 (see Figure 8.3). The surprising large impact of the six low inclination data sets had on the solution (where  $GEM-T1 = PGS-T2' + (6 \text{ low } i \text{ data sets})$ ) has already been shown (in terms of field accuracy) in Figure 10.2. Figure 10.15 directly shows the improvement the addition of these data had on the zonal harmonic recovery. A further assessment of the importance of these low inclination satellite data sets is the subject of this subsection.

A good approach for measuring the influence of the low inclination data on the GEM-T1 solution is through an evaluation of the solution "condition numbers" for the harmonics when models with and without these observations are compared. Here, condition number  $C_i$  is defined as:

$$C_i = D_{ii} \sigma_{ii} \quad (10.12)$$

where

$D_{ii}$  is the diagonal of the combined normal matrix (CN) given in equation (8.12), and

$\sigma_{ii}$  is the diagonal of the inverse of the CN matrix given in (8.13)

It can be shown that these condition numbers demonstrate the loss of significant digits on the solution parameters in the reduction of the matrix. ( $C_i = D_{ii} A_{ii}/\text{determinant}$  where  $A_{ii}$  is the cofactor for the element  $D_{ii}$ .)

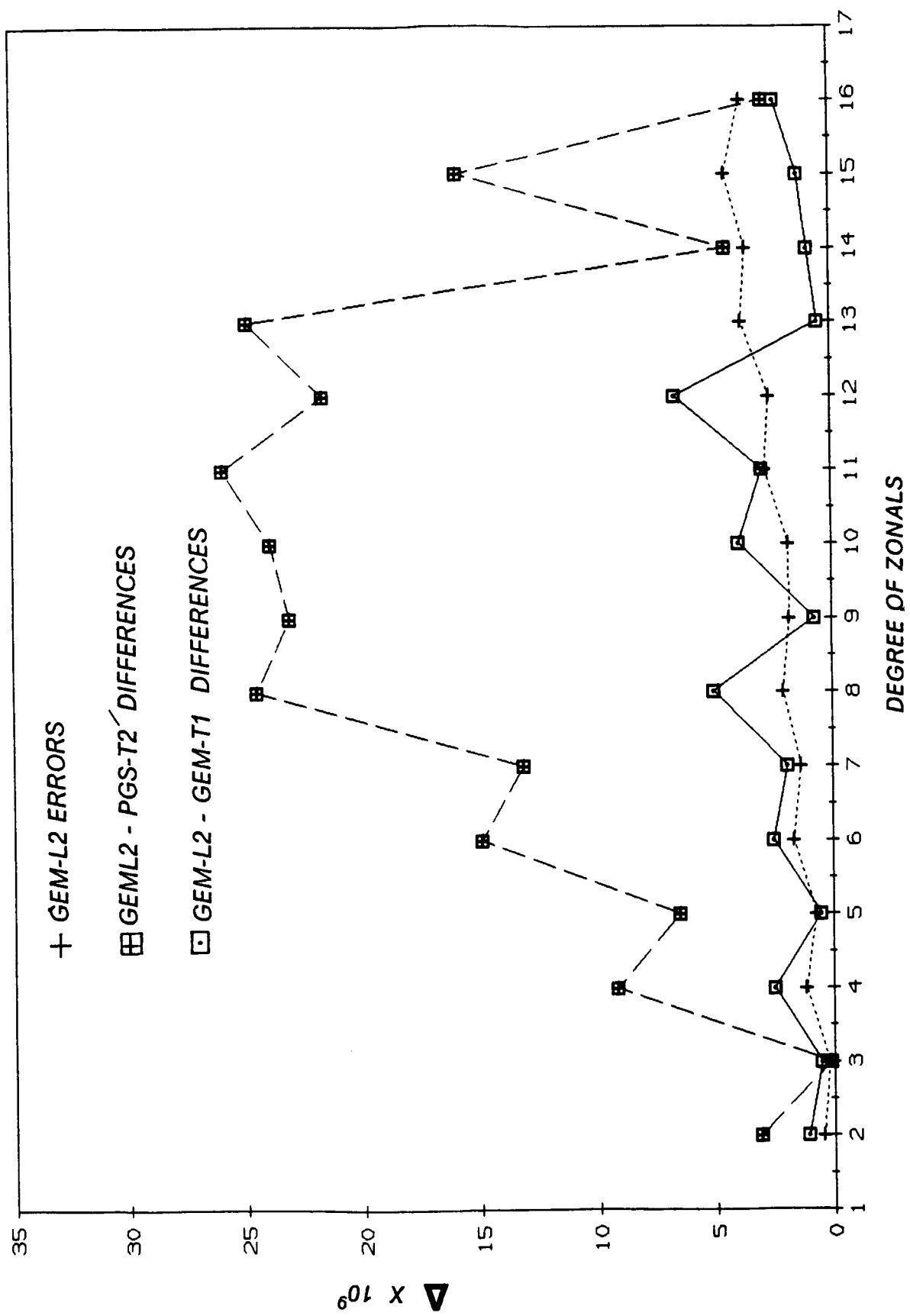


Figure 10.15. Zonal Coefficients.

Note that  $C_{ij}=1$ , if there is no correlation present (i.e.,  $\sigma_{ij}=0$  for  $i \neq j$ ) and

$$\sigma_{ii} = \frac{1}{D_{ii}} = \sigma_{ii}^{(o)} \quad \begin{array}{l} \text{Idealized error variances for} \\ \text{the case where there is zero} \\ \text{correlation present.} \end{array} \quad (10.13)$$

It can be shown that the condition number,  $C_i$ , will increase from unity depending on the extent of correlation in the inverse matrix (CN), and according to (10.12),  $\sigma_{ii}$  will increase as

$$\sigma_{ii} = C_i / D_{ii} = C_i \sigma_{ii}^{(o)} \quad (10.14)$$

Equation (10.14) shows that the size of the condition number reflects the extent that correlation in the solution causes the variance to increase over the idealized variance. Hence, if the condition numbers are significantly reduced in a matrix, then the error variances are proportionately reduced.

The condition numbers in the comparison below reveal an interesting statistical property about the loss of resolution in the answers, due to cross-correlations among the parameters. If one takes the condition numbers obtained in a model (like PGS-T2') which lacked the low inclination data and divides them by the condition numbers obtained in GEM-T1 (as was done to produce Figure 10.16) the full impact of these data can be assessed. It is clear that the off-diagonal conditioning provided by the low inclination data penetrated into the central mid-degree sections of the model allowing a better resolution of the harmonics extending beyond improving the zonal determination. Obviously, these low inclination observations played a significant role in the determination of GEM-T1 which is somewhat surprising, given their level of observation imprecision and the low weight these data had in the combined solution.

# GEM-T1 WITHOUT LOW INCLINATION SATELLITES OVER GEM-T1

| RMS  | DEGREE | ORDER |
|------|--------|-------|
| 3.0  | 2      | 0     |
| 3.6  | 3      | 1     |
| 3.4  | 4      | 2     |
| 3.9  | 5      | 3     |
| 37.0 | 6      | 4     |
| 36.2 | 7      | 5     |
| 8.1  | 8      | 6     |
| 28.8 | 9      | 7     |
| 10.9 | 10     | 8     |
| 14.0 | 11     | 9     |
| 7.6  | 12     | 10    |
| 7.0  | 13     | 11    |
| 5.0  | 14     | 12    |
| 3.8  | 15     | 13    |
| 3.0  | 16     | 14    |
| 2.6  | 17     | 15    |
| 2.1  | 18     | 16    |
| 2.4  | 19     | 17    |
| 2.2  | 20     | 18    |
| 1.3  | 21     | 19    |
| 1.9  | 22     | 20    |
| 1.2  | 23     | 21    |
| 1.1  | 24     | 22    |
| 1.2  | 25     | 23    |
| 1.1  | 26     | 24    |
| 1.2  | 27     | 25    |
| 1.1  | 28     | 26    |
| 1.1  | 29     | 27    |
| 1.0  | 30     | 28    |
| 1.1  | 31     | 29    |
| 1.1  | 32     | 30    |
| 1.1  | 33     | 31    |
| 1.1  | 34     | 32    |
| 1.1  | 35     | 33    |
| 1.1  | 36     | 34    |

Figure 10.16. Ratio of Condition Numbers.

## 10.5 SUMMARY

This section has described a method for calibrating the errors found within our GEM-T1 gravity solution. The scaled covariance matrix obtained for the GEM-T1 solution, we believe, reflects an accurate estimate of both gravitational and tidal model errors. A good deal of this effort was made possible by the availability of our vectorized software which allowed us to make a large number of experimental fields at nominal cost, and the fact that we have made a "satellite-only" model which could then be evaluated through the use of altimetry and surface gravimetry.

SECTION 11.0  
GRAVITY FIELD TESTING ON GEM-T1

11.1 ORBIT TESTING

One of the best ways, and in this project, one of the most relevant means for assessing the accuracy of the gravity model comes through tests using orbital tracking data. These tests typically fall into two categories: (a) orbital information extracted from previous analyses, such as "lumped harmonics" observed to explain the orbital evolution of deeply resonant objects, can be used to calibrate portions of the GEM-T1 field. And (b), the tracking data on various artificial satellites can readily be used to assess improvements and weaknesses in the gravity models when RMS of fits to these observations are obtained and the resulting residuals are analyzed. This second category of testing also includes fits to precise laser observations, re-calculation of reference orbits to assess radial errors detected through altimeter cross-over misclosures, and the use of new and unrepresented satellite data sets for orbital reductions. All of these approaches are undertaken herein.

In the past, Goddard Space Flight Center has had to rely on so-called "tailored" gravity models to satisfy certain orbital accuracy requirements. This represented an admission on our part, that errors in the general models could not be effectively minimized to a satisfactory level for all considered satellites. Therefore, certain data sets were given inordinately high weights in special solutions to provide satellite-specific minimization of gravity errors. The consequences of this intentional mis-balancing of the weights within a field were predictable. Firstly, the objective of having good performance on a specific satellite orbit was achieved. For example the PGS-1331 model which was "tailored" for STARLETTE, does indeed perform better on this

INCLINING PAGE 289 IN PAGE 288

satellite than any of the contemporary more general models. The same is true for the PGS-S4 model developed for SEASAT. However, this improvement was achieved at a cost, which is found in the aliasing of the coefficients within these "tailored" solutions--an aliasing which is considerably higher than that found in the general GEM models. It was hoped at the inception of this effort, that the good orbital performance seen with "tailored" models could be maintained with the development of an improved, general-purpose gravity solution. As shown in this section, GEM-T1 more than meets these earlier expectations.

Comparisons are made evaluating the performance of GEM-T1 with both general and "tailored" gravity models in the following subsections.

#### 11.1.1 Orbital Tests on Laser Satellites

The deployment of a worldwide network of laser stations has dramatically improved the capabilities of satellite geodesy. Special spacecraft have been designed and launched into near-earth orbit to take advantage of the unique accuracies provided by these tracking systems. Third generation lasers have a precision on the order of <5 cm for 1 point per second ranges. These high data rates can be condensed through the formation of "normal" points at sampled time intervals which, for most purposes, are nearly noiseless. Systematic errors may exist within the laser ranges, but colocation testing and prepass and postpass ranging calibrations limit these errors so that they seldom exceed 5 cm. With mobile instruments occupying globally distributed sites, the accumulated data from many satellite missions can provide a highly accurate set of observations for gravity model testing.

Of primary interest are two special laser satellites. LAGEOS and STARLETTE are unique in several respects. They are passive, dense spheres covered with retroreflectors, whose sole purposes are to serve

as space-based laser ranging targets. Both of these satellites, by careful design, have a limited sensitivity to non-conservative force model effects, and are extremely good satellites for gauging gravity modeling improvements. The STARLETTE and LAGEOS orbits are, however, quite different. LAGEOS orbits the earth at nearly an earth's radius and thereby senses only the longest wavelength portion of the earth's geopotential due to attenuation. STARLETTE, on the other hand, is in a somewhat eccentric orbit ( $e=.02$ ) with a perigee height of slightly more than 800km. In this orbit, STARLETTE experiences a much richer spectrum of gravity and tidal perturbations than does LAGEOS, especially those due to the shorter wavelength terms in the gravity model.

For LAGEOS orbits determined from a month's worth of tracking, gravity modeling is the dominant source of force model error. The orbit of LAGEOS is so clearly perturbed by the gravity field and little else, it is an ideal object for assessing long wavelength geopotential modeling accuracy. In order to isolate the gravity model error, LAGEOS monthly arcs require solution for the orbital state, a solar radiation pressure and along-track acceleration coefficient, as well as solution for earth orientation parameters. All of these were adjusted within each arc of LAGEOS used to test the fields.

Table 11.1 presents results from three typical monthly orbits found in the 1980-1984 time period. Intercompared are the RMS of fit to LAGEOS normal points (in cm) obtained within these orbital solutions when different general gravity models are used. GEM-T1 performs best with these data, with our GEM-L2 solution not far behind. The results from these two GSFC fields are considerably beyond the capabilities of other general fields shown for the determination of LAGEOS orbits. (In fact, GEM-L2 was adopted in 1984 for PROJECT MERIT's LAGEOS analyses). GEM-T1, however, included these observations. Table 11.2 intercompares GEM-T1 with GEM-L2 for an annual set of independent normal points, specifically those obtained during 1985. Again, GEM-T1 is shown to be

Table 11.1

**GRAVITY MODEL TESTS:  
LAGEOS (30<sup>D</sup> ARCS)**

RMS (cm)

| <u>MODEL</u> | <u>MAR. 81</u> | <u>AUG. 83</u> | <u>JUN. 84</u> |
|--------------|----------------|----------------|----------------|
| GEM-10B      | .162           | .165           | .184           |
| GEM-L2       | .084           | .070           | .131           |
| GRIM 3B      | .180           | .251           | .206           |
| GRIM 3L1     | .297           | .398           | .365           |
| GEM-T1       | .080           | .061           | .073           |

Table 11.2

**COMPARISON OF GRAVITY MODELS  
WITH LAGEOS LASER DATA:  
ANNUAL 1985 SOLUTIONS<sup>6</sup>**

| MODEL  | RMS (CM) FOR ANNUAL<br>SOLUTION |
|--------|---------------------------------|
| GEM-L2 | 7.4                             |
| GEM-T1 | 6.0                             |

- ✖ 1985 DATA HAS NOT BEEN UTILIZED IN EITHER  
GEM-L2 OR PGS-T2. ANNUAL SOLUTION ADJUSTS  
STATION COORDINATES AND POLAR MOTION.

Table 11.3

**GRAVITY MODEL TESTS:  
STARLETTE**

RMS (m)  
840122 (5<sup>D</sup>)

**MODEL**

|          |      |
|----------|------|
| GEM-10B  | 1.12 |
| GEM-L2   | 1.26 |
| GRIM 3B  | 3.65 |
| GRIM 3L1 | 3.07 |
| GEM-T1   | 0.16 |

an improved model. The 6 cm RMS of fit overall for the 1985 monthly arcs is quite good. At long wavelength, GEM-T1 seems to be a major advancement for LAGEOS orbit modeling.

STARLETTE is an excellent vehicle for field assessment. And by orbiting at a much lower orbit than LAGEOS, it complements LAGEOS for gravity field testing. Table 11.3 shows a sample STARLETTE five day orbit determined by various general gravity models. Surprisingly, GEM-T1 is nearly an order of magnitude improved over this complete set of recently published general fields. Test arcs spanning a variety of time periods are shown in Table 11.4 and Figure 11.1 where GEM-T1 is directly compared to the tailored model PGS-1331. The GEM-T1 model shows performance superior in every case by a factor of 2 to 3.

Other laser satellites, which are well represented in the general gravity models of the past five years, have also been used to test the performance of GEM-T1. Table 11.5 shows results for a sample five day arc using BE-C. Improvement comparable to that seen for both STARLETTE and LAGEOS is again seen for BE-C. BE-C was scheduled for high priority tracking to support crustal motion experiments in California. We have taken some of the short (two revolution) orbits which have been previously used in these investigations and re-computed them with GEM-T1. These results are shown in Table 11.6. GEM-T1 shows marked improvement in the ability to fit these BE-C observations, yielding results which are now at the noise levels of the laser instruments themselves in these two-revolution orbital arcs.

Tests using the GEOS-1,-2 and -3 satellites are shown in Table 11.7. In every case the RMS of fits are significantly better when GEM-T1 is used in the orbital modeling. The GEOS satellites are of special importance since their orbital inclinations are similar to that planned for TOPEX/POSEIDON.

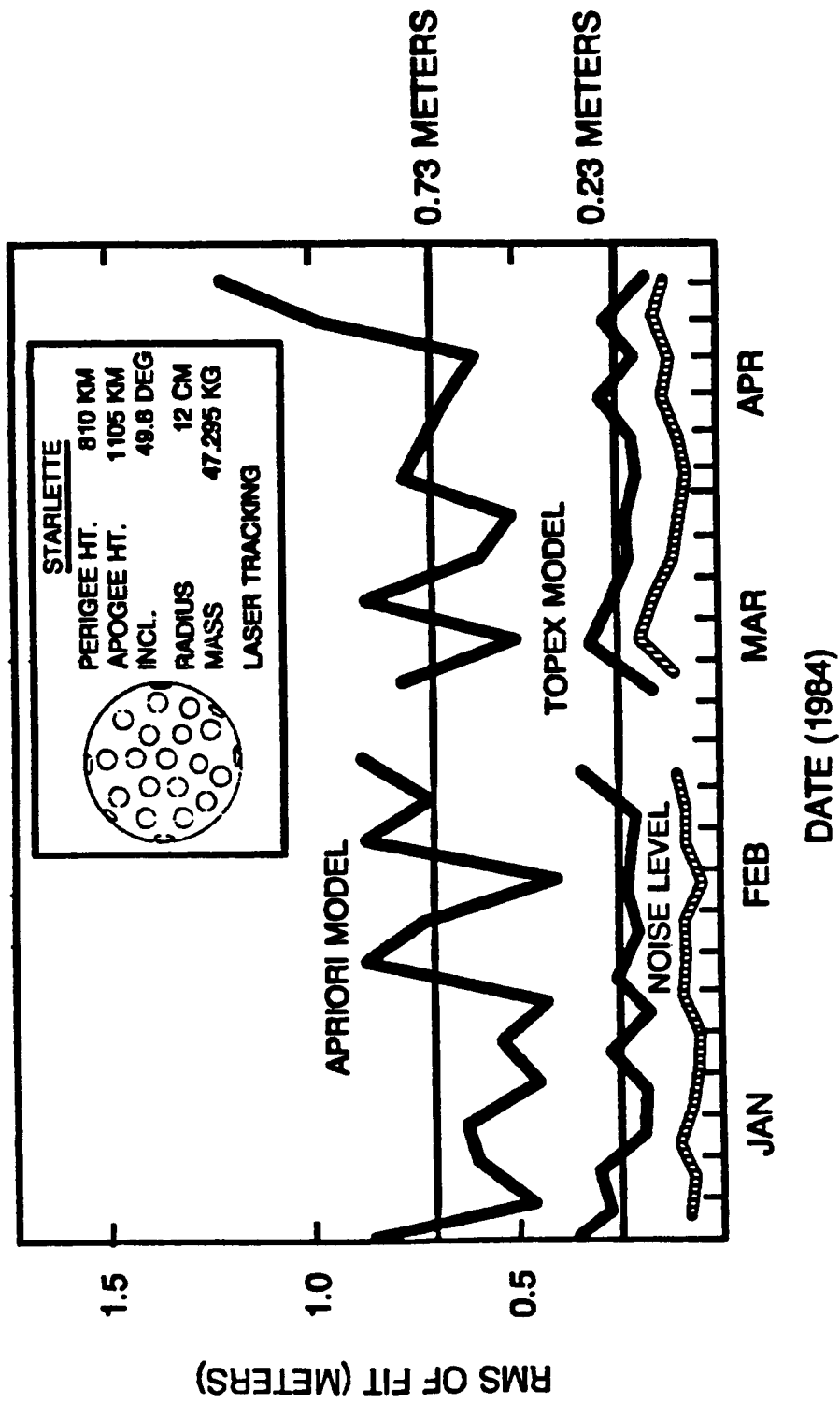


Figure 11.1. Precision Orbit Computations for the STARLETTE Satellite Using the May 1986 TOPEX Earth Gravity Model.

Table 11.4

**ORBIT TESTS ON  
STARLETTE**

| <u>DATE</u> | <u>RMS (cm)</u> |               |
|-------------|-----------------|---------------|
|             | <u>PGS-1331</u> | <u>GEM-T1</u> |
| 840112      | 64              | 20            |
| 840122      | 47              | 16            |
| 840206      | 56              | 18            |
| 840406      | 80              | 14            |
| 840511      | 93              | 20            |
| 840521      | 71              | 22            |
| 840526      | 76              | 19            |
| 840625      | 69              | 16            |
|             |                 |               |
| 761027      | 43              | 23            |
| 761116      | 46              | 18            |
|             |                 |               |
| 790320      | 49              | 25            |
| 790418      | 59              | 21            |

Table 11.5

**GRAVITY MODEL TESTS:**  
**BE-C**  
**SAMPLE 5 DAY ARC**  
**RMS (m)**

**MODEL**

|          |       |
|----------|-------|
| GEM-10B  | 0.75  |
| GEM-L2   | 0.91  |
| GRIM 3B  | 5.49  |
| GRIM 3L1 | 3.03  |
| GEM-T1   | 0.399 |

Table 11.6

**BE-C SHORT ARCS**  
**ORBITAL FITS ON INDEPENDENT**  
**DATA SETS**  
**(2 REVOLUTION ARCS)**

| <u>DATE</u>    | RMS (cm)<br>7062 |               | RMS (cm)<br>7051 |               |
|----------------|------------------|---------------|------------------|---------------|
|                | <u>GEM-9</u>     | <u>GEM-T1</u> | <u>GEM-9</u>     | <u>GEM-T1</u> |
| 740930         | 9.5              | 9.0           | 18.6             | 13.0          |
| 741001         | 14.6             | 9.9           | 14.5             | 13.0          |
| 741011         | 15.2             | 11.9          | 16.2             | 11.4          |
| 741017         | 12.5             | 11.1          | 18.8             | 10.4          |
| <b>AVERAGE</b> | <b>13.0</b>      | <b>10.5</b>   | <b>17.1</b>      | <b>12.0</b>   |
| 761028         | 12.7             | 8.5           | 22.1             | 12.4          |
| 761103         | 11.8             | 6.3           | 13.9             | 8.5           |
| 761104         | 13.8             | 10.5          | 11.5             | 11.3          |
| <b>AVERAGE</b> | <b>12.8</b>      | <b>8.5</b>    | <b>15.8</b>      | <b>10.7</b>   |
| 790414         | 16.9             | 6.8           | 23.5             | 6.6           |
| 790420         | 11.3             | 8.0           | 14.6             | 10.8          |
| 790421         | 14.7             | 7.9           | 18.7             | 11.3          |
| 790514         | 24.6             | 7.2           | 21.9             | 8.0           |
| <b>AVERAGE</b> | <b>14.1</b>      | <b>7.5</b>    | <b>19.7</b>      | <b>9.2</b>    |

Table 11.7

**GRAVITY MODEL TESTS:  
GEOS Satellites  
(5 DAY ARCS)  
RMS (m)**

| <u>MODEL</u> | <u>GEOS-1</u> | <u>GEOS-2</u> | <u>GEOS-3</u> |
|--------------|---------------|---------------|---------------|
| GEM-10B      | 0.84          | 1.34          | 1.37          |
| GEM-L2       | 0.95          | 1.06          | 1.57          |
| GRIM 3B      | 1.82          | 3.32          | 3.71          |
| GRIM 3L1     | 1.40          | 5.38          | 3.07          |
| GEM-T1       | 0.71          | 0.69          | 0.74          |

Table 11.8

ORBIT TESTS  
USING AJISAI\* LASER  
OBSERVATIONS

RMS (m)

| <u>EPOCH</u> | <u>GEM-T1</u> |            | <u>GEM-1OB</u> |            |
|--------------|---------------|------------|----------------|------------|
|              | <u>OBS</u>    | <u>RMS</u> | <u>OBS</u>     | <u>RMS</u> |
| 860818       | 14087         | 0.18       | 14617          | 0.63       |
| 860823       | 6373          | 0.17       | 6282           | 0.56       |
| 860828       | 3213          | 0.04       | 3212           | 0.41       |

\*

SEMI-MAJOR AXIS : 7870 KM  
ECCENTRICITY : 0.0006  
INCLINATION : 50°015

There are limited cases where laser data are available from a satellite which is not used in GEM-T1. The laser data overall, was considered essential in the development of this model. However, in the early summer of 1986, the Japanese launched a satellite called Ajisai which was equipped with laser retroreflectors. These data are not employed in any of the existent gravity models used for our analysis, and represent information on a unique orbit. Table 11.8 compares the RMS of fit we have obtained from two five-day arcs and one four-day arc using the Ajisai laser range data. When calibrating the orbits the estimated parameters included a daily drag coefficient ( $C_D$ ), one radiation pressure coefficient ( $C_R$ ) for each arc and one pole position at epoch, as well as the epoch state vector. The results of Table 11.8 show that the GEM-T1 field yields improvements ranging from a factor of 3 to a factor of 10 when compared to the GEM-10B field. Again, the results show more than a factor of three improvement obtained with the GEM-T1 field.

In summary, there is a very significant improvement in our ability to model the orbits of laser tracked satellites when using GEM-T1.

#### 11.1.2 Orbit Tests On Doppler Satellites

Data acquired by globally distributed Doppler stations have been used in GEM-T1. There are contributions from two satellites tracked by these systems. OSCAR-14 is in a polar orbit and for the first time gives the GEM models a strong orbit at this inclination. The altimeter bearing SEASAT satellite is very important for assessing the radial error in the model and for providing a recent satellite which was tracked by both laser and Doppler systems. Therefore, SEASAT uniquely allowed us to inter-relate the Doppler and laser station coordinates into a unified global datum.

Table 11.9

**GRAVITY MODEL TESTS:  
DOPPLER Satellites**

(6 DAY ARCS)

RMS (cm/sec)

| <u>MODEL</u> | <u>SEASAT</u> | <u>OSCAR</u> |
|--------------|---------------|--------------|
| GEM-10B      | 1.21          | 1.17         |
| GEM-L2       | 1.49          | 1.46         |
| GRIM 3B      | 2.56          | 2.34         |
| GRIM 3L1     | 1.86          | 1.87         |
| GEM-T1       | 0.62          | 1.16         |

There was only a limited amount of SEASAT and OSCAR Doppler data available, and all of it has been used in the development of the GEM-T1 field. Table 11.9 intercompares the performance of GEM-T1 against other global models with subsets of these Doppler data. However, in these comparisons, GEM-T1 has an advantage since these data were used in the solution. Therefore, while an improvement is noted, it is difficult to draw significant independent conclusions from these results. The PGS-S4 model is not a general field for it was "tailored" to the SEASAT orbit. To do so, this model used a significant amount of SEASAT altimetry. PGS-S4 is found to fit the SEASAT Doppler data at the same level as that shown for GEM-T1. Furthermore, it is difficult to achieve additional improvement beyond that seen with either of these fields given the apparent .6cm/sec noise seen for these Doppler observations.

There is a limited amount (6 days) of GEOSAT Doppler data which has been made available to us for test purposes. These observations have not been included in any of the gravity solutions. GEOSAT is in an orbit which is very similar to that of SEASAT, and fields which perform well on SEASAT would be expected to do well on GEOSAT. Table 11.10 confirms this speculation where the RMS of fit to the GEOSAT data is seen to be nearly equal for PGS-S4 and GEM-T1, with GEM-T1 doing slightly better. Both of these fields are a significant improvement over the results seen when using GEM-10B.

#### 11.1.3 Tests Using Low Inclination Data

The level of aliasing present in the PGS-T2' model, which lacked the low inclination observations, was large. The low inclination satellite data were subsequently added to the solution to produce GEM-T1. Table 11.11 shows the RMS of fit obtained on three of these satellite data sets when using GEM-10B (which utilized these satellites), GEM-T1 (which also used them) and PGS-T2' (which lacked

Table 11.10

**GRAVITY MODEL TESTS:  
GEOSAT (3<sup>D</sup> ARC)**

RMS (cm/sec)

**MODEL**

|         |      |
|---------|------|
| GEM-10B | 1.47 |
| PGS-S4  | 1.00 |
| GEM-T1  | 0.98 |

Table 11.11

**GRAVITY MODEL TESTS USING LASER TRACKING DATA  
FROM LOW INCLINATION SATELLITES**

| SATELLITE | EPOCH  | RMS IN METERS |                     |        |
|-----------|--------|---------------|---------------------|--------|
|           |        | GEM10B        | PGS-T2 <sup>*</sup> | GEM-T1 |
| DI-C      | 710615 | 2.58          | 2.42                | 1.65   |
|           | 710622 | 2.23          | 1.99                | 1.50   |
| DI-D      | 710507 | 1.93          | 1.76                | 1.22   |
|           | 710710 | 1.87          | .94                 | .94    |
| PEOLE     | 710304 | 1.73          | 5.20                | .89    |
|           | 710527 | 2.82          | 12.62               | .73    |

\* THIS GRAVITY MODEL DOES NOT CONTAIN LOW INCLINATION TRACKING DATA

contributions from any satellite inclinations below 40 degrees). The degradation of the fit for the PEOLE laser data when using PGS-T2' is especially large. Again, GEM-T1 has an improved capability for modeling these orbits.

#### 11.1.4 Radial Accuracy on SEASAT

Returning now to SEASAT, we have the ability to isolate the radial orbit modeling performance of different gravity fields through the use of altimeter data. The radial error can be assessed by evaluating the implied difference in the altimeter measured sea surface height at groundtrack crossover locations. Since the sea surface height is approximately equal to the geoid, (with small differences due to the general ocean circulation and errors due to mismodeled tides), its value at a specific geographical location would be expected to be nearly time-invariant. However, when the height of the sea surface above the reference ellipsoid at the same geographical point on the earth's surface is measured by crossing altimeter passes, the difference in the calculated sea surface heights is a reasonably strong measure of the non-geographically correlated radial orbit error. This assessment of radial error is incomplete, for there are correlated errors effecting both orbits equally. However, there remains a large time dependent radial error signal which can be detected and studied.

Table 11.12 gives a history of the altimeter crossover results which were obtained by GSFC during the efforts to "tailor" a field for SEASAT. Previously, the direct introduction of the SEASAT altimeter data into the solution was required to produce a model which gave better than 1m SEASAT radial orbit accuracy as measured by altimeter crossovers. As is shown by this table, GEM-T1, which lacks any altimeter data, performs significantly better than even the PGS-S4 field which used SEASAT altimeter data. Table 11.13 shows a comparison of the crossover performance on several test arcs using PGS-S4, the original PGS-T2,

Table 11.12

ALTIMETER CROSSOVER RESULTS  
FOR SEASAT

| MODEL  | DATA CONTENT  | RADIAL<br>ORBIT ERROR<br>(M) |
|--------|---|------------------------------|
| PGS-S1 | GEM-9+ SEASAT LASER                                     | 2.1                          |
| PGS-S2 | GEM-9+ SEASAT LASER<br>AND S-BAND RADAR                 | 1.8                          |
| PGS-S3 | GEM-10B (GEOS-3 ALT)<br>+ SEASAT LASER/S-BAND           | 1.2                          |
| PGS-S4 | PGS-S3 + SEASAT ALTIMETRY                               | 0.7                          |
| GEM-T1 | NEW SATELLITE ONLY MODEL<br>WITH SEASAT DOPPLER<br>DATA | 0.5                          |

Table 11.13

**SEASAT ALTIMETER CROSSOVER RESULTS:**  
**RMS (m) FOR 6 DAY ARCS**

| <u>EPOCH</u>                | <u>NO. OF<br/>Crossovers</u> | <u>PGS-S4</u> | <u>PGS-T2</u>  | <u>GEM-T1</u>  |
|-----------------------------|------------------------------|---------------|----------------|----------------|
|                             |                              | <u>1982</u>   | <u>AGU '86</u> | <u>+ ALTIM</u> |
| 780727                      | 1234                         | .623          |                | 0.933          |
| 780802                      | 1299                         | .868          |                | 0.688          |
| 780808                      | 1407                         | 1.316         | 0.841          | 0.695          |
| 780917                      | 1472                         | 1.249         | 0.722          | 0.632          |
| 780923                      | 1539                         | 1.215         | 0.730          | 0.675          |
| 780929                      | 1498                         | 0.922         | 0.786          | 0.710          |
| <u>AVERAGE</u> + $\sqrt{2}$ |                              | <b>0.72</b>   | <b>0.54</b>    | <b>0.42</b>    |
|                             |                              |               |                | <b>0.51</b>    |

GEM-T1 and a field which for test purposes combined GEM-T1 with SEASAT altimetry. The altimetry model represents only a preliminary attempt combining SEASAT altimeter data with the GEM-T1 satellite data base. A far more rigorous solution is in progress. Two conclusions can be drawn from this Table; first, GEM-T1 is a significant improvement over any field we have for modeling the radial trajectory of SEASAT. Second, when altimetry is added to the GEM-T1 model in the future, it will perform even better.

#### 11.1.5 Tests Using the Longitudinal Acceleration on Ten 24-Hour Satellites

Carl Wagner (private communications) has used the longitude accelerations observed on ten 24-hour satellites to evaluate the accuracy of the low degree and order portion of several recent gravity fields. The 24-hour orbits (all circular) are resonant with all terms where the difference (parity) between degree and order is even. However, since these objects orbit at very high altitude, the size of the effects attenuate quickly, leaving the strongest gravitational perturbations arising from the specific harmonics of C,S(2,2), C,S(3,1) and C,S(3,3). These satellites, well-distributed in longitude, provide a special case where their deeply resonant orbit perturbations provide a strong independent test of the low degree and order fields.

Table 11.14 compares the weighted RMS residual obtained for the calculated longitudinal accelerations from different gravity fields with the longitude accelerations observed on these ten satellites. A weighted RMS = 1 would indicate that the satellite models predict these accelerations to the noise level of the observations.

When reviewing Table 11.14, there is a large difference in the low degree and order accuracy of the earlier models, like GEM-9 and GEM-10B, which lacked LAGEOS tracking as compared to those containing these laser

Table 11.14

TESTS OF GRAVITY MODELS  
WITH  
24 - HOUR SATELLITE  
ACCELERATIONS

| <u>MODEL</u> | <u>RMS WEIGHTED<br/>RESIDUAL</u> |
|--------------|----------------------------------|
| GEM 9        | 5.42                             |
| GEM 10B      | 3.84                             |
| GEM L2       | 1.21                             |
| PGS-T2       | 1.65                             |
| GEM-T1       | 1.34                             |
| PGS- 3163    | 1.20                             |

range measurements. All of the other models found in Table 11.14 contained LAGEOS data. The longitude accelerations calculated from the LAGEOS fields predict those observed on these satellites to a accuracy level near to that by which they have been observed directly. Although the performances are quite similiar on the latest LAGEOS fields, GEM-L2 still yields the best result for a "satellite-only" model. However, the performance of GEM-T1 is still quite satisfactory. Note the addition of altimetry into the GEM-T1 solution, even when preliminary as was done to form PGS-3163, improves the field performance on this test substantially.

## 11.2 GEOID MODELING

An improvement in gravity modeling requires a better determination of the individual harmonic coefficients (geoid representation) as well as improved "lumped harmonics" for orbital calculations. Given the fact that the earth has a unique gravity field, genuine improvements in gravity modeling require better representation (in spherical harmonics) of this physical reality. Therefore, part of our gravity modeling activity was directed towards achieving an improved global geoid modeling capability. This is of special interest within the TOPEX/POSEIDON framework because knowledge of the marine geoid is of critical importance.

Recalling Section 10, we find that GEM-T1 yields an improved geoid modeling capability which exceeds that which was found in any previous GSFC "satellite-only" solution. This is most clearly seen in Figure 10.3.1, where GEM-T1 is evaluated using altimeter derived gravity anomalies and is a clear and dramatic improvement over GEM-L2. Figure 9 in Lerch et al, (1985) shows that GEM-L2 was significantly better than any of the earlier GEM models when compared to altimeter anomalies. Also of note, is that the estimated commission error at degree 22 (which

is the size of the complete GEM-L2 model) using surface gravity data indicates approximately a factor of two improvement for GEM-T1 over GEM-L2. This level of improvement in reduced coefficient uncertainty is shown directly in Figure 10.2.

These results indicate that GEM-T1 is a "satellite-only" model which has less geoidal distortion than earlier such models. As such, it can serve as an improved "base" field for use in combination with local surface gravity and altimetry data.

### 11.3 ESTIMATED TOPEX/POSEIDON ORBITAL ACCURACY

Estimates of the orbital accuracy achievable for TOPEX/POSEIDON based upon our best estimate of gravity model uncertainty can be ascertained. To make these calculations we used the GSFC ERODYN Program [Englar et al., 1978] which is capable of propagating the full gravity model covariance error statistically into an RSS position error of the satellite's trajectory as a function of time. The scaled covariance matrix for GEM-L2, GEM-T1 and PGS-3163 (as described in Section 10) was used in these assessments. In Section 8.3 we raised some questions about the reliability of the full GEM-T1 covariance. At this point in our investigation we have been unable to develop a gravity model entirely free of constraint. Therefore, the following study must be accepted with some caution due to the difficulty we have had in assessing the full effect of least squares collocation on the correlations in our solution. However, in studies using AJISAI, the predicted range error for test arcs is 10 to 15cm RMS when using the independent GEM-T1 covariance matrix. This is in quite good agreement with the orbital fits (Table 11.8) we are obtaining when using GEM-T1 and fitting the actual full rate Ajisai laser data. We therefore have reason to believe that the forthcoming simulation for TOPEX yields reliable gravity modeling error estimates.

To obtain a realistic TOPEX orbital study, we simulated 3 days worth of Doppler data from a global network of 40 stations using the best available estimate of the TOPEX nominal orbit. These observations were made without any consideration for tracking system errors, including noise, since the only error we sought to assess was that arising from geopotential sources. These data were then orbitally reduced, and a set of normal equations (with their variational partials in time) were output for use in ERODYN.

Table 11.15 presents a summary of the results. Shown in this table is the RMS radial error caused by imperfections in the gravity model, for the TOPEX/POSEIDON orbit, as calculated for 1/2 day, 1 day and 3 day arc lengths. The results, as a function of time, are shown in Figure 11.2 for the 3 day arc length. These estimates indicate that a major improvement has been made towards reaching the orbit modeling goals set forth for the TOPEX/POSEIDON Mission. While preliminary, they are grounds for cautious optimism.

Figure 11.3 shows a preliminary breakdown of the gravity model contributions to the radial errors estimated for TOPEX when taking subsets of the coefficients by both degree and by order. The strongest signal is seen from an evaluation of the geopotential error contributions by order where there are two very significant problems. These spikes indicate that the uncertainties of the  $m=1$  and  $m=13$  harmonics are the most significant sources of error within the GEM-T1 field for TOPEX. The  $m=13$  terms are at TOPEX's primary resonance. These terms should not present a problem for field improvement for even a little amount of TOPEX tracking data is capable of successfully resolving this orbital resonance. All of these  $m=13$  terms produce a single, dominating, well defined resonance perturbation (with two nearby and much smaller sideband effects). This primary resonance is easily corrected in a multi-day orbital arc. Likewise, the most likely cause of the  $m=1$  errors are those arising from the so-called " $m$ -daily" perturbations

*Table 11.15*

## **TOPEX PROJECTED RADIAL ERRORS**

**ERRORS IN CENTIMETERS**

**SAMPLE INTERVAL = 10 MIN.**

**GRAVITY MODEL      1/2 DAY ARC      1 DAY ARC      3 DAY ARC**

|                |             |             |             |
|----------------|-------------|-------------|-------------|
| <b>GEM-L2</b>  | <b>51.6</b> | <b>61.9</b> | <b>65.7</b> |
| <b>GEM-T1</b>  | <b>17.2</b> | <b>22.7</b> | <b>25.3</b> |
| <b>PGS3163</b> | <b>13.2</b> | <b>16.6</b> | <b>18.8</b> |

**( PGS3163 = GEM-T1 + SEASAT ALTIMETER )**

$RMS(\text{CM.}) \text{ GEM-L2} = 66, \text{ GEM-T1} = 25, PGS3163 = 19$

( PGS3163 : GEM-T1 + SEASAT ALTIMETER )

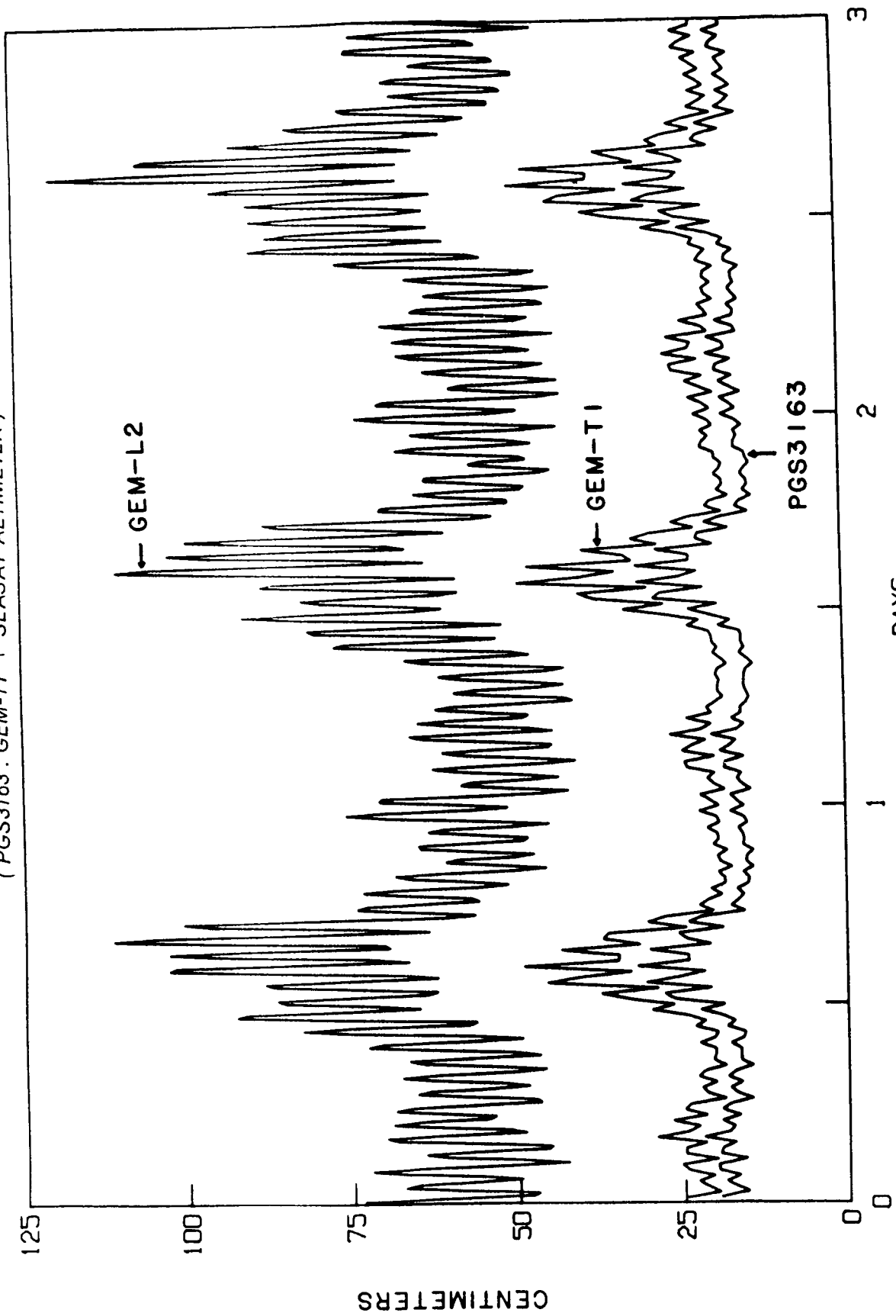
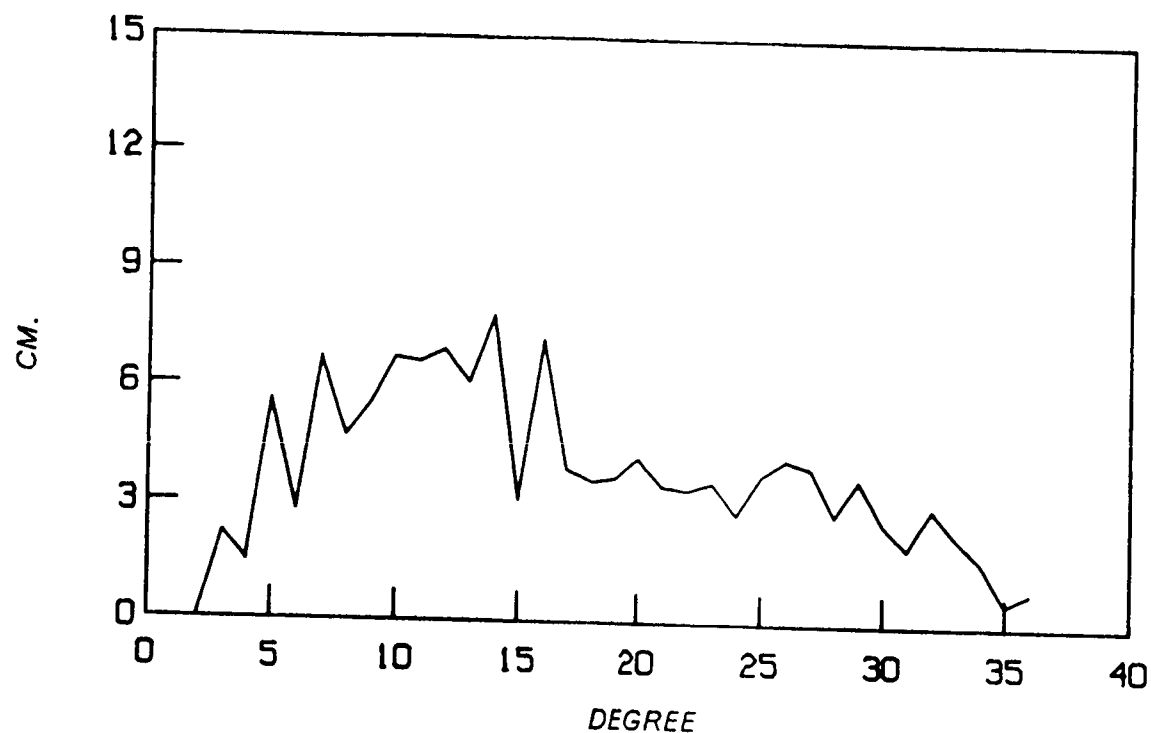


Figure 11.2. TOPEX Projected Radial Errors.

TOTAL RMS 25 CM.

RMS PER DEGREE



RMS PER ORDER

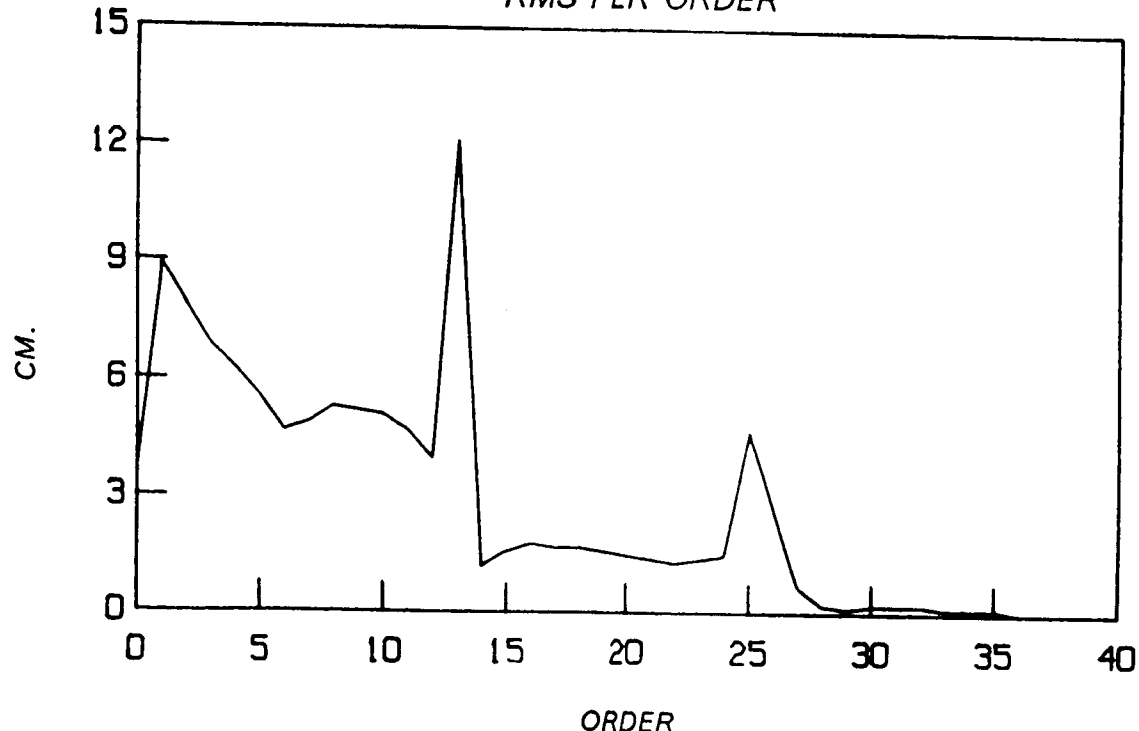


Figure 11.3. TOPEX Projected Radial Errors from GEM-T1.

which, for this order, have perturbations of one-cycle per day. These once per day cycles are clearly evident in Figure 11.2. Again, these m-daily terms should be modelled accurately if limited amounts of TOPEX/POSEIDON data are added to the gravity solution.

#### 11.4 ORTHOMETRIC HEIGHTS COMPARISONS

One of the quantities related to the gravity model which can provide an external check on the field is the undulation at tracking station locations. If the orthometric heights are accurately known from surveys and the geometric height of the instrument is determined from its geodetic coordinates, then these data can be used to calibrate the undulations inferred by global geopotential models. If  $N$  denotes the undulation,  $h$  the geometric height above the reference ellipsoid, and  $H$  the orthometric height, then :

$$N = h - H \quad (11.1)$$

The ellipsoidal heights are derived from the estimated center-of-mass referred three-dimensional station positions. The orthometric heights are obtained at the tracking sites from spirit levelling. Consequently we can independently determine the undulation  $N$  at specific points on the earth's surface. These values can be compared to the values obtained from the gravity models (taken to infinite degree and order) that expresses  $N$  in terms of the potential coefficients. In practice we only have a finite set of potential coefficients and can get only approximate values of  $N$ ; the error committed by omitting the coefficients above the truncation limit of the solution is termed omission error. The fact that the determined harmonics are in error, introduces an additional error, the so-called commission error. The mean sea level (orthometric) heights also have additional errors that vary, depending on the quality of the survey from which they were obtained. The surveying datum over the North American continent is expected to be of

good and of uniform accuracy. One of the comparisons we present here is for the Doppler-derived undulations at 750 North American stations compiled by NOAA's National Geodetic Survey. This data set has been used in other investigations such as [Tscherning and Goad, 1985], which has a detailed description of the data. The version which we used was obtained from Ohio State University (R.H. Rapp, private communication). Accompanying documentation from OSU indicates that the Doppler coordinates have been transformed into a geocentric system by applying the well known axial Z-shift of 4.0 meters, a scale change of -0.5 ppm and a Z-axis rotation of 0.5 mas. The undulations implied by various (recent) gravity field solutions were compared to those obtained from the Doppler sites. The mean differences and their RMS about the mean are listed in Table 11.16. The OSU fields are high degree expansions (to 180 x 180) and have much less omission error than the significantly smaller "satellite-only" fields. We have included them to provide some measure of the omission effects. It can be seen from this table that the new solutions compare favorably with others models. In most cases they are even better than satellite solutions which have included altimeter data and/or terrestrial gravity data (e.g. GEM10B, GRIM3).

A set of globally distributed undulations can also be used to infer the semi-major-axis of the best fitting ellipsoid. In theory the global undulation mean should be zero; one of the constraints in determining the size, shape and origin of the best fitting ellipsoid is having the undulations exactly mean to zero. In practice though we have only a limited number of point values where the geometric as well as the orthometric height are only approximately known. This determination therefore is only approximate and depends heavily on the distribution of the stations and the accuracy of the surveyed orthometric heights. The correction to the semi-major-axis is defined as the average misclosure in the equation relating  $N, h, H$  :

Table 11.16

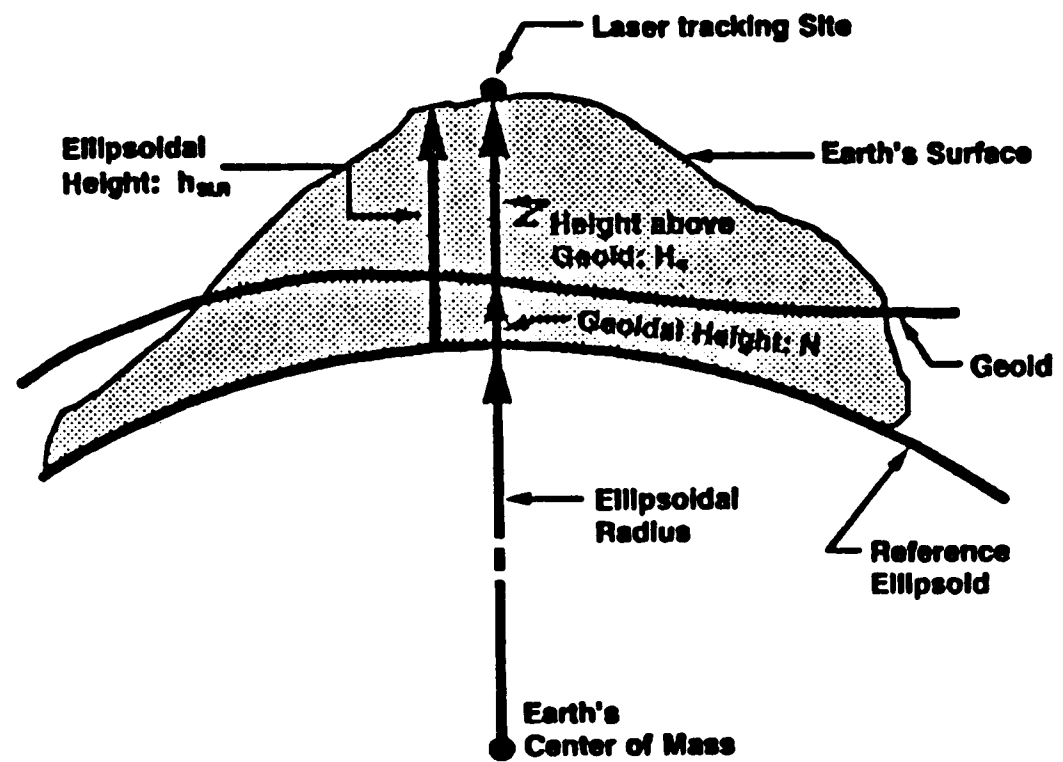
**GEOID HEIGHT COMPARISONS**  
**BASED ON 750 DOPPLER-DERIVED**  
**UNDULATIONS IN NORTH AMERICA**

| <b>FIELD<br/>DESIGNATION</b> | <b>MAXIMUM<br/>DEG. &amp; ORD.</b> | <b>MEAN DIFFERENCE<br/>[cm]</b> | <b>RMS DIFFERENCE<br/>[m]</b> |
|------------------------------|------------------------------------|---------------------------------|-------------------------------|
| * GEM-10B                    | 36, 36                             | -19                             | 3.6                           |
| * GRIM 3                     | 36, 36                             | -17                             | 3.8                           |
| * GRIM 3L1                   | 36, 36                             | -12                             | 3.3                           |
| * OSU '81                    | 36, 36                             | -6                              | 3.4                           |
| * OSU '78                    | 180, 180                           | -41                             | 2.9                           |
| GEM-L2                       | 20, 20                             | 13                              | 4.1                           |
| PGS-T2                       | 36, 36                             | 6                               | 3.4                           |
| GEM-T1                       | 36, 36                             | 15                              | 3.5                           |

\*COMBINATION FIELDS

$$\Delta a_e = h_{SLR} - H - N$$

For this comparison, we have restricted our global station network to those stations with SLR tracking. The geometric relationship of the above defined quantities is depicted in Figure 11.4 . The results of this computation at thirty five stations are given in Table 11.17. A six meter editing criterion was applied. We have thus eliminated some isolated points where a 36 x 36 field cannot model sudden high frequency changes of the local gravity field or there is some error in the local survey/station position. The value of  $a_e$  from the remaining thirty stations agrees very well (to a few centimeters) with that derived from LAGEOS solutions. The large standard deviation of the sample indicates that this is not a particularly strong test of the models, which is a known fact when station locations are considered. Many stations are located on islands or in mountainous regions where local gravity features can be steep. However, although the quality of the GEM-T1 field is not directly assessed, its performance against other contemporary models is shown to be quite good.



$$\Delta a_e = h_{\text{sun}} - H_o - N$$

Figure 11.4. Determination of Earth's Semi-Major Axis.

TABLE 11.17  
EARTH'S SEMI-MAJOR AXIS FROM GEM-T1

| SITE LOCATION | NO.  | ELLIPSOIDAL*<br>HEIGHT<br>m | MSL<br>HEIGHT<br>m | GEOIDAL**<br>HEIGHT<br>m | DELTA<br>$a_e$<br>m |
|---------------|------|-----------------------------|--------------------|--------------------------|---------------------|
| EASTER I.     | 7061 | 115.82                      | 119.14             | -4.72                    | 1.40                |
| OTAY MT.      | 7062 | 988.59                      | 1022.00            | -35.12                   | 1.71                |
| BEAR LAKE     | 7082 | 1962.89                     | 1976.51            | -12.16                   | -1.46               |
| FORT DAVIS    | 7086 | 1961.31                     | 1983.21            | -24.62                   | 2.72                |
| YARAGAEE      | 7090 | 241.30                      | 266.56             | -26.17                   | 0.91                |
| GREENBELT     | 7101 | 8.79                        | 42.43              | -34.63                   | 0.99                |
| GREENBELT     | 7102 | 17.95                       | 51.81              | -34.63                   | 0.77                |
| GREENBELT     | 7103 | 17.89                       | 51.80              | -34.63                   | 0.72                |
| GREENBELT     | 7105 | 19.13                       | 53.40              | -34.63                   | 0.72                |
| QUINCY        | 7109 | 1106.25                     | 1129.85            | -25.78                   | 2.18                |
| MON. PEAK     | 7110 | 1838.89                     | 1870.79            | -34.07                   | 3.17                |
| PLATTEVILLE   | 7112 | 1501.49                     | 1519.91            | -16.65                   | -1.77               |
| OWENS VAL.    | 7114 | 1178.00                     | 1203.80            | -28.04                   | 2.24                |
| HAWAII (M1)   | 7120 | 3067.73                     | 3048.25            | 4.30                     | 15.18E              |
| HUAHINE       | 7121 | 43.60                       | 34.20              | 4.10                     | 5.30E               |
| MAZATLAN      | 7122 | 30.74                       | 56.00              | -22.28                   | -2.98               |
| HAWAII        | 7210 | 3067.45                     | 3047.95            | 4.30                     | 15.20E              |
| TLRS MON.PK.  | 7220 | 1838.74                     | 1870.61            | -34.07                   | 2.20                |
| BARSTOW       | 7265 | 895.92                      | 926.72             | -30.04                   | -0.76               |
| SANTIAGO      | 7400 | 725.42                      | 690.36             | 21.40                    | 13.66E              |
| CERRA TOLLO   | 7401 | 2158.59                     | 2123.09            | 23.26                    | 12.24E              |
| FINLAND       | 7805 | 78.01                       | 59.23              | 19.95                    | -1.17               |
| KOOTWIJK      | 7833 | 93.42                       | 49.80              | 45.27                    | -1.65               |
| WETTZELL      | 7834 | 661.17                      | 614.44             | 46.55                    | 0.18                |
| SIMOSATO      | 7838 | 99.48                       | 60.43              | 36.52                    | 2.54                |
| GRAZ          | 7839 | 539.39                      | 494.36             | 46.57                    | -1.54               |
| GREENWICH     | 7840 | 75.33                       | 30.68              | 49.11                    | -4.46               |
| TLRS FT.DAVIS | 7885 | 1961.33                     | 1983.16            | -24.62                   | 2.79                |
| TLRS QUINCY   | 7886 | 1109.51                     | 1129.96            | -25.78                   | 5.33E               |
| VANDENBURG    | 7887 | 601.34                      | 636.45             | -35.57                   | 0.46                |
| VERNAL        | 7892 | 1590.01                     | 1607.70            | -13.54                   | -4.15               |
| AREQUIPA      | 7907 | 2492.25                     | 2452.27            | 35.79                    | 4.19                |
| MT. HOPKINS   | 7921 | 2352.49                     | 2383.38            | -28.89                   | -2.00               |
| MATERA        | 7939 | 535.86                      | 490.52             | 39.90                    | 5.44E               |
| ORRORAL       | 7943 | 948.89                      | 929.53             | 12.02                    | 7.34E               |

The average  $a_e$  (edited E): 6378137.29 ± .43

SECTION 12.0  
SUMMARY

The computation of GEM-T1 has been a major undertaking. To develop it, we have evaluated all of the overall solution design decisions made in the past for other GEM models and reconsidered them in light of the present state-of-the-art in Satellite Geodesy. As a result, we have achieved a level of internal consistency higher than for any earlier Goddard Earth Model. Moreover, this work was made possible by the redesign of our major software tools, GEODYN and SOLVE, for the Cyber 205 vector computer.

The GEM-T1 model provided a simultaneous solution for:

- o a gravity model in spherical harmonics complete to degree and order 36;
- o a subset of 66 ocean tidal coefficients for the long wavelength components of 12 major tides. This adjustment was made in the presence of 550 other ocean tidal coefficients representing 32 major and minor tides; and
- o 5-day averaged earth rotation and polar motion parameters for the 1980 period onwards.

The model was derived exclusively from satellite tracking data acquired on 17 different satellites which ranged in inclination from 15 degrees to polar. In all, almost 800,000 observations were used, half of which were from third generation laser systems. A calibration of the model accuracies has been performed showing GEM-T1 to be a major improvement over all earlier GSFC "satellite-only" models for both orbital calculations and geoidal representations. And for terms of low

PRECEDING PAGE BLANK NOT FILMED

degree and order (to 8 x 8) GEM-T1 is a major advancement over all GEM models, even those containing altimetry and surface gravimetry.

When a simulation of the TOPEX/POSEIDON orbit was made using the covariances of the GEM-T1 model, preliminary estimated radial error was reduced to a level below 20cm RMS as compared to more than 50cm when using GEM-L2. This simulation evaluated only errors arising from geopotential sources. GEM-L2 was the best available model for TOPEX prior to the work described herein. A major step towards more accurate gravity modeling for TOPEX/POSEIDON has been achieved in this first of an expected new series of Goddard Earth Models.

#### ACKNOWLEDGEMENTS

The authors wish to give their sincere thanks to the very capable group of scientists at the University of Texas' Center for Space Research under the direction of Prof. Byron D. Tapley, who, like ourselves, have embarked on the pursuit of gravity modeling at the level required for TOPEX/POSEIDON. Their interaction with us over the last four years has been a constant source of pleasure, intense interest and great food for thought. The Colorado Center for Astrodynamics Research at the University of Colorado, under the direction of Dr. George Born, played an important role in helping us evaluate the accuracy of GEM-T1. The authors would also like to acknowledge the contributions of two fine scientists, Carl Wagner of the National Geodetic Survey, and Ron Estes, of SAR Corporation, for their assistance in our field development. We also wish to thank Ralph Post of the National Science Data Center at GSFC for his tireless help in securing the vast amounts of archived data which made much of our work possible. Prof. Richard Rapp of The Ohio State University has kindly made his altimeter and surface gravity anomaly data available to us. And we would also like to thank him for his constructive comments on our models as their development progressed. In addition, this project was made possible due to the extensive GEODYN programming support we received from Dave Rowlands and Bill Eddy of EG&G, the SOLVE and ERODYN support from Dave Wildenhain, Ron Estes (while they were at BTS), Seth Grimes and Vas Mejer of BTS, and GEODYN benchmarking support from Susan Poulose and Susie Blackwell of RMS. Absolutely critical to the success of this endeavor was the support we received from Joe Bredekamp and his NASA Space and Earth Sciences Computing Center staff. They are responsible for keeping the Cyber 205 rolling and helping us fit comfortably within their system while meeting our production needs. Special thanks to Ray Sears of this Center for his assistance in handling the mass storage needs of our project are also acknowledged.

And last, but certainly in no way least, we would like to thank EG&G's Marge Payne and Nancy Gebicke for all of their patience when typing this material, and Jo Christodoulidis, for her wonderful help with the artwork and tables which made this work so presentable.

## REFERENCES

- Balmino, G., Reigber, C. and Moynot, B., "The GRIM 2 Earth Gravity Field Model; Determination and Evaluation," EOS (2), 34, pp.55-78, 1978.
- Barlier, F., Berger, C., Falin, K.L., Kockarts, G., Thuillier, G., "A Thermospheric Model Based Upon Satellite Drag Data," Ann. Geophys., +, 34, fasc1, 1978, pp. 9-24.
- Bomford, G., Geodesy, Oxford University Press, 1980.
- Christodoulidis, D.C., Smith, D.E., Klosko, S.M., & Dunn, P.J., "Solid Earth and Ocean Tide Paramters for LAGEOS", Proc. of the 10th International Symposium on Earth Tides (in press), 1986a.
- Christodoulidis, D.C., Williamson, R.G., Chinn, D. & Estes, R., "On the Prediction of Ocean Tides for Minor Constituents", Proc. of the 10th International Symposium on Earth Tides (in press), 1986b.
- Christodoulidis, D.C., Smith, D.E., Williamson, R.G. and Klosko, S.M., "Observed Tidal Braking in the Earth/Moon/Sun System," NASA Technical Memorandum 100677, June 1987.
- Englar, T.S., Estes, R.H., Chin, D.C., and Maslyar, G.A., "ERODYN Program Mathematical Description Version 7809," BTS Contractor Report BTS-TR-78-69, September 1978.
- Estes, R.H. and Majer, V., "SOLVE Program Mathematical Description," BTS Contractor Report prepared under NAS 5-27656, March 1986.

PRECEDING PAGE BLANK NOT FILMED

Gaposchkin, E.M., Smithsonian Standard Earth III S.A.O. Special Report, 353, 262-276, Smithsonian Astrophys. Observ., Cambridge, Mass., 1973.

Gaposchkin, E.M., "Gravity Field Determination From Laser Observations," Phil. Trans. R. Soc. A., 284, pp. 515-527, 1977.

Gaposchkin, E.M., "Pole Position Studied with Artificial Earth Satellites", in Rotation of the Earth, ed. by P. Melchoir & S. Yumi, pp.128-130, 1972.

Gilbert, F. & Dziewonski, A.M., "An Application of Normal Mode Theory to the Retrieval of Structural Parameters and Source Mechanisms from Seismic Spectra", Phil. Trans. R. Soc., Vol. A278, pp.187-269, 1975.

Heiskanen, W., and H. Moritz, 1967, Physical Geodesy, San Francisco, W.H. Freeman and Company.

Katsambalos, K.E., "The Effect of the Smoothing Operator on Potential Coefficient Determinations," Ohio State University, Dept. of Geodetic Science Report No. 287, 1979.

Kaula, W.M., Theory of Satellite Geodesy, Blaisdell Press, Waltham, Mass., 1966.

Kaula, W.M., "Tests of Satellite Determinations of the Gravity Field Against Gravimetry and Their Combination," Publication No. 509, Institute of Geophysics and Planetary Physics, University of California, 1966.

King-Hele, D.G. and D.M.C. Walker, "Evaluation of 15th Order Harmonics in the Geopotential From Analysis of Resonant Orbits," Proc. Roy. Soc., A379, 247-288, 1982.

Klosko, S.M. and Wagner, C.A., "Spherical Harmonic Representation of the Gravity Field From Dynamic Satellite Data," Planet Space Sci., Vol. 30, No. 1, pp. 5-28, 1982.

Lambeck, K., "Determination of the Earth's Pole of Rotation from Laser Range Observations to Satellites", Bull. Geod., Vol. 101, pp.263-281, 1971.

Lambeck, K. and Coleman, R. (1983), "The Earth's Shape and Gravity Field: A Report of Progress from 1958 to 1982," Geophys. J.R. Astr. Soc. (1983), 74, pp. 25-54.

Lambeck, K., "Polar Motion from the Tracking of Close Earth Satellites", in Rotation of the Earth, ed. by P. Melchoir & S. Yumi, pp.123-127, 1972.

Leick, A. & Van Gelder, B.H.W., "On Similarity Transformations and Geodetic Network Distortions based on Doppler Satellite Observations," Ohio State University, Dept. of Geodetic Science Report No. 235, 1975.

Lerch, F.J., Wagner, C.A., Richardson, J.A., Brownd, J.E., "Goddard Earth Models (5 and 6)," GSFC X-921-74-145, Greenbelt, Maryland, Dec. 1974.

Lerch, F.J., S.M. Klosko, R.E. Laubscher, and C.A. Wagner, "Gravity Model Improvement Using Geos 3," GSFC Document X-921-77-246, Goddard Space Flight Center, Greenbelt, Maryland, 1977.

Lerch, F.J., Klosko, S.M., Laubscher, R.E., Wagner, C.A., "Gravity Model Improvement Using GEOS-3 (GEM-9 and 10)," J. Geophys. Res., Vol. 84 (138), pp. 3897-3915, 1979.

Lerch, F.J., B.H. Putney, C.A. Wagner and S.M. Klosko, "Goddard Earth Models for Oceanographic Applications (GEM 10B and 10C)," Marine Geodesy, 5, 2, 145-187, 1981.

Lerch, F.J., Klosko, S.M., Patel, G.B., "Gravity Model Development From Lageos," Geophys. Res. Letters, Vol. 9, No. 11, pp. 1263-1266, 1982.

Lerch, F.J., Marsh, J.G., Klosko, S.M., Williamson, R.G., "Gravity Improvement for SEASAT," J. Geophys. Res., Vol. 87, No. C5, 3281-3296, April 30, 1982.

Lerch, F.J., "Error Spectrum of Goddard Satellite Models for the Gravity Field," Geodynamics Branch Annual Report-1984, NASA TM86223, August 1985a.

Lerch, F.J., Klosko, S.M., Wagner, C.A., & Patel, G.B., "On the Accuracy of Recent Goddard Gravity Models", J. Geophys. Res., Vol. 90, pp.9312-9334, 1985b.

Lerch, F.J., Klosko, S.M., & Wagner, C.A., "Comments on Lambeck and Coleman: 'The Earth's Shape and Gravity Field: A Report of Progress from 1958 to 1982'", Geophys. J. Roy. Astron. Soc., Vol. 86, pp.651-664, 1986.

Marsh, J.G., Lerch, F.J., & Williamson, R.G., "Precision Geodesy and Geodynamics Using Starlette Laser Ranging", J. Geophys. Res., V. 90, pp.9335-9345, 1985.

Marsh, J.G. et al, "An Improved Earth Gravity Model: A Status Report",  
EOS, V. 67, p.260 (abstract), 1986.

Marsh, J.G. & Born, G.H. TOPEX Gravity Model Development Team Activities  
During Fiscal Year 1984, NASA TM 86208, 1985.

Marsh, J.G. & Tapley, B.D. (editors), "TOPEX Gravity Model Improvement  
and Precision Orbit Determination Meeting Minutes," pp.A5-1 to  
A5-4, internal document, NASA/GSFC, 1985.

Marsh, J.G. et al., "A Global Station Coordinate Solution based upon  
Camera and Laser Data-GSFC 1973," NASA Report X-592-73-171, 1973,  
also published in Proceedings of the First International Symposium  
on the Use of Artificial Satellites for Geodesy and Geodynamics,  
Athens, Greece, May 1973.

Martin, T.V. & Eddy, W.F., "GEODYN System Documentation, Vol. 1," EG&G  
Washington Analytical Services Center, Inc., Prepared for  
B.H. Putney under contract NAS 5-22849, 1980.

Martin, T.V., Eddy, W.E., Rowlands, D.D., and Pavlis, D.E., "Volume 1 to  
5, GEODYN II System Description," EG&G Contractor Report, April  
1987.

McClure, P., "Diurnal Polar Motion," NASA document X-592-73-259, 1973.

Melbourne, W. Project MERIT Standards, Circular No. 167, U.S. Naval  
Observatory, Washington, D.C., 1983.

Moritz, H. "Least-Squares Collocation," Rev. of Geophysics & Space  
Physics, Vol. 16, 421-430, 1978.

Moritz, H., Advanced Physical Geodesy, Abacus Press, Tunbridge Wells Kent, Kent, England, 1980.

Munk, W.H. & Cartwright, D.E., "Tidal Spectroscopy and Prediction", Phil. Trans. R. Soc., Vol. A259, pp.533-581, 1977.

National Geodetic Satellite Program, NASA SP-365, Washington, D.C., 1977.

Putney, B.H., "General Theory for Dynamic Satellite Geodesy", in The National Geodetic Satellite Program, pp.319-334, NASA SP-365, 1977.

Rapp, R.H., "The Earth's Gravity Field to Degree and Order 180 Using Seasat Altimeter Data, Terrestrial Gravity Data, and Other Data," Dept. of Geodetic Science Report No. 322, The Ohio State University, Columbus, Ohio, Dec. 1981.

Rapp, R.H., "The Determination of Geoid Undulations and Gravity Anomalies from Seasat Altimeter Data," J. Geophys. Res., 88, C3, 1552-1562, 1983a.

Rapp, R.H., "The Development of the January 1983  $1^{\circ} \times 1^{\circ}$  Mean Free-Air Anomaly Data Tape," Department of Geodetic Science and Surveying, Internal Report Ohio State University, Columbus, Ohio, 1983b.

Rapp, R.H. Geometric Geodesy, Class notes, Dept. of Geodetic Science and Surveying, The Ohio State University, 1983.

Reigber, Ch., G. Balmino, B. Moynot and H. Mueller, "The GRIM3 Earth Gravity Field Model," Manuscripta Geodaetica, 8, 93-138, 1983.

Reigber, Ch., G. Balmino, B. Moynot, H. Mueller, Ch. Rizos and W. Bosch,  
"An Improved GRIM3 Earth Gravity Model (GRIM3B)," paper presented  
at XVIII IUGG-IAG General Assembly, Hamburg, 1983.

Safren, H.G., "Effect of a Drag Model Using a Variable Projected Area on  
the Orbit of the Beacon-Explorer C Satellite," NASA document  
X-921-75-210, 1975.

Schwarz, K.P., "Least-Squares Collocation for Large Systems," Bull.  
Geod. Sci., Aff., 35, 309-324, 1976.

Schwarz, K.P., "On the Application of Least-Squares Colloation Models to  
Physical Geodesy," in Approximation Methods in Geodesy, (H. Moritz  
and H. Sunkel, editors, H. Wichmann-Verlag, Karlsruhe, 1978.

Schwiderski, E.W. "Ocean Tides, Part I: Global Ocean Tide Equations",  
Marine Geodesy, Vol. 3, pp.161-217, 1980a.

Schwiderski, E.W. "Ocean Tides, Part II: Hydrodynamical Interpolation  
Model", Marine Geodesy, Vol. 3, pp.219-255, 1980b.

Smith, D.E., Kolenkiewicz, R., Dunn, P.J., & Torrence, M.H., "Determination  
of Station Coordinates from LAGEOS", in The Use of Artificial  
Satellites for Geodesy and Geodynamics, National Technical  
University, Athens, 1979.

Smith, D.E. et al, "Geodetic Applications of Laser Ranging", Phil.  
Trans. R. Soc., A284, pp.529-536, 1977.

Smith, D.E. et al., "A Global Geodetic Reference Frame from LAGEOS  
Ranging (SL5-1AP)," J. Geophys. Res., Vol. 90, pp. 9221-9235,  
1985.

Wahr, J.M., "The Tidal Motions of a Rotating, Elliptical, Elastic, and Oceanless Earth," PhD Thesis, University of Colorado, 1979.

Wagner, C.A. and S.M. Klosko, "Gravitational Harmonics from Shallow Resonant Orbits," Celestial Mechanics, (16), 1977.

Wagner, C.A. and F.J. Lerch, "The Accuracy of Geopotential Models," Planet. Space Sci., Vol. 26, pp. 1081-1140, 1978.

Wagner, C.A. and Colombo, O., "Gravitational Spectra From Direct Measurements, J. Geophys. Res., 84, 4709, 1979.

Wagner, C.A., "The Accuracy of the Low-Degree Geopotential: Implications for Ocean Dynamics," J. Geophys. Res., 88, B6, 5083-5090, 1983.

Wagner, C.A., Lerch, F.J., Brownd, J.E. & Richardson, J.A., "Improvement In the Geopotential derived from Satellite and Surface Data (GEM 7 and 8)," NASA document X-921-76-20, 1976.

Williamson, R.G. & Marsh, J.G., "Starlette Geodynamics: The Earth's Tidal Response", J. Geophys. Res., Vol. 90, pp.9346-9352, 1985.

**APPENDIX 1**

**APRIORI STATION POSITIONS  
FOR GEM-T1**

**LASER, DOPPLER, S-BAND  
TRACKING SITES**

**as of February 11, 1987**

TOPEX GEODETIC FILE CREATED 02/11/87  
SEMI-MAJOR AXIS: 6378137.00 FLATTENING: 1/298.257

| NAME      | I.D.                | X               | Y               | Z               | LATITUDE       | LONGITUDE     | HEIGHT   |
|-----------|---------------------|-----------------|-----------------|-----------------|----------------|---------------|----------|
| SJEDOP    | 8                   | 4083914.724000  | -4209803.344000 | -2499112.240000 | -23 13 2.8860  | 314 7 49.3899 | 613.1566 |
| MCDOP     | 19-1310713.158000   | 310460.103000   | -6213366.502000 | -77 50 51.7599  | 166 40 27.5094 | -13.2180      |          |
| MAHDOP    | 20 3602880.542000   | 5238222.012000  | -515939.533000  | -4 40 14.3724   | 55 28 46.4637  | 554.5197      |          |
| UCLDOP    | 21 4027832.421000   | 307023.842000   | 4919538.285000  | 50 47 55.0127   | 4 21 32.3079   | 158.9292      |          |
| SMGDP     | 22-3088047.508000   | 5333058.221000  | 1638811.523000  | 14 59 16.1057   | 120 4 21.0188  | 56.3766       |          |
| GWMDO     | 23-5059777.437000   | 3591210.689000  | 1472782.183000  | 13 26 22.8863   | 144 38 4.2689  | 95.3281       |          |
| TAFDOP    | 24-6100051.840000   | -997195.827000  | 1568316.404000  | -14 19 45.3734  | 189 17 3.1603  | 46.5015       |          |
| MSADOP    | 27-3857199.892000   | 3108659.442000  | 4004040.881000  | 39 8 6.5343     | 141 8 0.1677   | 118.7094      |          |
| PRTDOP    | 105 5051978.523000  | 2725637.921000  | -2774470.292000 | -25 56 48.6108  | 28 20 51.7217  | 1607.4999     |          |
| VIRDOP    | 107 1090140.067000  | -842520.407000  | 3991981.266000  | 38 59 43.7459   | 282 41 12.6096 | 85.5080       |          |
| STFDOP    | 112-3942240.273000  | 346854.279000   | -3608204.886000 | -34 40 26.4569  | 138 39 17.3545 | 36.1642       |          |
| NMXDOP    | 113-1556216.306000  | -5169444.382000 | 3387248.806000  | 32 16 43.9538   | 253 14 45.7264 | 1183.4823     |          |
| ANCDOP    | 114-2656164.201000  | -1544366.537000 | 5570655.093000  | 61 17 0.4578    | 210 10 29.6066 | 76.9700       |          |
| BSEDOP    | 116 4004964.422000  | -96559.816000   | 4946541.129000  | 51 11 4.5706    | 358 37 7.9124  | 125.5878      |          |
| TULDOP    | 118 539846.249000   | -1388555.301000 | 6180980.376000  | 76 32 9.0692    | 291 14 42.7896 | 69.2382       |          |
| ALTDOP    | 127-3850349.834000  | 397640.976000   | 5052349.435000  | 52 43 41.9001   | 174 6 13.4618  | 74.2770       |          |
| OTTDOP    | 128 1091450.380000  | -4351283.878000 | 4518704.850000  | 45 23 59.9346   | 284 4 52.3700  | 47.6656       |          |
| TEXDOP    | 192 -740293.270000  | -5457073.446000 | 3207244.281000  | 30 23 1.1196    | 262 16 28.3958 | 218.8637      |          |
| FLODOP    | 641 4522402.628000  | 898011.588000   | 4392486.373000  | 43 48 13.6779   | 11 13 51.9815  | 147.6731      |          |
| POTDAM    | 1181 3800618.509000 | 882010.731000   | 5028856.705000  | 52 22 48.9239   | 13 3 55.3462   | 144.7284      |          |
| MADSS     | 1425 4847873.416000 | -353562.114000  | 4117035.733000  | 40 27 15.6631   | 355 49 43.4091 | 819.4767      |          |
| ROSSST    | 1857 647216.476000  | -5178143.313000 | 3656423.608000  | 35 11 56.3641   | 277 7 28.0414  | 858.3802      |          |
| BDA3      | 6002 2308450.060000 | -4874293.259000 | 3393401.139000  | 32 21 4.8493    | 295 20 31.5201 | -13.8880      |          |
| QUIS      | 6006 1263459.520000 | -6255027.887000 | -68797.595000   | 0 37 18.6378    | 281 25 10.4892 | 3592.2966     |          |
| HAW3      | 6012-5543841.363000 | -2054556.810000 | 2387810.683000  | 22 7 34.6591    | 200 20 5.2415  | 1160.7495     |          |
| GDS3      | 6016-2354733.540000 | -4646742.113000 | 3669474.112000  | 35 20 32.0640   | 243 7 35.1027  | 933.0909      |          |
| ULA3      | 6018-2282487.586000 | -1453372.406000 | 5756710.824000  | 64 58 19.5128   | 212 29 12.9046 | 349.7586      |          |
| MAD3      | 6022 4847758.757000 | -353406.241000  | 4117201.143000  | 40 27 22.3866   | 355 49 49.6522 | 831.1639      |          |
| MAD8      | 6023 4847822.178000 | -353317.195000  | 4117139.507000  | 40 27 19.6721   | 355 49 53.6166 | 834.3747      |          |
| GWM3      | 6024-5068914.734000 | 3584103.540000  | 1458900.120000  | 13 18 38.2291   | 144 44 12.5497 | 140.8469      |          |
| GDS8      | 6028-2354766.548000 | -4646777.247000 | 3669390.480000  | 35 20 29.7765   | 243 7 34.5657  | 939.8022      |          |
| ROSS      | 6031 647202.274000  | -5178317.177000 | 3656144.291000  | 35 11 45.7653   | 277 7 26.6321  | 836.9229      |          |
| ORR3      | 6037-4447485.440000 | 2676856.637000  | -3695269.292000 | -35 37 40.6738  | 148 57 25.4426 | 947.3843      |          |
| MILA      | 6040 907138.484000  | -5535192.616000 | 3026104.975000  | 28 30 29.6131   | 279 18 25.9814 | -27.1839      |          |
| MI23      | 6041 907078.144000  | -5535232.599000 | 3026051.997000  | 28 30 27.6405   | 279 18 23.5539 | -26.3718      |          |
| AG03      | 6054 1769867.176000 | -504471.100000  | -3468390.273000 | -33 9 3.6279    | 289 20 0.8442  | 727.6853      |          |
| MIL3      | 6071 907076.114000  | -5535206.236000 | 3026102.214000  | 28 30 29.4823   | 279 18 23.6370 | -25.5543      |          |
| ETCA      | 6091 5219867.308000 | -4833147.503000 | 3992193.142000  | 38 59 54.2129   | 283 9 28.7975  | 23.5599       |          |
| IUNDAK    | 7034 -521692.957000 | -4242036.158000 | 4718733.840000  | 48 1 21.6883    | 262 59 19.9354 | 228.2115      |          |
| 1EDINB    | 7036 -828471.760000 | -5657444.892000 | 2816825.976000  | 26 22 46.9803   | 261 40 7.9202  | 31.3196       |          |
| 1COLBA    | 7037 -191272.927000 | -4967266.077000 | 3983269.628000  | 38 53 36.5000   | 267 47 41.3492 | 239.1561      |          |
| 1BERMD    | 7039 2308232.342000 | -4873587.010000 | 3394578.597000  | 32 21 49.8477   | 295 20 35.5563 | -1.6029       |          |
| 1PURIO    | 7040 2465070.227000 | -5534913.914000 | 1985531.452000  | 18 15 28.9988   | 294 0 23.8776  | 9.1055        |          |
| 1GSFCP    | 7043 1130730.821000 | -4831318.155000 | 3994143.543000  | 39 1 15.7027    | 283 10 21.0622 | 19.9526       |          |
| 1DENVR    | 7045-1240462.201000 | -4760221.025000 | 4048992.730000  | 39 38 48.2606   | 255 23 39.0016 | 1773.0005     |          |
| GODLAS    | 7050 1130692.438000 | -4831354.616000 | 3994112.117000  | 39 1 14.3647    | 283 10 19.1632 | 20.9531       |          |
| QUINCO51  | 7051-2516893.830000 | -4198389.747000 | 4076416.458000  | 39 58 24.7867   | 239 3 37.5502  | 1059.9437     |          |
| WALLAS    | 7052 1261570.901000 | -4881573.970000 | 3893171.501000  | 37 51 36.0935   | 284 29 24.7514 | -29.1658      |          |
| MOBLAS    | 7053 1130704.646000 | -4831318.517000 | 3994151.264000  | 39 1 16.0118    | 283 10 19.9993 | 20.4535       |          |
| CRMLAS    | 7054-2328184.126000 | 5299661.478000  | -2669470.815000 | -24 54 15.3778  | 113 42 58.5803 | 25.2383       |          |
| CMISLS    | 7060-5068966.309000 | 3584085.182000  | 1458762.160000  | 13 18 33.6245   | 144 44 14.0370 | 139.7523      |          |
| EASTER    | 7061-1884984.152000 | -5357610.236000 | -2892846.045000 | -27 8 51.9069   | 250 36 59.2013 | 115.8812      |          |
| OTAY MT   | 7062-2428826.443000 | -4799746.127000 | 3417278.409000  | 32 36 2.8875    | 243 9 32.8229  | 988.5455      |          |
| STALAS    | 7063 1130714.033000 | -4831362.670000 | 3994093.645000  | 39 1 13.6387    | 283 10 19.9610 | 19.2390       |          |
| GORF064   | 7064 1130678.096000 | -4831334.738000 | 3994134.113000  | 39 1 15.3807    | 283 10 18.7710 | 17.2255       |          |
| GORF065   | 7065 1130694.399000 | -4831348.899000 | 3994118.134000  | 39 1 14.6208    | 283 10 19.2967 | 20.7638       |          |
| WFCLAS    | 7066 1261612.031000 | -4881547.504000 | 3893201.667000  | 37 51 37.1712   | 284 29 26.6514 | -22.7571      |          |
| BDALAS    | 7067 2308538.082000 | -4874075.622000 | 3393635.082000  | 32 21 14.0276   | 295 20 38.1253 | -23.0299      |          |
| GRNTURK   | 7068 1920482.803000 | -5619475.234000 | 2318921.358000  | 21 27 38.0463   | 288 52 5.1988  | -18.6689      |          |
| RAMLAS    | 7069 917958.152000  | -5548366.753000 | 2998783.678000  | 28 13 40.9313   | 279 23 39.4468 | -23.5713      |          |
| WFCLMAS   | 7070 1261570.285000 | -4881564.364000 | 3893184.329000  | 37 51 36.6102   | 284 29 24.8254 | -28.7573      |          |
| 1JUM24    | 7071 976288.310000  | -5601387.375000 | 2880247.155000  | 27 1 14.3717    | 279 53 13.1683 | -17.1686      |          |
| 1JUM40    | 7072 976291.901000  | -5601381.235000 | 2880258.186000  | 27 1 14.7707    | 279 53 13.3413 | -16.9689      |          |
| 1JUPC1    | 7073 976298.392000  | -5601380.427000 | 2880256.241000  | 27 1 14.7097    | 279 53 13.5783 | -17.5688      |          |
| 1JUBC4    | 7074 976299.001000  | -5601377.656000 | 2880262.710000  | 27 1 14.9357    | 279 53 13.6173 | -16.9686      |          |
| 1SUDBR    | 7075 692632.551000  | -4347058.865000 | 4060492.858000  | 46 27 21.5533   | 279 3 10.9597  | 250.5663      |          |
| 1JAMAC    | 7076 1384174.482000 | -5905661.874000 | 1966555.590000  | 18 4 34.8917    | 283 11 27.3567 | 435.2710      |          |
| 1GSFCN    | 7077 1130077.869000 | -4833029.111000 | 399265.813000   | 38 59 57.4187   | 283 9 38.4381  | 16.9530       |          |
| WALHOT    | 7078 1261602.273000 | -4881343.277000 | 3893447.085000  | 37 51 47.4404   | 284 29 28.3556 | -30.1641      |          |
| 1CARVN    | 7079-2328603.726000 | 5299341.378000  | -2669685.615000 | -24 54 23.4100  | 113 43 16.8575 | 2.9745        |          |
| PATRICK   | 7081 917899.473000  | -5548370.254000 | 2998789.456000  | 28 13 41.1908   | 279 23 37.3025 | -26.2338      |          |
| BEARLAKE  | 7082-1735997.850000 | -4425042.770000 | 4241435.989000  | 41 56 1.1377    | 248 34 45.5581 | 1962.9933     |          |
| OWENS084  | 7084-2410591.023000 | -4477740.288000 | 3838653.927000  | 37 13 55.8799   | 241 42 15.1318 | 1178.0906     |          |
| GLDSTS085 | 7085-2353395.031000 | -4641524.591000 | 3676904.548000  | 35 25 28.1911   | 243 6 48.9479  | 965.4002      |          |
| MCDON086  | 7086-1330125.959000 | -5328522.319000 | 3236156.905000  | 30 40 37.5635   | 255 59 2.5634  | 1961.4090     |          |
| YARAGADE  | 7090-2389005.423000 | 5043325.366000  | -3078532.454000 | -29 2 47.6760   | 115 20 48.2987 | 241.3202      |          |

ORIGINAL PAGE IS  
OF POOR QUALITY

ORIGINAL PAGE IS  
OF POOR QUALITY

| NAME     | I.D.                | X               | Y               | Z               | LATITUDE       | LONGITUDE      | HEIGHT    |
|----------|---------------------|-----------------|-----------------|-----------------|----------------|----------------|-----------|
| HAYSTACK | 7091                | 1492452.890000  | -4457273.259000 | 4296821.737000  | 42 37 21.9617  | 288 30 44.5318 | 91.9873   |
| KWADJLAS | 7092-6143447.454000 | 1364701.263000  | 1034160.176000  | 9 23 37.5885    | 167 28 32.5869 | 32.8943        |           |
| SAMOALAS | 7096-6100045.486000 | -996205.338000  | -1568976.100000 | -14 20 7.5069   | 189 16 30.5733 | 48.9818        |           |
| GORF100  | 7100                | 1131355.271000  | -4831163.669000 | 3994137.992000  | 39 1 15.7277   | 283 10 47.8010 | 10.1821   |
| GORF101  | 7101                | 1131239.188000  | -4831174.383000 | 3994154.926000  | 39 1 16.4817   | 283 10 43.0010 | 8.3861    |
| GORF102  | 7102                | 1130685.810000  | -4831347.958000 | 3994117.232000  | 39 1 14.6568   | 283 10 18.9580 | 17.9634   |
| GORF103  | 7103                | 1130684.866000  | -4831343.606000 | 3994122.634000  | 39 1 14.8838   | 283 10 18.9610 | 17.9052   |
| GORF104  | 7104                | 1131095.124000  | -4831191.890000 | 3994176.935000  | 39 1 17.3588   | 283 10 37.0040 | 9.9705    |
| GORF105  | 7105                | 1130718.983000  | -4831345.460000 | 3994112.813000  | 39 1 14.4407   | 283 10 20.3244 | 19.1645   |
| QUINC109 | 7109-2517235.448000 | -4198550.859000 | 4076574.635000  | 39 58 30.2183   | 239 3 18.9461  | 1106.2919      |           |
| MONPEAK  | 7110-2386278.541000 | -4802349.879000 | 3444887.127000  | 32 53 30.4746   | 243 34 38.3005 | 1838.9476      |           |
| VANDENB  | 7111-2668830.842000 | -4530782.286000 | 3598709.230000  | 34 33 58.7920   | 239 30 0.1313  | 626.7517       |           |
| PLATVL   | 7112-1240679.001000 | -4720458.044000 | 4094486.505000  | 40 10 58.2580   | 255 16 26.3902 | 1501.5515      |           |
| OWENS114 | 7114-2410423.050000 | -4477797.657000 | 3838692.069000  | 37 13 57.4359   | 241 42 22.2338 | 1177.9945      |           |
| GLDST115 | 7115-2350862.271000 | -4655541.514000 | 3661003.506000  | 35 14 54.1284   | 243 12 28.9809 | 1038.5943      |           |
| MAUILAS  | 7120-5465998.744000 | -2404405.737000 | 2242230.454000  | 20 42 27.4667   | 203 44 38.1444 | 3067.7242      |           |
| HUAHINE  | 7121-5345864.877000 | -2958248.945000 | -1824620.993000 | -16 44 0.5754   | 208 57 32.0009 | 43.5516        |           |
| MAZATLAN | 7122-1660089.961000 | -5619097.054000 | 2511644.801000  | 23 20 34.5020   | 253 32 27.2487 | 30.8389        |           |
| GORF1251 | 7125                | 1130743.438000  | -4831365.212000 | 3994084.486000  | 39 1 13.2206   | 283 10 21.1271 | 20.6016   |
| HOLLAS   | 7210-5466006.852000 | -2404425.027000 | 2242189.498000  | 20 42 26.0470   | 203 44 38.6415 | 3067.4500      |           |
| MONPEAKT | 7220-2386292.850000 | -4802343.054000 | 3444886.538000  | 32 53 30.4541   | 243 34 37.6908 | 1838.8421      |           |
| BARSTOW  | 7265-2356476.472000 | -4646613.334000 | 3668430.278000  | 35 19 52.5993   | 243 6 31.2485  | 895.8857       |           |
| MTLAGUNA | 7274-2386291.134000 | -4802340.426000 | 3444886.484000  | 32 53 30.5076   | 243 34 37.7049 | 1836.1954      |           |
| SNTIAGOL | 7400                | 1769700.612000  | -5044619.215000 | -3468256.468000 | -33 8 58.4901  | 289 19 52.8881 | 725.3650  |
| CERROTL  | 7401                | 1815518.227000  | -5213470.794000 | -3187995.444000 | -30 10 20.6561 | 289 11 59.8451 | 2158.5624 |
| ASKITES  | 7510                | 4353445.920000  | 2082674.201000  | 4156503.948000  | 40 55 40.7134  | 25 33 58.6765  | 184.1009  |
| DIONYSOS | 7515                | 4595217.892000  | 2039442.831000  | 3912626.422000  | 38 4 42.7711   | 23 55 57.1260  | 512.1019  |
| ROUMELLI | 7517                | 4728694.568000  | 2174383.801000  | 3674569.898000  | 35 24 15.1174  | 24 41 39.3802  | 104.1018  |
| KARITZ   | 7520                | 4596043.243000  | 1733486.324000  | 4055718.246000  | 39 44 3.1556   | 20 39 53.7644  | 599.9742  |
| JRUSLM   | 7530                | 4366553.779000  | 3131126.067000  | 3353786.090000  | 31 44 2.6143   | 35 12 43.7988  | 757.9412  |
| MATERA40 | 7540                | 4641968.380000  | 1393063.494000  | 4133231.399000  | 40 38 55.0053  | 16 42 16.5601  | 516.7544  |
| MATERA41 | 7541                | 4641993.122000  | 1393048.174000  | 4133230.248000  | 40 38 54.5695  | 16 42 15.6330  | 530.6437  |
| PUNSAMEN | 7545                | 4893400.699000  | 772679.294000   | 4004140.157000  | 39 8 7.6904    | 8 58 22.9807   | 232.1879  |
| TRIESTE  | 7550                | 4336739.199000  | 1071281.849000  | 4537909.914000  | 45 38 34.5399  | 13 52 32.4804  | 448.4463  |
| MTGENERO | 7590                | 4390311.858000  | 696716.146000   | 4560853.602000  | 45 55 39.5797  | 9 1 4.3478     | 1663.4743 |
| WETZL596 | 7596                | 4075584.698000  | 931843.821000   | 4801558.909000  | 49 8 38.8751   | 12 52 43.5497  | 660.2469  |
| WETZL597 | 7597                | 4075604.248000  | 931833.091000   | 4801546.599000  | 49 8 38.2065   | 12 52 42.8187  | 661.8388  |
| WETZL599 | 7599                | 4075516.968000  | 931760.151000   | 4801629.999000  | 49 8 42.4533   | 12 52 40.2703  | 658.6266  |
| SAFLAS   | 7804                | 5105611.229000  | -555233.140000  | 3769639.160000  | 36 27 45.4103  | 353 47 36.5916 | 67.9012   |
| METSAHVI | 7805                | 2892595.047000  | 1311815.105000  | 5512609.368000  | 60 13 2.2114   | 24 23 40.8263  | 78.2898   |
| HAULAS   | 7809                | 4578354.440000  | 457992.130000   | 4403170.357000  | 43 55 56.3997  | 5 42 45.1244   | 706.5983  |
| ZIMRWALD | 7810                | 4331285.030000  | 567559.507000   | 4633143.586000  | 46 52 38.0360  | 7 27 55.2402   | 955.5510  |
| CANISL   | 7819                | 5440495.604000  | -1501675.583000 | 2961259.663000  | 27 50 37.4029  | 344 34 10.3013 | 121.2828  |
| DAKLAS   | 7820                | 5886274.041000  | -1845649.974000 | 1615245.180000  | 14 46 2.8382   | 342 35 27.9817 | 48.1843   |
| HELWAN   | 7831                | 4728281.385000  | 2879673.940000  | 3156890.992000  | 29 51 32.3280  | 31 20 33.8847  | 130.1489  |
| KOOTWIJK | 7833                | 3899223.487000  | 396749.080000   | 5015074.070000  | 52 10 42.2477  | 5 48 35.6243   | 93.4801   |
| WETZELL  | 7838                | 4075529.405000  | 931787.187000   | 4801617.581000  | 49 8 41.7460   | 12 52 41.4339  | 661.1067  |
| GRASSE   | 7835                | 4581691.193000  | 556164.708000   | 4389359.447000  | 43 45 16.8840  | 6 55 16.2747   | 1322.9373 |
| SHANGHAI | 7837-2831089.391000 | 4676208.174000  | 3275167.461000  | 31 5 50.9148    | 121 11 30.2116 | 29.2218        |           |
| SIMOSATO | 7838-3822387.162000 | 3699366.723000  | 3507566.454000  | 33 34 39.4932   | 135 56.13.2192 | 99.0526        |           |
| GRAZ     | 7839                | 4194426.092000  | 1162699.512000  | 4647245.773000  | 47 4 1.6445    | 15 29 36.3548  | 539.4764  |
| RCOLAS   | 7840                | 4033463.109000  | 23668.353000    | 4924305.460000  | 50 52 2.5912   | 0 20 10.3476   | 75.2802   |
| GRASSE   | 7842                | 4582050.519000  | 554736.161000   | 4389150.208000  | 43 45 7.8481   | 6 54 10.9638   | 1311.7171 |
| NATMAP   | 7843-4446475.905000 | 2678122.786000  | -3696256.267000 | -35 38 10.6996  | 148 56 21.6480 | 1350.2505      |           |
| CABSL882 | 7882-197742.190000  | -5528036.285000 | 2468364.902000  | 22 55 3.5269    | 250 8 7.9954   | 111.0910       |           |
| MCDON885 | 7885-1330126.074000 | -5328522.270000 | 3236156.903000  | 30 40 37.5638   | 255 59 2.5588  | 1961.3910      |           |
| QUINC886 | 7886-2517243.158000 | -4198548.760000 | 4076577.109000  | 39 58 30.2346   | 239 3 18.6220  | 1109.5399      |           |
| VANDN887 | 7887-2668868.722000 | -4530738.717000 | 3598690.293000  | 34 33 58.6232   | 239 29 57.9836 | 600.9262       |           |
| MTHOPKIN | 7888-1936744.915000 | -5077634.665000 | 3332000.152000  | 31 41 6.6096    | 249 7 18.5466  | 2331.2920      |           |
| GORF889  | 7889                | 1131364.030000  | -4831163.716000 | 3994135.281000  | 39 1 15.6177   | 283 10 48.1551 | 10.0624   |
| AUSTIN   | 7890                | -754162.717000  | -5459056.967000 | 3200750.958000  | 30 18 56.0496  | 262 8 3.9743   | 257.2461  |
| FLAGSTAF | 7891-1923977.301000 | -4850866.723000 | 3658580.761000  | 35 12 52.5769   | 248 21 55.6633 | 2144.2609      |           |
| VERNAL   | 7892-1631485.491000 | -4589128.521000 | 4106755.294000  | 40 19 36.8912   | 250 25 44.9131 | 1590.3207      |           |
| YUMA     | 7894-2196778.378000 | -4887334.614000 | 3448434.259000  | 32 56 21.1695   | 245 47 48.6551 | 241.6952       |           |
| JPLLAS   | 7896-2493212.494000 | -4655524.980000 | 3565580.077000  | 34 12 20.2046   | 241 49 39.7315 | 441.6185       |           |
| MCDON897 | 7897-1330802.109000 | -5328719.684000 | 3235713.110000  | 30 40 19.2891   | 255 58 39.7219 | 2040.5716      |           |
| GORF899  | 7899                | 1131364.030000  | -4831163.717000 | 3994135.282000  | 39 1 15.6177   | 283 10 48.1551 | 10.0638   |
| ORGLAS   | 7901-1535788.518000 | -516982.633000  | 3401042.783000  | 32 25 24.8068   | 253 26 47.0671 | 1626.6594      |           |
| OLILAS   | 7902                | 5056122.298000  | 2716520.205000  | -2775767.582000 | -25 57 36.0836 | 28 14 52.6461  | 1569.4682 |
| AREQUIPA | 7907                | 1942791.903000  | -5804080.070000 | -1796911.637000 | -16 27 56.4184 | 288 30 24.7320 | 2492.2662 |
| GORF18   | 7918                | 1130708.448000  | -4831340.981000 | 3994124.391000  | 39 1 14.8705   | 283 10 19.9404 | 21.2007   |
| GORF19   | 7919                | 1130693.793000  | -4831336.327000 | 3994133.143000  | 39 1 15.2517   | 283 10 19.3913 | 20.5958   |
| GORF20   | 7920                | 1130744.819000  | -4831365.034000 | 3994086.238000  | 39 1 13.2619   | 283 10 21.1847 | 21.8145   |
| HOPLAS   | 7921-1936760.950000 | -5077702.716000 | 3331929.098000  | 31 41 3.4660    | 249 7 18.8984  | 2352.9399      |           |
| NATAL    | 7929                | 5186467.775000  | -3653857.284000 | -654316.651000  | -5 55 39.9399  | 324 50 7.3422  | 39.5952   |
| GRELAS   | 7930                | 4595222.026000  | 2039459.557000  | 3912615.037000  | 38 4 42.2692   | 23 55 57.6844  | 513.3957  |
| DODAIR   | 7935-3910418.452000 | 3376364.722000  | 3272939.156000  | 36 0 20.2722    | 139 11 30.3195 | 902.9204       |           |
| MATERA   | 7939                | 4641964.690000  | 1393074.846000  | 4133261.132000  | 40 38 55.7423  | 16 42 17.0680  | 535.9172  |
| DIONYSOS | 7940                | 4599578.363000  | 2040864.682000  | 3906778.504000  | 38 0 42.2298   | 23 55 37.8905  | 501.1291  |
| ORRORAL  | 7943-4447547.753000 | 2677129.639000  | -3695000.954000 | -35 37 29.9285  | 148 57 17.4255 | 948.9088       |           |

| NAME     | I.D.     | X               | Y               | Z               | LATITUDE       | LONGITUDE      | HEIGHT    |
|----------|----------|-----------------|-----------------|-----------------|----------------|----------------|-----------|
| KOOT883  | 8833     | 3899237.136000  | 396775.269000   | 5015055.290000  | 52 10 41.4604  | 5 48 36.9228   | 88.5977   |
| OLISAO   | 9902     | 5056122.298000  | 2716520.205000  | -2775767.582000 | -25 57 36.0836 | 28 14 52.6461  | 1569.4682 |
| ARESAO   | 9907     | 1942791.903000  | -5804080.070000 | -1796911.637000 | -16 27 56.4184 | 288 30 24.7320 | 2492.2662 |
| HOPSAO   | 9921     | -1936760.950000 | -5077702.716000 | 3331929.098000  | 31 41 3.4660   | 249 7 18.8984  | 2352.9399 |
| NATSAO   | 9929     | 5186467.775000  | -3653857.284000 | -654316.649000  | -5 55 39.9399  | 324 50 7.3422  | 39.5950   |
| GRESAO   | 9940     | 4595214.996000  | 2039466.003000  | 3912612.430000  | 38 4 42.2788   | 23 55 58.0431  | 508.7882  |
| ACSDOP   | 10068    | 6119386.038000  | -1571424.522000 | -871688.464000  | -7 54 28.1129  | 345 35 52.6247 | 46.2993   |
| KWJDOP   | 10214    | -6160997.731000 | 1339618.542000  | 960416.572000   | 8 43 6.9791    | 167 43 58.1446 | 35.7283   |
| QUIDOP   | 30121    | 1280855.752000  | -6250961.609000 | -10805.525000   | 0 5 51.6484    | 281 34 47.7272 | 2711.6928 |
| SHIDOP   | 30123    | 6104423.692000  | -611086.597000  | -1740830.697000 | -15 56 34.8342 | 354 17 0.3124  | 603.3940  |
| HONDOP   | 30188    | -5511608.533000 | -2226970.519000 | 2303886.656000  | 21 18 52.5588  | 202 0 4.3794   | 20.4519   |
| STODOP   | 30280    | 1743940.474000  | -5022701.110000 | -3512033.120000 | -33 37 26.0082 | 289 8 51.3537  | 448.5113  |
| CALDOP   | 30414    | -1659604.189000 | -3676719.050000 | 4925498.638000  | 50 52 17.1118  | 245 42 23.2134 | 1248.3641 |
| NAPDOP   | 30448    | -4923683.543000 | 270895.598000   | -4031782.997000 | -39 27 31.6054 | 176 51 2.9697  | 18.7144   |
| EASDOP   | 30730    | -1888662.883000 | -5355677.851000 | -2893870.151000 | -27 9 30.4145  | 250 34 29.8655 | 48.9958   |
| TVEDOP   | 30793    | -5037686.750000 | 3301866.496000  | -2090790.183000 | -19 15 43.8524 | 146 45 28.2275 | 66.0787   |
| BGKDOP   | 30800    | -1139091.837000 | 6089774.901000  | 1510692.599000  | 13 47 32.9828  | 100 35 41.0666 | -13.3294  |
| DCCDOP   | 30939    | 1915631.725000  | 6030276.750000  | -801056.456000  | -7 15 49.0645  | 72 22 35.6272  | -57.4495  |
| LAJDOP   | 30966    | 4432069.966000  | -2268084.956000 | 3973470.407000  | 38 46 51.3245  | 332 53 57.0433 | 132.7341  |
| BDADOP   | 30967    | 2293704.122000  | -4883222.062000 | 3309598.216000  | 32 19 16.9668  | 295 9 35.8925  | -4.7505   |
| PERDOP   | 30968    | -2353567.078000 | 4877202.497000  | -3358333.914000 | -31 58 39.4446 | 115 45 37.1833 | 13.1668   |
| CNIDOP   | 30970    | 5384988.857000  | -1576474.618000 | 3023843.496000  | 28 28 54.5056  | 343 40 56.7134 | 626.5256  |
| UKIDOP   | 51960    | -2713391.456000 | -4144609.641000 | 4004304.887000  | 39 8 16.2157   | 236 47 16.9749 | 170.0838  |
| POTSDAM  | 18113901 | 3800618.509000  | 882010.731000   | 5028856.705000  | 52 22 48.9239  | 13 3 55.3462   | 144.7284  |
| QUINO511 | 70510101 | -2516895.280000 | -4198842.164000 | 4076418.824000  | 39 58 24.7868  | 239 3 37.5502  | 1063.6237 |
| QUINO512 | 70510202 | -2516895.254000 | -4198842.117000 | 4076418.769000  | 39 58 24.7865  | 239 3 37.5501  | 1063.5472 |
| QUINO513 | 70510203 | -2516895.254000 | -4198842.131000 | 4076418.778000  | 39 58 24.7865  | 239 3 37.5504  | 1063.5622 |
| QUINO514 | 70510804 | -2516895.110000 | -4198842.926000 | 4076418.548000  | 39 58 24.7860  | 239 3 37.5512  | 1063.2229 |
| EASTER1  | 70611201 | -1884984.664000 | -5357611.696000 | -2892846.837000 | -27 8 51.9068  | 250 36 59.2014 | 117.6193  |
| EASTER2  | 70611202 | -1884984.664000 | -5357611.696000 | -2892846.837000 | -27 8 51.9068  | 250 36 59.2014 | 117.6193  |
| OTAYMT1  | 70620201 | -2428827.802000 | -4799748.813000 | 3417280.328000  | 32 36 2.8873   | 243 9 32.8229  | 992.1153  |
| OTAYMT2  | 70620302 | -2428827.818000 | -4799748.845000 | 3417280.357000  | 32 36 2.8875   | 243 9 32.8230  | 992.1611  |
| OTAYMT3  | 70620303 | -2428827.812000 | -4799748.810000 | 3417280.322000  | 32 36 2.8871   | 243 9 32.8226  | 992.1136  |
| OTAYMT4  | 70621104 | -2428829.163000 | -4799747.956000 | 3417280.275000  | 32 36 2.8885   | 243 9 32.7615  | 991.9603  |
| OTAYMT5  | 70621205 | -2428827.125000 | -4799747.476000 | 3417279.376000  | 32 36 2.8875   | 243 9 32.8230  | 990.3399  |
| STALASI1 | 70632101 | 1130714.571000  | -4831364.967000 | 3994095.557000  | 39 1 13.6387   | 283 10 19.9610 | 22.2757   |
| GORF0641 | 70640101 | 1130678.623000  | -4831336.991000 | 3994135.988000  | 39 1 15.3807   | 283 10 18.7710 | 20.2036   |
| GORF0642 | 70640102 | 1130678.623000  | -4831336.980000 | 3994135.982000  | 39 1 15.3808   | 283 10 18.7711 | 20.1915   |
| GORF0651 | 70650201 | 1130695.004000  | -4831351.484000 | 3994120.285000  | 39 1 14.6208   | 283 10 19.2967 | 24.1806   |
| GORF0652 | 70650203 | 1130695.017000  | -4831351.530000 | 3994120.307000  | 39 1 14.6204   | 283 10 19.2968 | 24.2316   |
| GORF0653 | 70650302 | 1130694.853000  | -4831351.610000 | 3994120.252000  | 39 1 14.6182   | 283 10 19.2894 | 24.2285   |
| WFCL0661 | 70662701 | 1261613.824000  | -4881554.445000 | 3893207.239000  | 37 51 37.1712  | 284 29 26.6514 | -13.6775  |
| BDALAS1  | 70670101 | 2308539.420000  | -4874078.448000 | 3393637.063000  | 32 21 14.0276  | 295 20 38.1253 | -19.3284  |
| BDALAS2  | 70670102 | 2308539.410000  | -4874078.444000 | 3393637.052000  | 32 21 14.0274  | 295 20 38.1250 | -19.3410  |
| GTILAS1  | 70680201 | 1920483.885000  | -5619478.384000 | 2318922.667000  | 21 27 38.0463  | 288 52 5.1990  | -15.0903  |
| GTILAS2  | 70680202 | 1920483.882000  | -5619478.480000 | 2318922.712000  | 21 27 38.0466  | 288 52 5.1978  | -14.9902  |
| RAMLAS1  | 70692201 | 917958.646000   | -5548369.739000 | 2998785.303000  | 28 13 40.9313  | 279 23 39.4468 | -20.1361  |
| WFCL0701 | 70700201 | 1261570.949000  | -4881566.932000 | 3893186.391000  | 37 51 36.6102  | 284 29 24.8254 | -25.3976  |
| PATLAS1  | 70810201 | 917899.965000   | -5548373.228000 | 2998791.074000  | 28 13 41.1908  | 279 23 37.3025 | -22.8126  |
| BARLAS1  | 70820101 | -1735998.872000 | -4425045.384000 | 4241438.513000  | 41 56 1.1377   | 248 34 45.5583 | 1966.7679 |
| BARLAS2  | 70820102 | -1735998.883000 | -4425045.418000 | 4241438.537000  | 41 56 1.1376   | 248 34 45.5584 | 1966.8105 |
| BARLAS3  | 70821103 | -1735998.035000 | -4425046.288000 | 4241437.531000  | 41 56 1.1025   | 248 34 45.6064 | 1966.5103 |
| BARLAS4  | 70821104 | -1735997.926000 | -4425046.270000 | 4241437.600000  | 41 56 1.1054   | 248 34 45.6105 | 1966.5144 |
| OWNS0841 | 70840201 | -2410592.341000 | -4477742.737000 | 3838656.041000  | 37 13 55.8799  | 241 42 15.1318 | 1181.5839 |
| GLDS0851 | 70850101 | -2353396.463000 | -4641527.398000 | 3676906.786000  | 35 25 28.1911  | 243 6 48.9476  | 969.2653  |
| MCDN0861 | 70860101 | -1330126.754000 | -5328525.475000 | 3236158.844000  | 30 40 37.5638  | 255 59 2.5631  | 1965.1974 |
| MCDN0862 | 70861102 | -1330127.026000 | -5328526.018000 | 3236157.350000  | 30 40 37.5122  | 255 59 2.5582  | 1964.9449 |
| MCDN0863 | 70862403 | -1330121.606000 | -5328527.968000 | 3236153.351000  | 30 40 37.3910  | 255 59 2.7734  | 1963.4028 |
| YARAG1   | 70900501 | -2389006.624000 | 5043327.876000  | -3078534.003000 | -29 2 47.6761  | 115 20 48.2991 | 244.5048  |
| HAYSTK1  | 70910301 | 1492453.768000  | -4457275.873000 | 4296824.275000  | 42 37 21.9617  | 288 30 44.5319 | 95.7350   |
| HAYSTK2  | 70910702 | 1492453.680000  | -4457275.629000 | 4296824.015000  | 42 37 21.9612  | 288 30 44.5316 | 95.3681   |
| KWAJL1   | 70920801 | -6143450.492000 | 1364701.891000  | 1034160.674000  | 9 23 37.5881   | 167 28 32.5884 | 36.0359   |
| SAMOAL1  | 70960601 | -6100048.544000 | -996205.837000  | -1568976.891000 | -14 20 7.5069  | 189 16 30.5733 | 52.1796   |
| GORF1001 | 71000301 | 1131355.891000  | -4831166.327000 | 3994140.204000  | 39 1 15.7277   | 283 10 47.8009 | 13.6953   |
| GORF1002 | 71000402 | 1131355.856000  | -4831166.075000 | 3994140.005000  | 39 1 15.7279   | 283 10 47.8019 | 13.3732   |
| GORF1011 | 71010602 | 1131329.098000  | -4831176.841000 | 3994157.002000  | 39 1 16.4856   | 283 10 42.9741 | 11.5366   |
| GORF1012 | 71010801 | 1131239.046000  | -4831176.808000 | 3994157.029000  | 39 1 16.4872   | 283 10 42.9723 | 11.5194   |
| GORF1021 | 71020305 | 1130686.437000  | -4831350.557000 | 3994119.473000  | 39 1 14.6586   | 283 10 18.9587 | 21.4515   |
| GORF1022 | 71020402 | 1130686.374000  | -4831350.385000 | 3994119.248000  | 39 1 14.6567   | 283 10 18.9578 | 21.1685   |
| GORF1023 | 71020403 | 1130686.414000  | -4831350.328000 | 3994119.224000  | 39 1 14.6570   | 283 10 18.9600 | 21.1174   |
| GORF1024 | 71020404 | 1130686.420000  | -4831350.378000 | 3994119.229000  | 39 1 14.6561   | 283 10 18.9598 | 21.1594   |
| GORF1025 | 71020501 | 1130686.381000  | -4831350.390000 | 3994119.245000  | 39 1 14.6565   | 283 10 18.9581 | 21.1717   |
| GORF1031 | 71030601 | 1130685.399000  | -4831346.029000 | 3994124.644000  | 39 1 14.8837   | 283 10 18.9596 | 21.0980   |
| GORF1032 | 71030602 | 1130685.427000  | -4831346.031000 | 3994124.591000  | 39 1 14.8822   | 283 10 18.9607 | 21.0711   |
| GORF1041 | 71040701 | 1131095.729000  | -4831194.201000 | 3994178.959000  | 39 1 17.3610   | 283 10 37.0066 | 13.1002   |
| GORF1051 | 71050701 | 1130719.513000  | -4831347.838000 | 3994114.808000  | 39 1 14.4413   | 283 10 20.3233 | 22.3133   |
| GORF1052 | 71050702 | 1130719.513000  | -4831347.838000 | 3994114.808000  | 39 1 14.4413   | 283 10 20.3233 | 22.3133   |
| GORF1053 | 71050703 | 1130718.983000  | -4831345.460000 | 3994112.813000  | 39 1 14.4407   | 283 10 20.3244 | 19.1645   |
| GORF1054 | 71050704 | 1130718.983000  | -4831345.460000 | 3994112.813000  | 39 1 14.4407   | 283 10 20.3244 | 19.1645   |
| QUIN1051 | 71090601 | -2517236.706000 | -4198552.978000 | 4076576.716000  | 39 56 30.2166  | 239 5 18.9466  | 1109.5175 |

**CHART PAGE IS  
OF POOR QUALITY**

| NAME      | I.D.   | X                  | Y                      | Z                    | LATITUDE | LONGITUDE | HEIGHT |
|-----------|--|--------------------|------------------------|----------------------|----------|-----------|--------|
| QUIN1092  | 71090802-2517236.680000-4198552.934000                 | 4076576.619000     | 39 58 30.2173 239      | 3 18.9465 1109.4158  |          |           |        |
| QUIN1093  | 71091503-2517235.448000-4198550.859000                 | 4076574.635000     | 39 58 30.2183 239      | 3 18.9461 1106.2919  |          |           |        |
| LAGU1101  | 71100301-2386279.860000-4802352.528000                 | 3444889.032000     | 32 53 30.4744 243      | 34 38.3004 1842.4669 |          |           |        |
| LAGU1102  | 71100402-2386279.761000-4802352.301000                 | 3444888.842000     | 32 53 30.4736 243      | 34 38.2999 1842.1560 |          |           |        |
| VAND1111  | 71111101-2668830.288000-4530786.549000                 | 3598710.144000     | 34 33 58.7540 239      | 30 0.2349 630.0635   |          |           |        |
| PLATVL1   | 71120201-1240679.684000-4720460.634000                 | 4094488.774000     | 40 10 58.2581 255      | 16 26.3901 1505.0619 |          |           |        |
| OWNS1141  | 71140201-2410424.425000-4477800.195000                 | 3838694.258000     | 37 13 57.4358 241      | 42 22.2335 1181.6171 |          |           |        |
| OWNS1142  | 71141102-2410424.314000-4477799.072000                 | 3838695.370000     | 37 13 57.4850 241      | 42 22.2159 1181.4608 |          |           |        |
| OWNS1143  | 71141103-2410424.268000-4477799.144000                 | 3838695.409000     | 37 13 57.4852 241      | 42 22.2191 1181.5160 |          |           |        |
| GLDS1151  | 71150301-2350863.626000-4655544.133000                 | 3661005.598000     | 35 14 54.1287 243      | 12 28.9797 1042.2096 |          |           |        |
| MAUI1201  | 71200101-5466001.882000-2404407.104000                 | 2242231.716000     | 20 42 27.4663 203      | 44 38.1447 3071.3259 |          |           |        |
| UAHAME1   | 71210101-5345867.943000-2958250.684000                 | 1824622.047000     | -16 44 57.5754 208     | 57 32.0011 47.2137   |          |           |        |
| HAZATL1   | 71220601-1660090.795000-5619099.854000                 | 2511646.062000     | 23 20 34.5020 253      | 32 27.2484 34.0210   |          |           |        |
| CORF1251  | 71251501 1130743.438000-4813165.212000                 | 3994084.486000     | 39 1 13.2206 283       | 10 21.1271 20.6016   |          |           |        |
| HOLLAS1   | 72102301-5466007.345000-204425.239000                  | 2242190.501000     | 20 42 26.0714 203      | 44 38.6414 3068.3066 |          |           |        |
| MNPK2201  | 72201101-2386293.129000-4802345.089000                 | 3444889.510000     | 32 53 30.5008 243      | 34 37.7160 1842.0906 |          |           |        |
| MNPK2202  | 72201102-2386292.850000-4802343.054000                 | 3444886.538000     | 32 53 30.4541 243      | 34 37.6908 1838.8421 |          |           |        |
| BARSTOW1  | 72651101-2356478.931000-4646614.953000                 | 3668432.680000     | 35 19 52.6145 243      | 6 31.1890 899.3767   |          |           |        |
| MTLAGUNA  | 72741101-2386291.134000-4802340.426000                 | 3444886.484000     | 32 53 30.5076 243      | 34 37.7049 1836.1954 |          |           |        |
| SNTI4001  | 74001101 1769700.612000-5044619.215000-3468256.468000  | -33 8 58.4901 289  | 19 19 52.8881 725.3650 |                      |          |           |        |
| CERR4011  | 74011101 1815518.227000-5213470.794000-3187995.444000  | -30 10 20.6561 289 | 11 59.8451 2158.5624   |                      |          |           |        |
| ASKITES   | 75101501 4353445.920000 2082674.201000 4156503.948000  | 40 55 40.7134 25   | 33 58.6765 184.1009    |                      |          |           |        |
| DIONYS    | 75151501 4595217.892000 2039442.831000 3912626.421000  | 38 4 42.7711 23    | 55 57.1260 512.1012    |                      |          |           |        |
| ROUM1716  | 75171601 4728694.568000 2174383.801000 3674569.898000  | 35 24 15.1174 24   | 41 39.3802 104.1018    |                      |          |           |        |
| KARITZ    | 75215010 4596043.243000 1733486.324000 4055718.264000  | 39 44 3.1556 20    | 39 53.7644 599.9742    |                      |          |           |        |
| JRUSLM    | 75300000 436653.778000 3131126.067000 3335786.090000   | 31 44 2.6143 35    | 12 43.7988 757.9405    |                      |          |           |        |
| MATERA40  | 75401501 4641986.380000 1393063.949000 4133231.399000  | 40 38 54.6412 16   | 42 16.3399 529.8350    |                      |          |           |        |
| MATERA41  | 75411601 4641993.122000 1393048.174000 4133230.248000  | 40 38 54.5695 16   | 42 15.6330 530.6437    |                      |          |           |        |
| PUNSAMEN  | 75450000 4893400.699000 772679.294000 4004140.157000   | 39 8 7.6904 8      | 58 22.9807 232.1879    |                      |          |           |        |
| TRIESTE   | 75501601 4336739.199000 1071281.849000 4537909.914000  | 45 38 34.5399 13   | 52 32.4804 448.4463    |                      |          |           |        |
| MTGENERO  | 75900000 4390311.858000 696761.146000 4560835.602000   | 45 55 39.1743 9    | 1 4.3478 1650.5420     |                      |          |           |        |
| WET20106  | 75961502 4075584.698000 931843.821000 4801558.909000   | 49 8 38.8751 12    | 52 43.5497 660.2469    |                      |          |           |        |
| WET25961  | 75961601 4075584.698000 931843.821000 4801558.909000   | 49 8 38.8751 12    | 52 43.5497 660.2469    |                      |          |           |        |
| WET25971  | 75971501 4075604.248000 931833.091000 4801546.599000   | 49 8 38.2065 12    | 52 42.8187 661.8388    |                      |          |           |        |
| WET25991  | 75991501 4075516.968000 931760.151000 4801629.999000   | 49 8 42.4533 12    | 52 40.2703 658.6266    |                      |          |           |        |
| METZAHVI  | 78055301 2829595.047000 1311815.105000 5512609.368000  | 60 13 2.2114 24    | 23 40.8263 78.2898     |                      |          |           |        |
| ZIMRWLD1  | 78104801 4331285.030000 567559.507000 4633143.586000   | 46 52 38.0360 7    | 27 55.2402 955.5510    |                      |          |           |        |
| HELMANT   | 78314601 4728281.385000 2879673.940000 3156890.992000  | 29 51 32.3280 31   | 20 33.8847 130.1489    |                      |          |           |        |
| KOOTWIK1  | 78333201 3899223.487000 396749.080000 5015074.070000   | 52 10 42.2477 5    | 48 35.6243 93.4801     |                      |          |           |        |
| WETZELL   | 78343001 4075529.405000 931787.187000 4801617.581000   | 49 8 41.7460 12    | 52 41.4339 661.1067    |                      |          |           |        |
| GRASSE1   | 78353101 4581691.193000 556164.708000 4389359.447000   | 43 45 16.8840 6    | 55 16.2747 1322.9373   |                      |          |           |        |
| SHNGHA1   | 78373701-2831089.391000 4676208.174000 3275167.461000  | 31 5 50.9148 12    | 11 30.2116 29.2218     |                      |          |           |        |
| SIMOSATA  | 78383601-3822388.419000 3699367.939000 3507567.615000  | 33 34 39.4932 135  | 56 13.2192 101.1518    |                      |          |           |        |
| GRAZ1     | 78393401 4194426.092000 1162699.512000 4647245.773000  | 47 4 1.6445 15     | 29 36.3548 539.4764    |                      |          |           |        |
| RGOLASI   | 78403501 4033463.109000 23668.353000 4924305.460000    | 50 52 2.5912 0     | 20 10.3476 75.2802     |                      |          |           |        |
| NATHAP1   | 78432501 4464675.905000 2678122.786000-3696256.267000  | -35 38 10.6996 148 | 56 21.6480 1350.2505   |                      |          |           |        |
| CABO8821  | 78821201-1997242.723000-5528037.760000 2468365.566000  | 22 55 3.5270 250   | 8 7.9954 112.7941      |                      |          |           |        |
| MCDN8851  | 78851101-1330126.247000-5328524.621000 3236159.986000  | 30 40 37.6114 255  | 59 2.5738 1964.9618    |                      |          |           |        |
| QUIN8861  | 78861101-2517243.158000-4198548.760000 4076577.109000  | 39 58 30.2346 239  | 3 18.6220 1109.5399    |                      |          |           |        |
| QUIN8862  | 78861102-2517243.158000-4198548.760000 4076577.109000  | 39 58 30.2346 239  | 3 18.6220 1109.5399    |                      |          |           |        |
| VNDN8871  | 78871101-2668870.125000-4530742.080000 3598691.031000  | 34 33 58.5776 239  | 29 58.0017 604.2663    |                      |          |           |        |
| MTHOPKN1  | 78881101-1936745.913000-50077638.237000 3332000.678000 | 31 41 6.5612 249   | 7 18.5595 2334.7109    |                      |          |           |        |
| GOREF8891 | 78891201 1131364.574000-4831165.237000 3994138.563000  | 39 1 15.6676 283   | 10 48.1627 13.3757     |                      |          |           |        |
| GOREF8892 | 78891302 1131364.590000-4831165.242000 3994138.549000  | 39 1 15.6671 283   | 10 48.1633 13.3735     |                      |          |           |        |
| AUSTIN1   | 78901101 -754162.924000-5459060.531000 3200751.323000  | 30 18 56.0015 262  | 8 3.9849 260.5025      |                      |          |           |        |
| AUSTIN2   | 78901102 -754164.193000-5459059.415000 3200753.040000  | 30 18 56.0639 262  | 8 3.9321 260.5466      |                      |          |           |        |
| FLLGSTAT1 | 78911101-1923979.299000-4850868.905000 3685852.712000  | 35 12 52.5769 248  | 21 55.6216 2147.6448   |                      |          |           |        |
| VERNAL1   | 78921101-1631485.501000-4589131.270000 4106757.427000  | 40 19 36.8896 250  | 25 44.9517 1593.6783   |                      |          |           |        |
| VERNAL2   | 78921102-1631485.474000-4589131.208000 4106757.467000  | 40 19 36.8920 250  | 25 44.9519 1593.6528   |                      |          |           |        |
| YUMA1     | 78941101-2196778.378000-4887334.614000 3448434.259000  | 32 56 21.1695 245  | 47 48.6551 241.6952    |                      |          |           |        |
| JPL1      | 78961101-2493213.111000-4655226.798000 3565583.186000  | 34 12 20.2535 241  | 49 39.7438 444.9326    |                      |          |           |        |
| MCDN8971  | 78971101-1330802.872000-5328723.160000 3235713.379000  | 30 40 19.2377 255  | 58 39.7257 2043.7685   |                      |          |           |        |
| MCDN8972  | 78971102-1330802.873000-5328723.262000 3235713.478000  | 30 40 19.2388 255  | 58 39.7266 2043.9043   |                      |          |           |        |
| GOREF8991 | 78991101 1131364.574000-4831165.238000 3994138.563000  | 39 1 15.6676 283   | 10 48.1627 13.3765     |                      |          |           |        |
| GOREF8992 | 78991102 1131364.590000-4831165.242000 3994138.550000  | 39 1 15.6671 283   | 10 48.1633 13.3742     |                      |          |           |        |
| AREQUI171 | 79074001 1942791.873000-5077702.714000 3331929.105000  | -16 27 56.4185 288 | 30 24.7309 2492.2703   |                      |          |           |        |
| GOREF1813 | 79181301 1130708.884000-4831342.845000 3994125.943000  | 39 1 14.8705 283   | 10 19.9404 23.6651     |                      |          |           |        |
| GOREF1914 | 79191401 1130694.251000-4831338.287000 3994134.775000  | 39 1 15.2517 283   | 10 19.3913 23.1871     |                      |          |           |        |
| GOREF2011 | 79201101 1130745.039000-4831366.608000 3994089.505000  | 39 1 13.3119 283   | 10 21.1787 25.1010     |                      |          |           |        |
| GORE22011 | 79201102 1130744.819000-4831365.034000 3994086.238000  | 39 1 13.2619 283   | 10 21.1847 21.8145     |                      |          |           |        |
| HOPLAST1  | 79214031-1936760.949000-5077702.714000 3331929.105000  | 31 41 3.4662 249   | 7 18.8984 2352.9417    |                      |          |           |        |
| NATAL71   | 79294101 5186467.775000-3653857.284000 -654316.651000  | -5 55 39.9399 324  | 50 7.3422 39.5952      |                      |          |           |        |
| DODAIR1   | 79350000-3910418.452000 3376364.722000 3729239.156000  | 36 0 20.7222 139   | 11 30.3195 902.9204    |                      |          |           |        |
| MATERA1   | 79394101 4641964.690000 1393074.846000 4133261.132000  | 40 38 55.7423 16   | 42 17.0680 535.9172    |                      |          |           |        |
| DIONYS1   | 79404701 4599578.363000 2040864.682000 3906778.504000  | 38 0 42.2298 23    | 55 37.8905 501.1291    |                      |          |           |        |
| ORRORL1   | 79434201-4447547.753000 2677129.639000-3695000.954000  | -35 37 29.9285 148 | 57 17.4255 948.9088    |                      |          |           |        |
| KOOTB331  | 88331501 3899237.136000 396775.269000 5015055.290000   | 52 10 41.4604 5    | 48 36.9228 88.5977     |                      |          |           |        |
| KOOTB332  | 88331602 3899237.136000 396775.269000 5015055.290000   | 52 10 41.4604 5    | 48 36.9228 88.5977     |                      |          |           |        |
| KOOTB333  | 88331603 3899237.136000 396775.269000 5015055.290000   | 52 10 41.4604 5    | 48 36.9228 88.5977     |                      |          |           |        |
| OLIS902   | 99024001 5056122.298000 2716520.205000-2775767.582000  | -25 57 36.0836 28  | 14 52.6461 1569.4682   |                      |          |           |        |
| AREQUI191 | 99074001 1942791.873000-5804080.083000-1796911.642000  | -16 27 56.4185 288 | 30 24.7309 2492.2703   |                      |          |           |        |
| HOPLAS91  | 99214301-1936760.949000-5077702.714000 3331929.105000  | 31 41 3.4662 249   | 7 18.8984 2352.9417    |                      |          |           |        |
| NATAL91   | 99294101 5186467.775000-3653857.284000 -654316.651000  | -5 55 39.9399 324  | 50 7.3422 39.5952      |                      |          |           |        |
| DIONYS1   | 99404701 4595214.996000 2039466.003000 3912612.430000  | 38 4 42.2788 23    | 55 58.0431 508.7882    |                      |          |           |        |
| ORRORL91  | 99434201-4447547.753000 2677129.639000-3695000.954000  | -35 37 29.9285 148 | 57 17.4255 948.9088    |                      |          |           |        |

**APPENDIX 2**

**APRIORI STATION POSITIONS  
FOR GEM-T1**

**OPTICAL & DOPPLER  
TRACKING SITES**

**as of February 11, 1987**

**PRECEDING PAGE BLANK, NOT FILMED**

TOPEX GEODETIC FILE CREATED 02/11/87  
SEMI-MAJOR AXIS: 6378137.00 FLATTENING: 1/298.257

| NAME     | I.D. | X               | Y               | Z               | LATITUDE       | LONGITUDE      | HEIGHT    |
|----------|------|-----------------|-----------------|-----------------|----------------|----------------|-----------|
| 1BPOIN   | 1021 | 1118042.673000  | -4876303.718000 | 3942974.315000  | 38 25 50.1059  | 282 54 49.0319 | -35.1079  |
| 1FTMYR   | 1022 | 807877.886000   | -5651970.293000 | 2833513.886000  | 26 32 53.5470  | 278 8 4.5896   | -22.3786  |
| 1OOMER   | 1024 | -3977275.856000 | 3725643.767000  | -3302983.031000 | -31 23 25.1614 | 136 52 15.6789 | 135.9607  |
| 1SATAG   | 1028 | 1769719.956000  | -5044619.692000 | -3468246.138000 | -33 8 58.0878  | 289 19 53.5863 | 725.4544  |
| 1MOJAV   | 1030 | -2357228.652000 | -4646321.402000 | 3668322.198000  | 35 19 48.2390  | 243 5 59.4610  | 898.5917  |
| 1JOBUR   | 1031 | 5084791.750000  | 2670402.009000  | -2768144.919000 | -25 53 1.0486  | 27 42 26.2858  | 1550.2946 |
| 1NEWFL   | 1032 | 2602767.335000  | -3419137.999000 | 4697657.623000  | 47 44 29.6192  | 307 16 46.7707 | 77.0941   |
| 1COLEG   | 1033 | -2299248.779000 | -1445691.272000 | 5751818.453000  | 64 52 18.4528  | 212 9 37.1439  | 181.2022  |
| 1GFORK   | 1034 | -521692.908000  | -4242035.759000 | 4718733.398000  | 48 1 21.6883   | 262 59 19.9354 | 227.6111  |
| 1WNKFL   | 1035 | 3983119.138000  | -48488.686000   | 9946717.894000  | 51 26 45.9081  | 359 18 9.1498  | 117.3075  |
| 1ULASK   | 1036 | -2282348.390000 | -1452629.676000 | 5756906.658000  | 64 58 37.2922  | 212 28 30.8390 | 308.8093  |
| 1ROSKN   | 1037 | 647535.550000   | -5177922.122000 | 3656717.613000  | 35 12 7.5231   | 277 7 41.6406  | 880.8541  |
| 1ORORL   | 1038 | -4447486.306000 | 2677158.222000  | -3695055.561000 | -35 37 32.0848 | 148 57 15.1933 | 949.9060  |
| 1ROSMR   | 1042 | 647529.510000   | -5177922.522000 | 3656716.313000  | 35 12 7.4952   | 277 7 41.4017  | 879.8166  |
| 1TANAN   | 1043 | 4091868.993000  | 4434290.059000  | -2064734.326000 | -19 0 32.2311  | 47 17 59.3996  | 1374.9833 |
| MADGAR   | 1122 | 4091329.793000  | 4434216.058000  | -2065984.225000 | -19 1 15.1045  | 47 18 11.2313  | 1385.0988 |
| MADGAS   | 1123 | 4091343.393000  | 4434212.058000  | -2065970.925000 | -19 1 14.6291  | 47 18 10.7968  | 1386.7038 |
| ROS'RAN  | 1126 | 647205.415000   | -5178319.808000 | 3656150.566000  | 35 11 45.8756  | 277 7 26.7424  | 842.9914  |
| ULASKR   | 1128 | -2282490.491000 | -1453373.076000 | 5756716.860000  | 64 58 19.5130  | 212 29 12.8287 | 356.4167  |
| CARVON   | 1152 | -2328231.626000 | 5299695.978000  | -2669340.215000 | -24 54 10.8344 | 113 42 59.6354 | 16.2215   |
| MOROC    | 1804 | 5105598.670000  | -555231.211000  | 3769632.040000  | 36 27 45.4693  | 353 47 36.6141 | 53.4608   |
| CANARI   | 1819 | 5440484.420000  | -1501663.783000 | 2961260.039000  | 27 50 37.6249  | 344 34 10.6083 | 109.1496  |
| HOWARD   | 2001 | 1122551.680000  | -4823067.408000 | 4006490.821000  | 39 9 48.7587   | 283 6 7.6568   | 126.8940  |
| NEWMEX   | 2003 | -1555975.516000 | -5169337.536000 | 3387501.796000  | 32 16 53.8729  | 253 14 53.3592 | 1173.4164 |
| SANHES   | 2008 | 4083900.485000  | -4209792.868000 | -2499123.925000 | -23 13 3.4584  | 314 7 49.2870  | 601.7412  |
| MISAWA   | 2013 | -3779644.939000 | 3024716.790000  | 4138986.003000  | 40 43 13.9770  | 141 19 51.3907 | 51.4191   |
| ANCHOR   | 2014 | -2656171.683000 | -1544363.513000 | 5570648.254000  | 61 17 0.2115   | 210 10 29.1787 | 73.3496   |
| TAFUNA   | 2017 | -6100011.515000 | -997195.143000  | -1568454.805000 | -14 19 50.0579 | 189 17 3.3549  | 42.0909   |
| THOLEG   | 2018 | 539395.656000   | -1388369.682000 | 6181056.264000  | 76 32 20.1842  | 291 13 53.9457 | 64.7609   |
| MCMURD   | 2019 | -1310714.228000 | 310461.061000   | -6213364.320000 | -77 50 51.7053 | 166 40 27.4044 | -15.0854  |
| AUSTIN   | 2092 | -741620.291000  | -5462204.839000 | 3198143.740000  | 30 17 19.7384  | 262 16 5.0021  | 165.0000  |
| WAHIWA   | 2100 | -5504142.805000 | -2224142.821000 | 3232503.722000  | 21 31 15.5563  | 202 0 10.4627  | 411.0386  |
| LACRES   | 2103 | -1556205.009000 | -5169441.832000 | 3387263.869000  | 32 16 44.4660  | 253 14 46.1116 | 1186.7089 |
| LASHAM   | 2106 | 4005440.205000  | -71745.392000   | 4946709.632000  | 51 11 9.1373   | 358 58 25.7826 | 228.3128  |
| APLMND   | 2111 | 1122659.254000  | -4823035.989000 | 4006472.801000  | 39 9 48.4329   | 283 6 12.3176  | 110.6957  |
| SMITHL   | 2112 | -3942235.661000 | 3468855.745000  | -3608201.826000 | -34 40 26.4213 | 138 39 17.1916 | 32.3723   |
| PRETOR   | 2115 | 5051977.208000  | 2725634.308000  | -2774460.696000 | -25 56 48.3713 | 28 20 51.6299  | 1600.7180 |
| ASAMOA   | 2117 | -6100015.715000 | -997194.583000  | -1568457.905000 | -14 19 50.1229 | 189 17 3.3138  | 46.7867   |
| SANMIG   | 2121 | -3088055.247000 | 5333061.128000  | 1638815.384000  | 14 59 16.1733  | 120 4 21.1942  | 63.5512   |
| WALDOP   | 2203 | 1261687.864000  | -4881237.408000 | 3893561.151000  | 37 51 51.9753  | 284 29 32.8297 | -24.1640  |
| CANTON   | 2706 | -6303360.092000 | -923454.804000  | -308728.340000  | -2 47 35.2090  | 188 20 4.7574  | 34.5854   |
| MAHE     | 2717 | 3602875.617000  | 5238223.545000  | -515928.740000  | -4 40 14.0263  | 55 28 46.6236  | 552.1180  |
| ASCENS   | 2722 | 6118431.429000  | -1571559.409000 | -878444.905000  | -7 58 9.9380   | 345 35 40.6060 | 96.9358   |
| COCOS    | 2723 | -741966.658000  | 6190797.586000  | -1338588.853000 | -12 11 45.2618 | 96 50 3.4690   | -19.2995  |
| MOSLAK   | 2738 | -2127818.698000 | -3785834.127000 | 4656062.131000  | 47 11 7.6401   | 240 39 42.9984 | 355.2917  |
| SHEMAL   | 2739 | -3851514.689000 | 397264.310000   | 5051466.845000  | 52 42 55.7756  | 174 6 39.7958  | 50.3803   |
| BELTSV   | 2742 | 1130796.551000  | -4830813.278000 | 3994724.458000  | 39 1 40.0688   | 283 10 28.5062 | 15.4582   |
| STNVIL   | 2745 | -84982.690000   | -5327948.044000 | 3493465.591000  | 33 25 32.4685  | 269 5 10.2810  | 13.5933   |
| CARGIL   | 2809 | -4313785.893000 | 893041.467000   | -4596956.426000 | -46 24 43.7262 | 168 18 13.7845 | 5.3052    |
| PARIBO   | 2815 | 3623309.482000  | -5214208.718000 | 601537.041000   | 5 26 53.3756   | 304 47 42.3949 | -0.1532   |
| MESHERD  | 2817 | 2604359.352000  | 4444166.828000  | 3750327.345000  | 36 14 25.9684  | 59 37 44.2297  | 972.4892  |
| FRTLWY   | 2822 | 6023417.038000  | 1617938.536000  | 1331706.781000  | 12 7 53.8046   | 15 2 6.7821    | 316.7621  |
| NATLDP   | 2837 | 5186372.100000  | -3654218.808000 | -653027.495000  | -5 54 57.7605  | 324 49 55.9422 | 35.9026   |
| APLTWO   | 2911 | 1122714.880000  | -4823027.109000 | 4006482.121000  | 39 9 48.5861   | 283 6 14.6582  | 119.6539  |
| 1UNDAK   | 7034 | -521692.957000  | -242036.158000  | 4718733.844000  | 48 1 21.6883   | 262 59 19.9354 | 228.2115  |
| 1EDINB   | 7036 | -828471.760000  | -565744.892000  | 2816825.976000  | 26 22 46.9803  | 261 40 7.9202  | 31.3196   |
| 1COLBA   | 7037 | -191272.927000  | -4967266.077000 | 3983269.628000  | 38 53 36.5000  | 267 47 41.3492 | 239.1561  |
| 1BERMD   | 7039 | 2308232.342000  | -4873587.010000 | 3394578.597000  | 32 21 49.8477  | 295 20 35.5563 | -1.6029   |
| 1PURIO   | 7040 | 2465070.227000  | -5534913.914000 | 1985531.452000  | 18 15 28.9986  | 294 0 23.8776  | 9.1055    |
| 1GSFCP   | 7043 | 1130730.821000  | -4831318.155000 | 3994143.543000  | 39 1 15.7027   | 283 10 21.0622 | 19.9526   |
| 1DENVR   | 7045 | -1240462.201000 | -4760221.025000 | 4048992.730000  | 39 38 48.2606  | 255 23 39.0016 | 1773.0005 |
| GODLAS   | 7050 | 1130692.438000  | -4831354.616000 | 3994112.117000  | 39 1 14.3647   | 283 10 19.1632 | 20.9531   |
| QUINCO51 | 7051 | -2516893.830000 | -4198839.747000 | 4076416.458000  | 39 58 24.7867  | 239 3 37.5502  | 1059.9437 |
| WALLAS   | 7052 | 1261570.901000  | -4881573.970000 | 3893171.501000  | 37 51 36.0935  | 284 29 24.7514 | -29.1658  |
| MOBLAS   | 7053 | 1130704.646000  | -4831318.517000 | 3994151.264000  | 39 1 16.0118   | 283 10 19.9993 | 20.4535   |
| CRMLAS   | 7054 | -2328184.126000 | 5299661.478000  | -2669470.815000 | -24 54 15.3778 | 113 42 58.5803 | 25.2383   |
| GMISLS   | 7060 | -5068966.309000 | 3584085.182000  | 1458762.160000  | 13 18 33.6245  | 144 44 14.0370 | 139.7523  |
| EASTER   | 7061 | -1884984.612000 | -5357611.709000 | -2892846.844000 | -27 8 51.9071  | 250 36 59.2033 | 117.6181  |
| OTAY MT  | 7062 | -2428826.443000 | -4799746.127000 | 3417278.409000  | 32 36 2.8875   | 243 9 32.8229  | 988.5455  |
| STALAS   | 7063 | 1130714.033000  | -4831362.670000 | 3994093.645000  | 39 1 13.6387   | 283 10 19.9610 | 19.2390   |
| GORFO64  | 7064 | 1130678.096000  | -4831334.738000 | 3994134.113000  | 39 1 15.3807   | 283 10 18.7710 | 17.2255   |
| GORFO65  | 7065 | 1130694.399000  | -4831348.899000 | 3994118.134000  | 39 1 14.6208   | 283 10 19.2967 | 20.7638   |
| WFCLAS   | 7066 | 1261612.031000  | -4881547.504000 | 3893201.667000  | 37 51 37.1712  | 284 29 26.6514 | -22.7571  |
| BDALAS   | 7067 | 2308538.082000  | -4874075.622000 | 3393635.082000  | 32 21 14.0276  | 295 20 38.1253 | -23.0299  |
| GRNTURK  | 7068 | 1920482.803000  | -5619475.234000 | 2318921.358000  | 21 27 38.0463  | 288 52 5.1988  | -18.6689  |
| RAMLAS   | 7069 | 917958.152000   | -5548366.753000 | 2998783.678000  | 28 13 40.9313  | 279 23 39.4468 | -23.5713  |

**ORIGINAL PAGE IS  
OF POOR QUALITY**

| NAME     | I.D.                | X               | Y               | Z               | LATITUDE       | LONGITUDE      | HEIGHT    |
|----------|---------------------|-----------------|-----------------|-----------------|----------------|----------------|-----------|
| WFCMLAS  | 7070                | 1261570.285000  | -4881564.364000 | 3893184.329000  | 37 51 36.6102  | 284 29 24.8254 | -28.7573  |
| 1JUM24   | 7071                | 976288.131000   | -5601387.374000 | 2880247.155000  | 27 1 14.3717   | 279 53 13.1683 | -17.1695  |
| 1JUM40   | 7072                | 976291.901000   | -5601381.235000 | 2880258.186000  | 27 1 14.7707   | 279 53 13.3413 | -16.9689  |
| 1JUPC1   | 7073                | 976298.392000   | -5601380.427000 | 2880256.240000  | 27 1 14.7097   | 279 53 13.5783 | -17.5693  |
| 1JUBC4   | 7074                | 976299.006000   | -5601377.656000 | 2880262.710000  | 27 1 14.9357   | 279 53 13.6175 | -16.9678  |
| 1SUDBR   | 7075                | 692632.551000   | -4347058.865000 | 4600492.858000  | 46 27 21.5533  | 279 3 10.9597  | 250.5663  |
| 1JAMAC   | 7076                | 1384174.482000  | -5905661.874000 | 1966555.590000  | 18 4 34.8917   | 283 11 27.3567 | 435.2710  |
| 1GSFCN   | 7077                | 1130077.869000  | -4833029.111000 | 3992265.813000  | 38 59 57.4187  | 283 9 38.4381  | 16.9530   |
| WALMOT   | 7078                | 1261602.272000  | -4881343.277000 | 3893447.085000  | 37 51 47.4404  | 284 29 28.3556 | -30.1643  |
| 1CARVN   | 7079                | -2328603.726000 | 5299341.378000  | -2669685.615000 | -24 54 23.4104 | 113 43 16.8575 | 2.9745    |
| DELFTH   | 8009                | 3923405.024000  | 299909.552000   | 5002981.668000  | 52 0 6.3424    | 4 22 16.5137   | 73.1644   |
| ZIMWLD   | 8010                | 4331310.700000  | 567543.231000   | 4633125.666000  | 46 52 37.0879  | 7 27 54.3207   | 958.4242  |
| MALVRN   | 8011                | 3920168.247000  | -134706.054000  | 5012732.350000  | 52 8 35.9096   | 358 1 55.0516  | 161.5850  |
| HAUTEP   | 8015                | 4578328.737000  | 457997.648000   | 4403198.266000  | 43 55 57.6133  | 5 42 45.4853   | 707.9391  |
| NICEFR   | 8019                | 4579479.626000  | 5686622.290000  | 4386423.525000  | 43 43 32.8750  | 7 17 58.9994   | 431.3883  |
| MUDONI   | 8030                | 4205642.568000  | 163747.065000   | 4776554.051000  | 48 48 22.0630  | 2 13 46.8840   | 222.5547  |
| 1ORGAN   | 9001-1535736.898000 | -5166990.635000 | 3401055.124000  | 32 25 25.2673   | 253 26 49.0477 | 1627.3368      |           |
| 1OLFAN   | 9002                | 5056124.398000  | 27116514.805000 | -2775771.682000 | -25 57 36.2134 | 28 14 52.4394  | 1570.6283 |
| WOOMER   | 9003-3983793.232000 | 3743086.410000  | -3275536.467000 | -31 6 2.2261    | 136 47 3.4590  | 166.1201       |           |
| 1SPAIN   | 9004                | 5105596.429000  | -555212.070000  | 3769671.060000  | 36 27 46.5702  | 353 47 37.3686 | 73.1944   |
| 1TOKYO   | 9005-3946701.784000 | 3366284.120000  | 3698830.457000  | 35 40 22.6368   | 139 32 16.5965 | 97.4377        |           |
| 1NATAL   | 9006                | 1018193.658000  | 5471111.932000  | 3109615.511000  | 29 21 34.2701  | 79 27 27.5562  | 1881.9966 |
| 1QUIPA   | 9007                | 1942791.749000  | -5804079.617000 | -1796911.493000 | -16 27 56.4183 | 288 30 24.7320 | 2491.7665 |
| 1SHRAZ   | 9008                | 3376878.004000  | 4404003.001000  | 3136259.449000  | 29 38 13.5471  | 52 31 11.7222  | 1592.2059 |
| 1CURAC   | 9009                | 2251841.307000  | -5816910.568000 | 1327176.578000  | 12 5 25.3067   | 291 9 44.6674  | -9.8095   |
| 1JUPTR   | 9010                | 976306.929000   | -5601383.489000 | 2880250.753000  | 27 1 14.4847   | 279 53 13.8643 | -16.0690  |
| 1VILDO   | 9011                | 2280591.315000  | -4914582.504000 | -3355397.399000 | -31 56 34.4100 | 294 53 36.4518 | 638.7421  |
| 1MAUIO   | 9012-5466046.730000 | -2404297.754000 | 2242186.928000  | 20 42 26.1383   | 203 44 34.0628 | 3052.7508      |           |
| HOPKIN   | 9021-1936761.465000 | -5077706.425000 | 3331923.185000  | 31 41 3.2404    | 249 7 18.9303  | 2352.9393      |           |
| AUSBAK   | 9023-3977783.956000 | 3725095.767000  | -3303009.930000 | -31 23 25.9706  | 136 52 43.9634 | 146.7573       |           |
| DODAIR   | 9025-3910447.481000 | 3376358.232000  | 3729214.022000  | 36 0 19.7245    | 139 11 31.2730 | 902.4885       |           |
| DEZEIT   | 9028                | 4903753.689000  | 3965224.700000  | 963855.471000   | 8 44 50.8070   | 38 57 33.6719  | 1916.5855 |
| NATALB   | 9029                | 5186466.971000  | -3653856.721000 | -654316.421000  | -5 55 39.9358  | 324 50 7.3421  | 38.5952   |
| COMRIV   | 9031                | 1693805.245000  | -4112343.673000 | -4556637.708000 | -45 53 12.1867 | 292 23 9.3821  | 203.0141  |
| JUPGEO   | 9049                | 976296.864000   | -5601385.468000 | 2880245.476000  | 27 1 14.3287   | 279 53 13.4923 | -18.2692  |
| AGASSI   | 9050                | 1489749.695000  | -4467460.382000 | 4287314.575000  | 42 30 22.0210  | 288 26 30.5904 | 146.3939  |
| ATHENG   | 9051                | 4606872.302000  | 2029756.782000  | 3903548.846000  | 37 58 36.1806  | 23 46 40.6745  | 230.2932  |
| MALVRN   | 9080                | 3920171.696000  | -134721.226000  | 5012742.827000  | 52 8 36.0163   | 358 1 54.2604  | 172.2922  |
| GREECE   | 9091                | 4595164.574000  | 2039477.178000  | 3912661.522000  | 38 4 44.3632   | 23 55 59.3014  | 506.3560  |
| EDWAFB13 | 9113-2449990.048000 | -4624418.526000 | 3635038.437000  | 34 57 50.8759   | 242 5 8.2223   | 753.5172       |           |
| COLDLK14 | 9114-1264845.049000 | -3466885.553000 | 5185467.766000  | 54 44 33.9608   | 249 57 22.3359 | 687.6346       |           |
| OSLONR15 | 9115                | 3121281.524000  | 592659.860000   | 5512725.385000  | 60 12 39.0078  | 10 45 4.2127   | 623.0307  |
| JOHNST17 | 9117-6007406.974000 | -1111883.065000 | 1825753.157000  | 16 44 39.1301   | 190 29 9.4086  | 33.7610        |           |
| COLDLK24 | 9424-1264827.430000 | -3466879.952000 | 5185469.308000  | 54 44 34.2880   | 249 57 23.1537 | 682.3706       |           |
| EDWAFB25 | 9425-2449990.048000 | -4624418.526000 | 3635038.437000  | 34 57 50.8759   | 242 5 8.2223   | 753.5172       |           |
| OSLONR26 | 9426                | 3121281.524000  | 592659.860000   | 5512725.385000  | 60 12 39.0078  | 10 45 4.2127   | 623.0307  |
| JOHNST27 | 9427-6007406.974000 | -1111883.065000 | 1825753.157000  | 16 44 39.1301   | 190 29 9.4086  | 33.7610        |           |
| RIGLAT   | 9428                | 3183913.279000  | 1421526.773000  | 5322765.729000  | 56 56 53.3549  | 24 3 33.8538   | 14.7034   |
| RIGALA   | 9431                | 3183883.925000  | 1421491.579000  | 5322808.034000  | 56 56 55.2158  | 24 3 32.6607   | 27.7186   |
| UZHGOR   | 9432                | 3907416.268000  | 1602450.327000  | 4763917.190000  | 48 38 1.6238   | 22 17 55.5773  | 232.9081  |
| HELSIK   | 9435                | 2884535.666000  | 1342151.531000  | 5509526.419000  | 60 9 42.9720   | 24 57 7.8651   | 58.1214   |

## **APPENDIX 3**

# **APRIORI OCEAN TIDE MODEL**

**PRECEDING PAGE BLANK NOT FILMED**

| <u>Doodson<br/>Number</u> | <u>Tide<br/>Name</u> | <u>Degree &amp;<br/>Order No.</u> | <u>Interpolated Model<br/>C's</u> | <u>Model<br/>e's</u> | <u>Schwiderski Model<br/>C's</u> | <u>e's</u> |
|---------------------------|----------------------|-----------------------------------|-----------------------------------|----------------------|----------------------------------|------------|
|                           |                      | *                                 |                                   |                      |                                  |            |
| 056.5545                  | SA                   | 2 0                               | 0.092                             | 229.97               |                                  |            |
|                           |                      | 3 0                               | 0.006                             | 23.14                |                                  |            |
|                           |                      | 4 0                               | 0.021                             | 81.87                |                                  |            |
|                           |                      | 5 0                               | 0.041                             | 270.26               |                                  |            |
|                           |                      | 6 0                               | 0.054                             | 143.61               |                                  |            |
| 057.5555                  | SSA                  | 2 0                               | 0.566                             | 230.75               | 0.622                            | 221.72     |
|                           |                      | 3 0                               | 0.038                             | 25.47                | 0.031                            | 2.42       |
|                           |                      | 4 0                               | 0.129                             | 82.47                | 0.162                            | 92.88      |
|                           |                      | 5 0                               | 0.248                             | 269.77               | 0.262                            | 251.40     |
|                           |                      | 6 0                               | 0.320                             | 143.33               | 0.437                            | 145.84     |
| 058.5545                  |                      | 2 0                               | 0.032                             | 231.63               |                                  |            |
|                           |                      | 3 0                               | 0.002                             | 28.34                |                                  |            |
|                           |                      | 4 0                               | 0.007                             | 83.11                |                                  |            |
|                           |                      | 5 0                               | 0.014                             | 269.20               |                                  |            |
|                           |                      | 6 0                               | 0.018                             | 143.00               |                                  |            |
| 065.4555                  | MM                   | 2 0                               | 0.538                             | 241.96               | 0.532                            | 258.97     |
|                           |                      | 3 0                               | 0.024                             | 88.82                | 0.031                            | 94.48      |
|                           |                      | 4 0                               | 0.141                             | 89.76                | 0.099                            | 68.70      |
|                           |                      | 5 0                               | 0.205                             | 261.62               | 0.229                            | 292.14     |
|                           |                      | 6 0                               | 0.178                             | 136.37               | 0.065                            | 39.69      |
| 075.5555                  | MF                   | 2 0                               | 0.860                             | 261.07               | 0.853                            | 251.96     |
|                           |                      | 3 0                               | 0.104                             | 145.41               | 0.095                            | 148.22     |
|                           |                      | 4 0                               | 0.259                             | 99.12                | 0.298                            | 102.87     |
|                           |                      | 5 0                               | 0.241                             | 239.65               | 0.297                            | 223.21     |
|                           |                      | 6 0                               | 0.125                             | 8.99                 | 0.088                            | 107.99     |
| 075.5655                  |                      | 2 0                               | 0.354                             | 261.15               |                                  |            |
|                           |                      | 3 0                               | 0.043                             | 145.49               |                                  |            |
|                           |                      | 4 0                               | 0.107                             | 99.16                |                                  |            |
|                           |                      | 5 0                               | 0.099                             | 239.51               |                                  |            |
|                           |                      | 6 0                               | 0.052                             | 8.51                 |                                  |            |

- \* Due to symmetries in the harmonic expansion of the  $m=0$  tides (the prograde and retrograde components sum), the amplitude values shown require doubling when included in the tidal potential model.

| <u>Doodson<br/>Number</u> | <u>Tide<br/>Name</u> | <u>Degree &amp;<br/>Order No.</u> | <u>Interpolated Model</u> | <u>Schwiderski Model</u> |
|---------------------------|----------------------|-----------------------------------|---------------------------|--------------------------|
|                           |                      |                                   | C's                       | e's                      |
| 135.6555                  | Q1                   | 2 1                               | 0.530                     | 313.70                   |
|                           |                      | 3 1                               | 0.316                     | 104.18                   |
|                           |                      | 4 1                               | 0.293                     | 288.12                   |
|                           |                      | 5 1                               | 0.215                     | 112.27                   |
|                           |                      | 6 1                               | 0.041                     | 286.69                   |
|                           |                      | -2 1                              | 0.238                     | 165.27                   |
|                           |                      | -3 1                              | 0.210                     | 351.92                   |
|                           |                      | -4 1                              | 0.106                     | 338.07                   |
|                           |                      | -5 1                              | 0.081                     | 153.31                   |
|                           |                      | -6 1                              | 0.019                     | 195.21                   |
| 145.5455                  | O1F                  | 2 1                               | 0.466                     | 313.85                   |
|                           |                      | 3 1                               | 0.226                     | 93.70                    |
|                           |                      | 4 1                               | 0.267                     | 278.37                   |
|                           |                      | 5 1                               | 0.193                     | 110.02                   |
|                           |                      | 6 1                               | 0.034                     | 284.24                   |
|                           |                      | -2 1                              | 0.206                     | 156.40                   |
|                           |                      | -3 1                              | 0.192                     | 338.56                   |
|                           |                      | -4 1                              | 0.104                     | 330.63                   |
|                           |                      | -5 1                              | 0.081                     | 153.44                   |
|                           |                      | -6 1                              | 0.025                     | 202.63                   |
| 145.5555                  | O1                   | 2 1                               | 2.482                     | 313.85                   |
|                           |                      | 3 1                               | 1.202                     | 93.64                    |
|                           |                      | 4 1                               | 1.422                     | 278.32                   |
|                           |                      | 5 1                               | 1.029                     | 110.01                   |
|                           |                      | 6 1                               | 0.181                     | 284.23                   |
|                           |                      | -2 1                              | 1.099                     | 156.35                   |
|                           |                      | -3 1                              | 1.025                     | 338.50                   |
|                           |                      | -4 1                              | 0.554                     | 330.59                   |
|                           |                      | -5 1                              | 0.433                     | 153.44                   |
|                           |                      | -6 1                              | 0.132                     | 202.65                   |
| 155.4555                  | M1                   | 2 1                               | 0.060                     | 314.03                   |
|                           |                      | 3 1                               | 0.023                     | 72.46                    |
|                           |                      | 4 1                               | 0.037                     | 267.31                   |
|                           |                      | 5 1                               | 0.026                     | 107.30                   |
|                           |                      | 6 1                               | 0.004                     | 280.78                   |
|                           |                      | -2 1                              | 0.027                     | 145.08                   |
|                           |                      | -3 1                              | 0.026                     | 324.01                   |
|                           |                      | -4 1                              | 0.015                     | 323.22                   |
|                           |                      | -5 1                              | 0.012                     | 153.57                   |
|                           |                      | -6 1                              | 0.005                     | 206.96                   |
| 155.6555                  | M1F                  | 2 1                               | 0.172                     | 314.04                   |
|                           |                      | 3 1                               | 0.065                     | 71.92                    |
|                           |                      | 4 1                               | 0.107                     | 267.11                   |
|                           |                      | 5 1                               | 0.074                     | 107.25                   |
|                           |                      | 6 1                               | 0.012                     | 280.71                   |
|                           |                      | -2 1                              | 0.077                     | 144.86                   |
|                           |                      | -3 1                              | 0.080                     | 323.75                   |
|                           |                      | -4 1                              | 0.044                     | 323.09                   |
|                           |                      | -5 1                              | 0.035                     | 153.57                   |
|                           |                      | -6 1                              | 0.013                     | 207.02                   |

| <u>Doodson<br/>Number</u> | <u>Tide<br/>Name</u> | <u>Degree &amp;<br/>Order No.</u> | <u>Interpolated Model<br/>C's</u> | <u>Schwiderski Model<br/>c's</u> |
|---------------------------|----------------------|-----------------------------------|-----------------------------------|----------------------------------|
| 162.5565                  | PI1                  | 2 1                               | 0.054                             | 314.22                           |
|                           |                      | 3 1                               | 0.019                             | 43.09                            |
|                           |                      | 4 1                               | 0.037                             | 258.16                           |
|                           |                      | 5 1                               | 0.024                             | 104.77                           |
|                           |                      | 6 1                               | 0.003                             | 276.89                           |
|                           |                      | -2 1                              | 0.025                             | 134.56                           |
|                           |                      | -3 1                              | 0.029                             | 312.91                           |
|                           |                      | -4 1                              | 0.016                             | 317.60                           |
|                           |                      | -5 1                              | 0.012                             | 153.66                           |
|                           |                      | -6 1                              | 0.005                             | 209.25                           |
| 163.5555                  | P1                   | 2 1                               | 0.906                             | 314.24                           |
|                           |                      | 3 1                               | 0.326                             | 39.89                            |
|                           |                      | 4 1                               | 0.630                             | 257.28                           |
|                           |                      | 5 1                               | 0.401                             | 104.50                           |
|                           |                      | 6 1                               | 0.058                             | 276.45                           |
|                           |                      | -2 1                              | 0.432                             | 133.50                           |
|                           |                      | -3 1                              | 0.494                             | 311.91                           |
|                           |                      | -4 1                              | 0.269                             | 317.08                           |
|                           |                      | -5 1                              | 0.210                             | 153.67                           |
|                           |                      | -6 1                              | 0.093                             | 209.43                           |
| 164.5565                  | S1                   | 2 1                               | 0.021                             | 314.26                           |
|                           |                      | 3 1                               | 0.008                             | 36.68                            |
|                           |                      | 4 1                               | 0.015                             | 256.41                           |
|                           |                      | 5 1                               | 0.010                             | 104.24                           |
|                           |                      | 6 1                               | 0.001                             | 275.99                           |
|                           |                      | -2 1                              | 0.010                             | 132.43                           |
|                           |                      | -3 1                              | 0.012                             | 310.91                           |
|                           |                      | -4 1                              | 0.006                             | 316.56                           |
|                           |                      | -5 1                              | 0.005                             | 153.68                           |
|                           |                      | -6 1                              | 0.002                             | 209.61                           |
| 165.5455                  | K1F                  | 2 1                               | 0.053                             | 314.28                           |
|                           |                      | 3 1                               | 0.019                             | 33.66                            |
|                           |                      | 4 1                               | 0.038                             | 255.58                           |
|                           |                      | 5 1                               | 0.024                             | 103.98                           |
|                           |                      | 6 1                               | 0.003                             | 275.53                           |
|                           |                      | -2 1                              | 0.026                             | 131.41                           |
|                           |                      | -3 1                              | 0.030                             | 309.98                           |
|                           |                      | -4 1                              | 0.016                             | 316.07                           |
|                           |                      | -5 1                              | 0.013                             | 153.69                           |
|                           |                      | -6 1                              | 0.006                             | 209.77                           |
| 165.5555                  | K1                   | 2 1                               | 2.677                             | 314.28                           |
|                           |                      | 3 1                               | 0.990                             | 33.50                            |
|                           |                      | 4 1                               | 1.908                             | 255.54                           |
|                           |                      | 5 1                               | 1.195                             | 103.97                           |
|                           |                      | 6 1                               | 0.170                             | 275.51                           |
|                           |                      | -2 1                              | 1.296                             | 131.36                           |
|                           |                      | -3 1                              | 1.511                             | 309.93                           |
|                           |                      | -4 1                              | 0.817                             | 316.04                           |
|                           |                      | -5 1                              | 0.635                             | 153.69                           |
|                           |                      | -6 1                              | 0.288                             | 209.78                           |
|                           |                      |                                   |                                   | 2.816    315.16                  |
|                           |                      |                                   |                                   | 0.889    34.14                   |
|                           |                      |                                   |                                   | 1.912    254.20                  |
|                           |                      |                                   |                                   | 1.211    104.74                  |
|                           |                      |                                   |                                   | 0.164    282.14                  |
|                           |                      |                                   |                                   | 1.349    132.60                  |
|                           |                      |                                   |                                   | 1.524    310.96                  |
|                           |                      |                                   |                                   | 0.852    317.31                  |
|                           |                      |                                   |                                   | 0.656    156.16                  |
|                           |                      |                                   |                                   | 0.318    203.59                  |

| <u>Doodson<br/>Number</u> | <u>Tide<br/>Name</u> | <u>Degree &amp;<br/>Order No.</u> | <u>Interpolated Model<br/>C's</u> | <u>Schwiderski Model<br/>e's</u> |
|---------------------------|----------------------|-----------------------------------|-----------------------------------|----------------------------------|
| 165.5655                  | K1S                  | 2 1                               | 0.360                             | 314.28                           |
|                           |                      | 3 1                               | 0.133                             | 33.32                            |
|                           |                      | 4 1                               | 0.257                             | 255.49                           |
|                           |                      | 5 1                               | 0.161                             | 103.95                           |
|                           |                      | 6 1                               | 0.023                             | 275.48                           |
|                           |                      | -2 1                              | 0.174                             | 131.30                           |
|                           |                      | -3 1                              | 0.203                             | 309.87                           |
|                           |                      | -4 1                              | 0.110                             | 316.01                           |
|                           |                      | -5 1                              | 0.085                             | 153.69                           |
|                           |                      | -6 1                              | 0.039                             | 209.79                           |
| 166.5545                  | PSI1                 | 2 1                               | 0.021                             | 314.30                           |
|                           |                      | 3 1                               | 0.008                             | 30.34                            |
|                           |                      | 4 1                               | 0.015                             | 254.67                           |
|                           |                      | 5 1                               | 0.009                             | 103.69                           |
|                           |                      | 6 1                               | 0.001                             | 275.01                           |
|                           |                      | -2 1                              | 0.010                             | 130.27                           |
|                           |                      | -3 1                              | 0.012                             | 308.95                           |
|                           |                      | -4 1                              | 0.006                             | 315.53                           |
|                           |                      | -5 1                              | 0.005                             | 153.70                           |
|                           |                      | -6 1                              | 0.002                             | 209.95                           |
| 167.5555                  | PHI1                 | 2 1                               | 0.037                             | 314.32                           |
|                           |                      | 3 1                               | 0.014                             | 27.23                            |
|                           |                      | 4 1                               | 0.027                             | 253.80                           |
|                           |                      | 5 1                               | 0.017                             | 103.41                           |
|                           |                      | 6 1                               | 0.002                             | 274.50                           |
|                           |                      | -2 1                              | 0.018                             | 129.18                           |
|                           |                      | -3 1                              | 0.022                             | 307.99                           |
|                           |                      | -4 1                              | 0.012                             | 315.02                           |
|                           |                      | -5 1                              | 0.009                             | 153.70                           |
|                           |                      | -6 1                              | 0.004                             | 210.12                           |
| 175.4555                  | J1                   | 2 1                               | 0.127                             | 314.60                           |
|                           |                      | 3 1                               | 0.072                             | 359.10                           |
|                           |                      | 4 1                               | 0.110                             | 244.32                           |
|                           |                      | 5 1                               | 0.060                             | 99.94                            |
|                           |                      | 6 1                               | 0.007                             | 267.07                           |
|                           |                      | -2 1                              | 0.072                             | 116.76                           |
|                           |                      | -3 1                              | 0.093                             | 298.08                           |
|                           |                      | -4 1                              | 0.048                             | 309.50                           |
|                           |                      | -5 1                              | 0.036                             | 153.80                           |
|                           |                      | -6 1                              | 0.019                             | 211.71                           |
| 195.5555                  | 001                  | 2 1                               | 0.057                             | 315.08                           |
|                           |                      | 3 1                               | 0.057                             | 341.27                           |
|                           |                      | 4 1                               | 0.064                             | 234.05                           |
|                           |                      | 5 1                               | 0.029                             | 94.84                            |
|                           |                      | 6 1                               | 0.003                             | 251.77                           |
|                           |                      | -2 1                              | 0.041                             | 102.60                           |
|                           |                      | -3 1                              | 0.057                             | 288.45                           |
|                           |                      | -4 1                              | 0.027                             | 303.46                           |
|                           |                      | -5 1                              | 0.020                             | 153.91                           |
|                           |                      | -6 1                              | 0.012                             | 213.14                           |

| <u>Doodson<br/>Number</u> | <u>Tide<br/>Name</u> | <u>Degree &amp;<br/>Order No.</u> | <u>Interpolated Model</u> | <u>Schwiderski Model</u> |
|---------------------------|----------------------|-----------------------------------|---------------------------|--------------------------|
|                           |                      |                                   | C's                       | e's                      |
| 245.6555 N2               | 2                    | 2                                 | 0.651                     | 317.51                   |
|                           | 3                    | 2                                 | 0.089                     | 164.54                   |
|                           | 4                    | 2                                 | 0.215                     | 138.70                   |
|                           | 5                    | 2                                 | 0.073                     | 2.73                     |
|                           | 6                    | 2                                 | 0.077                     | 345.44                   |
|                           | -2                   | 2                                 | 0.155                     | 92.42                    |
|                           | -3                   | 2                                 | 0.057                     | 356.03                   |
|                           | -4                   | 2                                 | 0.132                     | 18.84                    |
|                           | -5                   | 2                                 | 0.160                     | 267.60                   |
|                           | -6                   | 2                                 | 0.030                     | 146.63                   |
| 255.5455 M2S              | 2                    | 2                                 | 0.109                     | 316.82                   |
|                           | 3                    | 2                                 | 0.019                     | 178.09                   |
|                           | 4                    | 2                                 | 0.037                     | 129.22                   |
|                           | 5                    | 2                                 | 0.013                     | 2.22                     |
|                           | 6                    | 2                                 | 0.013                     | 326.48                   |
|                           | -2                   | 2                                 | 0.023                     | 77.60                    |
|                           | -3                   | 2                                 | 0.006                     | 344.65                   |
|                           | -4                   | 2                                 | 0.018                     | 20.36                    |
|                           | -5                   | 2                                 | 0.026                     | 261.47                   |
|                           | -6                   | 2                                 | 0.005                     | 144.38                   |
| 255.5555 M2               | 2                    | 2                                 | 2.939                     | 316.81                   |
|                           | 3                    | 2                                 | 0.516                     | 178.13                   |
|                           | 4                    | 2                                 | 0.984                     | 129.18                   |
|                           | 5                    | 2                                 | 0.353                     | 2.22                     |
|                           | 6                    | 2                                 | 0.340                     | 326.40                   |
|                           | -2                   | 2                                 | 0.606                     | 77.52                    |
|                           | -3                   | 2                                 | 0.158                     | 344.56                   |
|                           | -4                   | 2                                 | 0.493                     | 20.37                    |
|                           | -5                   | 2                                 | 0.703                     | 261.44                   |
|                           | -6                   | 2                                 | 0.125                     | 144.37                   |
| 265.4555 L2               | 2                    | 2                                 | 0.070                     | 315.86                   |
|                           | 3                    | 2                                 | 0.017                     | 188.77                   |
|                           | 4                    | 2                                 | 0.025                     | 116.99                   |
|                           | 5                    | 2                                 | 0.009                     | 1.60                     |
|                           | 6                    | 2                                 | 0.009                     | 303.03                   |
|                           | -2                   | 2                                 | 0.014                     | 51.80                    |
|                           | -3                   | 2                                 | 0.002                     | 277.01                   |
|                           | -4                   | 2                                 | 0.008                     | 23.92                    |
|                           | -5                   | 2                                 | 0.017                     | 252.64                   |
|                           | -6                   | 2                                 | 0.003                     | 140.43                   |
| 271.5575                  | 2                    | 2                                 | 0.002                     | 314.93                   |
|                           | 3                    | 2                                 | 0.001                     | 194.75                   |
|                           | 4                    | 2                                 | 0.001                     | 106.75                   |
|                           | 5                    | 2                                 | 0.000                     | 1.08                     |
|                           | 6                    | 2                                 | 0.000                     | 287.22                   |
|                           | -2                   | 2                                 | 0.001                     | 28.18                    |
|                           | -3                   | 2                                 | 0.000                     | 219.53                   |
|                           | -4                   | 2                                 | 0.000                     | 31.80                    |
|                           | -5                   | 2                                 | 0.001                     | 243.98                   |
|                           | -6                   | 2                                 | 0.000                     | 135.25                   |

| <u>Doodson<br/>Number</u> | <u>Tide<br/>Name</u> | <u>Degree &amp;<br/>Order No.</u> | <u>Interpolated Model</u> | <u>Schwiderski Model</u> |       |
|---------------------------|----------------------|-----------------------------------|---------------------------|--------------------------|-------|
|                           |                      |                                   | C's                       | e's                      | C's   |
| 272.5565                  | T2                   | 2 2                               | 0.057                     | 314.91                   |       |
|                           |                      | 3 2                               | 0.018                     | 195.31                   |       |
|                           |                      | 4 2                               | 0.023                     | 105.61                   |       |
|                           |                      | 5 2                               | 0.008                     | 1.03                     |       |
|                           |                      | 6 2                               | 0.010                     | 265.71                   |       |
|                           |                      | -2 2                              | 0.013                     | 25.73                    |       |
|                           |                      | -3 2                              | 0.004                     | 217.09                   |       |
|                           |                      | -4 2                              | 0.004                     | 33.49                    |       |
|                           |                      | -5 2                              | 0.014                     | 242.92                   |       |
|                           |                      | -6 2                              | 0.002                     | 134.48                   |       |
| 273.5555                  | S2                   | 2 2                               | 0.969                     | 314.69                   | 0.931 |
|                           |                      | 3 2                               | 0.312                     | 195.86                   | 0.265 |
|                           |                      | 4 2                               | 0.386                     | 104.47                   | 0.372 |
|                           |                      | 5 2                               | 0.138                     | 0.97                     | 0.137 |
|                           |                      | 6 2                               | 0.169                     | 284.24                   | 0.172 |
|                           |                      | -2 2                              | 0.223                     | 23.33                    | 0.155 |
|                           |                      | -3 2                              | 0.067                     | 214.98                   | 0.096 |
|                           |                      | -4 2                              | 0.061                     | 35.54                    | 0.064 |
|                           |                      | -5 2                              | 0.232                     | 241.84                   | 0.213 |
|                           |                      | -6 2                              | 0.029                     | 133.66                   | 0.031 |
| 274.5545                  |                      | 2 2                               | 0.008                     | 314.57                   |       |
|                           |                      | 3 2                               | 0.003                     | 196.40                   |       |
|                           |                      | 4 2                               | 0.003                     | 103.32                   |       |
|                           |                      | 5 2                               | 0.001                     | 0.91                     |       |
|                           |                      | 6 2                               | 0.001                     | 282.81                   |       |
|                           |                      | -2 2                              | 0.002                     | 20.98                    |       |
|                           |                      | -3 2                              | 0.001                     | 213.14                   |       |
|                           |                      | -4 2                              | 0.000                     | 38.09                    |       |
|                           |                      | -5 2                              | 0.002                     | 240.73                   |       |
|                           |                      | -6 2                              | 0.000                     | 132.78                   |       |
| 275.5555                  | K2                   | 2 2                               | 0.255                     | 314.44                   | 0.260 |
|                           |                      | 3 2                               | 0.087                     | 196.92                   | 0.095 |
|                           |                      | 4 2                               | 0.104                     | 102.16                   | 0.106 |
|                           |                      | 5 2                               | 0.037                     | 0.84                     | 0.038 |
|                           |                      | 6 2                               | 0.047                     | 281.40                   | 0.047 |
|                           |                      | -2 2                              | 0.062                     | 18.68                    | 0.071 |
|                           |                      | -3 2                              | 0.021                     | 211.53                   | 0.019 |
|                           |                      | -4 2                              | 0.013                     | 41.29                    | 0.015 |
|                           |                      | -5 2                              | 0.061                     | 239.59                   | 0.064 |
|                           |                      | -6 2                              | 0.007                     | 131.82                   | 0.008 |
| 285.4555                  |                      | 2 2                               | 0.011                     | 312.22                   |       |
|                           |                      | 3 2                               | 0.006                     | 202.96                   |       |
|                           |                      | 4 2                               | 0.006                     | 86.66                    |       |
|                           |                      | 5 2                               | 0.002                     | 359.93                   |       |
|                           |                      | 6 2                               | 0.003                     | 266.16                   |       |
|                           |                      | -2 2                              | 0.004                     | 354.66                   |       |
|                           |                      | -3 2                              | 0.002                     | 200.63                   |       |
|                           |                      | -4 2                              | 0.001                     | 171.06                   |       |
|                           |                      | -5 2                              | 0.003                     | 221.65                   |       |
|                           |                      | -6 2                              | 0.000                     | 104.96                   |       |

| <u>Doodson<br/>Number</u> | <u>Tide<br/>Name</u> | <u>Degree &amp;<br/>Order No.</u> | <u>Interpolated Model</u> |            | <u>Schwiderski Model</u> |            |
|---------------------------|----------------------|-----------------------------------|---------------------------|------------|--------------------------|------------|
|                           |                      |                                   | <u>C's</u>                | <u>e's</u> | <u>C's</u>               | <u>e's</u> |
| 295.5555                  |                      | 2 2                               | 0.002                     | 308.07     |                          |            |
|                           |                      | 3 2                               | 0.002                     | 207.64     |                          |            |
|                           |                      | 4 2                               | 0.002                     | 72.13      |                          |            |
|                           |                      | 5 2                               | 0.000                     | 358.75     |                          |            |
|                           |                      | 6 2                               | 0.001                     | 255.90     |                          |            |
|                           |                      | -2 2                              | 0.002                     | 340.76     |                          |            |
|                           |                      | -3 2                              | 0.001                     | 196.63     |                          |            |
|                           |                      | -4 2                              | 0.001                     | 186.39     |                          |            |
|                           |                      | -5 2                              | 0.001                     | 199.95     |                          |            |
|                           |                      | -6 2                              | 0.000                     | 30.24      |                          |            |



## Report Documentation Page

|   |  |   |           |
|---|--|---|-----------|
| 1. Report No.<br>NASA TM 4019   | 2. Government Accession No.                          | 3. Recipient's Catalog No.  |           |
| 4. Title and Subtitle<br><b>An Improved Model of the Earth's Gravitational Field: GEM-T1</b>  |  | 5. Report Date<br>July 1987   |           |
|   |  | 6. Performing Organization Code<br>621.0                                      |           |
| 7. Author(s) J.G.Marsh, F.J.Lerch, D.C.Christodoulidis, B.H.Putney, T.L.Felsentreger, B.V.Sanchez, D.E.Smith, S.M.Klosko, T.V.Martin, E.C.Pavlis, J.W.Robbins, R.G.Williamson, O.L.Colombo, N.L.Chandler, K.E.Rachlin, G.B.Patel, S.Bhati, D.S.Chinn  |  | 8. Performing Organization Report No.<br>87B0451                              |           |
| 9. Performing Organization Name and Address<br>Goddard Space Flight Center<br>Greenbelt, Maryland 20771   |  | 10. Work Unit No.   |           |
|   |  | 11. Contract or Grant No.   |           |
| 12. Sponsoring Agency Name and Address<br>National Aeronautics and Space Administration<br>Washington, DC 20546-0001  |  | 13. Type of Report and Period Covered<br>Technical Memorandum                 |           |
|   |  | 14. Sponsoring Agency Code  |           |
| 15. Supplementary Notes<br>Authors Marsh through Smith are in the Geodynamics Branch of GSFC; authors Klosko through Rachlin are affiliated with EG&G Washington Analytical Services Center Inc. and authors Patel through Chinn are with Science Applications and Research Corporation   |  |   |           |
| 16. Abstract<br>A new generation of Goddard Earth Models is under development at the NASA/Goddard Space Flight Center to satisfy the requirements of future geodetic and oceanographic missions. GEM-T1, a model which has been developed from an analysis of direct satellite tracking observations, is the first in this series of models to be produced. GEM-T1 is complete to degree and order 36. It was developed using consistent reference parameters, extensive earth and ocean tidal models, and simultaneously solved for gravitational and tidal terms, earth orientation parameters and the orbital parameters of 580 individual satellite arcs. The solution used exclusively satellite tracking data acquired on 17 different satellites and is predominantly based upon the precise laser data taken by third generation systems. In total, 800,000 observations were used. A major improvement in field accuracy has been obtained with GEM-T1. For marine geodetic applications, nearly a factor of two improvement in long wavelength geoidal modeling has been achieved over that available from earlier "satellite-only" GEM models. Orbit determination accuracy has also been substantially advanced over a wide range of satellites which have been tested. |  |   |           |
| 17. Key Words (Suggested by Author(s))<br>gravitational models<br>geopotential<br>satellite geodesy<br>satellite data analysis<br>satellite laser ranging   |  | 18. Distribution Statement<br>Unclassified-Unlimited<br>Subject Category - 46 |           |
| 19. Security Classif. (of this report)<br>Unclassified  | 20. Security Classif. (of this page)<br>Unclassified | 21. No. of pages  | 22. Price |